

U.S. GLOBAL CHANGE RESEARCH PROGRAM CLIMATE SCIENCE SPECIAL REPORT (CSSR)

Public Comment Period
15 December 2016 – 3 February 2017
[revised end date]

Third-Order Draft (TOD)

COORDINATING LEAD AUTHORS

Donald Wuebbles
Office of Science & Technology Policy
Executive Office of the President

David Fahey
NOAA Earth System Research Lab

Kathleen Hibbard
NASA Headquarters

LEAD AUTHORS

Jeff Arnold, U.S. Army Corps of Engineers
Benjamin DeAngelo, U.S. Global Change Research Program
Sarah Doherty, University of Washington
David Easterling, NOAA National Centers for Environmental Information
James Edmonds, Pacific Northwest National Laboratory
Timothy Hall, NASA Goddard Institute for Space Studies
Katharine Hayhoe, Texas Tech University
Forrest Hoffman, Oak Ridge National Laboratory
Radley Horton, Columbia University
Deborah Huntzinger, Northern Arizona University
Libby Jewett, NOAA Ocean Acidification Program
Thomas Knutson, NOAA Geophysical Fluid Dynamics Lab
Robert Kopp, Rutgers University
James Kossin, NOAA National Centers for Environmental Information
Kenneth Kunkel, North Carolina State University

Allegra LeGrande, NASA Goddard Institute for Space Studies
L. Ruby Leung, Pacific Northwest National Laboratory
Wieslaw Maslowski, Naval Postgraduate School
Carl Mears, Remote Sensing Systems
Judith Perlwitz, NOAA Earth System Research Laboratory
Anastasia Romanou, Columbia University
Benjamin Sanderson, National Center for Atmospheric Research
William Sweet, NOAA National Ocean Service
Patrick Taylor, NASA Langley Research Center
Robert Trapp, University of Illinois at Urbana-Champaign
Russell Vose, NOAA National Centers for Environmental Information
Duane Waliser, NASA Jet Propulsion Laboratory
Chris Weaver, USEPA
Michael Wehner, Lawrence Berkeley National Laboratory
Tristram West, DOE Office of Science

CONTRIBUTING AUTHORS

Richard Alley, Penn State University
Shallin Busch, NOAA Ocean Acidification Program
Sarah Champion, North Carolina State University
Imke Durre, NOAA National Centers for Environmental Information
Dwight Gledhill, NOAA Ocean Acidification Program
Justin Goldstein, U.S. Global Change Research Program

Lisa Levin, University of California – San Diego
Allan Rhoades, University of California – Davis
Paul Ullrich, University of California – Davis
Eugene Wahl, NOAA National Centers for Environmental Information
John Walsh, University of Alaska Fairbanks

U.S. GLOBAL CHANGE RESEARCH PROGRAM CLIMATE SCIENCE SPECIAL REPORT (CSSR)

Third-Order Draft Table of Contents

Front Matter

About This Report	1
Guide to the Report	3
Executive Summary	11

Chapters

1. Our Globally Changing Climate	32
2. Physical Drivers of Climate Change	85
3. Detection and Attribution of Climate Change	139
4. Climate Models, Scenarios, and Projections	152
5. Large-Scale Circulation and Climate Variability	186
6. Temperature Changes in the United States	217
7. Precipitation Change in the United States	252
8. Droughts, Floods, and Hydrology	281
9. Extreme Storms	308
10. Changes in Land Cover and Terrestrial Biogeochemistry	337
11. Arctic Changes and their Effects on Alaska and the Rest of the United States	370
12. Sea Level Rise	411
13. Ocean Changes: Warming, Stratification, Circulation, Acidification, and Deoxygenation	452
14. Perspectives on Climate Change Mitigation	481
15. Potential Surprises: Compound Extremes and Tipping Elements	500

Appendices

A. Observational Datasets Used in Climate Studies	523
B. Weighting Strategy for the 4th National Climate Assessment	529
C. Acronyms and Units	539
D. Glossary	TBD

1 **About This Report**

2 As a key input into the Fourth National Climate Assessment (NCA4), the U.S. Global Change
3 Research Program (USGCRP) oversaw the production of this special, stand-alone report of the
4 state of science relating to climate change and its physical impacts. The Climate Science Special
5 Report (CSSR) serves several purposes for NCA4, including providing 1) an updated detailed
6 analysis of the findings of how climate change is affecting weather and climate across the United
7 States, 2) an executive summary that will be used as the basis for the science summary of NCA4,
8 and 3) foundational information and projections for climate change, including extremes, to
9 improve “end-to-end” consistency in sectoral, regional, and resilience analyses for NCA4. This
10 report allows NCA4 to focus more heavily on the human welfare, societal, and environmental
11 elements of climate change, in particular with regard to observed and projected risks, impacts,
12 adaptation options, regional analyses, and implications (such as avoided risks) of known
13 mitigation actions.

14 Much of this report is intended for a scientific and technically savvy audience, though the
15 Executive Summary is designed to be accessible to a broader audience.

16 **Report Development, Review, and Approval Process**

17 The National Oceanic and Atmospheric Administration (NOAA) served as the administrative
18 lead agency for the preparation of this report. The Science Steering Committee (SSC¹) comprises
19 representatives from three agencies (NOAA, NASA, and DOE) and the U.S. Global Change
20 Research Program (USGCRP),² and three Coordinating Lead Authors, all of whom were Federal
21 employees during the development of this report. Following a public notice for author
22 nominations, the SSC selected 30 Lead Authors, who are scientists representing Federal
23 agencies, national laboratories, universities, and the private sector. Contributing Authors were
24 later chosen to provide special input on select areas of the assessment.

25 **The Sustained National Climate Assessment**

26 The Climate Science Special Report has been developed as part of the USGCRP’s sustained
27 National Climate Assessment (NCA) process. This process facilitates continuous and transparent
28 participation of scientists and stakeholders across regions and sectors, enabling new information

¹ The Science Steering Committee is a federal advisory committee that oversees the production of the CSSR.

² The USGCRP is made up of 13 Federal departments and agencies that carry out research and support the Nation’s response to global change. The USGCRP is overseen by the Subcommittee on Global Change Research (SGCR) of the National Science and Technology Council’s Committee on Environment, Natural Resources, and Sustainability (CENRS), which in turn is overseen by the White House Office of Science and Technology Policy (OSTP). The agencies within USGCRP are the Department of Agriculture, the Department of Commerce (NOAA), the Department of Defense, the Department of Energy, the Department of Health and Human Services, the Department of the Interior, the Department of State, the Department of Transportation, the Environmental Protection Agency, the National Aeronautics and Space Administration, the National Science Foundation, the Smithsonian Institution, and the U.S. Agency for International Development.

and insights to be assessed as they emerge. Relative to other analyses done under the sustained assessment process, the Climate Science Special Report provides a more comprehensive assessment of the science underlying the changes occurring in the Earth's climate system, with a special focus on the United States.

Sources Used in this Report

The findings in this report are based on a large body of scientific, peer-reviewed research, as well as a number of other publicly available sources, including well-established and carefully evaluated observational and modeling datasets. The team of authors carefully reviewed these sources to ensure a reliable assessment of the state of scientific understanding. Each source of information was determined to meet the four parts of the IQA Guidance provided to authors: 1) utility, 2) transparency and traceability, 3) objectivity, and 4) integrity and security. Report authors assessed and synthesized information from peer-reviewed journal articles, technical reports produced by federal agencies, scientific assessments (such as IPCC 2013), reports of the National Academy of Sciences and its associated National Research Council, and various regional climate impact assessments, conference proceedings, and government statistics (such as population census and energy usage).

1 **Guide to the Report**

2 The following describes the format of the Climate Science Special Report and the overall
3 structure and features of the chapters.

4 **Executive Summary**

5 The Executive Summary describes the major findings from the Climate Science Special Report.
6 It summarizes the overall findings and includes some key figures and additional bullet points
7 covering overarching and especially noteworthy conclusions. The Executive Summary and the
8 majority of the Key Findings are written for the non-expert.

9 **Chapters**

10 **Key Findings and Traceable Accounts**

11 Each topical chapter includes Key Findings, which are based on the authors' expert judgment of
12 the synthesis of the assessed literature. Each Key Finding includes a confidence statement and, as
13 appropriate, framing of key scientific uncertainties, so as to better support assessment of
14 climate-related risks. (See "Documenting Uncertainty" below).

15 Each Key Finding is also accompanied by a Traceable Account that documents the supporting
16 evidence, process, and rationale the authors used in reaching these conclusions and provides
17 additional information on sources of uncertainty through confidence and likelihood statements.
18 The Traceable Accounts can be found at the end of each chapter.

19 **Regional Analyses**

20 Throughout the report, the regional analyses of climate changes for the United States are based
21 on ten different regions as shown in Figure 1. There are differences from the regions used in the
22 Third National Climate Assessment (Melillo et al. 2014): 1) the Great Plains are split into the
23 Northern Great Plains and Southern Great Plains; and 2) The U.S. islands in the Caribbean are
24 analyzed as a separate region apart from the Southeast.

25 **Chapter Text**

26 Each chapter assesses the state of the science for a particular aspect of the changing climate. The
27 first chapter gives a summary of the global changes occurring in the Earth's climate system. This
28 is followed in Chapter 2 by a summary of the scientific basis for climate change. Chapter 3 gives
29 an overview of the processes used in the detection and attribution of climate change and
30 associated studies using those techniques. Chapter 4 then discusses the scenarios for greenhouse
31 gases and particles and the modeling tools used to study future projections. Chapters 5 through 9
32 primarily focus on physical changes in climate occurring in the United States, including those
33 projected to occur in the future. Chapter 10 provides a focus on land use change and associated
34 feedbacks on climate. Chapter 11 addresses changes in Alaska in the Arctic, and how the latter

affects the United States. Chapters 12 and 13 discuss key issues connected with sea level rise and ocean changes, including ocean acidification, and their potential effects on the United States. Finally, Chapters 14 and 15 discuss some important perspectives on how mitigation activities could affect future changes in climate and provide perspectives on what surprises could be in store for the changing climate beyond the analyses already covered in the rest of the assessment. This report is designed to be an authoritative assessment of the science of climate change, with a focus on the United States, to serve as the foundation for efforts to assess climate-related risks and inform decision-making about responses. In accordance with this purpose, it does not include an assessment of literature on climate change mitigation, adaptation, economic valuation, or societal responses, nor does it include policy recommendations.

Throughout the report, results are presented in American units as well as in the International System of Units.

Reference time periods for graphics

There are many different types of graphics in the Climate Science Special Report. Some of the graphs in this report illustrate historical changes and future trends in climate compared to some reference period, with the choice of this period determined by the purpose of the graph and the availability of data. Where graphs were generated for this report, they are mostly based on one of two reference periods. The 1901–1960 reference period is particularly used for graphs that illustrate past changes in climate conditions, whether in observations or in model simulations. This 60-year time period was also used for analyses in the Third National Climate Assessment (NCA3; Melillo et al. 2014). The beginning date was chosen because earlier historical observations are generally considered to be less reliable. Thus, these graphs are able to highlight the recent, more rapid changes relative to the early part of the century (the reference period) and also reveal how well the climate models simulate these observed changes. In this report, this time period is used as the base period in most maps of observed trends and all time-varying, area-weighted averages that show both observed and projected quantities.

The other commonly used reference period in this report is 1976–2005. The choice of a 30-year period is consistent with the World Meteorological Organization’s recommendation for climate statistics. This period is used for graphs that illustrate projected changes simulated by climate models. The purpose of these graphs is to show projected changes compared to a period that allows stakeholders and decision makers to base fundamental planning and decisions on average and extreme climate conditions in a non-stationary climate; thus, a recent available 30-year period was chosen (Arguez and Vose 2011). The year 2005 was chosen as an end date because the historical period simulated by the models used in this assessment ends in that year.

For future projections, 30-year periods are again used for consistency. Projections are centered around 2030, 2050, and 2085 with an interval of plus and minus 15 years (for example, results for 2030 cover the period 2015–2045); Most model runs used here only project out to 2100 for

future scenarios, but where possible, results beyond 2100 are shown. Note that these time periods are different than those used in some of the graphics in NCA3. There are also exceptions for graphics that are based on existing publications.

For global results that may be dependent on findings from other assessments (such as those produced by the Intergovernmental Panel on Climate Change, or IPCC), and for other graphics that depend on specific published work, the use of other time periods was also allowed, but an attempt was made to keep them as similar to the selected periods as possible. For example, in the discussion of radiative forcing, the report uses the standard analyses from IPCC for the industrial era (1750 to 2011) (following IPCC 2013). And, of course, the paleoclimatic discussion of past climates goes back much further in time.

Model Results: Past Trends and Projected Futures

While the NCA3 included global modeling results from both the CMIP3 (Coupled Model Intercomparison Project, 3rd phase) models used in the 2007 international assessment (IPCC 2007) and the CMIP5 (Coupled Model Intercomparison Project, 5th phase) models used in the more recent international assessment (IPCC 2013), the primary focus in this assessment is the global model results and associated downscaled products from CMIP5. The CMIP5 models and the associated downscaled products are discussed in Chapter 4.

Treatment of Uncertainties: Likelihoods, Confidence, and Risk Framing

Throughout this report's assessment of the scientific understanding of climate change, the authors have assessed to the fullest extent possible the range of information in the scientific literature to arrive at a series of findings referred to as Key Findings. The approach used to represent the state of certainty in this understanding as represented in the Key Findings is done through two metrics:

- **Confidence** in the validity of a finding based on the type, amount, quality, strength, and consistency of evidence (such as mechanistic understanding, theory, data, models, and expert judgment); the skill, range, and consistency of model projections; and the degree of agreement within the body of literature.
- **Likelihood**, or probability of an effect or impact occurring, is based on measures of uncertainty expressed probabilistically (in other words, based on statistical analysis of observations or model results or on the authors' expert judgment).

The terminology used in the report associated with these metrics is shown in Figure 2. This language is based on that used in NCA3 (Melillo et al. 2014), the IPCC's Fifth Assessment Report (IPCC 2013), and most recently the USGCRP Climate and Health assessment (USGCRP 2016). Wherever used, the confidence and likelihood statements are italicized.

Assessments of confidence in the Key Findings are based on the expert judgment of the author team. Authors provide supporting evidence for each of the chapter's Key Findings in the Traceable Accounts. Confidence is expressed qualitatively and ranges from low confidence (inconclusive evidence or disagreement among experts) to very high confidence (strong evidence and high consensus) (see Figure 2). Confidence should not be interpreted probabilistically, as it is distinct from statistical likelihood.

In this report, likelihood is the chance of occurrence of an effect or impact based on measures of uncertainty expressed probabilistically (in other words, based on statistical analysis of observations or model results or on expert judgment). The authors used expert judgment based on the synthesis of the literature assessed to arrive at an estimation of the likelihood that a particular observed effect was related to human contributions to climate change or that a particular impact will occur within the range of possible outcomes. Where it is considered justified to report the likelihood of particular impacts within the range of possible outcomes, this report takes a plain-language approach to expressing the expert judgment of the chapter team, based on the best available evidence. For example, an outcome termed "likely" has at least a 66% chance of occurring; an outcome termed "very likely," at least a 90% chance. See Figure 2 for a complete list of the likelihood terminology used in this report.

Traceable Accounts for each Key Finding 1) document the process and rationale the authors used in reaching the conclusions in their Key Finding, 2) provide additional information to readers about the quality of the information used, 3) allow traceability to resources and data, and 4) describe the level of likelihood and confidence in the Key Finding. Thus, the Traceable Accounts represent a synthesis of the chapter author team's judgment of the validity of findings, as determined through evaluation of evidence and agreement in the scientific literature. The Traceable Accounts also identify areas where data are limited or emerging. Each Traceable Account includes 1) a description of the evidence base, 2) major uncertainties, and 3) an assessment of confidence based on evidence.

All Key Findings include a description of confidence. Where it is considered scientifically justified to report the likelihood of particular impacts within the range of possible outcomes, Key Findings also include a likelihood designation.

Confidence and likelihood levels are based on the expert assessment of the author team. They determined the appropriate level of confidence or likelihood by assessing the available literature, determining the quality and quantity of available evidence, and evaluating the level of agreement across different studies. Often, the underlying studies provided their own estimates of uncertainty and confidence intervals. When available, these confidence intervals were assessed by the authors in making their own expert judgments. For specific descriptions of the process by which the author team came to agreement on the Key Findings and the assessment of confidence and likelihood, see the Traceable Accounts in each chapter.

1 In addition to the use of systematic language to convey confidence and likelihood information,
2 this report attempts to highlight aspects of the science that are most relevant for supporting the
3 assessment (for example, in the upcoming fourth National Climate Assessment) of key societal
4 risks posed by climate change. This includes attention to the tails of the probability distribution
5 of future climate change and its proximate impacts (for example, on sea level or temperature and
6 precipitation extremes) and on defining plausible bounds for the magnitude of future changes,
7 since many key risks are disproportionately determined by low-probability, high-consequence
8 outcomes. Therefore, in addition to presenting the “most likely” or “best guess” range of
9 projected future climate outcomes, where appropriate, this report also provides information on
10 the outcomes lying outside this range which nevertheless cannot be ruled out, and may therefore
11 be relevant for assessing overall risk. In some cases, this involves an evaluation of the full range
12 of information contained in the ensemble of climate models used for this report, and in other
13 cases will involve the consideration of additional lines of scientific evidence beyond the models.

14 Complementing this use of risk-focused language and presentation around specific scientific
15 findings in the report, Chapter 15 provides an overview of potential surprises resulting from
16 climate change, including tipping elements in the climate system and the compounding effects of
17 multiple, interacting climate change impacts whose consequences may be much greater than the
18 sum of the individual impacts. Chapter 15 also highlights critical knowledge gaps that determine
19 the degree to which such high-risk tails and bounding scenarios can be precisely defined,
20 including missing processes and feedbacks that make it more likely than not that climate models
21 currently underestimate the potential for high-end changes, reinforcing the need to look beyond
22 the central tendencies of model projections to meaningfully assess climate change risk.

23

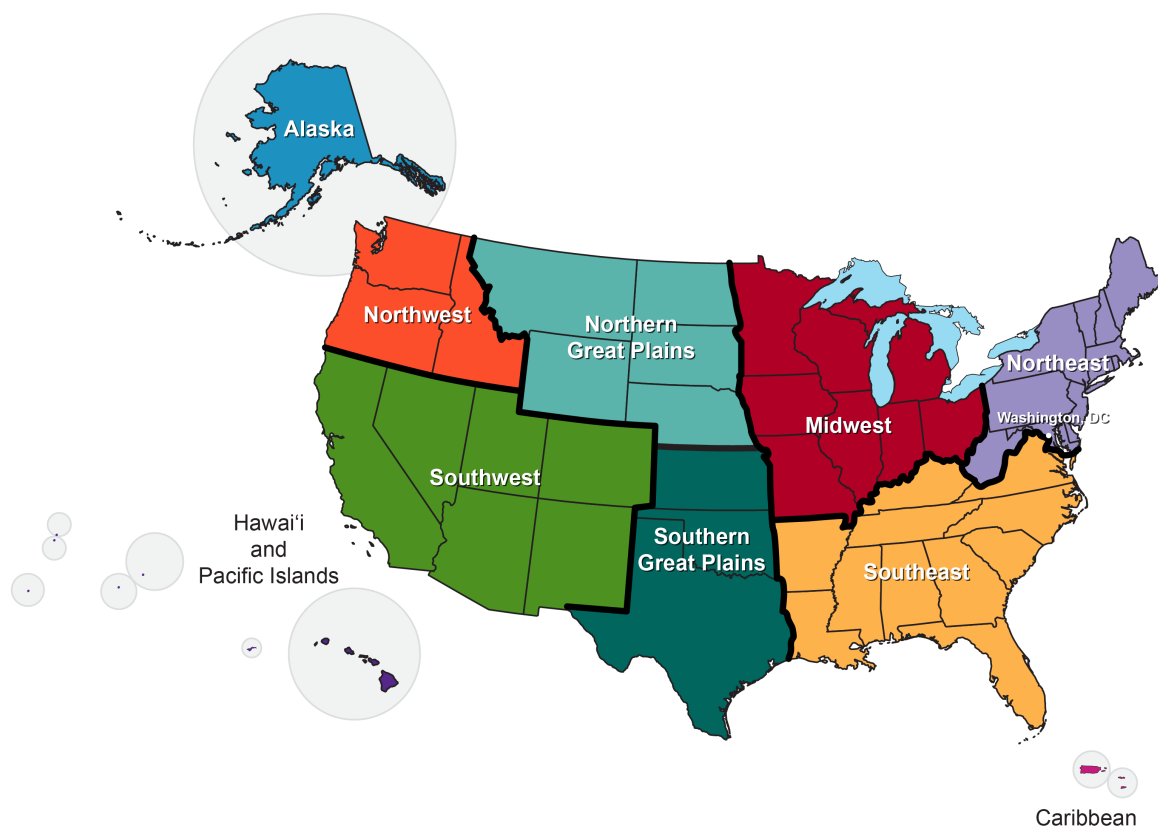


Figure 1. Map of the ten regions of the United States used throughout the Climate Science Special Report. Regions are similar to that used in the Third National Climate Assessment except that 1) the Great Plains are split into the Northern Great Plains and Southern Great Plains, and 2) the Caribbean islands have been split from the Southeast region. (Figure source: adapted from Melillo et al. 2014).

Confidence Level	Likelihood
Very High	Virtually Certain
Strong evidence (established theory, multiple sources, consistent results, well documented and accepted methods, etc.), high consensus	99%–100%
High	Extremely Likely
Moderate evidence (several sources, some consistency, methods vary and/or documentation limited, etc.), medium consensus	95%–100%
Medium	Very Likely
Suggestive evidence (a few sources, limited consistency, models incomplete, methods emerging, etc.), competing schools of thought	90%–100%
Low	Likely
Inconclusive evidence (limited sources, extrapolations, inconsistent findings, poor documentation and/or methods not tested, etc.), disagreement or lack of opinions among experts	66%–100%
	About as Likely as Not
	33%–66%
	Unlikely
	0%–33%
	Very Unlikely
	0%–10%
	Extremely Unlikely
	0%–5%
	Exceptionally Unlikely
	0%–1%

Figure 2. Confidence levels and likelihood statements used in the report. (Figure source: adapted from USGCRP 2016 and IPCC 2013).

Front Matter References

- Arguez, A. and R.S. Vose, 2011: The definition of the standard WMO climate normal: The key to deriving alternative climate normals. *Bulletin of the American Meteorological Society*, **92**, 699-704. <http://dx.doi.org/10.1175/2010BAMS2955.1>
- IPCC, 2007: *Climate Change 2007: The Physical Science Basis. Contribution of Working Group I to the Fourth Assessment Report of the Intergovernmental Panel on Climate Change*. Solomon, S., D. Qin, M. Manning, Z. Chen, M. Marquis, K.B. Averyt, M. Tignor, and H.L. Miller, Eds. Cambridge University Press, Cambridge, U.K., New York, NY, USA, 996 pp. www.ipcc.ch/publications_and_data/publications_ipcc_fourth_assessment_report_wg1_report_the_physical_science_basis.htm
- IPCC, 2013: *Climate Change 2013: The Physical Science Basis. Contribution of Working Group I to the Fifth Assessment Report of the Intergovernmental Panel on Climate Change*. Cambridge University Press, Cambridge, UK and New York, NY, 1535 pp. <http://dx.doi.org/10.1017/CBO9781107415324> www.climatechange2013.org
- Melillo, J.M., T.C. Richmond, and G.W. Yohe, eds. *Climate Change Impacts in the United States: The Third National Climate Assessment*. 2014, U.S. Global Change Research Program: Washington, D.C. 842. <http://dx.doi.org/10.7930/J0Z31WJ2>.
- OMB, 2002: Guidelines for Ensuring and Maximizing the Quality, Objectivity, Utility, and Integrity of Information Disseminated by Federal Agencies; Republication. *Federal Register*, **67**, 8452-8460. <https://www.whitehouse.gov/sites/default/files/omb/fedreg/reproducible2.pdf>
- USGCRP, 2016: *The Impacts of Climate Change on Human Health in the United States: A Scientific Assessment*. Crimmins, A., J. Balbus, J.L. Gamble, C.B. Beard, J.E. Bell, D. Dodgen, R.J. Eisen, N. Fann, M.D. Hawkins, S.C. Herring, L. Jantarasami, D.M. Mills, S. Saha, M.C. Sarofim, J. Trtanj, and L. Ziska, Eds. U.S. Global Change Research Program, Washington, DC, 312 pp. <http://dx.doi.org/10.7930/J0R49NQX>

U.S. GLOBAL CHANGE RESEARCH PROGRAM CLIMATE SCIENCE SPECIAL REPORT (CSSR)

Executive Summary

Introduction

New observations and new research have increased scientists' understanding of past, current, and future climate change since the Third U.S. National Climate Assessment (NCA3) was published in May 2014. This Climate Science Special Report (CSSR) is designed to capture that new information, build on the existing body of science, and summarize the current state of knowledge.

Predicting how climate will change in future decades is a different scientific issue from predicting weather a few weeks from now. Weather is what is happening in the atmosphere in a given location at a particular time—temperature, humidity, winds, clouds, and precipitation. Climate consists of the *patterns* exhibited by the weather—the averages and extremes of the indicated weather phenomena and how those averages and extremes vary from month to month over the course of a typical year—as observed over a period of decades. One can sensibly speak of the climate of a specific location (for example, Chicago) or a region (for example, the Midwest). Climate change means that these weather patterns—the averages and extremes and their timing—are shifting in consistent directions from decade to decade.

The world has warmed (globally and annually averaged surface air temperature) by about 1.6°F (0.9°C) over the last 150 years (1865–2015), and the spatial and temporal non-uniformity of the warming has triggered many other changes to the Earth's climate. Evidence for a changing climate abounds, from the top of the atmosphere to the depths of the oceans. Thousands of studies conducted by tens of thousands of scientists around the world have documented changes in surface, atmospheric, and oceanic temperatures; melting glaciers; disappearing snow cover; shrinking sea ice; rising sea level; and an increase in atmospheric water vapor. Many lines of evidence demonstrate that human activities, especially emissions of greenhouse (heat-trapping) gases, are primarily responsible for recent observed climate changes.

The last few years have also seen record-breaking, climate-related, weather extremes, as well as the warmest years on record for the globe. Periodically taking stock of the current state of knowledge about climate change and putting new weather extremes into context ensures that rigorous, scientifically based information is available to inform dialogue and decisions at every level.

Most of this special report is intended for those who have a technical background in climate science and is also designed to provide input to the authors of the Fourth U.S. National Climate Assessment (NCA4). In this executive summary, green boxes present highlights of the main report followed by related bullet points and selected figures covering more scientific

1 details. The summary material on each topic presents the most salient points of chapter
2 findings and therefore represents only a subset of the report contents. For more details, the
3 reader is referred to the content of individual chapters. This report discusses climate trends
4 and findings at several scales: global, nationwide for the United States, and according to ten
5 specific U.S. regions (shown in Figure 1 in the Guide to the Report). A statement of scientific
6 confidence also follows each bullet in the executive summary. The confidence scale is
7 described in the Guide to the Report.

8

9

DRAFT

Global and U.S. Temperatures Will Continue to Rise

Long-term temperature observations are among the most consistent and widespread evidence of a warming planet. Temperature (and, above all, its local averages and extremes) affects agricultural productivity, energy use, human health, infrastructure, natural ecosystems, and many other essential aspects of society and the natural environment. (Ch. 1)

Observed Global and U.S. Temperature

The global, long-term, and unambiguous warming trend has continued during recent years. Since the last National Climate Assessment was published, 2014 became the warmest year on record up to that time; 2015 surpassed 2014 by a wide margin; and 2016 is expected to surpass 2015. Fifteen of the last 16 years are the warmest years on record for the globe. (Ch.1; Fig ES.1)

- Global annual average temperature, measured over both land and ocean, has increased by more than 1.6°F (0.9°C) from 1880 through 2015 (*very high confidence*). Longer-term climate records indicate that average temperatures in recent decades over much of the world have been much higher than at any time in at least the past 1700 years (*high confidence*). (Ch.1)
- Many lines of evidence demonstrate that human activities, especially emissions of greenhouse gases, are primarily responsible for observed climate changes in the industrial era. There are no alternative explanations, and no natural cycles are found in the observational record that can explain the observed changes in climate. (*Very high confidence*) (Ch.1)
- The *likely* range of the human contribution to the global mean temperature increase over the period 1951–2010 is 1.1° to 1.3°F (0.6° to 0.7°C), which is close to the observed warming of 1.2°F (0.65°C) over this period (*high confidence*). It is *extremely likely* that most of the global mean temperature increase since 1951 was caused by human influence on climate (*high confidence*). The estimated influence of natural forcing and internal variability on globally and annually averaged temperatures over that period is small (*high confidence*). (Ch. 3)
- Natural variability, including El Niño events and other recurring patterns of ocean–atmosphere interactions, has important climate impacts on short time scales, but its influence is limited on global and regional climate trends over longer timescales (that is, a decade or more). (*Very high confidence*) (Ch. 1)
- The average annual temperature of the contiguous United States has increased by about 1.2°F (0.7°C) between 1901 and 2015. Surface and satellite data both show rapid warming

since the late 1970s, while paleo-temperature evidence shows that recent decades are the warmest in at least the past 1,500 years. (*High confidence*) (Ch. 6)

- For the contiguous United States, the largest temperature changes (from the average temperature in early 1900s compared to the average of the last 30 years) have occurred in the western United States, where average temperature increased by more than 1.5°F (0.8°C) across the Northwest and Southwest, and in the Northern Great Plains. (*Very high confidence*). (Ch. 6)

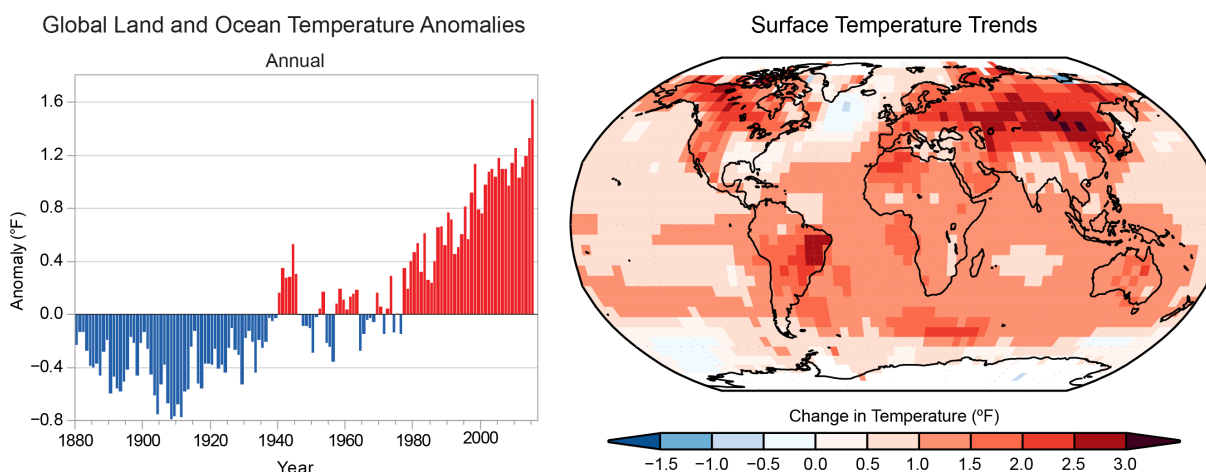


Figure ES.1 Global Temperatures Continue to Rise

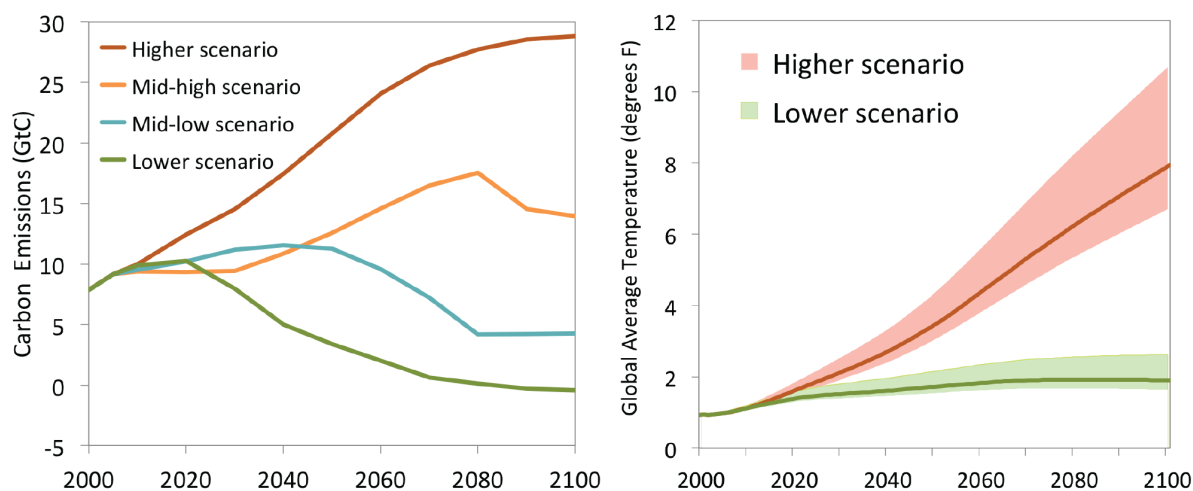
Left: Global annual average temperature has increased by more than 1.6°F (0.9°C) for the period 1986–2015 relative to 1901–1960. Red bars show temperatures above the long-term 1880–2015 average, and blue bars indicate temperatures below the long-term average. Right: Surface temperature trends (change in °F) for the period 1986–2015 relative to 1901–1960. *From Figures 1.2. and 1.3 in Ch. 1.*

Projected Global and U.S. Temperature

- Global climate is projected to continue to change over this century and beyond. Even if humans immediately ceased emitting greenhouse gases into the atmosphere, existing levels would commit the world to at least an additional 0.5°F (0.3°C) of warming over this century relative to today (*high confidence*). The magnitude of climate change beyond the next few decades depends primarily on the additional amount of greenhouse gases emitted globally, and on the sensitivity of Earth's climate to those emissions (*very high confidence*). (Ch. 1, 4; Fig ES.2)

The average annual temperature of the contiguous United States is projected to continue to rise throughout the century. (*Very high confidence*). (Ch.6; Fig ES.3)

- For the United States, near-term increases of at least 2.5°F (1.4°C) are projected over the next few decades even under significantly reduced future emissions, meaning that the temperatures of recent record-setting years will become relatively common in the near future. Increases will be much larger by late century (5.0°F [2.8°C] under a scenario with lower emissions and 8.7°F [4.8°C] under a scenario with higher emissions). (*High confidence*) (Ch.6; Fig ES.3)



ES.2 Figure ES.2. Greater Emissions Lead to Significantly More Warming

The two panels above show projected changes in annual carbon emissions in units of gigatons of carbon (GtC) per year (left) and temperature change that would result from the central estimate (lines) and the likely ranges (shaded areas) of climate sensitivity (right). See the main report for more details on these scenarios and implications. *Based on Figure 4.1 in Chapter 4.*

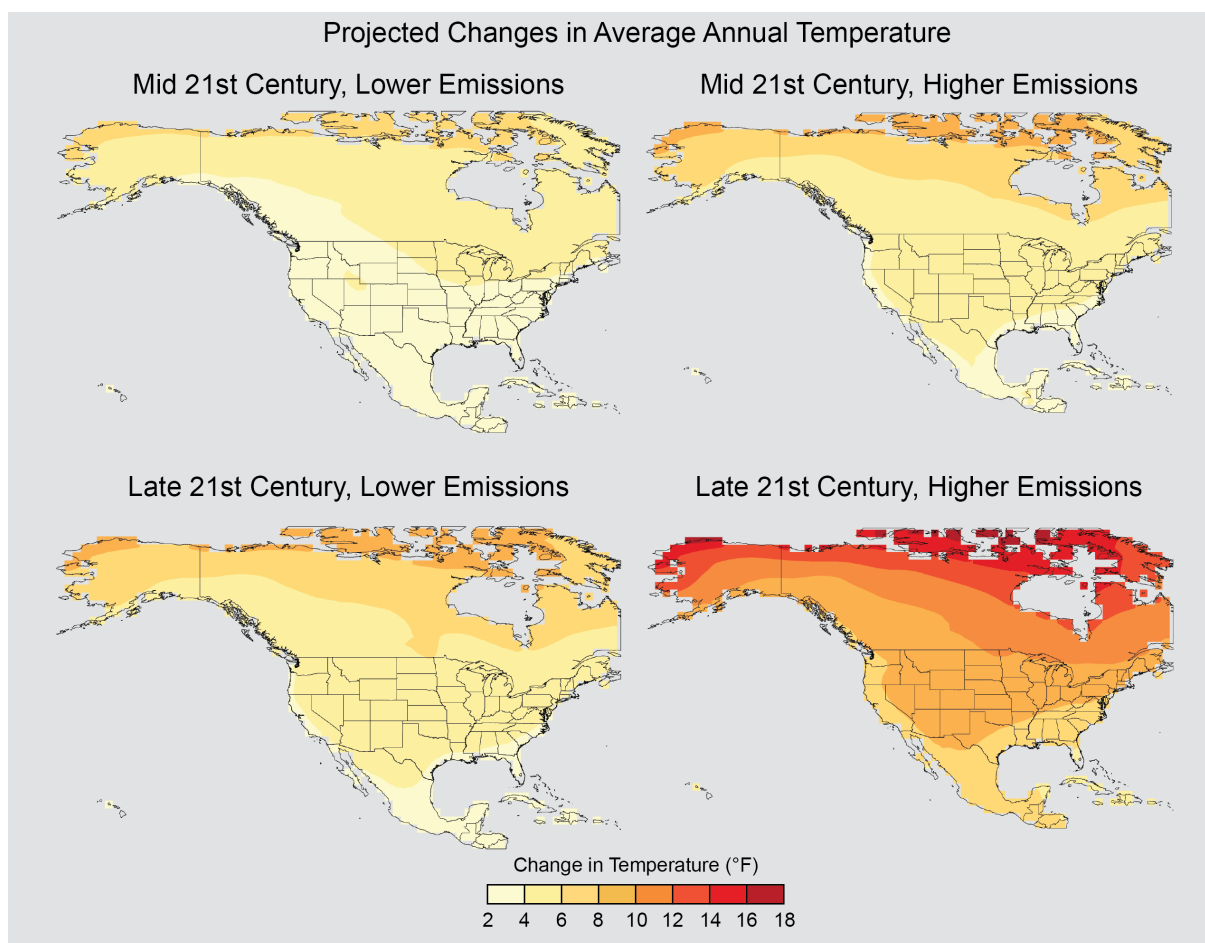


Figure ES.3 Significantly More Warming Occurs Under Higher Greenhouse Gas Concentrations

This figure shows the projected changes in annual average temperature for mid- and late-21st century for various future pathways. Changes are the difference between the average for mid-century (2036–2065; top), late-century (2071–2100; bottom), and the average for near-present (1976–2005). See Figure 6.7 in Chapter 6 for more details.

Many Temperature and Precipitation Extremes Are Becoming More Common

The increases in extreme weather that accompany global climate change are having significant, direct effects on the United States and the global economy and society. Temperature and precipitation extremes can affect water quality and availability, agricultural productivity, human health, vital infrastructure, iconic ecosystems and species, and the likelihood of disasters. Some extremes have already become more frequent, intense, or of longer duration, and many extremes are expected to continue to increase or worsen, presenting substantial challenges for built, agricultural, and natural systems. Some storm types such as hurricanes, tornadoes, and winter storms are also exhibiting changes that have been linked to climate change, although detailed understanding of these linkages is still insufficient in the current state of the science.

The frequency and intensity of heavy precipitation and extreme heat events are increasing in most regions of the world and will *very likely* continue to rise in the future. Trends for some other types of extreme events, such as floods, droughts, and severe storms, vary by region. (*Very high confidence*) (Ch.1)

- Extremely cold days have become warmer since the early 1900s, and extremely warm days have become warmer since the early 1960s. In recent decades, extreme cold waves have become less common while extreme heat waves have become more common. (*Very high confidence*) (Ch. 6)
- Heavy precipitation events across the United States have increased in both intensity and frequency since 1901. There are important regional differences in trends, with the largest increases occurring in the northeastern United States (*high confidence*). The frequency and intensity of heavy precipitation events are projected to continue to increase over the century (*high confidence*). (Ch.7)
- The frequency and severity of landfalling “atmospheric rivers” on the U.S. West Coast (narrow streams of moisture that account for 30%–40% of precipitation and snowpack in the region and are associated with severe flooding events) are projected to increase as a result of increasing evaporation and resulting higher atmospheric water vapor that occurs with increasing temperature. (*Medium confidence*) (Ch.9)
- Recent droughts and associated heat waves have reached record intensities in some regions of the United States, but, by geographical scale and duration, the Dust Bowl era of the 1930s remains the benchmark drought and extreme heat event in the U.S. historical record. (*Very high confidence*) (Ch. 8)

- Reductions in western U.S. winter and spring snowpack are projected as the climate warms. Under higher-emissions scenarios, and assuming no change to current water-resources management, chronic, long-lasting, hydrological drought is possible by end of century. (*Very high confidence*) (Ch. 8)
- For Atlantic and eastern North Pacific hurricanes and western North Pacific typhoons, increases are projected in precipitation rates (*high confidence*) and intensity (*medium confidence*). The frequency of the most intense storms is projected to increase in the Atlantic and western North Pacific (*low confidence*) and in the eastern North Pacific (*medium confidence*). (Ch. 9)

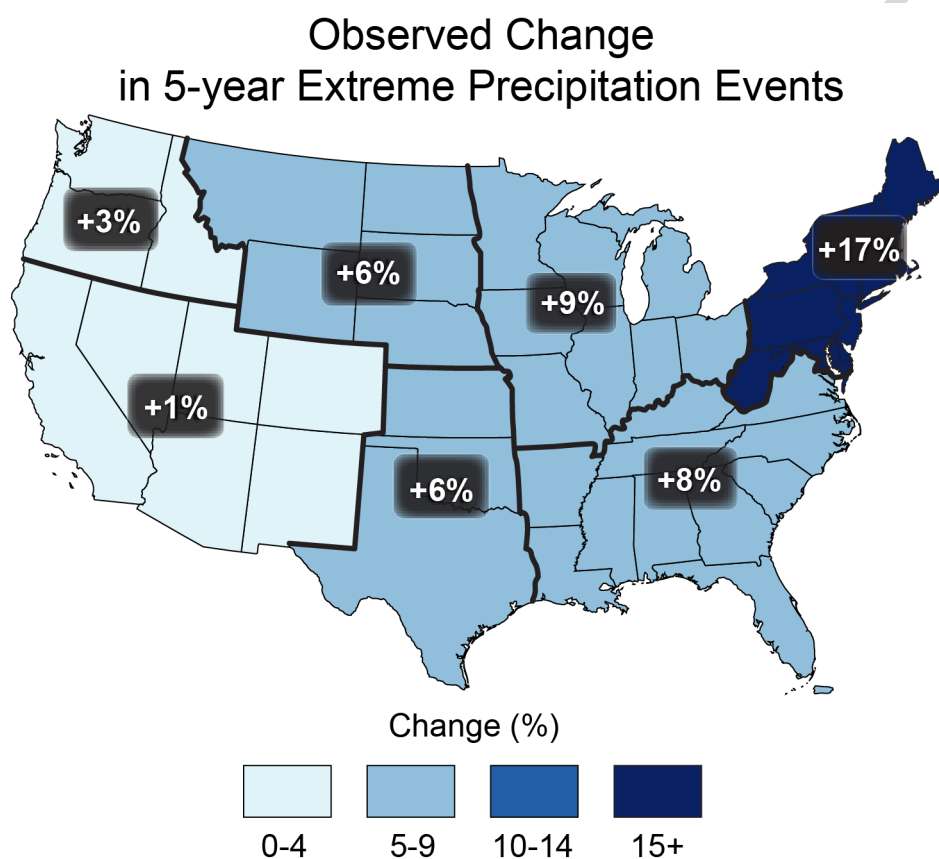


Figure ES.4: Extreme Precipitation Has Increased Across the United States

This figure shows the percentage difference between the 1901–1960 average and the 1981–2015 average of the top 20% of the annual maximum daily precipitation values in each period for events exceeding the threshold for a 5-year return period. The amount of precipitation falling in heavy events is greater across all regions in the entire contiguous United States. Based on figure 7.3 in Chapter 7.

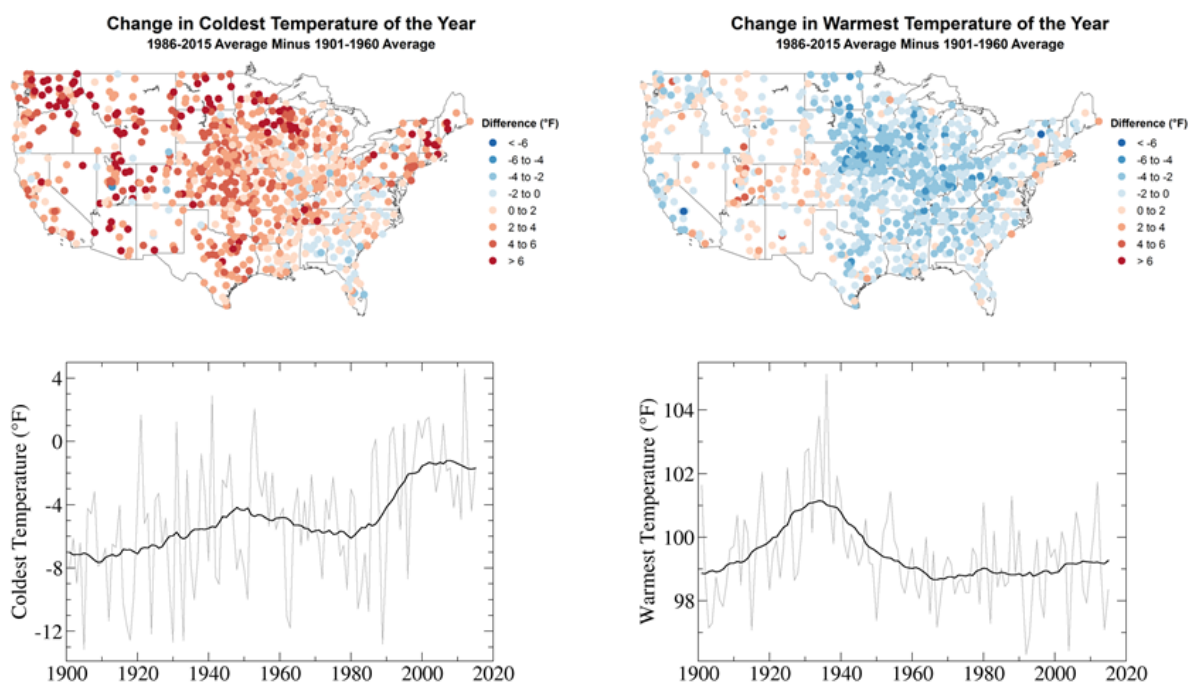


Figure ES.5 Extreme Cold Days Are Warming; Extreme Hot Days Dominated by 1930s Dust Bowl

Observed changes in the coldest and warmest daily temperatures (in °F) of the year. Maps (top) depict changes at stations; changes are the difference between the average for present-day (1986–2015) and the average for the first half of the last century (1901–1960). Time series (bottom) depict changes averaged over the contiguous United States. *Figure 6.3 from Chapter 6.*

****BOX ES.1 ****

The Connected Climate System: Changes Halfway Across the World Are Affecting the United States

Weather conditions and the ways they vary across regions and over the course of the year are influenced, in the United States as elsewhere, by a combination of fixed and variable factors, including local conditions (such as topography and urban heat islands), global trends (such as human-caused warming), and global and regional circulation patterns, including cyclical and chaotic patterns of natural variability within the climate system. For example, during an El Niño year, winters across the southwestern United States are typically wetter than average, and global temperatures are warmer than average. During a La Niña year, conditions across the southwestern United States are typically dry, and there tends to be a cooling effect on global temperatures.

El Niño is not the only repeating pattern of natural variability in the climate system. Other important patterns include the North Atlantic Oscillation (NAO)/Northern Annular Mode

(NAM) that particularly affects conditions on the U.S. East Coast, and the North Pacific Oscillation (NPO) and Pacific North American Pattern (PNA) that especially affect conditions in Alaska and the U.S. West Coast, all of which are closely linked to other atmospheric circulation phenomena like the position of the jet streams. The influences of human activities on the climate system are now so pervasive that the current and future behavior of these previous “natural” climate features can no longer be assumed to be independent of those human influences. (Ch.5)

Understanding the full scope of human impacts on climate requires a global focus because of the interconnected nature of the climate system. For example, the climate of the Arctic and the climate of the continental United States are strongly connected through atmospheric-circulation patterns. While the Arctic may seem physically remote to those living in other regions of the planet, the climatic effects of perturbations to Arctic sea ice, land ice, surface temperature, snow cover, and permafrost affect the amount of warming, sea level change, carbon cycle impacts, and potentially even weather patterns in the lower 48 states. The Arctic is warming at a rate approximately twice as fast as the global average and, if it continues to warm at the same rate, Septembers will be nearly ice-free in the Arctic Ocean sometime between now and the 2040s. The important influence of Arctic climate change on Alaska is apparent; understanding the details of how climate change in the Arctic is affecting the climate in the continental United States is an area of active research. (Ch. 11)

Changes in the tropics can also impact the rest of the globe, including the United States. There is growing evidence that the tropics have expanded over the past several decades, with an associated shift towards the poles of the subtropical dry zones in each hemisphere. The exact causes of this shift in the latitude of dry zones, and its implications, are not yet clear, although the shift is associated with projected drying of the American Southwest over the rest of the century. (Ch. 5)

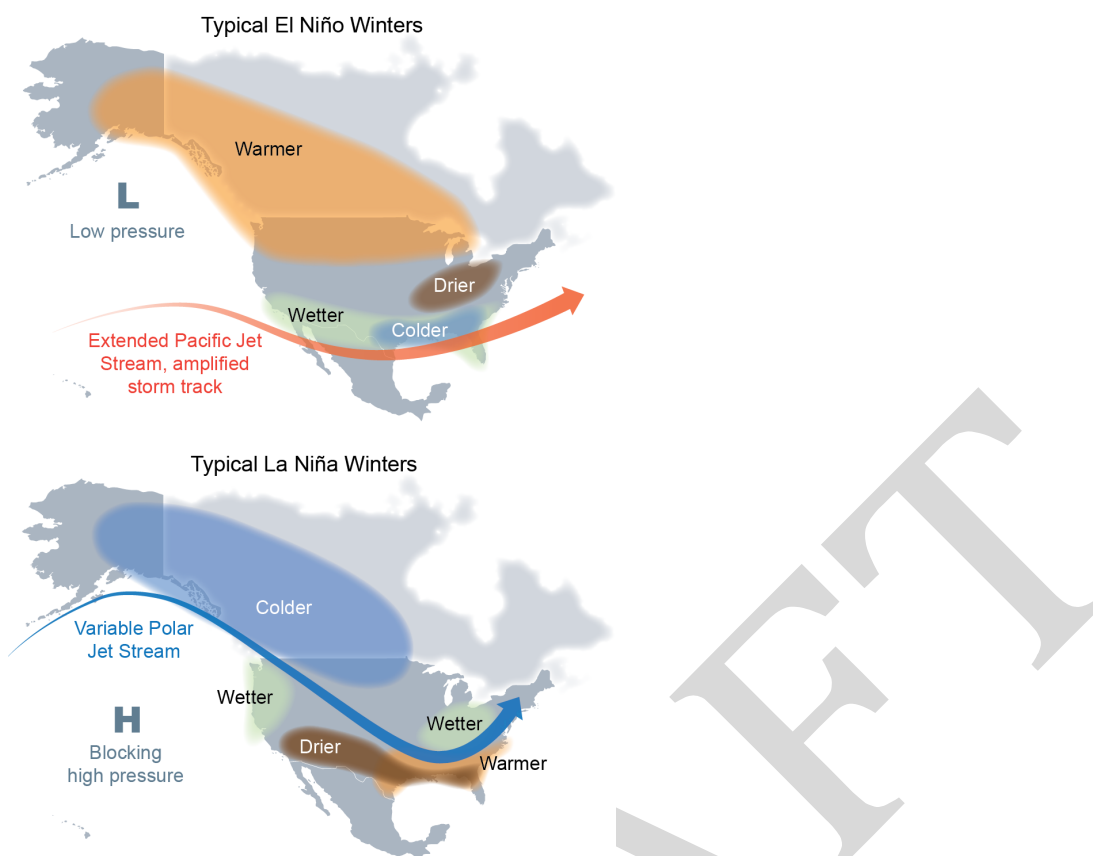


Figure ES.6. Large-Scale Patterns of Natural Variability, Now Being Influenced by Human Activities, Affect U.S. Climate

Typical January–March weather anomalies and atmospheric circulation during moderate to strong (top) El Niño, and (bottom) La Niña. *From Figure 5.2 in Chapter 5.*

****END BOX ES.1****

Oceans Are Rising, Warming, and Becoming More Acidic

Oceans occupy two thirds of the planet's surface and host unique ecosystems and species, including those important for global commercial and subsistence fishing. Understanding climate impacts on the ocean and the ocean's feedbacks to the climate system is critical for a comprehensive understanding of current and future changes in climate.

More than 90% percent of the extra heat being trapped inside the climate system by human emissions is being absorbed by the ocean (*very high confidence*), and the rate of acidification by uptake of CO₂ is faster than in at least the past 66 million years (*medium confidence*). (Ch. 13)

- Global mean sea level (GMSL) has risen by about 8–9 inches since 1880, with about 3 inches of that rise occurring since 1990 (*very high confidence*). Human-caused climate

change has made a substantial contribution to GMSL rise since 1900 (*high confidence*), contributing to a rate of rise faster than during any comparable period for at least 2800 years (*medium confidence*). (Ch. 12; Fig ES.7)

- Relative to the year 2000, GMSL is *very likely* to rise by 0.3–0.6 feet by 2030; 0.5–1.2 feet by 2050; and 1–4 feet by 2100 (*very high confidence in lower bounds of each of these predictions; medium confidence in upper bounds for 2030 and 2050; low confidence in upper bounds for 2100*). (Ch.12)
- Differences in emissions trajectories over the next two decades (see Fig. ES.2) and beyond are estimated to have little effect on the projected amount of GMSL rise over the next few decades, but significantly affect how much more GMSL should be expected by the end of the century (*high confidence*). Emerging scientific results regarding ice-sheet stability suggests that, under a higher scenario, a GMSL rise exceeding 8 feet by 2100 cannot be ruled out. (Ch.12)
- In most projections, GMSL will continue to rise beyond 2100 and even beyond 2200. The concept of a “sea level rise commitment” refers to the long-term projected sea level rise were the planet’s temperature stabilized at a given level. The paleo sea level record suggests that even 2°C (3.6°F) of warming above preindustrial global temperature may represent a commitment to six or more feet of rise (*high confidence*). (Ch. 12)
- Relative sea level (RSL) rise in this century will vary along U.S. coastlines due to vertical land motion and changes in ocean circulation, as well as changes in Earth’s gravitational field and rotation from melting of land ice (*very high confidence*). For almost all future scenarios, RSL rise is *likely* to be greater than the global average in the U.S. Northeast and the western Gulf of Mexico. In intermediate and low scenarios, RSL rise is *likely* to be less than the global average in much of the Pacific Northwest and Alaska. For high scenarios, RSL rise is *likely* to be higher than the global average along all U.S. coastlines outside Alaska (*high confidence*). (Ch. 12)
- Annual occurrences of daily tidal flooding—exceeding local thresholds for minor impacts to infrastructure—have increased 5- to 10-fold since the 1960s in several U.S. coastal cities (*very high confidence*). The changes in flood frequency over time are greatest where elevation is lower, local RSL rise is higher, or extreme variability is less (*very high confidence*). Tidal flooding will continue increasing in depth and frequency in similar manners this century (*very high confidence*). (Ch.12; Fig. ES. 8)
- The world’s oceans are currently absorbing about a quarter of the carbon dioxide emitted to the atmosphere annually from human activities (*very high confidence*), making them more acidic with potential detrimental impacts to marine ecosystems.
- The rate of acidification is unparalleled in at least the past 66 million years (*medium confidence*). Acidification is regionally higher along U.S. coastal systems as a result of

changes in seasonal upwelling (for example, the Pacific Northwest and Alaska), changes in freshwater inputs (for example, the Gulf of Maine), and nutrient input (for example, in urbanized estuaries) (*medium confidence*). (Ch. 11; Ch.13)

- Oxygen is essential to most life in the ocean, governing a host of biogeochemical and biological processes. Increasing sea surface temperatures, rising sea levels, and changing patterns of precipitation, winds, nutrients, and ocean circulation are all contributing to overall declining oxygen concentrations in ocean and coastal waters. Over the last half century, major oxygen losses have occurred in inland seas, estuaries, and in the coastal and open ocean. (*High confidence*) (Ch. 13)
- By 2100, global-average ocean-oxygen levels are projected to decrease from current levels by 2%–4% relative to current levels for a range of scenarios. Much larger losses are projected in some regions and in different water masses. Potential effects on ocean ecosystems could be significant, but are not well understood. (Ch. 13)

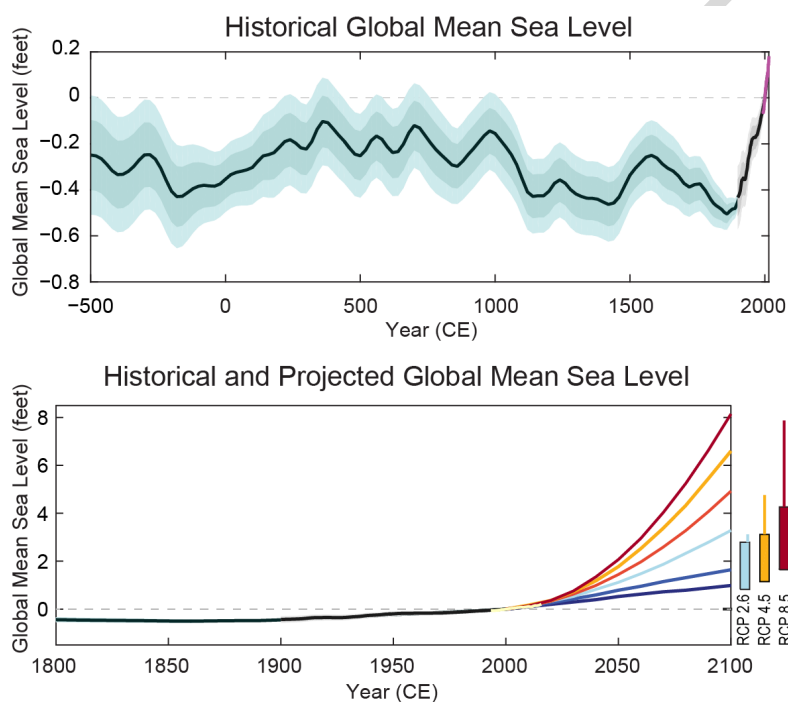


Figure ES.7 Recent Sea Level Rise Fastest for Over 2000 Years

The top panel shows observed and reconstructed mean sea level for the last 2500 years. The bottom panel shows projected mean sea level for six future scenarios, including a risk-based high scenario that assumes major ice melting on portions of Antarctica. *Based on Figure 12.1 in Chapter 12. See the main report for more details.*

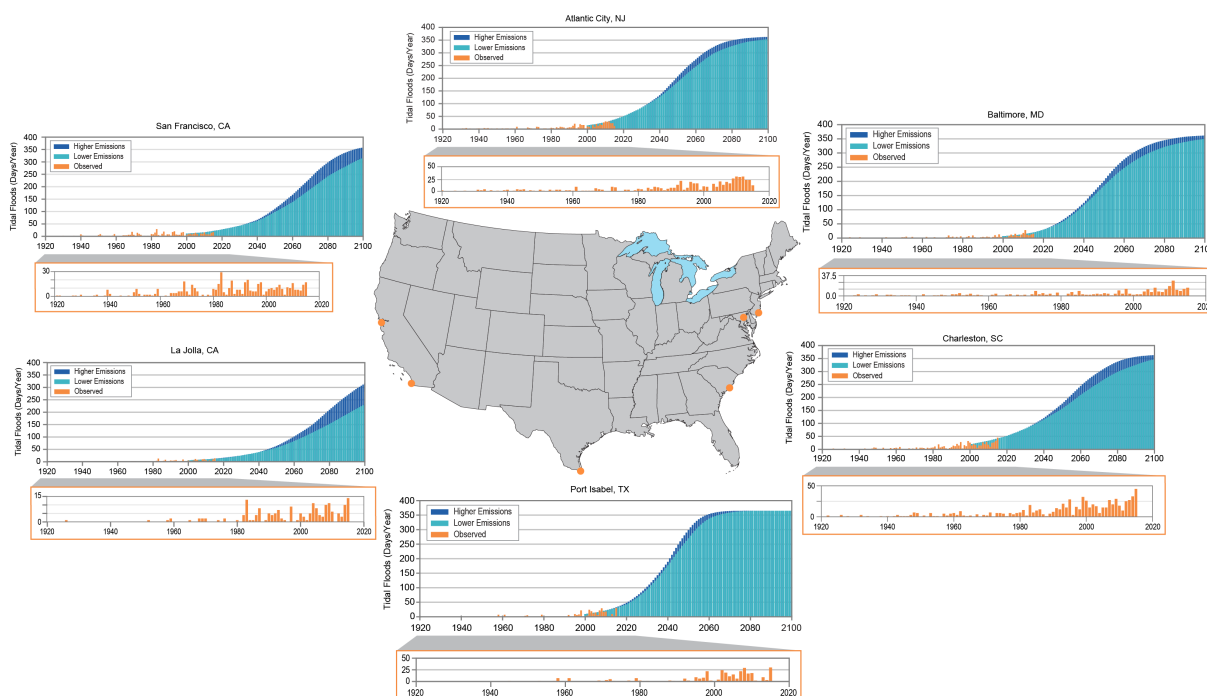


Figure ES. 8 “Nuisance Flooding” Increases Across the United States

Annual occurrences of daily tidal flooding, also called sunny-day or nuisance flooding, have increased for some U.S. coastal cities. Examples shown above include Atlantic City, NJ; Baltimore, MD; Charleston, SC; Port Isabel, TX; La Jolla, CA; and San Francisco, CA. *Based on data in Figure 12.3, Chapter 12.*

Climate Change in Alaska and across the Arctic Continues to Outpace Global Climate Change

Residents of Alaska are on the front lines of climate change. Crumbling buildings, roads, bridges, and eroding shorelines are commonplace. Accelerated melting of multiyear sea ice cover, mass loss from the Greenland Ice Sheet, reduced snow cover, and permafrost thawing are stark examples of the rapid changes occurring in the Arctic. The climate system is connected (see Box ES.1), meaning that changes in the Arctic influence climate conditions outside the Arctic.

Alaska and Arctic surface and air temperatures are rising more than twice as fast as the global average. (*Very high confidence*) (Ch. 11)

- Rising Alaskan temperatures are causing permafrost to thaw and become more discontinuous; these changes lead to release of carbon dioxide and methane from the decomposition of previously frozen organic matter, adding to the global greenhouse gas forcing that is driving climate change. (*High confidence*) (Ch.11)

- 1 • Losses of Arctic sea ice and Greenland Ice Sheet mass are accelerating, and Alaskan
2 mountain glaciers continue to steadily melt (*very high confidence*). Alaskan coastal sea-
3 ice loss rates exceed the Arctic average (*very high confidence*). Human activities have
4 contributed to these reductions in sea and land ice (*high confidence*).
- 5 • Observed sea- and land-ice losses across the Arctic are occurring faster than earlier
6 climate models predicted (*very high confidence*). Melting trends are expected to continue
7 with late summers becoming nearly ice-free for the Arctic Ocean by mid-century (*very*
8 *high confidence*). (Ch.11)
- 9 • Atmospheric circulation patterns connect the climates of the Arctic and the continental
10 United States. The midlatitude circulation influences Arctic climate change (*medium-high*
11 *confidence*). In turn, Arctic warming may be influencing midlatitude circulation over the
12 continental United States, affecting weather patterns (*low-medium confidence*). (Ch.11)

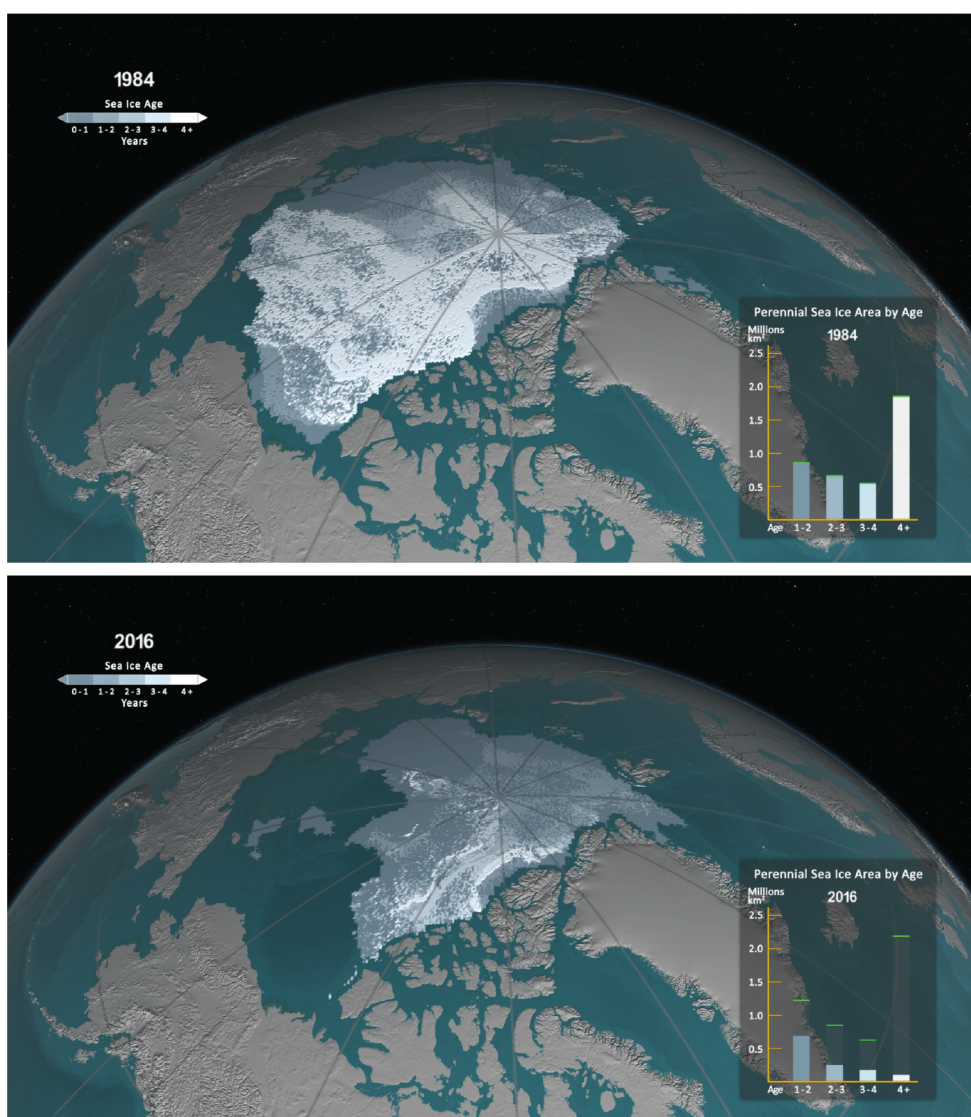


Figure ES.9 Multiyear Sea Ice Has Declined Dramatically

September sea ice extent and age (thickness) shown for 1984 (top) and 2016 (bottom), illustrating that significant reductions have occurred in sea ice extent and age. The bar graphs in the lower right of each panel illustrate the sea ice area covered within each age category. From Figure 11.1 in Chapter 11.

Limiting Globally Averaged Warming to 2°C (3.6°F) Will Require a Major Reduction in Emissions

Human activities are now the dominant cause of the observed changes in climate. For that reason, future climate projections are based on scenarios of how greenhouse gas emissions will continue to affect the climate over the remainder of this century and beyond. In 2016, significant steps were taken to limit future climate change in the form of three international agreements to reduce greenhouse-gas emissions: the Paris Agreement; an agreement to limit CO₂ emissions from aircraft under the International Civil Aviation Organization; and an

agreement to phase down hydrofluorocarbon (HFC) emissions under the Montreal Protocol (see Chapter 14 for more details on each). Despite the greenhouse-gas reductions planned under these agreements, there is still uncertainty about emissions due to changing economic, political, and demographic factors. For that reason, this report quantifies possible climate changes for a broad set of plausible future scenarios through the end of the century. (Chs. 4, 14)

Choices made today will determine the magnitude of climate change risks beyond the next few decades. (Chs. 4,14)

- There will be a delay of decades or longer between significant actions that reduce CO₂ emissions and reductions in atmospheric CO₂ concentrations that contribute to surface warming. This delay—the result of the long lifetime of CO₂ in the atmosphere and the time delay in the response of the climate system to changes in the atmosphere—means that near-term changes in climate will be largely determined by past and present greenhouse gas emissions, modified by natural variability. (*Very high confidence*) (Ch. 14)
- Limiting the global-mean temperature increase to 2°C (3.6°F) above preindustrial levels requires significant reductions in global CO₂ emissions relative to present-day emission rates. Cumulative emissions would likely have to stay below 1,000 gigatons carbon (GtC) for a 2°C objective, leaving about 400 GtC still to be emitted. Assuming future global emissions follow the RCP4.5 scenario (mid-low scenario in Fig ES.2), the total, cumulative emissions commensurate with the 2°C objective would likely be reached between 2051 and 2065, while under the RCP8.5 scenario (higher scenario in Fig ES.2), this point would likely be reached between 2043 and 2050. (*High confidence*). (Ch 14)
- If projected atmospheric CO₂ concentrations do not remain sufficiently low to prevent 2°C warming, climate-intervention strategies such as CO₂ removal or solar-radiation management could possibly offer additional means to limit or reduce temperature increases. Assessing the technical feasibility, costs, risks, co-benefits, and governance challenges of these additional measures, which are as-yet unproven at scale, would be of value to decision makers. (*Medium confidence*) (Ch. 14)
- Atmospheric CO₂ levels have now passed 400 ppm, last seen during the Pliocene, approximately 3 million years ago, when global mean temperatures were 3.6° to 6.3°F (2° to 3.5°C) higher than preindustrial and sea levels were 66 ± 33 feet (20 ± 10 meters) higher than today. (*High confidence*) (Ch. 4)

The observed acceleration in carbon emissions over the past 15–20 years is consistent with higher future scenarios (*very high confidence*); since 2014, growth rates have slowed as economic growth begins to uncouple from carbon emissions (*medium confidence*) but not yet at a rate that would stabilize climate at either the 1.5° or 2°C Paris objectives (*high confidence*). (Ch. 4)

- Continued growth in CO₂ emissions over this century and beyond would lead to concentrations not experienced in many millions of years. Present-day emissions rates of nearly 10 GtC per year, however, suggests that there is no precise past climate analogue for this century any time in at least the last 66 million years. (*Medium confidence*). (Ch.4)

There is a Significant Possibility for Unanticipated Changes

Humanity is conducting an unprecedented experiment with the Earth's climate system through emissions from large-scale fossil-fuel combustion, widespread deforestation, and other changes to the landscape. While scientists and policymakers rely on climate-model projections for a representative picture of the future Earth system under these conditions, there are still elements of the Earth system that models do not capture well. For this reason, there is significant potential for humankind's planetary experiment to result in unanticipated surprises—and the further and faster the Earth's climate system is changed, the greater the risk of such surprises.

There are at least two types of potential surprises: *compound events*, where multiple extreme climate events occur simultaneously or sequentially (creating greater overall impact), and *critical threshold* or *tipping point events*, where some critical threshold is crossed in the climate system (that can lead to large impacts). The probability of such surprises, as well as other more predictable but difficult-to-manage impacts, increases as the influence of human activities on the climate system increases. (Ch. 15)

Unanticipated changes are possible throughout the next century as tipping points are crossed and/or multiple climate-related extreme events occur simultaneously. (Ch. 15)

- Self-reinforcing cycles, or positive feedbacks, in the climate system have the potential to substantially accelerate human-induced climate change and even shift the Earth's climate system, in part or in whole, into new states that are very different from those experienced in the recent past—for example, ones with greatly diminished ice sheets or different large-scale patterns of atmosphere or ocean circulation. Some feedbacks and potential state shifts can be modeled and their probability of occurrence quantified; others can be

modeled or identified but not quantified; and some are probably still unknown (*very high confidence*). (Ch. 2 and 15)

- The physical and socioeconomic impacts of a compound extreme event (such as simultaneous heat and drought, wildfires associated with hot and dry conditions, or flooding associated with high precipitation on top of snow or water-saturated ground) can be greater than the sum of those from individual extreme events (*very high confidence*). Few analyses consider the spatial or temporal correlation between extreme events. (Ch. 15)
- Climate models are not yet able to include all of the processes that contribute to positive feedbacks, occurrence of extremes, and abrupt and/or irreversible changes. For this reason, future changes outside the range projected by current climate models cannot be ruled out (*very high confidence*), and climate models are more likely to underestimate than to overestimate the amount of future change (*medium confidence*). (Ch. 15)

****BOX ES.2****

A Summary of What's New Since NCA3

A more detailed summary of what's new since the release of the Third National Climate Assessment (NCA3) can be found at the end of Chapter 1, including the most notable advances in scientific understanding, new or improved tools and approaches, and changing context such as global-policy developments.

New Understanding

Detection and attribution: Significant advances have been made in the attribution of the human influence on individual climate and weather extreme events since NCA3. (Chapters 3, 6, 7, 8).

Atmospheric circulation and extreme events: The extent to which atmospheric circulation in the midlatitudes is changing or is projected to change is a new important area of research; this is particularly important for understanding changing extreme-climate conditions (Chapters 5, 6, 7).

Increased understanding of specific types of extreme events: The effects of climate change on specific types of extreme events in the United States is a key area where scientific understanding has advanced. (Chapter 9).

The so-called global warming hiatus: Since NCA3, many studies have investigated causes for the temporary slowdown in the rate of increase in near-surface global mean temperature from 2000 to 2013. This report provides a brief assessment of these studies. On the timescales relevant to human-induced climate change, the planet has continued to warm at a steady pace

as predicted by basic atmospheric physics and the well-documented buildup of heat-trapping gases in the atmosphere (Chapter 1).

Oceans and coastal waters: New research on ocean acidification, warming, and oxygen loss is included in this report. There is also growing evidence that the Atlantic meridional overturning circulation (AMOC), sometimes referred to as the ocean's conveyor belt, has slowed (Chapter 13).

Local sea-level-change projections: For the first time in the NCA process, sea level rise projections incorporate geographic variation based on factors such as local land subsidence, ocean currents, and changes in Earth's gravitational field (Chapter 12).

Accelerated ice-sheet loss and irreversibility: New observations from many different sources confirm that ice-sheet loss is accelerating (Chapters 1, 11, 12).

Slowing of the regrowth of Arctic sea ice extent: The annual Arctic sea ice-extent minimum for 2016 was the second lowest on record. In fall 2016, record-setting, slow ice regrowth may lead to record-low values in 2016–2017 winter ice volume as well (Chapter 11).

Potential surprises: Both large-scale state shifts in the climate system (sometimes called “tipping points”) and compound climate extremes (multiple simultaneous or sequential events) have the potential to generate unanticipated surprises. The discussion of these potential surprises in Chapter 15 marks the first extended treatment of this topic in an NCA report. (Chapter 15).

Better Tools and Approaches

Spatial downscaling: Modeled projections of climate changes are now statistically downscaled to a finer spatial resolution, generating temperature and precipitation predictions on a 1/16 degree latitude/longitude grid for the contiguous United States. (Chapters 4, 6, 7).

Risk-based framing: Highlighting aspects of climate science most relevant to assessment of key societal risks is included more completely than in prior NCA assessments.

Model weighting: For the first time, maps and plots of climate projections will use weighted averages of all available climate models. Individual model weights are based on their 1) historical performance relative to observations and 2) independence relative to other models. (Chapters 4, 6, 7).

High-resolution global climate model simulations: As computing resources have grown, more realistic simulations of intense weather systems, including hurricanes, are now possible. Even with the limited number of high-resolution models currently available, confidence has increased in projections of extreme weather (Chapter 9).

1 **Changing Global Context**

2 *The Paris Agreement:* The COP21 Paris Agreement, which entered into force November 4,
3 2016, provides a new framework for *all* nations to mitigate and adapt to climate change. The
4 present document addresses the global climate implications of the agreement objectives
5 (Chapter 4, 14).

6 ******End Box ES.2******

DRAFT

1. Our Globally Changing Climate

KEY FINDINGS

1. The global climate continues to change rapidly compared to the pace of the natural changes in climate that have occurred throughout Earth's history. Trends in globally-averaged temperature, sea-level rise, upper-ocean heat content, land-based ice melt, and other climate variables provide consistent evidence of a warming planet. These observed trends are robust, and have been confirmed by independent research groups around the world. (*Very high confidence*)
2. The frequency and intensity of heavy precipitation and extreme heat events are increasing in most regions of the world. These trends are consistent with expected physical responses to a warming climate and with climate model studies, although models tend to underestimate the observed trends. The frequency and intensity of such extreme events will *very likely* continue to rise in the future. Trends for some other types of extreme events, such as floods, droughts, and severe storms, have more regional characteristics. (*Very high confidence*)
3. Many lines of evidence demonstrate that human activities, especially emissions of greenhouse gases, are primarily responsible for the observed climate changes in the industrial era. There are no alternative explanations, and no natural cycles are found in the observational record that can explain the observed changes in climate. (*Very high confidence*)
4. Global climate is projected to continue to change over this century and beyond. The magnitude of climate change beyond the next few decades depends primarily on the amount of greenhouse (heat trapping) gases emitted globally and the sensitivity of Earth's climate to those emissions. (*Very high confidence*)
5. Natural variability, including El Niño events and other recurring patterns of ocean–atmosphere interactions, have important, but limited influences on global and regional climate over timescales ranging from months to decades. (*Very high confidence*)
6. Longer-term climate records indicate that average temperatures in recent decades over much of the world have been much higher than at any time in the past 1700 years or more. (*High confidence*)

1.1. Introduction

Since the Third U.S. National Climate Assessment (NCA3) was published in May 2014, new observations along multiple lines of evidence have strengthened the conclusion that Earth's climate is changing at a pace and in a pattern not explainable by natural influences. While this

report focuses especially on observed and projected future changes in the United States, it is important to understand those changes in the global context (this chapter).

The world has warmed over the last 150 years, and that warming has triggered many other changes to the Earth's climate. Evidence for a changing climate abounds, from the top of the atmosphere to the depths of the oceans. Thousands of studies conducted by tens of thousands of scientists around the world have documented changes in surface, atmospheric, and oceanic temperatures; melting glaciers; disappearing snow cover; shrinking sea ice; rising sea level; and an increase in atmospheric water vapor. Rainfall patterns and storms are changing and the occurrence of droughts is shifting.

Many lines of evidence demonstrate that human activities, especially emissions of greenhouse gases, are primarily responsible for the observed climate changes over the last 15 decades. There are no alternative explanations. There are no apparent natural cycles in the observational record that can explain the recent changes in climate (e.g., PAGES 2K 2013; Marcott et al. 2013). In addition, natural cycles within the Earth's climate system can only redistribute heat; they cannot be responsible for the observed increase in the overall heat content of the climate system (Church et al. 2011). Internal variability, alternative explanations, or even unknown forcing factors cannot explain the majority of the observed changes in climate (Anderson et al. 2012). The science underlying this evidence, along with the observed and projected changes in climate, is discussed in later chapters, starting with the basis for a human influence on climate in Chapter 2.

Predicting how climate will change in future decades is a different scientific issue from predicting weather a few weeks from now. Local weather is short term and chaotic, and determined by the complicated movement and interaction of high-pressure and low-pressure systems in the atmosphere, and thus it is difficult to predict day-to-day changes beyond about two weeks into the future. Climate, on the other hand, is the statistics of weather--meaning not just mean values but also the prevalence and intensity of extremes--as observed over a period of decades. Climate emerges from the interaction, over time, of rapidly and quite unpredictably changing local weather and more slowly changing and more predictable regional and global influences, such as the distribution of heat in the oceans, the amount of energy reaching Earth from the sun, and the composition of the atmosphere.

Throughout this report, there are many new findings relative to those found in NCA3 and other assessments of the science. Several of these are highlighted in a "What's New" box at the end of this chapter.

1.2. The Globally Changing Climate

1.2.1. Indicators of a Globally Changing Climate

Highly diverse types of direct measurements made on land, sea, and in the atmosphere over many decades have allowed scientists to conclude with high confidence that global mean

temperature is increasing. Observational datasets for many other climate variables support the conclusion with high confidence that the global climate is changing. Figure 1.1 depicts several of the indicators that demonstrate trends consistent with a warming planet over the last century. Temperatures in the lower atmosphere and oceans have increased, as have near-surface humidity and sea level. Basic physics tells us that a warmer atmosphere can hold more water vapor; this is exactly what is measured from satellite data. At the same time, a warmer world means higher evaporation rates and major changes to the hydrological cycle, including increases in the prevalence of torrential downpours. In addition, Arctic sea ice, mountain glaciers, and Northern Hemisphere spring snow cover have all decreased. The relatively small increase in Antarctic sea ice in the last 15 years appears to be best explained as being due to localized natural variability (see e.g., Meehl et al. 2016). The vast majority of the glaciers in the world are losing mass at significant rates. The two largest ice sheets on our planet—Greenland and Antarctica—are shrinking. Five different observational datasets show the heat content of the oceans is increasing.

Many other indicators of the changing climate have been determined from other observations—for example, changes in the growing season and the allergy season (see e.g., <https://www3.epa.gov/climatechange/science/indicators/>; <http://www.globalchange.gov/browse/indicators>). In general, the indicators demonstrate continuing changes in climate since the publication of NCA3. As with temperature, independent researchers have analyzed each of these indicators and come to the same conclusion: all of these changes paint a consistent and compelling picture of a warming planet.

[INSERT FIGURE 1.1 HERE:]

Figure 1.1. Examples of the observations from many different indicators of a changing climate. Anomalies are relative to 1976–2005 averages for the indicated variables. (Figure source: updated from Melillo et al. 2014). [Figure source: (top) adapted from NCEI 2016, (bottom) NOAA NCEI / CICS-NC]

1.2.2. Trends in Global Temperatures

Global annual average temperature (as measured over both land and oceans) has increased by more than 1.6°F (0.9°C) for the period from 1986-2015 relative to 1901-1960 (Figure 1.2). Global-average temperatures are not expected to increase smoothly in response to the human warming influences, because the warming trend is superimposed on natural variability associated with, e.g., the El Niño / La Niña ocean-heat oscillations and the cooling effects of particles emitted by volcanic eruptions. Even so, of the 16 warmest years in the ‘instrumental record’--the period, starting in the late 1800s, when coverage of thermometer measurements became adequate to calculate an global-average temperature for each year--15 occurred in the period from 2001 to 2015; and 2015 itself was the single warmest year in the entire instrumental record, eclipsing 2014 by 0.16°C (0.29°F), four times greater than the difference between 2014 and the next warmest year, 2010 (from NOAA data: <http://www.ncdc.noaa.gov/cag/>). As of November 2016, it appears that 2016 will eclipse 2015. According to NOAA’s temperature analyses, 2015 and

2014 were followed by 2010, 2013, 2005, 2009 and 1998 as the warmest years. Three of the four warmest years on record have occurred since the analyses through 2012 were reported in NCA3.

A strong El Nino contributed to 2015's record warmth (Blunden and Arndt 2016). It's instructive to note, however, that the then-record global temperature of 1998, to which the previous, even more powerful El Nino contributed, was much lower than that of 2015. This fact indicates that the human warming influence, not El Nino *per se*, is the dominant factor producing new record-high temperatures. It must only be added that the El Nino / La Nina cycle itself can no longer be considered to be entirely 'natural'; the human influence on Earth's climate system is now so pervasive that we must assume that virtually all weather and climate phenomena are being affected in one way or another (Trenberth 2015). It is the complex interaction of natural sources of variability with the continuously growing human warming influence that is now shaping the Earth's weather and climate.

Globally, the trend over the past 50 years far exceeds what can be accounted for by natural variability alone (IPCC 2013). That does not mean, of course, that natural sources of variability have become insignificant. They can be expected to continue to contribute a degree of "bumpiness" in the year-to-year global-average temperature trajectory, as well as influences on the average rate of warming that can last as much as a decade or so (Karl et al. 2015; Deser et al. 2012). For example, some combination of those natural sources of variability--and, perhaps, short- to medium-term changes in relation between human-caused warming and cooling effects--produced a much-discussed slowdown in the average pace of global warming in the early 2000s (see Box 1.1)."

[INSERT FIGURE 1.2 HERE:]

Figure 1.2. Top: Global annual average temperature (as measured over both land and oceans) has increased by more than 1.6°F (0.9°C) for the period from 1986-2015 relative to 1901-1960. Red bars show temperatures above the long-term 1880-2015 average, and blue bars indicate temperatures below the average over the entire period. While there is a clear long-term global warming trend, some years do not show a temperature increase relative to the previous year, and some years show greater changes than others. These year-to-year fluctuations in temperature are mainly due to natural sources of variability, such as the effects of El Niños, La Niñas, and volcanic eruptions. Based on the NCEI (NOAAGlobalTemp) data set 1880–2015 (updated from Vose et al. 2012). Bottom: Global average temperature averaged over decadal periods (1886–1895, 1896–1905, ..., 1996–2005, 2006–2015). Horizontal label indicates midpoint year of decadal period. Every decade since 1966–1975 has been warmer than the previous decade.]

Warming during the first half of the 1900s occurred mostly in the Northern Hemisphere (Delworth and Knutson 2000). The last three decades have seen greater warming in response to accelerating increases in greenhouse gas concentrations, particularly at high northern latitudes, and over land as compared to the oceans (see Figure 1.3). In general, winter is warming faster than summer (especially in northern latitudes). Also, nights are warming faster than days

(Alexander et al. 2006, Davy et al. 2016). There is also some evidence of faster warming at higher elevations (Mountain Research Initiative 2015).

A few regions, such as the North Atlantic Ocean, have experienced cooling over the last century, though these areas have warmed over recent decades. Regional climate variability is important (e.g., Hurrell and Deser 2009; Hoegh-Guldberg et al. 2014), but the effects of the increasing fresh water in the North Atlantic from melting of sea and land ice are also important (Rahmstorf et al. 2015). Even in the absence of significant ice melt, we could expect the North Atlantic to warm more slowly given the larger heat capacity of the ocean, leading to land–ocean differences in warming. As a result, the climate for land areas often responds more rapidly than the ocean areas, even though the forcing driving a change in climate occurs equally over land and the oceans (IPCC 2013).

[INSERT FIGURE 1.3 HERE:]

Figure 1.3. Surface temperature trends (change in °F) for the period 1986–2015 relative to 1901–1960 from the National Centers for Environmental Information’s (NCEI) surface temperature product. The relatively coarse (5.0° x 5.0°) resolution of these maps does not capture the finer details associated with mountains, coastlines, and other small-scale effects. (Figure source: updated from Vose et al. 2012).]

Figure 1.4 shows the projected changes in globally averaged temperature for a range of future pathways that vary from assuming strong continued dependence on fossil fuels in energy and transportation systems over the 21st century (the high scenario is Representative Concentration Pathway 8.5, or RCP8.5) to assuming major emission-reduction actions (the very low scenario, RCP2.6). Chapter 4 (Projections) describes the future scenarios and the models of the Earth’s climate system being used to quantify the impact of human choices and natural variability on future climate. Figure 1.4 suggests that global surface temperature increases for the end of the 21st century are *very likely* to exceed 1.5°C (2.7°F) relative to the 1850–1900 average for all projections except for RCP2.6 (IPCC 2013).

[INSERT FIGURE 1.4 HERE:]

Figure 1.4. Multimodel simulated time series from 1950 to 2100 for the change in global annual mean surface temperature relative to 1986–2005 for a range of future scenarios that account for the uncertainty in future emissions from human activities [as analyzed with the 20+ models from around the world used in the most recent international assessment (IPCC 2013)]. The mean and associated uncertainties [1.64 standard deviations (5%–95%) across the distribution of individual models (shading)] based on the averaged over 2081–2100 are given for all of the RCP scenarios as colored vertical bars. The numbers of models used to calculate the multimodel means are indicated. (Figure source: adapted from Walsh et al. 2014).]

----- **START BOX 1.1 HERE** -----

Box 1.1. Was there a “Hiatus” in Global Warming?

Over the past decade, there have been numerous assertions about a ‘hiatus’ (which means ‘pause’) in global warming. These assertions are explored here in the context of long-term climate change.

Statements about the hiatus often take the form of “there has been no global warming over the past X years,” where X is typically less than two decades. For relatively short periods of time, linear fits to the global mean temperature series can show zero or even slightly negative trends as a result of natural variability in the climate system (see Figure 1.5). However, since 1980, all periods exceeding 18 years (satellite data) or 13 years (surface data) have positive trends (Santer et al. 2016). In other words, surface and tropospheric temperature records do not support the assertion that long-term global warming ceased (Lewandowsky et al. 2016), a conclusion further reinforced by recently updated and improved datasets (Karl et al. 2015; Mears and Wentz 2016; Richardson et al. 2016).

[INSERT FIGURE 1.5 HERE:]

Figure 1.5. Panel A shows the annual mean temperature anomalies relative to a 1971–2000 baseline for global mean surface temperature and global mean tropospheric temperature. A previous period of relatively slow-to-no warming (the “Big Hiatus”) is obvious from the mid-1940s to the mid-1970s. Panel B shows the linear trend of 17-year overlapping periods (the maximum number of years historically for less than positive trends), plotted at the time of the center of the trend period. During the recent slowdown period, warming only ceased for two versions of the satellite data, and for a very narrow range of time periods. All 17-year trends are increasing rapidly as the effects of the 2015–2016 El Niño–Southern Oscillation (ENSO) event begin to affect the trends. Panel C shows the annual mean Pacific Decadal Oscillation (PDO) index. Temperature trends show a marked tendency to be lower during periods of generally negative PDO index, shown by the blue shading. (Figure source: adapted and updated from Trenberth 2015 and Santer et al. 2016; Panel B, © American Meteorological Society. Used with permission.)]

For the 15 years following the 1997–1998 ENSO event, the observed rate of warming was smaller than the underlying long-term increasing trend on 30-year climate time scales (Fyfe et al. 2016). Variation in the rate of warming on this time scale is not unexpected and can be the result of long-term internal variability in the climate system, or short-term changes in climate forcings such as aerosols or solar irradiance. Temporary periods similar or larger in magnitude to the current slowdown have occurred earlier in the historical record; almost no increase occurred in the “Big Hiatus” occurred from the mid 1940s to the mid 1970s, which is understood to mostly be due to an increase in anthropogenic and volcanic aerosols during this period. Shorter-term slowdowns also occur after major volcanic eruptions, such as Pinatubo’s eruption in 1991. Temporary speedups have also occurred, most notably in the 1930s and early 1940s, and in the late 1970s and early 1980s. Comparable slowdown and speedup events are also present in

climate simulations of both historical and future climate, even without decadal scale fluctuations in forcing (Easterling and Wehner 2009), and thus the recent slowdown is not particularly surprising from a statistical point of view.

Even though the slowdown of the early 2000s is not unexpected on statistical grounds, it has been used as informal evidence to cast doubt on the accuracy of climate projections from CMIP5 models, since the measured rate of warming in all surface and tropospheric temperature datasets from 2000–2015 was less than was expected given the results of the CMIP3 and CMIP5 historical climate simulations (Fyfe et al. 2016; Santer et al. 2016). Thus it is important to explore a physical explanation of the recent slowdown and to identify the relative contributions of different factors.

A number of studies have investigated the role of natural modes of variability and how they affected the flow of energy in the climate system of the post-2000 period (Balmaseda et al. 2013; England et al. 2014; Meehl et al. 2011; Kosaka and Xie 2013). For the 2000-2013 time period, they find:

- In the Pacific Ocean, a number of interrelated features, including cooler than expected tropical ocean surface temperatures, stronger than normal trade winds, and a shift to the cool phase of the Pacific Decadal Oscillation (PDO) led to cooler than expected surface temperatures in the Eastern Tropical Pacific, a region that has been shown to have a strong influence on global-scale climate (Kosaka and Xie 2013).
- For most of the world's oceans, an excess amount of heat was transferred from the surface into the deeper ocean (Balmaseda et al. 2013; Chen and Tung 2014; Nieves et al. 2015). The transfer of this heat to the deeper oceans removed heat from the atmosphere, causing a reduction in surface warming worldwide.
- Other studies attributed part of the cause of the measurement/model discrepancy to natural fluctuations in radiative forcings, such as stratospheric water vapor, solar output, or volcanic aerosols (add Solomon et al. 2010; Schmidt et al 2014; (Huber and Knutti 2014; Ridley et al. 2014; Santer et al. 2014).

When comparing model predictions with measurements, it is important to note that the CMIP5 runs used predicted values (not actual values) of these factors for time periods after 2000. Thus for these forcings, the model inputs were often different than what happened in the real-world, causing spurious warming in the model output. It is *very likely* that the early 2000s slowdown was caused by a combination of these factors, with natural internal variability in the world's oceans being the dominant factor (Trenberth 2015).

Although 2014 already set a new in globally averaged temperature record up to that time, in 2015–2016, the situation changed dramatically. A switch of the PDO to the positive phase, combined with a strong El Niño event during the fall and winter of 2015–2016, led to months of

record-breaking globally averaged temperatures in both the surface and satellite temperature records (see Figure 1.5; Trenberth 2015). A plot of the trends in 17-year intervals shows a marked increase for trends ending over the past several years, suggesting that the slowdown may be over.

On longer time scales, observed temperature changes are more consistent with model predictions and have been attributed to anthropogenic causes with high confidence (Bindoff et al. 2013). The pronounced globally averaged surface temperature record of 2015 appears to make recent observed temperature changes more consistent with model simulations—including with CMIP5 projections that were (notably) developed in advance of occurrence of the 2015 observed anomalies (Figure 1.6). A second important point illustrated by Figure 1.6 is the broad overall agreement between observations and models on the century timescale, which is robust to the shorter-term variations in trends in the past decade or so. Continued global warming and the frequent setting of new high global mean temperature records or near-records is consistent with expectations based on model projections of continued anthropogenic forcing toward warmer global mean conditions.

[INSERT FIGURE 1.6 HERE:]

Figure 1.6. Comparison of globally averaged temperature anomalies (°F) from observations (through 2015) and the CMIP5 multimodel ensemble (through 2016), using the reference period 1961–1990. The CMIP5 multimodel ensemble (black) is constructed from blended surface temperature and surface air temperature data from the models, masked where observations are not available in the HadCRUT4 dataset (Knutson et al. 2016; see also Richardson et al. 2016). The sources for the three observational indices are: HadCRUT4.5 (red): <http://www.metoffice.gov.uk/hadobs/hadcrut4/data/current/download.html>; NOAA (green): <https://www.ncdc.noaa.gov/monitoring-references/faq/anomalies.php>; and GISTEMP (blue): http://data.giss.nasa.gov/gistemp/tabledata_v3/GLB.Ts+dSST.txt (all downloaded on Oct. 3, 2016) (Figure source: adapted from Knutson et al. 2016).]

----- **END BOX 1.1 HERE** -----

1.2.3. Trends in Global Precipitation

Annual averaged precipitation across global land areas exhibits a slight rise over the past century along with ongoing increases in atmospheric moisture levels (see Figure 1.7). Interannual and interdecadal variability is clearly found in all precipitation reconstructions, owing to factors such as the North Atlantic Oscillation (NAO) and ENSO—the latter accounting for record-low global totals in 2015 in several major analyses; note that precipitation reconstructions are updated operationally by NOAA NCEI on a monthly basis (Becker et al. 2013; Adler et al. 2003).

[INSERT FIGURE 1.7 HERE:]

Figure 1.7. Surface annually-averaged precipitation trends (change in inches) for the period 1986–2015 relative to 1901–1960. The relatively coarse (0.5° x 0.5°) resolution of these maps

1 does not capture the finer details associated with mountains, coastlines, and other small-scale
2 effects. (Figure source: NOAA NCEI / CICS-NC).]

3 The hydrological cycle and the amount of global mean precipitation is primarily controlled by
4 energy budget considerations (Allen and Ingram 2002). The amount of global mean precipitation
5 also changes as a result of a mix of fast and slow atmospheric responses to the changing climate
6 (Collins et al. 2013). In the long term, increases in tropospheric radiative cooling due to CO₂
7 increases must be balanced by increased latent heating, resulting in precipitation increases of
8 approximately 1% to 3% per °C change (0.55% to 0.72% per °F) (IPCC 2013; Held and Soden
9 2006). Changes in global atmospheric water vapor, on the other hand, are controlled by the
10 Clausius-Clapeyron relationship (see Chapter 2: Science), increasing by about 6%–7% per °C of
11 warming. Satellite observations of changes in precipitable water over ocean have been detected
12 at about this rate and attributed to human changes in the atmosphere (Santer et al. 2007). Similar
13 observed changes in land-based measurements have also been attributed to the changes in
14 climate from greenhouse gases (Willet et al. 2010).

15 Earlier studies suggested a pattern from climate change of wet areas getting wetter and dry areas
16 getting dryer (e.g., Greve et al. 2014). While this behavior appears to be valid over ocean areas,
17 changes over land are more complicated. The wet versus dry pattern in observed precipitation
18 has only been attributed in a zonal mean sense (Zhang et al. 2007; Marvel and Bonfils 2013) due
19 to the large amount of spatial variation in precipitation changes as well as significant natural
20 variability. The detected signal in zonal mean is largest in the Northern Hemisphere, with
21 decreases in the sub-tropics and increases at high latitudes. As a result, changes in annual
22 averaged Arctic precipitation have been detected and attributed to human activities (Min et al.
23 2008).

24 **1.2.4. Global Trends in Extreme Weather Events**

25 A change in the frequency, duration, and/or magnitude of extreme weather events is one of the
26 most important consequences of a warming climate. In statistical terms, a small shift in the mean
27 of a weather variable occurring in concert with a change in the shape of its probability
28 distribution can cause a large increase or decrease in the probability of a value above or below an
29 extreme threshold (Katz and Brown 1992). Examples include extreme high-temperature events
30 and heavy precipitation events. Additionally, extreme events such as intense tropical cyclones,
31 mid-latitude cyclones, and hail and tornadoes associated with thunderstorms, can occur as
32 isolated events that are not generally studied in terms of extremes within a probability
33 distribution. Detecting trends in the frequency and intensity of extreme weather events is
34 challenging (Sardeshmukh et al. 2015). The most intense events are rare by definition, and
35 observations may be incomplete and suffer from reporting biases. Further discussion on trends
36 and projections of extreme events for the United States can be found in Chapter 9: Extreme
37 Storms.

Extreme Heat and Cold

The frequency of multiday heat waves and extreme high temperatures at both daytime and nighttime hours is increasing over the United States (Meehl et al. 2009) and over much of the global land areas (IPCC 2013). The land area experiencing daily highs above given thresholds (for example, 90° F) has been increasing since about 1998 (Seneviratne et al. 2014). At the same time, frequencies of cold waves and daytime and nighttime extremely low temperatures are decreasing over the United States and much of the Earth (IPCC 2013; Easterling et al. 2016).

The enhanced radiative forcing caused by greenhouse gases has a direct influence on heat extremes by shifting distributions of daily temperature (Min et al. 2013). Recent work indicates changes in atmospheric circulation may also play a significant role (See Chapter 5). For example, a recent study found that increasing anticyclonic circulations partially explain observed trends in heat events over North America and Eurasia, among other effects (Horton et al. 2015). Although the subject of significant study still, the observed changes in circulation may also be the result of human influences on climate.

Extreme Precipitation

A robust consequence of a warming climate is an increase in atmospheric water vapor, which exacerbates precipitation events under similar meteorological conditions, meaning that when rainfall occurs, the amount of rain falling in that event tends to be greater. As a result, extreme precipitation events globally are becoming more frequent (IPCC 2013; Asadieh and Krakauer 2015; Kunkel and Frankson 2015; Donat et al. 2016). On a global scale, the observational annual-maximum daily precipitation has increased by 8.5% over the last 110 years; global climate models also derive an increase in extreme precipitation globally but tend to underestimate the rate of the observed increase (Asadieh and Krakauer 2015; Donat et al. 2016). Extreme precipitation events are increasing globally in frequency over both wet and dry regions (Donat et al. 2016). Although more spatially heterogeneous than heat extremes, numerous studies have found increases in precipitation extremes on many regions using a variety of methods and threshold definitions (Kunkel et al. 2013), and those increases can be attributed to human-caused changes to the atmosphere (Min et al. 2011; Zhang et al., 2013). Finally, extreme precipitation associated with tropical cyclones (TCs) is expected to increase in the future (Knutson et al. 2015), but current trends are not clear (Kunkel et al. 2013).

The impact of extreme precipitation trends on flooding globally is complex because additional factors like soil moisture and changes in land cover are important (Berghuijs et al. 2016). Globally, there is low confidence in current river-flooding trends (Kundzewicz et al. 2014), but the magnitude and intensity of river flooding is projected to increase in the future (Arnell and Gosling 2014). More on flooding trends in the United States is in Chapter 8: Droughts, Floods, and Hydrology

Tornadoes and Thunderstorms

Increasing air temperature and moisture increase the risk of extreme convection, and there is evidence for a global increase in severe thunderstorm conditions (Sander et al. 2013). Strong convection, along with wind shear, represents favorable conditions for tornadoes. Thus, there is reason to expect increased tornado frequency and intensity in a warming climate (Diffenbaugh et al. 2013). Inferring current changes in tornado activity is hampered by changes in reporting standards, and trends remain highly uncertain (Kunkel et al. 2013).

Winter Storms

Winter storm tracks have shifted slightly northward in recent decades over the Northern Hemisphere (Bender et al. 2012). More generally, extra-tropical cyclone (ETC) activity is projected to change in complex ways under future climate scenarios, with increases in some regions and seasons and decreases in others. There was good general agreement on these points among CMIP5 climate models, although some models underestimated the current cyclone track density (Colle et al. 2013; Chang 2013).

Enhanced Arctic warming (arctic amplification), due in part to sea ice loss, reduces lower tropospheric meridional temperature gradients, diminishing baroclinicity (a measure of how misaligned the gradient of pressure is from the gradient of air density)—an important energy source for ETCs. At the same time, upper-level meridional temperature gradients will increase, due to a warming upper tropical troposphere and a cooling high-latitude lower stratosphere. While both effects counteract each other with respect to a projected change in mid-latitude storm tracks, the simulations indicate that the magnitude of arctic amplification is a controlling factor on circulation changes in the North Atlantic region (Barnes and Polvani 2015).

Tropical Cyclones

Detection of trends in past tropical cyclone activity is hampered by uncertainties in the data collected prior to the satellite era and by uncertainty in the relative contributions of natural variability and anthropogenic influences. Theoretical arguments and numerical modeling simulations support an expectation that radiative forcing by greenhouse gases and anthropogenic aerosols can affect tropical cyclone (TC) activity in a variety of ways, but robust formal detection and attribution for past observed changes has not yet been realized. Since the IPCC AR5 (2013), there is new evidence that the locations where TCs reach their peak intensity have migrated poleward in both the Northern and Southern Hemispheres, in concert with the independently measured expansion of the tropics (Kossin et al. 2014). In the western North Pacific, this migration has substantially changed the TC hazard exposure patterns in the region and appears to have occurred outside of the historically measured modes of regional natural variability (Kossin et al. 2016).

Whether global trends in high-intensity TCs are already observable is a topic of active debate. One study using the best-track data archive 1982–2009 found a significant positive global trend in lifetime maximum wind speed of high-intensity TCs, corroborating earlier work (Elsner et al. 2008; Kossin et al. 2013). When the same procedure is applied to a homogenized satellite record over the same period, the trends are no longer significant. However, the same study also demonstrated that the observed changes in the environment are *unlikely* to support a detectable trend over that period (Kossin et al. 2013). Other studies have suggested that aerosol pollution has masked the increase in TC intensity expected otherwise from greenhouse warming (Wang et al. 2014; Sobel et al. 2016).

TC intensities are expected to increase with warming, both on average and at the high end of the scale, as the range of achievable intensities expands, so that the most intense storms will exceed the intensity of any in the historical record (Sobel et al. 2016). Some studies have projected an overall increase in TC activity (Emanuel 2013). However studies with high-resolution models are giving a different result. For example, a high-resolution dynamical downscaling study of global TC activity under the RCP4.5 scenario projects an increased occurrence of the highest-intensity category TCs (Saffir-Simpson Categories 4 and 5), along with a reduced overall TC frequency, though there are considerable basin-to-basin differences (Knutson et al. 2015). Chapter 9 covers more on extreme storms affecting the United States.

1.2.5. Global Changes in Land Processes

Changes in land cover have had important effects on climate, while climate change also has important effects on land cover (IPCC 2013). In some case, there are changes in land cover that are both consequences of and influences on global climate change (e.g., declines in sea ice and snow cover, thawing permafrost). Other changes are currently mainly causes of climate change but in the future could become consequences (e.g., deforestation), while other changes are mainly consequences of climate change (e.g., effects of drought).

Northern Hemisphere snow cover extent has decreased, especially in spring, primarily due to earlier spring snowmelt (Kunkel et al. 2016), and this decrease since the 1970s is at least partially driven by anthropogenic influences (Rupp et al. 2013). Snow cover reductions, especially in the Arctic region in summer, have led to reduced seasonal albedo.

While global-scale trends in drought are uncertain due to lack of direct observations, regional trends indicate increased frequency and intensity of drought in the Mediterranean (Sousa et al. 2011; Hoerling et al. 2013) and West Africa (Dai 2013; Sheffield et al. 2012), and decreased frequency and intensity in central North America (Peterson et al. 2013) and northwest Australia (Dai 2013; Sheffield et al. 2012; Jones et al. 2009).

Anthropogenic land-use changes, such as deforestation and growing cropland extent, have increased the global land surface albedo, and a small amount of cooling can be attributed to this albedo change. Effects of other land use changes, including modifications of surface roughness,

latent heat flux, river runoff, and irrigation, are difficult to quantify, but may offset the direct land-use albedo changes (Bonan 2008; de Noblet-Ducoudré et al. 2012).

Globally, land-use change since 1750 has been typified by deforestation, driven by the growth in intensive farming and urban development. Global land-use change is estimated to have released 190 ± 65 PgC (petagrams of carbon) through 2014 (Le Quéré et al. 2015). Over the same period, cumulative fossil fuel and industrial emissions are estimated to have been 405 ± 20 PgC, yielding total anthropogenic emissions of 590 ± 70 PgC, of which cumulative land-use change emissions were about 32% (Le Quéré et al. 2015). Tropical deforestation is the dominant driver of land-use change emissions, estimated at 0.1–1.7 PgC per year. Global deforestation emissions of about 3 PgC per year are compensated by around 2 PgC per year of forest regrowth in some regions, mainly from abandoned agricultural land (Houghton et al. 2012; Pan et al. 2011).

Natural terrestrial ecosystems are gaining carbon through uptake of CO₂ by enhanced photosynthesis due to higher CO₂ levels, increased nitrogen deposition, and longer growing seasons in mid- and high latitudes. Anthropogenic atmospheric CO₂ absorbed by land ecosystems is stored as organic matter in live biomass (leaves, stems, and roots), dead biomass (litter and woody debris), and soil carbon.

Many studies have documented a lengthening growing (non-frozen) season, primarily due to the changing climate (Myneni et al. 1997; Parmesan and Yohe 2003; Menzel et al. 2006; Schwartz et al. 2006; Kim et al. 2012), and elevated CO₂ is expected to further lengthen the growing season (Reyes-Fox et al. 2014). In addition, a recent study has shown an overall increase in greening of the Earth in vegetated regions (Zhu et al. 2016), while another has demonstrated evidence that the greening of Northern Hemisphere extratropical vegetation is attributable to anthropogenic forcings, particularly rising atmospheric greenhouse gas levels (Mao et al. 2016). However, observations (Finzi et al. 2006; Palmroth et al. 2006; Norby et al. 2010) and models (Sokolov et al. 2008; Thornton et al. 2009; Zaehle and Friend 2010) indicate that nutrient limitations and land availability will constrain future land carbon sinks.

Modifications to the water, carbon, and biogeochemical cycles on land result in both positive and negative feedbacks to temperature increases (Betts et al. 2007; Bonan 2008; Bernier et al. 2011). Snow and ice albedo feedbacks are positive, leading to increased temperatures with loss of snow and ice extent. While land ecosystems are expected to have a net positive feedback due to reduced natural sinks of CO₂ in a warmer world, anthropogenically increased nitrogen deposition may reduce the magnitude of the net feedback (Churkina et al. 2009; Zaehle et al. 2010; Thornton et al. 2009). Increased temperature and reduced precipitation increase wildfire risk and susceptibility of terrestrial ecosystems to pests and disease, with resulting feedbacks on carbon storage. Increased temperature and precipitation, particularly at high latitudes, drives up soil decomposition, which leads to increased CO₂ and CH₄ emissions (Page et al. 2002; Ciais et al. 2005; Chambers et al. 2007; Kurz et al. 2008; Clark et al. 2010; van der Werf et al. 2010; Lewis et al. 2011). While some of these feedbacks are well known, others are not so well quantified and

yet others remain unknown; the potential for surprise is discussed further in Chapter 15: Potential Surprises.

1.2.6. Global Changes in Sea Ice, Glaciers, and Land Ice

Since NCA3 (Melillo et al. 2014), there have been significant advances in the understanding of changes in the cryosphere. Observations continue to show that Arctic sea ice extent and thickness, Northern Hemisphere snow cover, and the volume of mountain glaciers and continental ice sheets are all decreasing (Stroeve et al. 2014a,b; Comiso and Hall 2014). In many cases, evidence suggests that the net loss of mass from the global cryosphere is accelerating (Rignot et al. 2011, 2014; Williams et al. 2014; Zemp et al. 2015; Seo et al. 2015; Harig and Simons 2016). See Chapter 11 for more details on the Arctic and Alaska beyond the short discussion in this chapter.

Arctic Sea Ice

Arctic sea ice is a key component of the global climate system and appears to be in rapid transition. For example, sea-ice areal extent, thickness, and volume have been in decline since at least 1979 (IPCC 2013; Stroeve et al. 2014a,b; Comiso and Hall 2014), and annually averaged Arctic sea-ice extent has decreased since 1979 at a rate of 3.5%–4.1% per decade (IPCC 2013; <https://nsidc.org/arcticseaicenews/>). Reductions in Arctic sea ice are found in all months and are most rapid in summer and autumn (Stroeve et al. 2012b; Stroeve et al. 2014a; Comiso and Hall 2014). October 2016 was the slowest growth rate in Arctic sea ice in history for that month. Between 1979 and 2014, sea ice extent changes in March and September (the months of maximum and minimum extent) are –2.6% and –13.3% per decade, respectively (Perovich et al. 2015). At the same time, the age distribution of sea ice has also become younger since 1988 (Perovich et al. 2015).

The rate of perennial and multiyear sea ice loss has been $11.5\% \pm 2.1\%$ and $13.5\% \pm 2.5\%$ per decade, respectively, at the time of minimum extent (IPCC 2013). The thickness of the Arctic sea ice during winter has decreased between 1.3 and 2.3 meters (4 to 7.5 feet) (IPCC 2013). The length of the sea ice melt season has also increased by at least five days per decade since 1979 for much of the Arctic (Stroeve et al. 2014a; Parkinson 2014). Lastly, current generation climate models still exhibit difficulties in simulating changes in Arctic sea ice characteristics, simulating weaker reductions in sea ice volume and extent than observed (IPCC 2013; Stroeve et al. 2012a; Stroeve et al. 2014b; Zhang and Knutson 2013). See Chapter 11 for further discussion of the implications of changes in the Arctic.

Antarctic Sea Ice Extent

The area of sea ice around Antarctica has increased between 1979 and 2012 by 1.2% to 1.8% per decade (IPCC 2013), much smaller than the decrease in total sea ice area found in the Arctic summer. Strong regional differences in the sea ice growth rates around Antarctica are found, but

most (about 75%) of the sea ice area has expanded over the last 30 years (Zunz et al. 2013; IPCC 2013). Changes in wind patterns, ice–ocean feedbacks, and changes in freshwater flux have been investigated as contributing to the Antarctic sea ice growth, and there is still scientific debate around the physical cause (Zunz et al. 2013; Eisenman et al. 2014; Pauling et al. 2016). Scientific progress on understanding the observed changes in Antarctic sea ice extent is stymied by the short observational record; complex interactions between the sea ice, ocean, atmosphere, and Antarctic Ice Sheet; and large interannual variability. The most recent scientific evidence ties the increase in Antarctic sea ice extent to the negative phase of the Interdecadal Pacific Oscillation (IPO) climate variability pattern. The negative phase (1999–present) of the IPO resulted in cooler tropical Pacific sea surface temperatures, a slower warming trend, and a deepening of the Amundsen Sea Low near Antarctica, which contributed to regional circulation changes in the Ross Sea region and an expansion of sea ice (Meehl et al. 2016).

Continental Ice Sheets and Mountain Glaciers

Since the NCA3 (Mellilo et al. 2014), the Gravity Recovery and Climate Experiment (GRACE) constellation of satellites (e.g., Velicogna and Wahr 2013) has continued to provide a record of gravimetric measurements of land ice changes, advancing knowledge of recent mass loss to the global cryosphere. These measurements indicate that mass loss from the Antarctic Ice Sheet (AIS), Greenland Ice Sheet (GrIS), and mountain glaciers around the world continues.

The annual average net mass change from AIS is -92 ± 10 Gt per year since 2003 (Harig and Simons 2016). Strong spatial variations are found in mass loss; gains are found in the East Antarctic Ice Sheet (EAIS), and significant losses are found in the West Antarctic Ice Sheet (WAIS). Multiple data sources indicate that losses from WAIS outpace the EAIS gains (Rignot et al. 2014; Joughin et al. 2014; Williams et al. 2014; Harig and Simons 2015; Seo et al. 2015; Harig and Simons 2016). The WAIS ice shelves are undergoing rapid change due to ocean warming in this region from increased oceanic heat transport (Jenkins et al. 2010; Feldmann and Levermann 2015) contributing to the increase in flow rate of discharge glaciers.

Recent evidence has found that the grounding line retreat of glaciers in the Amundsen Sea sector has crossed a threshold and this sector is expected to eventually disintegrate entirely, with the potential to destabilize the entire WAIS (Rignot et al. 2014; Joughin et al. 2014; Feldmann and Levermann 2015). As a result, the evidence suggests an eventual committed global sea level rise from this disintegration could be at least 1.2 meters (about 4 feet) and possibly up to 3 meters (about 10 feet). The timescale over which the melt will occur is thought to be several centuries. However, recent analyses suggest that this could happen faster than previously thought, with a potential for an additional one or more feet of sea level rise during this century (DeConto and Pollard 2016; see Chapter 12: Sea Level Rise for further details). The potential for unanticipated rapid ice sheet melt and/or disintegration is discussed further in Chapter 15: Potential Surprises.

Average annual mass loss from GrIS between January 2003 and May 2013 was 244 ± 6 Gt per year (Harig and Simons 2016), an increase from 215 Gt per year for the period from 2002 to 2011 (IPCC 2013). Major GrIS melting events have been observed in recent years associated with increased surface air temperatures in response to variability in the atmospheric circulation (IPCC 2013; Lim et al. 2016). GrIS is rapidly losing mass at its edges and slightly gaining in its interior and has been the largest land ice contributor to global sea level rise over the last decade (Harig and Simons 2012; Jacob et al. 2012). The surface area of the Greenland Ice Sheet experiencing melt has increased significantly since 1980 (Tedesco et al. 2011; Fettweis et al. 2011; Tedesco et al. 2015). The Greenland surface melt recorded in 2012, where melt occurred over 98.6% of the ice sheet surface area on a single day in July, remains unprecedented (Nghiem et al. 2012; Tedesco et al. 2013). GRACE data indicate that the Greenland mass loss between April 2012 and April 2013 was 562 Gt—more than double the average annual rate found over recent decades.

The annually averaged ice mass from 37 global reference glaciers has decreased every year since 1984, and the rate of global glacier melt is accelerating (Pelto 2015; Zemp et al. 2015). This mountain glacier melt is contributing to sea level rise and will continue to contribute through the 21st Century (Mengel et al. 2016). Some of the greatest glacier mass losses are occurring in Alaska and the Pacific Northwest (IPCC 2013; Zemp et al. 2015). The current data also show strong imbalances in glaciers around the globe indicating additional ice loss even if climate were to stabilize (IPCC 2013; Zemp et al. 2015).

Arctic Snow Cover and Permafrost

Snow cover extent has decreased in the Northern Hemisphere, including over the United States; the decrease has been especially significant over the last decade (Derksen and Brown 2012). Observations indicate that between 1967 and 2012, Northern Hemisphere June snow cover extent has decreased by more than 50% (IPCC 2013). Reductions in May and June snow cover extent of 7.3% and 19.8% per decade, respectively, have occurred over the period from 1979 to 2014, while trends in snow cover duration show regions of both earlier and later snow cover onset (Derksen et al. 2015).

Annual mean temperature and thickness of the active soil layer—the layer experiencing seasonal thaw—are critical permafrost characteristics for the concerns about potential emissions of carbon dioxide and methane from thawing permafrost. Permafrost temperatures have increased in most regions of the Arctic. The rate of permafrost warming varies regionally; however, greater warming is consistently found for colder permafrost than for warmer permafrost (IPCC 2013; Romanovsky et al. 2015). Decadal trends in the permafrost active layer show strong regional variability (Shiklomanov et al. 2012); however, the thickness of the active layer is increasing in most areas across the Arctic (IPCC 2013; Romanovsky et al. 2015). The potentially large contribution of carbon and methane emissions from permafrost and the continental shelf in the Arctic to overall warming is discussed further in Chapter 15: Potential Surprises.

1.2.7. Global Changes in Sea Level

Statistical analyses of tide-gauge data indicate that global mean sea level has risen about 20–23 cm (8–9 inches) since 1880, with a rise rate of approximately 1.2–1.5 mm/year from 1901–1990 (~0.5–0.6 inches per decade; Church and White 2011; Hay et al. 2015; also see Chapter 12: Sea Level Rise). However, since the early 1990s, both tide gauges and satellite altimeters have recorded a faster rate of sea level rise of about 3 mm/year (approximately 0.12 inches per year; Church and White 2011; Nerem et al. 2010; Hay et al. 2015), resulting in about 8 cm (about 3 inches) of the global rise since the early 1990s. Nearly two-thirds of the sea level rise measured since 2005 has resulted from increases in ocean mass, primarily from land-based ice melt; the remaining one-third of the rise is in response to changes in density from increasing ocean temperatures (Merrifield et al. 2015).

Global sea level rise and its regional variability forced by climatic and ocean circulation patterns are contributing to significant increases in annual tidal-flood frequencies, which are measured by NOAA tide gauges and associated with minor infrastructure impacts; along some portions of the U.S. coast, frequency of the impacts from such events appear to be accelerating (Ezer and Atkinson 2014; Sweet and Park 2014; also see Chapter 12: Sea-Level Rise).

Future projections show that by 2100, global mean sea level is *very likely* to rise by 0.5–1.3 m (1.6–4.3 feet) under RCP8.5, 0.35–0.95 m (1.1–3.1 feet) under RCP4.5, and 0.24–0.79 m (0.8–2.6 feet) under RCP2.6 (see Chapter 4: Projections of Climate Change for a description of the scenarios) (Kopp et al. 2014). Sea level will not rise uniformly around the coasts of the United States and its overseas territories. Local sea level rise is *likely* to be greater than the global average along the U.S. Atlantic and Gulf Coasts and less than the global average in most of the Pacific Northwest. Emerging science suggests these projections may be underestimates, particularly for higher scenarios; a global mean sea level rise exceeding 2.4 m (8 feet) by 2100 cannot be excluded (see Chapter 12: Sea Level Rise), and even higher amounts are possible as a result of marine ice sheet instability (see Chapter 15: Potential Surprises). We have updated the global sea level rise scenarios for 2100 of Parris et al. (2012) accordingly (Sweet et al., In Prep), and also extended to year 2200 in Chapter 12: Sea-Level Rise. The scenarios are regionalized to better match the decision context needed for local risk framing purposes.

1.2.8. Recent Global Changes relative to Paleoclimates

Covering the last two millennia, referred to here as the “Common Era,” paleoclimate records provide a longer-term sample of the natural variability of modern climate, with a small overprint of human-forced climate change. The strongest drivers of climate in the last two thousand years have been volcanoes, land-use change (which has both albedo and greenhouse gas emissions effects), and emissions of greenhouse gases from fossil fuels and other human-related activities (Schmidt et al. 2011). Based on a number of proxies for temperature (for example, from tree rings, fossil pollen, corals, ocean and lake sediments, ice cores, etc.), temperature records are

available for the last 2000 years on hemispherical and continental scales (Figures 1.8 and 1.9) (Mann et al. 2008; PAGES 2K 2013). High-resolution temperature records for North America extend back less than half of this period, with temperatures in the early parts of the Common Era inferred from pollen archives. For this era, there is a general cooling trend, with a relatively rapid increase in temperature over the last 150–200 years (Figure 1.9, PAGES 2k 2013). For context, temperatures for 2015 are much higher than any period in the past 2000 years.

[INSERT FIGURE 1.8 HERE:]

Figure 1.8. Changes in the temperature of the Northern Hemisphere from surface observations (in red) and from proxies (in black; uncertainty range represented by shading) relative to 1961–1990 average temperature. These analyses suggest that current temperatures are higher than seen globally in at least the last 1700 years, and that the last decade (2006 to 2015) was the warmest decade on record. (Figure source: adapted and updated from Mann et al. 2008).]

[INSERT FIGURE 1.9 HERE:]

Figure 1.9. Proxy temperatures reconstructions for the seven regions of the PAGES-2K Network. Temperature anomalies are relative to the 1961–1990 reference period. Gray lines around expected-value estimates indicate uncertainty ranges as defined by each regional group (see PAGE 2K 2013 and related Supplementary Information). Note that the changes in temperature over the last century tend to occur at a much faster rate than found in the previous time periods. (Figure source: adapted from PAGES 2k et al. 2013)]

Global temperatures of the magnitude observed recently (and projected for the rest of this century) were *likely* last observed during the Eemian period—the last interglacial—125,000 years ago; at that time, global temperatures were, at their peak, about 1.8°–3.6°F (1°–2°C) warmer than preindustrial temperatures (Turney and Jones 2010). Coincident with these higher temperatures, sea levels were 6–9 meters (about 16–30 feet) higher than modern levels (Kopp et al. 2009; Dutton and Lambeck 2012). Modeling studies suggest that the Eemian period warming can be explained in part by increased solar insolation from orbital forcing as the Earth travels around the Sun (e.g., Kaspar et al. 2005). However, greenhouse gas concentrations were similar to preindustrial levels. Equilibrium climate with modern greenhouse gas concentrations (about 400 ppm CO₂) most recently occurred 3 million years ago during the Pliocene. During the warmest parts of this period, global temperatures were 5.4°–7.2°F (3°–4°C) higher than today, and sea levels were 25 meters (about 82 feet) higher (Haywood et al. 2013).

----- **START BOX 1.2 HERE** -----

Box 1.2: What's New in This Report

This assessment reflects both advances in scientific understanding and approach since NCA3, as well as global policy developments. Highlights of what's new include:

1 *Spatial downscaling*: Projections of climate changes are downscaled to a finer resolution than the
2 original global climate models using the Localized Constructed Analogs (LOCA) empirical
3 statistical downscaling model. The downscaling generates temperature and precipitation on a
4 1/16 degree latitude/longitude grid for the contiguous United States (Chapters 4,6,7).

5 *Risk-based framing*: Highlighting aspects of climate science most relevant to assessment of key
6 societal risks is included more here than in prior NCA assessments. This approach allows for
7 emphasis of possible outcomes that, while relatively unlikely to occur or characterized by high
8 uncertainty, would be particularly consequential, and thus associated with large risks.

9 *Detection and attribution*: Significant advances have been made in the attribution of the human
10 influence on individual climate and weather extreme events since NCA3. This assessment
11 contains extensive discussion of new and emerging findings in this area (Chapters 3,6,7,8).

12 *Atmospheric circulation and extreme events*: The extent to which atmospheric circulation in the
13 mid latitudes is changing or is projected to change, possibly in ways not captured by current
14 climate models, is a new important area of research. While still in its formative stages, this
15 research is critically important because of the implications of such changes for climate extremes
16 including extended cold air outbreaks, long-duration heat waves, and changes in storms and
17 drought patterns (Chapters 5,6,7).

18 *Increased understanding of specific types of extreme events*: How climate change may affect
19 specific types of extreme events in the United States is another key area where scientific
20 understanding has advanced. For example, this report highlights how intense flooding associated
21 with atmospheric rivers could increase dramatically as the atmosphere and oceans warm, or how
22 tornadoes could be concentrated into a smaller number of high-impact days (Chapter 9).

23 *Model weighting*: For the first time, maps and plots of climate projections will not show a
24 straight average of all available climate models. Rather, each model is given a weight based on
25 their 1) historical performance relative to observations and 2) independence relative to other
26 models. Although this is a more accurate way of representing model output, it does not
27 significantly alter the results: the weighting produces very similar trends and spatial patterns to
28 the equal-weighting-of-models approach used in prior assessments (Chapters 4,6,7).

29 *High-resolution global climate model simulations*: As computing resources have grown,
30 multidecadal simulations of global climate models are now being conducted at horizontal
31 resolutions on the order of 25 km (15 miles) that enable more realistic simulation of intense
32 weather systems, including hurricanes. Even the limited number of high-resolution models
33 currently available have increased confidence in projections of extreme weather (Chapter 9).

34 *The so-called global warming hiatus*: Since NCA3, many studies have investigated causes for
35 the temporary slowdown in the rate of increase in near-surface global mean temperature from
36 2000 to 2013. The slowdown, which ended with the record warmth in 2014-2016, is understood
37 to have been caused by a combination of internal variability, mostly in the heat exchange
38 between the ocean and the atmosphere, and short-term variations in external forcing factors, both

human and natural. On longer time scales relevant to human-induced climate change, the planet continues to warm at a steady pace as predicted by basic atmospheric physics and the well-documented increase in heat-trapping gases

Oceans and coastal waters: Concern over ocean acidification, warming, and oxygen loss is increasing as scientific understanding of the severity of their impacts grows. Both acidification and oxygen decreases may be magnified in some U.S. coastal waters relative to the global average, raising the risk of serious ecological and economic consequences. There is also growing evidence that the Atlantic Meridional Circulation (AMOC), sometimes referred to as the ocean's conveyor belt, has slowed down (Chapter 13).

Local sea-level change projections: For the first time in the NCA process, sea-level rise projections incorporate geographic variation based on factors such as local land subsidence, ocean currents, and changes in Earth's gravitational field (Chapter 12).

Accelerated ice-sheet loss and irreversibility: New observations from many different sources confirm that ice-sheet loss is accelerating. Combined with simultaneous advances in the physical understanding of ice sheets, scientists are now concluding that up to 8.5 feet of global sea-level rise is possible by 2100 under a high-emissions scenario, up from 6.6 feet in NCA3 (Chapter 12).

Slowing in Arctic sea-ice area extent regrowth: The annual Arctic sea ice extent minimum for 2016 was the second lowest on record. In fall 2016, record-setting slow ice regrowth put 2016–2017 winter ice volume records in jeopardy as well (Chapter 11).

Potential surprises: Both large-scale state shifts in the climate system (sometimes called “tipping points”) and compound extremes have the potential to generate unanticipated surprises. The further the earth system departs from historical climate forcings, and the more the climate changes, the greater the potential for these surprises. For the first time in the NCA process we include an extended discussion of these potential surprises (Chapter 15).

The Paris Agreement: The Paris Agreement, which entered into force November 4, 2016, provides a new framework for all nations to mitigate and adapt to climate change, and to periodically update and revisit their respective domestic commitments. The Agreement's long-term objective is to limit average global temperature change to well below 2°C (3.6°F) above preindustrial levels, with best efforts to limit it to 1.5°C (2.7°F), and this assessment addresses global climate implications of these objectives (Chapter 4, 14).

----- **END BOX 1.2 HERE** -----

TRACEABLE ACCOUNTS

Key Finding 1

The global climate continues to change rapidly compared to the pace of the natural changes in climate that have occurred throughout Earth's history. Trends in globally-averaged temperature, sea-level rise, upper-ocean heat content, land-based ice melt, and other climate variables provide consistent evidence of a warming planet. These observed trends are robust, and have been confirmed by independent research groups around the world.

Description of evidence base

The Key Finding and supporting text summarize extensive evidence documented in the climate science literature. Similar to statements made in previous national (NCA3; Melillo et al. 2014) and international (IPCC 2013) assessments.

Evidence for changes in global climate arises from multiple analyses of data from in-situ, satellite, and other records undertaken by many groups over several decades. These observational datasets are used throughout this chapter and are discussed further in Appendix 1 (e.g., updates of prior uses of these datasets by Vose et al. 2012; Karl et al. 2015). Changes in the mean state have been accompanied by changes in the frequency and nature of extreme events (e.g., Kunkel and Frankson 2015; Donat et al. 2016). A substantial body of analysis comparing the observed changes to a broad range of climate simulations consistently points to the necessity of invoking human-caused changes to adequately explain the observed climate system behavior. The influence of human impacts on the climate system has also been observed in a number of individual climate variables (attribution studies are discussed in Chapter 3 and in other chapters).

Major uncertainties

Key remaining uncertainties relate to the precise magnitude and nature of changes at global, and particularly regional, scales, and especially for extreme events and our ability to simulate and attribute such changes using climate models. Innovative new approaches to climate data analysis, continued improvements in climate modeling, and instigation and maintenance of reference quality observation networks such as the U.S. Climate Reference Network (<http://www.ncei.noaa.gov/crn/>) all have the potential to reduce uncertainties.

Assessment of confidence based on evidence and agreement, including short description of nature of evidence and level of agreement

x Very High

☐ High

☐ Medium

☐ Low

There is *very high confidence* that global climate is changing and this change is apparent across a wide range of observations, given the evidence base and remaining uncertainties. All

1 observational evidence is consistent with a warming climate since the late 1800s. There is *very*
2 *high confidence* that the global climate change of the past 50 years is primarily due to human
3 activities, given the evidence base and remaining uncertainties (IPCC 2013). Recent changes
4 have been consistently attributed in large part to human factors across a very broad range of
5 climate system characteristics.

6 **Summary sentence or paragraph that integrates the above information**

7 The key message and supporting text summarizes extensive evidence documented in the climate
8 science peer-reviewed literature. The trends described in NCA3 have continued and our
9 understanding of the observations related to climate and the ability to evaluate the many facets of
10 the climate system have increased substantially.

12 **Key Finding 2**

13 The frequency and intensity of heavy precipitation and extreme heat events are increasing in
14 most regions of the world. These trends are consistent with expected physical responses to a
15 warming climate and with climate model studies, although models tend to underestimate the
16 observed trends. The frequency and intensity of such extreme events will very likely continue to
17 rise in the future. Trends for some other types of extreme events, such as floods, droughts, and
18 severe storms, have more regional characteristics.

19 **Description of evidence base**

20 The Key Finding and supporting text summarizes extensive evidence documented in the climate
21 science literature and are similar to statements made in previous national (NCA3; Melillo et al.,
22 2014) and international (IPCC 2013) assessments. The analyses of past trends and future
23 projections in extreme events are also well substantiated through more recent peer review
24 literature as well (Seneviratne et al. 2014; Easterling et al. 2016; Kunkel and Frankson 2015;
25 Donat et al. 2016; Berghuijs et al. 2016; Arnell and Gosling 2014).

26 **Major uncertainties**

27 Key remaining uncertainties relate to the precise magnitude and nature of changes at global, and
28 particularly regional, scales, and especially for extreme events and our ability to simulate and
29 attribute such changes using climate models. Innovative new approaches to climate data analysis,
30 continued improvements in climate modeling, and instigation and maintenance of reference
31 quality observation networks such as the U.S. Climate Reference Network
32 (<http://www.ncei.noaa.gov/crn/>) all have the potential to reduce uncertainties.

33 **Assessment of confidence based on evidence and agreement, including short description of** 34 **nature of evidence and level of agreement**

35 x Very High

36 ☐ High

37 ☐ Medium

1 ☐ Low

2 There is *very high confidence*, based on the observational evidence and physical understanding,
3 that there are major trends in extreme events and significant projected changes for the future.

4 **Summary sentence or paragraph that integrates the above information**

5 The key message and supporting text summarizes extensive evidence documented in the climate
6 science peer-reviewed literature. The trends for extreme events that were described in the NCA3
7 and IPCC assessments have continued and our understanding of the data and ability to evaluate
8 the many facets of the climate system have increased substantially.

9

10 **Key Finding 3**

11 Many lines of evidence demonstrate that human activities, especially emissions of greenhouse
12 gases, are primarily responsible for the observed climate changes in the industrial era. There are
13 no alternative explanations, and no natural cycles are found in the observational record that can
14 explain the observed changes in climate.

15 **Description of evidence base**

16 The Key Finding and supporting text summarizes extensive evidence documented in the climate
17 science literature and are similar to statements made in previous national (NCA3; Melillo et al.
18 2014) and international (IPCC 2013) assessments. The human effects on climate have been well
19 documented through many papers in the peer reviewed scientific literature (e.g., see Chapters 2
20 and 3 for more discussion of supporting evidence).

21 **Major uncertainties**

22 Key remaining uncertainties relate to the precise magnitude and nature of changes at global, and
23 particularly regional, scales, and especially for extreme events and our ability to simulate and
24 attribute such changes using climate models. The exact effects from land use changes relative to
25 the effects from greenhouse gas emissions needs to be better understood.

26 **Assessment of confidence based on evidence and agreement, including short description of
27 nature of evidence and level of agreement**

28 x Very High

29 ☐ High

30 ☐ Medium

31 ☐ Low

32 There is *very high confidence* for a major human influence on climate.

33 **Summary sentence or paragraph that integrates the above information**

34 The key message and supporting text summarizes extensive evidence documented in the climate
35 science peer-reviewed literature. The analyses described in the NCA3 and IPCC assessments

support our findings and new observations and modeling studies have further substantiated these conclusions.

Key Finding 4

Global climate is projected to continue to change over this century and beyond. The magnitude of climate change beyond the next few decades depends primarily on the amount of greenhouse (heat trapping) gases emitted globally and the sensitivity of Earth's climate to those emissions.

Description of evidence base

The Key Finding and supporting text summarizes extensive evidence documented in the climate science literature and are similar to statements made in previous national (NCA3; Melillo et al. 2014) and international (IPCC 2013) assessments. The projections for future climate have been well documented through many papers in the peer reviewed scientific literature (e.g., see Chapter 4 for descriptions of the scenarios and the models used).

Major uncertainties

Key remaining uncertainties relate to the precise magnitude and nature of changes at global, and particularly regional, scales, and especially for extreme events and our ability to simulate and attribute such changes using climate models. Continued improvements in climate modeling to represent the physical processes affecting the Earth's climate system are aimed at reducing uncertainties. Monitoring and observation programs also can help improve the understanding needed to reduce uncertainties.

Assessment of confidence based on evidence and agreement, including short description of nature of evidence and level of agreement

☒ Very High

☐ High

☐ Medium

☐ Low

There is *very high confidence* for continued changes in climate.

Summary sentence or paragraph that integrates the above information

The key message and supporting text summarizes extensive evidence documented in the climate science peer-reviewed literature. The projections that were described in the NCA3 and IPCC assessments support our findings and new modeling studies have further substantiated these conclusions.

Key Finding 5

Natural variability, including El Niño events and other recurring patterns of ocean–atmosphere interactions, have important, but limited influences on global and regional climate over timescales ranging from months to decades.

Description of evidence base

The Key Finding and supporting text summarizes extensive evidence documented in the climate science literature and are similar to statements made in previous national (NCA3; Melillo et al. 2014) and international (IPCC 2013) assessments. The role of natural variability in climate trends has been extensively discussed in the peer reviewed literature (e.g., Karl et al. 2015; Rahmstorf et al. 2015; Lewandowsky et al. 2016; Mears and Wentz 2016; Trenberth et al. 2014; Santer et al. 2016).

Major uncertainties

Uncertainties still exist in the precise magnitude and nature of the full effects of individual ocean cycles and other aspects of natural variability on the climate system. Increased emphasis on monitoring should reduce this uncertainty significantly over the next few decades.

Assessment of confidence based on evidence and agreement, including short description of nature of evidence and level of agreement

x Very High

☐ High

☐ Medium

☐ Low

There is *very high confidence*, affected to some degree by limitations in the observational record, that the role of natural variability on future climate change is limited.

Summary sentence or paragraph that integrates the above information

The key message and supporting text summarizes extensive evidence documented in the climate science peer-reviewed literature. There has been an extensive increase in the understanding of the role of natural variability on the climate system over the last few decades, including a number of new findings since NCA3.

Key Finding 6

Longer-term climate records indicate that average temperatures in recent decades over much of the world have been much higher than at any time in the past 1700 years or more.

Description of evidence base

The Key Finding and supporting text summarizes extensive evidence documented in the climate science literature and are similar to statements made in previous national (NCA3; Melillo et al., 2014) and international (IPCC 2013) assessments. There are many recent studies of the

paleocliamte leading to this conclusion including those cited in the report (e.g., Mann et al. 2008; PAGE 2K 2013).

Major uncertainties

Despite the extensive increase in knowledge in the last few decades, there are still many uncertainties in understanding the hemispheric and global changes in climate over the Earth's history, including that of the last few millennia. Additional research efforts in this direction can help reduce those uncertainties.

Assessment of confidence based on evidence and agreement, including short description of nature of evidence and level of agreement

☐ Very High

x High

☐ Medium

☐ Low

There is *high confidence* for current temperatures to be higher than they have been in at least 1700 years and perhaps much longer.

Summary sentence or paragraph that integrates the above information

The key message and supporting text summarizes extensive evidence documented in the climate science peer-reviewed literature. There has been an extensive increase in the understanding of past climates on our planet, including a number of new findings since NCA3.

1 FIGURES

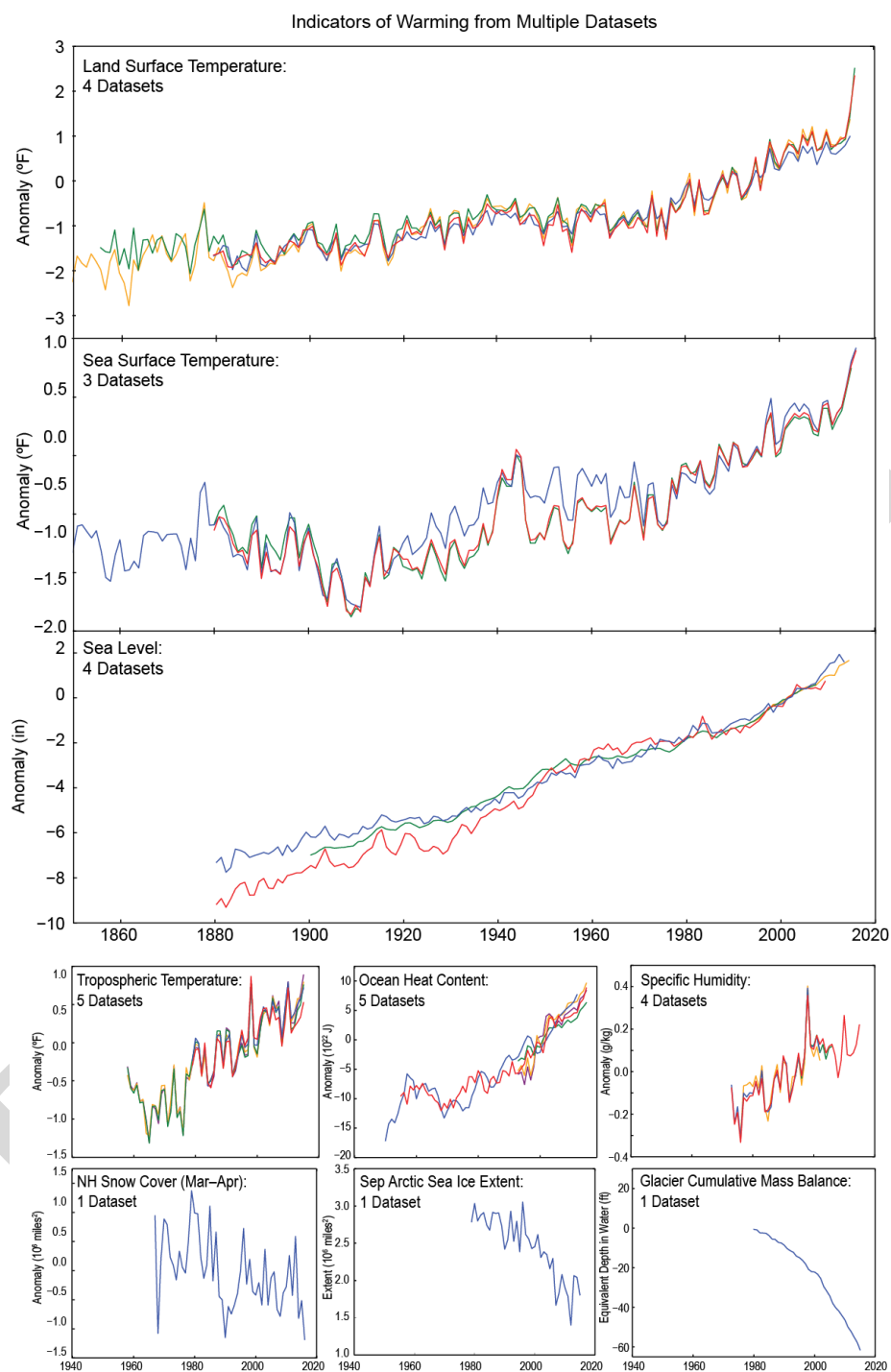


Figure 1.1. Examples of the observations from many different indicators of a changing climate. Anomalies are relative to 1976–2005 averages for the indicated variables. (Figure source: updated from Melillo et al. 2014).

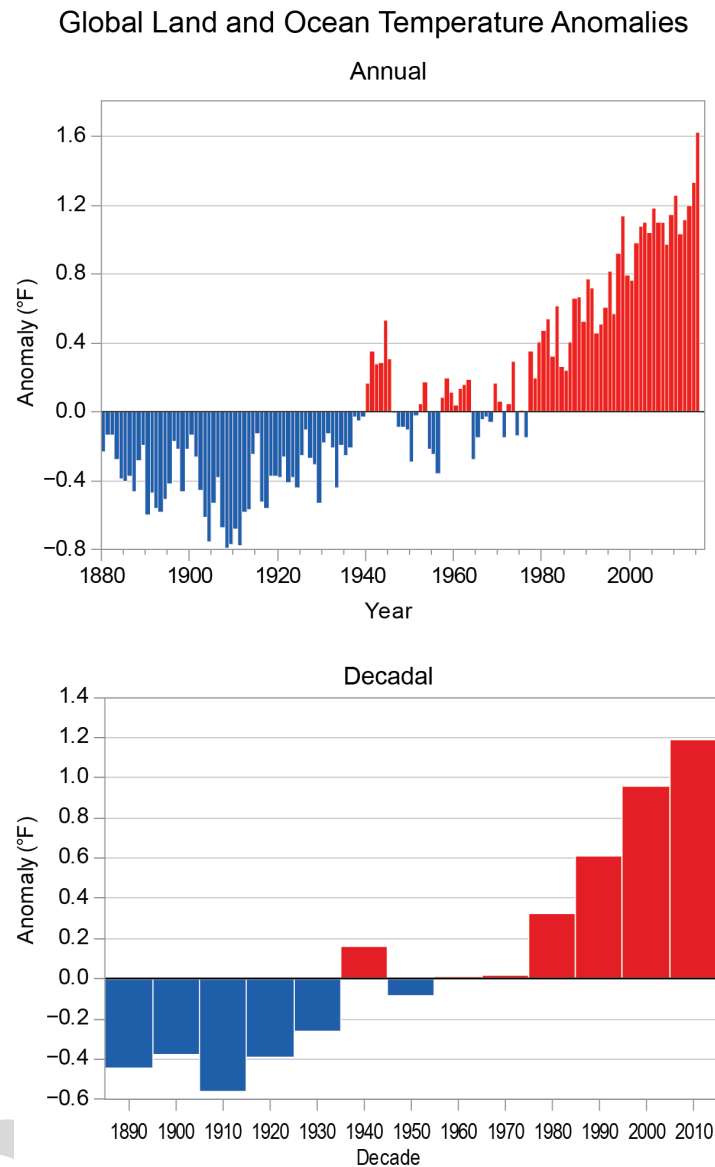


Figure 1.2. Top: Global annual average temperature (as measured over both land and oceans) has increased by more than 1.6°F (0.9°C) for the period from 1986–2015 relative to 1901–1960. Red bars show temperatures above the long-term 1880–2015 average, and blue bars indicate temperatures below the average over the entire period. While there is a clear long-term global warming trend, some years do not show a temperature increase relative to the previous year, and some years show greater changes than others. These year-to-year fluctuations in temperature are mainly due to natural sources of variability, such as the effects of El Niños, La Niñas, and volcanic eruptions. Based on the NCEI (NOAA GlobalTemp) data set 1901–2015 (updated from Vose et al. 2012). Bottom: Global average temperature averaged over decadal periods (1886–1895, 1896–1905, ..., 1996–2005, 2006–2015). Horizontal label indicates mid-point year of decadal period. Every decade since 1966–1975 has been warmer than the previous decade. (Figure source: (top) adapted from NCEI 2016, (bottom) NOAA NCEI / CICS-NC)

Surface Temperature Trends

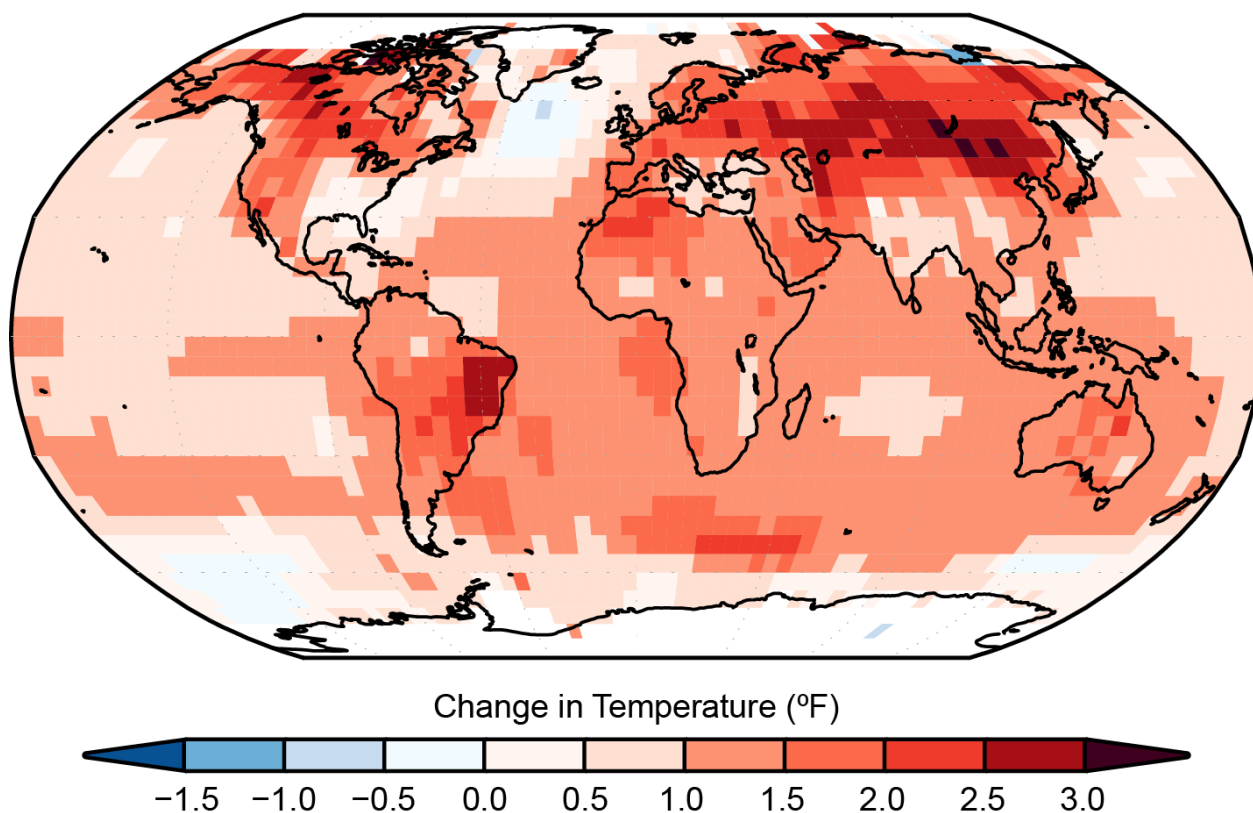


Figure 1.3. Surface temperature trends (change in °F) for the period 1986–2015 relative to 1901–1960 from the NOAA National Centers for Environmental Information’s (NCEI) surface temperature product. The relatively coarse (5.0° x 5.0°) resolution of these maps does not capture the finer details associated with mountains, coastlines, and other small-scale effects. (Figure source: updated from Vose et al. 2012).

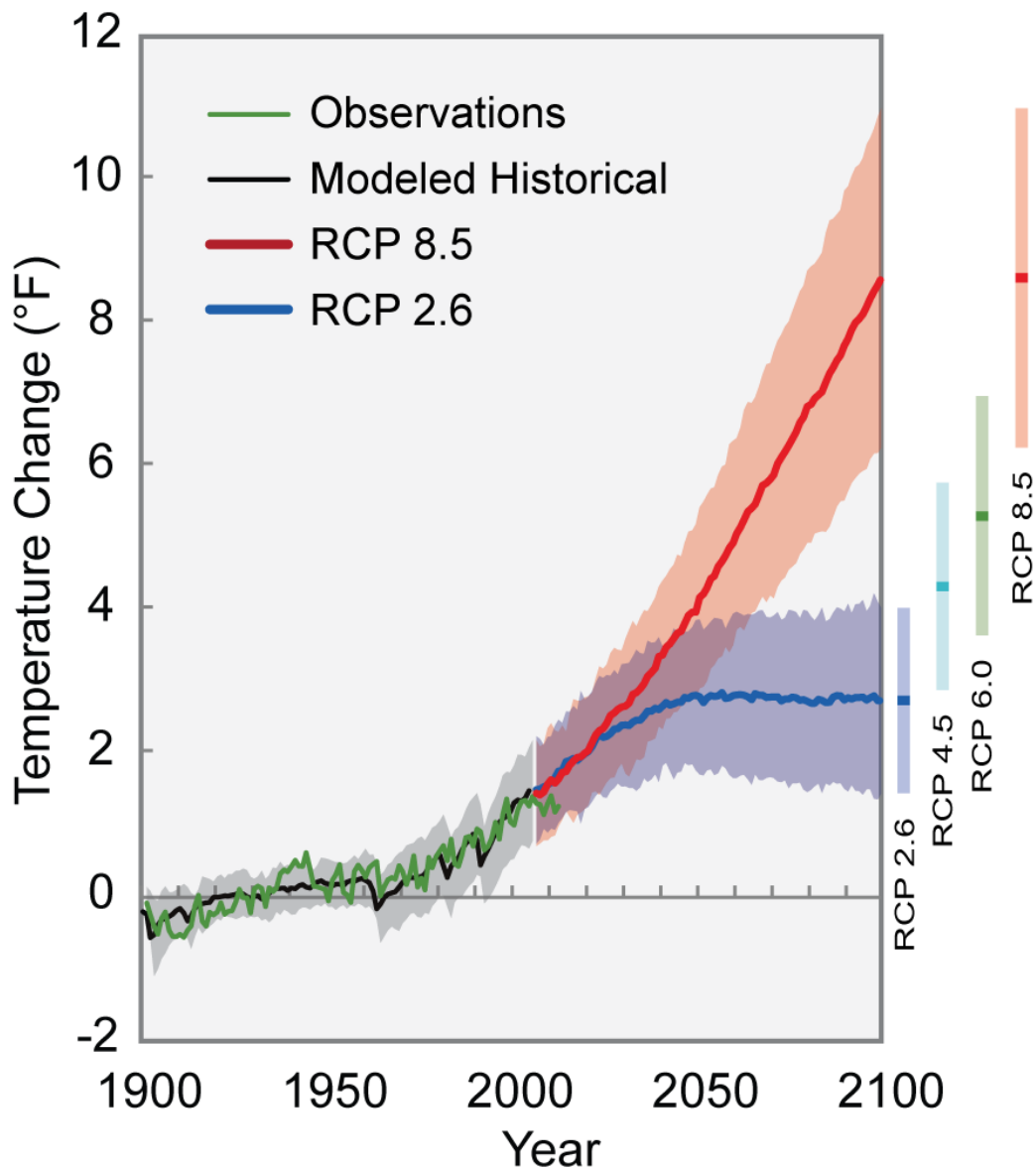


Figure 1.4. Multimodel simulated time series from 1950 to 2100 for the change in global annual mean surface temperature relative to 1986–2005 for a range of future emissions scenarios that account for the uncertainty in future emissions from human activities [as analyzed with the 20+ models from around the world used in the most recent international assessment (IPCC 2013)]. The mean and associated uncertainties [1.64 standard deviations (5%–95%) across the distribution of individual models (shading)] based on the averaged over 2081–2100 are given for all of the RCP scenarios as colored vertical bars. The numbers of models used to calculate the multimodel means are indicated. (Figure source: adapted from Walsh et al. 2014).

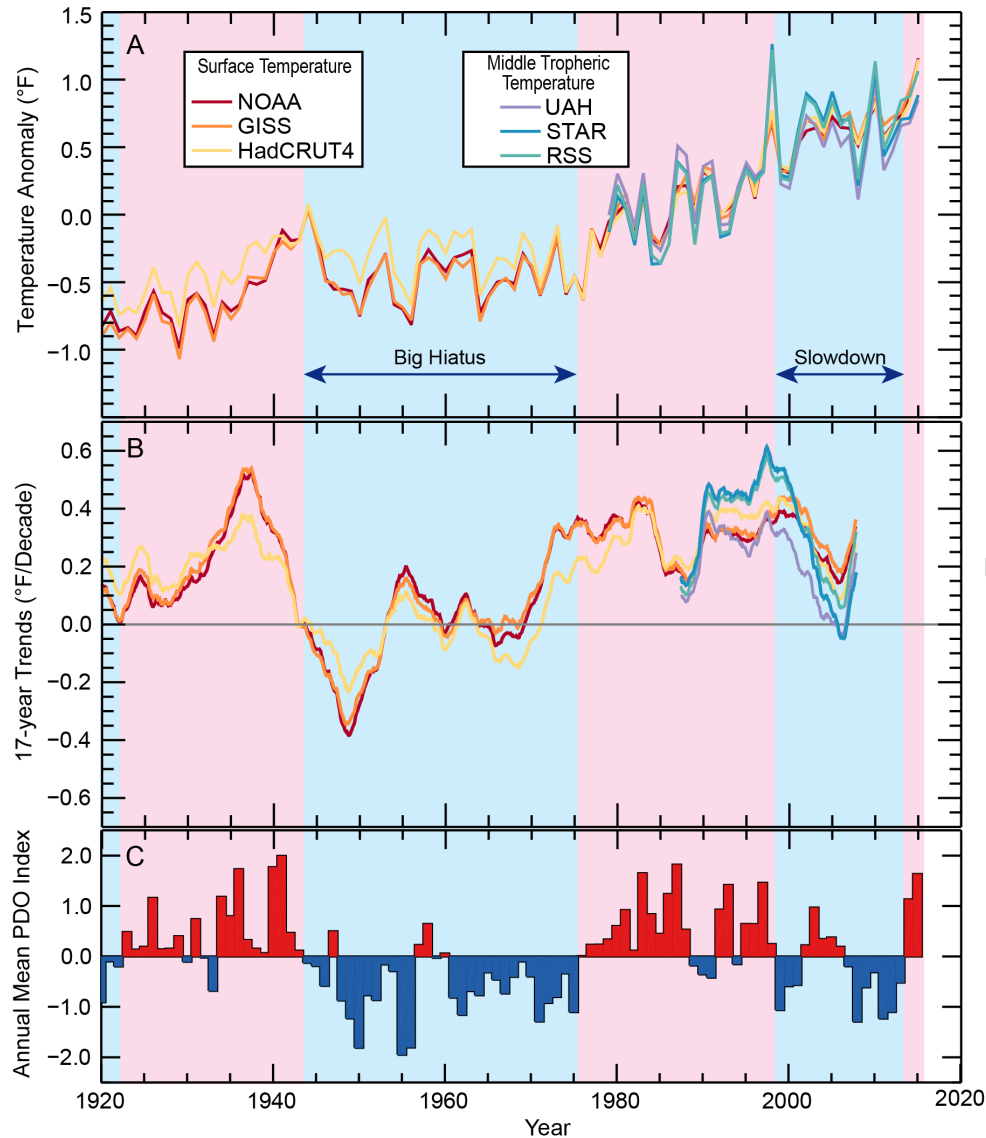


Figure 1.5. Panel A shows the annual mean temperature anomalies relative to a 1971–2000 baseline for global mean surface temperature and global mean tropospheric temperature. A previous period of relatively slow warming (the “Big Hiatus”) is obvious from the mid-1940s to the mid-1970s. Panel B shows the linear trend of 17-year overlapping periods (the maximum number of years historically for less than positive trends), plotted at the time of the center of the trend period. During the recent slowdown period, warming only ceased for two versions of the satellite data, and for a very narrow range of time periods. All 17-year trends are increasing rapidly as the effects of the 2015–2016 El Niño–Southern Oscillation (ENSO) event begin to affect the trends. Panel C shows the annual mean Pacific Decadal Oscillation (PDO) index. Temperature trends show a marked tendency to be lower during periods of generally negative PDO index, shown by the blue shading. (Figure source: adapted and updated from Trenberth 2015 and Santer et al. 2016; Panel B, © American Meteorological Society. Used with permission.)

Global Mean Temperature Anomalies

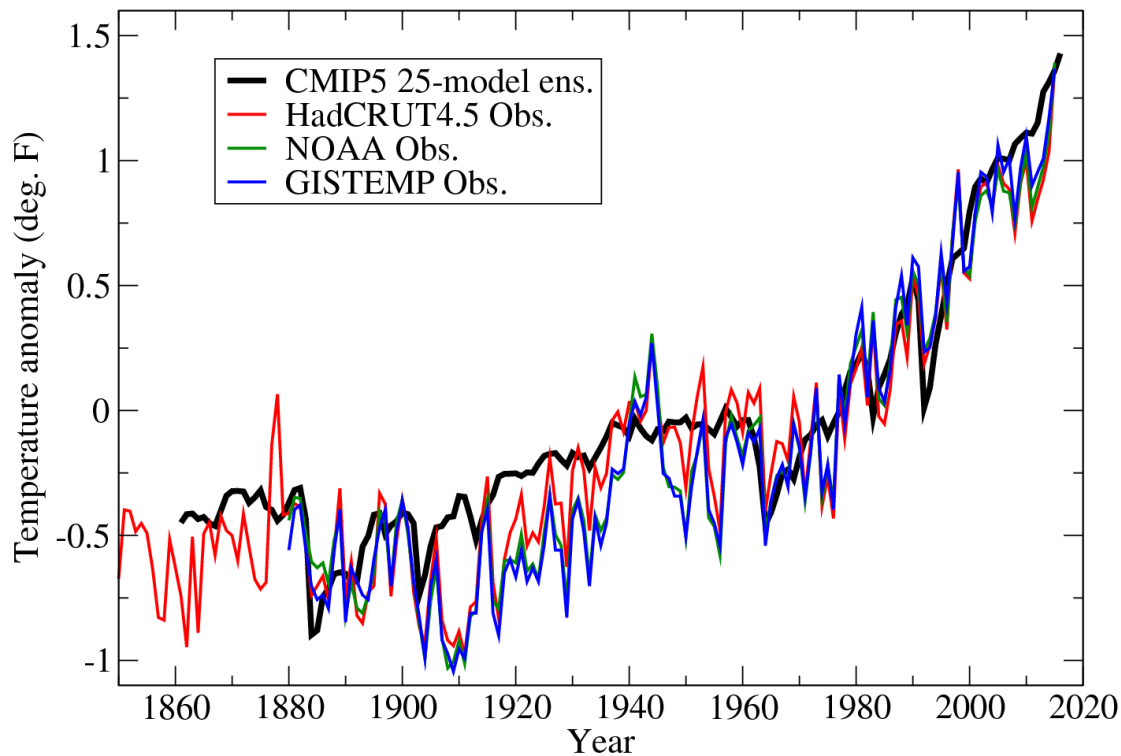
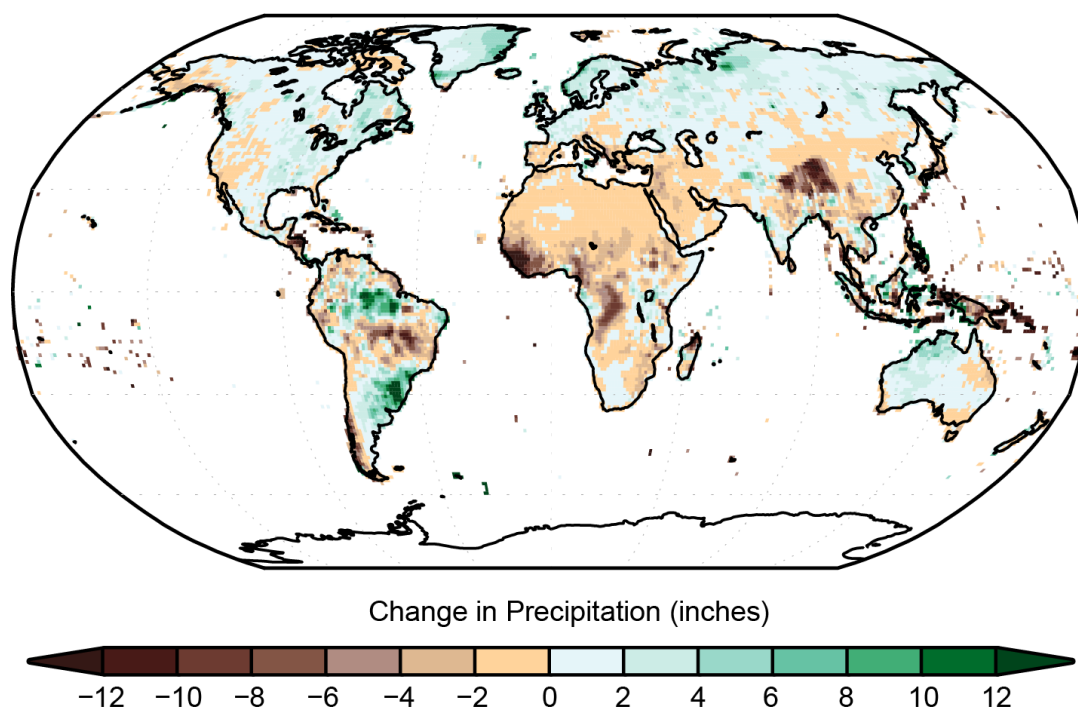


Figure 1.6. Comparison of global mean temperature anomalies ($^{\circ}\text{F}$) from observations (through 2015) and the CMIP5 multimodel ensemble (through 2016), using the reference period 1961–1990. The CMIP5 multimodel ensemble (black) is constructed from blended surface temperature and surface air temperature data from the models, masked where observations are not available in the HadCRUT4 dataset (Knutson et al. 2016; see also Richardson et al. 2016). The sources for the three observational indices are: HadCRUT4.5 (red): <http://www.metoffice.gov.uk/hadobs/hadcrut4/data/current/download.html>; NOAA (green): <https://www.ncdc.noaa.gov/monitoring-references/faq/anomalies.php>; and GISTEMP (blue): http://data.giss.nasa.gov/gistemp/tabledata_v3/GLB.Ts+dSST.txt (all downloaded on Oct. 3, 2016). (Figure source: adapted from Knutson et al. 2016)

1

Annually-averaged Precipitation Trends



2

3

4 **Figure 1.7.** Surface annually-averaged precipitation trends (change in inches) for the period
5 1986–2015 relative to 1901–1960. The relatively coarse ($0.5^\circ \times 0.5^\circ$) resolution of these maps
6 does not capture the finer details associated with mountains, coastlines, and other small-scale
7 effects. (Figure source: NOAA NCEI / CICS-NC).

8

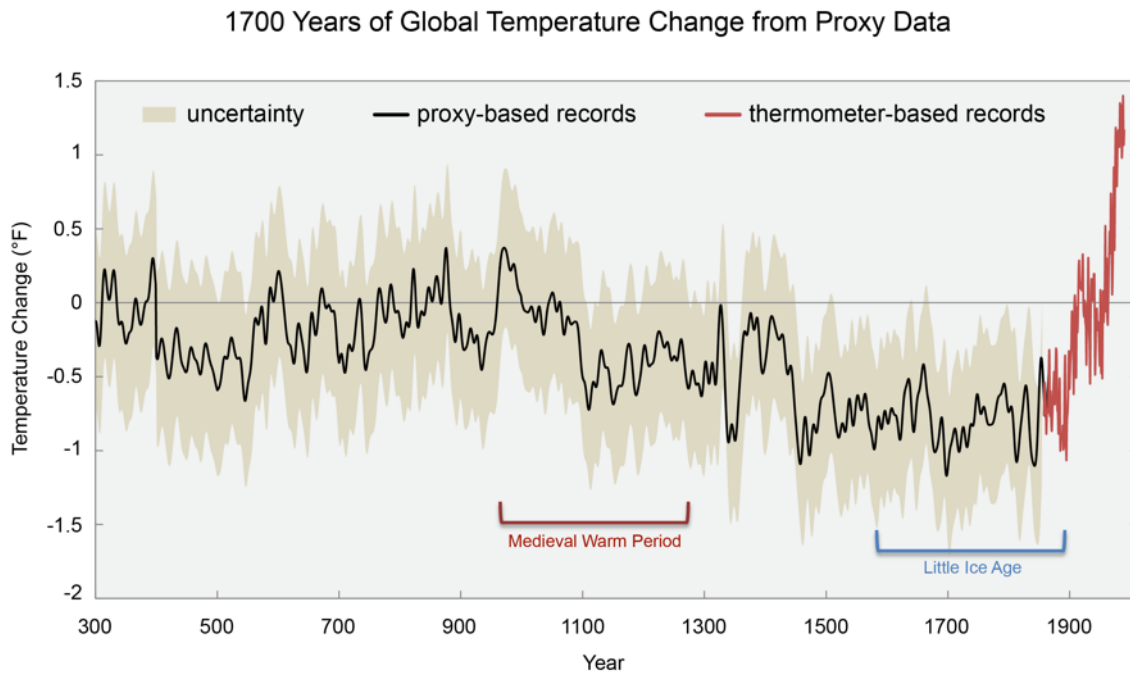


Figure 1.8. Changes in the temperature of the northern hemisphere from surface observations (in red) and from proxies (in black; uncertainty range represented by shading) relative to 1961-1990 average temperature. These analyses suggest that current temperatures are higher than seen globally in at least the last 1700 years, and that the last decade (2006 to 2015) was the warmest decade on record. (Figure source: adapted from Mann et al. 2008).

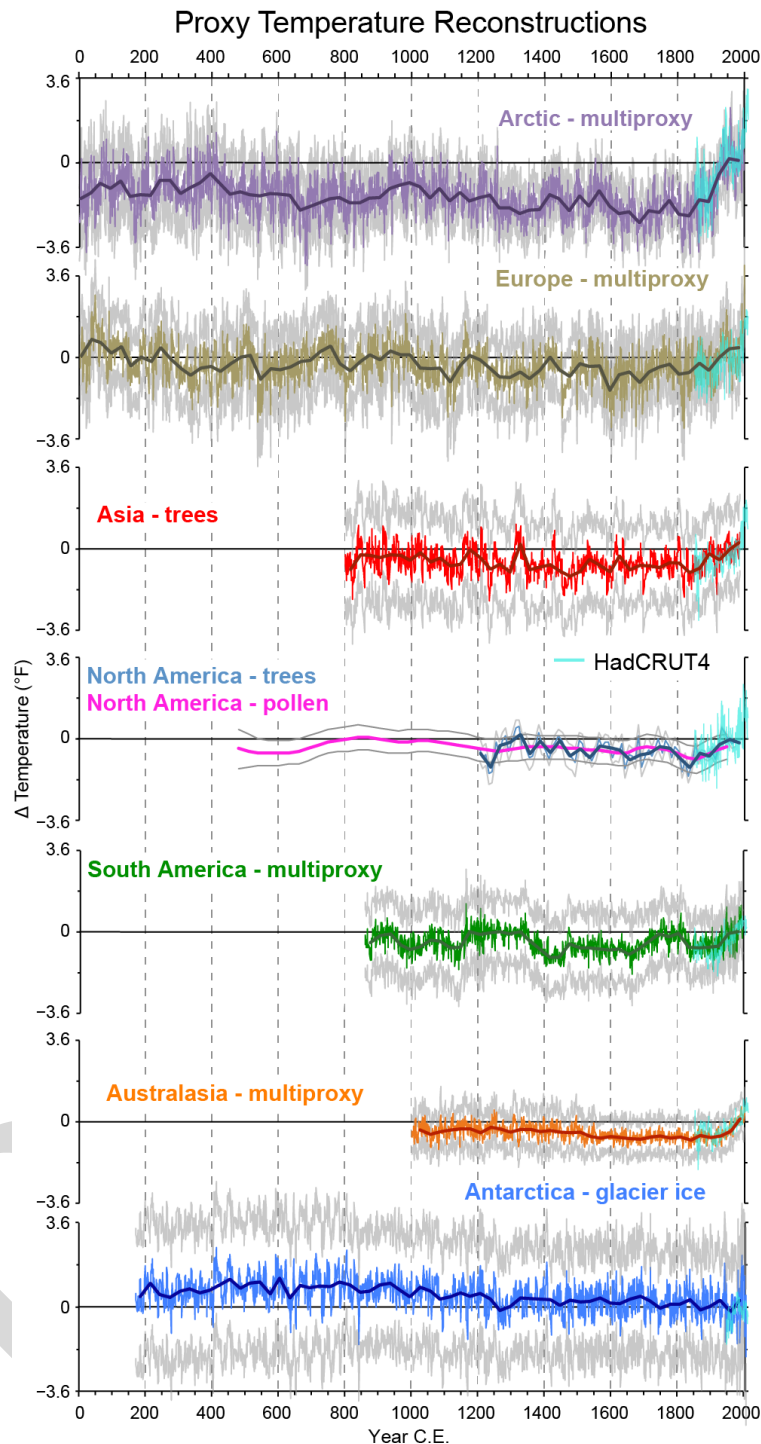


Figure 1.9. Proxy temperatures reconstructions for the seven regions of the PAGES 2K Network. Temperature anomalies are relative to the 1961–1990 reference period. Grey lines around expected-value estimates indicate uncertainty ranges as defined by each regional group (see PAGE 2K et al. 2013 and related Supplementary Information). Note that the changes in temperature over the last century tend to occur at a much faster rate than found in the previous time periods. (Figure source: adapted from PAGES 2k et al. 2013)

REFERENCES

- Adler, R.F., G.J. Huffman, A. Chang, R. Ferraro, P.-P. Xie, J. Janowiak, B. Rudolf, U. Schneider, S. Curtis, D. Bolvin, A. Gruber, J. Susskind, P. Arkin, and E. Nelkin, 2003: The version-2 Global Precipitation Climatology Project (GPCP) monthly precipitation analysis (1979–present). *Journal of Hydrometeorology*, **4**, 1147–1167. [http://dx.doi.org/10.1175/1525-7541\(2003\)004<1147:TVGPCP>2.0.CO;2](http://dx.doi.org/10.1175/1525-7541(2003)004<1147:TVGPCP>2.0.CO;2)
- Alexander, L.V., X. Zhang, T.C. Peterson, J. Caesar, B. Gleason, A.M.G. Klein Tank, M. Haylock, D. Collins, B. Trewin, F. Rahimzadeh, A. Tagipour, K. Rupa Kumar, J. Revadekar, G. Griffiths, L. Vincent, D.B. Stephenson, J. Burn, E. Aguilar, M. Brunet, M. Taylor, M. New, P. Zhai, M. Rusticucci, and J.L. Vazquez-Aguirre, 2006: Global observed changes in daily climate extremes of temperature and precipitation. *Journal of Geophysical Research*, **111**, 22. <http://dx.doi.org/10.1029/2005JD006290>
- Allen, M.R. and W.J. Ingram, 2002: Constraints on future changes in climate and the hydrologic cycle. *Nature*, **419**, 224–232. <http://dx.doi.org/10.1038/nature01092>
- Anderson, B.T., J.R. Knight, M.A. Ringer, J.-H. Yoon, and A. Cherchi, 2012: Testing for the Possible Influence of Unknown Climate Forcings upon Global Temperature Increases from 1950 to 2000. *Journal of Climate*, **25**, 7163–7172. <http://dx.doi.org/10.1175/jcli-d-11-00645.1>
- Arnell, N.W. and S.N. Gosling, 2016: The impacts of climate change on river flood risk at the global scale. *Climatic Change*, **134**, 387–401. <http://dx.doi.org/10.1007/s10584-014-1084-5>
- Asadieh, B. and N.Y. Krakauer, 2015: Global trends in extreme precipitation: climate models versus observations. *Hydrology and Earth System Sciences*, **19**, 877–891. <http://dx.doi.org/10.5194/hess-19-877-2015>
- Balmaseda, M.A., K.E. Trenberth, and E. Källén, 2013: Distinctive climate signals in reanalysis of global ocean heat content. *Geophysical Research Letters*, **40**, 1754–1759. <http://dx.doi.org/10.1002/grl.50382>
- Barnes, E.A. and L.M. Polvani, 2015: CMIP5 Projections of Arctic Amplification, of the North American/North Atlantic Circulation, and of Their Relationship. *Journal of Climate*, **28**, 5254–5271. <http://dx.doi.org/10.1175/JCLI-D-14-00589.1>
- Becker, A., P. Finger, A. Meyer-Christoffer, B. Rudolf, K. Schamm, U. Schneider, and M. Ziese, 2013: A description of the global land-surface precipitation data products of the Global Precipitation Climatology Centre with sample applications including centennial (trend) analysis from 1901–present. *Earth System Science Data*, **5**, 71–99. <http://dx.doi.org/10.5194/essd-5-71-2013>

- 1 Bender, F.A.-M., V. Ramanathan, and G. Tselioudis, 2012: Changes in extratropical storm track
2 cloudiness 1983–2008: observational support for a poleward shift. *Climate Dynamics*, **38**,
3 2037–2053. <http://dx.doi.org/10.1007/s00382-011-1065-6>
- 4 Berghuijs, W.R., R.A. Woods, C.J. Hutton, and M. Sivapalan, 2016: Dominant flood generating
5 mechanisms across the United States. *Geophysical Research Letters*, **43**, 4382–4390.
6 <http://dx.doi.org/10.1002/2016GL068070>
- 7 Bernier, P.Y., R.L. Desjardins, Y. Karimi-Zindashty, D. Worth, A. Beaudoin, Y. Luo, and S.
8 Wang, 2011: Boreal lichen woodlands: A possible negative feedback to climate change in
9 eastern North America. *Agricultural and Forest Meteorology*, **151**, 521–528.
10 <http://dx.doi.org/10.1016/j.agrformet.2010.12.013>
- 11 Betts, R.A., O. Boucher, M. Collins, P.M. Cox, P.D. Falloon, N. Gedney, D.L. Hemming, C.
12 Huntingford, C.D. Jones, D.M.H. Sexton, and M.J. Webb, 2007: Projected increase in
13 continental runoff due to plant responses to increasing carbon dioxide. *Nature*, **448**, 1037–
14 1041. <http://dx.doi.org/10.1038/nature06045>
- 15 Bindoff, N.L., P.A. Stott, K.M. AchutaRao, M.R. Allen, N. Gillett, D. Gutzler, K. Hansingo, G.
16 Hegerl, Y. Hu, S. Jain, I.I. Mokhov, J. Overland, J. Perlwitz, R. Sebbari, and X. Zhang, 2013:
17 Detection and Attribution of Climate Change: from Global to Regional. *Climate Change*
18 *2013: The Physical Science Basis. Contribution of Working Group I to the Fifth Assessment*
19 *Report of the Intergovernmental Panel on Climate Change*. Stocker, T.F., D. Qin, G.-K.
20 Plattner, M. Tignor, S.K. Allen, J. Boschung, A. Nauels, Y. Xia, V. Bex, and P.M. Midgley,
21 Eds. Cambridge University Press, Cambridge, United Kingdom and New York, NY, USA,
22 867–952. <http://dx.doi.org/10.1017/CBO9781107415324.022> www.climatechange2013.org
- 23 Blunden, J. and D.S. Arndt, 2016: State of the Climate in 2015. *Bulletin of the American*
24 *Meteorological Society*, **97**, Si-S275.
25 <http://dx.doi.org/10.1175/2016BAMSStateoftheClimate.1>
- 26 Bonan, G.B., 2008: Forests and Climate Change: Forcings, Feedbacks, and the Climate Benefits
27 of Forests. *Science*, **320**, 1444–1449. <http://dx.doi.org/10.1126/science.1155121>
- 28 Chambers, J.Q., J.I. Fisher, H. Zeng, E.L. Chapman, D.B. Baker, and G.C. Hurtt, 2007:
29 Hurricane Katrina's Carbon Footprint on U.S. Gulf Coast Forests. *Science*, **318**, 1107–1107.
30 <http://dx.doi.org/10.1126/science.1148913>
- 31 Chang, E.K.M., 2013: CMIP5 projection of significant reduction in extratropical cyclone activity
32 over North America. *Journal of Climate*, **26**, 9903–9922. [http://dx.doi.org/10.1175/JCLI-D-](http://dx.doi.org/10.1175/JCLI-D-13-00209.1)
33 [13-00209.1](http://dx.doi.org/10.1175/JCLI-D-13-00209.1)
- 34 Chen, X. and K.-K. Tung, 2014: Varying planetary heat sink led to global-warming slowdown
35 and acceleration. *Science*, **345**, 897–903. <http://dx.doi.org/10.1126/science.1254937>

- Church, J.A. and N.J. White, 2011: Sea-level rise from the late 19th to the early 21st century. *Surveys in Geophysics*, **32**, 585-602. <http://dx.doi.org/10.1007/s10712-011-9119-1>
- Church, J.A., N.J. White, L.F. Konikow, C.M. Domingues, J.G. Cogley, E. Rignot, J.M. Gregory, M.R. van den Broeke, A.J. Monaghan, and I. Velicogna, 2011: Revisiting the Earth's sea-level and energy budgets from 1961 to 2008. *Geophysical Research Letters*, **38**, L18601. <http://dx.doi.org/10.1029/2011GL048794>
- Churkina, G., V. Brovkin, W. von Bloh, K. Trusilova, M. Jung, and F. Dentener, 2009: Synergy of rising nitrogen depositions and atmospheric CO₂ on land carbon uptake moderately offsets global warming. *Global Biogeochemical Cycles*, **23**, n/a-n/a. <http://dx.doi.org/10.1029/2008GB003291>
- Ciais, P., M. Reichstein, N. Viovy, A. Granier, J. Ogee, V. Allard, M. Aubinet, N. Buchmann, C. Bernhofer, A. Carrara, F. Chevallier, N. De Noblet, A.D. Friend, P. Friedlingstein, T. Grunwald, B. Heinesch, P. Keronen, A. Knohl, G. Krinner, D. Loustau, G. Manca, G. Matteucci, F. Miglietta, J.M. Ourcival, D. Papale, K. Pilegaard, S. Rambal, G. Seufert, J.F. Soussana, M.J. Sanz, E.D. Schulze, T. Vesala, and R. Valentini, 2005: Europe-wide reduction in primary productivity caused by the heat and drought in 2003. *Nature*, **437**, 529-533. <http://dx.doi.org/10.1038/nature03972>
- Clark, D.B., D.A. Clark, and S.F. Oberbauer, 2010: Annual wood production in a tropical rain forest in NE Costa Rica linked to climatic variation but not to increasing CO₂. *Global Change Biology*, **16**, 747-759. <http://dx.doi.org/10.1111/j.1365-2486.2009.02004.x>
- Colle, B.A., Z. Zhang, K.A. Lombardo, E. Chang, P. Liu, and M. Zhang, 2013: Historical Evaluation and Future Prediction of Eastern North American and Western Atlantic Extratropical Cyclones in the CMIP5 Models during the Cool Season. *Journal of Climate*, **26**, 6882-6903. <http://dx.doi.org/10.1175/JCLI-D-12-00498.1>
- Collins, M., R. Knutti, J. Arblaster, J.-L. Dufresne, T. Fichefet, P. Friedlingstein, X. Gao, W.J. Gutowski, T. Johns, G. Krinner, M. Shongwe, C. Tebaldi, A.J. Weaver, and M. Wehner, 2013: Long-term Climate Change: Projections, Commitments and Irreversibility. *Climate Change 2013: The Physical Science Basis. Contribution of Working Group I to the Fifth Assessment Report of the Intergovernmental Panel on Climate Change*. Stocker, T.F., D. Qin, G.-K. Plattner, M. Tignor, S.K. Allen, J. Boschung, A. Nauels, Y. Xia, V. Bex, and P.M. Midgley, Eds. Cambridge University Press, Cambridge, United Kingdom and New York, NY, USA, 1029–1136. <http://dx.doi.org/10.1017/CBO9781107415324.024>
www.climatechange2013.org
- Comiso, J.C. and D.K. Hall, 2014: Climate trends in the Arctic as observed from space. *Wiley Interdisciplinary Reviews: Climate Change*, **5**, 389-409. <http://dx.doi.org/10.1002/wcc.277>

- 1 Dai, A., 2013: Increasing drought under global warming in observations and models. *Nature*
2 *Climate Change*, **3**, 52-58. <http://dx.doi.org/10.1038/nclimate1633>
- 3 Davy, R., I. Esau, A. Chernokulsky, S. Outten, and S. Zilitinkevich, 2016: Diurnal asymmetry to
4 the observed global warming. *International Journal of Climatology*, n/a-n/a.
5 <http://dx.doi.org/10.1002/joc.4688>
- 6 de Noblet-Ducoudré, N., J.-P. Boisier, A. Pitman, G.B. Bonan, V. Brovkin, F. Cruz, C. Delire,
7 V. Gayler, B.J.J.M.v.d. Hurk, P.J. Lawrence, M.K.v.d. Molen, C. Müller, C.H. Reick, B.J.
8 Strengers, and A. Voldoire, 2012: Determining Robust Impacts of Land-Use-Induced Land
9 Cover Changes on Surface Climate over North America and Eurasia: Results from the First
10 Set of LUCID Experiments. *Journal of Climate*, **25**, 3261-3281.
11 <http://dx.doi.org/10.1175/JCLI-D-11-00338.1>
- 12 DeConto, R.M. and D. Pollard, 2016: Contribution of Antarctica to past and future sea-level rise.
13 *Nature*, **531**, 591-597. <http://dx.doi.org/10.1038/nature17145>
- 14 Delworth, T.L. and T.R. Knutson, 2000: Simulation of Early 20th Century Global Warming.
15 *Science*, **287**, 2246-2250. <http://dx.doi.org/10.1126/science.287.5461.2246>
- 16 Derksen, C. and R. Brown, 2012: Spring snow cover extent reductions in the 2008–2012 period
17 exceeding climate model projections. *Geophysical Research Letters*, **39**, L19504.
18 <http://dx.doi.org/10.1029/2012gl053387>
- 19 Derksen, D., R. Brown, L. Mudryk, and K. Loujus, 2015: [The Arctic] Terrestrial snow cover
20 [in “State of the Climate in 2014”]. *Bulletin of the American Meteorological Society*, **96**,
21 S133-S135. <http://dx.doi.org/10.1175/2015BAMSStateoftheClimate.1>
- 22 Deser, C., R. Knutti, S. Solomon, and A.S. Phillips, 2012: Communication of the role of natural
23 variability in future North American climate. *Nature Climate Change*, **2**, 775-779.
24 <http://dx.doi.org/10.1038/nclimate1562>
25 http://www.nature.com/nclimate/journal/v2/n11/full/nclimate1562.html?WT.ec_id=NCLIM
26 ATE-201211
- 27 Diffenbaugh, N.S., M. Scherer, and R.J. Trapp, 2013: Robust increases in severe thunderstorm
28 environments in response to greenhouse forcing. *Proceedings of the National Academy of*
29 *Sciences*, **110**, 16361-16366. <http://dx.doi.org/10.1073/pnas.1307758110>
- 30 Donat, M.G., A.L. Lowry, L.V. Alexander, P.A. Ogorman, and N. Maher, 2016: More extreme
31 precipitation in the world’s dry and wet regions. *Nature Climate Change*, **6**, 508-513.
32 <http://dx.doi.org/10.1038/nclimate2941>
- 33 Dutton, A. and K. Lambeck, 2012: Ice Volume and Sea Level During the Last Interglacial.
34 *Science*, **337**, 216-219. <http://dx.doi.org/10.1126/science.1205749>

- 1 Easterling, D.R., K.E. Kunkel, M.F. Wehner, and L. Sun, 2016: Detection and attribution of
2 climate extremes in the observed record. *Weather and Climate Extremes*, **11**, 17-27.
3 <http://dx.doi.org/10.1016/j.wace.2016.01.001>
- 4 Easterling, D.R. and M.F. Wehner, 2009: Is the climate warming or cooling? *Geophysical*
5 *Research Letters*, **36**, 3. <http://dx.doi.org/10.1029/2009GL037810>
- 6 Eisenman, I., W.N. Meier, and J.R. Norris, 2014: A spurious jump in the satellite record: has
7 Antarctic sea ice expansion been overestimated? *The Cryosphere*, **8**, 1289-1296.
8 <http://dx.doi.org/10.5194/tc-8-1289-2014>
- 9 Elsner, J.B., J.P. Kossin, and T.H. Jagger, 2008: The increasing intensity of the strongest tropical
10 cyclones. *Nature*, **455**, 92-95. <http://dx.doi.org/10.1038/nature07234>
- 11 Emanuel, K.A., 2013: Downscaling CMIP5 climate models shows increased tropical cyclone
12 activity over the 21st century. *Proceedings of the National Academy of Sciences*, **110**, 12219-
13 12224. <http://dx.doi.org/10.1073/pnas.1301293110>
- 14 England, M.H., S. McGregor, P. Spence, G.A. Meehl, A. Timmermann, W. Cai, A.S. Gupta,
15 M.J. McPhaden, A. Purich, and A. Santoso, 2014: Recent intensification of wind-driven
16 circulation in the Pacific and the ongoing warming hiatus. *Nature Climate Change*, **4**, 222-
17 227. <http://dx.doi.org/10.1038/nclimate2106>
- 18 Ezer, T. and L.P. Atkinson, 2014: Accelerated flooding along the U.S. East Coast: On the impact
19 of sea-level rise, tides, storms, the Gulf Stream, and the North Atlantic Oscillations. *Earth's*
20 *Future*, **2**, 362-382. <http://dx.doi.org/10.1002/2014EF000252>
- 21 Feldmann, J. and A. Levermann, 2015: Collapse of the West Antarctic Ice Sheet after local
22 destabilization of the Amundsen Basin. *Proceedings of the National Academy of Sciences*,
23 **112**, 14191-14196. <http://dx.doi.org/10.1073/pnas.1512482112>
- 24 Fettweis, X., M. Tedesco, M. van den Broeke, and J. Ettema, 2011: Melting trends over the
25 Greenland ice sheet (1958–2009) from spaceborne microwave data and regional climate
26 models. *The Cryosphere*, **5**, 359-375. <http://dx.doi.org/10.5194/tc-5-359-2011>
- 27 Finzi, A.C., D.J.P. Moore, E.H. DeLucia, J. Lichter, K.S. Hofmockel, R.B. Jackson, H.-S. Kim,
28 R. Matamala, H.R. McCarthy, R. Oren, J.S. Pippen, and W.H. Schlesinger, 2006: Progressive
29 nitrogen limitation of ecosystem processes under elevated CO₂ in a warm-temperate forest.
30 *Ecology*, **87**, 15-25. <http://dx.doi.org/10.1890/04-1748>
- 31 Fyfe, J.C., G.A. Meehl, M.H. England, M.E. Mann, B.D. Santer, G.M. Flato, E. Hawkins, N.P.
32 Gillett, S.-P. Xie, Y. Kosaka, and N.C. Swart, 2016: Making sense of the early-2000s
33 warming slowdown. *Nature Climate Change*, **6**, 224-228.
34 <http://dx.doi.org/10.1038/nclimate2938>

- 1 Greve, P., B. Orlowsky, B. Mueller, J. Sheffield, M. Reichstein, and S.I. Seneviratne, 2014:
2 Global assessment of trends in wetting and drying over land. *Nature Geoscience*, **7**, 716-721.
3 <http://dx.doi.org/10.1038/ngeo2247>
- 4 Harig, C. and F.J. Simons, 2012: Mapping Greenland's mass loss in space and time. *Proceedings*
5 *of the National Academy of Sciences*, **109**, 19934-19937.
6 <http://dx.doi.org/10.1073/pnas.1206785109>
- 7 Harig, C. and F.J. Simons, 2015: Accelerated West Antarctic ice mass loss continues to outpace
8 East Antarctic gains. *Earth and Planetary Science Letters*, **415**, 134-141.
9 <http://dx.doi.org/10.1016/j.epsl.2015.01.029>
- 10 Harig, C. and F.J. Simons, 2016: Ice mass loss in Greenland, the Gulf of Alaska, and the
11 Canadian Archipelago: Seasonal cycles and decadal trends. *Geophysical Research Letters*,
12 **43**, 3150-3159. <http://dx.doi.org/10.1002/2016GL067759>
- 13 Hay, C.C., E. Morrow, R.E. Kopp, and J.X. Mitrovica, 2015: Probabilistic reanalysis of
14 twentieth-century sea-level rise. *Nature*, **517**, 481-484. <http://dx.doi.org/10.1038/nature14093>
- 15 Haywood, A.M., D.J. Hill, A.M. Dolan, B.L. Otto-Bliesner, F. Bragg, W.L. Chan, M.A.
16 Chandler, C. Contoux, H.J. Dowsett, A. Jost, Y. Kamae, G. Lohmann, D.J. Lunt, A. Abe-
17 Ouchi, S.J. Pickering, G. Ramstein, N.A. Rosenbloom, U. Salzmann, L. Sohl, C. Stepanek,
18 H. Ueda, Q. Yan, and Z. Zhang, 2013: Large-scale features of Pliocene climate: results from
19 the Pliocene Model Intercomparison Project. *Climate of the Past*, **9**, 191-209.
20 <http://dx.doi.org/10.5194/cp-9-191-2013>
- 21 Held, I.M. and B.J. Soden, 2006: Robust responses of the hydrological cycle to global warming.
22 *Journal of Climate*, **19**, 5686-5699. <http://dx.doi.org/10.1175/jcli3990.1>
- 23 Hoegh-Guldberg, O., R. Cai, E.S. Poloczanska, P.G. Brewer, S. Sundby, K. Hilmi, V.J. Fabry,
24 and S. Jung, 2014: The Ocean. *Climate Change 2014: Impacts, Adaptation, and*
25 *Vulnerability. Part B: Regional Aspects. Contribution of Working Group II to the Fifth*
26 *Assessment Report of the Intergovernmental Panel of Climate Change*. Barros, V.R., C.B.
27 Field, D.J. Dokken, M.D. Mastrandrea, K.J. Mach, T.E. Bilir, M. Chatterjee, K.L. Ebi, Y.O.
28 Estrada, R.C. Genova, B. Girma, E.S. Kissel, A.N. Levy, S. MacCracken, P.R. Mastrandrea,
29 and L.L. White, Eds. Cambridge University Press, Cambridge, United Kingdom and New
30 York, NY, USA, 1655-1731.
- 31 Hoerling, M., M. Chen, R. Dole, J. Eischeid, A. Kumar, J.W. Nielsen-Gammon, P. Pegion, J.
32 Perlwitz, X.-W. Quan, and T. Zhang, 2013: Anatomy of an extreme event. *Journal of*
33 *Climate*, **26**, 2811-2832. <http://dx.doi.org/10.1175/JCLI-D-12-00270.1>

- 1 Horton, D.E., N.C. Johnson, D. Singh, D.L. Swain, B. Rajaratnam, and N.S. Diffenbaugh, 2015:
2 Contribution of changes in atmospheric circulation patterns to extreme temperature trends.
3 *Nature*, **522**, 465-469. <http://dx.doi.org/10.1038/nature14550>
- 4 Houghton, R.A., J.I. House, J. Pongratz, G.R. van der Werf, R.S. DeFries, M.C. Hansen, C. Le
5 Quéré, and N. Ramankutty, 2012: Carbon emissions from land use and land-cover change.
6 *Biogeosciences*, **9**, 5125-5142. <http://dx.doi.org/10.5194/bg-9-5125-2012>
- 7 Huber, M. and R. Knutti, 2014: Natural variability, radiative forcing and climate response in the
8 recent hiatus reconciled. *Nature Geoscience*, **7**, 651-656. <http://dx.doi.org/10.1038/ngeo2228>
- 9 Hurrell, J.W. and C. Deser, 2009: North Atlantic climate variability: The role of the North
10 Atlantic Oscillation. *Journal of Marine Systems*, **78**, 28-41.
11 <http://dx.doi.org/10.1016/j.jmarsys.2008.11.026>
- 12 IPCC, 2013: *Climate Change 2013: The Physical Science Basis. Contribution of Working Group*
13 *I to the Fifth Assessment Report of the Intergovernmental Panel on Climate Change*.
14 Cambridge University Press, Cambridge, UK and New York, NY, 1535 pp.
15 <http://dx.doi.org/10.1017/CBO9781107415324> www.climatechange2013.org
- 16 Jacob, T., J. Wahr, W.T. Pfeffer, and S. Swenson, 2012: Recent contributions of glaciers and ice
17 caps to sea level rise. *Nature*, **482**, 514-518. <http://dx.doi.org/10.1038/nature10847>
- 18 Jenkins, A., P. Dutrieux, S.S. Jacobs, S.D. McPhail, J.R. Perrett, A.T. Webb, and D. White,
19 2010: Observations beneath Pine Island Glacier in West Antarctica and implications for its
20 retreat. *Nature Geoscience*, **3**, 468-472. <http://dx.doi.org/10.1038/ngeo890>
- 21 Jones, D.A., W. Wang, and R. Fawcett, 2009: High-quality spatial climate data-sets for
22 Australia. *Australian Meteorological and Oceanographic Journal*, **58**, 233-248.
- 23 Joughin, I., B.E. Smith, and B. Medley, 2014: Marine Ice Sheet Collapse Potentially Under Way
24 for the Thwaites Glacier Basin, West Antarctica. *Science*, **344**, 735-738.
25 <http://dx.doi.org/10.1126/science.1249055>
- 26 Karl, T.R., A. Arguez, B. Huang, J.H. Lawrimore, J.R. McMahon, M.J. Menne, T.C. Peterson,
27 R.S. Vose, and H.-M. Zhang, 2015: Possible artifacts of data biases in the recent global
28 surface warming hiatus. *Science*, **348**, 1469-1472. <http://dx.doi.org/10.1126/science.aaa5632>
- 29 Kaspar, F., N. Kühl, U. Cubasch, and T. Litt, 2005: A model-data comparison of European
30 temperatures in the Eemian interglacial. *Geophysical Research Letters*, **32**, n/a-n/a.
31 <http://dx.doi.org/10.1029/2005GL022456>
- 32 Katz, R.W. and B.G. Brown, 1992: Extreme events in a changing climate: Variability is more
33 important than averages. *Climatic Change*, **21**, 289-302.
34 <http://dx.doi.org/10.1007/bf00139728>

- 1 Kim, Y., J.S. Kimball, K. Zhang, and K.C. McDonald, 2012: Satellite detection of increasing
2 Northern Hemisphere non-frozen seasons from 1979 to 2008: Implications for regional
3 vegetation growth. *Remote Sensing of Environment*, **121**, 472-487.
4 <http://dx.doi.org/10.1016/j.rse.2012.02.014>
- 5 Knutson, T.R., J.J. Sirutis, M. Zhao, R.E. Tuleya, M. Bender, G.A. Vecchi, G. Villarini, and D.
6 Chavas, 2015: Global Projections of Intense Tropical Cyclone Activity for the Late Twenty-
7 First Century from Dynamical Downscaling of CMIP5/RCP4.5 Scenarios. *Journal of*
8 *Climate*, **28**, 7203-7224. <http://dx.doi.org/10.1175/JCLI-D-15-0129.1>
- 9 Knutson, T.R., R. Zhang, and L.W. Horowitz, 2016: Prospects for a prolonged slowdown in
10 global warming in the early 21st century. *Nature Communications*, **7**, 13676.
11 <http://dx.doi.org/10.1038/ncomms13676>
- 12 Kopp, R.E., R.M. Horton, C.M. Little, J.X. Mitrovica, M. Oppenheimer, D.J. Rasmussen, B.H.
13 Strauss, and C. Tebaldi, 2014: Probabilistic 21st and 22nd century sea-level projections at a
14 global network of tide-gauge sites. *Earth's Future*, **2**, 383-406.
15 <http://dx.doi.org/10.1002/2014EF000239>
- 16 Kopp, R.E., F.J. Simons, J.X. Mitrovica, A.C. Maloof, and M. Oppenheimer, 2009: Probabilistic
17 assessment of sea level during the last interglacial stage. *Nature*, **462**, 863-867.
18 <http://dx.doi.org/10.1038/nature08686>
- 19 Kosaka, Y. and S.-P. Xie, 2013: Recent global-warming hiatus tied to equatorial Pacific surface
20 cooling. *Nature*, **501**, 403-407. <http://dx.doi.org/10.1038/nature12534>
- 21 Kossin, J.P., K.A. Emanuel, and S.J. Camargo, 2016: Past and Projected Changes in Western
22 North Pacific Tropical Cyclone Exposure. *Journal of Climate*, **29**, 5725-5739.
23 <http://dx.doi.org/10.1175/JCLI-D-16-0076.1>
- 24 Kossin, J.P., K.A. Emanuel, and G.A. Vecchi, 2014: The poleward migration of the location of
25 tropical cyclone maximum intensity. *Nature*, **509**, 349-352.
26 <http://dx.doi.org/10.1038/nature13278>
- 27 Kossin, J.P., T.L. Olander, and K.R. Knapp, 2013: Trend analysis with a new global record of
28 tropical cyclone intensity. *Journal of Climate*, **26**, 9960-9976.
29 <http://dx.doi.org/10.1175/JCLI-D-13-00262.1>
- 30 Kundzewicz, Z.W., S. Kanae, S.I. Seneviratne, J. Handmer, N. Nicholls, P. Peduzzi, R. Mechler,
31 L.M. Bouwer, N. Arnell, K. Mach, R. Muir-Wood, G.R. Brakenridge, W. Kron, G. Benito,
32 Y. Honda, K. Takahashi, and B. Sherstyukov, 2014: Flood risk and climate change: global
33 and regional perspectives. *Hydrological Sciences Journal*, **59**, 1-28.
34 <http://dx.doi.org/10.1080/02626667.2013.857411>

- 1 Kunkel, K.E. and R.M. Frankson, 2015: Global Land Surface Extremes of Precipitation: Data
2 Limitations and Trends. *Journal of Extreme Events*, **02**, 1550004.
3 <http://dx.doi.org/10.1142/S2345737615500049>
- 4 Kunkel, K.E., T.R. Karl, H. Brooks, J. Kossin, J. Lawrimore, D. Arndt, L. Bosart, D. Changnon,
5 S.L. Cutter, N. Doesken, K. Emanuel, P.Y. Groisman, R.W. Katz, T. Knutson, J. O'Brien,
6 C.J. Paciorek, T.C. Peterson, K. Redmond, D. Robinson, J. Trapp, R. Vose, S. Weaver, M.
7 Wehner, K. Wolter, and D. Wuebbles, 2013: Monitoring and understanding trends in extreme
8 storms: State of knowledge. *Bulletin of the American Meteorological Society*, **94**.
9 <http://dx.doi.org/10.1175/BAMS-D-11-00262.1>
- 10 Kunkel, K.E., D.A. Robinson, S. Champion, X. Yin, T. Estilow, and R.M. Frankson, 2016:
11 Trends and Extremes in Northern Hemisphere Snow Characteristics. *Current Climate*
12 *Change Reports*, **2**, 65-73. <http://dx.doi.org/10.1007/s40641-016-0036-8>
- 13 Kurz, W.A., G. Stinson, G.J. Rampley, C.C. Dymond, and E.T. Neilson, 2008: Risk of natural
14 disturbances makes future contribution of Canada's forests to the global carbon cycle highly
15 uncertain. *Proceedings of the National Academy of Sciences*, **105**, 1551-1555.
16 <http://dx.doi.org/10.1073/pnas.0708133105>
- 17 Le Quéré, C., R. Moriarty, R.M. Andrew, J.G. Canadell, S. Sitch, J.I. Korsbakken, P.
18 Friedlingstein, G.P. Peters, R.J. Andres, T.A. Boden, R.A. Houghton, J.I. House, R.F.
19 Keeling, P. Tans, A. Arneeth, D.C.E. Bakker, L. Barbero, L. Bopp, J. Chang, F. Chevallier,
20 L.P. Chini, P. Ciais, M. Fader, R.A. Feely, T. Gkritzalis, I. Harris, J. Hauck, T. Ilyina, A.K.
21 Jain, E. Kato, V. Kitidis, K. Klein Goldewijk, C. Koven, P. Landschützer, S.K. Lauvset, N.
22 Lefèvre, A. Lenton, I.D. Lima, N. Metzl, F. Millero, D.R. Munro, A. Murata, J.E.M.S. Nabel,
23 S. Nakaoka, Y. Nojiri, K. O'Brien, A. Olsen, T. Ono, F.F. Pérez, B. Pfeil, D. Pierrot, B.
24 Poulter, G. Rehder, C. Rödenbeck, S. Saito, U. Schuster, J. Schwinger, R. Séférian, T.
25 Steinhoff, B.D. Stocker, A.J. Sutton, T. Takahashi, B. Tilbrook, I.T. van der Laan-Luijkx,
26 G.R. van der Werf, S. van Heuven, D. Vandemark, N. Viovy, A. Wiltshire, S. Zaehle, and N.
27 Zeng, 2015: Global Carbon Budget 2015. *Earth System Science Data*, **7**, 349-396.
28 <http://dx.doi.org/10.5194/essd-7-349-2015>
- 29 Lewandowsky, S., J.S. Risbey, and N. Oreskes, 2016: The "Pause" in Global Warming: Turning
30 a Routine Fluctuation into a Problem for Science. *Bulletin of the American Meteorological*
31 *Society*, **97**, 723-733. <http://dx.doi.org/10.1175/BAMS-D-14-00106.1>
- 32 Lewis, S.L., P.M. Brando, O.L. Phillips, G.M.F. van der Heijden, and D. Nepstad, 2011: The
33 2010 Amazon Drought. *Science*, **331**, 554-554. <http://dx.doi.org/10.1126/science.1200807>
- 34 Lim, Y.-K., D.S. Siegfried, M.J.N. Sophie, N.L. Jae, M.M. Andrea, I.C. Richard, Z. Bin, and V.
35 Isabella, 2016: Atmospheric summer teleconnections and Greenland Ice Sheet surface mass

- 1 variations: insights from MERRA-2. *Environmental Research Letters*, **11**, 024002.
2 <http://dx.doi.org/10.1088/1748-9326/11/2/024002>
- 3 Mann, M.E., Z. Zhang, M.K. Hughes, R.S. Bradley, S.K. Miller, S. Rutherford, and F. Ni, 2008:
4 Proxy-based reconstructions of hemispheric and global surface temperature variations over
5 the past two millennia. *Proceedings of the National Academy of Sciences*, **105**, 13252-13257.
6 <http://dx.doi.org/10.1073/pnas.0805721105>
- 7 Mao, J., A. Ribes, B. Yan, X. Shi, P.E. Thornton, R. Seferian, P. Ciais, R.B. Myneni, H.
8 Douville, S. Piao, Z. Zhu, R.E. Dickinson, Y. Dai, D.M. Ricciuto, M. Jin, F.M. Hoffman, B.
9 Wang, M. Huang, and X. Lian, 2016: Human-induced greening of the northern extratropical
10 land surface. *Nature Climate Change*, **advance online publication**.
11 <http://dx.doi.org/10.1038/nclimate3056>
- 12 Marcott, S.A., J.D. Shakun, P.U. Clark, and A.C. Mix, 2013: A reconstruction of regional and
13 global temperature for the past 11,300 years. *Science*, **339**, 1198-1201.
14 <http://dx.doi.org/10.1126/science.1228026>
- 15 Marvel, K. and C. Bonfils, 2013: Identifying external influences on global precipitation.
16 *Proceedings of the National Academy of Sciences*, **110**, 19301-19306.
17 <http://dx.doi.org/10.1073/pnas.1314382110>
- 18 Mears, C.A. and F.J. Wentz, 2016: Sensitivity of satellite-derived tropospheric temperature
19 trends to the diurnal cycle adjustment. *Journal of Climate*, **29**, 3629-3646.
20 <http://dx.doi.org/10.1175/JCLI-D-15-0744.1>
- 21 Meehl, G.A., J.M. Arblaster, C.M. Bitz, C.T.Y. Chung, and H. Teng, 2016: Antarctic sea-ice
22 expansion between 2000 and 2014 driven by tropical Pacific decadal climate variability.
23 *Nature Geoscience*, **9**, 590-595. <http://dx.doi.org/10.1038/ngeo2751>
- 24 Meehl, G.A., J.M. Arblaster, J.T. Fasullo, A. Hu, and K.E. Trenberth, 2011: Model-based
25 evidence of deep-ocean heat uptake during surface-temperature hiatus periods. *Nature*
26 *Climate Change*, **1**, 360-364. <http://dx.doi.org/10.1038/nclimate1229>
- 27 Meehl, G.A., C. Tebaldi, G. Walton, D. Easterling, and L. McDaniel, 2009: Relative increase of
28 record high maximum temperatures compared to record low minimum temperatures in the
29 US. *Geophysical Research Letters*, **36**, L23701. <http://dx.doi.org/10.1029/2009GL040736>
- 30 Melillo, J.M., T.C. Richmond, and G.W. Yohe, eds. *Climate Change Impacts in the United*
31 *States: The Third National Climate Assessment*. 2014, U.S. Global Change Research
32 Program: Washington, D.C. 842. <http://dx.doi.org/10.7930/J0Z31WJ2>.
- 33 Mengel, M., A. Levermann, K. Frieler, A. Robinson, B. Marzeion, and R. Winkelmann, 2016:
34 Future sea level rise constrained by observations and long-term commitment. *Proceedings of*

- 1 *the National Academy of Sciences*, **113**, 2597-2602.
- 2 <http://dx.doi.org/10.1073/pnas.1500515113>
- 3 Menzel, A., T.H. Sparks, N. Estrella, E. Koch, A. Aasa, R. Ahas, K. Alm-Kübler, P. Bissolli,
- 4 O.G. Braslavská, A. Briede, F.M. Chmielewski, Z. Crepinsek, Y. Curnel, Å. Dahl, C. Defila,
- 5 A. Donnelly, Y. Filella, K. Jatzak, F. Måge, A. Mestre, Ø. Nordli, J. Peñuelas, P. Pirinen, V.
- 6 Remišvá, H. Scheffinger, M. Striz, A. Susnik, A.J.H. Van Vliet, F.-E. Wielgolaski, S. Zach,
- 7 and A.N.A. Zust, 2006: European phenological response to climate change matches the
- 8 warming pattern. *Global Change Biology*, **12**, 1969-1976. [http://dx.doi.org/10.1111/j.1365-](http://dx.doi.org/10.1111/j.1365-2486.2006.01193.x)
- 9 2486.2006.01193.x
- 10 Merrifield, M.A., P. Thompson, E. Leuliette, G.T. Mitchum, D.P. Chambers, S. Jevrejeva, R.S.
- 11 Nerem, M. Menéndez, W. Sweet, B. Hamlington, and J.J. Marra, 2015: [Global Oceans] Sea
- 12 level variability and change [in “State of the Climate in 2014”]. *Bulletin of the American*
- 13 *Meteorological Society*, **96**, S82-S85.
- 14 <http://dx.doi.org/10.1175/2015BAMSStateoftheClimate.1>
- 15 Min, S.K., X. Zhang, F.W. Zwiers, and G.C. Hegerl, 2011: Human contribution to more-intense
- 16 precipitation extremes. *Nature*, **470**, 378-381. <http://dx.doi.org/10.1038/nature09763>
- 17 Min, S.-K., X. Zhang, and F. Zwiers, 2008: Human-Induced Arctic Moistening. *Science*, **320**,
- 18 518-520. <http://dx.doi.org/10.1126/science.1153468>
- 19 Min, S.-K., X. Zhang, F. Zwiers, H. Shiogama, Y.-S. Tung, and M. Wehner, 2013: Multimodel
- 20 Detection and Attribution of Extreme Temperature Changes. *Journal of Climate*, **26**, 7430-
- 21 7451. <http://dx.doi.org/10.1175/JCLI-D-12-00551.1>
- 22 Mountain Research Initiative, 2015: Elevation-dependent warming in mountain regions of the
- 23 world. *Nature Clim. Change*, **5**, 424-430. <http://dx.doi.org/10.1038/nclimate2563>
- 24 Myneni, R.B., C.D. Keeling, C.J. Tucker, G. Asrar, and R.R. Nemani, 1997: Increased plant
- 25 growth in the northern high latitudes from 1981 to 1991. *Nature*, **386**, 698-702.
- 26 <http://dx.doi.org/10.1038/386698a0>
- 27 NCEI, 2016: Climate at a glance. [www.ncdc.noaa.gov/cag/time-](http://www.ncdc.noaa.gov/cag/time-series/global/globe/land_ocean/ytd/12/1880-2015)
- 28 [series/global/globe/land_ocean/ytd/12/1880-2015](http://www.ncdc.noaa.gov/cag/time-series/global/globe/land_ocean/ytd/12/1880-2015)
- 29 Nerem, R.S., D.P. Chambers, C. Choe, and G.T. Mitchum, 2010: Estimating mean sea level
- 30 change from the TOPEX and Jason altimeter missions. *Marine Geodesy*, **33**, 435-446.
- 31 <http://dx.doi.org/10.1080/01490419.2010.491031>
- 32 Nghiem, S.V., D.K. Hall, T.L. Mote, M. Tedesco, M.R. Albert, K. Keegan, C.A. Shuman, N.E.
- 33 DiGirolamo, and G. Neumann, 2012: The extreme melt across the Greenland ice sheet in
- 34 2012. *Geophysical Research Letters*, **39**, L20502. <http://dx.doi.org/10.1029/2012GL053611>

- 1 Nieves, V., J.K. Willis, and W.C. Patzert, 2015: Recent hiatus caused by decadal shift in Indo-
2 Pacific heating. *Science*, **349**, 532-535. <http://dx.doi.org/10.1126/science.aaa4521>
- 3 Norby, R.J., J.M. Warren, C.M. Iversen, B.E. Medlyn, and R.E. McMurtrie, 2010: CO2
4 enhancement of forest productivity constrained by limited nitrogen availability. *Proceedings*
5 *of the National Academy of Sciences*, **107**, 19368-19373.
6 <http://dx.doi.org/10.1073/pnas.1006463107>
- 7 Page, S.E., F. Siegert, J.O. Rieley, H.-D.V. Boehm, A. Jaya, and S. Limin, 2002: The amount of
8 carbon released from peat and forest fires in Indonesia during 1997. *Nature*, **420**, 61-65.
9 <http://dx.doi.org/10.1038/nature01131>
- 10 PAGES 2K, 2013: Continental-scale temperature variability during the past two millennia.
11 *Nature Geoscience*, **6**, 339-346. <http://dx.doi.org/10.1038/ngeo1797>
- 12 Palmroth, S., R. Oren, H.R. McCarthy, K.H. Johnsen, A.C. Finzi, J.R. Butnor, M.G. Ryan, and
13 W.H. Schlesinger, 2006: Aboveground sink strength in forests controls the allocation of
14 carbon below ground and its [CO2]-induced enhancement. *Proceedings of the National*
15 *Academy of Sciences*, **103**, 19362-19367. <http://dx.doi.org/10.1073/pnas.0609492103>
- 16 Pan, Y., R.A. Birdsey, J. Fang, R. Houghton, P.E. Kauppi, W.A. Kurz, O.L. Phillips, A.
17 Shvidenko, S.L. Lewis, J.G. Canadell, P. Ciais, R.B. Jackson, S.W. Pacala, A.D. McGuire, S.
18 Piao, A. Rautiainen, S. Sitch, and D. Hayes, 2011: A large and persistent carbon sink in the
19 world's forests. *Science*, **333**, 988-93. <http://dx.doi.org/10.1126/science.1201609>
20 http://www.lter.uaf.edu/pdf/1545_Pan_Birdsey_2011.pdf
- 21 Parkinson, C.L., 2014: Spatially mapped reductions in the length of the Arctic sea ice season.
22 *Geophysical Research Letters*, **41**, 4316-4322. <http://dx.doi.org/10.1002/2014GL060434>
- 23 Parmesan, C. and G. Yohe, 2003: A globally coherent fingerprint of climate change impacts
24 across natural systems. *Nature*, **421**, 37-42. <http://dx.doi.org/10.1038/nature01286>
- 25 Parris, A., P. Bromirski, V. Burkett, D. Cayan, M. Culver, J. Hall, R. Horton, K. Knuuti, R.
26 Moss, J. Obeysekera, A. Sallenger, and J. Weiss, 2012: Global Sea Level Rise Scenarios for
27 the United States National Climate Assessment. NOAA Tech Memo OAR CPO-1. 37 pp.
28 National Oceanic and Atmospheric Administration, Silver Spring, MD.
29 http://scenarios.globalchange.gov/sites/default/files/NOAA_SLR_r3_0.pdf
- 30 Pauling, A.G., C.M. Bitz, I.J. Smith, and P.J. Langhorne, 2016: The Response of the Southern
31 Ocean and Antarctic Sea Ice to Freshwater from Ice Shelves in an Earth System Model.
32 *Journal of Climate*, **29**, 1655-1672. <http://dx.doi.org/10.1175/JCLI-D-15-0501.1>

- 1 Pelto, M.S., 2015: [Global Climate] Alpine glaciers [in “State of the Climate in 2014”]. *Bulletin*
2 *of the American Meteorological Society*, **96**, S19-S20.
3 <http://dx.doi.org/10.1175/2015BAMSStateoftheClimate.1>
- 4 Perovich, D., S. Gerlnad, S. Hendricks, W. Meier, M. Nicolaus, and M. Tschudi, 2015: [The
5 Arctic] Sea ice cover [in “State of the Climate in 2014”]. *Bulletin of the American*
6 *Meteorological Society*, **96**, S145-S146.
7 <http://dx.doi.org/10.1175/2015BAMSStateoftheClimate.1>
- 8 Peterson, T.C., R.R. Heim, R. Hirsch, D.P. Kaiser, H. Brooks, N.S. Diffenbaugh, R.M. Dole, J.P.
9 Giovannetone, K. Guirguis, T.R. Karl, R.W. Katz, K. Kunkel, D. Lettenmaier, G.J. McCabe,
10 C.J. Paciorek, K.R. Ryberg, S. Schubert, V.B.S. Silva, B.C. Stewart, A.V. Vecchia, G.
11 Villarini, R.S. Vose, J. Walsh, M. Wehner, D. Wolock, K. Wolter, C.A. Woodhouse, and D.
12 Wuebbles, 2013: Monitoring and understanding changes in heat waves, cold waves, floods
13 and droughts in the United States: State of knowledge. *Bulletin of the American*
14 *Meteorological Society*, **94**, 821-834. <http://dx.doi.org/10.1175/BAMS-D-12-00066.1>
- 15 Rahmstorf, S., J.E. Box, G. Feulner, M.E. Mann, A. Robinson, S. Rutherford, and E.J.
16 Schaffernicht, 2015: Exceptional twentieth-century slowdown in Atlantic Ocean overturning
17 circulation. *Nature Climate Change*, **5**, 475-480. <http://dx.doi.org/10.1038/nclimate2554>
- 18 Reyes-Fox, M., H. Steltzer, M.J. Trlica, G.S. McMaster, A.A. Andales, D.R. LeCain, and J.A.
19 Morgan, 2014: Elevated CO2 further lengthens growing season under warming conditions.
20 *Nature*, **510**, 259-262. <http://dx.doi.org/10.1038/nature13207>
- 21 Richardson, M., K. Cowtan, E. Hawkins, and M.B. Stolpe, 2016: Reconciled climate response
22 estimates from climate models and the energy budget of Earth. *Nature Climate Change*, **6**,
23 931-935. <http://dx.doi.org/10.1038/nclimate3066>
- 24 Ridley, D.A., S. Solomon, J.E. Barnes, V.D. Burlakov, T. Deshler, S.I. Dolgii, A.B. Herber, T.
25 Nagai, R.R. Neely, A.V. Nevzorov, C. Ritter, T. Sakai, B.D. Santer, M. Sato, A. Schmidt, O.
26 Uchino, and J.P. Vernier, 2014: Total volcanic stratospheric aerosol optical depths and
27 implications for global climate change. *Geophysical Research Letters*, **41**, 7763-7769.
28 <http://dx.doi.org/10.1002/2014GL061541>
- 29 Rignot, E., J. Mouginot, M. Morlighem, H. Seroussi, and B. Scheuchl, 2014: Widespread, rapid
30 grounding line retreat of Pine Island, Thwaites, Smith, and Kohler glaciers, West Antarctica,
31 from 1992 to 2011. *Geophysical Research Letters*, **41**, 3502-3509.
32 <http://dx.doi.org/10.1002/2014GL060140>
- 33 Rignot, E., I. Velicogna, M.R. van den Broeke, A. Monaghan, and J.T.M. Lenaerts, 2011:
34 Acceleration of the contribution of the Greenland and Antarctic ice sheets to sea level rise.
35 *Geophysical Research Letters*, **38**, L05503. <http://dx.doi.org/10.1029/2011GL046583>

- 1 Romanovsky, V.E., S.L. Smith, H.H. Christiansen, N.I. Shiklomanov, D.A. Streletskiy, D.S.
2 Drozdov, G.V. Malkova, N.G. Oberman, A.L. Kholodov, and S.S. Marchenko, 2015: [The
3 Arctic] Terrestrial permafrost [in “State of the Climate in 2014”]. *Bulletin of the American*
4 *Meteorological Society*, **96**, S139-S141.
5 <http://dx.doi.org/10.1175/2015BAMSSStateoftheClimate.1>
- 6 Rupp, D.E., P.W. Mote, N.L. Bindoff, P.A. Stott, and D.A. Robinson, 2013: Detection and
7 Attribution of Observed Changes in Northern Hemisphere Spring Snow Cover. *Journal of*
8 *Climate*, **26**, 6904-6914. <http://dx.doi.org/10.1175/JCLI-D-12-00563.1>
- 9 Sander, J., J.F. Eichner, E. Faust, and M. Steuer, 2013: Rising Variability in Thunderstorm-
10 Related U.S. Losses as a Reflection of Changes in Large-Scale Thunderstorm Forcing.
11 *Weather, Climate, and Society*, **5**, 317-331. <http://dx.doi.org/10.1175/WCAS-D-12-00023.1>
- 12 Santer, B.D., C. Bonfils, J.F. Painter, M.D. Zelinka, C. Mears, S. Solomon, G.A. Schmidt, J.C.
13 Fyfe, J.N.S. Cole, L. Nazarenko, K.E. Taylor, and F.J. Wentz, 2014: Volcanic contribution to
14 decadal changes in tropospheric temperature. *Nature Geoscience*, **7**, 185-189.
15 <http://dx.doi.org/10.1038/ngeo2098>
- 16 Santer, B.D., C. Mears, F.J. Wentz, K.E. Taylor, P.J. Gleckler, T.M.L. Wigley, T.P. Barnett, J.S.
17 Boyle, W. Brüggemann, N.P. Gillett, S.A. Klein, G.A. Meehl, T. Nozawa, D.W. Pierce, P.A.
18 Stott, W.M. Washington, and M.F. Wehner, 2007: Identification of human-induced changes
19 in atmospheric moisture content. *Proceedings of the National Academy of Sciences*, **104**,
20 15248-15253. <http://dx.doi.org/10.1073/pnas.0702872104>
21 <http://sa.indiaenvironmentportal.org.in/files/file/PNAS-2007-Santer-15248-53.pdf>
- 22 Santer, B.D., S. Solomon, G. Pallotta, C. Mears, S. Po-Chedley, Q. Fu, F. Wentz, C.-Z. Zou, J.
23 Painter, I. Cvijanovic, and C. Bonfils, Comparing tropospheric warming in climate models
24 and satellite data. *Journal of Climate*, **0**, null. <http://dx.doi.org/10.1175/JCLI-D-16-0333.1>
- 25 Sardeshmukh, P.D., G.P. Compo, and C. Penland, 2015: Need for Caution in Interpreting
26 Extreme Weather Statistics. *Journal of Climate*, **28**, 9166-9187.
27 <http://dx.doi.org/10.1175/JCLI-D-15-0020.1>
- 28 Schmidt, G.A., J.H. Jungclauss, C.M. Ammann, E. Bard, P. Braconnot, T.J. Crowley, G.
29 Delaygue, F. Joos, N.A. Krivova, R. Muscheler, B.L. Otto-Bliesner, J. Pongratz, D.T.
30 Shindell, S.K. Solanki, F. Steinhilber, and L.E.A. Vieira, 2011: Climate forcing
31 reconstructions for use in PMIP simulations of the last millennium (v1.0). *Geoscientific*
32 *Model Development*, **4**, 33-45. <http://dx.doi.org/10.5194/gmd-4-33-2011>
- 33 Schmidt, G.A., D.T. Shindell, and K. Tsigaridis, 2014: Reconciling warming trends. *Nature*
34 *Geoscience*, **7**, 158-160. <http://dx.doi.org/10.1038/ngeo2105>

- 1 Schwartz, M.D., R. Ahas, and A. Aasa, 2006: Onset of spring starting earlier across the Northern
2 Hemisphere. *Global Change Biology*, **12**, 343-351. <http://dx.doi.org/10.1111/j.1365->
3 [2486.2005.01097.x](http://dx.doi.org/10.1111/j.1365-2486.2005.01097.x)
- 4 Seneviratne, S.I., M.G. Donat, B. Mueller, and L.V. Alexander, 2014: No pause in the increase
5 of hot temperature extremes. *Nature Climate Change*, **4**, 161-163.
6 <http://dx.doi.org/10.1038/nclimate2145>
- 7 Seo, K.-W., C.R. Wilson, T. Scambos, B.-M. Kim, D.E. Waliser, B. Tian, B.-H. Kim, and J.
8 Eom, 2015: Surface mass balance contributions to acceleration of Antarctic ice mass loss
9 during 2003–2013. *Journal of Geophysical Research: Solid Earth*, **120**, 3617-3627.
10 <http://dx.doi.org/10.1002/2014JB011755>
- 11 Sheffield, J., E.F. Wood, and M.L. Roderick, 2012: Little change in global drought over the past
12 60 years. *Nature*, **491**, 435-438. <http://dx.doi.org/10.1038/nature11575>
- 13 Shiklomanov, N.E., D.A. Streletskiy, and F.E. Nelson. *Northern Hemisphere component of the*
14 *global Circumpolar Active Layer Monitory (CALM) program*. in *Proceedings of the 10th*
15 *International Conference on Permafrost*. 2012. Salekhard, Russia.
- 16 Sobel, A.H., S.J. Camargo, T.M. Hall, C.-Y. Lee, M.K. Tippett, and A.A. Wing, 2016: Human
17 influence on tropical cyclone intensity. *Science*, **353**, 242-246.
18 <http://dx.doi.org/10.1126/science.aaf6574>
- 19 Sokolov, A.P., D.W. Kicklighter, J.M. Melillo, B.S. Felzer, C.A. Schlosser, and T.W. Cronin,
20 2008: Consequences of Considering Carbon–Nitrogen Interactions on the Feedbacks between
21 Climate and the Terrestrial Carbon Cycle. *Journal of Climate*, **21**, 3776-3796.
22 <http://dx.doi.org/10.1175/2008JCLI2038.1>
- 23 Solomon, S., K.H. Rosenlof, R.W. Portmann, J.S. Daniel, S.M. Davis, T.J. Sanford, and G.-K.
24 Plattner, 2010: Contributions of Stratospheric Water Vapor to Decadal Changes in the Rate
25 of Global Warming. *Science*, **327**, 1219-1223. <http://dx.doi.org/10.1126/science.1182488>
- 26 Sousa, P.M., R.M. Trigo, P. Aizpurua, R. Nieto, L. Gimeno, and R. Garcia-Herrera, 2011:
27 Trends and extremes of drought indices throughout the 20th century in the Mediterranean.
28 *Natural Hazards and Earth System Sciences*, **11**, 33-51. <http://dx.doi.org/10.5194/nhess-11->
29 [33-2011](http://dx.doi.org/10.5194/nhess-11-33-2011)
- 30 Stroeve, J., A. Barrett, M. Serreze, and A. Schweiger, 2014: Using records from submarine,
31 aircraft and satellites to evaluate climate model simulations of Arctic sea ice thickness. *The*
32 *Cryosphere*, **8**, 1839-1854. <http://dx.doi.org/10.5194/tc-8-1839-2014>

- 1 Stroeve, J.C., V. Kattsov, A. Barrett, M. Serreze, T. Pavlova, M. Holland, and W.N. Meier,
2 2012: Trends in Arctic sea ice extent from CMIP5, CMIP3 and observations. *Geophysical*
3 *Research Letters*, **39**, L16502. <http://dx.doi.org/10.1029/2012GL052676>
- 4 Stroeve, J.C., T. Markus, L. Boisvert, J. Miller, and A. Barrett, 2014: Changes in Arctic melt
5 season and implications for sea ice loss. *Geophysical Research Letters*, **41**, 1216-1225.
6 <http://dx.doi.org/10.1002/2013GL058951>
- 7 Stroeve, J.C., M.C. Serreze, M.M. Holland, J.E. Kay, J. Malanik, and A.P. Barrett, 2012: The
8 Arctic's rapidly shrinking sea ice cover: A research synthesis. *Climatic Change*, **110**, 1005-
9 1027. <http://dx.doi.org/10.1007/s10584-011-0101-1>
- 10 Sweet, W.V., R.E. Kopp, C. Weaver, J. Obeysekera, R. Horton, E.R. Thieler, and C. Zervas, In
11 review: Global and Regional Sea Level Rise Scenarios for the United States. NOAA.
- 12 Sweet, W.V. and J. Park, 2014: From the extreme to the mean: Acceleration and tipping points
13 of coastal inundation from sea level rise. *Earth's Future*, **2**, 579-600.
14 <http://dx.doi.org/10.1002/2014EF000272>
- 15 Tedesco, M., E. Box, J. Cappelen, R.S. Fausto, X. Fettweis, K. Hansen, T. Mote, C.J.P.P.
16 Smeets, D.V. As, R.S.W.V.d. Wal, and J. Wahr, 2015: [The Arctic] Greenland ice sheet [in
17 "State of the Climate in 2014"]. *Bulletin of the American Meteorological Society*, **96**, S137-
18 S139. <http://dx.doi.org/10.1175/2015BAMSStateoftheClimate.1>
- 19 Tedesco, M., X. Fettweis, M.R.v.d. Broeke, R.S.W.v.d. Wal, C.J.P.P. Smeets, W.J.v.d. Berg,
20 M.C. Serreze, and J.E. Box, 2011: The role of albedo and accumulation in the 2010 melting
21 record in Greenland. *Environmental Research Letters*, **6**, 014005.
22 <http://dx.doi.org/10.1088/1748-9326/6/1/014005>
- 23 Tedesco, M., X. Fettweis, T. Mote, J. Wahr, P. Alexander, J.E. Box, and B. Wouters, 2013:
24 Evidence and analysis of 2012 Greenland records from spaceborne observations, a regional
25 climate model and reanalysis data. *The Cryosphere*, **7**, 615-630. [http://dx.doi.org/10.5194/tc-](http://dx.doi.org/10.5194/tc-7-615-2013)
26 [7-615-2013](http://dx.doi.org/10.5194/tc-7-615-2013)
- 27 Thornton, P.E., S.C. Doney, K. Lindsay, J.K. Moore, N. Mahowald, J.T. Randerson, I. Fung, J.F.
28 Lamarque, J.J. Feddema, and Y.H. Lee, 2009: Carbon-nitrogen interactions regulate climate-
29 carbon cycle feedbacks: results from an atmosphere-ocean general circulation model.
30 *Biogeosciences*, **6**, 2099-2120. <http://dx.doi.org/10.5194/bg-6-2099-2009>
- 31 Trenberth, K.E., 2015: Has there been a hiatus? *Science*, **349**, 691-692.
32 <http://dx.doi.org/10.1126/science.aac9225>

- 1 Trenberth, K.E., A. Dai, G. van der Schrier, P.D. Jones, J. Barichivich, K.R. Briffa, and J.
2 Sheffield, 2014: Global warming and changes in drought. *Nature Climate Change*, **4**, 17-22.
3 <http://dx.doi.org/10.1038/nclimate2067>
- 4 Turney, C.S.M. and R.T. Jones, 2010: Does the Agulhas Current amplify global temperatures
5 during super-interglacials? *Journal of Quaternary Science*, **25**, 839-843.
6 <http://dx.doi.org/10.1002/jqs.1423>
- 7 van der Werf, G.R., J.T. Randerson, L. Giglio, G.J. Collatz, M. Mu, P.S. Kasibhatla, D.C.
8 Morton, R.S. DeFries, Y. Jin, and T.T. van Leeuwen, 2010: Global fire emissions and the
9 contribution of deforestation, savanna, forest, agricultural, and peat fires (1997–2009).
10 *Atmospheric Chemistry and Physics*, **10**, 11707-11735. [http://dx.doi.org/10.5194/acp-10-](http://dx.doi.org/10.5194/acp-10-11707-2010)
11 [11707-2010](http://dx.doi.org/10.5194/acp-10-11707-2010)
- 12 Velicogna, I. and J. Wahr, 2013: Time-variable gravity observations of ice sheet mass balance:
13 Precision and limitations of the GRACE satellite data. *Geophysical Research Letters*, **40**,
14 3055-3063. <http://dx.doi.org/10.1002/grl.50527>
- 15 Vose, R.S., D. Arndt, V.F. Banzon, D.R. Easterling, B. Gleason, B. Huang, E. Kearns, J.H.
16 Lawrimore, M.J. Menne, T.C. Peterson, R.W. Reynolds, T.M. Smith, C.N. Williams, and
17 D.L. Wuertz, 2012: NOAA's Merged Land-Ocean Surface Temperature Analysis. *Bulletin of*
18 *the American Meteorological Society*, **93**, 1677-1685. [http://dx.doi.org/10.1175/BAMS-D-](http://dx.doi.org/10.1175/BAMS-D-11-00241.1)
19 [11-00241.1](http://dx.doi.org/10.1175/BAMS-D-11-00241.1)
- 20 Walsh, J., D. Wuebbles, K. Hayhoe, J. Kossin, K. Kunkel, G. Stephens, P. Thorne, R. Vose, M.
21 Wehner, J. Willis, D. Anderson, S. Doney, R. Feely, P. Hennon, V. Kharin, T. Knutson, F.
22 Landerer, T. Lenton, J. Kennedy, and R. Somerville, 2014: Ch. 2: Our changing climate.
23 *Climate Change Impacts in the United States: The Third National Climate Assessment*.
24 Melillo, J.M., T.C. Richmond, and G.W. Yohe, Eds. U.S. Global Change Research Program,
25 Washington, D.C., 19-67. <http://dx.doi.org/10.7930/J0KW5CXT>
- 26 Wang, C., L. Zhang, S.-K. Lee, L. Wu, and C.R. Mechoso, 2014: A global perspective on
27 CMIP5 climate model biases. *Nature Climate Change*, **4**, 201-205.
28 <http://dx.doi.org/10.1038/nclimate2118>
- 29 Willett, K.M., D.J. Philip, W.T. Peter, and P.G. Nathan, 2010: A comparison of large scale
30 changes in surface humidity over land in observations and CMIP3 general circulation
31 models. *Environmental Research Letters*, **5**, 025210. [http://dx.doi.org/10.1088/1748-](http://dx.doi.org/10.1088/1748-9326/5/2/025210)
32 [9326/5/2/025210](http://dx.doi.org/10.1088/1748-9326/5/2/025210)
- 33 Williams, S.D.P., P. Moore, M.A. King, and P.L. Whitehouse, 2014: Revisiting GRACE
34 Antarctic ice mass trends and accelerations considering autocorrelation. *Earth and Planetary*
35 *Science Letters*, **385**, 12-21. <http://dx.doi.org/10.1016/j.epsl.2013.10.016>

- 1 Zaehle, S., P. Friedlingstein, and A.D. Friend, 2010: Terrestrial nitrogen feedbacks may
2 accelerate future climate change. *Geophysical Research Letters*, **37**, L01401.
3 <http://dx.doi.org/10.1029/2009GL041345>
- 4 Zaehle, S. and A.D. Friend, 2010: Carbon and nitrogen cycle dynamics in the O-CN land surface
5 model: 1. Model description, site-scale evaluation, and sensitivity to parameter estimates.
6 *Global Biogeochemical Cycles*, **24**, n/a-n/a. <http://dx.doi.org/10.1029/2009GB003521>
- 7 Zemp, M., H. Frey, I. Gärtner-Roer, S.U. Nussbaumer, M. Hoelzle, F. Paul, W. Haeberli, F.
8 Denzinger, A.P. Ahlstrøm, B. Anderson, S. Bajracharya, C. Baroni, L.N. Braun, B.E.
9 Cáceres, G. Casassa, G. Cobos, L.R. Dávila, H. Delgado Granados, M.N. Demuth, L.
10 Espizua, A. Fischer, K. Fujita, B. Gadek, A. Ghazanfar, J.O. Hagen, P. Holmlund, N. Karimi,
11 Z. Li, M. Pelto, P. Pitte, V.V. Popovnin, C.A. Portocarrero, R. Prinz, C.V. Sangewar, I.
12 Severskiy, O. Sigurðsson, A. Soruco, R. Usabaliev, and C. Vincent, 2015: Historically
13 unprecedented global glacier decline in the early 21st century. *Journal of Glaciology*, **61**,
14 745-762. <http://dx.doi.org/10.3189/2015JoG15J017>
- 15 Zhang, R. and T.R. Knutson, 2013: The role of global climate change in the extreme low
16 summer Arctic sea ice extent in 2012 [in "Explaining Extremes of 2012 from a Climate
17 Perspective"]. *Bulletin of the American Meteorological Society*, **94**, S23-S26.
18 <http://dx.doi.org/10.1175/BAMS-D-13-00085.1>
- 19 Zhang, X., H. Wan, F.W. Zwiers, G.C. Hegerl, and S.-K. Min, 2013: Attributing intensification
20 of precipitation extremes to human influence. *Geophysical Research Letters*, **40**, 5252-5257.
21 <http://dx.doi.org/10.1002/grl.51010>
- 22 Zhang, X., F.W. Zwiers, G.C. Hegerl, F.H. Lambert, N.P. Gillett, S. Solomon, P.A. Stott, and T.
23 Nozawa, 2007: Detection of human influence on twentieth-century precipitation trends.
24 *Nature*, **448**, 461-465. <http://dx.doi.org/10.1038/nature06025>
- 25 Zhu, Z., S. Piao, R.B. Myneni, M. Huang, Z. Zeng, J.G. Canadell, P. Ciais, S. Sitch, P.
26 Friedlingstein, A. Arneth, C. Cao, L. Cheng, E. Kato, C. Koven, Y. Li, X. Lian, Y. Liu, R.
27 Liu, J. Mao, Y. Pan, S. Peng, J. Penuelas, B. Poulter, T.A.M. Pugh, B.D. Stocker, N. Viovy,
28 X. Wang, Y. Wang, Z. Xiao, H. Yang, S. Zaehle, and N. Zeng, 2016: Greening of the Earth
29 and its drivers. *Nature Climate Change*, **6**, 791-795. <http://dx.doi.org/10.1038/nclimate3004>
- 30 Zunz, V., H. Goosse, and F. Massonnet, 2013: How does internal variability influence the ability
31 of CMIP5 models to reproduce the recent trend in Southern Ocean sea ice extent? *The*
32 *Cryosphere*, **7**, 451-468. <http://dx.doi.org/10.5194/tc-7-451-2013>

2. Physical Drivers of Climate Change

Key Findings

1. Human activities continue to significantly affect Earth's climate by altering factors that change its radiative balance (known as a radiative forcing). These factors include greenhouse gases, small airborne particles (aerosols), and the reflectivity of the Earth's surface. In the industrial era, human activities have been and remain the dominant cause of climate warming and have far exceeded the relatively small net increase due to natural factors, which include changes in energy from the sun and the cooling effect of volcanic eruptions. (*Very high confidence*)
2. Aerosols caused by human activity play a profound and complex role in the climate system through direct radiative effects and indirect effects on cloud formation and properties. The combined forcing of aerosol–radiation and aerosol–cloud interactions is negative over the industrial era, substantially offsetting a substantial part of greenhouse gas forcing, which is currently the predominant human contribution (*high confidence*). The magnitude of this offset has declined in recent decades due to a decreasing trend in net aerosol forcing. (*Medium to high confidence*)
3. The climate system includes a number of positive and negative feedback processes that can either strengthen (positive feedback) or weaken (negative feedback) the system's responses to human and natural influences. These feedbacks operate on a range of timescales from very short (essentially instantaneous) to very long (centuries). While there are large uncertainties associated with some of these feedbacks, the net feedback effect over the industrial era has been positive (amplifying warming) and will continue to be positive in coming decades. (*High confidence*)

2.1 Earth's Energy Balance and the Greenhouse Effect

The temperature of the Earth system is determined by the amounts of incoming (short-wavelength) and outgoing (both short- and long-wavelength) radiation. In the modern era, the magnitudes of these flows are accurately determined from satellite measurements. Figure 2.1 shows that about a third of incoming, short-wavelength energy from the sun is reflected back to space and the remainder absorbed by the Earth system. The fraction of sunlight scattered back to space is determined by the reflectivity (albedo) of land surfaces (including snow and ice), oceans, and clouds and particles in the atmosphere. The amount and albedo of clouds, snow cover, and ice cover are particularly strong determinants of the amount of sunlight reflected back to space because their albedos are much higher than that of land and oceans.

In addition to reflected sunlight, the Earth loses energy through infrared (long-wavelength) radiation from the surface and atmosphere. Greenhouse gases in the atmosphere absorb some of this radiation, much of which is re-radiated back towards the surface (Figure 2.1) where it is absorbed, further heating the Earth; the remainder is emitted to space. The naturally occurring greenhouse gases in Earth's atmosphere--principally water vapor and carbon dioxide--keep the near-surface air temperature about 33°C (60°F) warmer than it would be in their absence. Geothermal heat from the Earth's interior, direct heating from energy production, and frictional heating through tidal flows also contribute to the amount of energy available for heating the Earth's surface and atmosphere, but their contribution is an extremely small fraction (<0.1%) of that due to net solar (shortwave) and infrared (longwave) radiation. (e.g., see Davies and Davies 2010; Flanner 2009; Munk and Wunsch 1998 for estimates of these forcings).

[INSERT FIGURE 2.1 HERE:]

Figure 2.1: Global mean energy budget of the Earth under present-day climate conditions. Numbers state magnitudes of the individual energy fluxes in watts per square meter (W/m^2) averaged over Earth's surface, adjusted within their uncertainty ranges to balance the energy budgets of the atmosphere and the surface. Numbers in parentheses attached to the energy fluxes cover the range of values in line with observational constraints. These constraints are largely provided by satellite-based observations, which have directly measured solar and infrared fluxes at the top of the atmosphere over nearly the whole globe since 1984 (Barkstrom 1984; Smith et al. 1994). More advanced satellite-based measurements focusing on the role of clouds in Earth's radiative fluxes, have been available since 1998 (Wielicki et al. 1995, 1996). (Figure source: IPCC 2013; © IPCC, used with permission).]

Thus, Earth's equilibrium temperature is controlled by a short list of factors: incoming sunlight, absorbed and reflected sunlight, emitted infrared radiation, and infrared radiation absorbed in the atmosphere, primarily by greenhouse gases. Changes in these factors affect Earth's radiative balance and therefore its climate, including but not limited to the average, near-surface air temperature. Anthropogenic activities have changed the Earth's radiative balance and its albedo by adding greenhouse gases, particles (aerosols), and aircraft contrails to the atmosphere, and through land-use changes.

Changes in the radiative balance produce changes in temperature, precipitation, and other climate variables through a complex set of physical processes, many of which are coupled (Figure 2.2). In the following sections, the principal components of the framework shown in Figure 2.2 are described. Climate models are structured to represent these processes; climate models, and their components and associated uncertainties, are discussed in more detail in Chapter 4: Projections.

[INSERT FIGURE 2.2 HERE:]

Figure 2.2 Simplified conceptual modeling framework for the climate system as implemented in many climate models (Chapter 4). Modeling components include forcing agents, feedback processes, carbon uptake processes and radiative forcing and balance. The lines indicate physical

interconnections (solid lines) and feedback pathways (dashed lines). Principal changes (blue boxes) lead to climate impacts (red box) and feedbacks. (Figure source: adapted from Knutti and Rugenstein 2015).]

The processes and feedbacks connecting changes in Earth's radiative balance to a climate response (Figure 2.2) operate on a large range of timescales. Reaching an equilibrium temperature distribution in response to anthropogenic activities takes decades or longer because the Earth system—in particular the oceans and cryosphere—are slow to respond due to their large thermal masses and the long timescale of circulation between the ocean surface and the deep ocean. Of the substantial energy gained in the combined ocean–atmosphere system over the previous four decades, over 90% of it has gone into ocean warming (Rhein et al. 2014; see Box 3.1 Fig 1). Even at equilibrium, internal variability in the Earth's climate system causes limited annual to decadal-scale variations in regional temperatures and other climate parameters that do not contribute to long-term trends. For example, it is *likely* that natural variability has led to between -0.1°C (-0.18°F) and 0.1°C (0.18°F) changes in surface temperatures from 1951 to 2010; by comparison, anthropogenic greenhouse gases have *likely* contributed between 0.5°C (0.9°F) and 1.3°C (2.3°F) to observed surface warming over this same period (Bindoff et al. 2013). Due to these longer timescale responses and natural variability, changes in Earth's radiative balance are not realized immediately as changes in climate, and even in equilibrium there will always be variability around mean trends.

2.2 Radiative Forcing (RF) and Effective Radiative Forcing (ERF)

Radiative forcing (RF) is widely used to quantify a radiative imbalance in Earth's atmosphere resulting from either natural changes or anthropogenic activities. It is expressed as a change in net radiative flux (W/m^2) at the tropopause or top of the atmosphere over the industrial era (Myhre et al. 2013). RF serves as a metric to compare present, past, or future perturbations to the climate system (e.g. Boer and Yu 2003; Gillett et al. 2004; Matthews et al. 2004; Meehl et al. 2004; Jones et al. 2007; Mahajan et al. 2013; Shiogama et al. 2013). The equilibrium surface temperature response (ΔT) to a forcing (RF) is given by $\Delta T = \lambda \text{ RF}$ where λ is the climate sensitivity factor (Knutti and Hegerl 2008; Flato et al. 2013). For clarity and consistency, RF calculations require that a time period be defined over which the forcing occurs. Here, this period is the industrial era, defined as beginning in 1750 and extending to 2011, unless otherwise noted. The 2011 end date is that adopted by the CMIP5 calculations, which are the basis of RF evaluations by the Intergovernmental Panel on Climate Change (IPCC; Myhre et al. 2013). In practice, the calculation of RF over a given period is defined in several ways based on where it is evaluated (tropopause or top of the atmosphere) and on assumptions concerning, for example, whether the surface or stratospheric temperature is allowed to respond (Myhre et al. 2013). In this report, we follow the IPCC recommendation that the RF caused by a forcing agent be evaluated as the net radiative flux change at the tropopause after stratospheric temperatures have adjusted to a new equilibrium while assuming all other variables (for example, temperatures and

cloud cover) are held fixed (Myhre et al. 2013). A change that results in a net increase in the downward flux at the tropopause constitutes a positive RF, normally resulting in a warming of the surface and/or atmosphere, and potentially changes in other climate parameters. Conversely, a change that yields an increase in the net upward flux constitutes a negative RF, leading to a cooling of the surface and/or atmosphere, and potentially changes in other climate parameters.

A refinement of the RF concept introduced in the latest IPCC assessment (IPCC 2013) is the use of effective radiative forcing (ERF). ERF for a climate driver is defined as its RF plus all rapid adjustment(s) to that RF (Myhre et al. 2013). These rapid adjustments occur on timescales much shorter than, for example, the response of ocean temperatures. For an important subset of climate drivers, ERF is more reliably correlated with the climate response to the forcing than is RF; as such, it is an increasingly used metric when discussing forcing. For atmospheric components, ERF includes rapid adjustments due to direct warming of the troposphere, which produces horizontal temperature variations, variations in the vertical lapse rate, and changes in clouds and vegetation, and it includes the microphysical effects of aerosols on cloud lifetime. Not included in ERF are climate responses driven by surface air temperature changes. For aerosols in surface snow, ERF includes the effects of direct warming of the snowpack by particulate absorption (for example, snow-grain size changes). The largest differences between RF and ERF occur for forcing by light-absorbing aerosols because of their influence on clouds and snow. Changes in these climate parameters can be quantified in terms of their impact on radiative fluxes (for example, albedo). For example, black carbon (BC) aerosol in the atmosphere absorbs sunlight, producing a positive RF. In addition, this absorption warms the atmosphere; on net this response is expected to increase cloud cover and therefore increase planetary albedo (the “semi-direct effect”). This “rapid response” lowers the ERF of atmospheric BC by approximately 15% relative to its RF from direct absorption alone (Bond et al. 2013). For BC deposited on snow, the ERF is a factor of three higher than the RF because of the positive feedbacks of reducing snow albedo and increasing snow melt (e.g., Flanner et al. 2009; Bond et al. 2013). For most non-aerosol climate drivers the differences are small.

2.3 Drivers of Climate Change over the Industrial Era

Climate drivers of significance over the industrial era include both those associated with anthropogenic activity and those of natural origin. The only significant natural climate drivers in the industrial era are changes in solar irradiance and volcanic eruptions. Natural emissions and sinks of greenhouse gases and aerosols have varied over the industrial era but have not contributed significantly to RF. Other known drivers of natural origin that operate on longer timescales are changes in Earth’s orbit (that is, the Milankovich cycles), asteroids, changes in atmospheric CO₂ via chemical weathering of rock, and potentially cosmic rays. Anthropogenic drivers can be divided into a number of categories, including well-mixed greenhouse gases (WMGHGs), short-lived climate forcers (SLCFs, which include methane, some hydrofluorocarbons [HFCs], ozone, and aerosols), contrails, and changes in albedo (for example,

land-use changes). Some WMGHGs are also considered SLCFs (for example, methane). Figure 2.3 summarizes RF and/or ERF for the principal climate drivers in the industrial era. Each is described briefly in the following.

[INSERT FIGURE 2.3 HERE:]

Figure 2.3 Bar chart for RF (hatched) and ERF (solid) for the period 1750–2011, where the total ERF is derived from IPCC. Uncertainties (5% to 95% confidence range) are given for RF (dotted lines) and ERF (solid lines). Volcanic forcing is not shown because this forcing is negligible over the industrial era. (Figure source: IPCC 2013© IPCC, used with permission).]

2.3.1 Natural Drivers

SOLAR IRRADIANCE

Solar irradiance changes directly impact the climate system because the irradiance is its primary source of energy (Lean 1997). At the century scale, the largest variations in total solar irradiance (TSI) are associated with the 11-year solar cycle (Frölich and Lean 2004; Gray et al. 2010), direct observations of which have been available since 1978 (Kopp 2014) though proxy indicators of solar cycles are available back to the early 1600s (Kopp et al. 2016). Although the variations in TSI amount to only 0.1% of the sun's total output of about 1360 W/m² (Kopp and Lean 2011), variations in irradiance at specific wavelengths can be much larger (tens of percent). Solar spectral irradiance (SSI) is most variable at near-ultraviolet (UV) and shorter wavelengths (Floyd et al. 2003), which are also the most important in driving changes in ozone (Ermolli et al. 2013; Bolduc et al. 2015). Variations in TSI and SSI can thus induce important changes in the stratosphere and troposphere, both through direct heating and through changes in stratospheric ozone that in turn further affect heating rates and both stratospheric and tropospheric circulation (Gray et al. 2010; Lockwood 2012; Seppälä et al. 2014). Further, the relationships between changes in TSI and changes in atmospheric composition, heating, and dynamics are complex. Changes in UV irradiance can be out of phase with changes in TSI with mixed consequences, for example, for the net production and destruction of stratospheric ozone (Ball et al. 2016). As a result, changes in TSI are not directly correlated with the resulting radiative flux changes (Ermolli et al. 2013; Xu and Powell 2013; Gao et al. 2015).

IPCC has provided an estimate of the TSI RF of 0.05 W/m² (range: 0.0 to 0.10 W/m²) (Myhre et al. 2013). This forcing does not account for radiative flux changes resulting from SSI-driven changes in stratospheric ozone. Understanding of the link between changes in SSI, stratospheric ozone, heating rates, and circulation changes has recently improved using, in particular, satellite data starting in 2002 that provide SSI measurements through the UV (Ermolli et al. 2013) along with a series of chemistry–climate modeling studies (Swartz et al. 2012; Chiodo et al. 2014; Dhomse et al. 2013; Ermolli et al. 2013; Bolduc et al. 2015). At the regional scale, circulation changes driven by SSI variations may be significant for some locations and seasons, but this is not yet sufficiently understood to quantify (Lockwood 2012). Despite remaining uncertainties,

there is *very high confidence* that solar radiance-induced changes in RF are small relative to RF from anthropogenic greenhouse gases over the industrial era (Myhre et al. 2013) (Figure 2.3). On millennial timescales, changes in solar output are expected to have influenced climate but there is uncertainty in extending the TSI and SSI records back in time.

VOLCANOES

Explosive volcanic eruptions inject sulfur dioxide (SO₂) and ash into the stratosphere, which leads to significant short-term climate effects (Myhre et al. 2013, and references therein). SO₂ oxidizes to form sulfuric acid (H₂SO₄) which condenses, forming new particles or adding mass to preexisting particles, thereby substantially enhancing the attenuation of sunlight transmitted through the stratosphere (that is, increasing the aerosol optical depth). These aerosols increase the Earth's albedo by scattering sunlight back to space, creating a negative RF that cools the planet (Andronova et al. 1999; Robock 2000). The RF persists for the lifetime of aerosol in the stratosphere, which is a few years, far exceeding that in the troposphere (about a week). Volcanic RF is integrated by the ocean, resulting in ocean cooling and associated changes in ocean circulation patterns that last for decades after major eruptions (for example, Mt. Tambora in 1815) (Stenchikov et al. 2009; Otterå et al. 2010; Zanchettin et al. 2012; Zhang et al. 2013). In addition to the direct RF, volcanic aerosol heats the stratosphere, altering circulation patterns and destroying ozone, which further changes heating and circulation. The resulting impacts on advective heat transport can be larger than the temperature impacts of the direct forcing (Robock 2000). Aerosol from both explosive and non-explosive eruptions also affects the troposphere through changes in diffuse radiation and through aerosol–cloud interactions, both through the initial emissions and later when volcanic aerosol eventually sediments out of the stratosphere. It has been proposed that major eruptions might “fertilize” the ocean with sufficient iron to affect phytoplankton production and therefore the ocean CO₂ sink, though this is a new area of research (Langmann 2014). Volcanoes also emit CO₂ and water vapor, although in small quantities relative to other emissions. Annual CO₂ emissions from volcanoes are conservatively estimated at <1% that from anthropogenic activities (Gerlach 2011). The magnitude of volcanic effects on climate depend on the number and strengths of eruptions, the latitude of injection and, for ocean temperature and circulation impacts, the timing of the eruption relative to ocean temperature and circulation patterns (Zanchettin et al. 2012; Zhang et al. 2013).

Volcanic eruptions are the largest natural forcings within the industrial era and in the last millennium caused multiyear transient episodes of negative RF of up to several W/m² (Figure 2.5). The RF of the last major volcanic eruption, Mt. Pinatubo in 1991, decayed to negligible values later in the 1990s, with the temperature signal lasting about twice as long due to the effects of changes in ocean heat uptake (Stenchikov et al. 2009). The present day volcanic RF evaluated for periods since 2000 yields values of about −0.1 W/m² or less due to several small non-explosive eruptions. A net volcanic RF has been omitted from the drivers of climate change in the industrial era in Figure 2.3 because the episodic short-term nature of volcanic RF is not comparable with the other climate drivers, which produce long-term effects. While future

explosive volcanic eruptions have the potential to again alter Earth's climate for periods of several years, predictions of occurrence, intensity, and location remain elusive.

2.3.2 Anthropogenic Drivers

PRINCIPAL WELL-MIXED GREENHOUSE GASES (WMGHGs)

The principal WMGHGs are carbon dioxide (CO₂), methane (CH₄), and nitrous oxide (N₂O). These gases have modest-to-small regional variabilities and, with atmospheric lifetimes of a decade or more, are circulated and mixed around the globe to yield small inter-hemispheric gradients. The atmospheric abundances and associated radiative forcings of WMGHGs have increased substantially over the industrial era (Figures 2.4–2.6). Contributions from natural sources of these constituents are accounted for in these industrial-era RF calculations.

[INSERT FIGURE 2.4 HERE:]

Figure 2.4 Atmospheric concentrations of carbon dioxide, methane, and nitrous oxide over the last 10,000 years (large panels) and since 1750 (inset panels). Measurements are shown from ice cores (symbols with different colors for different studies) and atmospheric samples (red lines). The corresponding radiative forcings are shown on the right-hand axes of the large panels. The concentrations of these gases have continued to increase in the 2000 to 2016 period (<http://www.esrl.noaa.gov/gmd/ccgg/aggi.html>). (Figure source: IPCC 2007© IPCC, used with permission)]

[INSERT FIGURE 2.5 HERE:]

Figure 2.5 (a) Radiative forcing (RF) from the major WMGHGs and groups of halocarbons (Others) from 1850 to 2011; (b) the data in (a) with a logarithmic scale; (c) RFs from the minor WMGHGs from 1850 to 2011 (logarithmic scale); (d) rate of change in forcing from the major WMGHGs and halocarbons from 1850 to 2011. (Figure source: IPCC 2013; © IPCC, used with permission).]

[INSERT FIGURE 2.6 HERE:]

Figure 2.6 Effective radiative forcing changes across the industrial era for anthropogenic and natural forcing mechanisms. Also shown are the sum of all forcings (Total) and the sum of anthropogenic forcings (Total Anthropogenic). Bars with the forcing and uncertainty ranges (5% to 95% confidence range) at present are given in the right part of the figure. For aerosol, the ERF due to aerosol–radiation interaction and total aerosol ERF are shown. The uncertainty ranges are for present (2011 versus 1750) and are given in Table 8.6. For aerosols, only the uncertainty in the total aerosol ERF is given. For several of the forcing agents the relative uncertainty may be larger for certain time periods compared to present. See IPCC AR5 Supplementary Material Table 8.SM.8 for further information on the forcing time evolutions. Forcing numbers provided in Annex II of this report. The total anthropogenic forcing was 0.57 (0.29 to 0.85) W/m² in 1950, 1.25 (0.64 to 1.86) W/m² in 1980 and 2.29 (1.13 to 3.33) W/m² in 2011. (Figure source: IPCC 2013; © IPCC, used with permission).]

CO₂ has substantial global sources and sinks (Figure 2.7). CO₂ emission sources have grown in the industrial era primarily from fossil fuel combustion (that is, coal, gas, oil), cement manufacturing, and land-use change from activities such as deforestation (Ciais et al. 2013). Processes that remove emitted CO₂ from the atmosphere include uptake in the oceans, residual land uptake, and ultimately rock weathering, thereby yielding an atmospheric lifetime of many decades to millennia, far greater than any other major GHG. Seasonal variations in CO₂ atmospheric concentrations occur in response to transpiration in the biosphere, and to a lesser degree due to seasonal variations in anthropogenic emissions. In addition to fossil fuel reserves, there are large natural reservoirs of carbon in the oceans, in vegetation and soils, and in permafrost. In the industrial era, the CO₂ atmospheric growth rate has been exponential (Figure 2.4), with the increase in atmospheric CO₂ approximately twice the ocean uptake. Over the last 50 years or more, CO₂ has shown the largest annual concentration and RF increases among all GHGs (Figures 2.4 and 2.5). The global average CO₂ concentration has increased by 40% over the industrial era, increasing from 278 parts per million (ppm) in 1750 to 390 ppm in 2011 (Ciais et al. 2013); it now exceeds 400 ppm (2016) (<http://www.esrl.noaa.gov/gmd/ccgg/trends/>). CO₂ has been chosen as the reference in defining the global warming potential (GWP) of other GHGs and climate agents. The GWP of a GHG is the integrated RF over a specified time period (for example, 100 years) from the emission of a given mass of the GHG divided by the integrated RF from the same mass emission of CO₂.

[INSERT FIGURE 2.7 HERE:]

Figure 2.7 | CO₂ sources and sinks (PgC/yr¹) over the industrial era (1750–2011). The partitioning of atmospheric emissions among the atmosphere, land, and ocean is shown as equivalent negative emissions in the lower panel; of these, the land and ocean terms are true sinks of atmospheric CO₂. The top panel shows an expanded view of emissions from fossil fuels and cement manufacturing. The atmospheric CO₂ growth rate is derived from atmospheric observations and ice core data. The ocean CO₂ sink is derived from a combination of models and observations. The land sink is the residual of the other terms in a balanced CO₂ budget, and represents the sink of anthropogenic CO₂ in natural land ecosystems. These terms only represent changes since 1750 and do not include natural CO₂ fluxes (for example, from weathering and outgassing from lakes and rivers). (Figure source: Ciais et al. 2014; © IPCC, used with permission)]

Methane concentrations and RF have also grown substantially in the industrial era (Figures 2.4 and 2.5). Methane is a much more potent greenhouse gas than CO₂ but it has a shorter atmospheric lifetime of about 12 years. Methane also has indirect climate effects through induced changes in CO₂, stratospheric water vapor and ozone (Lelieveld and Crutzen 1992). The 100-year GWP of methane is high (28, direct; 34 including indirect), and its 20-year GWP is even higher (84; 86) (Myhre et al. 2013 Table 8.7). With a current global value near 1840 parts per billion by volume (ppb), methane concentrations have increased by a factor of about 2.5 over

the industrial era. Variability in the methane annual growth rate over the past several decades has been larger than for CO₂ and N₂O, and occasionally negative for short periods.

Methane has a variety of natural and anthropogenic sources estimated to total 556 ± 56 Tg CH₄ per year in 2011, with the anthropogenic fraction estimated to be about 60% (Ciais et al. 2013). The methane budget is complicated by the variety of natural and anthropogenic sources and sinks that influence its atmospheric concentration. These include the global abundance of the hydroxyl radical (OH), which controls the methane atmospheric lifetime; changes in large-scale anthropogenic activities such as mining, natural gas extraction, animal husbandry, and agricultural practices; and natural wetland emissions. The remaining uncertainty in the cause(s) of the approximately 20-year negative trend in the methane annual growth rate starting in the mid-1980s reflects the budget complexity (IPCC 2013).

Growth in nitrous oxide concentrations and RF over the industrial era are smaller than for CO₂ and methane (Figures 2.4 and 2.5). Nitrous oxide is emitted in the nitrogen cycle in natural ecosystems and has a variety of anthropogenic sources, including the use of synthetic fertilizers in agriculture, motor vehicle exhaust, and some manufacturing processes. The current global value near 330 ppb reflects steady growth over the industrial era with average increases in recent decades of 0.75 ppb per year (Ciais et al. 2013) (Figure 2.4). Fertilization in global food production is estimated to be responsible for 80% of the growth rate. Anthropogenic sources account for approximately 40% of the annual N₂O emissions of 17.9 (8.1 to 30.7) TgN. Nitrous oxide has an atmospheric lifetime of about 120 years and GWP of 265 (direct; Myhre et al. 2013 Table 8.7). The primary sink of nitrous oxide is photochemical destruction in the stratosphere, which produces nitrogen oxides (NO_x) that catalytically destroy ozone (e.g. Skiba and Rees 2014). Small indirect climate effects, such as the response of stratospheric ozone, are generally not included in the nitrous oxide RF.

Nitrous oxide is a component of the larger global budget of total N comprising N₂O, ammonia (NH₃), and reactive nitrogen (NO_x). Significant uncertainties are associated with balancing this budget over oceans and land while accounting for deposition and emission processes (Ciais et al. 2013). Furthermore, changes in climate parameters such as temperature, moisture, and CO₂ concentrations are expected to affect the N₂O budget in the future, and perhaps atmospheric concentrations.

OTHER WELL-MIXED GREENHOUSE GASES

Other WMGHGs primarily include several categories of synthetic gases, including chlorofluorocarbons (CFCs), halons, hydrochlorofluorocarbons (HCFCs), hydrofluorocarbons (HFCs), perfluorocarbons (PFCs), and sulfur hexafluoride (SF₆). These gases entered the atmosphere as early as the mid-20th century, beginning with the expanded use of CFCs as refrigerants and in other applications. The rapid growth of CFCs declined beginning in the 1990s with their regulation as ozone-depleting substances under the United Nations Montreal Protocol

(Figure 2.4). All of these gases are greenhouse gases covering a wide range of GWPs, atmospheric concentrations, and trends. PFCs, SF₆, and HFCs are in the basket of gases covered under the United Nations Framework Convention on Climate Change. The United States has joined other countries in proposing that HFCs be controlled as a WMGHG under the Montreal Protocol because of their large projected future abundances (<http://m.state.gov/mc70621.htm>). In October 2016, the Montreal Protocol adopted an amendment to phase down global HFC production and consumption, avoiding emissions of an estimated 105 Gt CO₂-eq by 2100 (http://ozone.unep.org/sites/ozone/files/pdfs/FAQs_Kigali-Amendment.pdf). CFCs, HCFCs, HFCs, halons and a few other gases comprise atmospheric halocarbons. The atmospheric growth rates of some halocarbon concentrations are large (for example, SF₆ and HFC-134a), although their RF contributions remain small (Figure 2.4).

WATER VAPOR

Water vapor in the atmosphere acts as a powerful natural GHG, significantly increasing the Earth's equilibrium temperature. In the stratosphere, water vapor abundances are controlled by transport from the troposphere and from oxidation of methane. Increases in methane from anthropogenic activities therefore increase stratospheric water vapor, producing a positive RF (e.g. Solomon et al. 2010; Hegglin et al. 2014). Other less-important anthropogenic sources of stratospheric water vapor are hydrogen oxidation (le Texier et al. 1988), aircraft exhaust (Rosenlof et al. 2001; Morris et al. 2003), and explosive volcanic eruptions (Löffler et al. 2016). In the troposphere, changes in troposphere water vapor are considered a feedback in the climate system (see 2.6.1 and Figure 2.2). As GHGs warm the atmosphere, tropospheric water vapor concentrations increase, thereby amplifying the warming effect (Held and Soden 2000).

OZONE

Ozone is a naturally occurring GHG. Ozone changes in the troposphere and stratosphere in response to anthropogenic and natural emissions. The changes generally have substantial spatial and temporal variability due to the nature of the production, loss, and transport processes controlling ozone abundances. Ozone RF calculations are complex because ozone naturally occurs in both the troposphere and stratosphere and has a lifetime that varies by atmospheric region. In the global troposphere, photochemical ozone formation is increased by emissions of methane, NO_x, carbon monoxide (CO), and non-methane volatile organic compounds (VOCs), yielding a positive RF near and downwind of these precursor source emissions (e.g., Dentener et al. 2005). Stratospheric ozone is photochemically destroyed in reactions involving halogen species chlorine and bromine. Halogens are released in the stratosphere from the decomposition of synthetic halocarbons emitted at the surface (WMO 2014). Stratospheric ozone depletion, which is most notable in the polar regions, yields a net negative RF (Myhre et al. 2013).

AEROSOLS

Atmospheric aerosols are perhaps the most complex and are the most uncertain component of forcing due to anthropogenic activities (Myhre et al. 2013). Aerosols have diverse natural and anthropogenic sources, and emissions from these sources can interact in non-linear ways (Boucher et al. 2013). Aerosol types are categorized by composition; namely, sulfate, black carbon, organic aerosols, nitrate, dust, and sea salt. Individual particles generally include a mix of these components due to both chemical and physical transformations of aerosols and aerosol precursor gases following emission. Aerosol tropospheric lifetimes are days to weeks due to the general hygroscopic nature of primary and secondary particles and the ubiquity of cloud and precipitation systems in the troposphere. Particles which act as cloud condensation nuclei (CCN) or which are scavenged by cloud droplets are removed from the troposphere in precipitation. The heterogeneity of aerosol sources and locations combined with short aerosol lifetimes leads to the high spatial and temporal variabilities observed in global aerosol distributions and forcings.

Aerosols from anthropogenic activities influence RF in three primary ways: through the aerosol–radiation interaction (RF_{ari}), the aerosol–cloud interaction (RF_{aci}), and the albedo change from absorbing-aerosol deposition on snow and ice (Boucher et al. 2013). RF_{ari} is also known as the aerosol “direct effect,” involving absorption and scattering of longwave and shortwave radiation. RF_{aci} is also known as the cloud albedo “indirect effect” from changes in cloud particle number. Global net RF_{ari} and RF_{aci} are negative (Myhre et al. 2013), although light-absorbing aerosol components (for example, BC) have positive RF (Bond et al. 2013). The complexity of aerosol forcing increases with the use of ERF. ERF_{aci} incorporates the rapid adjustment from the semi-direct effect of absorbing aerosol (that is, the cloud response to atmospheric heating) and includes cloud lifetime effects (for example, glaciation and thermodynamic effects) (Boucher et al. 2013). Light-absorbing aerosols also affect climate when present in surface snow, by lowering surface albedo (e.g. Flanner et al. 2009). There is *very high confidence* that the RF from snow and ice albedo is positive; as noted above, the ERF of this forcing is significantly higher than its RF (Bond et al. 2013). Aerosol RF and ERF calculations and uncertainties continue to improve, as noted by IPCC (Boucher et al. 2013), as aerosol observations become more available and aerosol model skill improves.

LAND SURFACE

Land-cover changes (LCC) due to anthropogenic activities in the industrial era have changed the land surface brightness. There is strong evidence that these changes have increased Earth’s surface albedo, creating a globally averaged net-negative RF (Myhre et al. 2013). In specific regions, however, LCC has produced a positive RF by lowering surface albedo (for example through afforestation and pasture abandonment). In addition to the direct radiative forcing through albedo changes, land-cover changes also have indirect effects on climate, such as altering the hydrologic and carbon cycles and altering dust emissions. These effects are generally not included in the LCC RF calculations, and the sign of their forcing may be opposite that of the

LCC albedo forcing. Some of these responses, such as alteration of the carbon cycle, constitute climate feedbacks (Figure 2.2), as discussed more extensively in Chapter 10 (Changes in Land Cover and Terrestrial Biogeochemistry). The principal global terms in LCC are deforestation and afforestation. The increased use of satellite observations to quantify LCC has lowered recent estimates of the negative LCC RF (e.g., Ju and Masek 2016). In areas with significant irrigation, surface temperatures and precipitation are affected by a change in energy partitioning from sensible to latent heating. Direct RF due to irrigation is generally small and can be positive or negative, depending on the balance of long-wave (surface cooling or increases in water vapor) and short-wave (increased cloudiness) effects (Cook et al. 2015).

CONTRAILS

Persistent line-shaped (linear) contrails are formed in the wake of jet-engine aircraft operating in the mid to upper troposphere. Persistent contrail formation begins in the expanding exhaust plume on ambient or aircraft-induced aerosol and requires ambient ice-supersaturated conditions. As contrails spread and drift with the local winds after formation, they lose their linear feature while creating additional contrail cirrus cloudiness that is indistinguishable from background cloudiness. Contrails and contrail cirrus are additional forms of cirrus cloudiness, which interact with solar and thermal radiation to provide a global net positive RF and, thus, are visible evidence of an anthropogenic contribution to climate change (Burkhardt and Kärcher 2012).

2.4 Industrial-era Changes in Radiative Forcing Agents

The best estimates of present day RFs and ERFs from principal anthropogenic and natural climate drivers are shown in Figure 2.3 and in Table 2.1. The past changes in the industrial era leading up to present day RF are shown for anthropogenic gases in Figure 2.5 and for all climate drivers in Figure 2.6. The combined figures have several striking features. First, the sum of ERFs from CO₂ and non-CO₂ GHGs, tropospheric ozone, stratospheric water, contrails, and BC on snow shows a gradual, monotonic increase since 1750, with an accelerated trend in the past 50 years. The sum of aerosol effects, stratospheric ozone depletion, and land use show a gradual, monotonic decrease until near the end of the 20th century, followed by decades with no further decrease. Volcanic RFs reveal their episodic, short-lived characteristics along with large values that at times dominate the total RF.

Changes in total solar irradiance over the industrial era are dominated by the 11-year solar cycle and other short-term variations (Figure 2.6). Radiative forcing due to changes in solar irradiance are estimated at 0.05 (0.0 – 0.1) W/m² between 1745 and 2005 (Myhre et al. 2013). Inconsistencies among models, which all rely on proxies of solar irradiance to fit the industrial era, lead to the large relative uncertainty in solar RF.

The atmospheric concentrations of CO₂, CH₄, and N₂O are higher now than they have been in the past 800,000 years (Masson-Delmotte et al. 2014). All have increased monotonically over the industrial era, and are now 40%, 250%, and 20%, respectively, above their preindustrial

concentrations as reflected in the RF time series in Figure 2.5. Tropospheric ozone has increased in response to growth in precursor emissions in the industrial era. Synthetic GHG emissions have grown rapidly beginning in the mid-20th century, with many bringing halogens to the stratosphere and causing ozone depletion in subsequent decades. Aerosol RF effects are a sum over aerosol–radiation and aerosol–cloud interactions, which increased in the industrial era due to increased emissions of aerosol and aerosol precursors. These global trends average across disparate trends in concentrations at the regional scale, and to a lesser degree temporal trends in aerosol composition.

2.5 The Complex Relationship between Concentrations, Forcing, and Climate Response

Emissions, concentrations, forcing, and climate change metrics are often discussed at the global, annual-average scale. However, all vary both geographically and seasonally with the consequence that the associated patterns of concentration, forcing, and climate change do not strictly map to each other. In particular, feedbacks (Section 2.6) either amplify or dampen the direct effects of radiative forcing, as well as affecting the geographic and temporal patterns of climate response. As such, feedbacks are one reason that forcing and the climate change caused by that forcing are not linearly related.

The RF patterns of short-lived climate drivers with inhomogeneous source distributions, such as aerosols, ozone, contrails, and LCC, are leading examples of highly inhomogeneous forcings. Spatial variability in aerosol emissions is enhanced by factors associated with meteorology (for example, precipitation, temperature, and transport) and chemical transformation or formation (for example, primary to secondary aerosol formation). These factors highlight the additional inhomogeneity that exists, in general, in the temporal dimension. Even for relatively uniformly distributed species (for example, WMGHGs), RF patterns are less homogenous than their concentrations. The RF of a uniform CO₂ distribution, for example, is highly latitude and humidity dependent. With the added complexity and variability of regional forcings, the global mean RFs are known with more confidence than the regional RF patterns.

Quantifying the relationship between spatial RF patterns and regional and global responses is difficult because it requires distinguishing forcing responses from the inherent internal variability of the climate system, which acts on a range of time scales. In addition, studies have shown that the spatial pattern and timing of climate responses are not always well correlated with the spatial pattern and timing of radiative forcing, since adjustments within the climate system can determine much of the response (e.g., Shindell and Faluvegi 2009; Crook and Forster 2011; Knutti and Rugenstein 2015). The ability to test the accuracy of modeled responses to forcing patterns is limited by the sparsity of long-term observational records of regional climate variables. As a result there is *very low confidence* in our understanding of the qualitative and quantitative forcing–response relationship at the regional scale. However there is *medium to high confidence* in some more robust features, such as aerosol effects altering the location of the Inter

Tropical Convergence Zone (ITCZ) and the positive feedback to reductions snow and ice albedo changes at high latitudes (Boucher et al. 2013; Myhre et al. 2013).

2.6 Climate-forcing Feedbacks

Climate sensitivity is determined by the magnitude of the imposed forcings (ERFs) and by the climate responses to those forcings (Figure 2.2). All feedbacks can be quantified themselves as forcings, since each acts by affecting the Earth's albedo or its greenhouse effect. The responses to radiative forcing that constitute climate feedbacks are the largest source of uncertainty in climate sensitivity (Flato et al. 2013); namely, the response of clouds, the carbon cycle and, to a lesser extent, land and sea ice to surface temperature and precipitation changes driven by ERFs. These feedbacks operate on a range of time scales, and some may not be realized for decades or centuries. Near-term and long-term feedbacks are described in the following sections.

2.6.1 Near-term Feedbacks

PLANCK FEEDBACK

When the temperatures of Earth's surface and atmosphere increase in response to RF, more infrared radiation is emitted into the lower atmosphere; this serves to restore radiative balance at the tropopause. This radiative feedback, defined as the Planck feedback, only partially offsets the positive RF while triggering other feedbacks that affect radiative balance. The Planck feedback magnitude is $-3.20 \pm 0.04 \text{ W/m}^2$ per 1°C warming and is the strongest and primary stabilizing feedback in the climate system (Vial et al. 2013).

WATER VAPOR AND LAPSE RATE FEEDBACKS

Warmer air holds more moisture (water vapor) than cooler air—about 7% more per degree Celsius—as dictated by the Clausius-Clapeyron relationship (Allen and Ingram 2002). Thus, as global temperatures increase, the total amount of water vapor in the atmosphere increases, adding further to greenhouse warming—a positive feedback, adding approximately 1.6 W/m^2 per 1°C of warming (Flato et al. 2013, Table 9.5). The water vapor feedback is responsible for more than doubling the direct climate warming from CO_2 emissions alone (Bony et al. 2006; Soden and Held 2006; Vial et al. 2013). Observations confirm that global tropospheric water vapor has increased commensurate with measured warming (IPCC 2013, FAQ 3.2 and Figure 1a). Interannual variations and trends in stratospheric water vapor, while influenced by tropospheric abundances, are controlled largely by tropopause temperatures and dynamical processes (Dessler et al. 2014). Increases in tropospheric water vapor have a larger warming effect in the upper troposphere (where it is cooler) than in the lower troposphere, thereby decreasing the rate at which temperatures decrease with altitude (the lapse rate). Warmer temperatures aloft increase outgoing infrared radiation—a negative feedback. Water vapor and lapse rate feedback strengths are $1.71 \pm 0.13 \text{ W/m}^2$ per 1°C warming and $-0.66 \pm 0.17 \text{ W/m}^2$ per 1°C warming, respectively (Vial et al. 2013). These values remain largely unchanged between recent IPCC assessments

(IPCC 2007; 2013). Recent advances in both observations and models have increased confidence that the net effect of the water vapor and lapse rate feedbacks is a significant positive RF (Flato et al. 2013).

CLOUD FEEDBACKS

Increases in cloudiness have two direct impacts on radiative fluxes: increased scattering of sunlight, which increases Earth's albedo (the shortwave cloud radiative effect, SWCRE), and increased trapping of infrared radiation (the longwave cloud radiative effect, LWCRE), which warms the surface. Decreases in cloudiness have the opposite effects. The SWCRE has a larger effect on local albedo when clouds are over dark surfaces (for example, oceans) than when over higher albedo surfaces, such as sea ice and deserts. For clouds globally, the SWCRE is about -50 W/m^2 and the LWCRE about $+30 \text{ W/m}^2$, yielding a net cooling influence (Loeb et al. 2009; Sohn et al. 2010). The relative magnitudes of the SWCRE and LWCRE vary with cloud type as well as with location. Low-altitude, thick clouds (for example, stratus and stratocumulus) have a net cooling, whereas high-altitude, thin clouds (for example, cirrus) have a net warming (e.g. Hartmann et al. 1992; Chen et al. 2000). Therefore, increases in low clouds that result from RF are a negative feedback to forcing, while increases in high clouds are a positive feedback. Cloud feedbacks to RF have the potential to be significant because the potential magnitudes of cloud effects are large compared with global RF (see Section 2.4). Cloud feedbacks also influence natural variability within the climate system and may amplify atmospheric circulation patterns and the El Niño–Southern Oscillation (Rädel et al. 2016). The net effect of cloud feedbacks is estimated to be positive over the industrial era, with a value of $+0.27 \pm 0.42 \text{ W/m}^2$ per 1°C warming (Vial et al. 2013). The net cloud feedback can be broken into components, where the LW cloud feedback is positive ($+0.24 \pm 0.26 \text{ W/m}^2$ per 1°C warming) and the SW feedback is near-zero ($+0.14 \pm 0.40 \text{ W/m}^2$ per 1°C warming; Vial et al. 2013), though the two do not add linearly. The value of the SW cloud feedbacks shows a significant sensitivity to computation methodology (Taylor et al. 2011; Vial et al. 2013; Klocke et al. 2013). Uncertainty in cloud feedbacks remains the largest source of inter-model differences in calculated climate sensitivity (Vial et al. 2013; Boucher et al. 2013).

SNOW, ICE, AND SURFACE ALBEDO

Snow and ice are highly reflective of solar radiation relative to land surfaces and the ocean. Loss of snow cover, glaciers, ice sheets, and sea ice resulting from climate warming lowers Earth's surface albedo, which increases absorbed solar radiation and leads to further warming as well as changes in turbulent heat fluxes at the surface (Sejas et al. 2014). For ice sheets (for example, on Antarctica and Greenland [Ch. 11: Arctic Changes]), the positive radiative feedback is further amplified by dynamical feedbacks on ice sheet mass loss. Specifically, continental ice shelves limit the discharge rates of ice sheets into the ocean; melting of ice shelves results in an acceleration of the discharge rate and appears to be a positive feedback on the ice stream flow rate and total mass loss (e.g. Holland et al. 2008; Schoof 2010; Rignot et al. 2010; Joughin et al.

2012). Feedbacks related to ice sheet dynamics occur on longer timescales than other feedbacks—many centuries or longer. Significant ice sheet melt can also lead to changes in freshwater input to the oceans, which in turn can affect ocean temperatures and circulation, ocean–atmosphere heat exchange and moisture fluxes, and atmospheric circulation (Masson-Delmotte et al. 2014).

The complete contribution of ice sheet feedbacks on timescales of millennia are not generally included in CMIP5 climate simulations. These slow feedbacks are also not thought to change in proportion to global mean surface temperature change, implying that the climate sensitivity changes with time, making it difficult to fully understand climate sensitivity considering only the industrial age. This also implies a high likelihood for tipping points, as discussed further in Chapter 15.

The surface-albedo feedback is important to interannual variations in sea ice as well as to long-term climate change. While there is a significant range in estimates of the snow-albedo feedback, it is assessed as positive (Hall and Qu 2006; Fernandes et al. 2009; Vial et al. 2013), with a best estimate of $0.27 \pm 0.06 \text{ W/m}^2$ per 1°C of warming globally. This feedback acts only where snow and ice are present and, thus, is most effective in polar regions (Winton 2006; Taylor et al. 2011). However, there is evidence that the presence of a polar surface-albedo feedback influences the tropical climate as well (Hall 2004).

Changes in sea ice can also influence Arctic cloudiness. Recent work indicates that Arctic clouds have responded to sea ice loss in fall but not summer (Kay and Gettelman 2009; Kay et al. 2011; Taylor et al. 2015; Kay and L’Ecuyer 2013; Pistone et al. 2014). This has important implications for future climate change, as an increase in summer clouds could offset a portion of the amplifying surface albedo feedback, slowing down the rate of Arctic warming.

ATMOSPHERIC COMPOSITION

Climate change can alter the atmospheric abundance and distribution of some radiatively active species by changing natural emissions, atmospheric photochemical reaction rates, atmospheric lifetimes, transport patterns, or deposition rates. These changes in turn alter the associated ERFs, leading to further climate changes (Liao et al. 2009; Unger et al. 2009; Raes et al. 2010).

Important examples include climate-driven changes in temperature and precipitation that affect 1) natural sources of NO_x from soils and lightning and VOC sources from vegetation, all of which affect ozone abundances (Raes et al. 2010); 2) regional aridity, which influences surface dust sources as well as susceptibility to wildfires; and 3) surface winds, which control the emission of dust from the land surface and the emissions of sea salt and dimethyl sulfide—a natural precursor to sulfate aerosol—from the ocean surface.

Feedbacks through changes in composition occur through a variety of processes. Climate-driven ecosystem changes that alter the carbon cycle potentially impact atmospheric CO_2 and CH_4 abundances (Section 2.6.2). Atmospheric aerosols affect clouds and precipitation rates, which in

turn alter aerosol removal rates, lifetimes, and atmospheric abundances. Longwave radiative feedbacks and climate-driven circulation changes also alter stratospheric ozone abundance (Nowack et al. 2015). Investigation of these and other chemistry–climate interactions is an active area of research (e.g., John et al. 2012; Pacifico et al. 2012; Morgenstern et al. 2013; Holmes et al. 2013; Naik et al. 2013, Voulgarakis et al. 2013; Isaksen et al. 2014; Dietmuller et al. 2014; Banerjee et al. 2014). While understanding of key processes is improving, atmospheric chemistry feedbacks are absent or limited in many global climate modeling studies used to project future climate, though this is rapidly changing (<https://cmip.ucar.edu/aer-chem-mip>). For some chemistry–climate feedbacks involving shorter-lived constituents, the net effects may be near-zero at the global scale while significant at local to regional scales (e.g. Raes et al. 2010; Han et al. 2013).

2.6.2 Long-term Feedbacks

TERRESTRIAL ECOSYSTEMS AND CLIMATE CHANGE FEEDBACKS

The cycling of carbon through the climate system is an important long-term climate feedback that affects atmospheric CO₂ concentrations. Atmospheric CO₂ concentrations are determined by emissions from burning fossil fuels, wildfires, and permafrost thaw balanced against CO₂ uptake by the oceans and terrestrial biosphere (Ciais et al. 2013; Le Quéré et al. 2016) (Figure 2.2). About two-thirds of anthropogenic CO₂ is taken up by the terrestrial environment and the oceans, through photosynthesis and through direct diffusion into ocean surface waters, respectively. The ability of the land to continue uptake of CO₂ is uncertain and depends on land-use management through mitigation and/or policy and urbanization and ocean acidification processes (see Chapters 10 and 13). Altered uptake rates will affect atmospheric CO₂ abundances, forcing, and rates of climate change. Such changes are expected to evolve on the decadal and longer time-scale, though abrupt changes are possible.

Significant uncertainty exists in quantification of carbon cycle feedbacks. Differences in the assumed characteristics of the land carbon-cycle processes are the primary cause of the inter-model spread in modeling the present-day carbon cycle and a leading source of uncertainty. Significant uncertainties also exist in ocean carbon-cycle changes in future climate scenarios. Basic principles of carbon cycle dynamics in terrestrial ecosystems suggest that increased atmospheric CO₂ concentrations can directly enhance plant growth rates and, therefore, increase carbon uptake (the “CO₂ fertilization” effect), nominally sequestering much of the added carbon from fossil-fuel combustion (e.g., Wenzel et al. 2016). However, this effect is variable; sometimes plants acclimate so that higher CO₂ concentrations no longer enhance growth (e.g., Franks et al. 2013). In addition, CO₂ fertilization is often offset by other factors limiting plant growth, such as water and or nutrient availability, temperature, and incoming solar radiation that can be modified by changes in vegetation structure. Large-scale plant mortality through fire, soil moisture drought, and/or temperature changes also impact successional processes that contribute

to reestablishment and revegetation (or not) of disturbed ecosystems, altering the amount and distribution of plants available to uptake CO₂.

Climate-induced changes in the horizontal (for example, landscape to biome) and vertical (soils to canopy) structure of terrestrial ecosystems also alter the physical surface roughness and albedo, as well as biogeochemical (carbon, nitrogen) cycles and biophysical evapotranspiration and water demand. Combined, these responses constitute climate feedbacks by altering surface albedo and atmospheric GHG abundances. Drivers of these changes in terrestrial ecosystems include changes in the biophysical growing season, altered seasonality, wildfire patterns, and multiple other interacting factors (Chapter 10).

Determination of accurate future CO₂ stabilization scenarios depends on accounting for the significant role that the land biosphere plays in the global carbon cycle and feedbacks between climate change and the terrestrial carbon cycle (Hibbard et al. 2007). Earth System Models (ESMs) are increasing representation of terrestrial carbon cycle processes, including plant photosynthesis, plant and soil respiration and decomposition as well as CO₂ fertilization, with the latter based on the assumption that increased atmospheric CO₂ concentrations provide more substrate for photosynthesis and productivity. Recent advances in ESMs are beginning to account for other important factors such as nutrient limitations (Thornton et al. 2007; Brzostek et al. 2014; Wieder et al. 2015). ESMs that do include carbon-cycle feedbacks appear, on average, to overestimate terrestrial CO₂ uptake under the present-day climate (Anav et al. 2013; Smith et al. 2016) and underestimate nutrient limitations to CO₂ fertilization (Wieder et al. 2015). The sign of the land carbon-cycle feedback through 2100 remains unclear in the newest generation of ESMs (Friedlingstein et al. 2006, 2014; Wieder et al. 2015). Eleven CMIP5 ESMs forced with the same CO₂ emissions scenario—one consistent with RCP8.5 concentrations—produce a range of 795 to 1145 ppm for atmospheric CO₂ concentration in 2100. The majority of the ESMs (7 out of 11) simulated a CO₂ concentration larger (by 44 ppm on average) than their equivalent non-interactive carbon cycle counterpart (Friedlingstein et al. 2014). This difference in CO₂ equates to about 0.2°C more warming by 2100. The inclusion of carbon-cycle feedbacks does not alter the lower-end estimate of climate sensitivity, but in most climate models it pushes the upper bound higher (Friedlingstein et al. 2014).

OCEAN CHEMISTRY, ECOSYSTEM, AND CIRCULATION CHANGES

The ocean plays a critical role in regulating climate change by controlling the amount of greenhouse gases (including CO₂, water vapor, and nitrous oxide) and heat that remain in the atmosphere. The ocean also absorbs most of the net energy increase in the climate system from anthropogenic RF. This additional heat is stored predominantly (about 60%) in the upper 700 meters of the ocean (Johnson et al. 2016 and see Ch. 12: Sea Level Rise and Ch. 13: Ocean Acidification).

Marine ecosystems take up CO₂ from the atmosphere in the same way that plants do on land. About half of the global net primary production (NPP) is by marine plants (approximately 50 ± 28 PgC/year; Falkowski et al. 2004; Carr et al. 2006; Chavez et al. 2011). Phytoplankton NPP supports the biological pump, which transports 2–12 PgC/year of organic carbon to the deep sea (Doney 2010; Passow and Carlson 2012), where it is sequestered away from the atmospheric pool of carbon for 200–1500 years. Estimates of future changes in phytoplankton distributions and uptake of CO₂ vary significantly.

Remote sensing of sea surface temperature and chlorophyll as well as model simulations and sediment records suggest that global phytoplankton NPP may have increased over the last century as a consequence of decadal-scale natural climate variability such as the El Niño–Southern Oscillation, which promotes nutrient enrichment of the euphotic zone through vertical mixing and upwelling (Bidigare et al. 2009; Chavez et al. 2011; Zhai et al. 2013). In contrast, other analyses of chlorophyll distributions suggest that annual phytoplankton NPP in the global ocean has declined by more than 6% over the last three decades, mostly attributed to diatom changes (Gregg et al. 2003; Rousseaux and Gregg 2015). In contrast, other analyses suggest that phytoplankton NPP has decreased by about 1% per year over the last 100 years (Behrenfeld et al. 2006; Boyce et al. 2010; Capotondi et al. 2012). These results are consistent with model simulations indicating that both NPP and the biological pump have decreased by 6.6% and 8%, respectively, over the last five decades (Laufkötter et al. 2015), trends that are expected to continue through the end of this century (Steinacher et al. 2010). Consistent with this result, carbon cycle feedbacks in the ocean were positive across the suite of CMIP5 models.

In addition to being an important carbon sink, the ocean dominates the hydrological cycle, since most of the surface evaporation and rainfall occurs over the ocean (Trenberth et al. 2007; Schanze et al. 2010). The rate of evaporation, and thus the water vapor feedback, depends on surface wind stress and ocean temperature. Climate warming from radiative forcing also is associated with intensification of the water cycle (Ch. 7: Precipitation Changes). Over decadal timescales the surface ocean salinity has increased in areas of high salinity, such as the subtropical gyres, and decreased in areas of low salinity, such as the Warm Pool region (Durack and Wijfels 2010; Good et al. 2013). This increase in stratification in select regions and mixing in other regions leads to altered patterns of ocean circulation, which impacts uptake of anthropogenic heat and CO₂.

Increased ocean temperatures also affect ice sheet melt, particularly for the Antarctic Ice Sheet where basal sea ice melting is important relative to surface melting due to colder surface temperatures (Rignot and Thomas 2002). For the Greenland Ice Sheet, submarine melting at tidewater margins is also contributing to volume loss (van Den Broeke et al. 2009). In turn, changes in ice sheet melt rates change cold and fresh water inputs, altering ocean stratification. This affects ocean circulation and the ability of the ocean to absorb more greenhouse gases and heat (Enderlin and Hamilton 2014). Enhanced sea ice export to lower latitudes gives rise to local salinity anomalies (such as the Great Salinity Anomaly; Gelderloos et al. 2012) and therefore to

changes in ocean circulation and air–sea exchanges of momentum, heat, and freshwater, which in turn affect the atmospheric distribution of heat and greenhouse gases.

Additionally, as the ocean warms and freshens it becomes more stratified, inhibiting surface mixing, high-latitude convection, and deep water formation, thereby weakening the Meridional Overturning Circulation (MOC), the global ocean’s conveyor belt (Kostov et al. 2014; Andrews et al. 2012; see also Ch. 13: Ocean Acidification). Reduced deep water formation and slower overturning are associated with decreased heat and carbon sequestration at greater depths. Sporadic observations in the 1980s, 90s, and 2000s have led to the conclusion that there already is a slowdown (Lherminier et al. 2007). Other observational studies have not found any significant slowdown (Lumpkin et al., 2008). Recent continuous observations of MOC in the North Atlantic show that there are no detectable trends since 2004 (Cunningham and Marsh 2010). However, a recent analysis (Rahmstorf et al. 2015) finds that there has been an approximately 10% reduction in the strength of the overturning circulation over the 20th and early 21st Centuries. Future projections show that the strength of MOC will significantly decrease as the ocean warms and freshens and as upwelling in the Southern Ocean weakens due to storm track moving poleward (Rahmstorf et al. 2015; see also Ch. 13: Ocean Acidification). Such a slowdown of the ocean currents will impact the rate at which the ocean will absorb CO₂ and heat from the atmosphere.

PERMAFROST AND HYDRATES

Permafrost and methane hydrates contain large stores of carbon in the form of organic materials, mostly at northern high latitudes. With warming, this organic material can thaw, making previously frozen organic matter available for microbial decomposition, releasing CO₂ and methane to the atmosphere, providing additional radiative forcing and accelerating warming. This process defines the permafrost-carbon feedback. Combined data and modeling studies suggest that the permafrost-carbon feedback is *very likely* positive (Schaefer et al. 2014; Koven et al. 2015a; Schuur et al. 2015). This feedback was not included in the IPCC projections but is an active area of research. Accounting for permafrost-carbon release reduces the amount of emissions allowable from anthropogenic sources if future GHG mitigation targets are to be met (González-Eguino and Neumann 2016).

The permafrost-carbon feedback strength indicates a 120 ± 85 Gt release of carbon from permafrost by 2100, corresponding to a global temperature increase of $+0.94^\circ \pm 0.68^\circ\text{F}$ ($+0.52^\circ \pm 0.38^\circ\text{C}$) (Schaefer et al. 2014). A key feature of the permafrost feedback is that, once initiated, it continues for an extended period because emissions from decomposition occur slowly over decades and longer. In the coming few decades, enhanced plant growth at high latitudes and its associated CO₂ sink (Friedlingstein et al. 2006) are expected to partially offset the increased emissions from permafrost thaw (Schaefer et al. 2014; Schuur et al. 2015); thereafter, decomposition will dominate uptake. Recent evidence indicates that permafrost thaw is occurring faster than expected; poorly understood deep-soil carbon decomposition and ice wedge processes

1 *likely* contribute (Koven et al. 2015b; Liljedahl et al. 2016). Chapter 11 includes a more detailed
2 discussion of permafrost and methane hydrates in the Arctic. Future changes in permafrost
3 emissions and the potential for even greater emissions from methane hydrates in the continental
4 shelf are discussed further in Chapter 15.

5

DRAFT

TRACEABLE ACCOUNTS

Key Finding 1

Human activities continue to significantly affect Earth's climate by altering factors that change its radiative balance (known as a radiative forcing). These factors include greenhouse gases, small airborne particles (aerosols), and the reflectivity of the Earth's surface. In the industrial era, human activities have been and remain the dominant cause of climate warming and have far exceeded the relatively small net increase due to natural factors, which include changes in energy from the sun and the cooling effect of volcanic eruptions.

Description of evidence base

The Key Finding and supporting text summarizes extensive evidence documented in the climate science literature, including in previous national (NCA3; Melillo et al. 2014) and international (IPCC 2013) assessments. The assertion that Earth's climate is controlled by its radiative balance is a well-established physical property of the planet. Quantification of the changes in Earth's radiative balance come from a combination of observations and calculations. Satellite data are used directly to observe changes in Earth's outgoing visible and infrared radiation. Since 2002, observations of incoming sunlight include both total solar irradiance and solar spectral irradiance (Ermolli et al. 2013). Extensive in situ and remote sensing data are used to measure the concentrations of radiative forcing agents (greenhouse gases and aerosols) and changes in land cover, as well as the relevant properties of these agents (for example, aerosol microphysical and optical properties). Concentrations of long-lived greenhouse gases in particular are well-quantified through a limited number of observations because of their relatively high spatial homogeneity. Calculations of radiative forcing by greenhouse gases and aerosols are supported by observations of radiative fluxes from the surface, from airborne research platforms and from satellites. Both direct observations and modeling studies support the assertion that while volcanoes can have significant effects on climate over periods ranging from a couple of years (more moderate eruptions) to decades (very large eruptions), over the industrial era radiative forcing by volcanoes has been episodic and has not contributed significantly to forcing trends. Observations indicate a positive but small increase in solar input over the industrial era. Relatively higher variations in solar input at shorter (UV) wavelengths may be leading to indirect changes in Earth's radiative balance through their impact on ozone concentrations that are larger than the radiative impact of changes in total solar irradiance, but these changes are also small in comparison to anthropogenic greenhouse gas and aerosol forcing.

Major uncertainties

The largest source of uncertainty regarding changes in the Earth's radiative balance over the industrial era is quantifying forcing by aerosols. This has been a consistent finding across previous assessments (e.g., IPCC 2007; IPCC 2013). See discussion of major uncertainties associated with aerosol forcing in the Traceable Accounts for Key Finding 2 below.

Recent work has highlighted the potentially larger role of variations in UV solar irradiance, versus total solar irradiance, in solar forcing. However, this increase in solar forcing uncertainty is not sufficiently large to reduce confidence that anthropogenic activities dominate industrial-era forcing.

Assessment of confidence based on evidence and agreement, including short description of nature of evidence and level of agreement

x Very High

☐ **High**

☐ **Medium**

☐ **Low**

There is *very high confidence* that anthropogenic radiative forcing exceeds natural forcing over the industrial era. While there remain large uncertainties in aerosol radiative forcing in particular, natural forcing through solar irradiance changes and volcanic activity has been, with *very high confidence*, small over the industrial era relative to anthropogenic forcing. Estimates of anthropogenic industrial-era forcing have become larger and more positive with time: from the AR4 estimate (IPCC 2007) of anthropogenic forcing for the industrial era up to 2005 to the AR5 estimate (IPCC 2013) of forcing up to 2011, ERF increased by 43%. This is due to an increase in positive radiative forcing from greenhouse gas concentrations and improved understanding of forcing by aerosols that led to a reduction in the estimates of their negative forcing (IPCC 2013).

Summary sentence or paragraph that integrates the above information

This key finding is consistent with that in IPCC AR4 (IPCC 2007) and IPCC AR5 (IPCC 2013); namely, anthropogenic radiative forcing is positive (climate warming) and substantially larger than natural forcing from variations in solar input and volcanic emissions. Confidence in this finding has increased from AR4 to AR5, as anthropogenic greenhouse-gas forcings have continued to increase, whereas solar forcing remains small and volcanic forcing near-zero over decadal timescales.

Key Finding 2

Aerosols caused by human activity play a profound and complex role in the climate system through direct radiative effects and indirect effects on cloud formation and properties. The combined forcing of aerosol–radiation and aerosol–cloud interactions is negative over the industrial era, substantially offsetting a substantial part of greenhouse gas forcing, which is currently the predominant human contribution. The magnitude of this offset has declined in recent decades due to a decreasing trend in net aerosol forcing.

Description of evidence base

The Key Finding and supporting text summarize extensive evidence documented in the climate science literature, including in previous national (NCA3; Melillo et al. 2014) and international (IPCC 2013) assessments. Fundamental physics dictates that aerosols suspended in the atmosphere will scatter sunlight, and thereby reduce incoming solar radiation. Extensive in situ and remote sensing data are used to measure emission of aerosols and aerosol precursors from specific source types, the concentrations of aerosols in the atmosphere, aerosol microphysical and optical properties, and, via remote sensing, their direct impacts on radiative fluxes. Model calculations of aerosol forcing are constrained by these observations.

In addition to their direct impact on radiative fluxes, aerosols also act as cloud condensation nuclei. Multiple observational and modeling studies have concluded that increasing the number of aerosols in the atmosphere increases cloud albedo and lifetime, adding to the negative forcing (aerosol “indirect effects”) (e.g., Twohy 2005; Lohmann and Feichter 2005; Quaas et al. 2009; Rosenfeld et al. 2014). Particles that absorb sunlight increase atmospheric heating; if they are sufficiently dark, the net effect of scattering plus absorption can be a positive top-of-atmosphere radiative forcing. However, only a few very specific types of aerosols (for example, from diesel engines) are sufficiently dark that they have a positive radiative forcing (Bond et al. 2013). Modeling studies, combined with observational input, have investigated the thermodynamic response to aerosol absorption in the atmosphere (the “semi-direct effects”). Depending on aerosol location relative to the clouds and other factors the resulting changes in cloud properties can have a positive or negative effect on net downward radiative flux. The best estimate is that the semi-direct effect of aerosols is negative, offsetting approximately 15% of the positive radiative forcing by absorbing aerosols (specifically, black carbon) (Bond et al. 2013).

Major uncertainties

Aerosol–cloud interactions in particular are the largest source of uncertainty in both aerosol and total anthropogenic radiative forcing. These include the microphysical effects of aerosols on clouds (the “indirect effects”) and changes in clouds that result from the rapid response to absorption of sunlight by aerosols (the “semi-direct effects”). This has been a consistent finding of previous assessments (e.g., IPCC 2007; IPCC 2013). Aerosols affect the Earth’s albedo by directly interacting with solar radiation (scattering and absorbing sunlight) and by affecting cloud properties (albedo and lifetime). Aerosol cloud effects are, in particular, the most significant single source of uncertainty in anthropogenic ERF. This is due to poor understanding of how both natural and anthropogenic aerosol emissions have changed and how changing aerosol concentrations and composition affect cloud properties (albedo and lifetime) (Boucher et al. 2013; Carslaw et al. 2013). From a theoretical standpoint, aerosol–cloud these interactions are complex, and using observations to isolate the effects of aerosols on clouds is complicated by the fact that other factors (for example, the thermodynamic state of the atmosphere) also control cloud properties. Further, changes in aerosol properties and the atmospheric thermodynamic state are often correlated and interact in non-linear ways (Stevens and Feingold 2009).

While the indirect effects lead to negative forcing with *high confidence*, the semi-direct effects are uncertain in both sign and magnitude, but are assessed to be *likely* negative.

Assessment of confidence based on evidence and agreement, including short description of nature of evidence and level of agreement

☐ **Very High**

☒ **High**

☐ **Medium**

☐ **Low**

There is *very high confidence* that aerosol radiative forcing is negative on a global, annually averaged basis, *medium confidence* in the magnitude of the aerosol radiative forcing (RF), *high confidence* that aerosol effective radiative forcing (ERF) is also, on average, negative, and *low to medium confidence* in the magnitude of aerosol effective radiative forcing (ERF). Lower confidence in the magnitude of the aerosol ERF is due to large uncertainties in the effects of aerosols on clouds. Combined, we assess a *high level of confidence* that aerosol forcing is net-negative and sufficiently large to be substantially offsetting positive greenhouse gas forcing. Improvements in emissions estimates, observations (from both surface-based networks and satellites), and modeling capability give *medium to high confidence* in the finding that aerosol forcing trends are decreasing in recent decades.

Summary sentence or paragraph that integrates the above information

This key finding parallels the findings of IPCC AR5 (Myhre et al. 2013) that aerosols on net constitute a negative radiative forcing. While significant uncertainty remains in the quantification of aerosol ERF, we assess with *high confidence* that aerosols offset about half of the positive forcing by anthropogenic CO₂ and about a third of the forcing by all well-mixed anthropogenic greenhouse gases. The fraction of greenhouse gas forcing that is offset by aerosols has been decreasing over recent decades, as aerosol forcing has leveled off while greenhouse gas forcing continues to increase.

Key Finding 3

The climate system includes a number of positive and negative feedback processes that can either strengthen (positive feedback) or weaken (negative feedback) the system's responses to human and natural influences. These feedbacks operate on a range of timescales from very short (essentially instantaneous) to very long (centuries). While there are large uncertainties associated with some of these feedbacks, the net feedback effect over the industrial era has been positive (amplifying warming) and will continue to be positive in coming decades.

Description of evidence base

Fundamental physics dictates that the Planck feedback only partially offsets warming by increasing emitted infrared radiation. The largest feedback, the water vapor feedback, is again dictated by fundamental physics and with *very high confidence* is positive, approximately doubling the direct warming due to CO₂ emissions alone. The lapse rate feedback is, also with *very high confidence*, negative, but only partially offsets the water vapor feedback, with the two linked by the fact that both are driven by increases in atmospheric water vapor with warming. Estimates of this feedback strength have changed little across recent assessments (IPCC 2007; IPCC 2013). The snow and ice albedo feedback is also definitively positive in sign, with the magnitude of the feedback dependent in part on timescale of interest. Assessment of its strength has also not significantly changed since IPCC (2007). Cloud feedbacks can be either positive or negative, depending on the sign of the change in clouds with warming (increase or decrease) and the type of cloud that changes (low or high clouds). Recent international assessments (IPCC 2007; IPCC 2013) and a separate assessment specifically of feedbacks (Vial et al. 2013) all give best estimates of cloud feedbacks as positive on net, with uncertainty bounds allowing for a small negative feedback. Feedbacks via changes in atmospheric chemistry are an active area of research. They are not well-quantified, but are expected to be small relative to water-vapor-plus-lapse-rate, snow, and cloud feedbacks at the global scale. Carbon cycle feedbacks through changes in the land biosphere are currently of uncertain direction but uncertainties are asymmetric: they might be small and negative but could also be large and positive. Recent best estimates of ocean carbon cycle feedbacks are that they are positive, with significant uncertainty that includes allowance of a negative feedback for present-day CO₂ levels (Laufkötter et al. 2015; Steinacher et al. 2010). The thaw of permafrost with climate warming also has the potential to release large stores of carbon. While this source of CO₂ is currently likely small, the permafrost-carbon feedback is *very likely* positive, and as discussed in Chapter 15, could be a large positive feedback in longer term. Thus, while negative feedback processes exist the preponderance of evidence is that positive feedback processes dominate.

Major uncertainties

Cloud feedbacks carry the largest uncertainty of all the feedbacks, particularly on the decadal to century time-scale. This results from the fact cloud feedbacks can be either positive or negative, depending not only on the direction of change (more or less cloud) but also on the type of cloud affected and, to a lesser degree, the location of the cloud.

Assessment of confidence based on evidence and agreement, including short description of nature of evidence and level of agreement

☐ **Very High**

☒ **High**

☐ **Medium**

1 ☐ **Low**

2 There is *high confidence* that the net effect of all feedback processes in the climate system are
3 positive, i.e. reinforce warming. This is based on consistency across multiple assessments,
4 including IPCC AR5 (IPCC 2013 and references therein) of the magnitude of, in particular, the
5 largest feedbacks in the climate system, two of which (water vapor feedback and snow/ice
6 albedo feedback) are definitively positive in sign. While significant increases in low cloud cover
7 with climate warming would be a large negative feedback to warming, modeling and
8 observational studies do not support the idea of increases, on average, in low clouds with climate
9 warming.

10 **Summary sentence or paragraph that integrates the above information**

11 The net effect of all identified feedbacks to forcing is, by best current estimates, positive and
12 therefore reinforces climate warming. The various feedback processes operate on different
13 timescales with, in particular, carbon cycle and snow and ice albedo feedbacks operating on
14 longer timelines than water vapor, lapse rate, cloud, and atmospheric composition feedbacks.

15

1 **TABLES**2 Table 2.1. Global mean RF and ERF values in 2011 for the industrial era ^a

Climate forcing agent	Radiative forcing (W/m ²)	Effective radiative forcing (Wm ²) ^b
Well-mixed greenhouse gases (CO ₂ , CH ₄ , N ₂ O, and halocarbons)	+2.83 (2.54 to 3.12)	+2.83 (2.26 to 3.40)
Tropospheric ozone	+0.40 (0.20 to 0.60)	
Stratospheric ozone	-0.05 (-0.15 to +0.05)	
Stratospheric water vapor from CH ₄	+0.07 (+0.02 to +0.12)	
Aerosol–radiation interactions	-0.35 (-0.85 to +0.15)	-0.45 (-0.95 to +0.05)
Aerosol–cloud interactions	Not estimated	-0.45 (-1.2 to 0.0)
Surface albedo (land use)	-0.15 (-0.25 to -0.05)	
Surface albedo (black carbon aerosol on snow and ice)	+0.04 (+0.02 to +0.09)	
Contrails	+0.01 (+0.005 to +0.03)	
Combined contrails and contrail-induced cirrus	Not estimated	+0.05 (0.02 to 0.15)
Total anthropogenic	Not estimated	+2.3 (1.1 to 3.3)
Solar irradiance	+0.05 (0.0 to +0.10)	

3 ^a From IPCC (Myhre et al. 2013)4 ^b RF is a good estimate of ERF for most forcing agents except black carbon on snow and ice and
5 aerosol–cloud interactions.

6

7

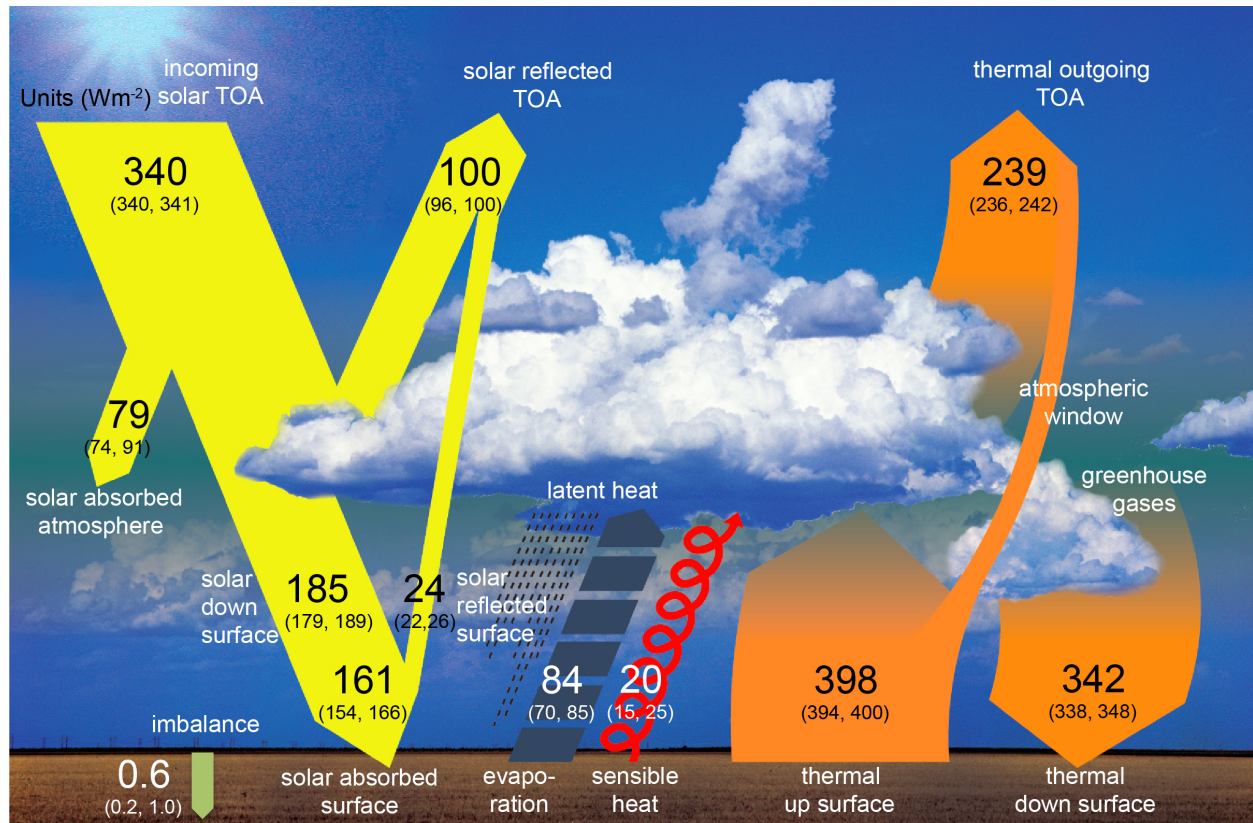
1 **FIGURES**

Figure 2.1: Global mean energy budget of the Earth under present-day climate conditions. Numbers state magnitudes of the individual energy fluxes in watts per square meter (W/m^2) averaged over Earth's surface, adjusted within their uncertainty ranges to balance the energy budgets of the atmosphere and the surface. Numbers in parentheses attached to the energy fluxes cover the range of values in line with observational constraints. These constraints are largely provided by satellite-based observations, which have directly measured solar and infrared fluxes at the top of the atmosphere over nearly the whole globe since 1984 (Barkstrom, 1984; Smith et al., 1994). More advanced satellite-based measurements focusing on the role of clouds in Earth's radiative fluxes have been available since 1998 (Wielicki et al., 1995 & 1996). (Figure source: Hartmann et al. 2013; © IPCC, used with permission).

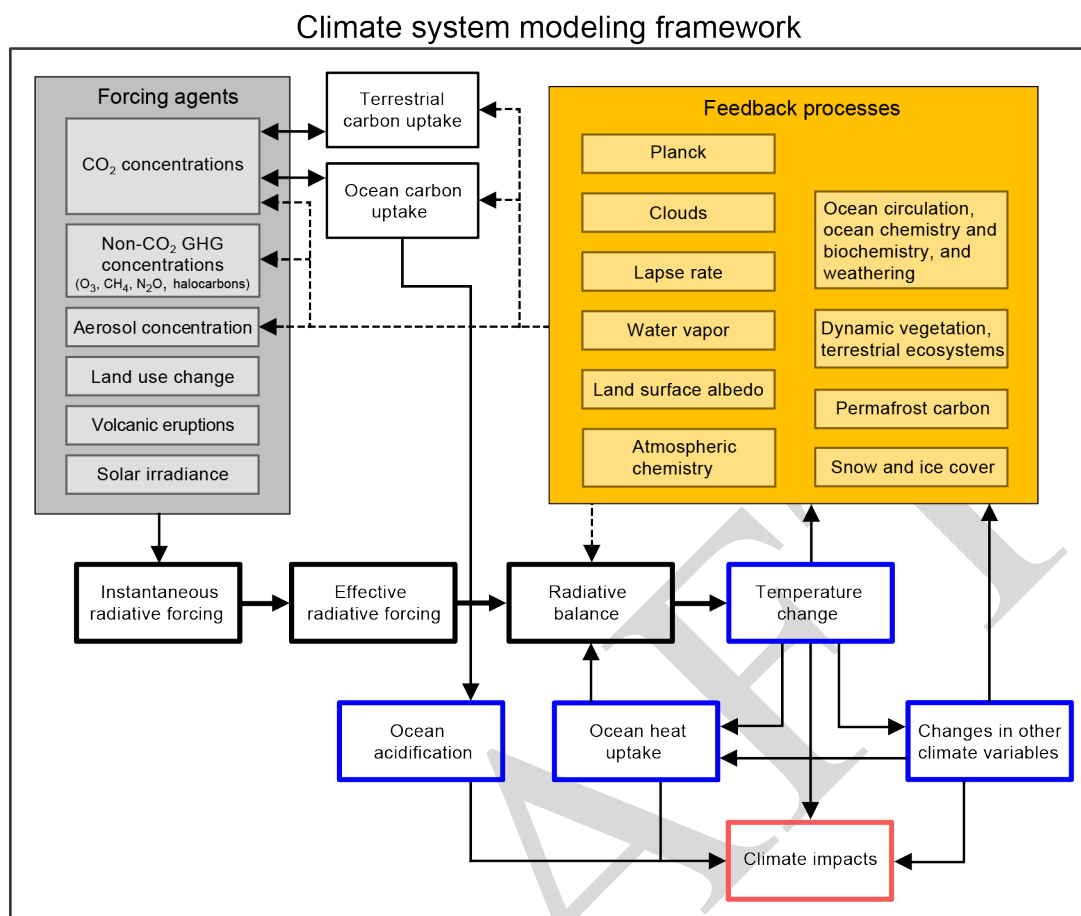


Figure 2.2: Simplified conceptual modeling framework for the climate system as implemented in many climate models (Chapter 4). Modeling components include forcing agents, feedback processes, carbon uptake processes and radiative forcing and balance. The lines indicate physical interconnections (solid lines) and feedback pathways (dashed lines). Principal changes (blue boxes) lead to climate impacts (red box) and feedbacks. (Figure source: adapted from Knutti and Rugenstein 2015).

Radiative Forcing of Climate Between 1750 and 2011

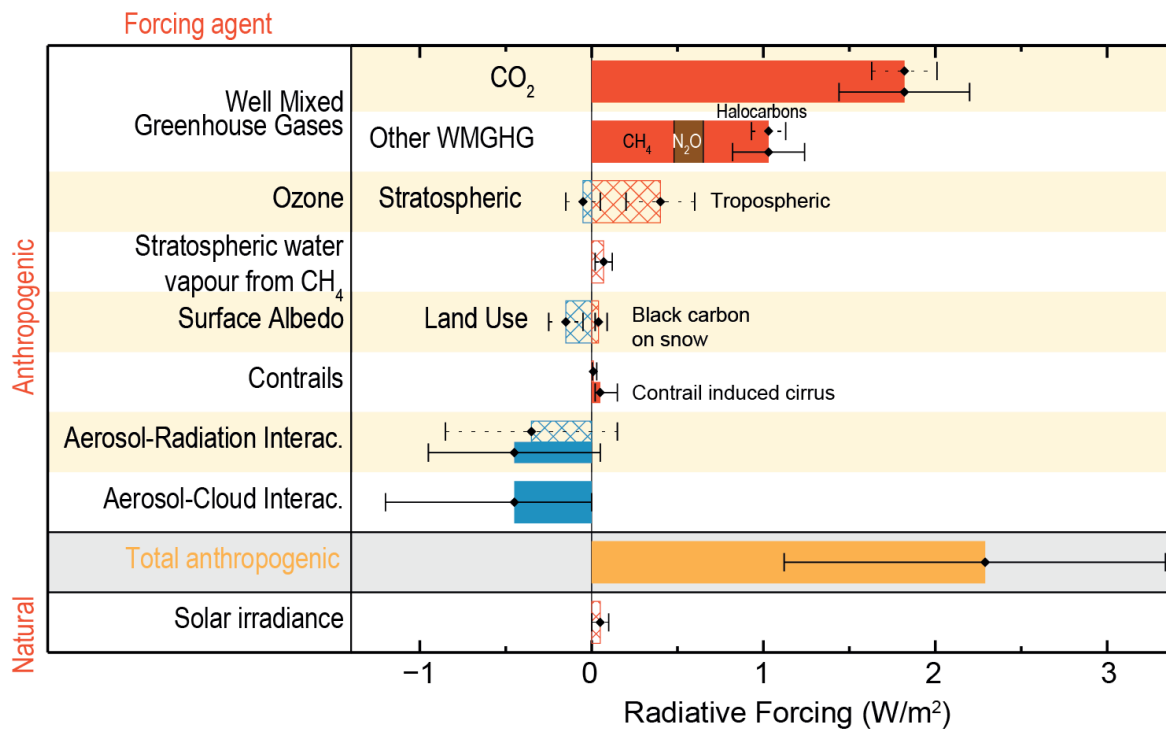
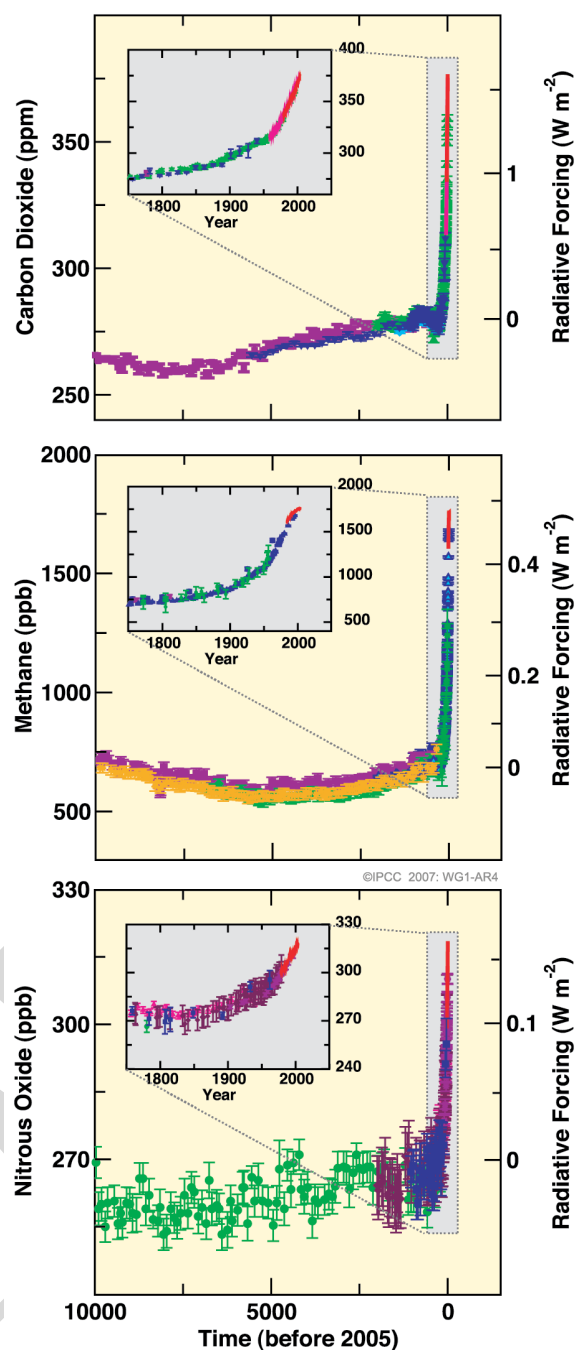


Figure 2.3: Bar chart for RF (hatched) and ERF (solid) for the period 1750–2011, where the total ERF is derived from IPCC. Uncertainties (5% to 95% confidence range) are given for RF (dotted lines) and ERF (solid lines). Volcanic forcing is not shown because this forcing is negligible over the industrial era. (Figure source: Myhre et al. 2013; © IPCC, used with permission).

1



2

3

4

5

6

7

8

9

Figure 2.4: Atmospheric concentrations of carbon dioxide, methane and nitrous oxide over the last 10,000 years (large panels) and since 1750 (inset panels). Measurements are shown from ice cores (symbols with different colors for different studies) and atmospheric samples (red lines). The corresponding radiative forcings are shown on the right hand axes of the large. The concentrations of these gases have continued to increase in the 2000 to 2016 period (<http://www.esrl.noaa.gov/gmd/ccgg/aggi.html>). (Figure source: IPCC 2007; © IPCC, used with permission)

Radiative Forcing of Well-mixed Greenhouse Gases

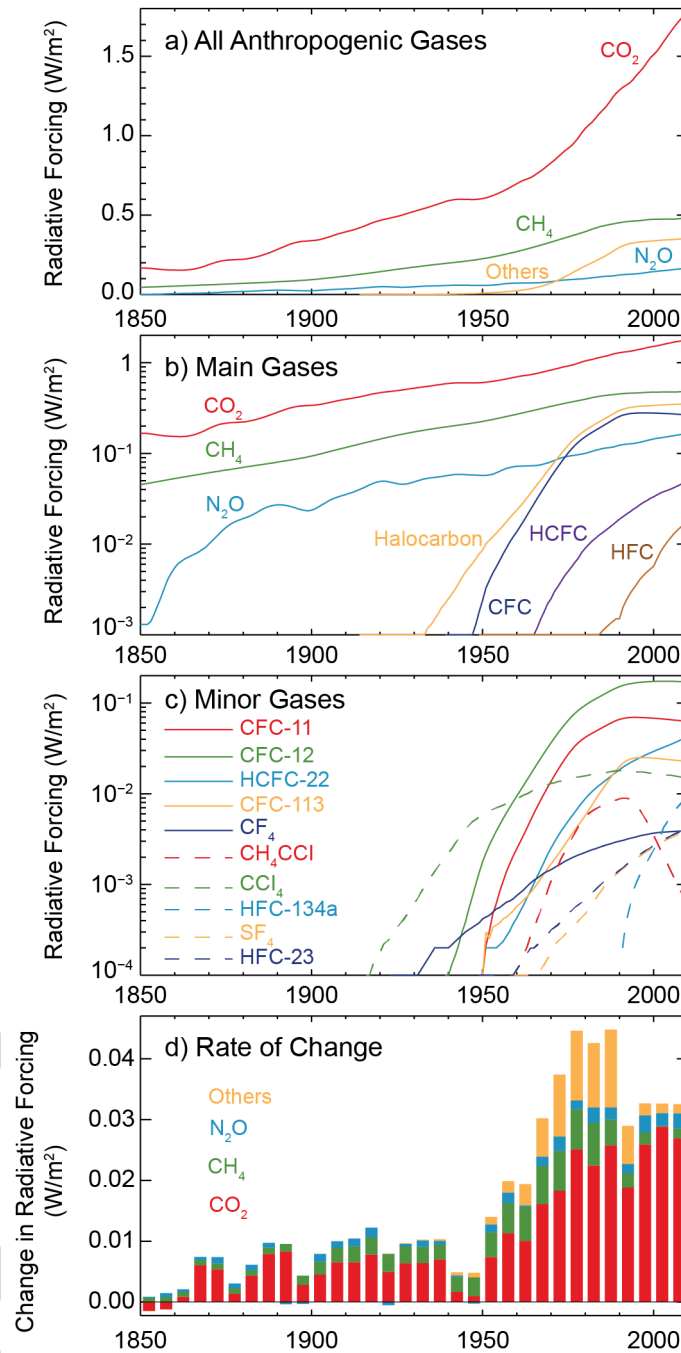


Figure 2.5: (a) Radiative forcing (RF) from the major WMGHGs and groups of halocarbons (Others) from 1850 to 2011; (b) the data in (a) with a logarithmic scale; (c) RFs from the minor WMGHGs from 1850 to 2011 (logarithmic scale); (d) rate of change in forcing from the major WMGHGs and halocarbons from 1850 to 2011. (Figure source: Myhre et al. 2013; © IPCC, used with permission).

Time Evolution of Forcings

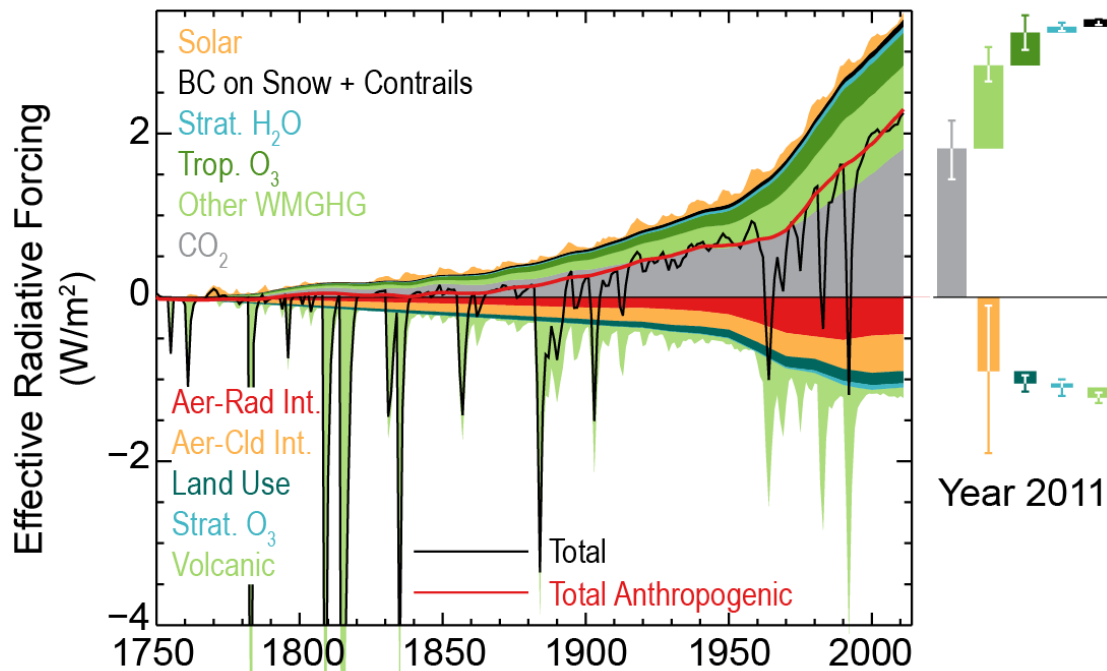


Figure 2.6: Effective radiative forcing changes across the industrial era for anthropogenic and natural forcing mechanisms. Also shown are the sum of all forcings (Total) and the sum of anthropogenic forcings (Total Anthropogenic). Bars with the forcing and uncertainty ranges (5 to 95% confidence range) at present are given in the right part of the figure. For aerosol the ERF due to aerosol–radiation interaction and total aerosol ERF are shown. The uncertainty ranges are for present (2011 versus 1750) and are given in Table 8.6. For aerosols, only the uncertainty in the total aerosol ERF is given. For several of the forcing agents the relative uncertainty may be larger for certain time periods compared to present. See IPCC AR5 Supplementary Material Table 8.SM.8 for further information on the forcing time evolutions. Forcing numbers provided in Annex II of this report. The total anthropogenic forcing was 0.57 (0.29 to 0.85) W m⁻² in 1950, 1.25 (0.64 to 1.86) W/m² in 1980 and 2.29 (1.13 to 3.33) W/m² in 2011. (Figure source: Myhre et al. 2013; © IPCC, used with permission).

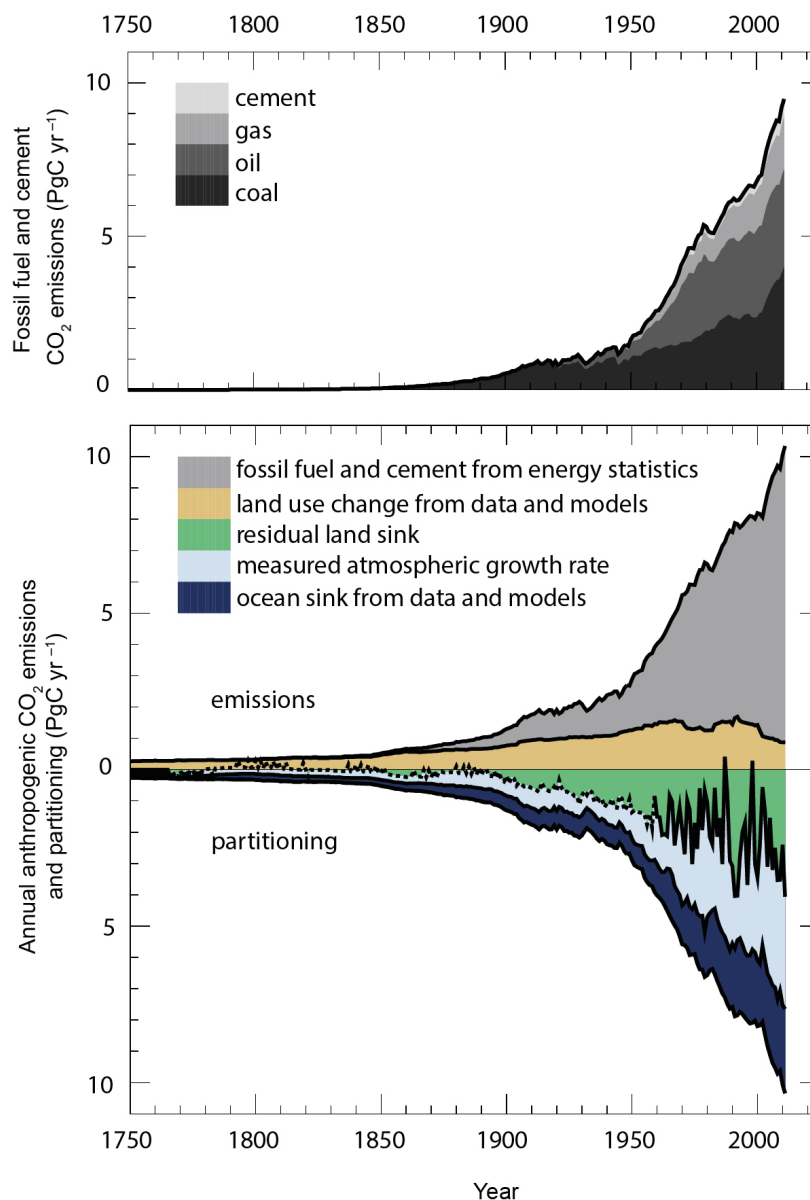


Figure 2.7: CO₂ sources and sinks (PgC/yr¹) over the industrial era (1750–2011). The partitioning of atmospheric emissions among the atmosphere, land and ocean is shown as equivalent negative emissions in the lower panel; of these, the land and ocean terms are true sinks of atmospheric CO₂. The top panel shows an expanded view of emissions from fossil fuels and cement manufacturing. The atmospheric CO₂ growth rate is derived from atmospheric observations and ice core data. The ocean CO₂ sink is derived from a combination of models and observations. The land sink is the residual of the other terms in a balanced CO₂ budget, and represents the sink of anthropogenic CO₂ in natural land ecosystems. These terms only represent changes since 1750 and do not include natural CO₂ fluxes (for example, from weathering and outgassing from lakes and rivers). (Figure source: Ciais et al. 2013; © IPCC, used with permission)

1 REFERENCES

- 2 Allen, M.R. and W.J. Ingram, 2002: Constraints on future changes in climate and the hydrologic
3 cycle. *Nature*, **419**, 224-232. <http://dx.doi.org/10.1038/nature01092>
- 4 Anav, A., P. Friedlingstein, M. Kidston, L. Bopp, P. Ciais, P. Cox, C. Jones, M. Jung, R.
5 Myneni, and Z. Zhu, 2013: Evaluating the Land and Ocean Components of the Global
6 Carbon Cycle in the CMIP5 Earth System Models. *Journal of Climate*, **26**, 6801-6843.
7 <http://dx.doi.org/10.1175/jcli-d-12-00417.1>
- 8 Andrews, T., J.M. Gregory, M.J. Webb, and K.E. Taylor, 2012: Forcing, feedbacks and climate
9 sensitivity in CMIP5 coupled atmosphere-ocean climate models. *Geophysical Research*
10 *Letters*, **39**, L09712. <http://dx.doi.org/10.1029/2012GL051607>
- 11 Andronova, N.G., E.V. Rozanov, F. Yang, M.E. Schlesinger, and G.L. Stenchikov, 1999:
12 Radiative forcing by volcanic aerosols from 1850 to 1994. *Journal of Geophysical Research:*
13 *Atmospheres*, **104**, 16807-16826. <http://dx.doi.org/10.1029/1999JD900165>
- 14 Ball, W.T., J.D. Haigh, E.V. Rozanov, A. Kuchar, T. Sukhodolov, F. Tummon, A.V. Shapiro,
15 and W. Schmutz, 2016: High solar cycle spectral variations inconsistent with stratospheric
16 ozone observations. *Nature Geoscience*, **9**, 206-209. <http://dx.doi.org/10.1038/ngeo2640>
- 17 Banerjee, A., A.T. Archibald, A.C. Maycock, P. Telford, N.L. Abraham, X. Yang, P. Braesicke,
18 and J.A. Pyle, 2014: Lightning NO_x, a key chemistry–climate interaction:
19 impacts of future climate change and consequences for tropospheric oxidising capacity.
20 *Atmospheric Chemistry and Physics*, **14**, 9871-9881. [http://dx.doi.org/10.5194/acp-14-9871-](http://dx.doi.org/10.5194/acp-14-9871-2014)
21 2014
- 22 Barkstrom, B.R., 1984: The Earth Radiation Budget Experiment (ERBE). *Bulletin of the*
23 *American Meteorological Society*, **65**, 1170-1185. [http://dx.doi.org/10.1175/1520-](http://dx.doi.org/10.1175/1520-0477(1984)065<1170:terbe>2.0.co;2)
24 0477(1984)065<1170:terbe>2.0.co;2
- 25 Behrenfeld, M.J., R.T. O'Malley, D.A. Siegel, C.R. McClain, J.L. Sarmiento, G.C. Feldman,
26 A.J. Milligan, P.G. Falkowski, R.M. Letelier, and E.S. Boss, 2006: Climate-driven trends in
27 contemporary ocean productivity. *Nature*, **444**, 752-755.
28 <http://dx.doi.org/10.1038/nature05317>
- 29 Bidigare, R.R., F. Chai, M.R. Landry, R. Lukas, C.C.S. Hannides, S.J. Christensen, D.M. Karl,
30 L. Shi, and Y. Chao, 2009: Subtropical ocean ecosystem structure changes forced by North
31 Pacific climate variations. *Journal of Plankton Research*, **31**, 1131-1139.
32 <http://dx.doi.org/10.1093/plankt/fbp064>
33 plankt.oxfordjournals.org/content/31/10/1131.abstract

- 1 Bindoff, N.L., P.A. Stott, K.M. AchutaRao, M.R. Allen, N. Gillett, D. Gutzler, K. Hansingo, G.
2 Hegerl, Y. Hu, S. Jain, I.I. Mokhov, J. Overland, J. Perlwitz, R. Sebbari, and X. Zhang, 2013:
3 Detection and Attribution of Climate Change: from Global to Regional. *Climate Change*
4 *2013: The Physical Science Basis. Contribution of Working Group I to the Fifth Assessment*
5 *Report of the Intergovernmental Panel on Climate Change*. Stocker, T.F., D. Qin, G.-K.
6 Plattner, M. Tignor, S.K. Allen, J. Boschung, A. Nauels, Y. Xia, V. Bex, and P.M. Midgley,
7 Eds. Cambridge University Press, Cambridge, United Kingdom and New York, NY, USA,
8 867–952. <http://dx.doi.org/10.1017/CBO9781107415324.022> www.climatechange2013.org
- 9 Boer, G. and B. Yu, 2003: Climate sensitivity and response. *Climate Dynamics*, **20**, 415-429.
10 <http://dx.doi.org/10.1007/s00382-002-0283-3>
- 11 Bolduc, C., M.S. Bourqui, and P. Charbonneau, 2015: A comparison of stratospheric
12 photochemical response to different reconstructions of solar ultraviolet radiative variability.
13 *Journal of Atmospheric and Solar-Terrestrial Physics*, **132**, 22-32.
14 <http://dx.doi.org/10.1016/j.jastp.2015.06.008>
- 15 Bond, T.C., S.J. Doherty, D.W. Fahey, P.M. Forster, T. Berntsen, B.J. DeAngelo, M.G. Flanner,
16 S. Ghan, B. Kärcher, D. Koch, S. Kinne, Y. Kondo, P.K. Quinn, M.C. Sarofim, M.G.
17 Schultz, M. Schulz, C. Venkataraman, H. Zhang, S. Zhang, N. Bellouin, S.K. Guttikunda,
18 P.K. Hopke, M.Z. Jacobson, J.W. Kaiser, Z. Klimont, U. Lohmann, J.P. Schwarz, D.
19 Shindell, T. Storelvmo, S.G. Warren, and C.S. Zender, 2013: Bounding the role of black
20 carbon in the climate system: A scientific assessment. *Journal of Geophysical Research:*
21 *Atmospheres*, **118**, 5380-5552. <http://dx.doi.org/10.1002/jgrd.50171>
- 22 Bony, S., R. Colman, V.M. Kattsov, R.P. Allan, C.S. Bretherton, J.-L. Dufresne, A. Hall, S.
23 Hallegatte, M.M. Holland, W. Ingram, D.A. Randall, B.J. Soden, G. Tselioudis, and M.J.
24 Webb, 2006: How Well Do We Understand and Evaluate Climate Change Feedback
25 Processes? *Journal of Climate*, **19**, 3445-3482. <http://dx.doi.org/10.1175/JCLI3819.1>
- 26 Boucher, O., D. Randall, P. Artaxo, C. Bretherton, G. Feingold, P. Forster, V.-M. Kerminen, Y.
27 Kondo, H. Liao, U. Lohmann, P. Rasch, S.K. Satheesh, S. Sherwood, B. Stevens, and X.Y.
28 Zhang, 2013: Clouds and Aerosols. *Climate Change 2013: The Physical Science Basis.*
29 *Contribution of Working Group I to the Fifth Assessment Report of the Intergovernmental*
30 *Panel on Climate Change*. Stocker, T.F., D. Qin, G.-K. Plattner, M. Tignor, S.K. Allen, J.
31 Boschung, A. Nauels, Y. Xia, V. Bex, and P.M. Midgley, Eds. Cambridge University Press,
32 Cambridge, United Kingdom and New York, NY, USA, 571–658.
33 <http://dx.doi.org/10.1017/CBO9781107415324.016> www.climatechange2013.org
- 34 Boyce, D.G., M.R. Lewis, and B. Worm, 2010: Global phytoplankton decline over the past
35 century. *Nature*, **466**, 591-596. <http://dx.doi.org/10.1038/nature09268>
36 www.nature.com/nature/journal/v466/n7306/pdf/nature09268.pdf

- Brzostek, E.R., J.B. Fisher, and R.P. Phillips, 2014: Modeling the carbon cost of plant nitrogen acquisition: Mycorrhizal trade-offs and multipath resistance uptake improve predictions of retranslocation. *Journal of Geophysical Research: Biogeosciences*, **119**, 1684-1697.
<http://dx.doi.org/10.1002/2014JG002660>
- Burkhardt, U. and B. Kärcher, 2011: Global radiative forcing from contrail cirrus. *Nature Climate Change*, **1**, 54-58. <http://dx.doi.org/10.1038/nclimate1068>
- Capotondi, A., M.A. Alexander, N.A. Bond, E.N. Curchitser, and J.D. Scott, 2012: Enhanced upper ocean stratification with climate change in the CMIP3 models. *Journal of Geophysical Research: Oceans*, **117**, n/a-n/a. <http://dx.doi.org/10.1029/2011JC007409>
- Carr, M.-E., M.A.M. Friedrichs, M. Schmeltz, M. Noguchi Aita, D. Antoine, K.R. Arrigo, I. Asanuma, O. Aumont, R. Barber, M. Behrenfeld, R. Bidigare, E.T. Buitenhuis, J. Campbell, A. Ciotti, H. Dierssen, M. Dowell, J. Dunne, W. Esaias, B. Gentili, W. Gregg, S. Groom, N. Hoepffner, J. Ishizaka, T. Kameda, C. Le Quéré, S. Lohrenz, J. Marra, F. Mélin, K. Moore, A. Morel, T.E. Reddy, J. Ryan, M. Scardi, T. Smyth, K. Turpie, G. Tilstone, K. Waters, and Y. Yamanaka, 2006: A comparison of global estimates of marine primary production from ocean color. *Deep Sea Research Part II: Topical Studies in Oceanography*, **53**, 741-770.
<http://dx.doi.org/10.1016/j.dsr2.2006.01.028>
www.sciencedirect.com/science/article/pii/S0967064506000555
- Carslaw, K.S., L.A. Lee, C.L. Reddington, K.J. Pringle, A. Rap, P.M. Forster, G.W. Mann, D.V. Spracklen, M.T. Woodhouse, L.A. Regayre, and J.R. Pierce, 2013: Large contribution of natural aerosols to uncertainty in indirect forcing. *Nature*, **503**, 67-71.
<http://dx.doi.org/10.1038/nature12674>
- Chavez, F.P., M. Messié, and J.T. Pennington, 2011: Marine primary production in relation to climate variability and change. *Annual Review of Marine Science*, **3**, 227-260.
<http://dx.doi.org/10.1146/annurev.marine.010908.163917>
- Chen, T., W.B. Rossow, and Y. Zhang, 2000: Radiative Effects of Cloud-Type Variations. *Journal of Climate*, **13**, 264-286. [http://dx.doi.org/10.1175/1520-0442\(2000\)013<0264:reoctv>2.0.co;2](http://dx.doi.org/10.1175/1520-0442(2000)013<0264:reoctv>2.0.co;2)
- Chiodo, G., D.R. Marsh, R. Garcia-Herrera, N. Calvo, and J.A. García, 2014: On the detection of the solar signal in the tropical stratosphere. *Atmospheric Chemistry and Physics*, **14**, 5251-5269. <http://dx.doi.org/10.5194/acp-14-5251-2014>
- Ciais, P., C. Sabine, G. Bala, L. Bopp, V. Brovkin, J. Canadell, A. Chhabra, R. DeFries, J. Galloway, M. Heimann, C. Jones, C. Le Quéré, R.B. Myneni, S. Piao, and P. Thornton, 2013: Carbon and Other Biogeochemical Cycles. *Climate Change 2013: The Physical Science Basis. Contribution of Working Group I to the Fifth Assessment Report of the*

- 1 *Intergovernmental Panel on Climate Change*. Stocker, T.F., D. Qin, G.-K. Plattner, M.
2 Tignor, S.K. Allen, J. Boschung, A. Nauels, Y. Xia, V. Bex, and P.M. Midgley, Eds.
3 Cambridge University Press, Cambridge, United Kingdom and New York, NY, USA, 465–
4 570. <http://dx.doi.org/10.1017/CBO9781107415324.015> www.climatechange2013.org
- 5 Cook, B.I., S.P. Shukla, M.J. Puma, and L.S. Nazarenko, 2015: Irrigation as an historical climate
6 forcing. *Climate Dynamics*, **44**, 1715-1730. <http://dx.doi.org/10.1007/s00382-014-2204-7>
- 7 Crook, J.A. and P.M. Forster, 2011: A balance between radiative forcing and climate feedback in
8 the modeled 20th century temperature response. *Journal of Geophysical Research:*
9 *Atmospheres*, **116**, n/a-n/a. <http://dx.doi.org/10.1029/2011JD015924>
- 10 Cunningham, S.A. and R. Marsh, 2010: Observing and modeling changes in the Atlantic MOC.
11 *Wiley Interdisciplinary Reviews: Climate Change*, **1**, 180-191.
12 <http://dx.doi.org/10.1002/wcc.22>
- 13 Davies, J.H. and D.R. Davies, 2010: Earth's surface heat flux. *Solid Earth*, **1**, 5-24.
14 <http://dx.doi.org/10.5194/se-1-5-2010> www.solid-earth.net/1/5/2010/
- 15 Dentener, F., D. Stevenson, J. Cofala, R. Mechler, M. Amann, P. Bergamaschi, F. Raes, and R.
16 Derwent, 2005: The impact of air pollutant and methane emission controls on tropospheric
17 ozone and radiative forcing: CTM calculations for the period 1990-2030. *Atmospheric*
18 *Chemistry and Physics*, **5**, 1731-1755. <http://dx.doi.org/10.5194/acp-5-1731-2005>
19 www.atmos-chem-phys.net/5/1731/2005/
- 20 Dessler, A.E., M.R. Schoeberl, T. Wang, S.M. Davis, K.H. Rosenlof, and J.P. Vernier, 2014:
21 Variations of stratospheric water vapor over the past three decades. *Journal of Geophysical*
22 *Research: Atmospheres*, **119**, 12,588-12,598. <http://dx.doi.org/10.1002/2014JD021712>
- 23 Dhomse, S.S., M.P. Chipperfield, W. Feng, W.T. Ball, Y.C. Unruh, J.D. Haigh, N.A. Krivova,
24 S.K. Solanki, and A.K. Smith, 2013: Stratospheric O₃ changes during
25 2001–2010: the small role of solar flux variations in a chemical transport model.
26 *Atmospheric Chemistry and Physics*, **13**, 10113-10123. [http://dx.doi.org/10.5194/acp-13-](http://dx.doi.org/10.5194/acp-13-10113-2013)
27 [10113-2013](http://dx.doi.org/10.5194/acp-13-10113-2013)
- 28 Dietmüller, S., M. Ponater, and R. Sausen, 2014: Interactive ozone induces a negative feedback
29 in CO₂-driven climate change simulations. *Journal of Geophysical Research: Atmospheres*,
30 **119**, 1796-1805. <http://dx.doi.org/10.1002/2013JD020575>
- 31 Doney, S.C., 2010: The growing human footprint on coastal and open-ocean biogeochemistry.
32 *Science*, **328**, 1512-6. <http://dx.doi.org/10.1126/science.1185198>

- 1 Durack, P.J. and S.E. Wijffels, 2010: Fifty-Year Trends in Global Ocean Salinities and Their
2 Relationship to Broad-Scale Warming. *Journal of Climate*, **23**, 4342-4362.
3 <http://dx.doi.org/10.1175/2010jcli3377.1>
- 4 Enderlin, E.M. and G.S. Hamilton, 2014: Estimates of iceberg submarine melting from high-
5 resolution digital elevation models: application to Sermilik Fjord, East Greenland. *Journal of*
6 *Glaciology*, **60**, 1084-1092. <http://dx.doi.org/10.3189/2014JoG14J085>
- 7 Ermolli, I., K. Matthes, T. Dudok de Wit, N.A. Krivova, K. Tourpali, M. Weber, Y.C. Unruh, L.
8 Gray, U. Langematz, P. Pilewskie, E. Rozanov, W. Schmutz, A. Shapiro, S.K. Solanki, and
9 T.N. Woods, 2013: Recent variability of the solar spectral irradiance and its impact on
10 climate modelling. *Atmospheric Chemistry and Physics*, **13**, 3945-3977.
11 <http://dx.doi.org/10.5194/acp-13-3945-2013>
- 12 Falkowski, P.G., M.E. Katz, A.H. Knoll, A. Quigg, J.A. Raven, O. Schofield, and F.J.R. Taylor,
13 2004: The Evolution of Modern Eukaryotic Phytoplankton. *Science*, **305**, 354-360.
14 <http://dx.doi.org/10.1126/science.1095964>
- 15 Fernandes, R., H. Zhao, X. Wang, J. Key, X. Qu, and A. Hall, 2009: Controls on Northern
16 Hemisphere snow albedo feedback quantified using satellite Earth observations. *Geophysical*
17 *Research Letters*, **36**, L21702. <http://dx.doi.org/10.1029/2009GL040057>
- 18 Flanner, M.G., 2009: Integrating anthropogenic heat flux with global climate models.
19 *Geophysical Research Letters*, **36**, L02801. <http://dx.doi.org/10.1029/2008gl036465>
- 20 Flanner, M.G., C.S. Zender, P.G. Hess, N.M. Mahowald, T.H. Painter, V. Ramanathan, and P.J.
21 Rasch, 2009: Springtime warming and reduced snow cover from carbonaceous particles.
22 *Atmospheric Chemistry and Physics*, **9**, 2481-2497. [http://dx.doi.org/10.5194/acp-9-2481-](http://dx.doi.org/10.5194/acp-9-2481-2009)
23 2009 www.atmos-chem-phys.net/9/2481/2009/
- 24 Flato, G., J. Marotzke, B. Abiodun, P. Braconnot, S.C. Chou, W. Collins, P. Cox, F. Driouech, S.
25 Emori, V. Eyring, C. Forest, P. Gleckler, E. Guilyardi, C. Jakob, V. Kattsov, C. Reason, and
26 M. Rummukainen, 2013: Evaluation of Climate Models. *Climate Change 2013: The Physical*
27 *Science Basis. Contribution of Working Group I to the Fifth Assessment Report of the*
28 *Intergovernmental Panel on Climate Change*. Stocker, T.F., D. Qin, G.-K. Plattner, M.
29 Tignor, S.K. Allen, J. Boschung, A. Nauels, Y. Xia, V. Bex, and P.M. Midgley, Eds.
30 Cambridge University Press, Cambridge, United Kingdom and New York, NY, USA, 741–
31 866. <http://dx.doi.org/10.1017/CBO9781107415324.020> www.climatechange2013.org
- 32 Floyd, L.E., J.W. Cook, L.C. Herring, and P.C. Crane, 2003: SUSIM'S 11-year observational
33 record of the solar UV irradiance. *Advances in Space Research*, **31**, 2111-2120.
34 [http://dx.doi.org/10.1016/S0273-1177\(03\)00148-0](http://dx.doi.org/10.1016/S0273-1177(03)00148-0)

- 1 Franks, P.J., M.A. Adams, J.S. Amthor, M.M. Barbour, J.A. Berry, D.S. Ellsworth, G.D.
2 Farquhar, O. Ghannoum, J. Lloyd, N. McDowell, R.J. Norby, D.T. Tissue, and S. von
3 Caemmerer, 2013: Sensitivity of plants to changing atmospheric CO₂ concentration: from
4 the geological past to the next century. *New Phytologist*, **197**, 1077-1094.
5 <http://dx.doi.org/10.1111/nph.12104>
- 6 Friedlingstein, P., P. Cox, R. Betts, L. Bopp, W.v. Bloh, V. Brovkin, P. Cadule, S. Doney, M.
7 Eby, I. Fung, G. Bala, J. John, C. Jones, F. Joos, T. Kato, M. Kawamiya, W. Knorr, K.
8 Lindsay, H.D. Matthews, T. Raddatz, P. Rayner, C. Reick, E. Roeckner, K.-G. Schnitzler, R.
9 Schnur, K. Strassmann, A.J. Weaver, C. Yoshikawa, and N. Zeng, 2006: Climate–Carbon
10 Cycle Feedback Analysis: Results from the C4MIP Model Intercomparison. *Journal of*
11 *Climate*, **19**, 3337-3353. <http://dx.doi.org/10.1175/JCLI3800.1>
- 12 Friedlingstein, P., M. Meinshausen, V.K. Arora, C.D. Jones, A. Anav, S.K. Liddicoat, and R.
13 Knutti, 2014: Uncertainties in CMIP5 Climate Projections due to Carbon Cycle Feedbacks.
14 *Journal of Climate*, **27**, 511-526. <http://dx.doi.org/10.1175/JCLI-D-12-00579.1>
- 15 Fröhlich, C. and J. Lean, 2004: Solar radiative output and its variability: evidence and
16 mechanisms. *The Astronomy and Astrophysics Review*, **12**, 273-320.
17 <http://dx.doi.org/10.1007/s00159-004-0024-1>
- 18 Gao, F.-L., L.-R. Tao, G.-M. Cui, J.-L. Xu, and T.-C. Hua, 2015: The influence of solar spectral
19 variations on global radiative balance. *Advances in Space Research*, **55**, 682-687.
20 <http://dx.doi.org/10.1016/j.asr.2014.10.028>
- 21 Gelderloos, R., F. Straneo, and C.A. Katsman, 2012: Mechanisms behind the Temporary
22 Shutdown of Deep Convection in the Labrador Sea: Lessons from the Great Salinity
23 Anomaly Years 1968–71. *Journal of Climate*, **25**, 6743-6755. [http://dx.doi.org/10.1175/jcli-](http://dx.doi.org/10.1175/jcli-d-11-00549.1)
24 [d-11-00549.1](http://dx.doi.org/10.1175/jcli-d-11-00549.1)
- 25 Gerlach, T., 2011: Volcanic versus anthropogenic carbon dioxide. *Eos, Transactions of the*
26 *American Geophysical Union*, **92**, 201-202. <http://dx.doi.org/10.1029/2011EO240001>
- 27 Gillett, N.P., M.F. Wehner, S.F.B. Tett, and A.J. Weaver, 2004: Testing the linearity of the
28 response to combined greenhouse gas and sulfate aerosol forcing. *Geophysical Research*
29 *Letters*, **31**, L14201. <http://dx.doi.org/10.1029/2004GL020111>
- 30 González-Eguino, M. and M.B. Neumann, 2016: Significant implications of permafrost thawing
31 for climate change control. *Climatic Change*, **136**, 381-388.
32 <http://dx.doi.org/10.1007/s10584-016-1666-5>
- 33 Good, P., J.M. Gregory, J.A. Lowe, and T. Andrews, 2013: Abrupt CO₂ experiments as tools for
34 predicting and understanding CMIP5 representative concentration pathway projections.
35 *Climate Dynamics*, **40**, 1041-1053. <http://dx.doi.org/10.1007/s00382-012-1410-4>

- Gray, L.J., J. Beer, M. Geller, J.D. Haigh, M. Lockwood, K. Matthes, U. Cubasch, D. Fleitmann, G. Harrison, L. Hood, J. Luterbacher, G.A. Meehl, D. Shindell, B. van Geel, and W. White, 2010: Solar influences on climate. *Reviews of Geophysics*, **48**, RG4001. <http://dx.doi.org/10.1029/2009RG000282>
- Gregg, W.W., M.E. Conkright, P. Ginoux, J.E. O'Reilly, and N.W. Casey, 2003: Ocean primary production and climate: Global decadal changes. *Geophysical Research Letters*, **30**, 1809. <http://dx.doi.org/10.1029/2003GL016889>
- Hall, A., 2004: The Role of Surface Albedo Feedback in Climate. *Journal of Climate*, **17**, 1550-1568. [http://dx.doi.org/10.1175/1520-0442\(2004\)017<1550:TROSAF>2.0.CO;2](http://dx.doi.org/10.1175/1520-0442(2004)017<1550:TROSAF>2.0.CO;2)
- Hall, A. and X. Qu, 2006: Using the current seasonal cycle to constrain snow albedo feedback in future climate change. *Geophysical Research Letters*, **33**, L03502. <http://dx.doi.org/10.1029/2005GL025127>
- Han, Z., J. Li, W. Guo, Z. Xiong, and W. Zhang, 2013: A study of dust radiative feedback on dust cycle and meteorology over East Asia by a coupled regional climate-chemistry-aerosol model. *Atmospheric Environment*, **68**, 54-63. <http://dx.doi.org/10.1016/j.atmosenv.2012.11.032>
- Hartmann, D.L., M.E. Ockert-Bell, and M.L. Michelsen, 1992: The Effect of Cloud Type on Earth's Energy Balance: Global Analysis. *Journal of Climate*, **5**, 1281-1304. [http://dx.doi.org/10.1175/1520-0442\(1992\)005<1281:teocto>2.0.co;2](http://dx.doi.org/10.1175/1520-0442(1992)005<1281:teocto>2.0.co;2)
- Hartmann, D.L., A.M.G. Klein Tank, M. Rusticucci, L.V. Alexander, S. Brönnimann, Y. Charabi, F.J. Dentener, E.J. Dlugokencky, D.R. Easterling, A. Kaplan, B.J. Soden, P.W. Thorne, M. Wild, and P.M. Zhai, 2013: Observations: Atmosphere and Surface. Climate Change 2013: The Physical Science Basis. Contribution of Working Group I to the Fifth Assessment Report of the Intergovernmental Panel on Climate Change. Stocker, T.F., D. Qin, G.-K. Plattner, M. Tignor, S.K. Allen, J. Boschung, A. Nauels, Y. Xia, V. Bex, and P.M. Midgley, Eds. Cambridge University Press, Cambridge, United Kingdom and New York, NY, USA, 159–254. <http://dx.doi.org/10.1017/CBO9781107415324.008> www.climatechange2013.org
- Hegglin, M.I., D.A. Plummer, T.G. Shepherd, J.F. Scinocca, J. Anderson, L. Froidevaux, B. Funke, D. Hurst, A. Rozanov, J. Urban, T. von Clarmann, K.A. Walker, H.J. Wang, S. Tegtmeier, and K. Weigel, 2014: Vertical structure of stratospheric water vapour trends derived from merged satellite data. *Nature Geoscience*, **7**, 768-776. <http://dx.doi.org/10.1038/ngeo2236>

- 1 Held, I.M. and K.M. Shell, 2012: Using Relative Humidity as a State Variable in Climate
2 Feedback Analysis. *Journal of Climate*, **25**, 2578-2582. [http://dx.doi.org/10.1175/JCLI-D-11-](http://dx.doi.org/10.1175/JCLI-D-11-00721.1)
3 [00721.1](http://dx.doi.org/10.1175/JCLI-D-11-00721.1)
- 4 Held, I.M. and B.J. Soden, 2000: Water vapor feedback and global warming. *Annual Review of*
5 *Energy and the Environment*, **25**, 441-475.
6 <http://dx.doi.org/10.1146/annurev.energy.25.1.441>
- 7 Hibbard, K.A., G.A. Meehl, P.M. Cox, and P. Friedlingstein, 2007: A strategy for climate change
8 stabilization experiments. *Eos, Transactions American Geophysical Union*, **88**, 217-221.
9 <http://dx.doi.org/10.1029/2007EO200002>
- 10 Holland, D.M., R.H. Thomas, B. de Young, M.H. Ribergaard, and B. Lyberth, 2008:
11 Acceleration of Jakobshavn Isbrae triggered by warm subsurface ocean waters. *Nature*
12 *Geoscience*, **1**, 659-664. <http://dx.doi.org/10.1038/ngeo316>
- 13 Holmes, C.D., M.J. Prather, O.A. Søvde, and G. Myhre, 2013: Future methane, hydroxyl, and
14 their uncertainties: key climate and emission parameters for future predictions. *Atmospheric*
15 *Chemistry and Physics*, **13**, 285-302. <http://dx.doi.org/10.5194/acp-13-285-2013>
- 16 IPCC, 2007: *Climate Change 2007: The Physical Science Basis. Contribution of Working Group*
17 *I to the Fourth Assessment Report of the Intergovernmental Panel on Climate Change*.
18 Solomon, S., D. Qin, M. Manning, Z. Chen, M. Marquis, K.B. Averyt, M. Tignor, and H.L.
19 Miller, Eds. Cambridge University Press, Cambridge. U.K, New York, NY, USA, 996 pp.
20 [www.ipcc.ch/publications_and_data/publications_ipcc_fourth_assessment_report_wg1_repor](http://www.ipcc.ch/publications_and_data/publications_ipcc_fourth_assessment_report_wg1_report_the_physical_science_basis.htm)
21 [t_the_physical_science_basis.htm](http://www.ipcc.ch/publications_and_data/publications_ipcc_fourth_assessment_report_wg1_report_the_physical_science_basis.htm)
- 22 IPCC, 2013: *Climate Change 2013: The Physical Science Basis. Contribution of Working Group*
23 *I to the Fifth Assessment Report of the Intergovernmental Panel on Climate Change*.
24 Cambridge University Press, Cambridge, UK and New York, NY, 1535 pp.
25 <http://dx.doi.org/10.1017/CBO9781107415324> www.climatechange2013.org
- 26 Isaksen, I., T. Berntsen, S. Dalsøren, K. Eleftheratos, Y. Orsolini, B. Rognerud, F. Stordal, O.
27 Søvde, C. Zerefos, and C. Holmes, 2014: Atmospheric Ozone and Methane in a Changing
28 Climate. *Atmosphere*, **5**, 518. <http://dx.doi.org/10.3390/atmos5030518> [www.mdpi.com/2073-](http://www.mdpi.com/2073-4433/5/3/518)
29 [4433/5/3/518](http://www.mdpi.com/2073-4433/5/3/518)
- 30 John, J.G., A.M. Fiore, V. Naik, L.W. Horowitz, and J.P. Dunne, 2012: Climate versus emission
31 drivers of methane lifetime against loss by tropospheric OH from 1860–2100. *Atmospheric*
32 *Chemistry and Physics*, **12**, 12021-12036. <http://dx.doi.org/10.5194/acp-12-12021-2012>
- 33 Johnson, G.C., J.M. Lyman, T. Boyer, C.M. Domingues, M. Ishii, R. Killick, D. Monselesan,
34 and S.E. Wijffels, 2016: [Global Oceans] Ocean heat content [in “State of the Climate in

2015”]. *Bulletin of the American Meteorological Society*, **97**, S66-S70.

<http://dx.doi.org/10.1175/2016BAMSSStateoftheClimate.1>

Jones, A., J.M. Haywood, and O. Boucher, 2007: Aerosol forcing, climate response and climate sensitivity in the Hadley Centre climate model. *Journal of Geophysical Research*, **112**, D20211. <http://dx.doi.org/10.1029/2007JD008688>

Joughin, I., R.B. Alley, and D.M. Holland, 2012: Ice-Sheet Response to Oceanic Forcing. *Science*, **338**, 1172-1176. <http://dx.doi.org/10.1126/science.1226481>

Ju, J. and J.G. Masek, 2016: The vegetation greenness trend in Canada and US Alaska from 1984–2012 Landsat data. *Remote Sensing of Environment*, **176**, 1-16.

<http://dx.doi.org/10.1016/j.rse.2016.01.001>

Kay, J.E. and A. Gettelman, 2009: Cloud influence on and response to seasonal Arctic sea ice loss. *Journal of Geophysical Research*, **114**, D18204.

<http://dx.doi.org/10.1029/2009JD011773>

Kay, J.E. and T. L'Ecuyer, 2013: Observational constraints on Arctic Ocean clouds and radiative fluxes during the early 21st century. *Journal of Geophysical Research: Atmospheres*, **118**,

7219-7236. <http://dx.doi.org/10.1002/jgrd.50489>

Kay, J.E., K. Raeder, A. Gettelman, and J. Anderson, 2011: The Boundary Layer Response to Recent Arctic Sea Ice Loss and Implications for High-Latitude Climate Feedbacks. *Journal of Climate*, **24**, 428-447. <http://dx.doi.org/10.1175/2010JCLI3651.1>

Klocke, D., J. Quaas, and B. Stevens, 2013: Assessment of different metrics for physical climate feedbacks. *Climate Dynamics*, **41**, 1173-1185. <http://dx.doi.org/10.1007/s00382-013-1757-1>

Knutti, R. and G.C. Hegerl, 2008: The equilibrium sensitivity of the Earth's temperature to radiation changes. *Nature Geoscience*, **1**, 735-743. <http://dx.doi.org/10.1038/ngeo337>

Knutti, R. and M.A.A. Rugenstein, 2015: Feedbacks, climate sensitivity and the limits of linear models. *Philosophical Transactions of the Royal Society A: Mathematical, Physical and Engineering Sciences*, **373**. <http://dx.doi.org/10.1098/rsta.2015.0146>

Kopp, G., 2014: An assessment of the solar irradiance record for climate studies. *Journal of Space Weather and Space Climate*, **4**, A14. <http://dx.doi.org/10.1051/swsc/2014012>

Kopp, G., N. Krivova, C.J. Wu, and J. Lean, 2016: The Impact of the Revised Sunspot Record on Solar Irradiance Reconstructions. *Solar Physics*, 1-15. <http://dx.doi.org/10.1007/s11207-016-0853-x>

- 1 Kopp, G. and J.L. Lean, 2011: A new, lower value of total solar irradiance: Evidence and climate
2 significance. *Geophysical Research Letters*, **38**, L01706.
3 <http://dx.doi.org/10.1029/2010GL045777>
- 4 Kostov, Y., K.C. Armour, and J. Marshall, 2014: Impact of the Atlantic meridional overturning
5 circulation on ocean heat storage and transient climate change. *Geophysical Research*
6 *Letters*, **41**, 2108-2116. <http://dx.doi.org/10.1002/2013GL058998>
- 7 Koven, C.D., D.M. Lawrence, and W.J. Riley, 2015: Permafrost carbon–climate feedback is
8 sensitive to deep soil carbon decomposability but not deep soil nitrogen dynamics.
9 *Proceedings of the National Academy of Sciences*, **112**, 3752-3757.
10 <http://dx.doi.org/10.1073/pnas.1415123112>
- 11 Koven, C.D., E.A.G. Schuur, C. Schädel, T.J. Bohn, E.J. Burke, G. Chen, X. Chen, P. Ciais, G.
12 Grosse, J.W. Harden, D.J. Hayes, G. Hugelius, E.E. Jafarov, G. Krinner, P. Kuhry, D.M.
13 Lawrence, A.H. MacDougall, S.S. Marchenko, A.D. McGuire, S.M. Natali, D.J. Nicolsky, D.
14 Olefeldt, S. Peng, V.E. Romanovsky, K.M. Schaefer, J. Strauss, C.C. Treat, and M. Turetsky,
15 2015: A simplified, data-constrained approach to estimate the permafrost carbon–climate
16 feedback. *Philosophical Transactions of the Royal Society A: Mathematical, Physical and*
17 *Engineering Sciences*, **373**. <http://dx.doi.org/10.1098/rsta.2014.0423>
- 18 Lambert, F.H. and P.C. Taylor, 2014: Regional variation of the tropical water vapor and lapse
19 rate feedbacks. *Geophysical Research Letters*, **41**, 7634-7641.
20 <http://dx.doi.org/10.1002/2014GL061987>
- 21 Langmann, B., 2014: On the Role of Climate Forcing by Volcanic Sulphate and Volcanic Ash.
22 *Advances in Meteorology*, **2014**, 17. <http://dx.doi.org/10.1155/2014/340123>
- 23 Laufkötter, C., M. Vogt, N. Gruber, M. Aita-Noguchi, O. Aumont, L. Bopp, E. Buitenhuis, S.C.
24 Doney, J. Dunne, T. Hashioka, J. Hauck, T. Hirata, J. John, C. Le Quéré, I.D. Lima, H.
25 Nakano, R. Seferian, I. Totterdell, M. Vichi, and C. Völker, 2015: Drivers and uncertainties
26 of future global marine primary production in marine ecosystem models. *Biogeosciences*, **12**,
27 6955-6984. <http://dx.doi.org/10.5194/bg-12-6955-2015>
28 www.biogeosciences.net/12/6955/2015/
- 29 Le Quéré, C., R.M. Andrew, J.G. Canadell, S. Sitch, J.I. Korsbakken, G.P. Peters, A.C. Manning,
30 T.A. Boden, P.P. Tans, R.A. Houghton, R.F. Keeling, S. Alin, O.D. Andrews, P. Anthoni, L.
31 Barbero, L. Bopp, F. Chevallier, L.P. Chini, P. Ciais, K. Currie, C. Delire, S.C. Doney, P.
32 Friedlingstein, T. Gkritzalis, I. Harris, J. Hauck, V. Haverd, M. Hoppema, K. Klein
33 Goldewijk, A.K. Jain, E. Kato, A. Körtzinger, P. Landschützer, N. Lefèvre, A. Lenton, S.
34 Lienert, D. Lombardozzi, J.R. Melton, N. Metzl, F. Millero, P.M.S. Monteiro, D.R. Munro,
35 J.E.M.S. Nabel, S.I. Nakaoka, K. O'Brien, A. Olsen, A.M. Omar, T. Ono, D. Pierrot, B.
36 Poulter, C. Rödenbeck, J. Salisbury, U. Schuster, J. Schwinger, R. Séférian, I. Skjelvan, B.D.

- 1 Stocker, A.J. Sutton, T. Takahashi, H. Tian, B. Tilbrook, I.T. van der Laan-Luijkx, G.R. van
2 der Werf, N. Viovy, A.P. Walker, A.J. Wiltshire, and S. Zaehle, 2016: Global Carbon Budget
3 2016. *Earth System Science Data*, **8**, 605-649. <http://dx.doi.org/10.5194/essd-8-605-2016>
4 www.earth-syst-sci-data.net/8/605/2016/
- 5 le Texier, H., S. Solomon, and R.R. Garcia, 1988: The role of molecular hydrogen and methane
6 oxidation in the water vapour budget of the stratosphere. *Quarterly Journal of the Royal*
7 *Meteorological Society*, **114**, 281-295. <http://dx.doi.org/10.1002/qj.49711448002>
- 8 Lean, J., 1997: The sun's variable radiation and its relevance for earth. *Annual Review of*
9 *Astronomy and Astrophysics*, **35**, 33-67. <http://dx.doi.org/10.1146/annurev.astro.35.1.33>
- 10 Lelieveld, J. and P.J. Crutzen, 1992: Indirect chemical effects of methane on climate warming.
11 *Nature*, **355**, 339-342.
- 12 Lherminier, P., H. Mercier, C. Gourcuff, M. Alvarez, S. Bacon, and C. Kermabon, 2007:
13 Transports across the 2002 Greenland-Portugal Ovide section and comparison with 1997.
14 *Journal of Geophysical Research: Oceans*, **112**, C07003.
15 <http://dx.doi.org/10.1029/2006JC003716>
- 16 Liao, H., Y. Zhang, W.-T. Chen, F. Raes, and J.H. Seinfeld, 2009: Effect of chemistry-aerosol-
17 climate coupling on predictions of future climate and future levels of tropospheric ozone and
18 aerosols. *Journal of Geophysical Research: Atmospheres*, **114**, D10306.
19 <http://dx.doi.org/10.1029/2008JD010984>
- 20 Liljedahl, A.K., J. Boike, R.P. Daanen, A.N. Fedorov, G.V. Frost, G. Grosse, L.D. Hinzman, Y.
21 Iijima, J.C. Jorgenson, N. Matveyeva, M. Necsoiu, M.K. Reynolds, V.E. Romanovsky, J.
22 Schulla, K.D. Tape, D.A. Walker, C.J. Wilson, H. Yabuki, and D. Zona, 2016: Pan-Arctic
23 ice-wedge degradation in warming permafrost and its influence on tundra hydrology. *Nature*
24 *Geoscience*, **9**, 312-318. <http://dx.doi.org/10.1038/ngeo2674>
- 25 Lockwood, M., 2012: Solar Influence on Global and Regional Climates. *Surveys in Geophysics*,
26 **33**, 503-534. <http://dx.doi.org/10.1007/s10712-012-9181-3>
- 27 Loeb, N.G., B.A. Wielicki, D.R. Doelling, G.L. Smith, D.F. Keyes, S. Kato, N. Manalo-Smith,
28 and T. Wong, 2009: Toward Optimal Closure of the Earth's Top-of-Atmosphere Radiation
29 Budget. *Journal of Climate*, **22**, 748-766. <http://dx.doi.org/10.1175/2008JCLI2637.1>
- 30 Löffler, M., S. Brinkop, and P. Jöckel, 2016: Impact of major volcanic eruptions on stratospheric
31 water vapour. *Atmospheric Chemistry and Physics*, **16**, 6547-6562.
32 <http://dx.doi.org/10.5194/acp-16-6547-2016> www.atmos-chem-phys.net/16/6547/2016/

- 1 Lohmann, U. and J. Feichter, 2005: Global indirect aerosol effects: a review. *Atmospheric*
2 *Chemistry and Physics*, **5**, 715-737. <http://dx.doi.org/10.5194/acp-5-715-2005> [www.atmos-](http://www.atmos-chem-phys.net/5/715/2005/)
3 [chem-phys.net/5/715/2005/](http://www.atmos-chem-phys.net/5/715/2005/)
- 4 Lumpkin, R., K.G. Speer, and K.P. Koltermann, 2008: Transport across 48°N in the Atlantic
5 Ocean. *Journal of Physical Oceanography*, **38**, 733-752.
6 <http://dx.doi.org/10.1175/2007jpo3636.1>
- 7 Mahajan, S., K.J. Evans, J.J. Hack, and J.E. Truesdale, 2013: Linearity of Climate Response to
8 Increases in Black Carbon Aerosols. *Journal of Climate*, **26**, 8223-8237.
9 <http://dx.doi.org/10.1175/JCLI-D-12-00715.1>
- 10 Masson-Delmotte, V., M. Schulz, A. Abe-Ouchi, J. Beer, A. Ganopolski, J.F. González Rouco,
11 E. Jansen, K. Lambeck, J. Luterbacher, T. Naish, T. Osborn, B. Otto-Bliesner, T. Quinn, R.
12 Ramesh, M. Rojas, X. Shao, and A. Timmermann, 2013: Information from Paleoclimate
13 Archives. *Climate Change 2013: The Physical Science Basis. Contribution of Working*
14 *Group I to the Fifth Assessment Report of the Intergovernmental Panel on Climate Change*.
15 Stocker, T.F., D. Qin, G.-K. Plattner, M. Tignor, S.K. Allen, J. Boschung, A. Nauels, Y. Xia,
16 V. Bex, and P.M. Midgley, Eds. Cambridge University Press, Cambridge, United Kingdom
17 and New York, NY, USA, 383–464. <http://dx.doi.org/10.1017/CBO9781107415324.013>
18 www.climatechange2013.org
- 19 Matthews, H.D., A.J. Weaver, K.J. Meissner, N.P. Gillett, and M. Eby, 2004: Natural and
20 anthropogenic climate change: incorporating historical land cover change, vegetation
21 dynamics and the global carbon cycle. *Climate Dynamics*, **22**, 461-479.
22 <http://dx.doi.org/10.1007/s00382-004-0392-2>
- 23 Meehl, G.A., W.M. Washington, C.M. Ammann, J.M. Arblaster, T.M.L. Wigley, and C. Tebaldi,
24 2004: Combinations of Natural and Anthropogenic Forcings in Twentieth-Century Climate.
25 *Journal of Climate*, **17**, 3721-3727. [http://dx.doi.org/10.1175/1520-](http://dx.doi.org/10.1175/1520-0442(2004)017<3721:CONAAF>2.0.CO;2)
26 [0442\(2004\)017<3721:CONAAF>2.0.CO;2](http://dx.doi.org/10.1175/1520-0442(2004)017<3721:CONAAF>2.0.CO;2)
- 27 Melillo, J.M., T.C. Richmond, and G.W. Yohe, eds. *Climate Change Impacts in the United*
28 *States: The Third National Climate Assessment*. 2014, U.S. Global Change Research
29 Program: Washington, D.C. 842. <http://dx.doi.org/10.7930/J0Z31WJ2>.
- 30 Morgenstern, O., G. Zeng, N. Luke Abraham, P.J. Telford, P. Braesicke, J.A. Pyle, S.C.
31 Hardiman, F.M. O'Connor, and C.E. Johnson, 2013: Impacts of climate change, ozone
32 recovery, and increasing methane on surface ozone and the tropospheric oxidizing capacity.
33 *Journal of Geophysical Research: Atmospheres*, **118**, 1028-1041.
34 <http://dx.doi.org/10.1029/2012JD018382>

- 1 Morris, G.A., J.E. Rosenfield, M.R. Schoeberl, and C.H. Jackman, 2003: Potential impact of
2 subsonic and supersonic aircraft exhaust on water vapor in the lower stratosphere assessed
3 via a trajectory model. *Journal of Geophysical Research: Atmospheres*, **108**, 4103.
4 <http://dx.doi.org/10.1029/2002JD002614>
- 5 Munk, W. and C. Wunsch, 1998: Abyssal recipes II: energetics of tidal and wind mixing. *Deep*
6 *Sea Research Part I: Oceanographic Research Papers*, **45**, 1977-2010.
7 [http://dx.doi.org/10.1016/S0967-0637\(98\)00070-3](http://dx.doi.org/10.1016/S0967-0637(98)00070-3)
8 www.sciencedirect.com/science/article/pii/S0967063798000703
- 9 Myhre, G., D. Shindell, F.-M. Bréon, W. Collins, J. Fuglestad, J. Huang, D. Koch, J.-F.
10 Lamarque, D. Lee, B. Mendoza, T. Nakajima, A. Robock, G. Stephens, T. Takemura, and H.
11 Zhang, 2013: Anthropogenic and Natural Radiative Forcing. *Climate Change 2013: The*
12 *Physical Science Basis. Contribution of Working Group I to the Fifth Assessment Report of*
13 *the Intergovernmental Panel on Climate Change*. Stocker, T.F., D. Qin, G.-K. Plattner, M.
14 Tignor, S.K. Allen, J. Boschung, A. Nauels, Y. Xia, V. Bex, and P.M. Midgley, Eds.
15 Cambridge University Press, Cambridge, United Kingdom and New York, NY, USA, 659–
16 740. <http://dx.doi.org/10.1017/CBO9781107415324.018> www.climatechange2013.org
- 17 Naik, V., A. Voulgarakis, A.M. Fiore, L.W. Horowitz, J.F. Lamarque, M. Lin, M.J. Prather, P.J.
18 Young, D. Bergmann, P.J. Cameron-Smith, I. Cionni, W.J. Collins, S.B. Dalsøren, R.
19 Doherty, V. Eyring, G. Faluvegi, G.A. Folberth, B. Josse, Y.H. Lee, I.A. MacKenzie, T.
20 Nagashima, T.P.C. van Noije, D.A. Plummer, M. Righi, S.T. Rumbold, R. Skeie, D.T.
21 Shindell, D.S. Stevenson, S. Strode, K. Sudo, S. Szopa, and G. Zeng, 2013: Preindustrial to
22 present-day changes in tropospheric hydroxyl radical and methane lifetime from the
23 Atmospheric Chemistry and Climate Model Intercomparison Project (ACCMIP).
24 *Atmospheric Chemistry and Physics*, **13**, 5277-5298. [http://dx.doi.org/10.5194/acp-13-5277-](http://dx.doi.org/10.5194/acp-13-5277-2013)
25 2013
- 26 Nowack, P.J., N. Luke Abraham, A.C. Maycock, P. Braesicke, J.M. Gregory, M.M. Joshi, A.
27 Osprey, and J.A. Pyle, 2015: A large ozone-circulation feedback and its implications for
28 global warming assessments. *Nature Climate Change*, **5**, 41-45.
29 <http://dx.doi.org/10.1038/nclimate2451>
- 30 Otterå, O.H., M. Bentsen, H. Drange, and L. Suo, 2010: External forcing as a metronome for
31 Atlantic multidecadal variability. *Nature Geoscience*, **3**, 688-694.
32 <http://dx.doi.org/10.1038/ngeo955>
- 33 Pacifico, F., G.A. Folberth, C.D. Jones, S.P. Harrison, and W.J. Collins, 2012: Sensitivity of
34 biogenic isoprene emissions to past, present, and future environmental conditions and
35 implications for atmospheric chemistry. *Journal of Geophysical Research*, **117**, D22302.
36 <http://dx.doi.org/10.1029/2012JD018276>

- 1 Passow, U. and C.A. Carlson, 2012: The biological pump in a high CO₂ world. *Marine Ecology*
2 *Progress Series*, **470**, 249-271. www.int-res.com/abstracts/meps/v470/p249-271/
- 3 Pistone, K., I. Eisenman, and V. Ramanathan, 2014: Observational determination of albedo
4 decrease caused by vanishing Arctic sea ice. *Proceedings of the National Academy of*
5 *Sciences*, **111**, 3322-3326. <http://dx.doi.org/10.1073/pnas.1318201111>
- 6 Quaas, J., Y. Ming, S. Menon, T. Takemura, M. Wang, J.E. Penner, A. Gettelman, U. Lohmann,
7 N. Bellouin, O. Boucher, A.M. Sayer, G.E. Thomas, A. McComiskey, G. Feingold, C.
8 Hoose, J.E. Kristjánsson, X. Liu, Y. Balkanski, L.J. Donner, P.A. Ginoux, P. Stier, B.
9 Grandey, J. Feichter, I. Sednev, S.E. Bauer, D. Koch, R.G. Grainger, Kirkev, aring, A. g, T.
10 Iversen, Ø. Seland, R. Easter, S.J. Ghan, P.J. Rasch, H. Morrison, J.F. Lamarque, M.J.
11 Iacono, S. Kinne, and M. Schulz, 2009: Aerosol indirect effects – general circulation model
12 intercomparison and evaluation with satellite data. *Atmospheric Chemistry and Physics*, **9**,
13 8697-8717. <http://dx.doi.org/10.5194/acp-9-8697-2009> [www.atmos-chem-](http://www.atmos-chem-phys.net/9/8697/2009/)
14 [phys.net/9/8697/2009/](http://www.atmos-chem-phys.net/9/8697/2009/)
- 15 Rädcl, G., T. Mauritsen, B. Stevens, D. Dommenges, D. Matei, K. Bellomo, and A. Clement,
16 2016: Amplification of El Nino by cloud longwave coupling to atmospheric circulation.
17 *Nature Geoscience*, **9**, 106-110. <http://dx.doi.org/10.1038/ngeo2630>
- 18 Raes, F., H. Liao, W.-T. Chen, and J.H. Seinfeld, 2010: Atmospheric chemistry-climate
19 feedbacks. *Journal of Geophysical Research*, **115**, D12121.
20 <http://dx.doi.org/10.1029/2009JD013300>
- 21 Rahmstorf, S., J.E. Box, G. Feulner, M.E. Mann, A. Robinson, S. Rutherford, and E.J.
22 Schaffernicht, 2015: Exceptional twentieth-century slowdown in Atlantic Ocean overturning
23 circulation. *Nature Climate Change*, **5**, 475-480. <http://dx.doi.org/10.1038/nclimate2554>
- 24 Rhein, M., S.R. Rintoul, S. Aoki, E. Campos, D. Chambers, R.A. Feely, S. Gulev, G.C. Johnson,
25 S.A. Josey, A. Kostianoy, C. Mauritzen, D. Roemmich, L.D. Talley, and F. Wang, 2013:
26 Observations: Ocean. *Climate Change 2013: The Physical Science Basis. Contribution of*
27 *Working Group I to the Fifth Assessment Report of the Intergovernmental Panel on Climate*
28 *Change*. Stocker, T.F., D. Qin, G.-K. Plattner, M. Tignor, S.K. Allen, J. Boschung, A.
29 Nauels, Y. Xia, V. Bex, and P.M. Midgley, Eds. Cambridge University Press, Cambridge,
30 United Kingdom and New York, NY, USA, 255–316.
31 <http://dx.doi.org/10.1017/CBO9781107415324.010> www.climatechange2013.org
- 32 Rignot, E., M. Koppes, and I. Velicogna, 2010: Rapid submarine melting of the calving faces of
33 West Greenland glaciers. *Nature Geoscience*, **3**, 187-191. <http://dx.doi.org/10.1038/ngeo765>
- 34 Rignot, E. and R.H. Thomas, 2002: Mass Balance of Polar Ice Sheets. *Science*, **297**, 1502-1506.
35 <http://dx.doi.org/10.1126/science.1073888>

- 1 Robock, A., 2000: Volcanic eruptions and climate. *Reviews of Geophysics*, **38**, 191-219.
2 <http://dx.doi.org/10.1029/1998RG000054>
- 3 Rosenfeld, D., M.O. Andreae, A. Asmi, M. Chin, G. de Leeuw, D.P. Donovan, R. Kahn, S.
4 Kinne, N. Kivekäs, M. Kulmala, W. Lau, K.S. Schmidt, T. Suni, T. Wagner, M. Wild, and J.
5 Quaas, 2014: Global observations of aerosol-cloud-precipitation-climate interactions.
6 *Reviews of Geophysics*, **52**, 750-808. <http://dx.doi.org/10.1002/2013RG000441>
- 7 Rosenlof, K.H., S.J. Oltmans, D. Kley, J.M. Russell, E.W. Chiou, W.P. Chu, D.G. Johnson, K.K.
8 Kelly, H.A. Michelsen, G.E. Nedoluha, E.E. Remsberg, G.C. Toon, and M.P. McCormick,
9 2001: Stratospheric water vapor increases over the past half-century. *Geophysical Research*
10 *Letters*, **28**, 1195-1198. <http://dx.doi.org/10.1029/2000GL012502>
- 11 Rousseaux, C.S. and W.W. Gregg, 2015: Recent decadal trends in global phytoplankton
12 composition. *Global Biogeochemical Cycles*, **29**, 1674-1688.
13 <http://dx.doi.org/10.1002/2015GB005139>
- 14 Schaefer, K., H. Lantuit, E.R. Vladimir, E.A.G. Schuur, and R. Witt, 2014: The impact of the
15 permafrost carbon feedback on global climate. *Environmental Research Letters*, **9**, 085003.
16 <http://dx.doi.org/10.1088/1748-9326/9/8/085003>
- 17 Schanze, J.J., R.W. Schmitt, and L.L. Yu, 2010: The global oceanic freshwater cycle: A state-of-
18 the-art quantification. *Journal of Marine Research*, **68**, 569-595.
19 <http://dx.doi.org/10.1357/002224010794657164>
- 20 Schoof, C., 2010: Ice-sheet acceleration driven by melt supply variability. *Nature*, **468**, 803-806.
21 <http://dx.doi.org/10.1038/nature09618>
- 22 Schuur, E.A.G., A.D. McGuire, C. Schadel, G. Grosse, J.W. Harden, D.J. Hayes, G. Hugelius,
23 C.D. Koven, P. Kuhry, D.M. Lawrence, S.M. Natali, D. Olefeldt, V.E. Romanovsky, K.
24 Schaefer, M.R. Turetsky, C.C. Treat, and J.E. Vonk, 2015: Climate change and the
25 permafrost carbon feedback. *Nature*, **520**, 171-179. <http://dx.doi.org/10.1038/nature14338>
- 26 Sejas, S.A., M. Cai, A. Hu, G.A. Meehl, W. Washington, and P.C. Taylor, 2014: Individual
27 Feedback Contributions to the Seasonality of Surface Warming. *Journal of Climate*, **27**,
28 5653-5669. <http://dx.doi.org/10.1175/JCLI-D-13-00658.1>
- 29 Seppälä, A., K. Matthes, C.E. Randall, and I.A. Mironova, 2014: What is the solar influence on
30 climate? Overview of activities during CAWSES-II. *Progress in Earth and Planetary*
31 *Science*, **1**, 1-12. <http://dx.doi.org/10.1186/s40645-014-0024-3>
- 32 Shindell, D. and G. Faluvegi, 2009: Climate response to regional radiative forcing during the
33 twentieth century. *Nature Geoscience*, **2**, 294-300. <http://dx.doi.org/10.1038/ngeo473>

- Shiogama, H., D.A. Stone, T. Nagashima, T. Nozawa, and S. Emori, 2013: On the linear additivity of climate forcing-response relationships at global and continental scales. *International Journal of Climatology*, **33**, 2542-2550. <http://dx.doi.org/10.1002/joc.3607>
- Skiba, U.M. and R.M. Rees, 2014: Nitrous oxide, climate change and agriculture. *CAB Reviews*, **9**, 7. <http://dx.doi.org/10.1079/PAVSNNR20149010>
- Smith, G.L., B.R. Barkstrom, E.F. Harrison, R.B. Lee, and B.A. Wielicki, 1994: Radiation budget measurements for the eighties and nineties. *Advances in Space Research*, **14**, 81-84. [http://dx.doi.org/10.1016/0273-1177\(94\)90351-4](http://dx.doi.org/10.1016/0273-1177(94)90351-4)
www.sciencedirect.com/science/article/pii/0273117794903514
- Smith, W.K., S.C. Reed, C.C. Cleveland, A.P. Ballantyne, W.R.L. Anderegg, W.R. Wieder, Y.Y. Liu, and S.W. Running, 2016: Large divergence of satellite and Earth system model estimates of global terrestrial CO₂ fertilization. *Nature Climate Change*, **6**, 306-310. <http://dx.doi.org/10.1038/nclimate2879>
- Soden, B.J. and I.M. Held, 2006: An Assessment of Climate Feedbacks in Coupled Ocean–Atmosphere Models. *Journal of Climate*, **19**, 3354-3360. <http://dx.doi.org/10.1175/JCLI3799.1>
- Sohn, B.J., T. Nakajima, M. Satoh, and H.S. Jang, 2010: Impact of different definitions of clear-sky flux on the determination of longwave cloud radiative forcing: NICAM simulation results. *Atmospheric Chemistry and Physics*, **10**, 11641-11646. <http://dx.doi.org/10.5194/acp-10-11641-2010>
- Solomon, S., K.H. Rosenlof, R.W. Portmann, J.S. Daniel, S.M. Davis, T.J. Sanford, and G.-K. Plattner, 2010: Contributions of Stratospheric Water Vapor to Decadal Changes in the Rate of Global Warming. *Science*, **327**, 1219-1223. <http://dx.doi.org/10.1126/science.1182488>
- Steinacher, M., F. Joos, T.L. Frölicher, L. Bopp, P. Cadule, V. Cocco, S.C. Doney, M. Gehlen, K. Lindsay, and J.K. Moore, 2010: Projected 21st century decrease in marine productivity: A multi-model analysis. *Biogeosciences*, **7**, 979-1005. <http://dx.doi.org/10.5194/bg-7-979-2010>
- Stenchikov, G., T.L. Delworth, V. Ramaswamy, R.J. Stouffer, A. Wittenberg, and F. Zeng, 2009: Volcanic signals in oceans. *Journal of Geophysical Research*, **114**, D16104. <http://dx.doi.org/10.1029/2008JD011673>
- Stevens, B. and G. Feingold, 2009: Untangling aerosol effects on clouds and precipitation in a buffered system. *Nature*, **461**, 607-613.
- Swartz, W.H., R.S. Stolarski, L.D. Oman, E.L. Fleming, and C.H. Jackman, 2012: Middle atmosphere response to different descriptions of the 11-yr solar cycle in spectral irradiance in

- 1 a chemistry-climate model. *Atmospheric Chemistry and Physics*, **12**, 5937-5948.
2 <http://dx.doi.org/10.5194/acp-12-5937-2012>
- 3 Taylor, P.C., R.G. Ellingson, and M. Cai, 2011: Geographical Distribution of Climate Feedbacks
4 in the NCAR CCSM3.0. *Journal of Climate*, **24**, 2737-2753.
5 <http://dx.doi.org/10.1175/2010JCLI3788.1>
- 6 Taylor, P.C., S. Kato, K.-M. Xu, and M. Cai, 2015: Covariance between Arctic sea ice and
7 clouds within atmospheric state regimes at the satellite footprint level. *Journal of*
8 *Geophysical Research: Atmospheres*, **120**, 12656-12678.
9 <http://dx.doi.org/10.1002/2015JD023520>
- 10 Thornton, P.E., J.-F. Lamarque, N.A. Rosenbloom, and N.M. Mahowald, 2007: Influence of
11 carbon-nitrogen cycle coupling on land model response to CO₂ fertilization and climate
12 variability. *Global Biogeochemical Cycles*, **21**, GB4018.
13 <http://dx.doi.org/10.1029/2006GB002868>
- 14 Trenberth, K.E., P.D. Jones, P. Ambenje, R. Bojariu, D. Easterling, A.K. Tank, D. Parker, F.
15 Rahimzadeh, J.A. Renwick, M. Rusticucci, B. Soden, and P. Zhai, 2007: Observations:
16 Surface and atmospheric climate change. *Climate Change 2007: The Physical Science Basis.*
17 *Contribution of Working Group I to the Fourth Assessment Report of the Intergovernmental*
18 *Panel on Climate Change*. Solomon, S., D. Qin, M. Manning, Z. Chen, M. Marquis, K.B.
19 Averyt, M. Tignor, and H.L. Miller, Eds. Cambridge University Press, Cambridge, United
20 Kingdom and New York, NY, USA.
21 www.ipcc.ch/publications_and_data/ar4/wg1/en/ch3.html
- 22 Twohy, C.H., M.D. Petters, J.R. Snider, B. Stevens, W. Tahnk, M. Wetzel, L. Russell, and F.
23 Burnet, 2005: Evaluation of the aerosol indirect effect in marine stratocumulus clouds:
24 Droplet number, size, liquid water path, and radiative impact. *Journal of Geophysical*
25 *Research: Atmospheres*, **110**, D08203. <http://dx.doi.org/10.1029/2004JD005116>
- 26 Unger, N., S. Menon, D.M. Koch, and D.T. Shindell, 2009: Impacts of aerosol-cloud interactions
27 on past and future changes in tropospheric composition. *Atmospheric Chemistry and Physics*,
28 **9**, 4115-4129. <http://dx.doi.org/10.5194/acp-9-4115-2009> [www.atmos-chem-](http://www.atmos-chem-phys.net/9/4115/2009/)
29 [phys.net/9/4115/2009/](http://www.atmos-chem-phys.net/9/4115/2009/)
- 30 van den Broeke, M., J. Bamber, J. Ettema, E. Rignot, E. Schrama, W.J. van de Berg, E. van
31 Meijgaard, I. Velicogna, and B. Wouters, 2009: Partitioning Recent Greenland Mass Loss.
32 *Science*, **326**, 984-986. <http://dx.doi.org/10.1126/science.1178176>
- 33 Vial, J., J.-L. Dufresne, and S. Bony, 2013: On the interpretation of inter-model spread in CMIP5
34 climate sensitivity estimates. *Climate Dynamics*, **41**, 3339-3362.
35 <http://dx.doi.org/10.1007/s00382-013-1725-9>

- 1 Voulgarakis, A., V. Naik, J.F. Lamarque, D.T. Shindell, P.J. Young, M.J. Prather, O. Wild, R.D.
2 Field, D. Bergmann, P. Cameron-Smith, I. Cionni, W.J. Collins, S.B. Dalsøren, R.M.
3 Doherty, V. Eyring, G. Faluvegi, G.A. Folberth, L.W. Horowitz, B. Josse, I.A. MacKenzie,
4 T. Nagashima, D.A. Plummer, M. Righi, S.T. Rumbold, D.S. Stevenson, S.A. Strode, K.
5 Sudo, S. Szopa, and G. Zeng, 2013: Analysis of present day and future OH and methane
6 lifetime in the ACCMIP simulations. *Atmospheric Chemistry and Physics*, **13**, 2563-2587.
7 <http://dx.doi.org/10.5194/acp-13-2563-2013>
- 8 Wenzel, S., P.M. Cox, V. Eyring, and P. Friedlingstein, 2016: Projected land photosynthesis
9 constrained by changes in the seasonal cycle of atmospheric CO₂. *Nature*, **538**, 499-501.
10 <http://dx.doi.org/10.1038/nature19772>
- 11 Wieder, W.R., C.C. Cleveland, W.K. Smith, and K. Todd-Brown, 2015: Future productivity and
12 carbon storage limited by terrestrial nutrient availability. *Nature Geoscience*, **8**, 441-444.
13 <http://dx.doi.org/10.1038/ngeo2413>
- 14 Wielicki, B.A., B.R. Barkstrom, E.F. Harrison, R.B.L. III, G.L. Smith, and J.E. Cooper, 1996:
15 Clouds and the Earth's Radiant Energy System (CERES): An Earth Observing System
16 Experiment. *Bulletin of the American Meteorological Society*, **77**, 853-868.
17 [http://dx.doi.org/10.1175/1520-0477\(1996\)077<0853:catere>2.0.co;2](http://dx.doi.org/10.1175/1520-0477(1996)077<0853:catere>2.0.co;2)
- 18 Wielicki, B.A., E.F. Harrison, R.D. Cess, M.D. King, and D.A. Randall, 1995: Mission to Planet
19 Earth: Role of Clouds and Radiation in Climate. *Bulletin of the American Meteorological*
20 *Society*, **76**, 2125-2153. [http://dx.doi.org/10.1175/1520-](http://dx.doi.org/10.1175/1520-0477(1995)076<2125:mtpero>2.0.co;2)
21 [0477\(1995\)076<2125:mtpero>2.0.co;2](http://dx.doi.org/10.1175/1520-0477(1995)076<2125:mtpero>2.0.co;2)
- 22 Winton, M., 2006: Surface Albedo Feedback Estimates for the AR4 Climate Models. *Journal of*
23 *Climate*, **19**, 359-365. <http://dx.doi.org/10.1175/JCLI3624.1>
- 24 WMO, 2014: Scientific Assessment of Ozone Depletion: 2014. 416 pp. World Meteorological
25 Organization Geneva, Switzerland. <http://www.esrl.noaa.gov/csd/assessments/ozone/2014/>
- 26 Xu, J. and A.M. Powell, 2013: What happened to surface temperature with sunspot activity in the
27 past 130 years? *Theoretical and Applied Climatology*, **111**, 609-622.
28 <http://dx.doi.org/10.1007/s00704-012-0694-y>
- 29 Zanchettin, D., C. Timmreck, H.-F. Graf, A. Rubino, S. Lorenz, K. Lohmann, K. Krüger, and
30 J.H. Jungclaus, 2012: Bi-decadal variability excited in the coupled ocean-atmosphere system
31 by strong tropical volcanic eruptions. *Climate Dynamics*, **39**, 419-444.
32 <http://dx.doi.org/10.1007/s00382-011-1167-1>
- 33 Zhai, P.-W., Y. Hu, C.A. Hostetler, B. Cairns, R.A. Ferrare, K.D. Knobelspiesse, D.B. Josset,
34 C.R. Trepte, P.L. Lucker, and J. Chowdhary, 2013: Uncertainty and interpretation of aerosol
35 remote sensing due to vertical inhomogeneity. *Journal of Quantitative Spectroscopy and*

- 1 *Radiative Transfer*, **114**, 91-100. <http://dx.doi.org/10.1016/j.jqsrt.2012.08.006>
2 www.sciencedirect.com/science/article/pii/S0022407312003706
- 3 Zhang, D., R. Blender, and K. Fraedrich, 2013: Volcanoes and ENSO in millennium simulations:
4 global impacts and regional reconstructions in East Asia. *Theoretical and Applied*
5 *Climatology*, **111**, 437-454. <http://dx.doi.org/10.1007/s00704-012-0670-6>

DRAFT

3. Detection and Attribution of Climate Change

Key Findings

1. The *likely* range of the human contribution to the global mean temperature increase over the period 1951–2010 is 1.1° to 1.3°F (0.6° to 0.7°C), which is close to the observed warming of 1.2°F (0.65°C) (*high confidence*). It is *extremely likely* that more than half of the global mean temperature increase since 1951 was caused by human influence on climate (*high confidence*). The estimated influence of natural forcing and internal variability on global temperatures over that period is minor (*high confidence*)

3.1 Introduction

Detection and attribution of climate change involves assessing the causes of observed changes in the climate system through systematic comparison of climate models and observations using various statistical methods. Attributing an observed change or an event partly to a causal factor (such as anthropogenic climate forcing) normally requires that the change first be detectable (Hegerl et al. 2010). A detectable change is one in which an observed change is distinguishable from natural variability in some defined statistical sense, again without necessarily ascribing a cause. An attributable change refers to a change in which the relative contribution of causal factors has been evaluated along with an assignment of statistical confidence (e.g., Bindoff et al. 2013; Hegerl et al. 2010).

More confident statements about attribution are underpinned by a thorough understanding of the physical processes involved. Since the release of the Intergovernmental Panel on Climate Change's Fifth Assessment Report (IPCC AR5) and the Third National Climate Assessment (NCA3; Melillo et al. 2014), there have been some advances in the science of detection and attribution of climate change. The IPCC AR5 presented an assessment of detection and attribution research at the global to regional scale (Bindoff et al. 2013) which is briefly summarized here. An emerging area in the science of detection and attribution is the attribution of extreme weather and climate events (NAS 2016; Stott 2016; Easterling et al. 2016).

A growing number of climate change and extreme event attribution studies use a multi-step attribution (Hegerl et al. 2010) or attribution without detection approaches. These are methods that attribute a climate change or a change in the likelihood of occurrence of an event to a causal factor without detecting a change in the phenomenon itself. Detection, for example, would mean demonstrating that a long-term trend or change in a phenomenon is highly unusual compared to natural variability. For the multi-step approach, the attribution may be based on a change in climate conditions that are closely related to a given type of event. As an example, some attribution statements for phenomena such as droughts or hurricane activity—where there are not necessarily detectable trends—are based on models and on detected changes in related variables such as surface temperature, as well as an understanding of the relevant physical processes.

Possible anthropogenic influence on an extreme event can be assessed using a risk-based approach, which examines whether the odds of occurrence of a type of extreme event have changed, or through an ingredients-based or conditional attribution approach. In the latter case, for example, an investigator may look for changes in occurrence of atmospheric circulation and weather patterns relevant to the extreme event, or at the impact of certain environmental changes (for example, greater atmospheric moisture) on the character of an extreme event (Trenberth et al. 2015; Shepherd 2016; Horton et al. 2016). An example of the conditional attribution approach, as applied to Hurricane Sandy, assumes that the weather patterns in which the storm was embedded, and the storm itself, could have occurred in a preindustrial climate, and the event is re-simulated changing only some aspects of the large-scale environment (for example, sea surface temperatures, atmospheric temperatures and moisture) by an estimated anthropogenic climate change signal. One study using this approach found that anthropogenic climate change to date did not have a statistically significant influence on the intensity of Hurricane Sandy (Lackmann 2015).

There are reasons why attribution without detection statements can be appropriate, despite the lower confidence typically associated with such statements as compared to attribution statements that are supported by detection of a change in the phenomenon itself. The event may be so rare that a trend analysis for similar events is not practical. Including attribution without detection events in analysis of climate change impacts reduces the chances of a false negative, that is, incorrectly concluding that climate change had no influence on a given extreme events (Anderegg et al. 2014) in a case where it did have an influence. However, avoiding this type of error through attribution without detection comes at the risk of increasing the rate of false positives, where one incorrectly concludes that anthropogenic climate change had a certain type of influence on an extreme event when in fact it did not have such an influence.

Review of Key Detection and Attribution Findings in IPCC AR5

Key attribution assessment results for global mean temperature are summarized in Figure 3.1 (from Bindoff et al. 2013), which shows assessed likely ranges and midpoint estimates for several factors contributing to increases in global mean temperature. According to Bindoff et al., it is extremely likely that anthropogenic forcings caused more than half of the warming for 1951–2010, with a likely contribution range of 0.6° to 0.7°C (1.1°F to 1.3°F), compared with the observed warming of about 0.65°C (1.2°F). The estimated likely contribution ranges for natural forcing and internal variability were both much smaller (–0.1° to 0.1°C, or –0.2° to 0.2°F).

[INSERT FIGURE 3.1 HERE:]

Figure 3.1: Attributable warming likely ranges (bar-whisker plots) and midpoint values (colored bars) for global mean temperature trends (degrees Celsius) over 1951–2010 from IPCC AR5 (Bindoff et al. 2013). Observations are from HadCRUT4, along with observational uncertainty (5% to 95%) error bars (Morice et al. 2012). GHG refers to well-mixed greenhouse gases, OA to other anthropogenic forcings, NAT to natural forcings, and ANT to all anthropogenic forcings

combined. The ranges within which the true value is extremely likely to occur are broader than the likely ranges shown in the figure, which is why the term “more than half” is used to characterize the fraction of warming that is *extremely likely* due on anthropogenic influence, despite the fact that the midpoint of the likely range of the anthropogenic forcing contribution is close to the observed warming value. Likely ranges are broader for contributions from well-mixed greenhouse gases or other anthropogenic forcings, assessed separately, than for the contributions from all anthropogenic forcings, as it is more difficult to quantitatively constrain the separate contributions of the various anthropogenic forcing agents. (Figure source: redrawn from Bindoff et al. 2013; © IPCC. Used with permission.)]

Likely or very likely attributable human contributions have also been reported by IPCC AR5 for warming over all continents except Antarctica, and, globally, changes in daily temperature extremes, ocean surface and subsurface temperature and salinity, and sea level pressure patterns; Arctic sea ice loss; northern hemispheric snow cover decrease; global mean sea level rise; and ocean acidification (Bindoff et al. 2013). IPCC AR5 also reported medium confidence in anthropogenic contributions to increased atmospheric specific humidity, zonal mean precipitation over northern hemisphere mid to high latitudes, and intensification or heavy precipitation over land regions. IPCC AR5 had weaker attribution conclusions than IPCC AR4 on some phenomena, including tropical cyclone and drought changes. The present assessment does not change any of the IPCC AR5 conclusions, although we make some additional attribution statements in the relevant chapters of this report regarding regional temperature, extreme precipitation, and flooding frequency increases over parts of the United States.

3.2 Extreme Event Attribution

Attribution of extreme weather events under a changing climate is an important aspect of climate science. The European heat wave of 2003 (Stott et al. 2004) and Australia’s extreme temperatures and heat indices of 2013 (e.g., Arblaster et al. 2014; King et al. 2014; Knutson et al. 2014; Lewis and Karoly 2014; Perkins et al. 2014) are examples of extreme weather or climate events where relatively strong evidence for a human contribution to the event has been found for cases outside of the United States. The science of event attribution for weather and climate extremes over the United States has also significantly evolved since the NCA3. For example, following several extreme climate events, such as the 2011 Texas heat wave and drought or the recent/ongoing California drought, investigators have attempted to determine, using various methods discussed in this chapter, whether human-caused climate change contributed to the event. Several recent reports have extensively reviewed the topic of extreme event attribution (NAS 2016; Easterling et al. 2016). While this topic cannot be comprehensively reviewed here, a few highlighted statements from the National Academy of Sciences study (NAS 2016) are given here:

- Event attribution is more reliable when based on sound physical principles, consistent evidence from observations, and numerical models that can replicate the event.

- Confidence in attribution findings of anthropogenic influence is greatest for extreme events that are related to an aspect of temperature.
- Statements about attribution are sensitive to the way the questions are posed (that is, framing)

In addition, the National Academies noted that conclusions would be more robust in cases where observed changes in the event being examined are consistent with expectations from model-based attribution studies. Typically, there is less confidence in such an attribution-without-detection statement than one where a detectable anthropogenic influence (for example, a detectable and attributable long-term trend or increase in variability) on the phenomenon itself had also been demonstrated. An example would be stating that a change in the probability or magnitude of a heat wave in the southeastern United States was attributable to greenhouse gases when there is not a detectable trend in either long-term temperature or in temperature variability in the data in that region, as discussed below. No extreme weather event observed to date has been found to have zero probability of occurrence in a preindustrial climate according to climate model simulations. Therefore, the causes of attributed extreme events are a combination of natural variations in the climate system compounded (or alleviated) by the anthropogenic change to the climate system. Event attribution statements quantify the relative contribution of these human and natural causal factors.

As an example illustrating different methods of event attribution, for the 2011 Texas heat wave/meteorological drought, Hoerling et al. (2013) found that the event was primarily caused by antecedent and concurrent negative rainfall anomalies due mainly to natural variability and the La Niña conditions at the time of the event, but with a relatively small (not detected) warming contribution from anthropogenic forcing. The anthropogenic contribution nonetheless doubled the chances of reaching a new temperature record in 2011 compared to the 1981–2010 reference period, according to their study. Rupp et al. (2012), meanwhile, concluded that extreme heat events in Texas were about 20 times more likely for 2008 La Niña conditions than similar conditions during the 1960s. This pair of studies illustrates how the framing of the attribution question can matter. The Hoerling et al. analysis focused more on what caused most of the magnitude of the anomalies, whereas Rupp et al. focused more on the changes in the probability of the event. Otto et al. (2012) show how such approaches can give seemingly conflicting results yet have no fundamental contradiction. In this case, we conclude that there is *medium* confidence that anthropogenic forcing contributed to the Texas heat wave of 2011, both in terms of a small contribution to the anomaly magnitude and a significant increase in the probability of occurrence of the event.

In this report, we do not assess all individual weather or climate extreme events for which an attributable anthropogenic climate change has been claimed in a published study, as there are now many such studies. A few selected individual United States studies are discussed in more

1 detail either in this chapter or in Chapters 6, 7, 8, and 9, which focus on particular weather and
2 climate phenomena.

3 3.3 Updated Detection and Attribution Summaries

4 In general, detection and attribution at regional scales are more challenging than at the global
5 scale for a number of reasons. Regional changes typically have smaller signal-to-noise ratios
6 than changes at global scales. Also, there is less spatial pattern information for distinguishing
7 contributions from different forcings. Omitted forcings in climate models, such as land-use
8 change, could be more important at regional scales, and simulated internal variability may be less
9 reliable (Bindoff et al. 2013).

10 In the various phenomena chapters of this report, updated detection attribution statements
11 focusing on the United States region are presented.

DRAFT

TRACEABLE ACCOUNTS

Key Finding 1

The *likely* range of the human contribution to the global mean temperature increase over the period 1951–2010 is 1.1° to 1.3°F (0.6° to 0.7°C), which is close to the observed warming of 1.2°F (0.65°C) (*high confidence*). It is *extremely likely* that more than half of the global mean temperature increase since 1951 was caused by human influence on climate (*high confidence*). The estimated influence of natural forcing and internal variability on global temperatures over that period is minor (*high confidence*).

Description of evidence base

This Key Finding summarizes key detection and attribution evidence documented in the climate science literature and in the IPCC AR5 (Bindoff et al. 2013), and references therein. The Key Finding is essentially the same as the summary assessment of IPCC AR5. The attribution of temperature increases since 1951 is based on the detection and attribution analyses of Gillett et al. (2013), Jones et al. (2013), and consideration of Ribes and Terray (2013), Huber and Knutti (2011), Wigley and Santer (2013), and IPCC AR4 (Hegerl et al. 2007). The estimated potential influence of internal variability is based on Knutson et al. (2013) and Huber and Knutti (2011), with consideration of the above references. Moreover, simulated global temperature multidecadal variability is assessed to be adequate (Bindoff et al. 2013), with *high confidence* that models reproduce global and northern hemisphere temperature variability across a range of timescales (Flato et al. 2013). Further support for these assessments comes from paleoclimate data (Masson-Delmotte et al. 2013) and physical understanding of the climate system (IPCC 2013). A more detailed traceable account is contained in Bindoff et al. (2013). Post IPCC AR5 supporting evidence includes additional analyses showing unusual nature of observed global warming compared to simulated internal climate variability (Knutson et al., in press) and recent occurrence of new record high global mean temperatures, consistent with model projections of continued warming on multidecadal scales (for example, Chapter 1).

Major uncertainties

The transient climate response (TCR) is defined as the global mean surface temperature change at the time of CO₂ doubling in a 1%/year CO₂ transient increase experiment. The TCR of the climate system to greenhouse gas increases remains uncertain, with ranges of 0.9° to 2.0°C (1.6° to 3.6°F) and 0.9° to 2.5°C (1.6° to 4.5°F) in two recent assessments (Otto et al. 2013 and Lewis and Curry 2014, respectively). The climate system response to aerosol forcing (direct and indirect effects combined) remains highly uncertain (Myhre et al. 2013), because although more of the relevant processes are being included in models, confidence in these representations remains low (Boucher et al. 2013). Therefore, there is considerable uncertainty in quantifying the attributable warming contributions of greenhouse gases and aerosols separately. There is uncertainty in the possible levels of internal climate variability, but current estimates (likely range of $\pm 0.1^{\circ}\text{C}$, or 0.2°F , over 60 years) would have to be too low by more than a factor or

two or three for the observed trend to be explainable by internal variability (e.g., Knutson et al. 2013; Huber and Knutti 2011).

Assessment of confidence based on evidence and agreement, including short description of nature of evidence and level of agreement

☒ Very High

☒ High

☐ Medium

☐ Low

There is *very high confidence* that global temperature has been increasing and that anthropogenic forcings have played a major role in the increase observed over the past 60 years, with strong evidence from several studies using well-established detection and attribution techniques. There is *high confidence* that the role of internal variability is minor, as climate models simulate only a minor role and the models have been assessed as adequate for the purpose of estimating the potential role of internal variability.

If appropriate, estimate likelihood of impact or consequence, including short description of basis of estimate

☒ Greater than 9 in 10 / Very Likely

☐ Greater than 2 in 3 / Likely

☐ About 1 in 2 / As Likely as Not

☐ Less than 1 in 3 / Unlikely

☐ Less than 1 in 10 / Very Unlikely

Summary sentence or paragraph that integrates the above information

Detection and attribution studies, climate models, observations, paleoclimate data, and physical understanding lead to *high confidence (extremely likely)* that more half of the observed global mean warming since 1951 was caused by humans, and *high confidence* that internal climate variability played only a minor role (and possibly even a negative contribution) in the observed warming. The key message and supporting text summarizes extensive evidence documented in the peer-reviewed detection and attribution literature, including in the IPCC AR5.

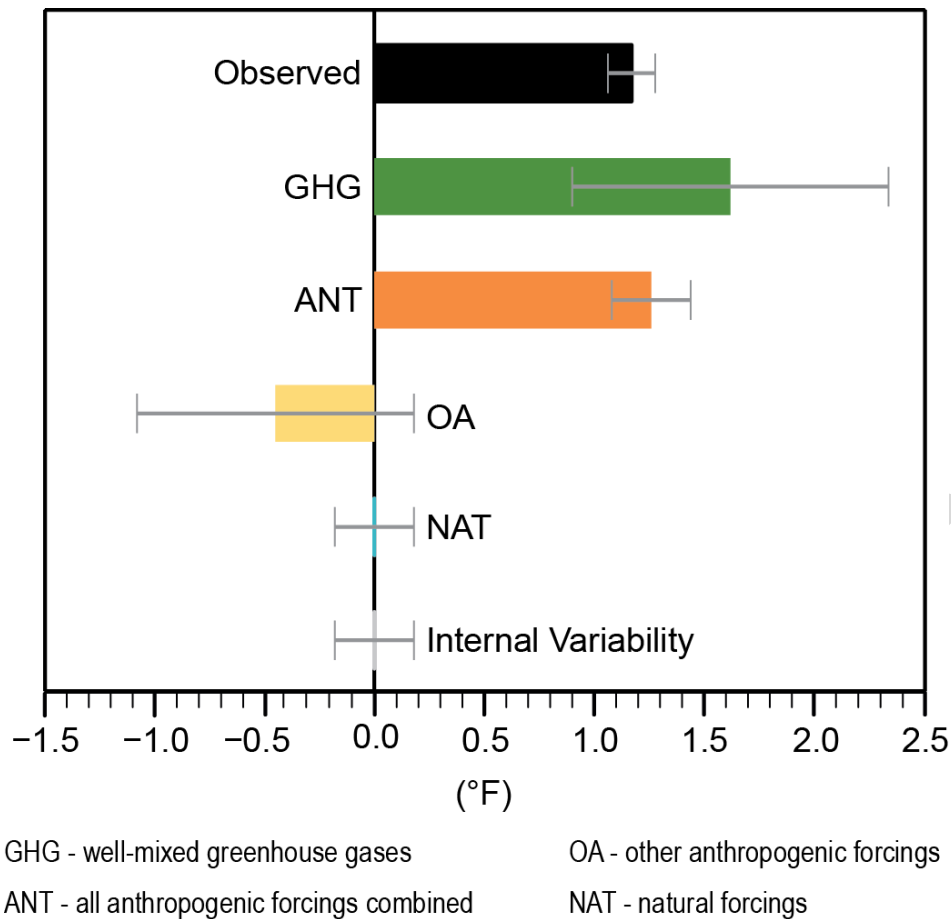
1 **FIGURES**

Figure 3.1: Attributable warming likely ranges (bar-whisker plots) and midpoint values (colored bars) for global mean temperature trends (degrees Celsius) over 1951–2010 from IPCC AR5 (Bindoff et al. 2013). Observations are from HadCRUT4, along with observational uncertainty (5% to 95%) error bars (Morice et al. 2012). GHG refers to well-mixed greenhouse gases, OA to other anthropogenic forcings, NAT to natural forcings, and ANT to all anthropogenic forcings combined. The ranges within which the true value is extremely likely to occur are broader than the likely ranges shown in the figure, which is why the term “more than half” is used to characterize the fraction of warming that is *extremely likely* due on anthropogenic influence, despite the fact that the midpoint of the likely range of the anthropogenic forcing contribution is close to the observed warming value. Likely ranges are broader for contributions from well-mixed greenhouse gases or other anthropogenic forcings, assessed separately, than for the contributions from all anthropogenic forcings, as it is more difficult to quantitatively constrain the separate contributions of the various anthropogenic forcing agents. (Figure source: redrawn from Bindoff et al. 2013; © IPCC. Used with permission.)

REFERENCES

- Anderegg, W.R.L., E.S. Callaway, M.T. Boykoff, G. Yohe, and T.y.L. Root, 2014: Awareness of both type 1 and 2 errors in climate science and assessment. *Bulletin of the American Meteorological Society*, **95**, 1445-1451. <http://dx.doi.org/10.1175/BAMS-D-13-00115.1>
- Arblaster, J.M., E.-P. Lim, H.H. Hendon, B.C. Trewin, M.C. Wheeler, G. Liu, and K. Braganza, 2014: Understanding Australia's hottest September on record [in "Explaining Extremes of 2013 from a Climate Perspective"]. *Bulletin of the American Meteorological Society*, **95**, S37-S41. <http://dx.doi.org/10.1175/1520-0477-95.9.S1.1>
- Bindoff, N.L., P.A. Stott, K.M. AchutaRao, M.R. Allen, N. Gillett, D. Gutzler, K. Hansingo, G. Hegerl, Y. Hu, S. Jain, I.I. Mokhov, J. Overland, J. Perlwitz, R. Sebbari, and X. Zhang, 2013: Detection and Attribution of Climate Change: from Global to Regional. *Climate Change 2013: The Physical Science Basis. Contribution of Working Group I to the Fifth Assessment Report of the Intergovernmental Panel on Climate Change*. Stocker, T.F., D. Qin, G.-K. Plattner, M. Tignor, S.K. Allen, J. Boschung, A. Nauels, Y. Xia, V. Bex, and P.M. Midgley, Eds. Cambridge University Press, Cambridge, United Kingdom and New York, NY, USA, 867–952. <http://dx.doi.org/10.1017/CBO9781107415324.022> www.climatechange2013.org
- Boucher, O., D. Randall, P. Artaxo, C. Bretherton, G. Feingold, P. Forster, V.-M. Kerminen, Y. Kondo, H. Liao, U. Lohmann, P. Rasch, S.K. Satheesh, S. Sherwood, B. Stevens, and X.Y. Zhang, 2013: Clouds and Aerosols. *Climate Change 2013: The Physical Science Basis. Contribution of Working Group I to the Fifth Assessment Report of the Intergovernmental Panel on Climate Change*. Stocker, T.F., D. Qin, G.-K. Plattner, M. Tignor, S.K. Allen, J. Boschung, A. Nauels, Y. Xia, V. Bex, and P.M. Midgley, Eds. Cambridge University Press, Cambridge, United Kingdom and New York, NY, USA, 571–658. <http://dx.doi.org/10.1017/CBO9781107415324.016> www.climatechange2013.org
- Easterling, D.R., K.E. Kunkel, M.F. Wehner, and L. Sun, 2016: Detection and attribution of climate extremes in the observed record. *Weather and Climate Extremes*, **11**, 17-27. <http://dx.doi.org/10.1016/j.wace.2016.01.001>
- Flato, G., J. Marotzke, B. Abiodun, P. Braconnot, S.C. Chou, W. Collins, P. Cox, F. Driouech, S. Emori, V. Eyring, C. Forest, P. Gleckler, E. Guilyardi, C. Jakob, V. Kattsov, C. Reason, and M. Rummukainen, 2013: Evaluation of Climate Models. *Climate Change 2013: The Physical Science Basis. Contribution of Working Group I to the Fifth Assessment Report of the Intergovernmental Panel on Climate Change*. Stocker, T.F., D. Qin, G.-K. Plattner, M. Tignor, S.K. Allen, J. Boschung, A. Nauels, Y. Xia, V. Bex, and P.M. Midgley, Eds. Cambridge University Press, Cambridge, United Kingdom and New York, NY, USA, 741–866. <http://dx.doi.org/10.1017/CBO9781107415324.020> www.climatechange2013.org

- 1 Gillett, N.P., J.C. Fyfe, and D.E. Parker, 2013: Attribution of observed sea level pressure trends
2 to greenhouse gas, aerosol, and ozone changes. *Geophysical Research Letters*, **40**, 2302-
3 2306. <http://dx.doi.org/10.1002/grl.50500>
- 4 Hegerl, G.C., O. Hoegh-Guldberg, G. Casassa, M.P. Hoerling, R.S. Kovats, C. Parmesan, D.W.
5 Pierce, and P.A. Stott, 2010: Good Practice Guidance Paper on Detection and Attribution
6 Related to Anthropogenic Climate Change. *Meeting Report of the Intergovernmental*
7 *Panel on Climate Change Expert Meeting on Detection and Attribution of*
8 *Anthropogenic Climate Change*. Stocker, T.F., C.B. Field, D. Qin, V. Barros, G.-K. Plattner,
9 M. Tignor, P.M. Midgley, and K.L. Ebi, Eds. IPCC Working Group I Technical Support
10 Unit, University of Bern, Bern, Switzerland, 1-8. [http://www.ipcc.ch/pdf/supporting-](http://www.ipcc.ch/pdf/supporting-material/ipcc_good_practice_guidance_paper_anthropogenic.pdf)
11 [material/ipcc_good_practice_guidance_paper_anthropogenic.pdf](http://www.ipcc.ch/pdf/supporting-material/ipcc_good_practice_guidance_paper_anthropogenic.pdf)
- 12 Hegerl, G.C., F.W. Zwiers, P. Braconnot, N.P. Gillett, Y. Luo, J.A.M. Orsini, N. Nicholls, J.E.
13 Penner, and P.A. Stott, 2007: Understanding and attributing climate change. *Climate Change*
14 *2007: The Physical Science Basis. Contribution of Working Group I to the Fourth*
15 *Assessment Report of the Intergovernmental Panel on Climate Change*. Solomon, S., D. Qin,
16 M. Manning, Z. Chen, M. Marquis, K.B. Averyt, M. Tignor, and H.L. Miller, Eds.
17 Cambridge University Press, Cambridge, United Kingdom and New York, NY, USA, 663-
18 745. http://www.ipcc.ch/publications_and_data/ar4/wg1/en/ch9.html
- 19 Hoerling, M., M. Chen, R. Dole, J. Eischeid, A. Kumar, J.W. Nielsen-Gammon, P. Pegion, J.
20 Perlwitz, X.-W. Quan, and T. Zhang, 2013: Anatomy of an extreme event. *Journal of*
21 *Climate*, **26**, 2811–2832. <http://dx.doi.org/10.1175/JCLI-D-12-00270.1>
- 22 Horton, R.M., J.S. Mankin, C. Lesk, E. Coffel, and C. Raymond, 2016: A Review of Recent
23 Advances in Research on Extreme Heat Events. *Current Climate Change Reports*, 1-18.
24 <http://dx.doi.org/10.1007/s40641-016-0042-x>
- 25 Huber, M. and R. Knutti, 2012: Anthropogenic and natural warming inferred from changes in
26 Earth's energy balance. *Nature Geoscience*, **5**, 31-36. <http://dx.doi.org/10.1038/ngeo1327>
- 27 IPCC, 2013: *Climate Change 2013: The Physical Science Basis. Contribution of Working Group*
28 *I to the Fifth Assessment Report of the Intergovernmental Panel on Climate Change*.
29 Cambridge University Press, Cambridge, UK and New York, NY, 1535 pp.
30 <http://dx.doi.org/10.1017/CBO9781107415324> www.climatechange2013.org
- 31 Jones, G.S., P.A. Stott, and N. Christidis, 2013: Attribution of observed historical near surface
32 temperature variations to anthropogenic and natural causes using CMIP5 simulations.
33 *Journal of Geophysical Research*, **118**, 4001-4024. <http://dx.doi.org/10.1002/jgrd.50239>
- 34 King, A.D., D.J. Karoly, M.G. Donat, and L.V. Alexander, 2014: Climate change turns
35 Australia's 2013 Big Dry into a year of record-breaking heat [in "Explaining Extremes of

- 2013 from a Climate Perspective"]. *Bulletin of the American Meteorological Society*, **95**, S41-S45. <http://dx.doi.org/10.1175/1520-0477-95.9.S1.1>
- Knutson, T.R., F. Zeng, and A.T. Wittenberg, 2013: Multimodel Assessment of Regional Surface Temperature Trends: CMIP3 and CMIP5 Twentieth-Century Simulations. *Journal of Climate*, **26**, 8709-8743. <http://dx.doi.org/10.1175/JCLI-D-12-00567.1>
- Knutson, T.R., F. Zeng, and A.T. Wittenberg, 2014: Multimodel assessment of extreme annual-mean warm anomalies during 2013 over regions of Australia and the western tropical Pacific [in "Explaining Extremes of 2013 from a Climate Perspective"]. *Bulletin of the American Meteorological Society*, **95**, S26-S30. <http://dx.doi.org/10.1175/1520-0477-95.9.S1.1>
- Knutson, T.R., R. Zhang, and L.W. Horowitz, 2016: Prospects for a prolonged slowdown in global warming in the early 21st century. *Nature Communications*, **7**, 13676. <http://dx.doi.org/10.1038/ncomms13676>
- Lackmann, G.M., 2015: Hurricane Sandy before 1900 and after 2100. *Bulletin of the American Meteorological Society*, **96**, 547-560. <http://dx.doi.org/10.1175/BAMS-D-14-00123.1>
- Lewis, N. and J.A. Curry, 2015: The implications for climate sensitivity of AR5 forcing and heat uptake estimates. *Climate Dynamics*, **45**, 1009-1023. <http://dx.doi.org/10.1007/s00382-014-2342-y>
- Lewis, S. and D.J. Karoly, 2014: The role of anthropogenic forcing in the record 2013 Australia-wide annual and spring temperatures [in "Explaining Extremes of 2013 from a Climate Perspective"]. *Bulletin of the American Meteorological Society*, **95**, S31-S33. <http://dx.doi.org/10.1175/1520-0477-95.9.S1.1>
- Masson-Delmotte, V., M. Schulz, A. Abe-Ouchi, J. Beer, A. Ganopolski, J.F. González Rouco, E. Jansen, K. Lambeck, J. Luterbacher, T. Naish, T. Osborn, B. Otto-Bliesner, T. Quinn, R. Ramesh, M. Rojas, X. Shao, and A. Timmermann, 2013: Information from Paleoclimate Archives. *Climate Change 2013: The Physical Science Basis. Contribution of Working Group I to the Fifth Assessment Report of the Intergovernmental Panel on Climate Change*. Stocker, T.F., D. Qin, G.-K. Plattner, M. Tignor, S.K. Allen, J. Boschung, A. Nauels, Y. Xia, V. Bex, and P.M. Midgley, Eds. Cambridge University Press, Cambridge, United Kingdom and New York, NY, USA, 383–464. <http://dx.doi.org/10.1017/CBO9781107415324.013>
www.climatechange2013.org
- Melillo, J.M., T.C. Richmond, and G.W. Yohe, eds. *Climate Change Impacts in the United States: The Third National Climate Assessment*. 2014, U.S. Global Change Research Program: Washington, D.C. 842. <http://dx.doi.org/10.7930/J0Z31WJ2>.
- Morice, C.P., J.J. Kennedy, N.A. Rayner, and P.D. Jones, 2012: Quantifying uncertainties in global and regional temperature change using an ensemble of observational estimates: The

- 1 HadCRUT4 dataset. *Journal of Geophysical Research*, **117**, D08101.
2 <http://dx.doi.org/10.1029/2011JD017187>
- 3 Myhre, G., D. Shindell, F.-M. Bréon, W. Collins, J. Fuglestedt, J. Huang, D. Koch, J.-F.
4 Lamarque, D. Lee, B. Mendoza, T. Nakajima, A. Robock, G. Stephens, T. Takemura, and H.
5 Zhang, 2013: Anthropogenic and Natural Radiative Forcing. *Climate Change 2013: The*
6 *Physical Science Basis. Contribution of Working Group I to the Fifth Assessment Report of*
7 *the Intergovernmental Panel on Climate Change*. Stocker, T.F., D. Qin, G.-K. Plattner, M.
8 Tignor, S.K. Allen, J. Boschung, A. Nauels, Y. Xia, V. Bex, and P.M. Midgley, Eds.
9 Cambridge University Press, Cambridge, United Kingdom and New York, NY, USA, 659–
10 740. <http://dx.doi.org/10.1017/CBO9781107415324.018> www.climatechange2013.org
- 11 National Academies of Sciences, E., and Medicine, 2016: *Attribution of Extreme Weather Events*
12 *in the Context of Climate Change*. The National Academies Press, Washington, DC, 186 pp.
13 <http://dx.doi.org/10.17226/21852>
- 14 Otto, A., F.E.L. Otto, O. Boucher, J. Church, G. Hegerl, P.M. Forster, N.P. Gillett, J. Gregory,
15 G.C. Johnson, R. Knutti, N. Lewis, U. Lohmann, J. Marotzke, G. Myhre, D. Shindell, B.
16 Stevens, and M.R. Allen, 2013: Energy budget constraints on climate response. *Nature*
17 *Geoscience*, **6**, 415–416. <http://dx.doi.org/10.1038/ngeo1836>
- 18 Otto, F.E.L., N. Massey, G.J. van Oldenborgh, R.G. Jones, and M.R. Allen, 2012: Reconciling
19 two approaches to attribution of the 2010 Russian heat wave. *Geophysical Research Letters*,
20 **39**, L04702. <http://dx.doi.org/10.1029/2011GL050422>
- 21 Perkins, S.E., S.C. Lewis, A.D. King, and L.V. Alexander, 2014: Increased simulated risk of the
22 hot Australian summer of 2012/13 due to anthropogenic activity as measured by heat wave
23 frequency and intensity [in "Explaining Extremes of 2013 from a Climate Perspective"].
24 *Bulletin of the American Meteorological Society*, **95**, S34–S37.
25 <http://dx.doi.org/10.1175/1520-0477-95.9.S1.1>
- 26 Perlwitz, J., M. Hoerling, and R. Dole, 2015: Arctic Tropospheric Warming: Causes and
27 Linkages to Lower Latitudes. *Journal of Climate*, **28**, 2154–2167.
28 <http://dx.doi.org/10.1175/JCLI-D-14-00095.1>
- 29 Pierce, D.W., T.P. Barnett, B.D. Santer, and P.J. Gleckler, 2009: Selecting global climate models
30 for regional climate change studies. *Proceedings of the National Academy of Sciences*, **106**,
31 8441–8446. <http://dx.doi.org/10.1073/pnas.0900094106>
- 32 Ribes, A. and L. Terray, 2013: Application of regularised optimal fingerprinting to attribution.
33 Part II: application to global near-surface temperature. *Climate Dynamics*, **41**, 2837–2853.
34 <http://dx.doi.org/10.1007/s00382-013-1736-6>

- 1 Rupp, D.E., P.W. Mote, N. Massey, C.J. Rye, R. Jones, and M.R. Allen, 2012: Did human
2 influence on climate make the 2011 Texas drought more probable? [in Explaining extreme
3 events of 2011 from a climate perspective]. *Bulletin of the American Meteorological Society*,
4 **93**, 1052-1054. <http://dx.doi.org/10.1175/BAMS-D-12-00021.1>
- 5 Shepherd, T.G., 2016: A Common Framework for Approaches to Extreme Event Attribution.
6 *Current Climate Change Reports*, **2**, 28-38. <http://dx.doi.org/10.1007/s40641-016-0033-y>
- 7 Stott, P., 2016: How climate change affects extreme weather events. *Science*, **352**, 1517-1518.
8 <http://dx.doi.org/10.1126/science.aaf7271>
- 9 Stott, P.A., D.A. Stone, and M.R. Allen, 2004: Human contribution to the European heatwave of
10 2003. *Nature*, **432**, 610-614. <http://dx.doi.org/10.1038/nature03089>
- 11 Trenberth, K.E., J.T. Fasullo, and T.G. Shepherd, 2015: Attribution of climate extreme events.
12 *Nature Climate Change*, **5**, 725-730. <http://dx.doi.org/10.1038/nclimate2657>
- 13 Walsh, J., D. Wuebbles, K. Hayhoe, J. Kossin, K. Kunkel, G. Stephens, P. Thorne, R. Vose, M.
14 Wehner, J. Willis, D. Anderson, S. Doney, R. Feely, P. Hennon, V. Kharin, T. Knutson, F.
15 Landerer, T. Lenton, J. Kennedy, and R. Somerville, 2014: Ch. 2: Our changing climate.
16 *Climate Change Impacts in the United States: The Third National Climate Assessment*.
17 Melillo, J.M., T.C. Richmond, and G.W. Yohe, Eds. U.S. Global Change Research Program,
18 Washington, D.C., 19-67. <http://dx.doi.org/10.7930/J0KW5CXT>
- 19 Wigley, T.M.L. and B.D. Santer, 2013: A probabilistic quantification of the anthropogenic
20 component of twentieth century global warming. *Climate Dynamics*, **40**, 1087-1102.
21 <http://dx.doi.org/10.1007/s00382-012-1585-8>

4. Climate Models, Scenarios, and Projections

KEY FINDINGS

1. Merely maintaining present-day levels of greenhouse (heat-trapping) gases in the atmosphere would commit the world to at least an additional 0.3°C (0.5°F) of warming over this century relative to today (*high confidence*). Projections over the next three decades differ modestly, primarily due to uncertainties in natural sources of variability. Past mid-century, the amount of climate change depends primarily on future emissions and the sensitivity of the climate system to those emissions.
2. Atmospheric carbon dioxide (CO₂) levels have now passed 400 ppm, a concentration last seen about 3 million years ago, when average temperature and sea level were significantly higher than today. Continued growth in CO₂ emissions over this century and beyond would lead to concentrations not experienced in tens to hundreds of millions of years. The rapid present-day emissions rate of nearly 10 GtC per year, however, suggests that there is no precise past climate analogue for this century any time in at least the last 66 million years. (*Medium confidence*)
3. The observed acceleration in carbon emissions over the past 15–20 years is consistent with higher future scenarios (*very high confidence*). Since 2014, growth rates have slowed as economic growth begins to uncouple from carbon emissions (*medium confidence*) but not yet at a rate that, were it to continue, would limit atmospheric temperature increase to the 2009 Copenhagen goal of 2°C (3.6°F), let alone the 1.5°C (2.7°F) target of the 2015 Paris Agreement (*high confidence*).
4. Combining output from global climate models and dynamical and statistical downscaling models using advanced averaging, weighting, and pattern scaling approaches can result in more relevant and robust future projections. These techniques also allow the scientific community to provide better guidance on the use of climate projections for quantifying regional-scale impacts (*medium to high confidence*).

4.1. The Human Role in Future Climate

The Earth's climate, past and future, is not static; it changes in response to both natural and anthropogenic drivers (see Ch. 2: Scientific Basis). Since the industrial era, human emissions of carbon dioxide (CO₂), methane (CH₄), and other greenhouse gases now overwhelm the influence of natural drivers on the external forcing of the Earth's climate (see Ch. 3: Detection and Attribution). For this reason, projections of changes in Earth's climate over this century and beyond focus primarily on its response to emissions of greenhouse gases, particulates, and other radiatively-active species from human activities.

Climate change and ocean acidification (see Ch. 13: Ocean Acidification) are already occurring due to the buildup of atmospheric CO₂ in the industrial era (Hartmann et al. 2013; Rhein et al. 2013). If atmospheric levels of greenhouse gases were frozen at current levels, temperature would continue to increase by an estimated 0.3°C (0.54°F) over this century (Collins et al. 2013). However, climate change over this century and beyond is primarily a function of future emissions and the response of the climate system to those emissions (see Ch. 2: Scientific Basis). For that reason, climate projections are not predictions; instead, they consist of a range of plausible scenarios or pathways that can be expressed in terms of population, energy sources, technology, emissions, atmospheric concentrations, radiative forcing, and/or global temperature change. For a given scenario, it is possible to estimate the range in potential climate change—as determined by climate sensitivity, which is the response of global temperature to a natural or anthropogenic forcing (see Ch. 2: Scientific Basis)—that would result at the global and regional scale (Collins et al. 2013).

Over the past 15–20 years, growth rates in carbon emissions from human activities of 3%–4% per year largely tracked with those projected under higher scenarios, in large part to growing contributions from developing economies (Raupach et al. 2007; Le Quéré et al. 2009). Since 2014, however, growth rates have flattened, a trend cautiously attributed to declining coal use in China, despite large uncertainties in emissions reporting (Jackson et al. 2016; Korsbakken et al. 2016). Carbon emissions and economic growth may be beginning to decouple, as global economies led by China and the United States phase out coal and begin the transition to renewable, non-carbon energy (IEA 2016; Green and Stern 2016). In the 2015 Paris Agreement, signatories agree to “holding the increase in the global average temperature to well below 2°C (3.6°F) above preindustrial levels and pursuing efforts to limit the temperature increase to 1.5°C (2.7°F) above preindustrial levels” (UNFCCC 2015). To stabilize climate, however, it is not enough to halt the growth in annual carbon emissions; global net carbon emissions would eventually need to reach zero (Collins et al. 2013) and most recent economic scenarios require negative emissions for a greater than 50% chance of limiting warming below 2°C (3.6°F) (Smith et al. 2016; see also Ch. 14 Mitigation for a discussion of negative emission technologies).

4.2. Future Scenarios

4.2.1. Representative Concentration Pathways

Over the last 25 years, the climate modeling community has based its simulations on standard sets of scenarios that correspond with possible future emissions of greenhouse gases, aerosols, and other species. Developed by the integrated assessment modeling community, these sets of standard scenarios have become more comprehensive with each new generation: the IS92 emission scenarios of the 1990s (Leggett et al. 1992); after 2000, the Special Report on Emission Scenarios (SRES; Nakicenovic et al. 2000); and today, the Representative Concentration Pathways (RCPs; Moss et al. 2010).

The SRES scenarios began with a storyline that lays out a consistent picture of demographics, international trade, flow of information and technology; these assumptions are then fed through socioeconomic and Integrated Assessment Models (IAMs) to derive emissions. In turn, emissions were used as input to carbon cycle or earth system models to calculate resulting atmospheric concentrations and radiative forcing. In contrast, RCP scenarios are tied to one value: the change in radiative forcing at the tropopause by 2100. The four RCPs are numbered according to specific changes in radiative forcing at the tropopause from preindustrial conditions to 2100: +2.6, +4.5, +6.0 and +8.5 watts per square meter (W/m^2). From this value, it is possible to work backwards to derive a range of emissions trajectories and corresponding policies and technological strategies that would achieve the same ultimate impact on radiative forcing.

Although there are multiple emissions pathways that would lead to the same radiative forcing target, an associated pathway of annual carbon dioxide and other anthropogenic emissions of greenhouse gases, aerosols, air pollutants, and other short-lived species has been identified for each RCP to use as input to future climate model simulations (e.g., Riahi et al. 2011; Cubasch et al. 2013). In addition, RCPs provide climate modelers with gridded trajectories of land use and land cover. Using the RCPs as input, climate models produce trajectories of future climate change including global and regional changes in temperature, precipitation, and other physical characteristics of the climate system (Collins et al. 2013; Kirtman et al. 2013; see also Ch. 6-7).

Within the RCP family, individual scenarios have no likelihood attached to them. Higher-numbered scenarios correspond to higher emissions, and a larger and more rapid global temperature change (Figure 4.1); the range of values covered by the scenarios was chosen to reflect the then-current range in the open literature. Since the choice of scenario constrains the magnitudes of future changes, most assessments (including this one; see Ch. 6: Temperature Change) quantify the impacts under a range of future scenarios that reflect the uncertainty in the consequences of human choices over the coming century.

The higher RCP8.5 scenario corresponds to a future where carbon emissions continue to rise as a result of fossil fuel use, albeit with significant declines in emission growth rates over the second half of the century (Figure 4.1) and modest improvements in energy intensity and technological change (Riahi et al. 2011). Atmospheric carbon dioxide levels rise from current-day levels of 400 up to 936 parts per million (ppm) and global temperature increases by 3° to 5.5°C (5.4° to 9.9°F) by 2100 relative to the 1986–2005 average. RCP8.5 reflects the upper range of the open literature on emissions, but is not intended to serve as an upper limit on possible emissions nor as a business as usual or reference scenario for the other three scenarios.

Projections based on SRES scenarios, such as those used in the Second and Third National Climate Assessments (NCA2 and NCA3; Karl et al. 2009; Melillo et al. 2014), are not necessarily incompatible with new RCP-based ones; RCP8.5 is similar to SRES A1fi, RCP6.0 is similar to SRES A1B, and RCP4.5 is similar to SRES B1. While none of the SRES scenarios

included a scenario with explicit policies and measures to limit climate forcing, however, the three lower RCP scenarios (2.6, 4.5, and 6.0) are climate-policy scenarios.

Under the RCP4.5 and 2.6 scenarios, for example, atmospheric CO₂ levels remain below 550 and 450 ppm by 2100, respectively. The RCP2.6 scenario is much lower than any SRES scenario because it includes the option of using policies to achieve net negative carbon dioxide emissions before the end of the century, while SRES scenarios do not. The lower the atmospheric concentrations of CO₂, the greater the chance that projected global temperature change will remain below 2°C (3.6°F) relative to preindustrial levels, consistent with the Paris Agreement. Under RCP4.5, global temperature change is more likely than not to exceed 2°C (3.6°F) (<https://tntcat.iiasa.ac.at/RcpDb/dsd?Action=htmlpage&page=compare>; Collins et al. 2013), whereas under RCP2.6 it is likely to remain below 2°C (Sanderson et al. 2016; Collins et al. 2013). RCPs do not consider climate forcing in the range of 2.0 W/m², a level consistent with limiting global mean surface temperature change to 1.5°C (2.7°F); it is estimated that a 66% chance of achieving this target would require net zero greenhouse gas emissions by 2050—or 2060, if global temperature is permitted to temporarily exceed 1.5°C for up to 50 years (Sanderson et al. 2016).

[INSERT FIGURE 4.1 HERE:]

Figure 4.1: The climate projections used in this report are based on the 2010 Representative Concentration Pathways (RCP, right). They are largely consistent with scenarios used in previous assessments, the 2000 Special Report on Emission Scenarios (SRES, left). This figure compares SRES and RCP annual carbon emissions (top), carbon dioxide equivalent levels in the atmosphere (middle), and temperature change that would result from the central estimate (lines) and the likely range (shaded areas) of climate sensitivity (bottom). (Data from CMIP3 and CMIP5). (Figure source: Walsh et al. 2014)]

4.2.2. Shared Socioeconomic Pathways

Shared Socioeconomic Pathways (SSPs) are a set of socioeconomic scenarios that include assumptions regarding demographics, urbanization, economic growth and technology development. These scenarios were designed to meet the needs of the impacts, adaptation, and vulnerability (IAV) communities, enabling them to explore the socioeconomic challenges to emissions mitigation and adaptation to climate change (O'Neill et al. 2014). Five SSP scenarios have been developed: SSP1 (“Sustainability”; low challenges to mitigation and adaptation), SSP2 (“Middle of the Road”; middle challenges to mitigation and adaptation), SSP3 (“Regional Rivalry”; high challenges to mitigation and adaptation), SSP4 (“Inequality”; low challenges to mitigation, high challenges to adaptation), and SSP5 (“Fossil-fueled Development”; high challenges to mitigation, low challenges to adaptation). Each of the scenarios has an underlying SSP narrative, as well as a consistent quantification of demographic, urbanization, economic growth and technology development assumptions.

To allow IAV researchers to couple alternative socioeconomic scenarios with the climate scenarios developed using RCPs, SSP-driven scenarios have been constrained using emissions limitations policies consistent with the underlying SSP story lines to create new scenarios with climate forcing that matches RCP values, but a range of five alternative socioeconomic underpinnings. Only SSP5 produces a reference scenario that matches RCP8.5; the other SSPs have no-climate-policy reference scenarios with climate forcing below 8.5 W/m^2 . Similarly, the nature of SSP3 makes it impossible for that scenario to produce a climate forcing as low as 2.6 W/m^2 . While new research is under way to explore scenarios that limit climate forcing to 2.0 W/m^2 , neither the RCPs nor the SSPs have produced scenarios in that range.

4.2.3. Global Mean Temperature Scenarios and Pattern Scaling Approaches

RCP scenarios and their associated SSPs provide the input for the global climate model simulations described in section 4.3 below. The output from these simulations is typically summarized over a range of future climatological time periods (for example, temperature change in 2040–2079 or 2070–2099 relative to 1980–2009). The time-slice approach has the advantage of developing projections for a given time horizon. It has the disadvantage, however, of including a broad range of uncertainty regarding what may occur over a given time frame, due to both scenario uncertainty and climate sensitivity. This uncertainty increases, the further out in time the projections go. A scenario-based approach is also increasingly disconnected with the framing of many climate targets, including the Paris Agreement, that are expressed in terms of global mean temperature rather than a given scenario, pathway, or time frame. This is one reason why the Paris Agreement requested that the IPCC provide a special report on the impacts of a 1.5°C (2.7°F) world.

Global mean temperature (GMT) scenarios provide a way to connect model-based projections to climate targets, using pre-existing RCP or SRES-based climate model simulations. Traditional RCP or SRES-based simulations can be transformed into GMT scenarios by calculating the projected changes and resulting impacts that would occur under a transient warming of 1° , 2° , or 3°C (1.8° , 3.6° , or 5.4°F) or more. The climatological time slice in each individual model simulation that corresponds to a given increase in global mean temperature can then be extracted. This increase can be defined relative to the desired baseline such as preindustrial, for example, or a more recent time period such as 1976–2005 (Figure 4.2).

Many physical changes and impacts have been shown to scale with GMT, including shifts in average precipitation, extreme heat, runoff, drought risk, wildfire, temperature-related crop yield changes, and even risk of coral bleaching (e.g., NRC 2011; Collins et al. 2013; Frieler et al. 2013; Swain and Hayhoe 2015) and this approach has been found to reduce the multimodel spread of future projections (Herger et al. 2015; Swain and Hayhoe 2015). By quantifying projected changes for a given amount of warming, regardless of when it may be reached, this approach de-emphasizes the uncertainty due to both scenarios and climate sensitivity. Instead,

GMT scenarios highlight other aspects of scientific uncertainty regarding the response of the Earth's climate system (which can be large, particularly at the regional scale) to human-induced change when a given global warming threshold or target is achieved. GMT scenarios are less useful for impacts such as species migration, however, that are more dependent on the rate than the magnitude of change.

Pattern scaling techniques (Mitchell 2003) are based on a similar assumption, namely that large-scale patterns of regional change will scale with the amount of forcing. These techniques can be used to quantify regional change for scenarios that are not readily available in preexisting databases of global climate model simulations (as described in section 4.3.1 below), including changes in both mean and extremes (e.g., Fix et al. 2016). A comprehensive assessment both confirms and constrains the validity of applying pattern scaling to quantify climate response to a range of forcings (Tebaldi and Arblaster 2014). As the world moves towards quantifiable climate targets, it is expected that these pattern scaling frames or GMT scenarios will become more commonly used.

[INSERT FIGURE 4.2 HERE:]

Figure 4.2: Global mean surface temperature anomalies (°C) relative to 1976–2005 for four RCP scenarios, 2.6 (green), 4.5 (yellow), 6.0 (orange), and 8.5 (red), calculated in 0.5°C increments. Each line represents an individual simulation from the CMIP5 archive; every RCP-based simulation with annual or monthly temperature outputs available was used here. (Figure source: adapted from Swain and Hayhoe 2015)]

4.2.4. Cumulative Carbon Emissions

The SRES, RCP, and global mean temperature scenarios described above all contain a component of time: how much will climate change, and by when? Ultimately, however, the magnitude of human-induced climate change depends less on the year-to-year emissions than it does on the net amount of carbon, or cumulative carbon, produced. To date, human activities, including burning fossil fuels and deforestation, have emitted more than 600 gigatons of carbon (GtC) into the atmosphere since preindustrial times. Unless substantial amounts are removed from the atmosphere via carbon sequestration, this amount has already committed the world to at least an additional 0.3°C (0.5°F) of warming over this century, relative to today.

In order to meet the ambitious 1.5°C (2.7°F) target in the Paris Agreement, only 150 GtC more of carbon can be emitted globally. To meet the higher 2°C (3.6°F) target, approximately 400 GtC more can be emitted. At current emission rates of just under 10 GtC per year, that would permit just 15 years for the lower target and around 40 more years of carbon emissions under the higher target. Under the RCP4.5 pathway, cumulative emissions totaling 1000 GtC, consistent with a 2°C (3.6°F) target, would likely be reached between 2051 and 2065, while under the RCP8.5 pathway, this level would likely be reached between 2043 and 2050. For the lower 1.5°C (2.7°F) target, the cumulative carbon limit of 750 GtC would likely be reached following the RCP4.5

pathway sometime between 2028 and 2041, and, following the RCP8.5 pathway, between 2026 and 2036. When non-CO₂ greenhouse gases such as methane and nitrous oxide (whose warming potentials differ over time, relative to CO₂) are included, exactly when a given temperature threshold would be exceeded becomes even more uncertain.

The cumulative carbon emissions that would allow the world to meet a given global temperature target can also be compared to known fossil fuel reserves to calculate how much of their carbon would have to “stay in the ground” to meet these targets, in the absence of widespread carbon capture and storage (see Ch. 14). It is estimated that to meet the 2°C (3.6°F) target, two thirds of known global fossil fuel reserves would need to remain in the ground (McGlade and Ekins 2015). Accounting for the differing carbon content of various types of fuels, in order to meet the 2°C target one third of oil reserves, half of gas reserves, and over 80% of coal reserves would need to remain unused, as well as any new unconventional, undeveloped, or undiscovered resources (McGlade and Ekins 2015).

4.2.5. Paleoclimate Analogues for Long-Term Equilibrium Change

Most CMIP5 simulations project transient changes in climate through 2100; a few simulations extend to 2200, 2300 or beyond. The long-term impact of human activities on the carbon cycle and the Earth’s climate, however, can only be assessed by considering changes that occur over multiple centuries and even millennia, after net human emissions have reached zero, atmospheric carbon dioxide levels have stabilized, and the carbon cycle has re-balanced (NRC 2011).

In the past, there have been several extended periods of “hothouse” climates where carbon dioxide concentrations and/or global mean temperatures were similar to preindustrial, current, or plausible future levels. These periods are sometimes referenced as analogues, albeit imperfect and incomplete, of future climate (e.g., Crowley 1990).

The last interglacial period, approximately 125,000 years ago, is known as the Eemian. During that time, CO₂ levels were similar to preindustrial, around 280 ppm (Schneider et al. 2013). Global mean temperature was approximately 1° to 2°C (1.8° to 3.6°F) higher than preindustrial levels (Lunt et al. 2012; Otto-Bleisner et al. 2013), the poles were significantly warmer (NEEM 2013; Jouzel et al. 2007), and sea level was 6 to 9 meters (20 to 30 feet) higher than today (Fig. 4.3; Kopp et al. 2009). During the Pliocene, approximately 3 million years ago, long-term CO₂ levels were similar to today’s, around 400 ppm (Seki et al. 2010) – although those concentrations were sustained over long periods of time, whereas ours are increasing rapidly. Global mean temperature in the Pliocene was approximately 2° to 3.5°C (3.6° to 6.3°F) above preindustrial, and sea level was somewhere between 20 ± 10 meters (66 ± 33 feet) higher than today (Fig. 4.3; Haywood et al. 2013; Dutton et al. 2015; Miller et al. 2012).

Under the higher RCP8.5 scenario, CO₂ concentrations are projected to exceed 900 ppm before 2100. During the Eocene, 35 to 55 million years ago, CO₂ levels were between 680 and 1260

1 ppm, or two and a half to four and a half times above preindustrial levels (Jagniecki et al. 2015).
2 Using Eocene conditions as an analogue, this suggests that if the CO₂ concentrations projected to
3 occur under the RCP8.5 scenario by 2100 were sustained over long periods of time, they would
4 result in global temperatures approximately 5° to 8°C (9° to 14°F) above preindustrial levels
5 (Royer 2014). During the Eocene, there were no permanent land-based ice sheets; Antarctic
6 glaciation did not begin until approximately 34 million years ago (Pagani et al. 2011).
7 Calibrating sea level rise models against these and other past climate conditions suggests that,
8 under the RCP8.5 scenario, Antarctica could contribute 1 meter of sea level rise by 2100 and 15
9 meters by 2500 (DeConto and Pollard 2016). If atmospheric CO₂ were sustained at levels
10 approximately two to three times above preindustrial for tens of thousands of years, it's
11 estimated that Greenland and Antarctic ice sheets could melt entirely (Gasson et al. 2014),
12 resulting in approximately 65 meters (215 feet) of sea level rise relative to present-day (Vaughn
13 et al. 2013).

14 An analog for the rapid pace of change occurring today is the relatively abrupt warming of 5° to
15 8°C (9° to 14°F) that occurred during the Paleocene-Eocene Thermal Maximum (PETM),
16 approximately 55–56 million years ago (Bowen et al. 2015; Kirtland Turner et al. 2014; Penman
17 et al. 2014; Crowley et al. 1990). However, new analyses reveal that this carbon was released
18 over some 4000 years or so, and the rate of maximum sustained carbon release during that period
19 was less than 1.1 GtC per year (Zeebe et al. 2016). In comparison, industrial era emissions have
20 occurred over a few centuries, at rates now approaching 10 GtC per year. This suggests that there
21 is no real past analogue any time in the last 66 million years that could help to constrain
22 projections of future climate (Zeebe et al. 2016; Crowley et al. 1990).

23 **[INSERT FIGURE 4.3 HERE:]**

24 **Figure 4.3:** Putting present-day global mean temperature, CO₂ concentrations, and sea level into
25 context, this figure summarizes what is known about the range in peak global mean temperature,
26 atmospheric CO₂, maximum global mean sea level (GMSL), and source(s) of meltwater over
27 three periods in the past with CO₂ levels similar to pre-industrial levels (around 270 ppm) or
28 today (around 400 ppm). Light blue shading indicates uncertainty of GMSL maximum. Red pie
29 charts over Greenland and Antarctica denote fraction, not location, of ice retreat. (Figure source:
30 Dutton et al. 2015)]

31 **4.3. Modeling Tools**

32 **4.3.1. Global Climate Models**

33 Climate scientists use a wide range of observational and computational tools to understand the
34 complexity of the Earth's climate system and to study how that system responds to external
35 forces, including human activities. Computational tools include models that simulate different
36 components of the climate system, including the atmosphere, ocean, land, and sea ice (see Ch. 2:
37 Scientific Basis). The most sophisticated computational tools used by climate scientists are

global climate models, or GCMs (previously referred to as “general circulation models” when they included only the physics needed to simulate the general circulation of the atmosphere and oceans). Models that include an interactive carbon cycle and/or biogeochemistry component are sometimes also referred to as Earth System Models (ESMs).

Global climate models are mathematical models originally built on fundamental equations of physics that include the conservation of energy, mass, and momentum, and how these are exchanged among different components of the climate system. Using these fundamental relationships, the models generate many important features that are evident in the Earth’s climate system: the jet stream that circles the globe 30,000 feet above the Earth’s surface; the Gulf Stream and other ocean currents that transport heat from the tropics to the poles; and even hurricanes in the Atlantic Ocean and typhoons in the Pacific Ocean when the models are run at a fine enough spatial resolution.

[INSERT FIGURE 4.4 HERE:]

Figure 4.4: As climate modeling has evolved over the last 120 years, increasing amounts of physical science have been incorporated into the models. This figure shows the evolution from simple energy balance models through atmosphere–ocean general circulation models to today’s earth system models.]

In addition to expanding the number of processes in the models and improving the treatment of existing processes, the average horizontal spatial resolution of GCMs has increased over time, as computers become more powerful, and with each successive version of the World Climate Research Programme’s (WCRP’s) Coupled Model Intercomparison Project (CMIP). CMIP5 provides output from over 50 GCMs with spatial resolutions ranging from about 50 to 300 km (30 to 200 miles) per horizontal size, and variable vertical resolution on the order of hundreds of meters in the troposphere or lower atmosphere. Versions 3 and 5 are currently available, and Version 6 is underway [Note: we will update CMIP6 progress in subsequent drafts]. These simulations provide output from a large ensemble of different climate models and future scenarios to quantify future climate change at global, continental, and broad regional scales.

GCMs are constantly being expanded to include more physics, chemistry, and, increasingly, even the biology and biogeochemistry at work in the climate system (Figure 4.4). However, these models build on previous generations and are not independent from each other. Many share both ideas and model components or code, complicating the interpretation of multi-model ensembles that often are assumed to be independent (Knutti et al. 2013; Sanderson et al. 2015). This is one of the key pieces of information going into the weighting approach used in this report (see Weighting Appendix). And even with new experimental high-resolution simulations at 25 km (15 miles) per horizontal grid cell, there are still important fine-scale processes occurring at regional to local scales that GCMs are unable to simulate.

To translate global projections into the higher-resolution information often required for impact assessment, climate impact studies often use the statistical or dynamical downscaling methods discussed above. Regional climate models can directly simulate the response of regional climate processes to global change, while statistical models can remove biases in simulations relative to observations. While some new approaches are combining dynamical and statistical methods into a hybrid framework, most assessments still tend to rely on one or the other type of downscaling, where the choice is based on the needs of the assessment.

4.3.2. Regional Climate Models

Dynamical downscaling models are often referred to as regional climate models (RCMs), since they include many of the same physical processes that make up a global climate model, but simulate these processes at higher resolution over smaller rectangular regions, such as the western or eastern United States. Regional climate modeling can improve understanding of regional climate change by modeling areas with complex terrain, such as coastlines or mountains. They can also incorporate changes in land use, land cover, or hydrology into local climate at spatial scales relevant to planning and decision-making at the regional level.

RCMs are computationally intensive because of the higher resolution, but provide a broad range of output variables that resolve regional climate features important for assessing climate impacts. The size of individual grid cells can be as fine as 1 to 2 km (0.6 to 1.2 miles) per horizontal side in some studies, but more commonly range from about 10 to 50 km (6 to 30 miles). Despite the differences in resolution, RCMs are still subject to many of the same types of uncertainty as GCMs, such as not fully resolving physical processes that occur at even smaller scales than the model is able to resolve. One additional source of uncertainty unique to RCMs arises from the fact that at their boundaries RCMs require output from GCMs to provide large-scale circulation such as winds, temperature, and moisture.

The North America Coordinated Regional Climate Downscaling Experiment (CORDEX; Note: in progress, will need to be updated in subsequent drafts) is currently generating a set of high-resolution RCM simulations for North America at spatial resolutions ranging from 10 to 50 km (6 to 30 miles) with 3-hour outputs for more than 60 different surface and upper-air variables. Currently-available simulations from the North American Regional Climate Change Assessment Program are useful for examining certain impacts over North America but, as they are based on simulations from four CMIP3 GCMS for a single mid-high SRES scenario, do not encompass the full range of uncertainty in future projections due to both human activities and climate sensitivity, as represented by the range of CMIP5 GCMs and RCP scenarios.

If the study is a sensitivity analysis, where using one or two future simulations is not a limitation, or if it requires many climate variables as input, then regional climate modeling may be more appropriate than statistical modeling. Kotamarthi et al. (2016) provides a full discussion of the

issues surrounding selecting and applying dynamical and statistical downscaling methods to assess climate impacts.

[INSERT FIGURE 4.5 HERE:]

Figure 4.5: Global climate models typically operate at coarser horizontal spatial scales, while regional climate models have much finer resolutions. This figure compares annual average precipitation for the historical period 1979–2008 using (a) a resolution of 25 km or 15 miles with (b) a resolution of 250 km or 150 miles, to illustrate the importance of spatial scale in resolving key topographical features, particularly along the coasts and in mountainous areas. In this case, both simulations are by the GFDL HIRAM model, an experimental high-resolution model. (Figure source: adapted from Dixon et al. 2016; © American Meteorological Society, used with permission)]

4.3.3. Empirical Statistical Downscaling Models

Empirical statistical downscaling models (ESDMs) combine GCM output with historical observations to translate large-scale predictors or patterns into high-resolution projections at the scale of observations. The observations used in an ESDM can range from individual weather stations to gridded datasets. As output, they can generate a range of products, from large grids to analyses optimized for a specific location, variable, or decision-context. The statistical techniques are even more varied, from simple difference or delta approaches (subtracting historical simulated values from future values, and adding the resulting delta to historical observations, as used in the First National Climate Assessment) to complex clustering and neural network techniques that can rival dynamical downscaling in their demand for computational resources (see review by Kotamarthi et al. 2016).

Statistical models are generally flexible and less computationally demanding than RCMs. A number of databases provide statistically downscaled projections for a continuous period from 1960 to 2100 using many global models and a range of higher and lower future scenarios. ESDMs are also effective at removing biases in historical simulated values, leading to a good match between the average (multidecadal) statistics of observed and statistically downscaled climate at the spatial scale and over the historical period of the observational data used to train the statistical model. With the exception of methods that simultaneously downscale multiple variables, however, bias correction will remove the physical interdependence between variables.

ESDMs are also limited in that they require observational data as input; the longer and more complete the record, the greater the confidence that the ESDM is being trained on a representative sample of climatic conditions for that location. Application of ESDMs to remote locations with sparse temporal and/or spatial records is challenging though in many cases reanalysis (Brands et al. 2012) or even monthly satellite data (Thrasher et al. 2013) can be used in lieu of in situ observations. Lack of data availability can also limit their use in applications that require more variables than temperature and precipitation.

Finally, statistical models are based on the key assumption that the relationship between large-scale weather systems and local climate or the spatial pattern of surface climate will remain stationary over the time horizon of the projections. This assumption may not hold if climate change alters local feedback processes that affect these relationships; initial analyses have demonstrated that the assumption of stationarity can vary significantly by ESDM method, by quantile, and by the time scale (daily or monthly) of the GCM input (Dixon et al. 2016).

ESDMs are best suited for analyses that require a broad range of future projections of standard, near-surface variables such as temperature and precipitation, at the scale of observations that may already be used for planning purposes. If the study needs to resolve the full range of projected changes under multiple models and scenarios or is more constrained by practical resources, then statistical downscaling may be more appropriate than dynamical downscaling. However, even within statistical downscaling, selecting an appropriate method for any given study depends on the questions being asked; these issues are discussed in greater detail by Kotamarthi et al. (2016).

4.3.4. Averaging, Weighting, and Selection of Global Models

Individual climate model simulations using the same inputs can differ from each other over several years to several decades. These differences are the result of normal, natural variability as well as the different ways models characterize various small-scale processes. Although decadal predictability is an active research area, the timing of natural variations is largely unpredictable beyond several seasons. For this reason, multimodel simulations are generally averaged (as the last stage in any analysis before preparing, for example, figures showing projected changes in annual or seasonal temperature or precipitation; see Ch. 6 and 7) to remove the effects of randomly occurring natural variations from long-term trends and make it easier to discern the impact of external drivers, both human and natural, on the Earth's climate. The effect of averaging on the systematic errors depends on the extent to which models have similar errors or offsetting errors. For that reason, on time series plots, we also show a range of outcomes across GCMs, quantify the risks inherent to a given scenario.

Previous assessments have used a simple average to calculate the multimodel ensemble. Such approach implicitly assumes each climate model is independent from the others and of equal ability. Neither of these assumptions, however, are completely valid. As noted previously, some models share many components with other models in the CMIP5 archive, whereas others have been developed largely in isolation (Knutti et al. 2013; Sanderson et al. 2015). Also, some models are more successful than others: at replicating observed climate and trends over the past century; at simulating the large-scale dynamical features responsible for creating or affecting the average climate conditions over a certain region, such as the Arctic or the Caribbean (e.g., Wang et al. 2007, 2014; Ryu and Hayhoe 2014); or at simulating past climates with very different states than present day (Braconnot et al. 2012). Evaluation of models' success often depends on the variable or metric being considered in the analysis, with some models performing better than

others for certain regions or variables. However, all future simulations agree that both global and regional temperatures will increase over this century in response to increasing emissions of greenhouse gases from human activities.

For the first time in an official U.S. Global Change Research Program report, this assessment uses model weighting to refine future climate change projections (see Appendix B: Model Weighting). The weighting approach takes into account the interdependence of individual climate models and their relative abilities in simulating North American climate. Understanding of model history, together with the fingerprints of particular model biases, has been used to identify model pairs that are not independent. In this report, model independence and selected global and North American model quality metrics are considered in order to determine the weighting parameters (Sanderson et al. in prep).

Sensitivity studies in the implementation of the weighting scheme show that global-scale temperature response is not significantly constrained by the weighting strategy, although there are small regional differences in significance. The choice of metric used to evaluate models has very little effect on the independence weighting, and some moderate influence on the skill weighting if only a small number of variables are used to assess model quality. Because a large number of variables are combined to produce a comprehensive “skill metric,” the metric is not highly sensitive to any single variable.

4.4. Uncertainty in Future Projections

The magnitude of future climate change depends on human choices (see Section 4.2), natural variability, and scientific uncertainty (Hawkins and Sutton 2009, 2011; Deser et al. 2012). Scientific uncertainty in turn encompasses multiple factors. The first is parametric uncertainty—the ability of GCMs to simulate processes that occur on spatial or temporal scales smaller than they can resolve. The second is structural uncertainty—whether GCMs include and accurately represent all the important physical processes occurring on scales they can resolve. Structural uncertainty can arise because a process is not yet recognized—such as “tipping points” or mechanisms of abrupt change, as discussed in Ch.15, Potential Surprises—or because it is known but is not yet understood well enough to be modeled accurately—such as dynamical mechanisms that are important to melting ice sheets. The third is climate sensitivity—a measure of the response of the planet to increasing levels of CO₂, formally defined as the equilibrium temperature change resulting from a doubling of CO₂ levels in the atmosphere relative to preindustrial levels. Various lines of evidence constrain the likely value of climate sensitivity. These include historical warming (in the instrumental record, as well as events in the paleo-climate record, such as the transition from the Last Glacial Maximum to today), and combining analysis of aspects of present-day climate with physical modeling of the climate system to constrain possible feedbacks such as how clouds might change in a warmer world (Knutti and Hegerl 2008). Combining this evidence, climate sensitivity is likely to lie between 2°C and 4.5°C (3.6°F and 8.1°F; IPCC 2013b).

1 Which of these sources of uncertainty—human, natural, and scientific—is most important
2 depends on the time frame and the variable considered. For temperature, it is clear that
3 increasing greenhouse gas emissions from human activities will drive increases in global and
4 most regional temperatures and that these rising temperatures will increase with the magnitude of
5 future emissions, particularly past mid-century (Hawkins and Sutton 2009). Uncertainty in
6 projected temperature change is generally smaller than uncertainty in projected changes in
7 precipitation or other aspects of climate. For precipitation, the processes that form precipitation
8 happen below the scale of the models, requiring a significant amount of parameterization. For
9 that reason, scientific uncertainty tends to dominate in precipitation projections throughout the
10 entire century (Hawkins and Sutton 2011).

11 Over the next few decades, the greater part of the range or uncertainty in projected global and
12 regional change is the result of a combination of natural variability (mostly related to uncertainty
13 in specifying the initial conditions of the state of the ocean) and scientific limitations in our
14 ability to model and understand the Earth's climate system (Figure 4.6). Differences in forcing
15 scenarios, shown in orange in Figure 4.6, represent the scenarios, or human uncertainty. Over the
16 short term, these differences are relatively small. As time progresses, however, differences in
17 emissions become larger and the delayed ocean response to these differences begins to be
18 realized. By about 2030, the human source of uncertainty becomes increasingly important in
19 determining the magnitude and patterns of future change. Even though natural variability will
20 continue to occur, most of the difference between present and future climates will be determined
21 by choices that society makes today and over the next few decades. The further out in time we
22 look, the greater the influence of these differences in human choices are on the differences in
23 magnitude of future change.

24 **[INSERT FIGURE 4.6 HERE:]**

25 **Figure 4.6:** The fraction of total variance in decadal mean surface air temperature predictions
26 explained by the three components of total uncertainty is shown for (a) Alaska, (b) Hawai'i, and
27 (c) the lower 48 states. Orange regions represent human or scenario uncertainty, blue regions
28 represent model uncertainty, and green regions represent the internal variability component. As
29 the size of the region is reduced, the relative importance of internal variability increases. In
30 interpreting this figure, it is important to remember that it shows the fractional sources of
31 uncertainty. Total uncertainty increases as time progresses. (Figure source: adapted from
32 Hawkins and Sutton 2009)]

TRACEABLE ACCOUNTS

Key Finding 1

Merely maintaining present-day levels of greenhouse (heat-trapping) gases in the atmosphere would commit the world to at least an additional 0.3°C (0.5°F) of warming over this century relative to today (*high confidence*). Projections over the next three decades differ modestly, primarily due to uncertainties in natural sources of variability. Past mid-century, the amount of climate change depends primarily on future emissions and the sensitivity of the climate system to those emissions.

Description of evidence base

The basic physics underlying the impact of human emissions on global climate, and the role of climate sensitivity in moderating the impact of those emissions on global temperature, has been documented since the 1800s in a series of peer-reviewed journal articles that is summarized in a collection titled, “The Warming Papers: The Scientific Foundation for the Climate Change Forecast” (Archer and Pierrehumbert 2011).

IPCC AR5 WG1 SPM states “Total radiative forcing is positive, and has led to an uptake of energy by the climate system. The largest contribution to total radiative forcing is caused by the increase in the atmospheric concentration of CO₂ since 1750” (C, page 13) and “Observational and model studies of temperature change, climate feedbacks and changes in the Earth’s energy budget together provide confidence in the magnitude of global warming in response to past and future forcing.” (IPCC 2013b, D.2, page 16)

The estimate of committed warming at constant atmospheric concentrations is based on IPCC AR5 WG1, Collins et al. 2013.

Analysis of the sources of uncertainty in near-term versus long-term projections have been made by Hawkins & Sutton (2009, 2011) and Deser et al. (2012).

Major uncertainties

In the statement, virtually none. In future emissions and climate sensitivity, there are significant uncertainties as reflected by the focus of this Key Message.

Assessment of confidence based on evidence and agreement, including short description of nature of evidence and level of agreement

X Certain (100%)

☐ Very High

X High

☐ Medium

☐ Low

The first statement regarding additional warming has *high confidence* in the amount of warming; the second is *virtually certain*, as understanding of the radiative properties of greenhouse gases

and the existence of both positive and negative feedbacks in the climate system is basic physics, dating to the 19th century.

Summary sentence or paragraph that integrates the above information

The key finding is based on basic physics that has been well established for decades to centuries and is referenced in every IPCC report from FAR to AR5.

Key Finding 2

Atmospheric carbon dioxide (CO₂) levels have now passed 400 ppm, a concentration last seen about 3 million years ago, when average temperature and sea level were significantly higher than today. Continued growth in CO₂ emissions over this century and beyond would lead to concentrations not experienced in tens to hundreds of millions of years. The rapid present-day emissions rate of nearly 10 GtC per year, however, suggests that there is no precise past climate analogue for this century any time in at least the last 66 million years. (*Medium confidence*)

Description of evidence base

The Key Finding is based on a large body of research including Crowley (1990), Schneider et al. (2013), Lunt et al. (2012), Otto-Bleisner et al. (2013), NEEM (2013), Jouzel et al. (2007), Dutton et al. (2015), Seki et al. (2010), Haywood et al. (2013), Miller et al. (2012), Royer (2014), Bowen et al. (2015), Kirtland Turner et al. (2014), Penman et al. (2014), Zeebe et al. (2016), and summarized in NRC (2011) and Masson-Delmotte et al. (2013).

Major uncertainties

The largest uncertainty is the measurement of past sea level, given the contributions of not only changes in land ice mass, but also in solid earth, mantle, isostatic adjustments, etc. that occur on timescales of millions of years. This uncertainty increases the further back in time we go; however, the signal (and forcing) size is also much greater. There are also associated uncertainties in precise quantification of past global mean temperature and carbon dioxide levels. There is uncertainty in the age models used to determine rates of change and coincidence of response at shorter, sub-millennial timescales.

Assessment of confidence based on evidence and agreement, including short description of nature of evidence and level of agreement

☐ Very High

☐ High

X Medium

☐ Low

Medium confidence in the likelihood statement that past global mean temperature and sea level rise were higher with similar or higher CO₂ concentrations is based on Masson-Delmotte et al. (2013) in IPCC AR5. *Medium confidence* that no precise analog exists in 66 million years is

based on Zeebe et al. (2016) as well as the larger body of literature summarized in Masson-Delmotte et al. (2013).

Summary sentence or paragraph that integrates the above information

The key finding is based on a vast body of literature that summarizes the results of observations, paleoclimate analyses, and paleoclimate modeling over the past 50 years and more.

Key Finding 3

The observed acceleration in carbon emissions over the past 15–20 years is consistent with higher future scenarios (*very high confidence*). Since 2014, growth rates have slowed as economic growth begins to uncouple from carbon emissions (*medium confidence*) but not yet at a rate that, were it to continue, would limit atmospheric temperature increase to the 2009 Copenhagen goal of 2°C (3.6°F), let alone the 1.5°C (2.7°F) target of the 2015 Paris Agreement (*high confidence*).

Description of Evidence Base

Observed emissions for 2014 and 2015 and estimated emissions for 2016 suggest a decrease in the growth rate and possibly even emissions of carbon; this shift is attributed primarily to decreased coal use in China although with significant uncertainty as noted in the references in the text.

All credible climate models assessed in Chapter 9 of the IPCC WG1 AR5 (IPCC 2013a) from the simplest to the most complex respond with elevated global mean temperature, the simplest indicator of climate change, when greenhouse gases increase. It follows then that an emissions pathway that tracks or exceeds RCP8.5 would lead to larger amounts of climate change.

The evidence that actual emission rates track or exceed the RCP8.5 scenario are as follows. The actual emission of CO₂ from fossil fuel consumption and concrete manufacture over the period 2005–2014 is 90.11 Pg (Le Quéré et al. 2015) The RCP8.5 emissions over the same period assuming linear trends between years in the specification is 89.01 Pg.

Actual emissions: <http://www.globalcarbonproject.org/carbonbudget/15/data.htm> and Le Quere et al. (2015).

RCP8.5 emissions

<http://tntcat.iiasa.ac.at:8787/RcpDb/dsd?Action=htmlpage&page=compare>

The actual numbers (red is estimated).

	RCP8.5	Actual	difference
2005	7.971	8.076	0.105
2006	8.162	8.363	0.201
2007	8.353	8.532	0.179
2008	8.544	8.74	0.196
2009	8.735	8.7	-0.035
2010	8.9256	9.14	0.2144
2011	9.18716	9.449	0.26184
2012	9.44832	9.575025506	0.126705506
2013	9.70948	9.735033958	0.025553958
2014	9.97064	9.795211382	-0.175428618
total	89.0062	90.10527085	1.099070845

Major Uncertainties

None

Assessment of confidence based on evidence and agreement, including short description of nature of evidence and level of agreement

☐ Certain (100%)

☒ Very High

☒ High

☒ Medium

☐ Low

Very high confidence in increasing emissions over the last 20 years and *high confidence* in the fact that recent emission trends will not be sufficient to avoid 2°C. *Medium confidence* in recent findings that the growth rate is slowing and/or emissions are plateauing soon. Climate change scales with the amount of anthropogenic greenhouse gas in the atmosphere. If emissions exceed RCP8.5, the likely range of changes temperatures and climate variables will be larger than projected.

Summary sentence or paragraph that integrates the above information

The key finding is based on basic physics relating emissions to concentrations, radiative forcing, and resulting change in global mean temperature as well as on IEA data on national emissions as reported in the peer-reviewed literature.

Key Finding 4

Combining output from global climate models and dynamical and statistical downscaling models using advanced averaging, weighting, and pattern scaling approaches can result in more relevant and robust future projections. These techniques also allow the scientific community to provide better guidance on the use of climate projections for quantifying regional-scale impacts (*medium to high confidence*).

Description of evidence base

The contribution of weighting and pattern scaling to improving the robustness of multimodel ensemble projections is described and quantified by a large body of literature as summarized in the text. The state of the art of dynamical and statistical downscaling and the scientific community's ability to provide guidance regarding the application of climate projections to regional impact assessments is summarized in Kotamarthi et al. (2016). This peer-reviewed DOD SERDP report documents new advances in testing and evaluating empirical statistical downscaling methods. This is the best available reference at this time, as downscaling receives only cursory mention in IPCC AR5 and—despite proposals for a report on this topic—has yet to be the focus of an NAS report.

Major uncertainties

Regional climate models are subject to the same structural and parametric uncertainties as global models, as well as the uncertainty due to incorporating boundary conditions. The primary source of error in application of empirical statistical downscaling methods is inappropriate application, followed by stationarity.

Assessment of confidence based on evidence and agreement, including short description of nature of evidence and level of agreement

☐ Very High

☐ High

X Medium

☐ Low

Advanced weighting techniques have significantly improved over previous Bayesian approaches; confidence in their ability to improve the robustness of multi-model ensembles, while currently rated as *medium*, is likely to grow in coming years. Downscaling has evolved significantly over the last decade and is now broadly viewed as a robust source for high-resolution climate projections that can be used as input to regional impact assessments.

Summary sentence or paragraph that integrates the above information

Scientific understanding of climate projections, downscaling, multi-model ensembles, and weighting has evolved significantly over the last decades to the extent that appropriate methods are now broadly viewed as robust sources for climate projections that can be used as input to regional impact assessments.

1 FIGURES

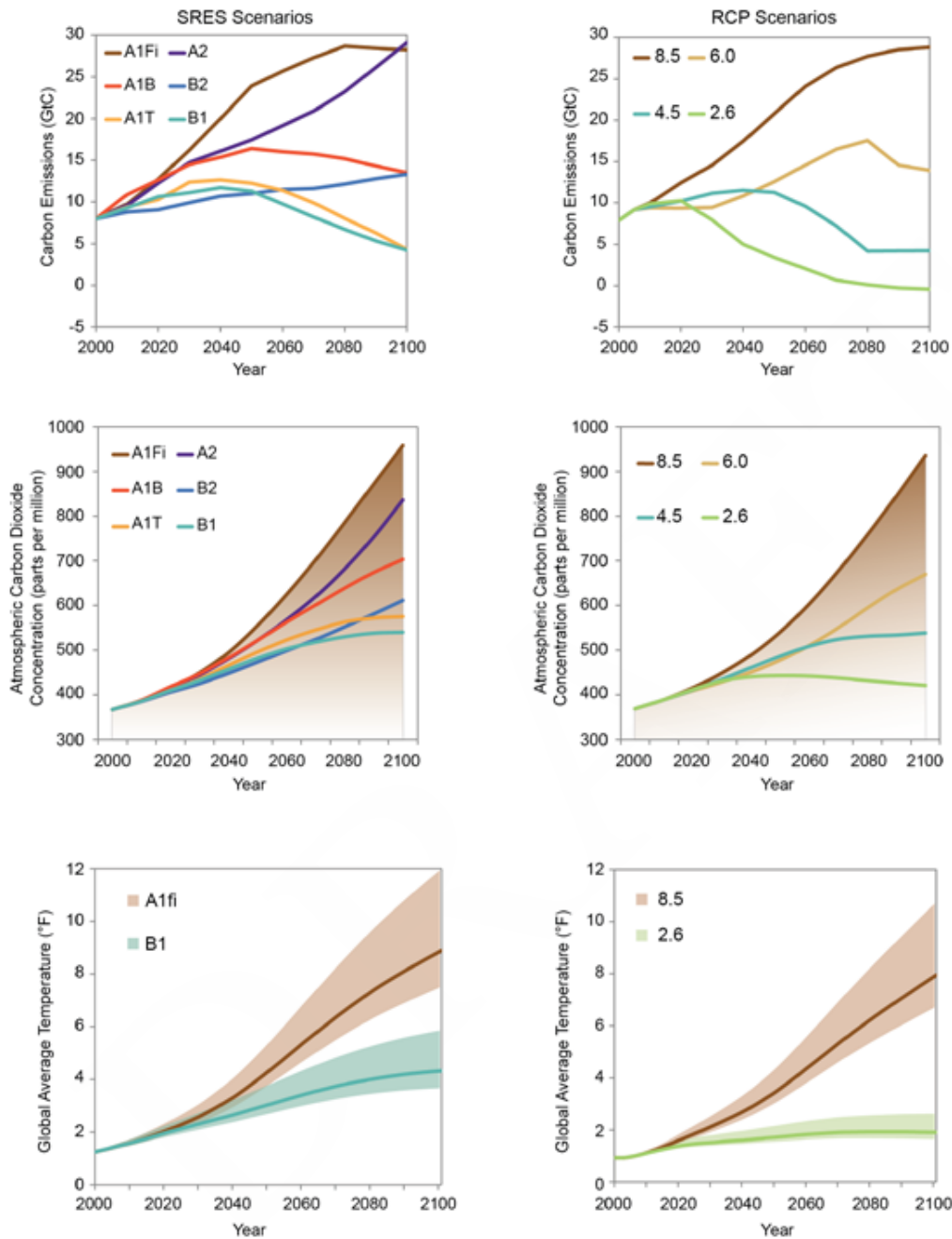


Figure 4.1: The climate projections used in this report are based on the 2010 Representative Concentration Pathways (RCP, right). They are largely consistent with scenarios used in previous assessments, the 2000 Special Report on Emission Scenarios (SRES, left). This figure compares SRES and RCP annual carbon emissions (top), carbon dioxide equivalent levels in the atmosphere (middle), and temperature change that would result from the central estimate (lines) and the likely range (shaded areas) of climate sensitivity (bottom). (Data from CMIP3 and CMIP5). (Figure source: Walsh et al. 2014)

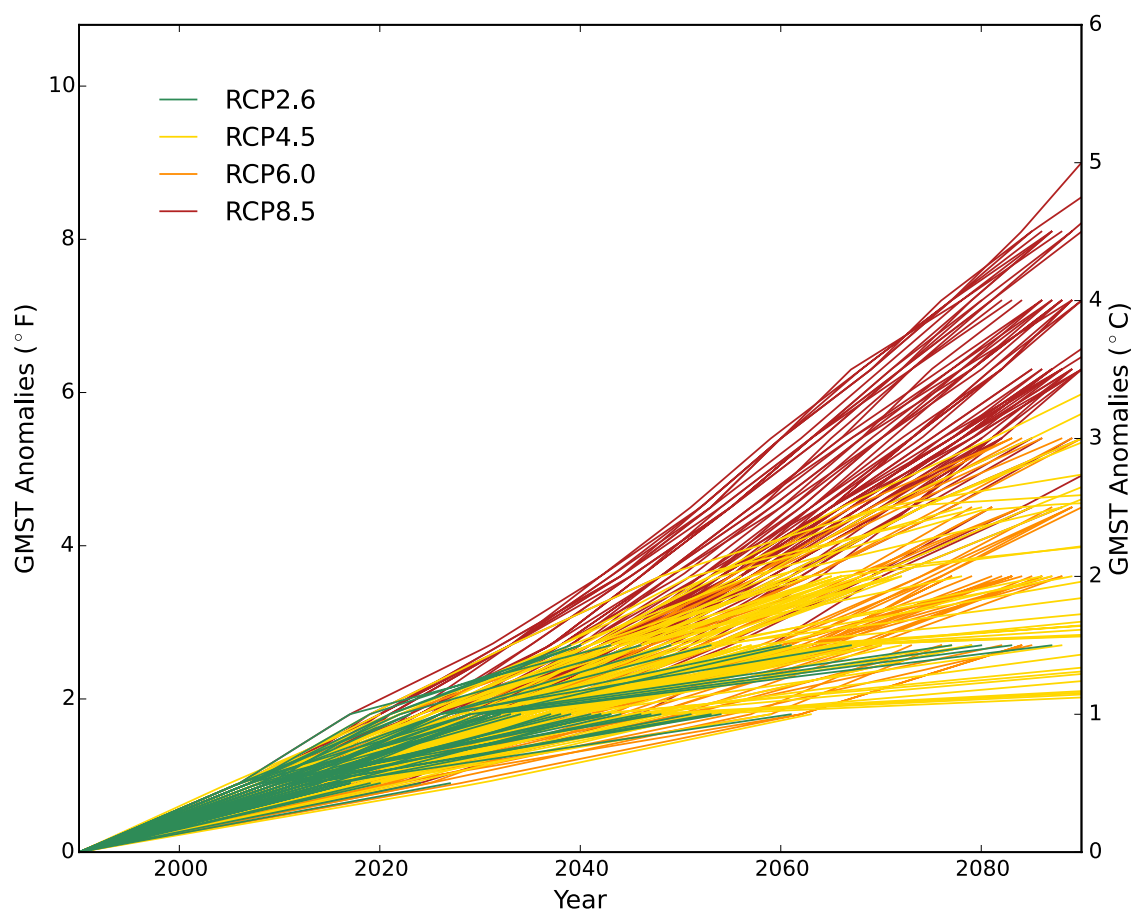
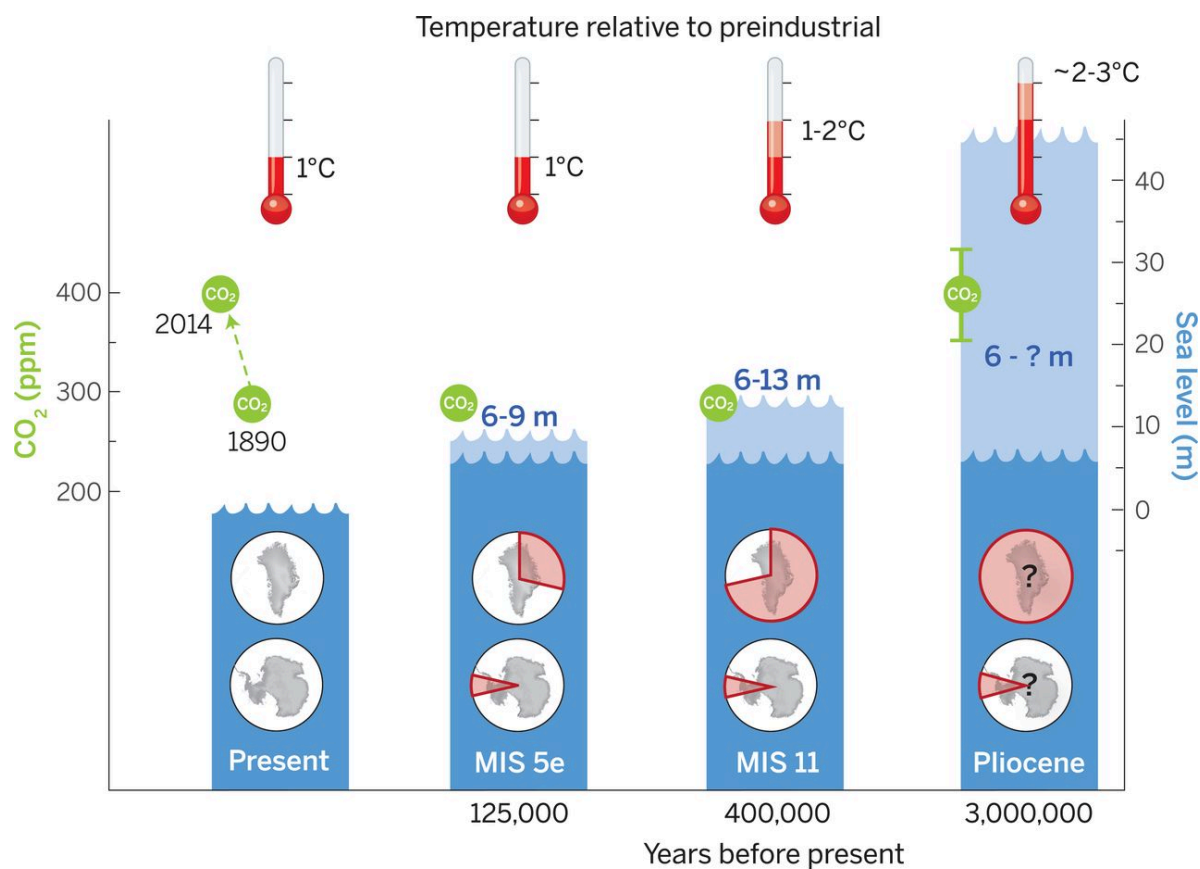


Figure 4.2: Global mean surface temperature anomalies (°C) relative to 1976–2005 for four RCP scenarios, 2.6 (green), 4.5 (yellow), 6.0 (orange), and 8.5 (red), calculated in 0.5°C increments. Each line represents an individual simulation from the CMIP5 archive; every RCP-based CMIP5 simulation with annual or monthly temperature outputs available was used here. (Figure source: adapted from Swain and Hayhoe 2015)



2
3
4 **Figure 4.3:** Putting present-day global mean temperature, CO₂ concentrations, and sea level into
5 context, this figure summarizes what is known about the range in peak global mean temperature,
6 atmospheric CO₂, maximum global mean sea level (GMSL), and source(s) of meltwater over
7 three periods in the past with CO₂ levels similar to pre-industrial levels (around 270 ppm) or
8 today (around 400 ppm). Light blue shading indicates uncertainty of GMSL maximum. Red pie
9 charts over Greenland and Antarctica denote fraction, not location, of ice retreat. (Figure source:
10 Dutton et al. 2015)
11

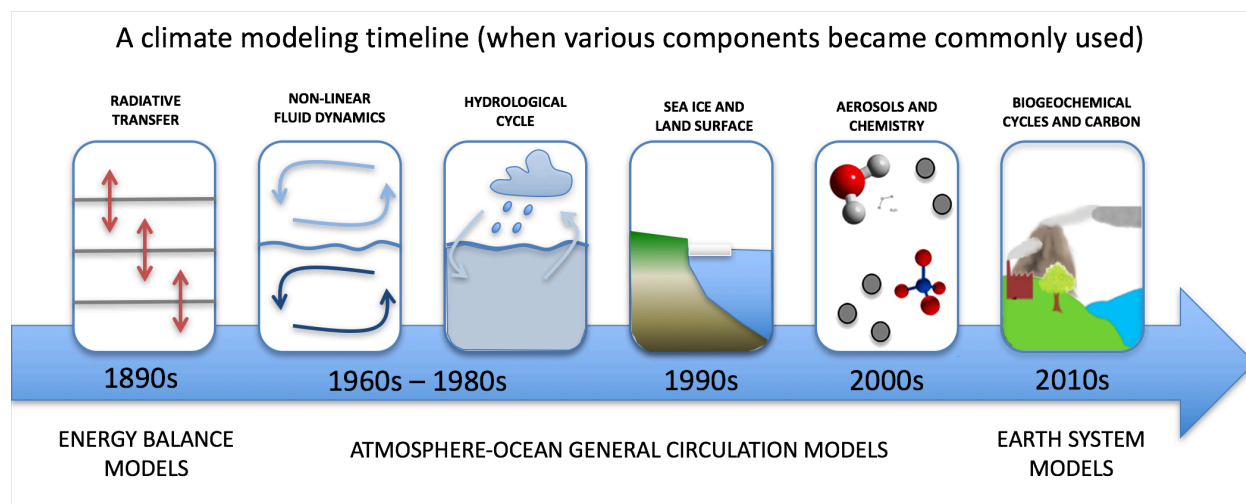


Figure 4.4: As climate modeling has evolved over the last 120 years, increasing amounts of physical science have been incorporated into the models. This figure shows the evolution from simple energy balance models through atmosphere–ocean general circulation models to today’s earth system models.

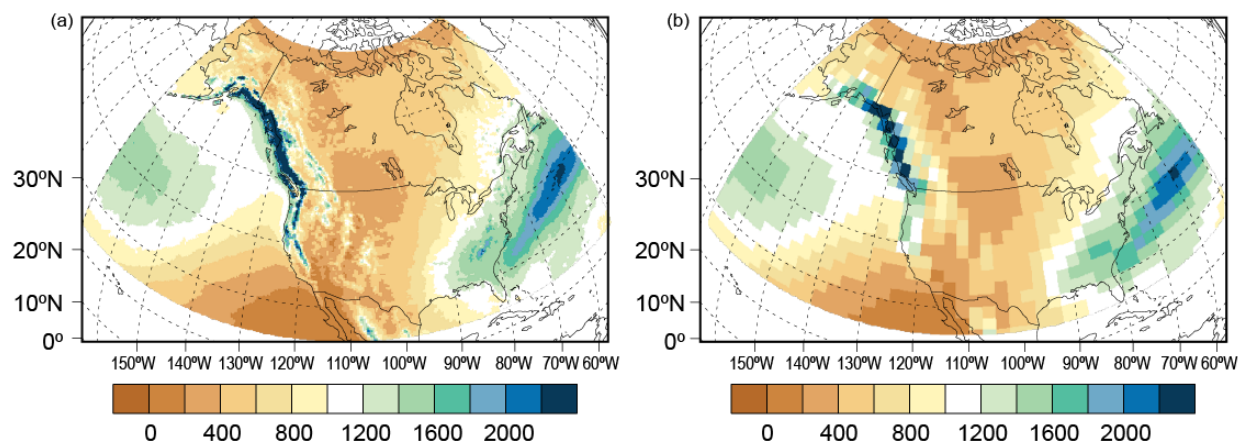


Figure 4.5: Global climate models typically operate at coarser horizontal spatial scales, while regional climate models have much finer resolutions. This figure compares annual average precipitation for the historical period 1979–2008 using (a) a resolution of 25 km or 15 miles with (b) a resolution of 250 km or 150 miles, to illustrate the importance of spatial scale in resolving key topographical features, particularly along the coasts and in mountainous areas. In this case, both simulations are by the GFDL HIRAM model, an experimental high-resolution model. (Figure source: adapted from Dixon et al. 2016; © American Meteorological Society, used with permission)

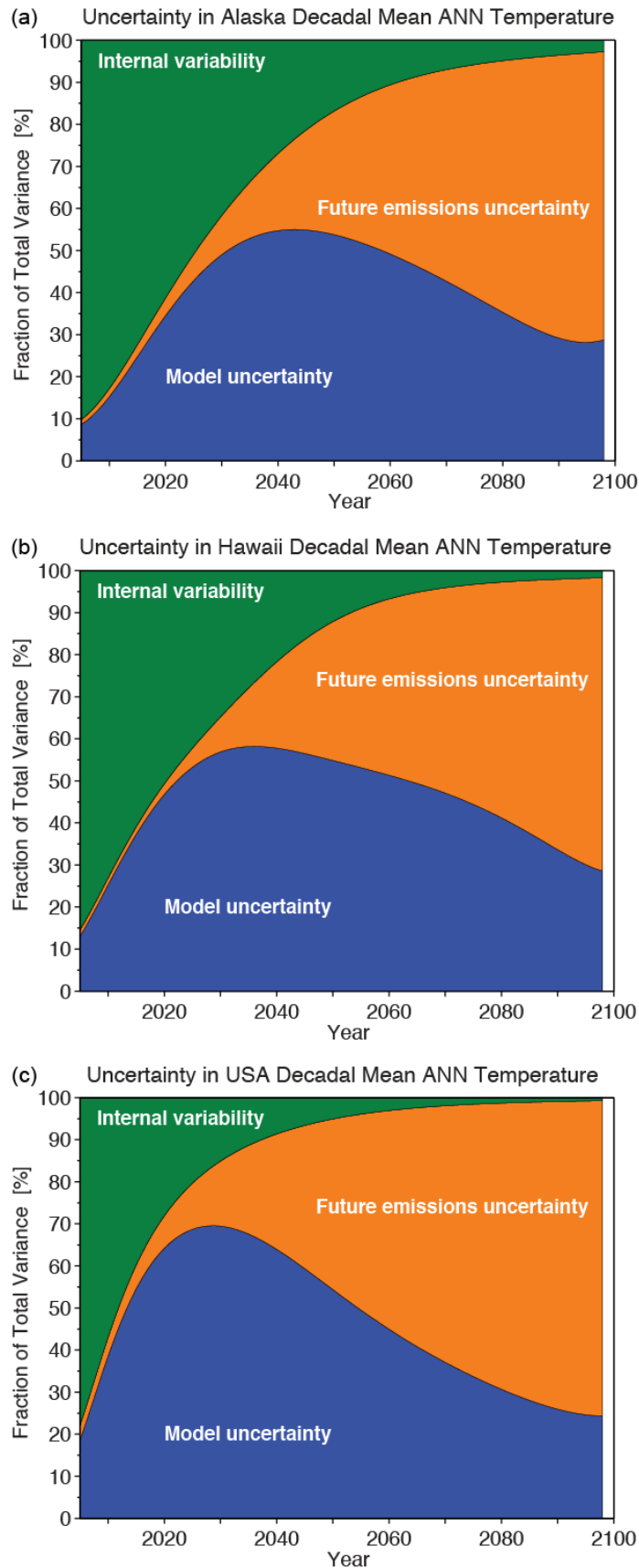


Figure 4.6: The fraction of total variance in decadal mean surface air temperature predictions explained by the three components of total uncertainty is shown for (a) Alaska, (b) Hawai’I, and (c) the lower 48 states (bottom). Orange regions represent human or scenario uncertainty, blue regions represent model uncertainty, and green regions represent the internal variability component. As the size of the region is reduced, the relative importance of internal variability increases. In interpreting this figure, it is important to remember that it shows the fractional sources of uncertainty. Total uncertainty increases as time progresses. (Figure source: adapted from Hawkins and Sutton 2009)

1 REFERENCES

- 2 Archer, D. and R. Pierrehumbert, eds. *The Warming Papers: The Scientific Foundation for the*
3 *Climate Change Forecast*. 2011, Wiley-Blackwell: Oxford, UK. 432.
- 4 Bowen, G.J., B.J. Maibauer, M.J. Kraus, U. Rohl, T. Westerhold, A. Steimke, P.D. Gingerich,
5 S.L. Wing, and W.C. Clyde, 2015: Two massive, rapid releases of carbon during the onset of
6 the Palaeocene-Eocene thermal maximum. *Nature Geosci*, **8**, 44-47.
7 <http://dx.doi.org/10.1038/ngeo2316>
- 8 Braconnot, P., S.P. Harrison, M. Kageyama, P.J. Bartlein, V. Masson-Delmotte, A. Abe-Ouchi,
9 B. Otto-Bliesner, and Y. Zhao, 2012: Evaluation of climate models using palaeoclimatic
10 data. *Nature Clim. Change*, **2**, 417-424. <http://dx.doi.org/10.1038/nclimate1456>
- 11 Brands, S., J.M. Gutiérrez, S. Herrera, and A.S. Cofiño, 2012: On the Use of Reanalysis Data for
12 Downscaling. *Journal of Climate*, **25**, 2517-2526. <http://dx.doi.org/10.1175/jcli-d-11-00251.1>
- 13 Collins, M., R. Knutti, J. Arblaster, J.-L. Dufresne, T. Fichefet, P. Friedlingstein, X. Gao, W.J.
14 Gutowski, T. Johns, G. Krinner, M. Shongwe, C. Tebaldi, A.J. Weaver, and M. Wehner,
15 2013: Long-term Climate Change: Projections, Commitments and Irreversibility. *Climate*
16 *Change 2013: The Physical Science Basis. Contribution of Working Group I to the Fifth*
17 *Assessment Report of the Intergovernmental Panel on Climate Change*. Stocker, T.F., D.
18 Qin, G.-K. Plattner, M. Tignor, S.K. Allen, J. Boschung, A. Nauels, Y. Xia, V. Bex, and
19 P.M. Midgley, Eds. Cambridge University Press, Cambridge, United Kingdom and New
20 York, NY, USA, 1029–1136. <http://dx.doi.org/10.1017/CBO9781107415324.024>
21 www.climatechange2013.org
- 22 Crowley, T.J., 1990: Are There Any Satisfactory Geologic Analogs for a Future Greenhouse
23 Warming? *Journal of Climate*, **3**, 1282-1292. [http://dx.doi.org/10.1175/1520-](http://dx.doi.org/10.1175/1520-0442(1990)003<1282:atasga>2.0.co;2)
24 [0442\(1990\)003<1282:atasga>2.0.co;2](http://dx.doi.org/10.1175/1520-0442(1990)003<1282:atasga>2.0.co;2)
- 25 Cubasch, U., D. Wuebbles, D. Chen, M.C. Facchini, D. Frame, N. Mahowald, and J.-G. Winther,
26 2013: Introduction. *Climate Change 2013: The Physical Science Basis. Contribution of*
27 *Working Group I to the Fifth Assessment Report of the Intergovernmental Panel on Climate*
28 *Change*. Stocker, T.F., D. Qin, G.-K. Plattner, M. Tignor, S.K. Allen, J. Boschung, A.
29 Nauels, Y. Xia, V. Bex, and P.M. Midgley, Eds. Cambridge University Press, Cambridge,
30 United Kingdom and New York, NY, USA, 119–158.
31 <http://dx.doi.org/10.1017/CBO9781107415324.007> www.climatechange2013.org
- 32 DeConto, R.M. and D. Pollard, 2016: Contribution of Antarctica to past and future sea-level rise.
33 *Nature*, 531, 591-597. <http://dx.doi.org/10.1038/nature17145>

- Deser, C., A. Phillips, V. Bourdette, and H. Teng, 2012: Uncertainty in climate change projections: The role of internal variability. *Climate Dynamics*, **38**, 527-546. <http://dx.doi.org/10.1007/s00382-010-0977-x>
- Dixon, K.W., J.R. Lanzante, M.J. Nath, K. Hayhoe, A. Stoner, A. Radhakrishnan, V. Balaji, and C.F. Gaitán, 2016: Evaluating the stationarity assumption in statistically downscaled climate projections: is past performance an indicator of future results? *Climatic Change*, **135**, 395-408. <http://dx.doi.org/10.1007/s10584-016-1598-0>
- Dutton, A., A.E. Carlson, A.J. Long, G.A. Milne, P.U. Clark, R. DeConto, B.P. Horton, S. Rahmstorf, and M.E. Raymo, 2015: Sea-level rise due to polar ice-sheet mass loss during past warm periods. *Science*, **349**. <http://dx.doi.org/10.1126/science.aaa4019>
- Fix, M.J., D. Cooley, S.R. Sain, and C. Tebaldi, 2016: A comparison of U.S. precipitation extremes under RCP8.5 and RCP4.5 with an application of pattern scaling. *Climatic Change*, 1-13. <http://dx.doi.org/10.1007/s10584-016-1656-7>
- Frieler, K., M. Meinshausen, A. Golly, M. Mengel, K. Lebek, S.D. Donner, and O. Hoegh-Guldberg, 2013: Limiting global warming to 2°C is unlikely to save most coral reefs. *Nature Climate Change*, **3**, 165-170. <http://dx.doi.org/10.1038/nclimate1674>
- Gasson, E., D.J. Lunt, R. DeConto, A. Goldner, M. Heinemann, M. Huber, A.N. LeGrande, D. Pollard, N. Sagoo, M. Siddall, A. Winguth, and P.J. Valdes, 2014: Uncertainties in the modelled CO₂ threshold for Antarctic glaciation. *Climate of the Past*, **10**, 451-466. <http://dx.doi.org/10.5194/cp-10-451-2014> <http://www.clim-past.net/10/451/2014/>
- Green, F. and N. Stern, 2016: China's changing economy: implications for its carbon dioxide emissions. *Climate Policy*, 1-15. <http://dx.doi.org/10.1080/14693062.2016.1156515>
- Hartmann, D.L., A.M.G. Klein Tank, M. Rusticucci, L.V. Alexander, S. Brönnimann, Y. Charabi, F.J. Dentener, E.J. Dlugokencky, D.R. Easterling, A. Kaplan, B.J. Soden, P.W. Thorne, M. Wild, and P.M. Zhai, 2013: Observations: Atmosphere and Surface. *Climate Change 2013: The Physical Science Basis. Contribution of Working Group I to the Fifth Assessment Report of the Intergovernmental Panel on Climate Change*. Stocker, T.F., D. Qin, G.-K. Plattner, M. Tignor, S.K. Allen, J. Boschung, A. Nauels, Y. Xia, V. Bex, and P.M. Midgley, Eds. Cambridge University Press, Cambridge, United Kingdom and New York, NY, USA, 159–254. <http://dx.doi.org/10.1017/CBO9781107415324.008> www.climatechange2013.org
- Hawkins, E. and R. Sutton, 2009: The potential to narrow uncertainty in regional climate predictions. *Bulletin of the American Meteorological Society*, **90**, 1095-1107. <http://dx.doi.org/10.1175/2009BAMS2607.1>

- 1 Hawkins, E. and R. Sutton, 2011: The potential to narrow uncertainty in projections of regional
2 precipitation change. *Climate Dynamics*, **37**, 407-418. [http://dx.doi.org/10.1007/s00382-010-](http://dx.doi.org/10.1007/s00382-010-0810-6)
3 0810-6
- 4 Haywood, A.M., D.J. Hill, A.M. Dolan, B.L. Otto-Bliesner, F. Bragg, W.L. Chan, M.A.
5 Chandler, C. Contoux, H.J. Dowsett, A. Jost, Y. Kamae, G. Lohmann, D.J. Lunt, A. Abe-
6 Ouchi, S.J. Pickering, G. Ramstein, N.A. Rosenbloom, U. Salzmann, L. Sohl, C. Stepanek,
7 H. Ueda, Q. Yan, and Z. Zhang, 2013: Large-scale features of Pliocene climate: results from
8 the Pliocene Model Intercomparison Project. *Climate of the Past*, **9**, 191-209.
9 <http://dx.doi.org/10.5194/cp-9-191-2013>
- 10 Herger, N., B.M. Sanderson, and R. Knutti, 2015: Improved pattern scaling approaches for the
11 use in climate impact studies. *Geophysical Research Letters*, **42**, 3486-3494.
12 <http://dx.doi.org/10.1002/2015GL063569>
- 13 IEA, 2016: Decoupling of global emissions and economic growth confirmed. International
14 Energy Agency, March 16.
15 [https://www.iea.org/newsroomandevents/pressreleases/2016/march/decoupling-of-global-](https://www.iea.org/newsroomandevents/pressreleases/2016/march/decoupling-of-global-emissions-and-economic-growth-confirmed.html)
16 [emissions-and-economic-growth-confirmed.html](https://www.iea.org/newsroomandevents/pressreleases/2016/march/decoupling-of-global-emissions-and-economic-growth-confirmed.html)
- 17 IPCC, 2013: *Climate Change 2013: The Physical Science Basis. Contribution of Working Group*
18 *I to the Fifth Assessment Report of the Intergovernmental Panel on Climate Change*.
19 Cambridge University Press, Cambridge, UK and New York, NY, 1535 pp.
20 <http://dx.doi.org/10.1017/CBO9781107415324> www.climatechange2013.org
- 21 IPCC, 2013: Summary for policymakers. *Climate Change 2013: The Physical Science Basis.*
22 *Contribution of Working Group I to the Fifth Assessment Report of the Intergovernmental*
23 *Panel on Climate Change*. Stocker, T.F., D. Qin, G.-K. Plattner, M. Tignor, S.K. Allen, J.
24 Boschung, A. Nauels, Y. Xia, V. Bex, and P.M. Midgley, Eds. Cambridge University Press,
25 Cambridge, United Kingdom and New York, NY, USA, 1–30.
26 <http://dx.doi.org/10.1017/CBO9781107415324.004>
- 27 Jackson, R.B., J.G. Canadell, C. Le Quere, R.M. Andrew, J.I. Korsbakken, G.P. Peters, and N.
28 Nakicenovic, 2016: Reaching peak emissions. *Nature Climate Change*, **6**, 7-10.
29 <http://dx.doi.org/10.1038/nclimate2892>
- 30 Jagiecki, E.A., T.K. Lowenstein, D.M. Jenkins, and R.V. Demicco, 2015: Eocene atmospheric
31 CO₂ from the nahcolite proxy. *Geology*. <http://dx.doi.org/10.1130/g36886.1>
32 <http://geology.gsapubs.org/content/early/2015/10/23/G36886.1.abstract>
- 33 Jouzel, J., V. Masson-Delmotte, O. Cattani, G. Dreyfus, S. Falourd, G. Hoffmann, B. Minster, J.
34 Nouet, J.M. Barnola, J. Chappellaz, H. Fischer, J.C. Gallet, S. Johnsen, M. Leuenberger, L.
35 Loulergue, D. Luethi, H. Oerter, F. Parrenin, G. Raisbeck, D. Raynaud, A. Schilt, J.

- 1 Schwander, E. Selmo, R. Souchez, R. Spahni, B. Stauffer, J.P. Steffensen, B. Stenni, T.F.
2 Stocker, J.L. Tison, M. Werner, and E.W. Wolff, 2007: Orbital and Millennial Antarctic
3 Climate Variability over the Past 800,000 Years. *Science*, **317**, 793-796.
4 <http://dx.doi.org/10.1126/science.1141038>
- 5 Karl, T.R., J.M. Melillo, and T.C. Peterson, 2009: Global Climate Change Impacts in the United
6 States. 189 pp., New York. [http://downloads.globalchange.gov/usimpacts/pdfs/climate-](http://downloads.globalchange.gov/usimpacts/pdfs/climate-impacts-report.pdf)
7 [impacts-report.pdf](http://downloads.globalchange.gov/usimpacts/pdfs/climate-impacts-report.pdf)
- 8 Kirtland Turner, S., P.F. Sexton, C.D. Charles, and R.D. Norris, 2014: Persistence of carbon
9 release events through the peak of early Eocene global warmth. *Nature Geosci*, **7**, 748-751.
10 <http://dx.doi.org/10.1038/ngeo2240>
- 11 Kirtman, B., S.B. Power, J.A. Adedoyin, G.J. Boer, R. Bojariu, I. Camilloni, F.J. Doblas-Reyes,
12 A.M. Fiore, M. Kimoto, G.A. Meehl, M. Prather, A. Sarr, C. Schär, R. Sutton, G.J.
13 van Oldenborgh, G. Vecchi, and H.J. Wang, 2013: Near-term climate change: Projections
14 and predictability. *Climate Change 2013: The Physical Science Basis. Contribution of*
15 *Working Group I to the Fifth Assessment Report of the Intergovernmental Panel on Climate*
16 *Change*. Stocker, T.F., D. Qin, G.-K. Plattner, M. Tignor, S.K. Allen, J. Boschung, A.
17 Nauels, Y. Xia, V. Bex, and P.M. Midgley, Eds. Cambridge University Press, Cambridge,
18 UK and New York, NY, USA, 953–1028.
19 <http://dx.doi.org/10.1017/CBO9781107415324.023>
- 20 Knutti, R. and G.C. Hegerl, 2008: The equilibrium sensitivity of the Earth's temperature to
21 radiation changes. *Nature Geoscience*, **1**, 735-743. <http://dx.doi.org/10.1038/ngeo337>
- 22 Knutti, R., D. Masson, and A. Gettelman, 2013: Climate model genealogy: Generation CMIP5
23 and how we got there. *Geophysical Research Letters*, **40**, 1194-1199.
24 <http://dx.doi.org/10.1002/grl.50256>
- 25 Kopp, R.E., F.J. Simons, J.X. Mitrovica, A.C. Maloof, and M. Oppenheimer, 2009: Probabilistic
26 assessment of sea level during the last interglacial stage. *Nature*, **462**, 863-867.
27 <http://dx.doi.org/10.1038/nature08686>
- 28 Korsbakken, J.I., G.P. Peters, and R.M. Andrew, 2016: Uncertainties around reductions in
29 China's coal use and CO2 emissions. *Nature Climate Change*, **6**, 687-690.
30 <http://dx.doi.org/10.1038/nclimate2963>
- 31 Kotamarthi, R., L. Mearns, K. Hayhoe, C. Castro, and D. Wuebbles, 2016: Use of Climate
32 Information for Decision-Making and Impact Research. 55 pp. U.S. Department of Defense,
33 Strategic Environment Research and Development Program Report.
- 34 Le Quéré, C., R. Moriarty, R.M. Andrew, J.G. Canadell, S. Sitch, J.I. Korsbakken, P.
35 Friedlingstein, G.P. Peters, R.J. Andres, T.A. Boden, R.A. Houghton, J.I. House, R.F.

- Keeling, P. Tans, A. Arneeth, D.C.E. Bakker, L. Barbero, L. Bopp, J. Chang, F. Chevallier, L.P. Chini, P. Ciais, M. Fader, R.A. Feely, T. Gkritzalis, I. Harris, J. Hauck, T. Ilyina, A.K. Jain, E. Kato, V. Kitidis, K. Klein Goldewijk, C. Koven, P. Landschützer, S.K. Lauvset, N. Lefèvre, A. Lenton, I.D. Lima, N. Metzl, F. Millero, D.R. Munro, A. Murata, J.E.M.S. Nabel, S. Nakaoka, Y. Nojiri, K. O'Brien, A. Olsen, T. Ono, F.F. Pérez, B. Pfeil, D. Pierrot, B. Poulter, G. Rehder, C. Rödenbeck, S. Saito, U. Schuster, J. Schwinger, R. Séférian, T. Steinhoff, B.D. Stocker, A.J. Sutton, T. Takahashi, B. Tilbrook, I.T. van der Laan-Luijkx, G.R. van der Werf, S. van Heuven, D. Vandemark, N. Viovy, A. Wiltshire, S. Zaehle, and N. Zeng, 2015: Global Carbon Budget 2015. *Earth System Science Data*, **7**, 349-396. <http://dx.doi.org/10.5194/essd-7-349-2015>
- Le Quéré, C., M.R. Raupach, J.G. Canadell, G. Marland, L. Bopp, P. Ciais, T.J. Conway, S.C. Doney, R.A. Feely, P. Foster, P. Friedlingstein, K. Gurney, R.A. Houghton, J.I. House, C. Huntingford, P.E. Levy, M.R. Lomas, J. Majkut, N. Metzl, J.P. Ometto, G.P. Peters, I.C. Prentice, J.T. Randerson, S.W. Running, J.L. Sarmiento, U. Schuster, S. Sitch, T. Takahashi, N. Viovy, G.R. van der Werf, and F.I. Woodward, 2009: Trends in the sources and sinks of carbon dioxide. *Nature Geoscience*, **2**, 831-836. <http://dx.doi.org/10.1038/ngeo689>
- Leggett, J., W.J. Pepper, R.J. Swart, J. Edmonds, L.G.M. Filho, I. Mintzer, M.X. Wang, and J. Watson, 1992: Emissions Scenarios for the IPCC: an Update. *Climate Change 1992: The Supplementary Report to the IPCC Scientific Assessment*. Houghton, J.T., B.A. Callander, and S.K. Varney, Eds. Cambridge University Press, Cambridge, United Kingdom, New York, NY, USA, and Victoria, Australia, 73-95.
- Lunt, D.J., T. Dunkley Jones, M. Heinemann, M. Huber, A. LeGrande, A. Winguth, C. Loptson, J. Marotzke, C.D. Roberts, J. Tindall, P. Valdes, and C. Winguth, 2012: A model–data comparison for a multi-model ensemble of early Eocene atmosphere–ocean simulations: EoMIP. *Climate of the Past*, **8**, 1717-1736. <http://dx.doi.org/10.5194/cp-8-1717-2012>
- Masson-Delmotte, V., M. Schulz, A. Abe-Ouchi, J. Beer, A. Ganopolski, J.F. González Rouco, E. Jansen, K. Lambeck, J. Luterbacher, T. Naish, T. Osborn, B. Otto-Bliesner, T. Quinn, R. Ramesh, M. Rojas, X. Shao, and A. Timmermann, 2013: Information from Paleoclimate Archives. *Climate Change 2013: The Physical Science Basis. Contribution of Working Group I to the Fifth Assessment Report of the Intergovernmental Panel on Climate Change*. Stocker, T.F., D. Qin, G.-K. Plattner, M. Tignor, S.K. Allen, J. Boschung, A. Nauels, Y. Xia, V. Bex, and P.M. Midgley, Eds. Cambridge University Press, Cambridge, United Kingdom and New York, NY, USA, 383–464. <http://dx.doi.org/10.1017/CBO9781107415324.013> www.climatechange2013.org
- McGlade, C. and P. Ekins, 2015: The geographical distribution of fossil fuels unused when limiting global warming to 2 [deg]C. *Nature*, **517**, 187-190. <http://dx.doi.org/10.1038/nature14016>

- 1 Melillo, J.M., T.C. Richmond, and G.W. Yohe, eds. *Climate Change Impacts in the United*
2 *States: The Third National Climate Assessment*. 2014, U.S. Global Change Research
3 Program: Washington, D.C. 842. <http://dx.doi.org/10.7930/J0Z31WJ2>.
- 4 Miller, K.G., J.D. Wright, J.V. Browning, A. Kulpecz, M. Kominz, T.R. Naish, B.S. Cramer, Y.
5 Rosenthal, W.R. Peltier, and S. Sosdian, 2012: High tide of the warm Pliocene: Implications
6 of global sea level for Antarctic deglaciation. *Geology*. <http://dx.doi.org/10.1130/g32869.1>
- 7 Mitchell, T.D., 2003: Pattern Scaling: An Examination of the Accuracy of the Technique for
8 Describing Future Climates. *Climatic Change*, **60**, 217-242.
9 <http://dx.doi.org/10.1023/a:1026035305597>
- 10 Moss, R.H., J.A. Edmonds, K.A. Hibbard, M.R. Manning, S.K. Rose, D.P. van Vuuren, T.R.
11 Carter, S. Emori, M. Kainuma, T. Kram, G.A. Meehl, J.F.B. Mitchell, N. Nakicenovic, K.
12 Riahi, S.J. Smith, R.J. Stouffer, A.M. Thomson, J.P. Weyant, and T.J. Wilbanks, 2010: The
13 next generation of scenarios for climate change research and assessment. *Nature*, **463**, 747-
14 756. <http://dx.doi.org/10.1038/nature08823>
- 15 Nakicenovic, N., J. Alcamo, G. Davis, B.d. Vries, J. Fenhann, S. Gaffin, K. Gregory, A. Grübler,
16 T.Y. Jung, T. Kram, E.L.L. Rovere, L. Michaelis, S. Mori, T. Morita, W. Pepper, H. Pitcher,
17 L. Price, K. Riahi, A. Roehrl, H.-H. Rogner, A. Sankovski, M. Schlesinger, P. Shukla, S.
18 Smith, R. Swart, S.v. Rooijen, N. Victor, and Z. Dadi, 2000: IPCC Special Report on
19 Emissions Scenarios. Cambridge University Press,
- 20 NEEM, 2013: Eemian interglacial reconstructed from a Greenland folded ice core. *Nature*, **493**,
21 489-494. <http://dx.doi.org/10.1038/nature11789>
- 22 NRC, 2011: *Climate Stabilization Targets: Emissions, Concentrations, and Impacts over*
23 *Decades to Millennia*. National Research Council. The National Academies Press,
24 Washington, D.C., 298 pp. <http://dx.doi.org/10.17226/12877>
- 25 O'Neill, B.C., E. Kriegler, K. Riahi, K.L. Ebi, S. Hallegatte, T.R. Carter, R. Mathur, and D.P.
26 van Vuuren, 2014: A new scenario framework for climate change research: The concept of
27 shared socioeconomic pathways. *Climatic Change*, **122**, 387-400.
28 <http://dx.doi.org/10.1007/s10584-013-0905-2>
- 29 Otto-Bliesner, B.L., N. Rosenbloom, E.J. Stone, N.P. McKay, D.J. Lunt, E.C. Brady, and J.T.
30 Overpeck, 2013: How warm was the last interglacial? New model–data comparisons.
31 *Philosophical Transactions of the Royal Society A: Mathematical, Physical and Engineering*
32 *Sciences*, **371**. <http://dx.doi.org/10.1098/rsta.2013.0097>
- 33 Pagani, M., M. Huber, Z. Liu, S.M. Bohaty, J. Henderiks, W. Sijp, S. Krishnan, and R.M.
34 DeConto, 2011: The Role of Carbon Dioxide During the Onset of Antarctic Glaciation.
35 *Science*, **334**, 1261-1264. <http://dx.doi.org/10.1126/science.1203909>

- 1 Penman, D.E., B. Hönlisch, R.E. Zeebe, E. Thomas, and J.C. Zachos, 2014: Rapid and sustained
2 surface ocean acidification during the Paleocene-Eocene Thermal Maximum.
3 *Paleoceanography*, **29**, 357-369. <http://dx.doi.org/10.1002/2014PA002621>
- 4 Raupach, M.R., G. Marland, P. Ciais, C. Le Quéré, J.G. Canadell, G. Klepper, and C.B. Field,
5 2007: Global and regional drivers of accelerating CO₂ emissions. *Proceedings of the*
6 *National Academy of Sciences*, **104**, 10288-10293.
7 <http://dx.doi.org/10.1073/pnas.0700609104>
- 8 Rhein, M., S.R. Rintoul, S. Aoki, E. Campos, D. Chambers, R.A. Feely, S. Gulev, G.C. Johnson,
9 S.A. Josey, A. Kostianoy, C. Mauritzen, D. Roemmich, L.D. Talley, and F. Wang, 2013:
10 Observations: Ocean. *Climate Change 2013: The Physical Science Basis. Contribution of*
11 *Working Group I to the Fifth Assessment Report of the Intergovernmental Panel on Climate*
12 *Change*. Stocker, T.F., D. Qin, G.-K. Plattner, M. Tignor, S.K. Allen, J. Boschung, A.
13 Nauels, Y. Xia, V. Bex, and P.M. Midgley, Eds. Cambridge University Press, Cambridge,
14 United Kingdom and New York, NY, USA, 255–316.
15 <http://dx.doi.org/10.1017/CBO9781107415324.010> www.climatechange2013.org
- 16 Riahi, K., S. Rao, V. Krey, C. Cho, V. Chirkov, G. Fischer, G. Kindermann, N. Nakicenovic, and
17 P. Rafaj, 2011: RCP 8.5—A scenario of comparatively high greenhouse gas emissions.
18 *Climatic Change*, **109**, 33-57. <http://dx.doi.org/10.1007/s10584-011-0149-y>
- 19 Royer, D.L., 2014: 6.11 - Atmospheric CO₂ and O₂ During the Phanerozoic: Tools, Patterns,
20 and Impacts A2 - Holland, Heinrich D. *Treatise on Geochemistry (Second Edition)*.
21 Turekian, K.K., Ed. Elsevier, Oxford, 251-267. [http://dx.doi.org/10.1016/B978-0-08-095975-](http://dx.doi.org/10.1016/B978-0-08-095975-7.01311-5)
22 [7.01311-5 http://www.sciencedirect.com/science/article/pii/B9780080959757013115](http://www.sciencedirect.com/science/article/pii/B9780080959757013115)
- 23 Ryu, J.-H. and K. Hayhoe, 2013: Understanding the sources of Caribbean precipitation biases in
24 CMIP3 and CMIP5 simulations. *Climate Dynamics*, 1-20. [http://dx.doi.org/10.1007/s00382-](http://dx.doi.org/10.1007/s00382-013-1801-1)
25 [013-1801-1](http://dx.doi.org/10.1007/s00382-013-1801-1)
- 26 Sanderson, B.M., R. Knutti, and P. Caldwell, 2015: A Representative Democracy to Reduce
27 Interdependency in a Multimodel Ensemble. *Journal of Climate*, **28**, 5171-5194.
28 <http://dx.doi.org/10.1175/JCLI-D-14-00362.1>
- 29 Sanderson, B.M., B.C. O'Neill, and C. Tebaldi, 2016: What would it take to achieve the Paris
30 temperature targets? *Geophysical Research Letters*, **43**, 7133-7142.
31 <http://dx.doi.org/10.1002/2016GL069563>
- 32 Sanderson, B.M., M. Wehner, and R. Knutti, 2016: Skill and Independence weighting for multi-
33 model Assessment. *Geoscientific Model Development* **Submitted**.
- 34 Schneider, R., J. Schmitt, P. Köhler, F. Joos, and H. Fischer, 2013: A reconstruction of
35 atmospheric carbon dioxide and its stable carbon isotopic composition from the penultimate

- glacial maximum to the last glacial inception. *Clim. Past*, **9**, 2507-2523.
<http://dx.doi.org/10.5194/cp-9-2507-2013> <http://www.clim-past.net/9/2507/2013/>
- Seki, O., G.L. Foster, D.N. Schmidt, A. Mackensen, K. Kawamura, and R.D. Pancost, 2010: Alkenone and boron-based Pliocene pCO₂ records. *Earth and Planetary Science Letters*, **292**, 201-211. <http://dx.doi.org/10.1016/j.epsl.2010.01.037>
<http://www.sciencedirect.com/science/article/pii/S0012821X10000816>
- Smith, P., S.J. Davis, F. Creutzig, S. Fuss, J. Minx, B. Gabrielle, E. Kato, R.B. Jackson, A. Cowie, E. Kriegler, D.P. van Vuuren, J. Rogelj, P. Ciais, J. Milne, J.G. Canadell, D. McCollum, G. Peters, R. Andrew, V. Krey, G. Shrestha, P. Friedlingstein, T. Gasser, A. Grubler, W.K. Heidug, M. Jonas, C.D. Jones, F. Kraxner, E. Littleton, J. Lowe, J.R. Moreira, N. Nakicenovic, M. Obersteiner, A. Patwardhan, M. Rogner, E. Rubin, A. Sharifi, A. Torvanger, Y. Yamagata, J. Edmonds, and C. Yongsung, 2015: Biophysical and economic limits to negative CO₂ emissions. *Nature Climate Change*, **6**, 42-50.
<http://dx.doi.org/10.1038/nclimate2870>
- Swain, S. and K. Hayhoe, 2015: CMIP5 projected changes in spring and summer drought and wet conditions over North America. *Climate Dynamics*, **44**, 2737-2750.
<http://dx.doi.org/10.1007/s00382-014-2255-9>
- Tebaldi, C. and J.M. Arblaster, 2014: Pattern scaling: Its strengths and limitations, and an update on the latest model simulations. *Climatic Change*, **122**, 459-471.
<http://dx.doi.org/10.1007/s10584-013-1032-9>
- Thrasher, B., J. Xiong, W. Wang, F. Melton, A. Michaelis, and R. Nemani, 2013: Downscaled Climate Projections Suitable for Resource Management. *Eos, Transactions of the American Geophysical Union*, **94**, 321-323. <http://dx.doi.org/10.1002/2013EO370002>
- UNFCCC, 2015: Paris Agreement. United Nations Framework Convention on Climate Change, [Bonn, Germany].
- Vaughan, D.G., J.C. Comiso, I. Allison, J. Carrasco, G. Kaser, R. Kwok, P. Mote, T. Murray, F. Paul, J. Ren, E. Rignot, O. Solomina, K. Steffen, and T. Zhang, 2013: Observations: Cryosphere. *Climate Change 2013: The Physical Science Basis. Contribution of Working Group I to the Fifth Assessment Report of the Intergovernmental Panel on Climate Change*. Stocker, T.F., D. Qin, G.-K. Plattner, M. Tignor, S.K. Allen, J. Boschung, A. Nauels, Y. Xia, V. Bex, and P.M. Midgley, Eds. Cambridge University Press, Cambridge, United Kingdom and New York, NY, USA, 317-382. <http://dx.doi.org/10.1017/CBO9781107415324.012>
www.climatechange2013.org
- Walsh, J., D. Wuebbles, K. Hayhoe, J. Kossin, K. Kunkel, G. Stephens, P. Thorne, R. Vose, M. Wehner, J. Willis, D. Anderson, S. Doney, R. Feely, P. Hennon, V. Kharin, T. Knutson, F.

- 1 Landerer, T. Lenton, J. Kennedy, and R. Somerville, 2014: Ch. 2: Our changing climate.
2 *Climate Change Impacts in the United States: The Third National Climate Assessment*.
3 Melillo, J.M., T.C. Richmond, and G.W. Yohe, Eds. U.S. Global Change Research Program,
4 Washington, D.C., 19-67. <http://dx.doi.org/10.7930/J0KW5CXT>
- 5 Wang, C., L. Zhang, S.-K. Lee, L. Wu, and C.R. Mechoso, 2014: A global perspective on
6 CMIP5 climate model biases. *Nature Climate Change*, **4**, 201-205.
7 <http://dx.doi.org/10.1038/nclimate2118>
- 8 Wang, M., J.E. Overland, V. Kattsov, J.E. Walsh, X. Zhang, and T. Pavlova, 2007: Intrinsic
9 versus Forced Variation in Coupled Climate Model Simulations over the Arctic during the
10 Twentieth Century. *Journal of Climate*, **20**, 1093-1107. <http://dx.doi.org/10.1175/JCLI4043.1>
- 11 Zeebe, R.E., A. Ridgwell, and J.C. Zachos, 2016: Anthropogenic carbon release rate
12 unprecedented during the past 66 million years. *Nature Geoscience*, **9**, 325-329.
13 <http://dx.doi.org/10.1038/ngeo2681>

5. Large-Scale Circulation and Climate Variability

KEY FINDINGS

1. Under increased greenhouse gas concentrations, the tropics are *likely* to expand with an accompanying poleward shift of the subtropical dry zones and midlatitude jets in each hemisphere (*medium to high confidence*). While it is *likely* that tropics have expanded since 1979 (*medium confidence*), uncertainties remain regarding the attribution of these changes to human activities.
2. Recurring patterns of variability in large-scale atmospheric circulation (such as the North Atlantic Oscillation and Northern Annular Mode) and the atmosphere–ocean system (such as El Niño–Southern Oscillation) cause year-to-year variations in U.S. temperatures and precipitation (*high confidence*). Changes in the occurrence of these patterns or their properties have contributed to recent U.S. temperature and precipitation trends (*medium confidence*) although uncertainties remain about the size of the role of human influences in these changes.
3. Increasing temperatures and atmospheric specific humidity are already having important influences on extremes (*high confidence*). It is still unclear, however, to what extent increasing temperatures and humidity have influenced and will influence persistent circulation patterns, which in turn influence these extremes.

5.1. Introduction

The causes of regional climate trends cannot be understood without considering the impact of changes in large-scale atmospheric circulation and an assessment of the role of internally generated climate variability. There are contributions to regional climate trends from changes in large-scale latitudinal circulation, which is generally organized into three cells in each hemisphere—Hadley Cell, Ferrell Cell and Polar Cell—and which determines the location of subtropical dry zones and midlatitude jet streams. These circulation cells are expected to shift poleward during warmer periods (Frierson et al. 2007; Sun et al. 2013; Vallis et al. 2015), which could result in poleward shifts in precipitation patterns affecting natural ecosystems, agriculture, and water resources (Seidel et al. 2008; Feng and Fu 2013).

In addition, regional climate can be strongly affected by non-local response to recurring patterns (or modes) of variability of the atmospheric circulation or the coupled atmosphere–ocean system. These modes of variability represent preferred spatial patterns and their temporal variation and account for gross features in variance and for teleconnections. Modes of variability are often described as a product of a spatial climate pattern and an associated climate index time series that are identified based on statistical methods like Principle Component Analysis (PC analysis),

which is also called Empirical Orthogonal Function Analysis (EOF analysis), and cluster analysis.

[INSERT FIGURE 5.1 HERE:]

Figure 5.1: (*Top*) Plan and (*bottom*) cross section schematic view representation of the general circulation of the atmosphere. Three main circulations exist between the equator and poles due to solar heating and the earth's rotation.

Hadley cell (1) – Low-latitude air moves toward the equator. Due to solar heating, air near the equator rises vertically and moves poleward in the upper atmosphere.

Ferrel cell (2) – A midlatitude mean atmospheric circulation cell. In this cell, the air flows poleward and eastward near the surface and equatorward and westward at higher levels.

Polar cell (3) – Air rises, diverges, and travels toward the poles. Once over the poles, the air sinks, forming the polar highs. At the surface, air diverges outward from the polar highs. Surface winds in the polar cell are easterly (polar easterlies).

A high pressure band is located at about 30° N/S latitude, leading to dry/hot weather due to descending air motion (subtropical dry zones are indicated in orange in the schematic views).

Expanding tropics (indicted by orange arrows) are associated with a poleward shift of the subtropical dry zones. A low pressure band is found at 50°–60° N/S, with rainy and stormy weather in relation to the polar jet stream bands of strong westerly wind in the upper levels of the atmosphere. (Figure source: adapted from NWS 2016)]

On intra-seasonal to interannual time scales, the climate of the United States is strongly affected by modes of atmospheric circulation variability like the North Atlantic Oscillation (NAO)/Northern Annular Mode (NAM), North Pacific Oscillation (NPO), and Pacific North American Pattern (PNA). They are closely linked to other atmospheric circulation phenomena like blocking and quasi-stationary wave patterns and jet streams. On an interannual time scale, coupled atmosphere–ocean phenomena like El Niño–Southern Oscillation (ENSO) have a prominent effect. On longer time scales, U.S. climate anomalies are linked to slow variations of sea surface temperature related to the Pacific Decadal Oscillation (PDO) and the Atlantic Multidecadal Oscillation (AMO).

In general, the influences of human activities on the climate system are now so widespread that the current and future behavior of these previous ‘natural’ climate features can no longer be assumed independent of those human influences. Climate response to external forcing appears to project strongly onto these existing recurring modes of variability, although the regional temperature and precipitation impacts of these modes can be modified due to a changed background climate. However, modes of internal variability of the climate system also contribute to observed decadal and multidecadal temperature and precipitation trends on local scales, masking possible systematic changes due to an anthropogenic influence. Recent studies point out though, that there are still large uncertainties in our understanding of the impact of human-induced climate change on atmospheric circulation, and the predictability of large-scale circulation changes might be limited (Shepherd 2014; Vallis et al. 2015).

5.2 Modes of Variability: Past and Projected Changes

5.2.1 Width of the Tropics and Global Circulation

Sea level pressure gives an indication of surface changes in atmospheric circulation.

Contributions of greenhouse gas, ozone, and aerosol changes on the seasonal and geographical patterns of trends in global sea level pressure over 1951–2011 are detectable (Gillett et al. 2013). On regional scales and particularly at higher latitudes, internal variability has been found to play a large role in uncertainties of future sea level pressure projections (Deser et al. 2012).

Evidence continues to mount for an expansion of the tropics over the past several decades, with a poleward expansion of the Hadley cell and an associated poleward shift of the subtropical dry zones in each hemisphere, although the rate of expansion is uncertain and depends on the metrics used (Birner et al. 2014; Brönnimann et al. 2015; Davis and Birner 2013; Feng and Fu 2013; Garfinkel et al. 2015; Karnauskas and Ummenhofer 2014; Lucas et al. 2014; Quan et al. 2014; Reichler 2016). While the roles of stratospheric ozone depletion in the Southern Hemisphere (Waugh et al. 2015) and anthropogenic aerosols in the Northern Hemisphere (Allen et al. 2012; Kovilakam and Mahajan 2015) have been implicated as contributors in the expansion, there is uncertainty in the relative contributions of natural and anthropogenic factors, and natural variability may be dominating (Adam et al. 2014; Allen et al. 2014; Garfinkel et al. 2015).

Most of the previous work on tropical expansion to date has focused on zonally-averaged changes. There are only a few recent studies that diagnose regional characteristics of tropical expansion. The findings depend on analysis methods and datasets. For example, a northward expansion of the tropics in most regions of the Northern Hemisphere, including the Eastern Pacific with impact on drying in the American Southwest, is found based on diagnosing outgoing longwave radiation (Chen et al. 2014). However, other studies do not find a significant poleward expansion of the tropics over the Eastern Pacific and North America (Schwendike et al. 2015; Lucas and Nguyen 2015). Thus, the implications of the recent widening of the tropics for the climate of the United States and thus observed drying of the Southwest (Feng and Fu 2013; Prein et al. 2016) are not clear.

Due to human-induced greenhouse gas increases, the Hadley cell is likely to widen in the future with an accompanying poleward shift in the subtropical dry zones and midlatitude jets (Collins et al. 2013; Barnes and Polvani 2013; Scheff and Frierson 2012a; Scheff and Frierson 2012b; Vallis et al. 2015; Feng and Fu 2013). Large uncertainties remain in projected changes in non-zonal to regional circulation components and related changes in precipitation patterns (Simpson et al. 2014; Barnes and Polvani 2013; Shepherd 2014; Simpson et al. 2016). Uncertainties in projected changes in midlatitude jets are also related to projected rate of arctic amplification and changes in the stratospheric polar vortex. Both factors could shift the mid-latitude jet equatorward especially in the North Atlantic region (Barnes and Polvani 2015; Scaife et al. 2012; Karpechko and Manzini 2012).

5.2.2 El Niño-Southern Oscillation

El Niño–Southern Oscillation (ENSO) is a main source of climate variability, with a 2–7 year timescale, originating from coupled ocean–atmosphere interactions in the tropical Pacific and affecting weather patterns over many parts of the globe through atmospheric teleconnections. It strongly affects precipitation and temperature in the United States (Figure 5.2) (Halpert and Ropelewski 1992; Hoerling et al. 2001; Kiladis and Diaz 1989; Ropelewski and Halpert 1987).

[INSERT FIGURE 5.2 HERE:]

Figure 5.2: El Niño- and La Niña-related winter features over North America. Shown are typical January to March weather anomalies and atmospheric circulation during moderate to strong El Niño and La Niña conditions: (top) During El Niño, there is a tendency for a strong jet stream and storm track across the southern part of the United States. The southern tier of Alaska and the U.S. Pacific Northwest tend to be warmer than average, whereas the southern tier of U.S. states tends to be cooler and wetter than average. During La Niña, there is a tendency of a very wave-like jet stream flow over the United States and Canada, with colder and stormier than average conditions across the North, and warmer and less stormy conditions across the South. (Figure source: adapted from Lindsey 2016)]

El Niño teleconnections are modulated by the location of maximum anomalous tropical Pacific sea surface temperatures (SST). Eastern Pacific (EP) El Niño events affect winter temperatures primarily over the Great Lakes, Northeast, and Southwest, while Central Pacific (CP) events influence temperatures primarily over the northwestern and southeastern United States (Yu et al. 2012). The CP El Niño also enhances the drying effect, but weakens the wetting effect, typically produced by traditional EP El Niño events on the United States winter precipitation (Yu and Zou 2013). It is not clear whether observed decadal-scale modulations of ENSO properties, including an increase in ENSO amplitude (Li et al. 2011) and an increase in frequency of CP El Niño events (Lee and McPhaden 2010; Yeh et al. 2009), are due to internal variability or anthropogenic forcing. There are at least a couple of reasons for this uncertainty. First, comprehensive observations that allow investigation of ENSO-related coupled atmosphere–ocean feedbacks go back only to the late 1970s (Christensen et al. 2013). Second, unforced global climate model simulations show that decadal to centennial modulations of ENSO can be generated without any change in external forcing (Capatondi et al. 2015).

While there is high confidence that ENSO will remain a preferred mode of natural climate variability in the 21st century, only low confidence is indicated for specific projected changes in ENSO variability (Christensen et al. 2013). This low confidence is the result of the fact that models do not agree on the projected changes in El Niño intensity or on changes in the zonal gradient of tropical Pacific sea surface temperatures. Recent studies suggest a near doubling in frequency of occurrence of both extreme El Niño and La Niña events due to human-induced greenhouse gas increases for the 21st century relative to the 20th century, as determined by a subset of CMIP model simulations (Cai et al. 2014, 2015a,b).

There is robust evidence of an eastward shift of ENSO-induced teleconnection patterns due to greenhouse gas-induced climate change (Kug et al. 2010; Meehl and Teng 2007; Stevenson 2012; Zhou et al. 2014). However, the impact of this shift on ENSO-induced climate anomalies in the United States is not well understood (Seager et al. 2012; Zhou et al. 2014).

5.2.3 Extra-tropical Modes of Variability and Phenomena

NORTH ATLANTIC OSCILLATION AND NORTHERN ANNULAR MODE

The North Atlantic Oscillation (NAO), the leading recurring mode of variability in the extra-tropical North Atlantic region, describes an opposite variation in sea level pressure between the Atlantic subtropical high and the Iceland/Arctic low. Variations in the NAO are accompanied by changes in the location and intensity of the Atlantic midlatitude storm track and blocking activity that affect climate over the North Atlantic and surrounding continents. A negative NAO phase is related to anomalously cold conditions and an enhanced number of cold outbreaks in the eastern United States, while a strong positive phase of the NAO tends to be associated with above-normal temperatures in this region (Hurrell and Deser 2009; Thompson and Wallace 2001). The positive phase of the NAO is associated with increased precipitation frequency and positive daily rainfall anomalies, including extreme daily precipitation anomalies in the northeastern United States (Durkee et al. 2008; Archambault et al. 2008).

The Northern Annular Mode/Arctic Oscillation (NAM/AO) is closely related to the NAO. It describes a pressure seesaw between mid and high latitudes on a hemispheric scale and thus includes a third anomaly center over the North Pacific Ocean (Thompson and Wallace 1998; Thompson and Wallace 2000). The time series of the NAO and NAM/AO are highly correlated, with persistent NAO and NAM/AO events being indistinguishable (Deser 2000; Feldstein and Franzke 2006).

The wintertime NAO/NAM index exhibits pronounced variability on multidecadal time scales, with an increase from the 1960s to the 1990s, a shift to a more negative phase since the 1990s due to a series of winters like 2009–2010 and 2010–2011 (which had exceptionally low index values), and a return to more positive values after 2011 (Bindoff et al. 2013). Decadal scale temperature trends in the eastern United States, including occurrence of cold outbreaks during recent years, are linked to these changes in the NAO/NAM (Hurrell 1995; Cohen and Barlow 2005; Overland and Wang 2015; Overland et al. 2015).

The CMIP5 models on average simulate a progressive shift of the NAO/NAM towards its positive phase due to human-induced climate change (Gillett and Fyfe 2013). However, the spread between model simulations is larger than the projected multimodel increase, and shifts between preferred periods of positive and negative NAO phase will continue to occur similar to those observed in the past (Deser et al. 2012; Christensen et al. 2013).

The NAO's influence on the ocean occurs through changes in heat content, gyre circulations, mixed layer depth, salinity, high-latitude deep water formation, and sea ice cover (Hurrell and Deser 2009). Climate model simulations show that multidecadal variation in the NAO induce multidecadal variations in the Atlantic meridional overturning circulation and poleward ocean heat transport in the Atlantic that is extending to the Arctic. It has been suggested that these variations have contributed to the observed rapid loss of Arctic sea ice and Northern Hemisphere warming, especially in the late 1990s and early 2000s, and thus enhanced the long-term trends in Arctic sea ice loss and hemispheric warming that are mainly caused by anthropogenic forcing (Delworth et al. 2016).

NORTH PACIFIC OSCILLATION/WEST PACIFIC OSCILLATION

The North Pacific Oscillation (NPO) is the leading mode of variability in the extratropical North Pacific region and is characterized by a north-south seesaw in sea level pressure. NPO effects on U.S. hydroclimate and marginal ice zone extent in the Arctic seas have been reported (Linkin and Nigam 2008). However, 21st century climate projections suggest no major changes in the NPO (Furtado et al. 2011).

PACIFIC/NORTH AMERICAN PATTERN

The Pacific/North American (PNA) pattern is the leading recurring mode of internal atmospheric variability over the North Pacific and the North American continent, especially during the cold season. It describes a quadripole pattern of mid-tropospheric height anomalies, with anomalies of similar sign located over the subtropical northeastern Pacific and northwestern North America and of the opposite sign centered over the Gulf of Alaska and the southeastern United States. The PNA pattern is associated with strong fluctuations in the strength and location of the East Asian jet stream. The positive phase of the PNA pattern is associated with above-average temperatures over the western and northwestern United States, and below-average temperatures across the south-central and southeastern United States, including enhanced occurrence of extreme cold temperatures (Leathers et al. 1991; Loikith and Broccoli 2012; Ning and Bradley 2016).

Significant negative correlation between the PNA and winter precipitation over the Ohio River Valley has been documented (Leathers et al. 1991; Coleman and Rogers 2003; Ning and Bradley 2016).

The PNA is related to ENSO events (Nigam 2003) and also serves as a bridge linking ENSO and NAO variability (Li and Lau 2012). A single model sensitivity study suggests that the PNA mode of atmospheric internal variability remains largely unchanged in pattern in a warmer climate (Zhou et al. 2014).

BLOCKING AND QUASI-STATIONARY WAVES

Anomalous atmospheric flow patterns in the extratropics that remain in place for an extended period of time (for example, blocking and quasi-stationary Rossby waves)—and thus affect a

1 region with similar weather conditions like rain or clear sky for several days to weeks—can lead
2 to flooding, drought, heat waves, and cold waves (Grotjahn et al. 2016; Whan et al. 2016;
3 Petoukhov et al. 2013). Specifically, blocking describes large-scale, persistent high pressure
4 systems that interrupt the typical westerly flow, while planetary waves (Rossby waves) describe
5 large meandering of the atmospheric jet stream.

6 A persistent pattern of high pressure in the circulation off the west coast of the United States has
7 been associated with the California drought (Ch.8; Swain et al. 2014; Seager et al. 2015).
8 Blocking in the Alaskan region, which is enhanced during La Niña winters (Figure 5.2)
9 (Renwick and Wallace 1996), is associated with higher temperatures in western Alaska but a
10 shift to lower mean and extreme surface temperatures from the Yukon southward to the southern
11 Plains (Carrera et al. 2004). The anomalously cold winters of 2009–2010 and 2010–2011 in the
12 United States are linked to the blocked (or negative) phase of the NAO (Guirguis et al. 2011).
13 Stationary Rossby wave patterns may have contributed to the North American temperature
14 extremes during summers like 2011 (Wang et al. 2014). It has been suggested that arctic
15 amplification has already led to weakened westerly winds and hence more slowly moving and
16 amplified wave patterns and enhanced occurrence of blocking (Francis and Vavrus 2012; Francis
17 et al. 2016; Ch. 11: Arctic Changes).

18 While a study based on a homogenized/extended Greenland Blocking Index (GBI) identified a
19 significant increase in the frequency of blocking events over Greenland since 1981 in all seasons
20 as well as in the annual mean (Hanna et al. 2016), a series of other studies did not find a
21 significant increase in the frequency of blocking, based on various blocking metrics in specific
22 regions and seasons and on various reanalysis products (Barnes 2013; Barnes et al. 2014).
23 Various metrics have been applied to diagnose recent changes in the amplitude of midlatitude
24 planetary waves (Francis and Vavrus 2012; Screen and Simmonds 2013) that differ in their
25 conclusions. While a metric based on the maximum latitude of selected 500 mb geopotential
26 height (Z_{500}) isopleths exhibits a statistical significant increase (Francis and Vavrus 2012), a
27 metric based on midlatitude meridional wave amplitude at 500 mb does not show significant
28 changes (Screen and Simmonds 2013).

29 A decrease of blocking frequency with climate change is found in CMIP3, CMIP5, and higher-
30 resolution models (Christensen et al. 2013; Hoskins and Woollings 2015; Kennedy et al. 2016).
31 However, CMIP5 models still underestimate observed blocking activity in the North Atlantic
32 sector while they tend to overestimate activity in the North Pacific, although with a large
33 intermodel spread (Christensen et al. 2013). Climate models robustly project a change in
34 Northern Hemisphere winter quasi-stationary wave fields that are linked to a wetting of the
35 North American West Coast (Brandefelt and Körnich 2008; Haarsma and Selten 2012; Simpson
36 et al. 2014), due to a strengthening of the zonal mean westerlies in the subtropical upper
37 troposphere. However, most of the climate models are found to overestimate the climate change
38 related response because of biases in the representation of relevant waves (Simpson et al. 2016).

Therefore, there is low confidence in projected changes in atmospheric blocking and wintertime quasi-stationary waves.

5.2.4 Modes of Variability on Decadal to Multidecadal Time Scales

PACIFIC DECADEAL OSCILLATION (PDO)/INTERDECADEAL PACIFIC OSCILLATION (IPO)

The Pacific Decadal Oscillation (PDO) is the leading year-round pattern of monthly North Pacific sea surface temperature variability, with a characteristic time scale of 40 to 60 years. Interdecadal Pacific Oscillation (IPO) refers to the same phenomenon based on Pacific-wide sea surface temperatures. PDO/IPO represents not a single phenomenon but rather a combination of processes that span the tropics and extratropics, including both remote tropical forcing and local North Pacific atmosphere–ocean interactions (Newman et al. 2016). Consequently, PDO-related impacts on temperature and precipitation of the United States are very similar to phenomena on interannual time scales like ENSO and variations in the strength of the Aleutian low (North Pacific Index, NPI), as shown in Figure 5.3. A PDO-related impact on Alaska temperatures is also apparent (Hartmann and Wendler 2005; McAfee 2014).

[INSERT FIGURE 5.3 HERE:

Cold season relationship between climate indices and U.S. precipitation and temperature anomalies determined from U.S. climate division data (Vose et al. 2014), for the years 1901–2014. November–March mean U.S. precipitation anomalies correlated with (a) the PDO index, (b) the ENSO index, and (c) the North Pacific Index. November–March U.S. temperature anomalies correlated with (d) the PDO index, (e) the ENSO index, and (f) the NPI. Decadal impacts related to the Pacific Decadal Oscillation (PDO) on temperature and precipitation of the United States are very similar to the impact of phenomena on interannual time scales like ENSO and variations in the strength of the Aleutian low characterized by the North Pacific Index (NPI). (Figure source: Newman et al. 2016; © American Meteorological Society, used with permission)]

Studies on future changes in the PDO/IPO are available based on CMIP3 models. It is found that most of these models do not exhibit significant changes in spatial and temporal characteristics in the PDO/IPO (Furtado et al. 2011), while some models suggest that the PDO/IPO becomes weaker and more frequent by the end of the 21st century (Lapp et al. 2012). Future emission changes have been suggested to also impact the PDO/IPO (Allen and Ajoku 2016). Therefore, there is only low confidence in projected future changes in the PDO/IPO.

ATLANTIC MULTI-DECADEAL OSCILLATION (AMO)

The Atlantic Multi-Decadal Oscillation (AMO) is one of the principal features of multidecadal variability in the instrumental climate record, with a coherent pattern of 50- to 70-year variability in surface temperature centered on the North Atlantic Ocean. Cool AMO phases occurred in the

1900s–1920s and 1960s–1980s, while a warm phase occurred in the 1930s–1950s and has been observed since the mid-1990s. During AMO warm periods, less than normal precipitation is found in most of the United States, including the most severe 20th century droughts in the 1930s and 1950s (Enfield et al. 2001; Seager et al. 2008; Feng et al. 2011). It is suggested that the warm phase of the AMO strengthens the North Atlantic tropical cyclone activity (Goldenberg et al. 2001; Chylek and Lesins 2008; Zhang and Delworth 2009).

Long-lived Atlantic multidecadal variability is found in long control simulations carried out with climate models (Menary et al. 2012), and CMIP3 models do not show any fundamental change in the characteristics of the AMO in the 21st century as compared to the 20th century or preindustrial climate (Ting et al. 2011).

INTERNALLY-GENERATED VERSUS EXTERNALLY-FORCED DECADEAL CLIMATE VARIABILITY

Several studies suggest that climate patterns in response to natural forcings (such as volcanic aerosols) and anthropogenic forcings (such as aerosols and greenhouse gases) project onto AMO- and PDO/IPO-related climate variability patterns (Boo et al. 2015; Booth et al. 2012; Evan et al. 2009; Mann and Emanuel 2006; Meehl et al. 2013). For example, historical aerosol cooling combined with global ocean warming due to increasing greenhouse gases could explain a large fraction of Atlantic multidecadal variability (Booth et al. 2012). Changes in aerosols are also found to coincide with PDO-like variability in North Pacific sea surface temperatures (Boo et al. 2015). Furthermore, it has been determined that periods with near zero warming trends of global mean temperature and periods of accelerated temperatures result from the interplay between internally generated PDO/IPO-like cooling and warming in the tropical Pacific Ocean and greenhouse gas-induced ocean warming (Meehl et al. 2013). These findings have implications for the attribution of causes of trends in global and regional mean temperatures, width of the tropics, droughts, and tropical cyclones (Ch. 1, 3, 8, 9 and Section 5.2.1). For example, studies that assign an entirely natural forcing component to regional patterns that resemble PDO/IPO may underestimate the role of human forcing, while studies that did not account for the impact of the PDO/IPO may overestimate the role of human-induced forcing (Abatzoglou et al. 2014a; Abatzoglou et al. 2014b; Johnstone and Mantua 2014a; Johnstone and Mantua 2014b). Furthermore, it is likely that PDO/IPO and AMO-like variability will continue to occur in the future, modulating anthropogenic forcing and its climate impacts on the United States and globally.

5.3. Quantifying the Role of Internal Variability on Past and Future U.S. Climate Trends

The role of internal variability in masking trends is substantially increased on regional and local scales relative to the global scale, and in the extratropics relative to the tropics (Ch. 4: Projections). Approaches are developed to better quantify the externally forced and internally

driven contributions to observed and future climate trends and variability and further separate these contributions into thermodynamically and dynamically driven factors (Wallace et al. 2015). Specifically, large “initial condition” climate model ensembles with 30 ensemble members and more (Deser et al. 2012; Deser et al. 2014; Wettstein and Deser 2014) and long control runs (Thompson et al. 2015) have been shown to be useful tools to characterize uncertainties in climate change projections at local/regional scales.

North American temperature and precipitation trends on timescales of up to a few decades are strongly affected by intrinsic atmospheric circulation variability (Deser et al. 2014; Wallace et al. 2015; Deser et al. 2016). For example, it is estimated that internal circulation trends account for approximately one-third of the observed wintertime warming over North America during the past 50 years. In a few areas, such as the central Rocky Mountains and far western Alaska, internal dynamics have offset the warming trend by 10%–30% (Deser et al. 2016). Natural climate variability superimposed upon forced climate change will result in a large range of possible trends for surface air temperature and precipitation in the United States over the next 50 years (Figure 5.4) (Deser et al. 2014).

[INSERT FIGURE 5.4 HERE:]

Figure 5.4: (left) Total 2010–60 winter trends decomposed into (center) internal and (right) forced components for two contrasting CCSM3 ensemble members (runs 29 and 6) for (a) SAT [color shading; $^{\circ}\text{F} (51 \text{ years})^{-1}$] and SLP (contours) and (b) precipitation [color shading; inches per day $(51 \text{ years})^{-1}$] and SLP (contours). SLP contour interval is 1 hPa $(51 \text{ years})^{-1}$, with solid (dashed) contours for positive (negative) values; the zero contour is thickened. The same climate model (CCSM3) simulates a large range of possible trends in North American climate over the 2010–2060 period because of the influence of internal climate variability superposed upon forced climate trends. (Figure source: adapted from Deser et al. 2014; © American Meteorological Society, used with permission)

Climate models are evaluated with respect to their proper simulation of internal decadal variability. Comparing observed and simulated variability estimates at time scales longer than 10 years suggest that models tend to overestimate the internal variability in the northern extratropics, including over the continental United States, but underestimate it over much of the tropics and subtropical ocean regions (Deser et al. 2012; Knutson et al. 2013). Such biases affect signal-to-noise estimates of regional scale climate change response and thus assessment of internally driven contributions to regional/local trends.

TRACEABLE ACCOUNTS

Key Finding 1

Under increased greenhouse gas concentrations, the tropics are *likely* to expand with an accompanying poleward shift of the subtropical dry zones and midlatitude jets in each hemisphere (*medium to high confidence*). While it is *likely* that tropics have expanded since 1979 (*medium confidence*), uncertainties remain regarding the attribution of these changes to human activities.

Description of evidence base

The Key Finding is supported by statements of the previous international IPCC AR5 assessment (IPCC 2013). Further evidence of an impact of greenhouse gas increases on the widening of the tropical belt and poleward shifts of the mid-latitude jets is provided by the diagnosis of CMIP5 simulations (Vallis et al. 2015, Barnes and Polvani 2013). Recent studies on estimates of changes in the width of the tropics provide additional evidence that the tropics has widened since 1979 (Birner et al. 2014; Davis and Birner 2013; Feng and Fu 2013; Garfinkel et al. 2015; Karneuskas and Ummenhofer 2014; Lucas et al. 2014; Quan et al. 2014; Reichler 2016). Recent studies provide new evidence on the significance of internal variability on recent changes in the tropical width (Adam et al. 2014; Allen et al. 2014; Garfinkel et al. 2015). These studies are discussed in the text.

Major uncertainties

The rate of observed expansion of tropics is uncertain and depends on the metrics used. Uncertainties also result from the utilizing of reanalysis to determine trends and limited observational records. There are major uncertainty in the estimates of the relative contribution of anthropogenic factors and internal variability to recent trends. Uncertainties in modeling future changes in global circulation arises from the presentation of stratosphere as well as simulated Arctic amplification.

Assessment of confidence based on evidence and agreement, including short description of nature of evidence and level of agreement

☐ Very High

☒ High

☒ Medium

☒ Low

There is high confidence that increased greenhouse gases cause a poleward expansion of the Hadley circulation. This is based on the agreement of a large number of studies utilizing modeling of different complexity and theoretical considerations. There is only medium confidence in future changes of mid-latitude jets specifically in the Northern Hemisphere due to the potential impact of other factors (Arctic amplification, stratospheric circulation change) that can push the mid-latitude jets equatorward. Uncertainties in the causes of recent trends result

from uncertainties in the magnitude of observed widening and a possibly large contribution of internal variability.

If appropriate, estimate likelihood of impact or consequence, including short description of basis of estimate

☐ Greater than 9 in 10 / Very Likely

x Greater than 2 in 3 / Likely

☐ About 1 in 2 / As Likely as Not

☐ Less than 1 in 3 / Unlikely

☐ Less than 1 in 10 / Very Unlikely

Estimate is based on the assessment of a large number of studies that diagnose past changes in global circulation and the impact of increased greenhouse gas concentration on tropical width and mid-latitude jets. A poleward shift of global circulation results in poleward expansion of tropical dry zones and mid-latitude circulation patterns that affect natural ecosystems, agriculture, and water resources.

Summary sentence or paragraph that integrates the above information

This Key Finding is supported by a large amount of observational and modeling evidence documented in the climate science peer-reviewed literature. Compared to the previous international assessment (IPCC AR5) the confidence is increased for an observed poleward shift of circulation features since 1979 due to additional observational studies. Uncertainties regarding the attribution of the observed tropical widening results from both uncertainties in the magnitude of observed trends and the contribution of internal variability.

Key Finding 2

Recurring patterns of variability in large-scale atmospheric circulation (such as the North Atlantic Oscillation and Northern Annular Mode) and the atmosphere–ocean system (such as El Niño–Southern Oscillation) cause year-to-year variations in U.S. temperatures and precipitation (*high confidence*). Changes in the occurrence of these patterns or their properties have contributed to recent U.S. temperature and precipitation trends (*medium confidence*) although uncertainties remain about the size of the role of human influences in these changes.

Description of evidence base

The Key Finding is supported by multiple studies as described in the text that diagnose recurring patterns of variability and their changes, as well as their impact on temperature and precipitation of the United States. These included studies on changes in the Northern Atlantic Oscillation/Northern Annular Mode (Hurrell 1995; Cohen and Barlow 2005; Overland and Wang 2015; Overland et al. 2015) as well as studies on the observed decadal modification of ENSO (Yu et al. 2012; Yu and Zou 2013; Li et al. 2011; Lee and McPhaden 2010; Yeh et al. 2009; Capantoni et al. 2013). The uncertainties in the attribution of changes in these preferred patterns

of variability results from limited observational records and the findings from long climate simulations showing that decadal to multi-decadal variations of El Nino–Southern Oscillation and Northern Annular Mode can be generated without any change in external forcing (Capantoni et al. 2013; Deser et al. 2012; IPCC 2013). These studies are discussed in the text.

Major uncertainties

A key uncertainty is related to limited observational records and our capability to properly simulate climate variability on decadal to multidecadal time scale, as well as properly simulate modes of climate variability including El Nino–Southern Oscillation and Northern Hemisphere Annular Mode–North Atlantic Oscillation.

Assessment of confidence based on evidence and agreement, including short description of nature of evidence and level of agreement

☐ Very High

x High

x Medium

☐ Low

There is high confidence that preferred modes of variability affect U.S. temperature on year-to-year time scale and medium confidence on their impact on decadal time scales based on a large number of studies that diagnose observational data records and long simulations with climate models for a various of preferred modes of variability.

If appropriate, estimate likelihood of impact or consequence, including short description of basis of estimate

☐ Greater than 9 in 10 / Very Likely

☐ Greater than 2 in 3 / Likely

☐ About 1 in 2 / As Likely as Not

☐ Less than 1 in 3 / Unlikely

☐ Less than 1 in 10 / Very Unlikely

Summary sentence or paragraph that integrates the above information

The Key Finding is supported by multiple studies that diagnose recurring patterns of variability and their changes, as well as their impact on temperature and precipitation of the United States. The causes of these changes are uncertain due to the limited observational record.

Key Finding 3

Increasing temperatures and atmospheric specific humidity are already having important influences on extremes (*high confidence*). It is still unclear, however, to what extent increasing temperatures and humidity have influenced and will influence persistent circulation patterns, which in turn influence these extremes.

Description of evidence base

The Key Finding integrates assessment from Chapters 5 and 6, regarding the impact of increasing temperatures and atmospheric specific humidity on extremes with the assessment of this chapter on circulation changes. The key finding on the low confidence the impact of increasing temperatures and humidity on quasi-persistent circulation patterns supported by statements of the previous international assessment (IPCC 2013) and recent studies on changes in atmospheric blocking and stationary waves in observation and climate models (Barnes 2013; Barnes et al. 2014, Francis and Vavrus 2012; Screen and Simmonds 2013; Simpson et al. 2016; Kennedy et al. 2016), and theoretical considerations (Hoskins and Woollings 2015). These studies are discussed in the text.

Major uncertainties

Key uncertainties result from the lack of climate models to properly simulate quasi-stationary circulation patterns like atmospheric blocking and quasi-stationary waves and limited records of observations.

Assessment of confidence based on evidence and agreement, including short description of nature of evidence and level of agreement

☐ Very High

☒ High

☐ Medium

☒ Low

Low confidence in the impact of changes of temperature and specific humidity on circulation patterns results from the lack of detectability of robust trends of changes in persistent circulation patterns in observational records as well as model biases that limit the confidence in projected trends.

If appropriate, estimate likelihood of impact or consequence, including short description of basis of estimate

☐ Greater than 9 in 10 / Very Likely

☐ Greater than 2 in 3 / Likely

☐ About 1 in 2 / As Likely as Not

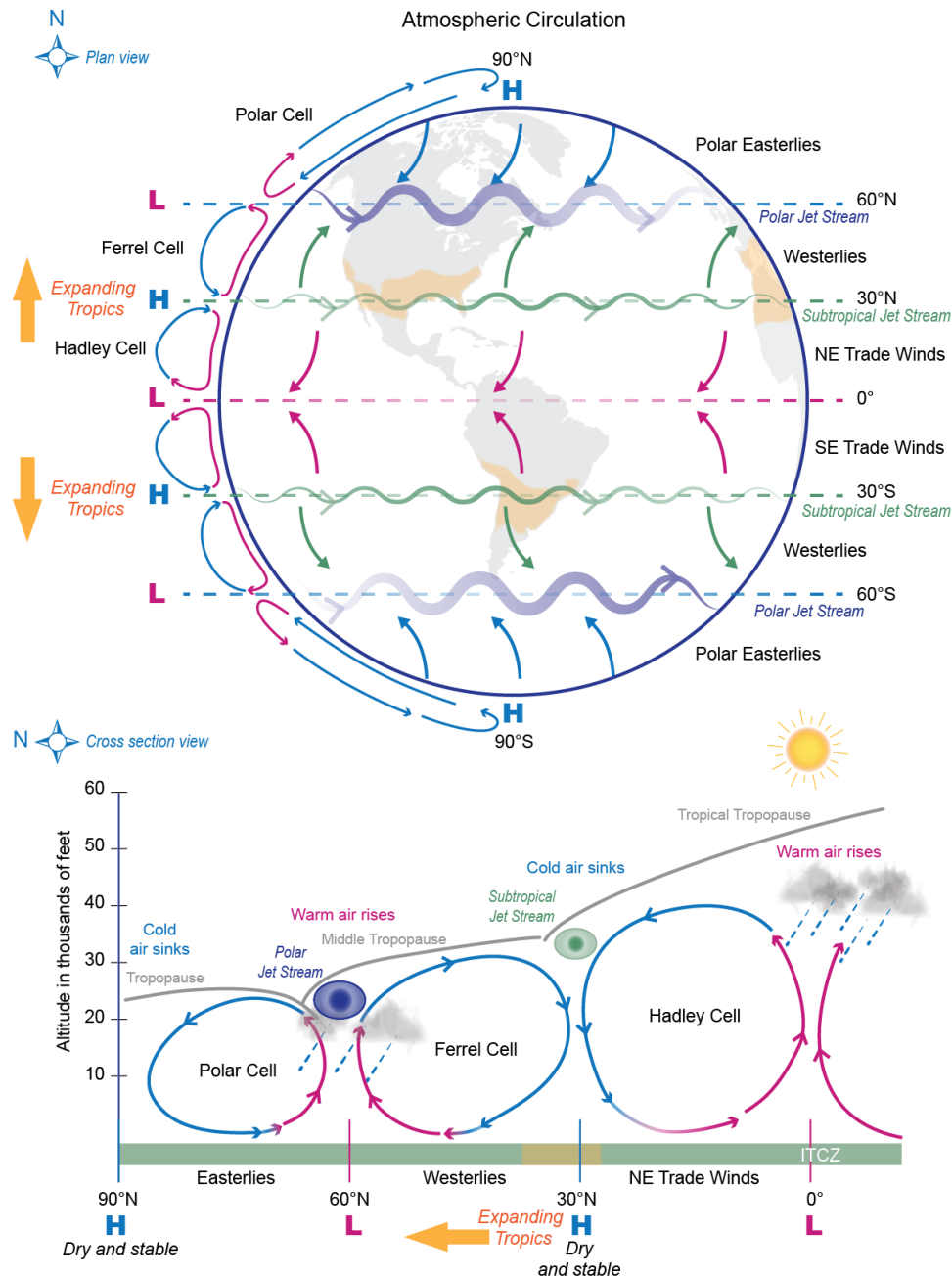
☐ Less than 1 in 3 / Unlikely

☐ Less than 1 in 10 / Very Unlikely

Summary sentence or paragraph that integrates the above information

Our confidence is low on the impact of changes in observed and future changes in temperature and specific humidity on persistent circulation patterns that could affect extremes. Uncertainty is large because of lack of robust detectability of past trends in these persistent circulation patterns and model biases in simulating these patterns that limit our confidence in simulated changes.

1 FIGURES



2

3 **Figure 5.1:**(*Top*) Plan and (*bottom*) cross section schematic view representation of the general
 4 circulation of the atmosphere. Three main circulations exist between the equator and poles due to
 5 solar heating and the earth's rotation.

6 **Hadley cell (1)** – Low-latitude air moves toward the equator. Due to solar heating, air near the
 7 equator rises vertically and moves poleward in the upper atmosphere.

8 **Ferrel cell (2)** – A midlatitude mean atmospheric circulation cell. In this cell, the air flows
 9 poleward and eastward near the surface and equatorward and westward at higher levels.

1 **Polar cell (3)** – Air rises, diverges, and travels toward the poles. Once over the poles, the air
2 sinks, forming the polar highs. At the surface, air diverges outward from the polar highs. Surface
3 winds in the polar cell are easterly (polar easterlies).
4 A high pressure band is located at about 30° N/S latitude, leading to dry/hot weather due to
5 descending air motion (subtropical dry zones are indicated in orange in the schematic views).
6 Expanding tropics (indicted by orange arrows) are associated with a poleward shift of the
7 subtropical dry zones. A low pressure band is found at 50°–60° N/S, with rainy and stormy
8 weather in relation to the polar jet stream bands of strong westerly wind in the upper levels of the
9 atmosphere. (Figure source: adapted from NWS 2016)

10

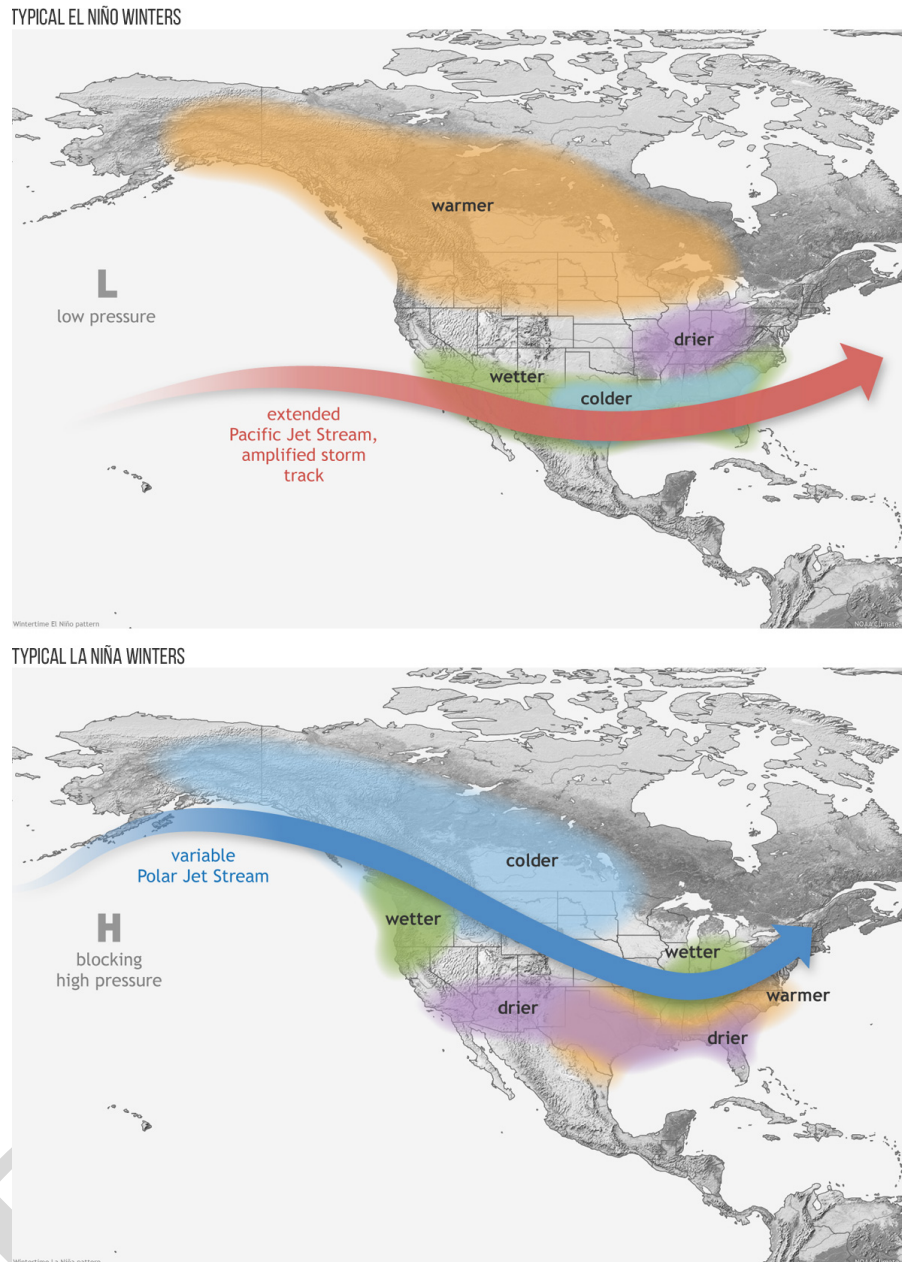


Figure 5.2: El Niño- and La Niña-related winter features over North America. Shown are typical January to March weather anomalies and atmospheric circulation during moderate to strong El Niño and La Niña conditions: (top) During El Niño, there is a tendency for a strong jet stream and storm track across the southern part of the United States. The southern tier of Alaska and the U.S. Pacific Northwest tend to be warmer than average, whereas the southern tier of U.S. states tends to be cooler and wetter than average. During La Niña, there is a tendency of a very wave-like jet stream flow over the United States and Canada, with colder and stormier than average conditions across the North, and warmer and less stormy conditions across the South. (Figure source: adapted from Lindsey 2016)

Cold Season Relationship between Climate Indices and Precipitation/Temperature Anomalies

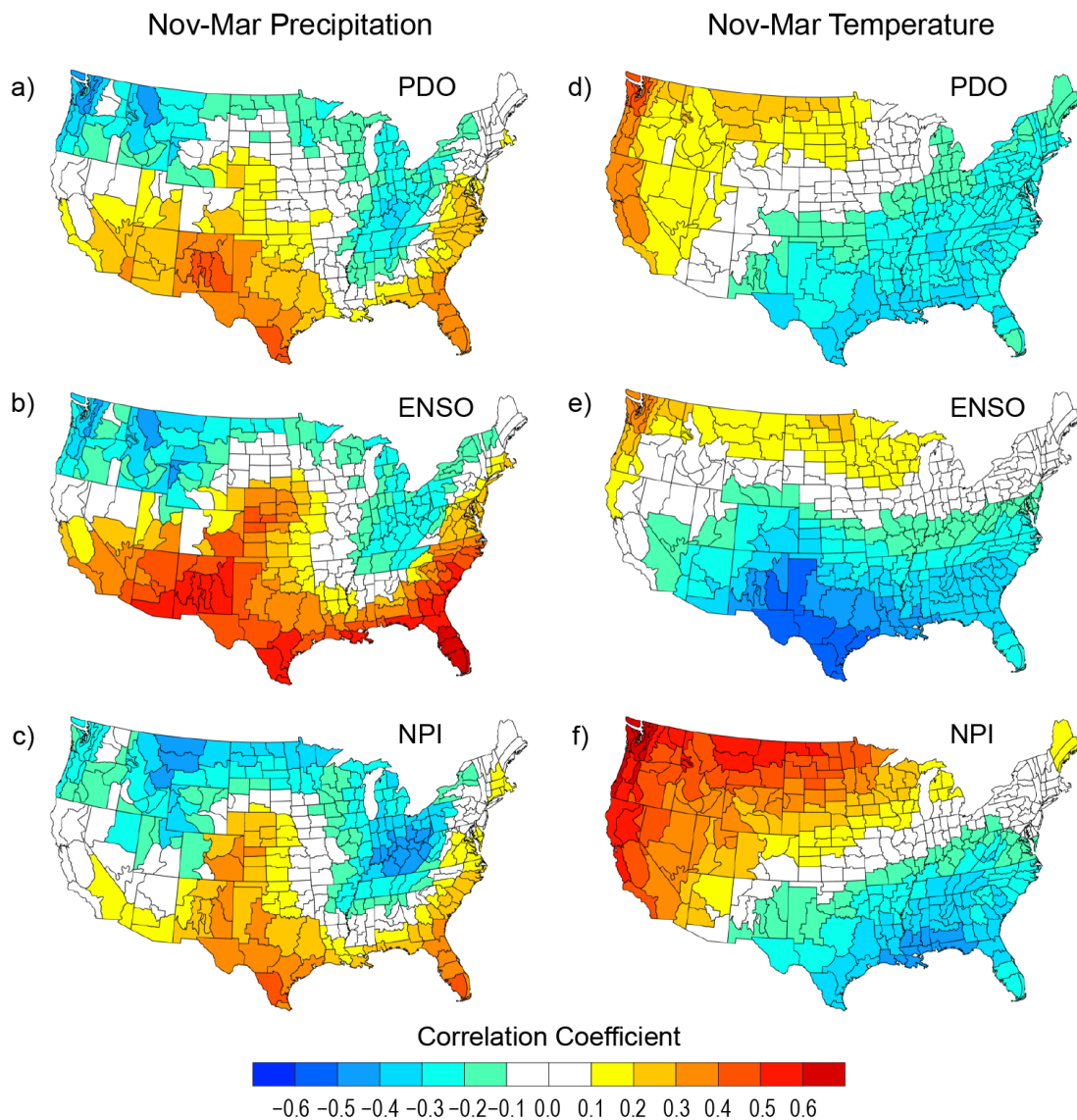
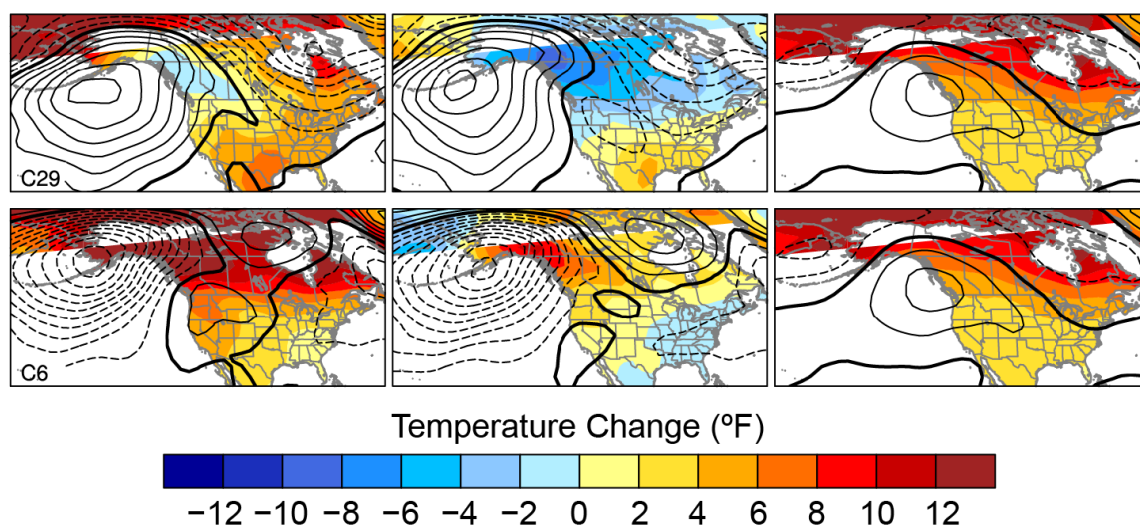


Figure 5.3: Cold season relationship between climate indices and U.S. precipitation and temperature anomalies determined from U.S. climate division data (Vose et al. 2014), for the years 1901–2014. November–March mean U.S. precipitation anomalies correlated with (a) the PDO index, (b) the ENSO index, and (c) the North Pacific Index. November–March U.S. temperature anomalies correlated with (d) the PDO index, (e) the ENSO index, and (f) the NPI. Decadal impacts related to the Pacific Decadal Oscillation (PDO) on temperature and precipitation of the United States are very similar to the impact of phenomena on interannual time scales like ENSO and variations in the strength of the Aleutian low characterized by the North Pacific Index (NPI). (Figure source: Newman et al. 2016; © American Meteorological Society, used with permission)

a) Winter surface air temperature and sea level pressure



b) Winter precipitation and sea level pressure

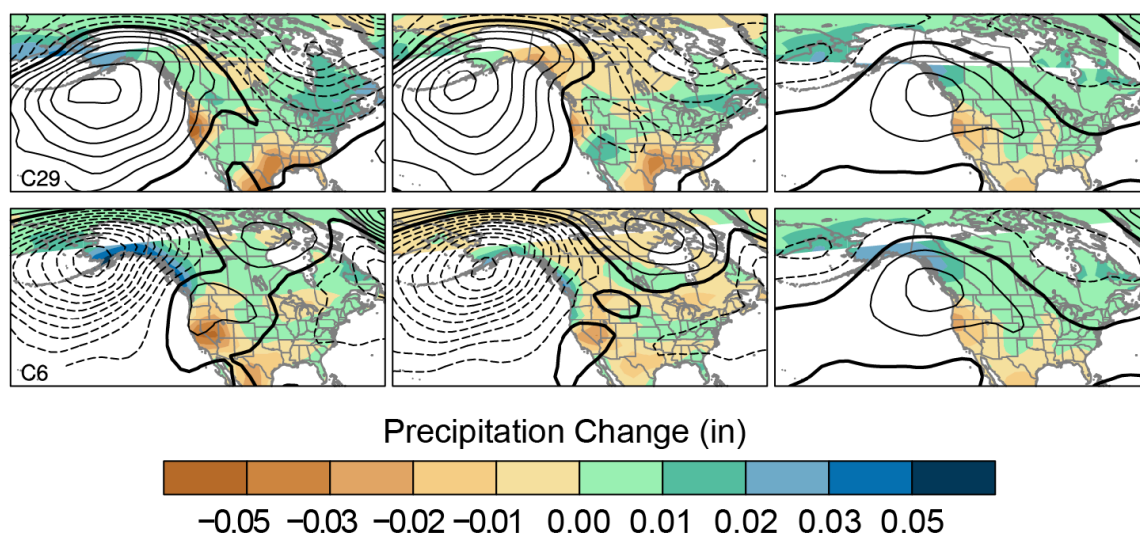


Figure 5.4: (left) Total 2010–2060 winter trends decomposed into (center) internal and (right) forced components for two contrasting CCSM3 ensemble members (runs 29 and 6) for (a) SAT [color shading; °F (51 years)⁻¹] and SLP (contours) and (b) precipitation [color shading; inches per day (51 years)⁻¹] and SLP (contours). SLP contour interval is 1 hPa (51 years)⁻¹, with solid (dashed) contours for positive (negative) values; the zero contour is thickened. The same climate model (CCSM3) simulates a large range of possible trends in North American climate over the 2010–2060 period because of the influence of internal climate variability superposed upon forced climate trends. (Figure source: adapted from Deser et al. 2014; © American Meteorological Society, used with permission.)

1 **REFERENCES**

- 2 Abatzoglou, J.T., D.E. Rupp, and P.W. Mote, 2014: Seasonal Climate Variability and Change in
3 the Pacific Northwest of the United States. *Journal of Climate*, **27**, 2125-2142.
4 <http://dx.doi.org/10.1175/jcli-d-13-00218.1>
- 5 Abatzoglou, J.T., D.E. Rupp, and P.W. Mote, 2014: Questionable evidence of natural warming
6 of the northwestern United States. *Proceedings of the National Academy of Sciences*, **111**,
7 E5605-E5606. <http://dx.doi.org/10.1073/pnas.1421311112>
8 <http://www.pnas.org/content/111/52/E5605.short>
- 9 Adam, O., T. Schneider, and N. Harnik, 2014: Role of changes in mean temperatures versus
10 temperature gradients in the recent widening of the Hadley circulation. *Journal of Climate*,
11 **27**, 7450-7461. <http://dx.doi.org/10.1175/JCLI-D-14-00140.1>
- 12 Allen, R.J. and O. Ajoku, 2016: Future aerosol reductions and widening of the northern tropical
13 belt. *Journal of Geophysical Research: Atmospheres*, **121**, 6765-6786.
14 <http://dx.doi.org/10.1002/2016JD024803>
- 15 Allen, R.J., J.R. Norris, and M. Kovilakam, 2014: Influence of anthropogenic aerosols and the
16 Pacific decadal oscillation on tropical belt width. *Nature Geoscience*, **7**, 270-274.
17 <http://dx.doi.org/10.1038/ngeo2091>
- 18 Allen, R.J., S.C. Sherwood, J.R. Norris, and C.S. Zender, 2012: Recent Northern Hemisphere
19 tropical expansion primarily driven by black carbon and tropospheric ozone. *Nature*, **485**,
20 350-354. <http://dx.doi.org/10.1038/nature11097>
- 21 Archambault, H.M., L.F. Bosart, D. Keyser, and A.R. Aiyyer, 2008: Influence of large-scale
22 flow regimes on cool-season precipitation in the northeastern United States. *Monthly*
23 *Weather Review*, **136**, 2945-2963. <http://dx.doi.org/10.1175/2007MWR2308.1>
- 24 Barnes, E.A., 2013: Revisiting the evidence linking Arctic amplification to extreme weather in
25 midlatitudes. *Geophysical Research Letters*, **40**, 4734-4739.
26 <http://dx.doi.org/10.1002/grl.50880>
- 27 Barnes, E.A., E. Dunn-Sigouin, G. Masato, and T. Woollings, 2014: Exploring recent trends in
28 Northern Hemisphere blocking. *Geophysical Research Letters*, **41**, 638-644.
29 <http://dx.doi.org/10.1002/2013GL058745>
- 30 Barnes, E.A. and L. Polvani, 2013: Response of the Midlatitude Jets, and of Their Variability, to
31 Increased Greenhouse Gases in the CMIP5 Models. *Journal of Climate*, **26**, 7117-7135.
32 <http://dx.doi.org/10.1175/JCLI-D-12-00536.1>

- 1 Bindoff, N.L., P.A. Stott, K.M. AchutaRao, M.R. Allen, N. Gillett, D. Gutzler, K. Hansingo, G.
 2 Hegerl, Y. Hu, S. Jain, I.I. Mokhov, J. Overland, J. Perlwitz, R. Sebbari, and X. Zhang, 2013:
 3 Detection and Attribution of Climate Change: from Global to Regional. *Climate Change*
 4 *2013: The Physical Science Basis. Contribution of Working Group I to the Fifth Assessment*
 5 *Report of the Intergovernmental Panel on Climate Change*. Stocker, T.F., D. Qin, G.-K.
 6 Plattner, M. Tignor, S.K. Allen, J. Boschung, A. Nauels, Y. Xia, V. Bex, and P.M. Midgley,
 7 Eds. Cambridge University Press, Cambridge, United Kingdom and New York, NY, USA,
 8 867–952. <http://dx.doi.org/10.1017/CBO9781107415324.022> www.climatechange2013.org
- 9 Birner, T., S.M. Davis, and D.J. Seidel, 2014: The changing width of Earth's tropical belt.
 10 *Physcis Today*, **67**, 38-44. <http://dx.doi.org/10.1063/PT.3.2620>
- 11 Boo, K.-O., B.B.B. Booth, Y.-H. Byun, J. Lee, C. Cho, S. Shim, and K.-T. Kim, 2015: Influence
 12 of aerosols in multidecadal SST variability simulations over the North Pacific. *Journal of*
 13 *Geophysical Research: Atmospheres*, **120**, 517-531. <http://dx.doi.org/10.1002/2014JD021933>
- 14 Booth, B.B.B., N.J. Dunstone, P.R. Halloran, T. Andrews, and N. Bellouin, 2012: Aerosols
 15 implicated as a prime driver of twentieth-century North Atlantic climate variability. *Nature*,
 16 **484**, 228-232. <http://dx.doi.org/10.1038/nature10946>
- 17 Brandefelt, J. and H. Körnich, 2008: Northern Hemisphere Stationary Waves in Future Climate
 18 Projections. *Journal of Climate*, **21**, 6341-6353. <http://dx.doi.org/10.1175/2008JCLI2373.1>
- 19 Brönnimann, S., A.M. Fischer, E. Rozanov, P. Poli, G.P. Compo, and P.D. Sardeshmukh, 2015:
 20 Southward shift of the northern tropical belt from 1945 to 1980. *Nature Geoscience*, **8**, 969-
 21 974. <http://dx.doi.org/10.1038/ngeo2568>
- 22 Cai, W., S. Borlace, M. Lengaigne, P. van Rensch, M. Collins, G. Vecchi, A. Timmermann, A.
 23 Santoso, M.J. McPhaden, L. Wu, M.H. England, G. Wang, E. Guilyardi, and F.-F. Jin, 2014:
 24 Increasing frequency of extreme El Nino events due to greenhouse warming. *Nature Climate*
 25 *Change*, **4**, 111-116. <http://dx.doi.org/10.1038/nclimate2100>
- 26 Cai, W., A. Santoso, G. Wang, S.-W. Yeh, S.-I. An, K.M. Cobb, M. Collins, E. Guilyardi, F.-F.
 27 Jin, J.-S. Kug, M. Lengaigne, M.J. McPhaden, K. Takahashi, A. Timmermann, G. Vecchi,
 28 M. Watanabe, and L. Wu, 2015: ENSO and greenhouse warming. *Nature Climate Change*, **5**,
 29 849-859. <http://dx.doi.org/10.1038/nclimate2743>
- 30 Cai, W., G. Wang, A. Santoso, M.J. McPhaden, L. Wu, F.-F. Jin, A. Timmermann, M. Collins,
 31 G. Vecchi, M. Lengaigne, M.H. England, D. Dommenget, K. Takahashi, and E. Guilyardi,
 32 2015: Increased frequency of extreme La Nina events under greenhouse warming. *Nature*
 33 *Climate Change*, **5**, 132-137. <http://dx.doi.org/10.1038/nclimate2492>
- 34 Capotondi, A., A.T. Wittenberg, M. Newman, E.D. Lorenzo, J.-Y. Yu, P. Braconnot, J. Cole, B.
 35 Dewitte, B. Giese, E. Guilyardi, F.-F. Jin, K. Karnauskas, B. Kirtman, T. Lee, N. Schneider,

- 1 Y. Xue, and S.-W. Yeh, 2015: Understanding ENSO Diversity. *Bulletin of the American*
 2 *Meteorological Society*, **96**, 921-938. <http://dx.doi.org/10.1175/BAMS-D-13-00117.1>
- 3 Carrera, M.L., R.W. Higgins, and V.E. Kousky, 2004: Downstream Weather Impacts Associated
 4 with Atmospheric Blocking over the Northeast Pacific. *Journal of Climate*, **17**, 4823-4839.
 5 <http://dx.doi.org/10.1175/JCLI-3237.1>
- 6 Chen, S., K. Wei, W. Chen, and L. Song, 2014: Regional changes in the annual mean Hadley
 7 circulation in recent decades. *Journal of Geophysical Research: Atmospheres*, **119**, 7815-
 8 7832. <http://dx.doi.org/10.1002/2014JD021540>
- 9 Christensen, J.H., K. Krishna Kumar, E. Aldrian, S.-I. An, I.F.A. Cavalcanti, M. de Castro, W.
 10 Dong, P. Goswami, A. Hall, J.K. Kanyanga, A. Kitoh, J. Kossin, N.-C. Lau, J. Renwick, D.B.
 11 Stephenson, S.-P. Xie, and T. Zhou, 2013: Climate Phenomena and their Relevance for
 12 Future Regional Climate Change. *Climate Change 2013: The Physical Science Basis.*
 13 *Contribution of Working Group I to the Fifth Assessment Report of the Intergovernmental*
 14 *Panel on Climate Change*. Stocker, T.F., D. Qin, G.-K. Plattner, M. Tignor, S.K. Allen, J.
 15 Boschung, A. Nauels, Y. Xia, V. Bex, and P.M. Midgley, Eds. Cambridge University Press,
 16 Cambridge, United Kingdom and New York, NY, USA, 1217-1308.
 17 <http://dx.doi.org/10.1017/CBO9781107415324.028> www.climatechange2013.org
- 18 Chylek, P. and G. Lesins, 2008: Multidecadal variability of Atlantic hurricane activity: 1851-
 19 2007. *Journal of Geophysical Research*, **113**, D22106.
 20 <http://dx.doi.org/10.1029/2008JD010036>
- 21 Cohen, J. and M. Barlow, 2005: The NAO, the AO, and Global Warming: How Closely Related?
 22 *Journal of Climate*, **18**, 4498-4513. <http://dx.doi.org/10.1175/jcli3530.1>
- 23 Coleman, J.S.M. and J.C. Rogers, 2003: Ohio River Valley Winter Moisture Conditions
 24 Associated with the Pacific-North American Teleconnection Pattern. *Journal of Climate*, **16**,
 25 969-981. [http://dx.doi.org/10.1175/1520-0442\(2003\)016<0969:ORVWMC>2.0.CO;2](http://dx.doi.org/10.1175/1520-0442(2003)016<0969:ORVWMC>2.0.CO;2)
- 26 Collins, M., R. Knutti, J. Arblaster, J.-L. Dufresne, T. Fiechfet, P. Friedlingstein, X. Gao, W.J.
 27 Gutowski, T. Johns, G. Krinner, M. Shongwe, C. Tebaldi, A.J. Weaver, and M. Wehner,
 28 2013: Long-term Climate Change: Projections, Commitments and Irreversibility. *Climate*
 29 *Change 2013: The Physical Science Basis. Contribution of Working Group I to the Fifth*
 30 *Assessment Report of the Intergovernmental Panel on Climate Change*. Stocker, T.F., D.
 31 Qin, G.-K. Plattner, M. Tignor, S.K. Allen, J. Boschung, A. Nauels, Y. Xia, V. Bex, and
 32 P.M. Midgley, Eds. Cambridge University Press, Cambridge, United Kingdom and New
 33 York, NY, USA, 1029-1136. <http://dx.doi.org/10.1017/CBO9781107415324.024>
 34 www.climatechange2013.org

- 1 Davis, N.A. and T. Birner, 2013: Seasonal to multidecadal variability of the width of the tropical
2 belt. *Journal of Geophysical Research: Atmospheres*, **118**, 7773-7787.
3 <http://dx.doi.org/10.1002/jgrd.50610>
- 4 Delworth, T.L., F. Zeng, G.A. Vecchi, X. Yang, L. Zhang, and R. Zhang, 2016: The North
5 Atlantic Oscillation as a driver of rapid climate change in the Northern Hemisphere. *Nature*
6 *Geoscience*, **9**, 509-512. <http://dx.doi.org/10.1038/ngeo2738>
- 7 Deser, C., 2000: On the teleconnectivity of the “Arctic Oscillation”. *Geophysical Research*
8 *Letters*, **27**, 779-782. <http://dx.doi.org/10.1029/1999GL010945>
- 9 Deser, C., A. Phillips, V. Bourdette, and H. Teng, 2012: Uncertainty in climate change
10 projections: The role of internal variability. *Climate Dynamics*, **38**, 527-546.
11 <http://dx.doi.org/10.1007/s00382-010-0977-x>
- 12 Deser, C., A.S. Phillips, M.A. Alexander, and B.V. Smoliak, 2014: Projecting North American
13 Climate over the Next 50 Years: Uncertainty due to Internal Variability. *Journal of Climate*,
14 **27**, 2271-2296. <http://dx.doi.org/10.1175/JCLI-D-13-00451.1>
- 15 Deser, C., L. Terray, and A.S. Phillips, 2016: Forced and Internal Components of Winter Air
16 Temperature Trends over North America during the past 50 Years: Mechanisms and
17 Implications. *Journal of Climate*, **29**, 2237-2258. [http://dx.doi.org/10.1175/JCLI-D-15-](http://dx.doi.org/10.1175/JCLI-D-15-0304.1)
18 [0304.1](http://dx.doi.org/10.1175/JCLI-D-15-0304.1)
- 19 Durkee, J.D., J.D. Frye, C.M. Fuhrmann, M.C. Lacke, H.G. Jeong, and T.L. Mote, 2008: Effects
20 of the North Atlantic Oscillation on precipitation-type frequency and distribution in the
21 eastern United States. *Theoretical and Applied Climatology*, **94**, 51-65.
22 <http://dx.doi.org/10.1007/s00704-007-0345-x>
- 23 Enfield, D.B., A.M. Mestas-Núñez, and P.J. Trimble, 2001: The Atlantic Multidecadal
24 Oscillation and its relation to rainfall and river flows in the continental U.S. *Geophysical*
25 *Research Letters*, **28**, 2077-2080. <http://dx.doi.org/10.1029/2000GL012745>
- 26 Evan, A.T., D.J. Vimont, A.K. Heidinger, J.P. Kossin, and R. Bennartz, 2009: The role of
27 aerosols in the evolution of tropical North Atlantic Ocean temperature anomalies. *Science*,
28 **324**, 778-781. <http://dx.doi.org/10.1126/science.1167404>
- 29 Feldstein, S.B. and C. Franzke, 2006: Are the North Atlantic Oscillation and the Northern
30 Annular Mode Distinguishable? *Journal of the Atmospheric Sciences*, **63**, 2915-2930.
31 <http://dx.doi.org/10.1175/JAS3798.1>
- 32 Feng, S. and Q. Fu, 2013: Expansion of global drylands under a warming climate. *Atmospheric*
33 *Chemistry and Physics*, **13**, 10081-10094. <http://dx.doi.org/10.5194/acp-13-10081-2013>

- 1 Feng, S., Q. Hu, and R.J. Oglesby, 2011: Influence of Atlantic sea surface temperatures on
2 persistent drought in North America. *Climate Dynamics*, **37**, 569-586.
3 <http://dx.doi.org/10.1007/s00382-010-0835-x>
- 4 Francis, J.A. and S.J. Vavrus, 2012: Evidence linking Arctic amplification to extreme weather in
5 mid-latitudes. *Geophysical Research Letters*, **39**, L06801.
6 <http://dx.doi.org/10.1029/2012GL051000>
- 7 Francis, J.A., S.J. Vavrus, and J. Cohen, 2016: Amplified Arctic Warming and Mid-Latitude
8 Weather: Emerging ConnectionsWiRes. *WIREs*, **Submitted**.
- 9 Frierson, D.M.W., J. Lu, and G. Chen, 2007: Width of the Hadley cell in simple and
10 comprehensive general circulation models. *Geophysical Research Letters*, **34**, n/a-n/a.
11 <http://dx.doi.org/10.1029/2007GL031115>
- 12 Furtado, J.C., E.D. Lorenzo, N. Schneider, and N.A. Bond, 2011: North Pacific Decadal
13 Variability and Climate Change in the IPCC AR4 Models. *Journal of Climate*, **24**, 3049-
14 3067. <http://dx.doi.org/10.1175/2010JCLI3584.1>
- 15 Garfinkel, C.I., D.W. Waugh, and L.M. Polvani, 2015: Recent Hadley cell expansion: The role
16 of internal atmospheric variability in reconciling modeled and observed trends. *Geophysical
17 Research Letters*, **42**, 10,824-10,831. <http://dx.doi.org/10.1002/2015GL066942>
- 18 Gillett, N.P. and J.C. Fyfe, 2013: Annular mode changes in the CMIP5 simulations. *Geophysical
19 Research Letters*, **40**, 1189-1193. <http://dx.doi.org/10.1002/grl.50249>
- 20 Gillett, N.P., J.C. Fyfe, and D.E. Parker, 2013: Attribution of observed sea level pressure trends
21 to greenhouse gas, aerosol, and ozone changes. *Geophysical Research Letters*, **40**, 2302-
22 2306. <http://dx.doi.org/10.1002/grl.50500>
- 23 Goldenberg, S.B., C.W. Landsea, A.M. Mestas-Nuñez, and W.M. Gray, 2001: The Recent
24 Increase in Atlantic Hurricane Activity: Causes and Implications. *Science*, **293**, 474-479.
25 <http://dx.doi.org/10.1126/science.1060040>
- 26 Grotjahn, R., R. Black, R. Leung, M.F. Wehner, M. Barlow, M. Bosilovich, A. Gershunov, W.J.
27 Gutowski, J.R. Gyakum, R.W. Katz, Y.-Y. Lee, Y.-K. Lim, and Prabhat, 2016: North
28 American extreme temperature events and related large scale meteorological patterns: a
29 review of statistical methods, dynamics, modeling, and trends. *Climate Dynamics*, **46**, 1151-
30 1184. <http://dx.doi.org/10.1007/s00382-015-2638-6>
- 31 Guirguis, K., A. Gershunov, R. Schwartz, and S. Bennett, 2011: Recent warm and cold daily
32 winter temperature extremes in the Northern Hemisphere. *Geophysical Research Letters*, **38**,
33 n/a-n/a. <http://dx.doi.org/10.1029/2011GL048762>

- 1 Haarsma, R.J. and F. Selten, 2012: Anthropogenic changes in the Walker circulation and their
2 impact on the extra-tropical planetary wave structure in the Northern Hemisphere. *Climate*
3 *Dynamics*, **39**, 1781-1799. <http://dx.doi.org/10.1007/s00382-012-1308-1>
- 4 Halpert, M.S. and C.F. Ropelewski, 1992: Surface Temperature Patterns Associated with the
5 Southern Oscillation. *Journal of Climate*, **5**, 577-593. [http://dx.doi.org/10.1175/1520-0442\(1992\)005<0577:STPAWT>2.0.CO;2](http://dx.doi.org/10.1175/1520-0442(1992)005<0577:STPAWT>2.0.CO;2)
- 7 Hanna, E., T.E. Cropper, R.J. Hall, and J. Cappelen, 2016: Greenland Blocking Index 1851–
8 2015: a regional climate change signal. *International Journal of Climatology*, n/a-n/a.
9 <http://dx.doi.org/10.1002/joc.4673>
- 10 Hartmann, B. and G. Wendler, 2005: The Significance of the 1976 Pacific Climate Shift in the
11 Climatology of Alaska. *Journal of Climate*, **18**, 4824-4839.
12 <http://dx.doi.org/10.1175/JCLI3532.1>
- 13 Hoerling, M.P., A. Kumar, and T. Xu, 2001: Robustness of the Nonlinear Climate Response to
14 ENSO's Extreme Phases. *Journal of Climate*, **14**, 1277-1293. [http://dx.doi.org/10.1175/1520-0442\(2001\)014<1277:ROTNCR>2.0.CO;2](http://dx.doi.org/10.1175/1520-0442(2001)014<1277:ROTNCR>2.0.CO;2)
- 16 Hoskins, B. and T. Woollings, 2015: Persistent Extratropical Regimes and Climate Extremes.
17 *Current Climate Change Reports*, **1**, 115-124. <http://dx.doi.org/10.1007/s40641-015-0020-8>
- 18 Hurrell, J.W., 1995: Decadal Trends in the North Atlantic Oscillation: Regional Temperatures
19 and Precipitation. *Science*, **269**, 676-679. <http://dx.doi.org/10.1126/science.269.5224.676>
- 20 Hurrell, J.W. and C. Deser, 2009: North Atlantic climate variability: The role of the North
21 Atlantic Oscillation. *Journal of Marine Systems*, **78**, 28-41.
22 <http://dx.doi.org/10.1016/j.jmarsys.2008.11.026>
- 23 IPCC, 2013: *Climate Change 2013: The Physical Science Basis. Contribution of Working Group*
24 *I to the Fifth Assessment Report of the Intergovernmental Panel on Climate Change*.
25 Cambridge University Press, Cambridge, UK and New York, NY, 1535 pp.
26 <http://dx.doi.org/10.1017/CBO9781107415324> www.climatechange2013.org
- 27 Johnstone, J.A. and N.J. Mantua, 2014: Atmospheric controls on northeast Pacific temperature
28 variability and change, 1900–2012. *Proceedings of the National Academy of Sciences*, **111**,
29 14360-14365. <http://dx.doi.org/10.1073/pnas.1318371111>
30 <http://www.pnas.org/content/111/40/14360.abstract>
- 31 Johnstone, J.A. and N.J. Mantua, 2014: Reply to Abatzoglou et al.: Atmospheric controls on
32 northwest United States air temperatures, 1948–2012. *Proceedings of the National Academy*
33 *of Sciences*, **111**, E5607-E5608. <http://dx.doi.org/10.1073/pnas.1421618112>
34 <http://www.pnas.org/content/111/52/E5607.short>

- 1 Karnauskas, K.B. and C.C. Ummenhofer, 2014: On the dynamics of the Hadley circulation and
2 subtropical drying. *Climate Dynamics*, **42**, 2259-2269. [http://dx.doi.org/10.1007/s00382-014-](http://dx.doi.org/10.1007/s00382-014-2129-1)
3 2129-1
- 4 Karpechko, A.Y. and E. Manzini, 2012: Stratospheric influence on tropospheric climate change
5 in the Northern Hemisphere. *Journal of Geophysical Research: Atmospheres*, **117**, n/a-n/a.
6 <http://dx.doi.org/10.1029/2011JD017036>
- 7 Kiladis, G.N. and H.F. Diaz, 1989: Global Climatic Anomalies Associated with Extremes in the
8 Southern Oscillation. *Journal of Climate*, **2**, 1069-1090. [http://dx.doi.org/10.1175/1520-](http://dx.doi.org/10.1175/1520-0442(1989)002<1069:GCAAWE>2.0.CO;2)
9 0442(1989)002<1069:GCAAWE>2.0.CO;2
- 10 Kennedy, D., T. Parker, T. Woollings, B. Harvey, and L. Shaffrey, 2016: The response of high-
11 impact blocking weather systems to climate change, *Geophys. Res. Lett.*, **43**, 7250–7258,
12 <http://dx.doi.org/10.1002/2016GL069725>
- 13 Knutson, T.R., F. Zeng, and A.T. Wittenberg, 2013: Multimodel Assessment of Regional
14 Surface Temperature Trends: CMIP3 and CMIP5 Twentieth-Century Simulations. *Journal of*
15 *Climate*, **26**, 8709-8743. <http://dx.doi.org/10.1175/JCLI-D-12-00567.1>
- 16 Kovilakam, M. and S. Mahajan, 2015: Black carbon aerosol-induced Northern Hemisphere
17 tropical expansion. *Geophysical Research Letters*, **42**, 4964-4972.
18 <http://dx.doi.org/10.1002/2015GL064559>
- 19 Kug, J.-S., S.-I. An, Y.-G. Ham, and I.-S. Kang, 2010: Changes in El Niño and La Niña
20 teleconnections over North Pacific–America in the global warming simulations. *Theoretical*
21 *and Applied Climatology*, **100**, 275-282. <http://dx.doi.org/10.1007/s00704-009-0183-0>
- 22 Lapp, S.L., J.-M. St. Jacques, E.M. Barrow, and D.J. Sauchyn, 2012: GCM projections for the
23 Pacific Decadal Oscillation under greenhouse forcing for the early 21st century. *International*
24 *Journal of Climatology*, **32**, 1423-1442. <http://dx.doi.org/10.1002/joc.2364>
- 25 Leathers, D.J., B. Yarnal, and M.A. Palecki, 1991: The Pacific/North American Teleconnection
26 Pattern and United States Climate. Part I: Regional Temperature and Precipitation
27 Associations. *Journal of Climate*, **4**, 517-528. [http://dx.doi.org/10.1175/1520-](http://dx.doi.org/10.1175/1520-0442(1991)004<0517:TPATPA>2.0.CO;2)
28 0442(1991)004<0517:TPATPA>2.0.CO;2
- 29 Lee, T. and M.J. McPhaden, 2010: Increasing intensity of El Niño in the central-equatorial
30 Pacific. *Geophysical Research Letters*, **37**, n/a-n/a. <http://dx.doi.org/10.1029/2010GL044007>
- 31 Li, J., S.-P. Xie, E.R. Cook, G. Huang, R. D'Arrigo, F. Liu, J. Ma, and X.-T. Zheng, 2011:
32 Interdecadal modulation of El Nino amplitude during the past millennium. *Nature Climate*
33 *Change*, **1**, 114-118. <http://dx.doi.org/10.1038/nclimate1086>

- 1 Li, Y. and N.-C. Lau, 2012: Impact of ENSO on the Atmospheric Variability over the North
2 Atlantic in Late Winter—Role of Transient Eddies. *Journal of Climate*, **25**, 320-342.
3 <http://dx.doi.org/10.1175/JCLI-D-11-00037.1>
- 4 Lindsey, R., 2016: How El Niño and La Niña affect the winter jet stream and U.S. climate.
5 Climate.gov. [https://www.climate.gov/news-features/featured-images/how-el-ni%C3%B1o-](https://www.climate.gov/news-features/featured-images/how-el-ni%C3%B1o-and-la-ni%C3%B1a-affect-winter-jet-stream-and-us-climate)
6 [and-la-ni%C3%B1a-affect-winter-jet-stream-and-us-climate](https://www.climate.gov/news-features/featured-images/how-el-ni%C3%B1o-and-la-ni%C3%B1a-affect-winter-jet-stream-and-us-climate)
- 7 Linkin, M.E. and S. Nigam, 2008: The North Pacific Oscillation–West Pacific Teleconnection
8 Pattern: Mature-Phase Structure and Winter Impacts. *Journal of Climate*, **21**, 1979-1997.
9 <http://dx.doi.org/10.1175/2007JCLI2048.1>
- 10 Loikith, P.C. and A.J. Broccoli, 2012: Characteristics of Observed Atmospheric Circulation
11 Patterns Associated with Temperature Extremes over North America. *Journal of Climate*, **25**,
12 7266-7281. <http://dx.doi.org/10.1175/JCLI-D-11-00709.1>
- 13 Lucas, C. and H. Nguyen, 2015: Regional characteristics of tropical expansion and the role of
14 climate variability. *Journal of Geophysical Research: Atmospheres*, **120**, 6809-6824.
15 <http://dx.doi.org/10.1002/2015JD023130>
- 16 Lucas, C., B. Timbal, and H. Nguyen, 2014: The expanding tropics: a critical assessment of the
17 observational and modeling studies. *Wiley Interdisciplinary Reviews: Climate Change*, **5**, 89-
18 112. <http://dx.doi.org/10.1002/wcc.251>
- 19 Mann, M.E. and K.A. Emanuel, 2006: Atlantic hurricane trends linked to climate change. *Eos*,
20 *Transactions of the American Geophysical Union*, **87**, 233-244.
21 <http://dx.doi.org/10.1029/2006EO240001>
- 22 McAfee, S.A., 2014: Consistency and the Lack Thereof in Pacific Decadal Oscillation Impacts
23 on North American Winter Climate. *Journal of Climate*, **27**, 7410-7431.
24 <http://dx.doi.org/10.1175/JCLI-D-14-00143.1>
- 25 Meehl, G.A., A. Hu, J.M. Arblaster, J. Fasullo, and K.E. Trenberth, 2013: Externally Forced and
26 Internally Generated Decadal Climate Variability Associated with the Interdecadal Pacific
27 Oscillation. *Journal of Climate*, **26**, 7298-7310. [http://dx.doi.org/10.1175/JCLI-D-12-](http://dx.doi.org/10.1175/JCLI-D-12-00548.1)
28 [00548.1](http://dx.doi.org/10.1175/JCLI-D-12-00548.1)
- 29 Meehl, G.A. and H. Teng, 2007: Multi-model changes in El Niño teleconnections over North
30 America in a future warmer climate. *Climate Dynamics*, **29**, 779-790.
31 <http://dx.doi.org/10.1007/s00382-007-0268-3>
- 32 Menary, M.B., W. Park, K. Lohmann, M. Vellinga, M.D. Palmer, M. Latif, and J.H. Jungclauss,
33 2012: A multimodel comparison of centennial Atlantic meridional overturning circulation
34 variability. *Climate Dynamics*, **38**, 2377-2388. <http://dx.doi.org/10.1007/s00382-011-1172-4>

- Newman, M., M.A. Alexander, T.R. Ault, K.M. Cobb, C. Deser, E.D. Lorenzo, N.J. Mantua, A.J. Miller, S. Minobe, H. Nakamura, N. Schneider, D.J. Vimont, A.S. Phillips, J.D. Scott, and C.A. Smith, 2016: The Pacific Decadal Oscillation, Revisited. *Journal of Climate*, **29**, 4399-4427. <http://dx.doi.org/10.1175/JCLI-D-15-0508.1>
- Nigam, S., 2003: Teleconnections. *Encyclopedia of Atmospheric Sciences*. Holton, J.R., Ed. Academic Press, 2243-2269.
- Ning, L. and R.S. Bradley, 2016: NAO and PNA influences on winter temperature and precipitation over the eastern United States in CMIP5 GCMs. *Climate Dynamics*, **46**, 1257-1276. <http://dx.doi.org/10.1007/s00382-015-2643-9>
- Overland, J., J.A. Francis, R. Hall, E. Hanna, S.-J. Kim, and T. Vihma, 2015: The Melting Arctic and Midlatitude Weather Patterns: Are They Connected? *Journal of Climate*, **28**, 7917-7932. <http://dx.doi.org/10.1175/JCLI-D-14-00822.1>
- Overland, J.E. and M. Wang, 2015: Increased Variability in the Early Winter Subarctic North American Atmospheric Circulation. *Journal of Climate*, **28**, 7297-7305. <http://dx.doi.org/10.1175/jcli-d-15-0395.1>
- Petoukhov, V., S. Rahmstorf, S. Petri, and H.J. Schellnhuber, 2013: Quasiresonant amplification of planetary waves and recent Northern Hemisphere weather extremes. *Proceedings of the National Academy of Sciences*, **110**, 5336-5341. <http://dx.doi.org/10.1073/pnas.1222000110>
- Prein, A.F., G.J. Holland, R.M. Rasmussen, M.P. Clark, and M.R. Tye, 2016: Running dry: The U.S. Southwest's drift into a drier climate state. *Geophysical Research Letters*, **43**, 1272-1279. <http://dx.doi.org/10.1002/2015GL066727>
- Quan, X.-W., M.P. Hoerling, J. Perlwitz, H.F. Diaz, and T. Xu, 2014: How Fast Are the Tropics Expanding? *Journal of Climate*, **27**, 1999-2013. <http://dx.doi.org/10.1175/JCLI-D-13-00287.1>
- Reichler, T., 2016: Chapter 6 - Poleward Expansion of the Atmospheric Circulation *Climate Change (Second Edition)*. Letcher, T.M., Ed. Elsevier, Boston, 79-104. <http://dx.doi.org/10.1016/B978-0-444-63524-2.00006-3>
- Renwick, J.A. and J.M. Wallace, 1996: Relationships between North Pacific Wintertime Blocking, El Niño, and the PNA Pattern. *Monthly Weather Review*, **124**, 2071-2076. [http://dx.doi.org/10.1175/1520-0493\(1996\)124<2071:RBNPWB>2.0.CO;2](http://dx.doi.org/10.1175/1520-0493(1996)124<2071:RBNPWB>2.0.CO;2)
- Ropelewski, C.F. and M.S. Halpert, 1987: Global and Regional Scale Precipitation Patterns Associated with the El Niño/Southern Oscillation. *Monthly Weather Review*, **115**, 1606-1626. [http://dx.doi.org/10.1175/1520-0493\(1987\)115<1606:GARSPP>2.0.CO;2](http://dx.doi.org/10.1175/1520-0493(1987)115<1606:GARSPP>2.0.CO;2)

- 1 Scaife, A.A., T. Spanghel, D.R. Fereday, U. Cubasch, U. Langematz, H. Akiyoshi, S. Bekki, P.
2 Braesicke, N. Butchart, M.P. Chipperfield, A. Gettelman, S.C. Hardiman, M. Michou, E.
3 Rozanov, and T.G. Shepherd, 2012: Climate change projections and stratosphere–
4 troposphere interaction. *Climate Dynamics*, **38**, 2089–2097.
5 <http://dx.doi.org/10.1007/s00382-011-1080-7>
- 6 Scheff, J. and D. Frierson, 2012: Twenty-First-Century Multimodel Subtropical Precipitation
7 Declines Are Mostly Midlatitude Shifts. *Journal of Climate*, **25**, 4330–4347.
8 <http://dx.doi.org/10.1175/JCLI-D-11-00393.1>
- 9 Scheff, J. and D.M.W. Frierson, 2012: Robust future precipitation declines in CMIP5 largely
10 reflect the poleward expansion of model subtropical dry zones. *Geophysical Research*
11 *Letters*, **39**, L18704. <http://dx.doi.org/10.1029/2012GL052910>
- 12 Schwendike, J., G.J. Berry, M.J. Reeder, C. Jakob, P. Govekar, and R. Wardle, 2015: Trends in
13 the local Hadley and local Walker circulations. *Journal of Geophysical Research:*
14 *Atmospheres*, **120**, 7599–7618. <http://dx.doi.org/10.1002/2014JD022652>
- 15 Screen, J.A. and I. Simmonds, 2013: Exploring links between Arctic amplification and mid-
16 latitude weather. *Geophysical Research Letters*, **40**, 959–964.
17 <http://dx.doi.org/10.1002/grl.50174>
- 18 Seager, R., M. Hoerling, S. Schubert, H. Wang, B. Lyon, A. Kumar, J. Nakamura, and N.
19 Henderson, 2015: Causes of the 2011–14 California Drought. *Journal of Climate*, **28**, 6997–
20 7024. <http://dx.doi.org/10.1175/JCLI-D-14-00860.1>
- 21 Seager, R., Y. Kushnir, M. Ting, M. Cane, N. Naik, and J. Miller, 2008: Would Advance
22 Knowledge of 1930s SSTs Have Allowed Prediction of the Dust Bowl Drought? *Journal of*
23 *Climate*, **21**, 3261–3281. <http://dx.doi.org/10.1175/2007JCLI2134.1>
- 24 Seager, R., N. Naik, and L. Vogel, 2012: Does Global Warming Cause Intensified Interannual
25 Hydroclimate Variability? *Journal of Climate*, **25**, 3355–3372.
26 <http://dx.doi.org/10.1175/JCLI-D-11-00363.1>
- 27 Seidel, D.J., Q. Fu, W.J. Randel, and T.J. Reichler, 2008: Widening of the tropical belt in a
28 changing climate. *Nature Geosci*, **1**, 21–24. <http://dx.doi.org/10.1038/ngeo.2007.38>
- 29 Shepherd, T.G., 2014: Atmospheric circulation as a source of uncertainty in climate change
30 projections. *Nature Geoscience*, **7**, 703–708. <http://dx.doi.org/10.1038/ngeo2253>
- 31 Simpson, I.R., R. Seager, M. Ting, and T.A. Shaw, 2016: Causes of change in Northern
32 Hemisphere winter meridional winds and regional hydroclimate. *Nature Climate Change*, **6**,
33 65–70. <http://dx.doi.org/10.1038/nclimate2783>

- 1 Simpson, I.R., T.A. Shaw, and R. Seager, 2014: A Diagnosis of the Seasonally and
2 Longitudinally Varying Midlatitude Circulation Response to Global Warming. *Journal of the*
3 *Atmospheric Sciences*, **71**, 2489-2515. <http://dx.doi.org/10.1175/JAS-D-13-0325.1>
- 4 Stevenson, S.L., 2012: Significant changes to ENSO strength and impacts in the twenty-first
5 century: Results from CMIP5. *Geophysical Research Letters*, **39**, L17703.
6 <http://dx.doi.org/10.1029/2012GL052759>
- 7 Sun, Y., G. Ramstein, C. Contoux, and T. Zhou, 2013: A comparative study of large-scale
8 atmospheric circulation in the context of a future scenario (RCP4.5) and past warmth (mid-
9 Pliocene). *Climate of the Past*, **9**, 1613-1627. <http://dx.doi.org/10.5194/cp-9-1613-2013>
- 10 Swain, D., M. Tsiang, M. Haughen, D. Singh, A. Charland, B. Rajarthan, and N.S. Diffenbaugh,
11 2014: The extraordinary California drought of 2013/14: Character, context and the role of
12 climate change [in "Explaining Extremes of 2013 from a Climate Perspective"]. *Bulletin of*
13 *the American Meteorological Society*, **95**, S3-S6. [http://dx.doi.org/10.1175/1520-0477-](http://dx.doi.org/10.1175/1520-0477-95.9.S1.1)
14 [95.9.S1.1](http://dx.doi.org/10.1175/1520-0477-95.9.S1.1)
- 15 Thompson, D.W.J., E.A. Barnes, C. Deser, W.E. Foust, and A.S. Phillips, 2015: Quantifying the
16 Role of Internal Climate Variability in Future Climate Trends. *Journal of Climate*, **28**, 6443-
17 6456. <http://dx.doi.org/10.1175/JCLI-D-14-00830.1>
- 18 Thompson, D.W.J. and J.M. Wallace, 1998: The Arctic oscillation signature in the wintertime
19 geopotential height and temperature fields. *Geophysical Research Letters*, **25**, 1297-1300.
20 <http://dx.doi.org/10.1029/98GL00950>
- 21 Thompson, D.W.J. and J.M. Wallace, 2000: Annular Modes in the Extratropical Circulation. Part
22 I: Month-to-Month Variability. *Journal of Climate*, **13**, 1000-1016.
23 [http://dx.doi.org/10.1175/1520-0442\(2000\)013<1000:AMITEC>2.0.CO;2](http://dx.doi.org/10.1175/1520-0442(2000)013<1000:AMITEC>2.0.CO;2)
- 24 Thompson, D.W.J. and J.M. Wallace, 2001: Regional Climate Impacts of the Northern
25 Hemisphere Annular Mode. *Science*, **293**, 85-89. <http://dx.doi.org/10.1126/science.1058958>
- 26 Ting, M., Y. Kushnir, R. Seager, and C. Li, 2011: Robust features of Atlantic multi-decadal
27 variability and its climate impacts. *Geophysical Research Letters*, **38**, L17705.
28 <http://dx.doi.org/10.1029/2011GL048712>
- 29 Vallis, G.K., P. Zurita-Gotor, C. Cairns, and J. Kidston, 2015: Response of the large-scale
30 structure of the atmosphere to global warming. *Quarterly Journal of the Royal*
31 *Meteorological Society*, **141**, 1479-1501. <http://dx.doi.org/10.1002/qj.2456>
- 32 Vose, R.S., S. Applequist, M. Squires, I. Durre, M.J. Menne, C.N.W. Jr., C. Fenimore, K.
33 Gleason, and D. Arndt, 2014: Improved Historical Temperature and Precipitation Time

- 1 Series for U.S. Climate Divisions. *Journal of Applied Meteorology and Climatology*, **53**,
2 1232-1251. <http://dx.doi.org/10.1175/JAMC-D-13-0248.1>
- 3 Wallace, J.M., C. Deser, B.V. Smoliak, and A.S. Phillips, 2015: Attribution of Climate Change
4 in the Presence of Internal Variability. *Climate Change: Multidecadal and Beyond*. WORLD
5 SCIENTIFIC, 1-29. http://dx.doi.org/10.1142/9789814579933_0001
- 6 Wang, H., S. Schubert, R. Koster, Y.-G. Ham, and M. Suarez, 2014: On the Role of SST Forcing
7 in the 2011 and 2012 Extreme U.S. Heat and Drought: A Study in Contrasts. *Journal of*
8 *Hydrometeorology*, **15**, 1255-1273. <http://dx.doi.org/10.1175/JHM-D-13-069.1>
- 9 Waugh, D.W., C.I. Garfinkel, and L.M. Polvani, 2015: Drivers of the Recent Tropical Expansion
10 in the Southern Hemisphere: Changing SSTs or Ozone Depletion? *Journal of Climate*, **28**,
11 6581-6586. <http://dx.doi.org/10.1175/JCLI-D-15-0138.1>
- 12 Wettstein, J.J. and C. Deser, 2014: Internal Variability in Projections of Twenty-First-Century
13 Arctic Sea Ice Loss: Role of the Large-Scale Atmospheric Circulation. *Journal of Climate*,
14 **27**, 527-550. <http://dx.doi.org/10.1175/JCLI-D-12-00839.1>
- 15 Whan, K., F. Zwiers, and J. Sillmann, 2016: The Influence of Atmospheric Blocking on Extreme
16 Winter Minimum Temperatures in North America. *Journal of Climate*, **29**, 4361-4381.
17 <http://dx.doi.org/10.1175/JCLI-D-15-0493.1>
- 18 Yeh, S.-W., J.-S. Kug, B. Dewitte, M.-H. Kwon, B.P. Kirtman, and F.-F. Jin, 2009: El Nino in a
19 changing climate. *Nature*, **461**, 511-514. <http://dx.doi.org/10.1038/nature08316>
- 20 Yu, J.-Y. and Y. Zou, 2013: The enhanced drying effect of Central-Pacific El Niño on US
21 winter. *Environmental Research Letters*, **8**, 014019. [http://dx.doi.org/10.1088/1748-](http://dx.doi.org/10.1088/1748-9326/8/1/014019)
22 [9326/8/1/014019](http://dx.doi.org/10.1088/1748-9326/8/1/014019)
- 23 Yu, J.-Y., Y. Zou, S.T. Kim, and T. Lee, 2012: The changing impact of El Niño on US winter
24 temperatures. *Geophysical Research Letters*, **39**, L15702.
25 <http://dx.doi.org/10.1029/2012GL052483>
- 26 Zhang, R. and T.L. Delworth, 2009: A new method for attributing climate variations over the
27 Atlantic Hurricane Basin's main development region. *Geophysical Research Letters*, **36**,
28 L06701. <http://dx.doi.org/10.1029/2009GL037260>
- 29 Zhou, Z.-Q., S.-P. Xie, X.-T. Zheng, Q. Liu, and H. Wang, 2014: Global Warming-Induced
30 Changes in El Niño Teleconnections over the North Pacific and North America. *Journal of*
31 *Climate*, **27**, 9050-9064. <http://dx.doi.org/10.1175/JCLI-D-14-00254.1>

6. Temperature Changes in the United States

KEY FINDINGS

1. The annual-average, near-surface air temperature over the contiguous United States has increased by about 1.2°F (0.7°C) between 1901 and 2015. Surface and satellite data both show rapid warming since the late 1970s, while paleo-temperature evidence shows that recent decades have been the warmest in at least the past 1,500 years. (*Extremely likely, High confidence*)
2. Accompanying the rise in average temperatures, there have been – as is to be expected – increases in extreme temperature events in most parts of the United States. Since the early 1900s, the temperature of extremely cold days has increased throughout the contiguous United States, and the temperature of extremely warm days has increased across much of the West. In recent decades, intense cold waves have become less common while intense heat waves have become more common. (*Extremely likely, Very high confidence*)
3. The average annual temperature of the contiguous United States is projected to rise throughout the century. Increases of at least 2.5°F (1.4°C) are projected over the next few decades, meaning that recent record-setting years will be relatively “common” in the near future. Increases of 5.0°–7.5°F (2.8°–4.8°C) are projected by late century depending upon the level of future emissions. (*Extremely likely, Very high confidence*)
4. Extreme temperatures are projected to increase even more than average temperatures. The temperatures of extremely cold days and extremely warm days are both projected to increase. Cold waves are projected to become less intense while heat waves will become more intense. (*Extremely likely, Very high confidence*)

Introduction

Temperature is among the most important climatic elements used in decision-making. For example, builders and insurers use temperature data for planning and risk management. Energy companies and regulators use temperature data to predict demand and set utility rates. Farmers use temperature data to select crop types and determine planting times.

Temperature is also a key indicator of climate change: recent increases are apparent over the land, ocean, and troposphere, and substantial changes are expected for this century. This chapter summarizes the major observed and projected changes in near-surface air temperature over the United States, emphasizing new data sets and model projections since NCA3. Changes are depicted using a spectrum of observations, including surface weather stations, moored ocean buoys, polar-orbiting satellites, and temperature-sensitive proxies. Projections are based on global models and downscaled products from CMIP5 (Coupled Model Intercomparison Project

Phase 5) using a suite of Representative Concentration Pathways (RCPs; see Chapter 4 for more on RCPs and future scenarios).

6.1 Historical Changes

6.1.1. Average Temperatures

Changes in temperature are described using a suite of observational datasets. As in the Third National Climate Assessment (NCA3), the primary dataset for the contiguous United States is nClimGrid (Vose et al. 2014), but new datasets are now available to address changes in Alaska, Hawai‘i, and the Caribbean (Vose et al. submitted). Along U.S. coastlines, changes in sea surface temperatures are quantified using a new reconstruction (Huang et al. 2015), which now forms the ocean component of the NOAA Global Temperature dataset (Vose et al. 2012). Changes in middle tropospheric temperature are assessed using several recently improved satellite datasets.

Average annual temperature across the United States increased by about 0.7°C (1.2°F) between 1901 and 2015, very slightly less than reported in NCA3 (Table 6.1). This difference stems from the use of different time periods to represent present-day climate in each report. In particular, NCA3 defined present-day as the average of 1991-2012, which was slightly warmer than the 1986-2015 period used here. (The reference period in both assessments is 1901-1960.)

[INSERT TABLE 6.1 HERE:]

Table 6.1. Observed changes in average annual temperature (°F) for each NCA region. Changes are the difference between the average for present-day (1986–2015) and the average for the first half of the last century (1901–1960).

Each NCA region experienced a net warming through 2015 (Table 6.1). The largest changes were in the western United States, where average temperature increased by more than 0.8°C (1.50°F) in Alaska, the Northwest, the Southwest, and also in the Northern Great Plains. As noted in NCA3, the Southeast had the least warming, driven by a combination of natural variations and human influences. Across all regions, average minimum temperature increased at a slightly higher rate than average maximum temperature, with the Midwest having the largest discrepancy. This differential rate of warming resulted in a continuing decrease in the diurnal temperature range that is consistent with other parts of the globe (Thorne et al. 2016). Average sea surface temperature also increased along all regional coastlines (see Figure 1.3), though changes were generally smaller than over land owing to the higher heat capacity of water. Increases were largest in Alaska (greater than 0.6°C [1.0°F]) while increases were smallest (less than 0.3°C [0.5°F]) in coastal areas of the Southeast.

More than 97% of the land surface of the United States had an increase in average temperature from 1900 to 2015 (Figure 6.1). In contrast, only small (and somewhat dispersed) parts of the Southeast and Southern Great Plains experienced cooling. From a seasonal perspective, warming was greatest and most widespread in winter, with increases of over 0.8°C (1.5°F) in most areas.

In summer, warming was less extensive (mainly along the East Coast and in the western third of the Nation), while cooling was evident in parts of the Southeast, Midwest, and Great Plains.

[INSERT FIGURE 6.1 HERE:]

Figure 6.1. Observed changes in annual, winter, and summer temperature (°F). Observed changes in annual, winter, and summer temperature (°F). Changes are the difference between the average for present-day (1986–2015) and the average for the first half of the last century (1901–1960 for the contiguous United States, 1925–1960 for Alaska and Hawai‘i). (Figure source: NOAA/NCEI)].

There has been a rapid increase in the average temperature of the contiguous United States over the past several decades. There is general consistency on this point between the surface thermometer record from NOAA (Vose et al. 2014) and the middle tropospheric satellite records from Remote Sensing Systems (RSS; Mears and Wentz 2016), NOAA’s Center for Satellite Applications and Research (STAR; Zou and Li 2014), and the University of Alabama in Huntsville (UAH; Christy et al. 2011). In particular, for the period 1979–2015, the rate of warming in the surface record was 0.256°C (0.460°F) per decade, versus trends of 0.223°C (0.401°F), 0.210°C (0.378°F), and 0.130 °C (0.234°F) per decade for RSS version 4, STAR version 3, and UAH version 6, respectively (after accounting for stratospheric influences). All trends are statistically significant. For the contiguous United States, the year 2015 was the second-warmest on record at the surface and the warmest on record for the middle troposphere. Generally speaking, surface and satellite records do not have identical trends because they do not represent the same physical quantity; surface measurements are made using thermometers in shelters about 1.5 meters (4–5 feet) above the ground whereas satellite measurements are mass-weighted averages of microwave emissions from deep atmospheric layers. The UAH record likely has a lower trend because it differs from the other satellite products in the treatment of target temperatures from the NOAA-9 satellite as well as in the correction for diurnal drift (Po-Chedley et al. 2015).

Recent paleo-temperature evidence confirms the unusual character of wide-scale warming during the past few decades as determined from the instrumental record. The most important new paleoclimate study since NCA3 showed that for each of the seven continental regions, the reconstructed area-weighted average temperature for 1971–2000 was higher than for any other time in nearly 1,400 years (PAGES 2K 2013), although with significant uncertainty around the central estimate that leads to this conclusion. Recent (up to 2006) 30-year smoothed temperatures across temperate North America (including most of the continental United States) are similarly reconstructed as the warmest over the past 1,500 years (Trouet et al. 2013) (Figure 6.3). Unlike the PAGES 2k seven-continent result mentioned above, this conclusion for North America is robust in relation to the estimated uncertainty range. Reconstruction data since 1500 for western temperate North America show the same conclusion at the annual time scale for 1986–2005. This time period and the running 20-year periods thereafter are warmer than all possible

continuous 20-year sequences in a 1,000-member statistical reconstruction ensemble (Wahl and Smerdon 2012).

[INSERT FIGURE 6.2 HERE:]

Figure 6.2. Pollen-based temperature reconstruction for temperate North America. Pollen-based temperature reconstruction for temperate North America. The blue curve depicts the pollen-based reconstruction of 30-year averages (as anomalies from 1904 to 1980) for the temperate region (30°–55°N, 7°5–130°W). The red curve shows the corresponding tree ring-based decadal average reconstruction, which was smoothed and used to calibrate the lower-frequency pollen-based estimate. Light (medium) blue zones indicate 2 standard error (1 standard error) uncertainty estimations associated with each 30-year value. The black curve shows comparably smoothed instrumental temperature values up to 1980. The dashed black line represents the average temperature anomaly of comparably smoothed instrumental data for the period 2000–2006. (Figure source: NOAA/NCEI)]

6.1.2. Temperature Extremes

Shifts in temperature extremes are examined using a suite of societally relevant climate change indices (Zhang et al. 2011) derived from long-term observations of daily surface temperature (Menne et al. 2012). The coldest and warmest temperatures of the year are of particular relevance given their widespread use in engineering, agricultural, and other sectoral applications (for example, extreme annual design conditions by the American Society of Heating, Refrigeration, and Air Conditioning; plant hardiness zones by the U.S. Department of Agriculture). Cold and warm spells (that is, extended periods of below- or above-normal temperature) are likewise of great importance because of their numerous societal and environmental impacts, which span from human health to plant phenology. Changes are considered for a spectrum of event frequencies and intensities, ranging from the typical annual extreme to the 1-in-10 year event (an extreme that only has a 10% chance of occurrence in any given year). Generally speaking, changes in many extremes have been larger than changes in average temperature.

The coldest daily temperature of the year increased at most locations in the contiguous United States through 2015 (Figure 6.3). All regions experienced net increases (Table 6.2), with the largest rises in the Northern Great Plains and the Northwest (roughly 2.8°C [5.0°F]), and the smallest in the Southeast (about 0.6°C [1.0°F]). In general, there were increases throughout the period of record, with a slight acceleration in the past few decades (Figure 6.3). The temperature of extremely warm days (1-in-10 year events) generally exhibited the same pattern of increases as the coldest daily temperature of the year. Consistent with these increases, the number of cool nights per year (those with a minimum temperature below the 10th percentile) declined in all regions, with much of the West having decreases of roughly two weeks.

[INSERT TABLE 6.2 HERE:]

Table 6.2. Observed changes in temperature extremes (°F) for each NCA region. Changes are the difference between the average for present-day (1986–2015) and the average for the first half of the last century (1901–1960).].

[INSERT FIGURE 6.3 HERE:]

Figure 6.3. Observed changes in the coldest and warmest daily temperatures (°F) of the year. Maps (top) depict changes at stations; changes are the difference between the average for present-day (1986–2015) and the average for the first half of the last century (1901–1960). Time series (bottom) depict changes over the contiguous United States. (Figure source: NOAA/NCEI)].

The warmest daily temperature of the year generally increased at locations throughout the West (Figure 6.3), as did the temperature of extremely warm days (1-in-10 year events) and the number of warm days per year (those with a maximum temperature above the 90th percentile). The largest regional increases were in the Southwest (Table 6.2). In contrast, there were decreases in maximum temperatures in almost all locations east of the Rocky Mountains; the decreases were actually larger for the 1-in-10 year events than for the warmest day of the year. The decreases in the eastern half of Nation (Figure 6.3) are generally tied to the hot summers in the 1930s Dust Bowl era, particularly across the Great Plains, where extreme agricultural drought and land mismanagement resulted in denuded landscapes, depleted soil moisture, and reduced evaporative cooling. Since the mid-1960s, however, there has been a slight increase in the warmest daily temperature of the year.

The frequency of cold spells (brief periods of below-normal temperatures) has steadily fallen across the contiguous United States during the past century (Figure 6.4). The frequency of intense cold waves (1-in-5 year events) peaked in the 1980s in all regions (including Alaska) and then reached record-low levels in the 2000s (Peterson et al. 2013). Nationally, the average temperature of extreme cold waves (5-day, 1-in-10 year events) was about 1.0 °C (1.8°F) warmer in the past three decades than in the first half of the 20th century, with increases in excess of 1.7°C (3.0°F) in the Southwest, Northwest, and Northern Great Plains (Table 6.2).

[INSERT FIGURE 6.4 HERE:]

Figure 6.4. Observed changes in cold and warm spells in the contiguous United States. The top panel depicts changes in the frequency of cold spells, the middle panel depicts changes in the frequency of warm spells, and the bottom panel depicts changes in the intensity of heat waves. (Figure source: NOAA/NCEI)]

Warm spells (brief periods of above-normal temperatures) increased in frequency until the mid-1930s, became somewhat less common through the mid-1960s, and increased in frequency again thereafter (Figure 6.4). As with warm daily temperatures, the peak period for heat waves was the 1930s in most regions except the West. Nationwide, the average temperature of extreme heat

waves (5-day, 1-in-10 year events) was about 0.8°C (1.5°F) warmer in the first half of the 20th century than in the past three decades, with the Midwest having the largest regional difference (Table 6.2). The frequency of intense heat waves (1-in-5 year events) has generally increased since the 1960s in most regions except the Midwest and the Great Plains (Peterson et al. 2013; Smith et al. 2013). Since the early 1980s (Figure 6.4), there is suggestive evidence of a slight increase in the intensity of heat waves nationwide (Russo et al. 2014) as well as an increase in the concurrence of droughts and heat waves (Mazdiyasni and AghaKouchak 2015). Recent warm spells have generally been longer in duration than those in the 1930s, as evidenced by the multi-month heat waves in the Midwest in 2012.

6.2 Detection and Attribution

6.2.1 Average Temperatures

While a confident attribution of global temperature increases to anthropogenic forcing has been made (Bindoff et al. 2013), detection and attribution assessment statements for smaller regions are generally much weaker. Nevertheless, some detectable anthropogenic influences on average temperature have been reported for North America and parts of the United States (e.g., Christidis et al. 2010; Bonfils et al. 2008; Pierce et al. 2009). Figure 6.5 shows an example for 1901–2015 temperature trends, indicating a detectable anthropogenic warming since 1901 over the western and northern regions of the contiguous United States for the CMIP5 multi-model ensemble—a condition that was also met for most of the individual models (Knutson et al. 2013a). The Southeast stands out as the only region with no “detectable” warming since 1901; observed trends there were inconsistent with CMIP5 All Forcing historical runs (Knutson et al. 2013a). The cause of this “warming hole,” or lack of a long-term warming trend, remains uncertain, though it is likely a combination of natural and human causes. Some studies conclude that changes in anthropogenic aerosols have played a crucial role (e.g., Leibensperger et al. 2012a, b; Yu et al. 2014), whereas other studies infer a possible large role for internal climate variability (e.g., Meehl et al. 2012; Knutson et al. 2013a) as well as changes in land use (e.g., Goldstein et al. 2009; Xu et al. 2015). Notably, the Southeast has been warming rapidly since the early 1960s (Walsh et al. 2014; Pan et al. 2013).

[INSERT FIGURE 6.5 HERE:]

Figure 6.5. Detection and attribution assessment of trends in average annual temperature (°F). Grid-box values indicate whether trends for 1901–2015 are detectable (that is, distinct from natural variability) and/or consistent with CMIP5 historical All-Forcing runs. If the grid-box trend is found to be both detectable and either consistent with or greater than the warming in the All-Forcing runs, then the grid box is assessed as having a detectable anthropogenic contribution to warming over the period. (Figure source: updated from Knutson et al. 2013; © American Meteorological Society, used with permission)]

6.2.2 Temperature Extremes

IPCC AR5 (Bindoff et al. 2013) concluded that it is very likely that human influence has contributed to the observed changes in frequency and intensity of temperature extremes on the global scale since the mid-20th century. The combined influence of anthropogenic and natural forcings was also detectable over large subregions of North America (e.g., Zwiers et al. 2011; Min et al. 2013). In general, however, results for the contiguous United States are not as compelling as for global land areas, in part because detection of changes in U.S. regional temperature extremes is affected by extreme temperature in the 1930s (Peterson et al. 2013). Table 6.3 summarizes available attribution statements for recent extreme U.S. temperature events. As an example, the recent record or near-record high March–May average temperatures occurring in 2012 over the eastern United States were attributed in part to external (natural plus anthropogenic) forcing (Knutson et al. 2013b); the century-scale trend response of temperature to external forcing is typically a close approximation to the anthropogenic forcing response alone. Another study found that although the extreme March 2012 warm anomalies over the United States were mostly due to natural variability, anthropogenic warming contributed to the severity (Dole et al. 2014). Such statements reveal that both natural and anthropogenic factors influence the severity of extreme temperature events. Nearly every modern analysis of current extreme hot and cold events reveals some degree of attributable human influence.

[INSERT TABLE 6.3 HERE:]

Table 6.3. Extreme temperature events in the United States for which attribution statements have been made. There are three possible attribution statements: “+” shows an attributable human-induced increase in frequency or intensity, “–” shows an attributable human-induced decrease in frequency or intensity, “0” shows no attributable human contribution.]

6.3 Projected Changes

6.3.1 Average Temperatures

Temperature projections are based on global model results and associated downscaled products from CMIP5 using a suite of Representative Concentration Pathways (RCPs). In contrast to NCA3, model weighting is employed to refine projections of temperature for each RCP (Ch. 4: Projections; Appendix B: Model Weighting). Weighting parameters are based on model independence and model skill over North America for seasonal temperature and annual extremes (Figure 6.5). Unless stated otherwise, all changes presented here represent the weighted multi-model mean. The weighting scheme helps refine confidence and likelihood statements, but projections of U.S. surface air temperature remain very similar to those in NCA3. Generally speaking, extreme temperatures are projected to increase at a greater rate than changes in average temperatures (Collins et al. 2013).

[INSERT FIGURE 6.6 HERE:]

Figure 6.6. Relative performance of the CMIP5 models used in this study in simulating observed

North American temperature indices. The first four rows depict performance for extremes while the next four rows depict performance for seasonal averages. The last row depicts the combined performance for all metrics. Models are ordered from left (best) to worst (right) based upon this combined metric. (Figure source: adapted from Sanderson et al., submitted 2016)]

The average annual temperature of the contiguous United States is projected to rise throughout the century. Near-term increases will be about 1.4°C (2.5°F) for RCP4.5 and 1.6°C (2.9°F) for RCP8.5; the similarity in warming reflects the similarity in greenhouse gas concentrations during this period (Figure 4.1). Notably, a 1.4°C (2.5°F) increase makes the near-term average roughly comparable to the hottest year in the historical record (2012). In other words, recent record-breaking years could be “normal” by about 2030. By late-century, the RCPs diverge in a statistically significant sense, leading to very different rates of warming: approximately 2.8°C (5.0°F) for RCP4.5 and 4.8°C (8.7°F) for RCP8.5. Unforced internal variations will continue to be evident in future U.S. temperatures, particularly in the near-term. Slightly larger increases are projected for summer than winter (except for Alaska), and average maximum temperature will rise slightly faster than average minimum temperature.

Warming is projected for all parts of the United States by mid- and late-century (Figure 6.7). The largest changes are in Alaska (5.5°C [10°F] or more by late-century under RCP8.5), in part due to decreases in surface albedo as snow cover declines. In the contiguous United States, northern regions (the Northeast, Midwest, and Northern Great Plains) have slightly more warming than elsewhere, consistent with polar amplification (Table 6.4). The Southeast has slightly less warming because anthropogenic effects are partially offset by latent heat release from increases in evapotranspiration (as is already evident in the observed record). From a sub-regional perspective, less warming is projected along the coasts due to the moderating effects of the ocean, although the temperature increases are still substantial. In addition, anthropogenic warming at higher elevations may be underestimated because the resolution of the CMIP5 models does not capture orography in detail, with important implications for future snowpack in the mountainous West.

[INSERT FIGURE 6.7 HERE:]

Figure 6.7. Projected changes in average annual temperature (°F) for mid- and late-21st century. Changes are the difference between the average for mid-century (2036–2065; top) or late-century (2071–2100, bottom) and the average for near-present (1976–2005). (Figure source: CICS-NC / NOAA/NCEI).]

[INSERT TABLE 6.4 HERE:]

Table 6.4. Projected changes in average annual temperature (°F) for each NCA region. Changes are the difference between the average in the future (either mid- or late-century) and the average for near-present (1976–2005).]

6.3.2 Temperature Extremes

The coldest and warmest daily temperatures of the year are projected to increase substantially over the coming decades (Figure 6.8). Under RCP8.5, increases in most areas exceed 2.8°C [5°F] by mid-century (Fischer et al. 2013), rising to 5.5°C [10°F] or more by late-century (Sillmann et al. 2013). From a regional perspective, the coldest temperatures will increase the most in Alaska and in the northern half of the contiguous United States whereas the warmest temperatures will exhibit somewhat more uniform changes geographically (Table 6.5). Changes in “very rare” temperature extremes are particularly dramatic under RCP8.5; by late century, current 1-in-20 year maximums are projected to occur every year, while current 1-in-20 year minimums are not projected to occur at all over the contiguous United States (Wuebbles et al. 2014). Finally, there is a substantial projected decrease in the number of days with a minimum temperature below freezing, particularly in the West, and a marked increase in the number days with a maximum over 38°C [100°F], particularly in the Southwest, Great Plains, and Southeast (Figure 6.9).

[INSERT FIGURE 6.8 HERE:]

Figure 6.8. Projected changes in the coldest and warmest daily temperatures (°F) of the year. Changes are the difference between the average for mid-century (2036–2065) and the average for near-present (1976–2005) under RCP8.5. (Figure source: CICS-NC / NOAA/NCEI)]

[INSERT FIGURE 6.9 HERE:]

Figure 6.9. Projected changes in the number of days per year with a minimum temperature below 32°F (left) and a maximum temperature above 100°F (right). Changes are the difference between the average for mid-century (2036–2065) and the average for near-present (1976–2005) under RCP8.5. (Figure source: CICS-NC / NOAA/NCEI)]

[INSERT TABLE 6.5 HERE:]

Table 6.5. Projected changes in temperature extremes (°F) for each NCA region. Changes are the difference between the average for mid-century and the average for near-present (1976–2005) under RCP8.5.]

The frequency and intensity of cold spells is projected to decrease while the frequency and intensity of warm spells is projected to increase throughout the century. The frequency of cold spells will decrease the most in Alaska and the least in the Northeast while the frequency of warm spells will increase in all regions, particularly the Southeast, Southwest, and Alaska. By mid-century, decreases in the frequency of cold spells are similar across RCPs whereas increases in the frequency of warm spells are about 50% greater in RCP8.5 than RCP4.5 (Sun et al. 2015). The intensity of cold waves and heat waves is also projected to increase dramatically, particularly under RCP8.5. By mid-century, both extreme cold waves and extreme heat waves (5-day, 1-in-10 year events) are projected to have temperature increases of at least 6°C [11°F] nationwide, with larger increases in northern regions (the Northeast, Midwest, Northern Great Plains, and Northwest; Table 6.5). Changes in land surface properties will play an important role

1 in the changes in warm spells. In the stagnant air conditions associated with prolonged heat
2 waves, soils will dry out faster in a warmer climate. The reduction in evaporative cooling then
3 compounds the average warming during the heat wave.

4

DRAFT

TRACEABLE ACCOUNTS

Key Finding 1

The annual-average, near-surface air temperature over the contiguous United States has increased by about 1.2°F (0.7°C) between 1901 and 2015. Surface and satellite data both show rapid warming since the late 1970s, while paleo-temperature evidence shows that recent decades have been the warmest in at least the past 1,500 years. (*Extremely likely, High confidence*)

Description of Evidence Base

The key finding and supporting text summarize extensive evidence documented in the climate science literature. Similar statements about changes have also been made in other national assessments (such as NCA3) and in reports by the Climate Change Science Program (such as SAP1.1: Temperature trends in the lower atmosphere, and SAP 1.6: Global Climate Change Impacts in the United States). Statements about annual events and extremes are documented in the State of the Climate Reports by the *Bulletin of the American Meteorological Society*.

Evidence for changes in U.S. climate arises from multiple analyses of data from in-situ, satellite, and other records undertaken by many groups over several decades. The primary dataset for surface temperatures in the contiguous United States is nClimGrid (Vose et al. 2014), with other recently released datasets for Alaska and other areas. Changes in sea surface temperatures are derived from the NOAA Global Temperature dataset (Vose et al. 2012), which now uses the Extended Reconstructed Sea Surface Temperature Dataset version 4 (Huang et al. 2015). Several recently improved satellite datasets document changes in middle tropospheric temperatures (Mears and Wentz 2016; Zou and Li 2016; Christy et al. 2011). Longer-term changes are depicted using multiple paleo analyses (e.g., Wahl and Smerdon 2012, Truett et al. 2013).

Major Uncertainties

The primary uncertainties for surface data relate to historical changes in station location, temperature instrumentation, observing practice, and spatial sampling. Satellite records are similarly impacted by non-climatic changes such as orbital decay, diurnal sampling, and instrument calibration to target temperatures. Several uncertainties are inherent in temperature-sensitive proxies, such as dating techniques and spatial sampling.

Assessment of Confidence

Very High

Likelihood of Impact

Extremely Likely

Summary Sentence

There is very high confidence in observed changes in average temperature over the United States based upon the convergence of evidence from multiple data sources, analyses, and assessments.

Key Finding 2

Accompanying the rise in average temperatures, there have been – as is to be expected – increases in extreme temperature events in most parts of the United States. Since the early 1900s, the temperature of extremely cold days has increased throughout the contiguous United States, and the temperature of extremely warm days has increased across much of the West. In recent decades, intense cold waves have become less common while intense heat waves have become more common. (*Extremely likely, Very high confidence*)

Description of Evidence Base

The key finding and supporting text summarize extensive evidence documented in the climate science literature. Similar statements about changes have also been made in other national assessments (such as NCA3) and in reports by the Climate Change Science Program (such as SAP3.3: Weather and Climate Extremes in a Changing Climate) and the IPCC Special Report on Managing the Risks of Extreme Events and Disasters to Advance Climate Change Adaptation. Statements about annual events and extremes are documented in the State of the Climate Reports and the Explaining Extreme Events Reports by the *Bulletin of the American Meteorological Society*.

Evidence for changes in U.S. climate arises from multiple analyses of in situ data and atmospheric reanalyses using widely published climate extremes indices. The primary source of in situ data is the Global Historical Climatology Network – Daily dataset (Menne et al. 2011), the largest collection of U.S. and global temperature data in the world. Climate extremes indices, comprehensively documented in Zhang et al. 2011, have been employed in numerous publications and assessments.

Major Uncertainties

The primary uncertainties for in situ data relate to historical changes in station location, temperature instrumentation, observing practice, and spatial sampling (particularly the precision of estimates of change in areas and periods with low station density, such as the intermountain West in the early 20th century).

Assessment of Confidence

Very High

Likelihood of Impact

Extremely Likely

Summary Sentence

There is very high confidence in observed changes in temperature extremes over the United States based upon the convergence of evidence from multiple data sources, analyses, and assessments.

Key Finding 3

The average annual temperature of the contiguous United States is projected to rise throughout the century. Increases of at least 2.5°F (1.4°C) are projected over the next few decades, meaning that recent record-setting years will be relatively “common” in the near future. Increases of 5.0°–7.5°F (2.8°–4.8°C) are projected by late century depending upon the level of future emissions. (*Extremely likely, Very high confidence*)

Description of Evidence Base

The key finding and supporting text summarize extensive evidence documented in the climate science literature. Similar statements about changes have also been made in other national assessments (such as NCA3) and in reports by the Climate Change Science Program (such as SAP 1.6: Global Climate Change Impacts in the United States). The basic physics underlying the impact of human emissions on global climate has also been documented in every IPCC assessment.

Major Uncertainties

Global climate models are subject to structural and parametric uncertainty, resulting in a range of estimates of future changes in average temperature. This is partially mitigated through the use of model weighting and pattern scaling. Furthermore, virtually every ensemble member of every model projection contains an increase in temperature by mid- and late-century. Empirical downscaling introduces additional uncertainty (e.g., with respect to stationarity). Projections will improve in the future along with improvements in model physics and resolution.

Assessment of Confidence

Very High

Likelihood of Impact

Extremely likely

Summary Sentence

There is high confidence in projected changes in average temperature over the United States based upon the convergence of evidence from multiple model simulations, analyses, and assessments.

Key Finding 4

Extreme temperatures are projected to increase even more than average temperatures. The temperatures of extremely cold days and extremely warm days are both projected to increase. Cold waves are projected to become less intense while heat waves will become more intense. (*Extremely likely, Very high confidence*)

Description of Evidence Base

The key finding and supporting text summarize extensive evidence documented in the climate science literature. Similar statements about changes have also been made in other national assessments (such as NCA3) and in reports by the Climate Change Science Program (such as SAP 3,3: Weather and Climate Extremes in a Changing Climate). The basic physics underlying the impact of human emissions on global climate has also been documented in every IPCC assessment.

Major Uncertainties

Global climate models are subject to structural and parametric uncertainty, resulting in a range of estimates of future changes in temperature extremes. This is partially mitigated through the use of model weighting and pattern scaling. Furthermore, virtually every ensemble member of every model projection contains an increase in temperature by mid- and late-century. Empirical downscaling introduces additional uncertainty (e.g., with respect to stationarity). Projections will improve in the future along with improvements in model physics and resolution.

Assessment of Confidence

Very High

Likelihood of Impact

Extremely likely

Summary Sentence

There is high confidence in projected changes in temperature extremes over the United States based upon the convergence of evidence from multiple model simulations, analyses, and assessments.

1 **TABLES**

2 **Table 6.1.** Observed changes in average annual temperature (°F) for each NCA region. Changes
 3 are the difference between the average for present-day (1986–2015) and the average for the first
 4 half of the last century (1901–1960).

NCA Region	Average Annual Temperature	Average Annual Maximum Temperature	Average Annual Minimum Temperature
Contiguous U.S.	1.18	1.00	1.35
Northeast	1.37	1.09	1.65
Southeast	0.40	0.10	0.70
Midwest	1.18	0.71	1.66
Great Plains North	1.62	1.59	1.65
Great Plains South	0.70	0.50	0.90
Southwest	1.56	1.57	1.56
Northwest	1.51	1.48	1.52
Alaska	1.52	1.29	1.76
Hawaii	0.75	-	-

5

- 1 **Table 6.2.** Observed changes in temperature extremes (°F) for each NCA region. Changes are
 2 the difference between the average for present-day (1986–2015) and the average for the first half
 3 of the last century (1901–1960).

NCA Region	Coldest Day of the Year	Coldest 5-Day 1-in-10 Year Event	Warmest Day of the Year	Warmest 5-Day 1-in-10 Year Event
Northeast	3.04	1.13	-0.99	-1.85
Southeast	1.13	0.43	-1.53	-1.64
Midwest	3.04	-1.32	-2.26	-4.12
Great Plains North	4.80	3.16	-1.16	-1.45
Great Plains South	3.44	1.55	-1.16	-1.10
Southwest	4.12	3.31	0.40	0.14
Northwest	5.00	3.53	-0.22	-0.85

4

Table 6.3. Extreme temperature events in the United States for which attribution statements have been made. There are three possible attribution statements: “+” shows an attributable human-induced increase in frequency or intensity, “–” shows an attributable human-induced decrease in frequency or intensity, “0” shows no attributable human contribution.

Study	Period	Region	Type	Statement
Rupp et al. 2012	Spring/Summer 2011	Texas	Hot	+
Angelil et al. 2016				+
Hoerling et al. 2013	Summer 2011	Texas	Hot	+
Diffenbaugh and Scherer 2013	July 2012	Northcentral and Northeast	Hot	+
Angelil et al. 2016				+
Cattiaux and Yiou 2013	Spring 2012	East.	Hot	0
Angelil et al. 2016				+
Knutson et al. 2013	Spring 2012	East	Hot	+
Angelil et al. 2016				+
Jeon et al 2016	Summer 2011	Texas/Oklahoma	Hot	+
Dole et al. 2014	March 2012	Upper Midwest	Hot	+
Seager et al. 2014	2011-2014	California	Hot	+
Wolter et al. 2015	Winter 2014	Midwest	Cold	–
Trenary et al. 2015	Winter 2014	East	Cold	0

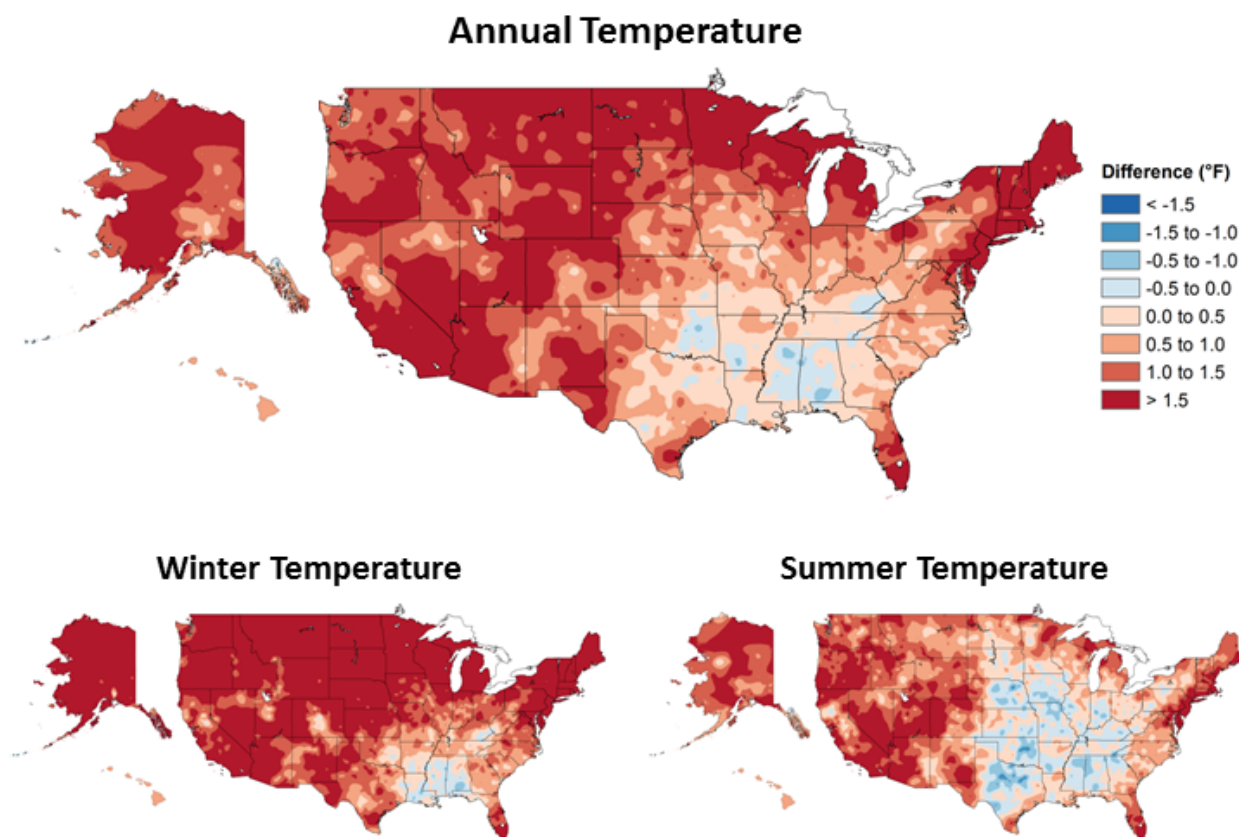
- 1 **Table 6.4.** Projected changes in average annual temperature (°F) for each NCA region. Changes
 2 are the difference between the average in the future (either mid- or late-century) and the average
 3 for near-present (1976-2005).

NCA Region	RCP4.5 Mid-Century (2036-2065)	RCP 8.5 Mid-Century (2036-2065)	RCP 4.5 Late-Century (2071-2100)	RCP 8.5 Late-Century (2071-2100)
Contiguous U.S.	3.79	4.83	5.03	8.72
Northeast	3.98	5.09	5.27	9.11
Southeast	3.40	4.30	4.43	7.72
Midwest	4.21	5.29	5.57	9.49
Great Plains North	4.05	5.10	5.44	9.37
Great Plains South	3.62	4.61	4.78	8.44
Southwest	3.72	4.80	4.93	8.65
Northwest	3.66	4.67	4.99	8.51

- 1 **Table 6.5.** Projected changes in temperature extremes (°F) for each NCA region. Changes are the
 2 difference between the average for mid-century and the average for near-present (1976–2005)
 3 under RCP8.5.

NCA Region	Coldest Day of the Year	Coldest 5-Day 1-in-10 Year Event	Warmest Day of the Year	Warmest 5-Day 1-in-10 Year Event
Northeast	9.51	15.93	6.51	12.88
Southeast	4.97	8.84	5.79	11.09
Midwest	9.44	15.52	6.71	13.02
Great Plains North	8.01	12.01	6.48	12.00
Great Plains South	5.49	9.41	5.70	10.73
Southwest	6.13	10.20	5.85	11.17
Northwest	7.33	10.95	6.25	12.31

4

1 **FIGURES**

2

3

4 **Figure 6.1.** Observed changes in annual, winter, and summer temperature (°F). Changes are the
5 difference between the average for present-day (1986–2015) and the average for the first half of
6 the last century (1901–1960 for the contiguous United States, 1925–1960 for Alaska and
7 Hawai‘i). (Figure source: NOAA/NCEI)

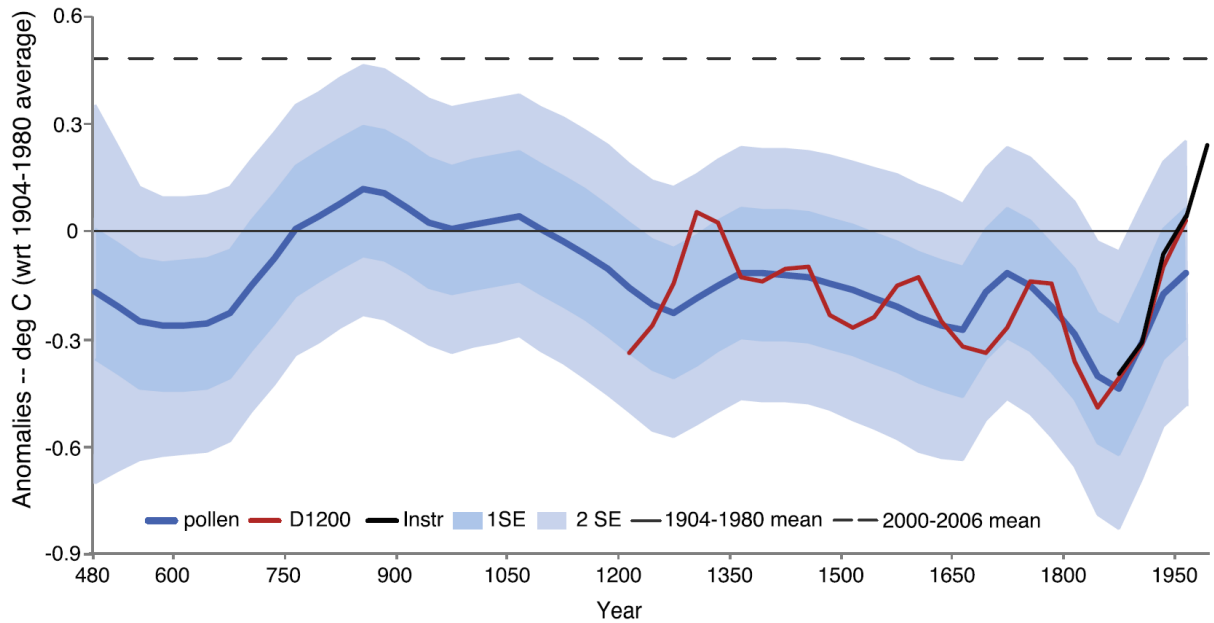


Figure 6.2. Pollen-based temperature reconstruction for temperate North America. The blue curve depicts the pollen-based reconstruction of 30-year averages (as anomalies from 1904 to 1980) for the temperate region (30°–55°N, 7°5–130°W). The red curve shows the corresponding tree ring-based decadal average reconstruction, which was smoothed and used to calibrate the lower-frequency pollen-based estimate. Light (medium) blue zones indicate 2 standard error (1 standard error) uncertainty estimations associated with each 30-year value. The black curve shows comparably smoothed instrumental temperature values up to 1980. The dashed black line represents the average temperature anomaly of comparably smoothed instrumental data for the period 2000–2006. (Figure source: NOAA/NCEI)

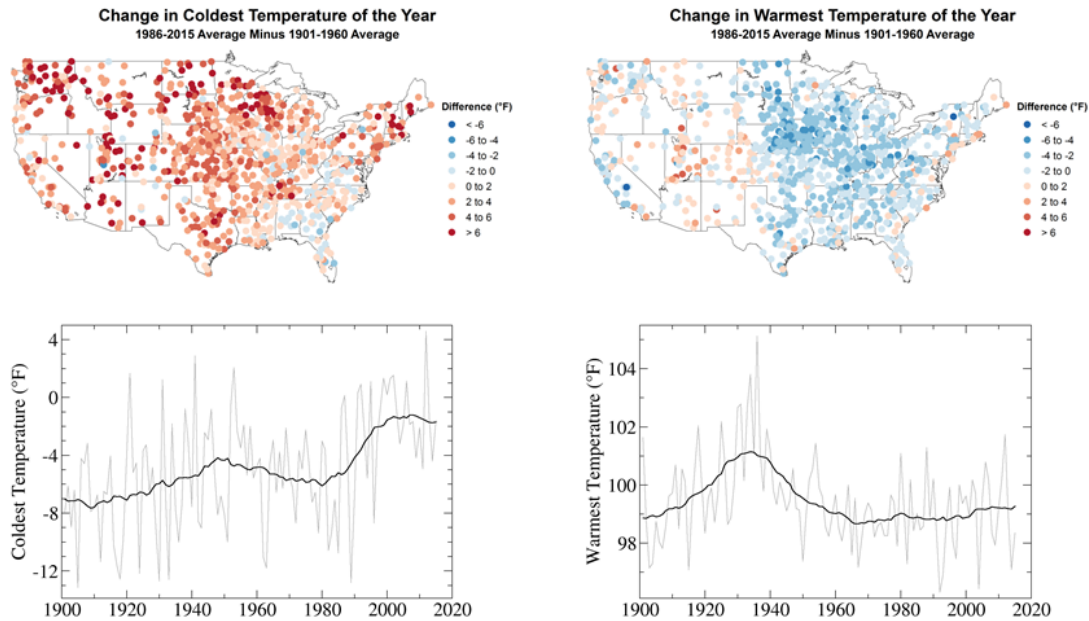


Figure 6.3. Observed changes in the coldest and warmest daily temperatures (°F) of the year. Maps (top) depict changes at stations; changes are the difference between the average for present-day (1986–2015) and the average for the first half of the last century (1901–1960). Time series (bottom) depict changes over the contiguous United States. (Figure source: NOAA/NCEI)

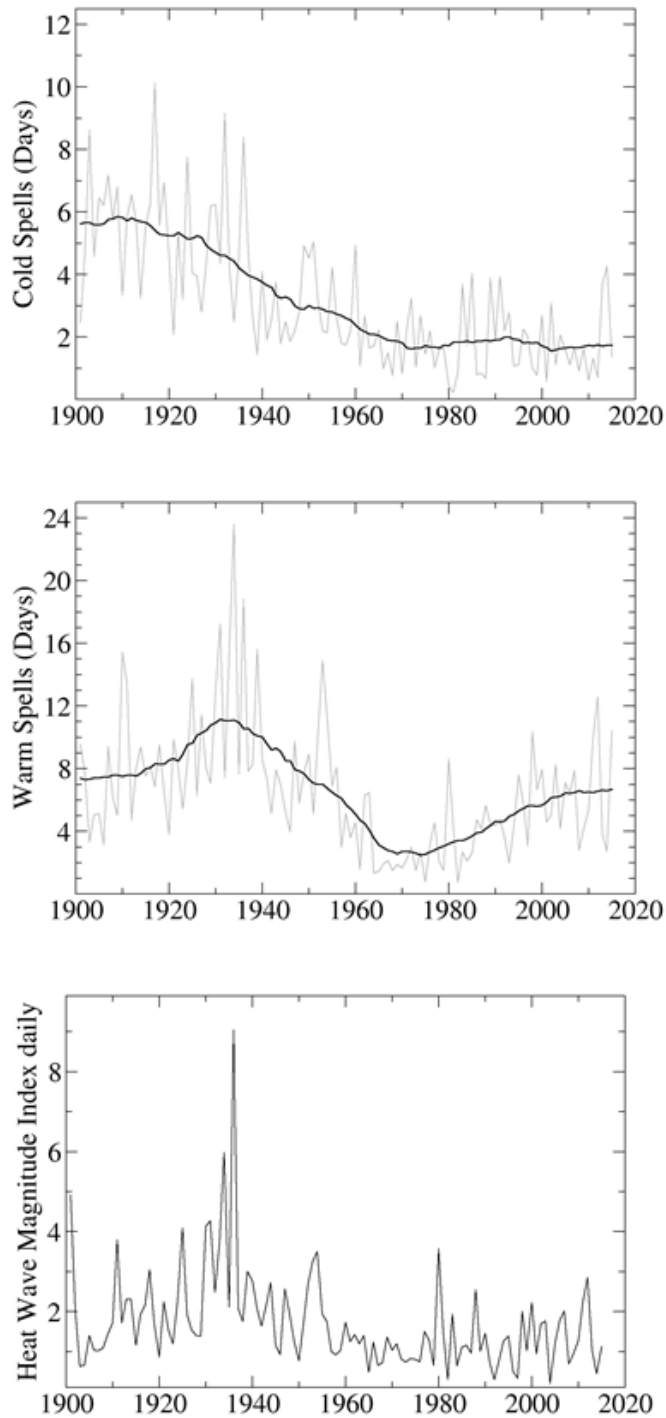


Figure 6.4. Observed changes in cold and warm spells in the contiguous United States. The top panel depicts changes in the frequency of cold spells, the middle panel depicts changes in the frequency of warm spells, and the bottom panel depicts changes in the intensity of heat waves. (Figure source: NOAA/NCEI)

Assessment of Annual Surface Temperature Trends (1901–2015)

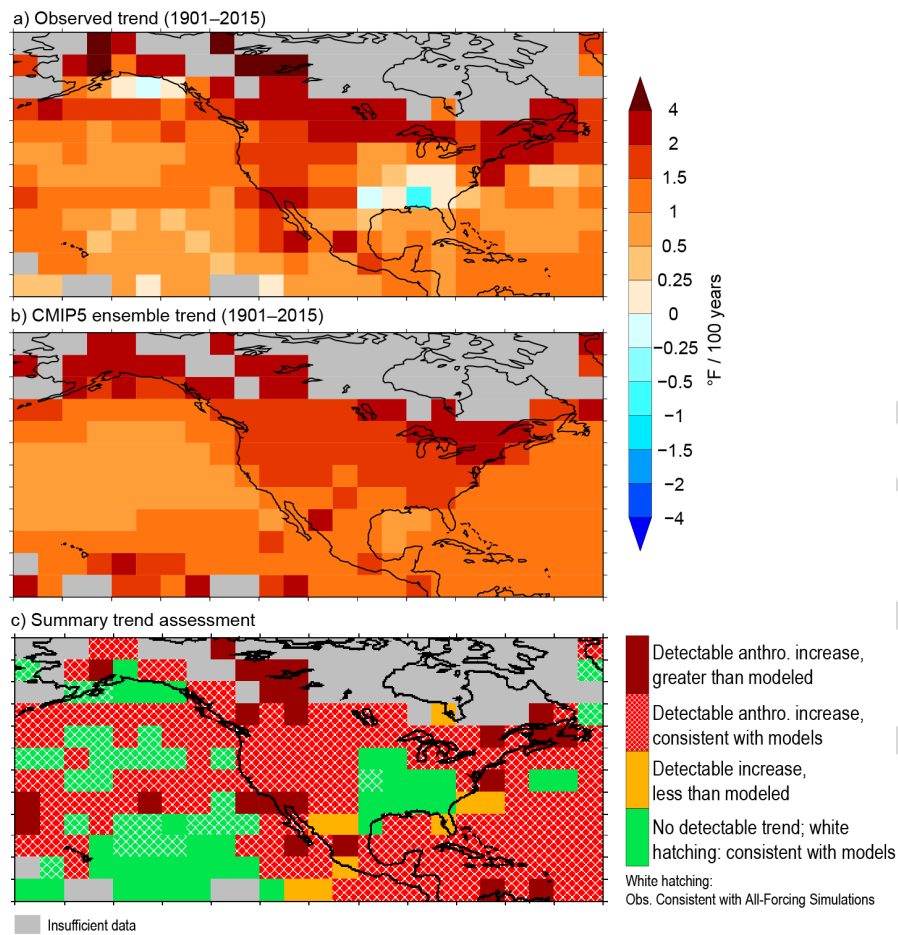


Figure 6.5. Detection and attribution assessment of trends in average annual temperature (°F). Grid-box values indicate whether trends for 1901–2015 are detectable (that is, distinct from natural variability) and/or consistent with CMIP5 historical All-Forcing runs. If the grid-box trend is found to be both detectable and either consistent with or greater than the warming in the All-Forcing runs, then the grid box is assessed as having a detectable anthropogenic contribution to warming over the period. (Figure source: updated from Knutson et al. 2013; © American Meteorological Society. Used with permission.)

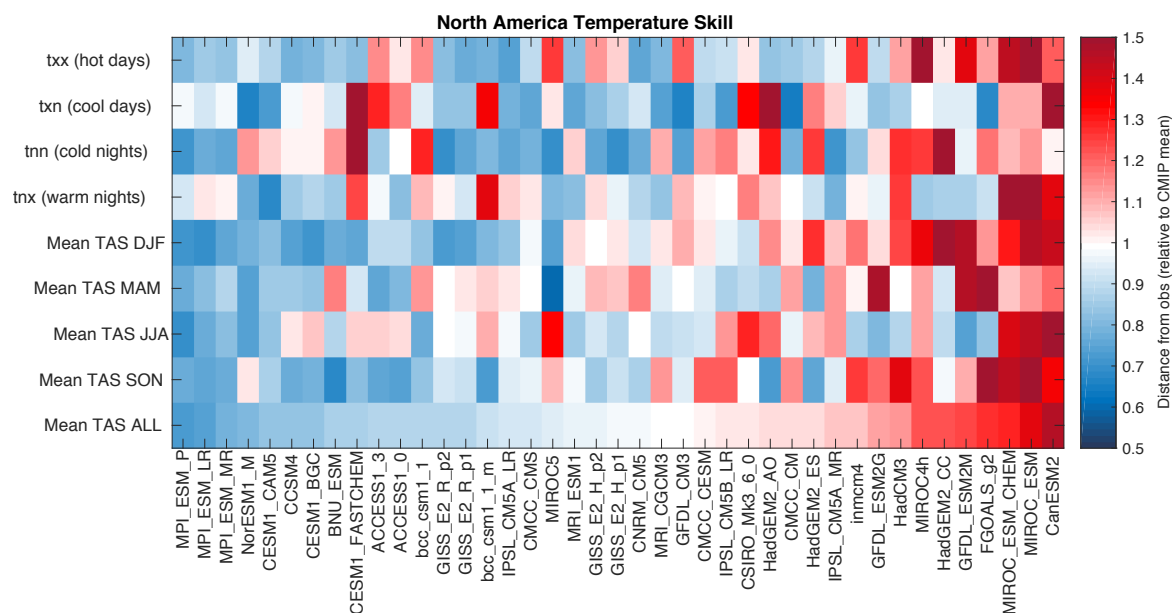


Figure 6.6. Relative performance of the CMIP5 models used in this study in simulating observed North American temperature indices. The first four rows depict performance for extremes while the next four rows depict performance for seasonal averages. The last row depicts the combined performance for all metrics. Models are ordered from left (best) to worst (right) based upon this combined metric. (Figure source: adapted from Sanderson et al., submitted 2016)

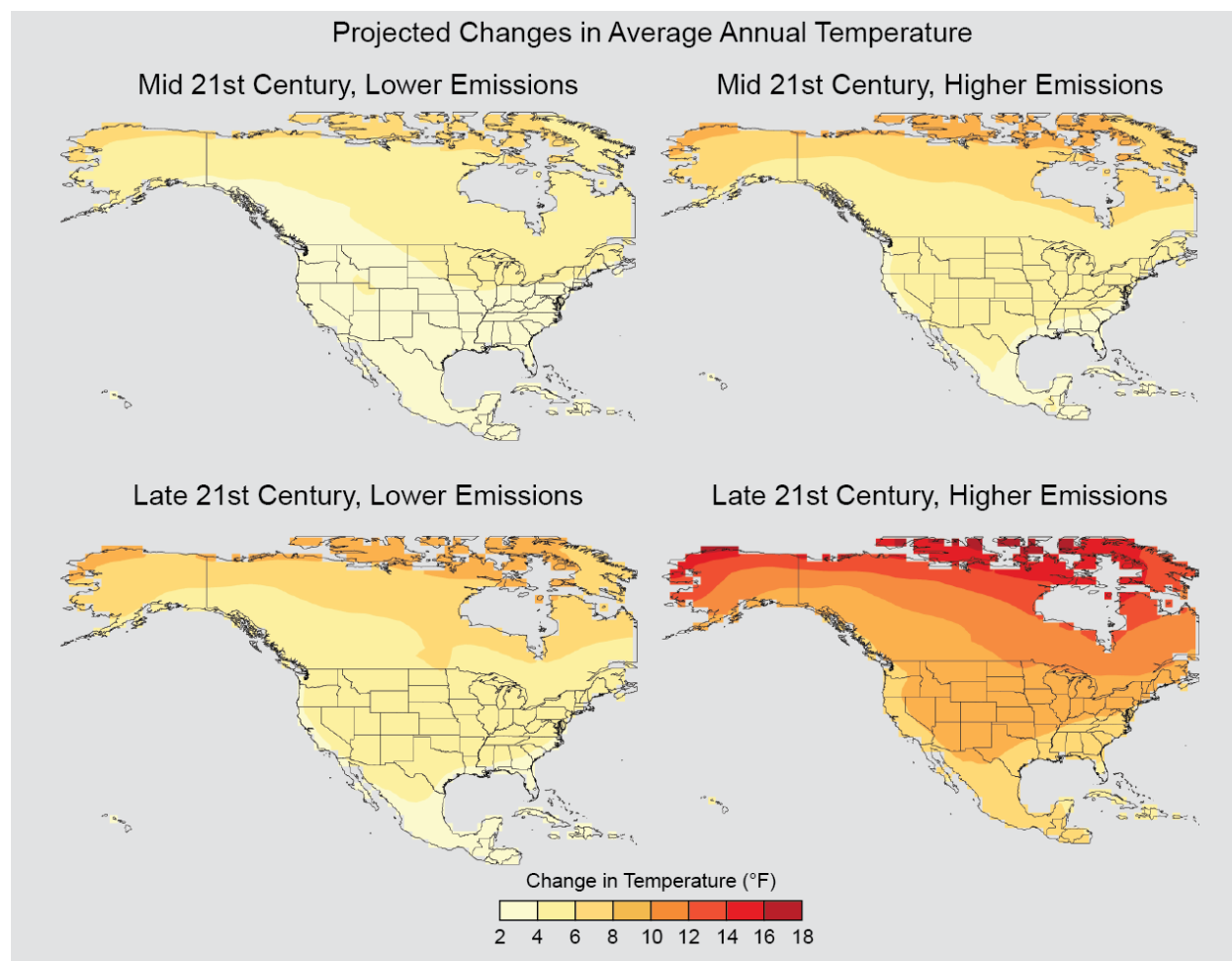


Figure 6.7. Projected changes in average annual temperature (°F) for mid- and late-21st century. Changes are the difference between the average for mid-century (2036–2065; top) or late-century (2071–2100, bottom) and the average for near-present (1976–2005). (Figure source: CICS-NC / NOAA/NCEI)

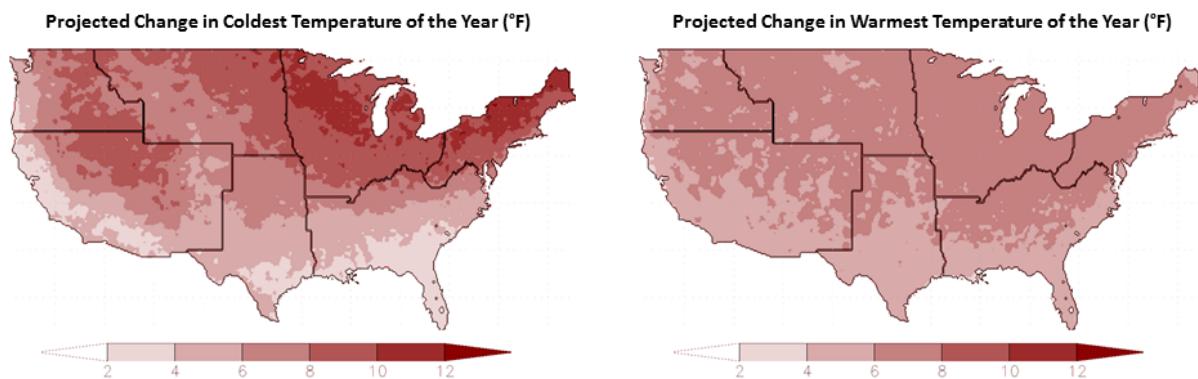


Figure 6.8. Projected changes in the coldest and warmest daily temperatures (°F) of the year. Changes are the difference between the average for mid-century (2036–2065) and the average for near-present (1976–2005) under RCP8.5. (Figure source: CICS-NC / NOAA/NCEI)

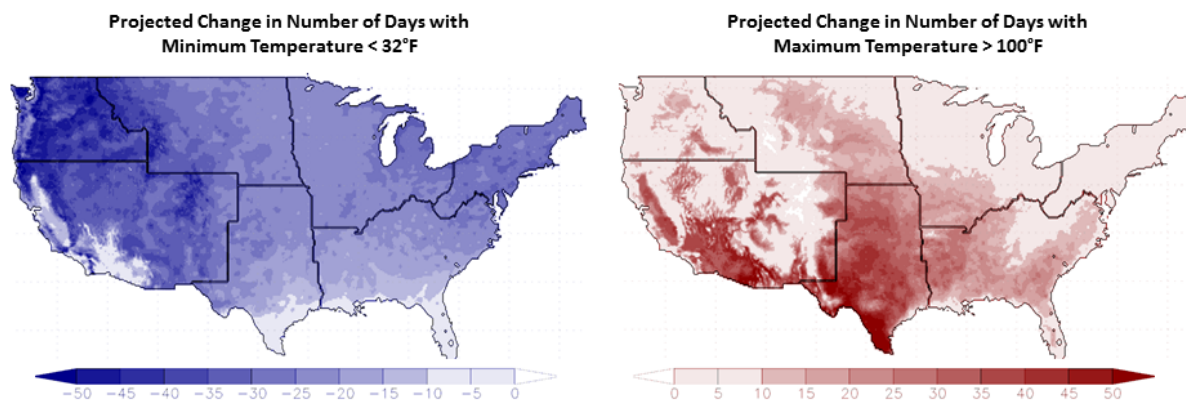


Figure 6.9. Projected changes in the number of days per year with a minimum temperature below 32°F (left) and a maximum temperature above 100°F (right). Changes are the difference between the average for mid-century (2036–2065) and the average for near-present (1976–2005) under RCP8.5. (Figure source: CICS-NC / NOAA/NCEI)

1 REFERENCES

- 2 Angéllil, O., D. Stone, M. Wehner, C.J. Paciorek, H. Krishnan, and W. Collins, 2016: An
 3 independent assessment of anthropogenic attribution statements for recent extreme
 4 temperature and rainfall events. *Journal of Climate*, **in press**, null.
 5 <http://dx.doi.org/10.1175/JCLI-D-16-0077.1>
- 6 Bindoff, N.L., P.A. Stott, K.M. AchutaRao, M.R. Allen, N. Gillett, D. Gutzler, K. Hansingo, G.
 7 Hegerl, Y. Hu, S. Jain, I.I. Mokhov, J. Overland, J. Perlwitz, R. Sebbari, and X. Zhang, 2013:
 8 Detection and Attribution of Climate Change: from Global to Regional. *Climate Change*
 9 *2013: The Physical Science Basis. Contribution of Working Group I to the Fifth Assessment*
 10 *Report of the Intergovernmental Panel on Climate Change*. Stocker, T.F., D. Qin, G.-K.
 11 Plattner, M. Tignor, S.K. Allen, J. Boschung, A. Nauels, Y. Xia, V. Bex, and P.M. Midgley,
 12 Eds. Cambridge University Press, Cambridge, United Kingdom and New York, NY, USA,
 13 867–952. <http://dx.doi.org/10.1017/CBO9781107415324.022> www.climatechange2013.org
- 14 Bonfils, C., P.B. Duffy, B.D. Santer, T.M.L. Wigley, D.B. Lobell, T.J. Phillips, and C.
 15 Doutriaux, 2008: Identification of external influences on temperatures in California. *Climatic*
 16 *Change*, **87**, 43-55. <http://dx.doi.org/10.1007/s10584-007-9374-9>
- 17 Cattiaux, J. and P. Yiou, 2013: U.S. heat waves of spring and summer 2012 from the flow
 18 analogue perspective [in "Explaining Extremes of 2012 from a Climate Perspective"].
 19 *Bulletin of the American Meteorological Society*, **94**, S10-S13.
 20 <http://dx.doi.org/10.1175/BAMS-D-13-00085.1>
- 21 Christidis, N., P.A. Stott, F.W. Zwiers, H. Shiogama, and T. Nozawa, 2010: Probabilistic
 22 estimates of recent changes in temperature: a multi-scale attribution analysis. *Climate*
 23 *Dynamics*, **34**, 1139-1156. <http://dx.doi.org/10.1007/s00382-009-0615-7>
- 24 Christy, J.R., R.W. Spencer, and W.B. Norris, 2011: The role of remote sensing in monitoring
 25 global bulk tropospheric temperatures. *International Journal of Remote Sensing*, **32**, 671-
 26 685. <http://dx.doi.org/10.1080/01431161.2010.517803>
- 27 Collins, M., R. Knutti, J. Arblaster, J.-L. Dufresne, T. Fichet, P. Friedlingstein, X. Gao, W.J.
 28 Gutowski, T. Johns, G. Krinner, M. Shongwe, C. Tebaldi, A.J. Weaver, and M. Wehner,
 29 2013: Long-term Climate Change: Projections, Commitments and Irreversibility. *Climate*
 30 *Change 2013: The Physical Science Basis. Contribution of Working Group I to the Fifth*
 31 *Assessment Report of the Intergovernmental Panel on Climate Change*. Stocker, T.F., D.
 32 Qin, G.-K. Plattner, M. Tignor, S.K. Allen, J. Boschung, A. Nauels, Y. Xia, V. Bex, and
 33 P.M. Midgley, Eds. Cambridge University Press, Cambridge, United Kingdom and New
 34 York, NY, USA, 1029–1136. <http://dx.doi.org/10.1017/CBO9781107415324.024>
 35 www.climatechange2013.org

- 1 Diffenbaugh, N.S. and M. Scherer, 2013: Likelihood of July 2012 U.S. temperatures in pre-
2 industrial and current forcing regimes [in "Explaining Extremes of 2012 from a Climate
3 Perspective"]. *Bulletin of the American Meteorological Society*, **94**, S6-S9.
4 <http://dx.doi.org/10.1175/BAMS-D-13-00085.1>
- 5 Dole, R., M. Hoerling, A. Kumar, J. Eischeid, J. Perlwitz, X.-W. Quan, G. Kiladis, R. Webb, D.
6 Murray, M. Chen, K. Wolter, and T. Zhang, 2014: The Making of an Extreme Event: Putting
7 the Pieces Together. *Bulletin of the American Meteorological Society*, **95**, 427-440.
8 <http://dx.doi.org/10.1175/BAMS-D-12-00069.1>
- 9 Fischer, E.M., U. Beyerle, and R. Knutti, 2013: Robust spatially aggregated projections of
10 climate extremes. *Nature Climate Change*, **3**, 1033-1038.
11 <http://dx.doi.org/10.1038/nclimate2051>
- 12 Goldstein, A.H., C.D. Koven, C.L. Heald, and I.Y. Fung, 2009: Biogenic carbon and
13 anthropogenic pollutants combine to form a cooling haze over the southeastern United States.
14 *Proceedings of the National Academy of Sciences*, **106**, 8835-8840.
15 <http://dx.doi.org/10.1073/pnas.0904128106>
16 <http://www.pnas.org/content/106/22/8835.abstract>
- 17 Hoerling, M., M. Chen, R. Dole, J. Eischeid, A. Kumar, J.W. Nielsen-Gammon, P. Pegion, J.
18 Perlwitz, X.-W. Quan, and T. Zhang, 2013: Anatomy of an extreme event. *Journal of*
19 *Climate*, **26**, 2811-2832. <http://dx.doi.org/10.1175/JCLI-D-12-00270.1>
- 20 Huang, B., V.F. Banzon, E. Freeman, J. Lawrimore, W. Liu, T.C. Peterson, T.M. Smith, P.W.
21 Thorne, S.D. Woodruff, and H.-M. Zhang, 2015: Extended Reconstructed Sea Surface
22 Temperature Version 4 (ERSST.v4). Part I: Upgrades and Intercomparisons. *Journal of*
23 *Climate*, **28**, 911-930. <http://dx.doi.org/10.1175/JCLI-D-14-00006.1>
- 24 IPCC, 2013: *Climate Change 2013: The Physical Science Basis. Contribution of Working Group*
25 *I to the Fifth Assessment Report of the Intergovernmental Panel on Climate Change*.
26 Cambridge University Press, Cambridge, UK and New York, NY, 1535 pp.
27 <http://dx.doi.org/10.1017/CBO9781107415324> www.climatechange2013.org
- 28 Jeon, S., C.J. Paciorek, and M.F. Wehner, 2016: Quantile-based bias correction and uncertainty
29 quantification of extreme event attribution statements. *Weather and Climate Extremes*, **12**,
30 24-32. <http://dx.doi.org/10.1016/j.wace.2016.02.001>
31 <http://www.sciencedirect.com/science/article/pii/S2212094715300220>
- 32 Jones, G.S., P.A. Stott, and N. Christidis, 2013: Attribution of observed historical near surface
33 temperature variations to anthropogenic and natural causes using CMIP5 simulations. *Journal*
34 *of Geophysical Research*, 118, 4001-4024. <http://dx.doi.org/10.1002/jgrd.50239>

- 1 Knutson, T.R., F. Zeng, and A.T. Wittenberg, 2013a: Multimodel Assessment of Regional
2 Surface Temperature Trends: CMIP3 and CMIP5 Twentieth-Century Simulations. *Journal of*
3 *Climate*, **26**, 8709-8743. <http://dx.doi.org/10.1175/JCLI-D-12-00567.1>
- 4 Knutson, T.R., F. Zeng, and A.T. Wittenberg, 2013b: The extreme March-May 2012 warm
5 anomaly over the eastern United States: Global context and multimodel trend analysis [in
6 "Explaining Extremes of 2012 from a Climate Perspective"]. *Bulletin of the American*
7 *Meteorological Society*, **94**, S13-S17. <http://dx.doi.org/10.1175/BAMS-D-13-00085.1>
- 8 Leibensperger, E.M., L.J. Mickley, D.J. Jacob, W.T. Chen, J.H. Seinfeld, A. Nenes, P.J. Adams,
9 D.G. Streets, N. Kumar, and D. Rind, 2012: Climatic effects of 1950-2050 changes in US
10 anthropogenic aerosols - Part 1: Aerosol trends and radiative forcing. *Atmospheric Chemistry*
11 *and Physics* **12**, 3333-3348. <http://dx.doi.org/10.5194/acp-12-3333-2012>
- 12 Leibensperger, E.M., L.J. Mickley, D.J. Jacob, W.T. Chen, J.H. Seinfeld, A. Nenes, P.J. Adams,
13 D.G. Streets, N. Kumar, and D. Rind, 2012: Climatic effects of 1950–2050 changes in
14 US anthropogenic aerosols – Part 2: Climate response. *Atmospheric Chemistry and*
15 *Physics*, **12**, 3349-3362. <http://dx.doi.org/10.5194/acp-12-3349-2012>
- 16 Mazdiyasni, O. and A. AghaKouchak, 2015: Substantial increase in concurrent droughts and
17 heatwaves in the United States. *Proceedings of the National Academy of Sciences*, **112**,
18 11484-11489. <http://dx.doi.org/10.1073/pnas.1422945112>
- 19 Mears, C.A. and F.J. Wentz, 2016?: Sensitivity of satellite-derived tropospheric temperature
20 trends to the diurnal cycle adjustment. *Journal of Climate*, **29**, 3629-3646.
21 <http://dx.doi.org/10.1175/JCLI-D-15-0744.1>
- 22 Meehl, G.A., J.M. Arblaster, and G. Branstator, 2012: Mechanisms contributing to the warming
23 hole and the consequent US east-west differential of heat extremes. *Journal of Climate*, **25**,
24 6394-6408. <http://dx.doi.org/10.1175/JCLI-D-11-00655.1>
- 25 Menne, M.J., I. Durre, R.S. Vose, B.E. Gleason, and T.G. Houston, 2012: An overview of the
26 global historical climatology network-daily database. *Journal of Atmospheric and Oceanic*
27 *Technology*, **29**, 897-910. <http://dx.doi.org/10.1175/JTECH-D-11-00103.1>
- 28 Min, S.-K., X. Zhang, F. Zwiers, H. Shioyama, Y.-S. Tung, and M. Wehner, 2013: Multimodel
29 Detection and Attribution of Extreme Temperature Changes. *Journal of Climate*, **26**, 7430-
30 7451. <http://dx.doi.org/10.1175/JCLI-D-12-00551.1>
- 31 PAGES 2K, 2013: Continental-scale temperature variability during the past two millennia.
32 *Nature Geoscience*, **6**, 339-346. <http://dx.doi.org/10.1038/ngeo1797>
- 33 Pan, Z., X. Liu, S. Kumar, Z. Gao, and J. Kinter, 2013: Intermodel Variability and Mechanism
34 Attribution of Central and Southeastern U.S. Anomalous Cooling in the Twentieth Century

- as Simulated by CMIP5 Models. *Journal of Climate*, **26**, 6215-6237.
<http://dx.doi.org/doi:10.1175/JCLI-D-12-00559.1>
<http://journals.ametsoc.org/doi/abs/10.1175/JCLI-D-12-00559.1>
- Peterson, T.C., R.R. Heim, R. Hirsch, D.P. Kaiser, H. Brooks, N.S. Diffenbaugh, R.M. Dole, J.P. Giovannettone, K. Guirguis, T.R. Karl, R.W. Katz, K. Kunkel, D. Lettenmaier, G.J. McCabe, C.J. Paciorek, K.R. Ryberg, S. Schubert, V.B.S. Silva, B.C. Stewart, A.V. Vecchia, G. Villarini, R.S. Vose, J. Walsh, M. Wehner, D. Wolock, K. Wolter, C.A. Woodhouse, and D. Wuebbles, 2013: Monitoring and understanding changes in heat waves, cold waves, floods and droughts in the United States: State of knowledge. *Bulletin of the American Meteorological Society*, **94**, 821-834. <http://dx.doi.org/10.1175/BAMS-D-12-00066.1>
- Pierce, D.W., T.P. Barnett, B.D. Santer, and P.J. Gleckler, 2009: Selecting global climate models for regional climate change studies. *Proceedings of the National Academy of Sciences*, **106**, 8441-8446. <http://dx.doi.org/10.1073/pnas.0900094106>
- Po-Chedley, S., T.J. Thorsen, and Q. Fu, 2015: Removing diurnal cycle contamination in satellite-derived tropospheric temperatures: Understanding tropical tropospheric trend discrepancies. *Journal of Climate*, **28**, 2274-2290. <http://dx.doi.org/10.1175/JCLI-D-13-00767.1>
- Rupp, D.E., P.W. Mote, N. Massey, C.J. Rye, R. Jones, and M.R. Allen, 2012: Did human influence on climate make the 2011 Texas drought more probable? [in Explaining extreme events of 2011 from a climate perspective]. *Bulletin of the American Meteorological Society*, **93**, 1052-1054. <http://dx.doi.org/10.1175/BAMS-D-12-00021.1>
- Russo, S., A. Dosio, R.G. Graversen, J. Sillmann, H. Carrao, M.B. Dunbar, A. Singleton, P. Montagna, P. Barbola, and J.V. Vogt, 2014: Magnitude of extreme heat waves in present climate and their projection in a warming world. *Journal of Geophysical Research: Atmospheres*, **119**, 12,500-12,512. <http://dx.doi.org/10.1002/2014JD022098>
- Seager, R., M. Hoerling, D.S. Siegfried, h. Wang, B. Lyon, A. Kumar, J. Nakamura, and N. Henderson, 2014: Causes and predictability of the 2011-14 California drought. 40 pp. NOAA Drought Task Force Narrative Team. http://docs.lib.noaa.gov/noaa_documents/OAR/CPO/MAPP/california_drought_2011-2014.pdf
- Sillmann, J., V.V. Kharin, F.W. Zwiers, X. Zhang, and D. Bronaugh, 2013: Climate extremes indices in the CMIP5 multimodel ensemble: Part 2. Future climate projections. *Journal of Geophysical Research: Atmospheres*, **118**, 2473-2493. <http://dx.doi.org/10.1002/jgrd.50188>

- 1 Smith, T.T., B.F. Zaitchik, and J.M. Gohlke, 2013: Heat waves in the United States: Definitions,
2 patterns and trends. *Climatic Change*, **118**, 811-825. [http://dx.doi.org/10.1007/s10584-012-](http://dx.doi.org/10.1007/s10584-012-0659-2)
3 [0659-2](http://dx.doi.org/10.1007/s10584-012-0659-2)
- 4 Sun, L., K.E. Kunkel, L.E. Stevens, A. Buddenberg, J.G. Dobson, and D.R. Easterling, 2015:
5 Regional Surface Climate Conditions in CMIP3 and CMIP5 for the United States:
6 Differences, Similarities, and Implications for the U.S. National Climate Assessment. NOAA
7 Technical Report NESDIS 144, 111 pp. National Oceanic and Atmospheric Administration,
8 National Environmental Satellite, Data, and Information Service.
9 [http://www.nesdis.noaa.gov/technical_reports/NOAA NESDIS Technical Report 144.pdf](http://www.nesdis.noaa.gov/technical_reports/NOAA_NESDIS_Technical_Report_144.pdf)
- 10 Thorne, P.W., M.G. Donat, R.J.H. Dunn, C.N. Williams, L.V. Alexander, J. Caesar, I. Durre, I.
11 Harris, Z. Hausfather, P.D. Jones, M.J. Menne, R. Rohde, R.S. Vose, R. Davy, A.M.G.
12 Klein-Tank, J.H. Lawrimore, T.C. Peterson, and J.J. Rennie, 2016: Reassessing changes in
13 diurnal temperature range: Intercomparison and evaluation of existing global data set
14 estimates. *Journal of Geophysical Research: Atmospheres*, **121**, 5138-5158.
15 <http://dx.doi.org/10.1002/2015JD024584>
- 16 Trenary, L., T. DelSole, B. Doty, and M.K. Tippett, 2015: Was the Cold Eastern Us Winter of
17 2014 Due to Increased Variability? *Bulletin of the American Meteorological Society*, **96**,
18 S15-S19. <http://dx.doi.org/10.1175/bams-d-15-00138.1>
- 19 Trouet, V., H.F. Diaz, E.R. Wahl, A.E. Viau, R. Graham, N. Graham, and E.R. Cook, 2013: A
20 1500-year reconstruction of annual mean temperature for temperate North America on
21 decadal-to-multidecadal time scales. *Environmental Research Letters*, **8**, 024008.
22 <http://dx.doi.org/10.1088/1748-9326/8/2/024008>
- 23 Vose, R.S., S. Applequist, M. Squires, I. Durre, M.J. Menne, C.N. Williams, C. Fenimore, K.
24 Gleason, and D. Arndt, 2016: Improved historical temperature and precipitation time series
25 for Alaska climate divisions. *Journal of Applied Meteorology and Climatology* Submitted.
- 26 Vose, R.S., S. Applequist, M. Squires, I. Durre, M.J. Menne, C.N.W. Jr., C. Fenimore, K.
27 Gleason, and D. Arndt, 2014: Improved Historical Temperature and Precipitation Time
28 Series for U.S. Climate Divisions. *Journal of Applied Meteorology and Climatology*, **53**,
29 1232-1251. <http://dx.doi.org/10.1175/JAMC-D-13-0248.1>
- 30 Vose, R.S., D. Arndt, V.F. Banzon, D.R. Easterling, B. Gleason, B. Huang, E. Kearns, J.H.
31 Lawrimore, M.J. Menne, T.C. Peterson, R.W. Reynolds, T.M. Smith, C.N. Williams, and
32 D.L. Wuertz, 2012: NOAA's Merged Land-Ocean Surface Temperature Analysis. *Bulletin of*
33 *the American Meteorological Society*, **93**, 1677-1685. [http://dx.doi.org/10.1175/BAMS-D-](http://dx.doi.org/10.1175/BAMS-D-11-00241.1)
34 [11-00241.1](http://dx.doi.org/10.1175/BAMS-D-11-00241.1)

- 1 Wahl, E.R. and J.E. Smerdon, 2012: Comparative performance of paleoclimate field and index
2 reconstructions derived from climate proxies and noise-only predictors. *Geophysical*
3 *Research Letters*, **39**, L06703. <http://dx.doi.org/10.1029/2012GL051086>
- 4 Walsh, J., D. Wuebbles, K. Hayhoe, J. Kossin, K. Kunkel, G. Stephens, P. Thorne, R. Vose, M.
5 Wehner, J. Willis, D. Anderson, S. Doney, R. Feely, P. Hennon, V. Kharin, T. Knutson, F.
6 Landerer, T. Lenton, J. Kennedy, and R. Somerville, 2014: Ch. 2: Our changing climate.
7 *Climate Change Impacts in the United States: The Third National Climate Assessment*.
8 Melillo, J.M., T.C. Richmond, and G.W. Yohe, Eds. U.S. Global Change Research Program,
9 Washington, D.C., 19-67. <http://dx.doi.org/10.7930/J0KW5CXT>
- 10 Wolter, K., J.K. Eischeid, X.-W. Quan, T.N. Chase, M. Hoerling, R.M. Dole, G.J.V.
11 Oldenborgh, and J.E. Walsh, 2015: How Unusual was the Cold Winter of 2013/14 in the
12 Upper Midwest? *Bulletin of the American Meteorological Society*, **96**, S10-S14.
13 <http://dx.doi.org/10.1175/bams-d-15-00126.1>
- 14 Wuebbles, D., G. Meehl, K. Hayhoe, T.R. Karl, K. Kunkel, B. Santer, M. Wehner, B. Colle,
15 E.M. Fischer, R. Fu, A. Goodman, E. Janssen, V. Kharin, H. Lee, W. Li, L.N. Long, S.C.
16 Olsen, Z. Pan, A. Seth, J. Sheffield, and L. Sun, 2014: CMIP5 Climate Model Analyses:
17 Climate Extremes in the United States. *Bulletin of the American Meteorological Society*, **95**,
18 571-583. <http://dx.doi.org/10.1175/BAMS-D-12-00172.1>
- 19 Xu, L., H. Guo, C.M. Boyd, M. Klein, A. Bougiatioti, K.M. Cerully, J.R. Hite, G. Isaacman-
20 VanWertz, N.M. Kreisberg, C. Knote, K. Olson, A. Koss, A.H. Goldstein, S.V. Hering, J. de
21 Gouw, K. Baumann, S.-H. Lee, A. Nenes, R.J. Weber, and N.L. Ng, 2015: Effects of
22 anthropogenic emissions on aerosol formation from isoprene and monoterpenes in the
23 southeastern United States. *Proceedings of the National Academy of Sciences*, **112**, 37-42.
24 <http://dx.doi.org/10.1073/pnas.1417609112> <http://www.pnas.org/content/112/1/37.abstract>
- 25 Yu, S., K. Alapaty, R. Mathur, J. Pleim, Y. Zhang, C. Nolte, B. Eder, K. Foley, and T.
26 Nagashima, 2014: Attribution of the United States “warming hole”: Aerosol indirect effect
27 and precipitable water vapor. *Scientific Reports*, **4**, 6929. <http://dx.doi.org/10.1038/srep06929>
- 28 Zhang, X., L. Alexander, G.C. Hegerl, P. Jones, A.K. Tank, T.C. Peterson, B. Trewin, and F.W.
29 Zwiers, 2011: Indices for monitoring changes in extremes based on daily temperature and
30 precipitation data. *Wiley Interdisciplinary Reviews: Climate Change*, **2**, 851-870.
31 <http://dx.doi.org/10.1002/wcc.147>
- 32 Zou, C.-Z. and J. Li, 2014: NOAA MSU Mean Layer Temperature. 35 pp.
33 NOAA/NESDIS/STAR.
34 http://www.star.nesdis.noaa.gov/smcd/emb/mscat/documents/MSU_TCDR_CATBD_Zou_Li
35 .pdf

- 1 Zwiers, F.W., X.B. Zhang, and Y. Feng, 2011: Anthropogenic Influence on Long Return Period
- 2 Daily Temperature Extremes at Regional Scales. *Journal of Climate*, **24**, 881-892.
- 3 <http://dx.doi.org/10.1175/2010jcli3908.1>

DRAFT

7. Precipitation Change in the United States

KEY FINDINGS

1. There are sizeable regional and seasonal differences in precipitation changes since 1901. Annual precipitation has decreased in much of the West, Southwest and Southeast, and increased in most of the Northern and Southern Plains, Midwest and Northeast. A national average increase of 4% in annual precipitation since 1901 is mostly a result of large increases in the fall season. (*Medium confidence*)
2. Heavy precipitation events across the United States have increased in both intensity and frequency since 1901. There are important regional differences in trends, with the largest increases occurring in the northeastern United States. (*High confidence*)
3. The frequency and intensity of heavy precipitation events are projected to continue to increase over the 21st century (*high confidence*). However, there are regional and seasonal differences in projected changes in total precipitation with the northern United States, including Alaska getting wetter in the winter and spring, and parts of the southwest United States getting drier in the winter and spring (*medium confidence*).
4. Northern Hemisphere spring snow cover extent, North America maximum snow depth, and extreme snowfall years in the southern and western United States. have all declined while extreme snowfall years in parts of the northern United States. have increased (*medium confidence*). Projections indicate large declines in snowpack in the western United States and shifts to more precipitation falling as rain than snow in the cold season in many parts of the central and eastern United States (*high confidence*).

Introduction

Changes in precipitation are one of the most important potential outcomes of a warming world, because precipitation is integral to the very nature of society and ecosystems. These systems have developed and adapted to the past envelope of precipitation variations. Any large changes beyond the historical envelope may have profound societal and ecological impacts.

Historical variations in precipitation, as observed from both instrumental and proxy records, establish the context around which future projected changes can be interpreted because it is within that context that systems have evolved. Long-term station observations from core climate networks serve as a primary source to establish observed changes in both means and extremes. Proxy records, which are used to reconstruct past climate conditions, are varied and include sources such as tree ring and ice core data. Projected changes are examined using the Coupled Model Intercomparison Project Phase 5 (CMIP5) suite of model simulations. They establish the likelihood of distinct regional and seasonal patterns of change.

7.1 Historical Changes

7.1.1 Mean Changes

Annual precipitation averaged across the United States has increased approximately 4% over the 1901–2015 period, slightly less than the 5% increase reported in the Third National Climate Assessment (NCA3) over the 1901–2012 period (Walsh et al. 2014). This slight decrease appears to be the result of the recent lingering droughts in the western and southwestern United States (NOAA 2016a; Barnston and Lyon 2016). The current meteorological drought in California began in late 2011 (Seager et al. 2015; NOAA 2016b). Further, there continue to be important regional and seasonal differences in precipitation changes (Figure 7.1). Seasonally, national increases are largest in the fall, while little change is observed for winter. Regional differences are apparent, as the Northeast, Midwest, and Great Plains have had increases while parts of the Southwest and Southeast have had decreases. The year 2015 was the third wettest on record, just behind 1973 and 1983 (all of which were years marked by El Niño events). Interannual variability is substantial, as evidenced by large multiyear meteorological and agricultural droughts in the 1930s and 1950s.

[INSERT FIGURE 7.1 HERE:]

Figure 7.1: Annual and seasonal changes in precipitation over the contiguous United States. Changes are the average for present-day (1986–2015) minus the average for the first half of the last century (1901–1960 for the contiguous United States, 1925–1960 for Alaska and Hawaii) divided by the average for the first half of the century. (Figure source: Panel 1: adapted from Peterson et al. 2013, © American Meteorological Society. Used with permission; Panels 2–5: NOAA NCEI, data source: nCLIMDiv)].

Trends differ markedly across the seasons, as do regional patterns of increases and decreases. Fall exhibits the largest (10%) and most widespread increase, exceeding 15% in much of the Northern Great Plains, Southeast, and Northeast. Winter has the smallest increase (2%), with drying over most of the western United States as well as parts of the Southeast. Spring and summer have comparable increases (about 3.5%) but substantially different patterns. In spring, the northern half of the contiguous United States has become wetter and the southern half has become drier. In summer, there is a mixture of increases and decreases across the Nation. Alaska shows little change in annual precipitation (+1.5%), however in all seasons central Alaska shows declines, and the panhandle shows increases. Hawai‘i shows a decline of more than 15% in annual precipitation.

7.1.2 Snow

Changes in snow cover extent (SCE) in the Northern Hemisphere exhibit a strong seasonal dependence. There has been little change since the 1960s (when the first satellite records became available) in the winter, while fall SCE has increased. However, spring SCE has declined, due in

part to higher temperatures that shorten the time snow spends on the ground in the spring. This tendency is highlighted by the recent occurrences of both unusually high and unusually low monthly (October–June) SCE values, including top 5 highest and top 5 lowest values in the 48 years of data. From 2010 onward, 7 of the 45 highest monthly SCE values occurred, all in the fall or winter (mostly in November and December), while 9 of the 10 lowest May and June values occurred. This reflects the trend toward earlier spring snowmelt, particularly at high latitudes, while little trend is noted in extreme fall SCE (Kunkel et al. 2016). The seasonal maximum snow depth has decreased and shifted to an earlier date over North America since 1951 (Kunkel et al. 2016). There has been a decrease in the frequency of large snowfall years (years exceeding the 90th percentile) in the southern United States and the U.S. Pacific Northwest and an increase in the frequency of large snowfall years in the northern United States (Kluver and Leathers 2015). In the snow belts of the Great Lakes, lake effect snowfall has increased overall since the early 20th Century for Lakes Superior, Michigan-Huron, and Erie (Kunkel et al. 2010). However, individual studies for Lakes Michigan (Bard and Kristovich 2012) and Ontario (Harnett et al. 2014) indicate that this increase has not been continuous. In both cases, upward trends were observed till the 1970s/early 1980s. However, since then lake effect snowfall has decreased in these regions.

7.1.3 Observed changes in U.S. seasonal extreme precipitation.

Extreme precipitation events occur when the air is nearly completely saturated. Hence, extreme precipitation events are generally observed to increase in intensity by about 6% to 7% for each degree Celsius of temperature increase, as dictated by the Clausius-Clapeyron relation. Figure 7.2 shows the observed change in the 20-year return value of the seasonal maximum 5-day precipitation totals (rx5day) over the period 1948 to 2015. A mix of increases and decreases in individual weather stations is observed. However, well over two-thirds of the stations exhibit statistically significant increases, consistent with theoretical expectations and the observed changes in atmospheric moisture content.

[INSERT FIGURE 7.2 HERE:]

Figure 7.2: Observed changes in the 20-year return value of the seasonal daily precipitation totals over the period 1948 to 2015 using data from the Global Historical Climatology Network (GHCN) dataset. (Figure source: adapted from Kunkel et al. 2013; © American Meteorological Society. Used with permission.)]

Another metric of extreme precipitation, the annual maximum daily precipitation total, was calculated for the period 1901–2015. Those events exceeding a 5-year return value (essentially the top 20% of all annual maximum values) were averaged for 1986–2015 and 1901–1960. The difference between these two periods (Figure 7.3) indicates substantial increases over the eastern United States, particularly the northeast United States. The increases are much smaller over the western United States, with the southwest and northwest United States showing little increase.

[INSERT FIGURE 7.3 HERE:]

Figure 7.3: Percentage difference between 1901–1960 average and 1981–2015 average of top 20% (events exceeding the threshold for a 5-year return period) of annual maximum daily precipitation values in each period using 930 U.S. stations from the Global Historical Climatology Network (GHCN). The percentages are first calculated for individual stations, then averaged over 2° latitude by 2° longitude grid boxes, and finally averaged over each NCA4 region. (Figure source: CICS-NC / NOAA NCEI)]

Figure 7.4 shows an update of a U.S. index of extreme precipitation from NCA3. This is the number of 2-day precipitation events exceeding the threshold for a 5-year recurrence, calculated over the period of 1896–2015. The number of events has been well above average for the last three decades. The slight drop from 2006–2010 to 2011–2015 reflects a below average number during the widespread severe meteorological drought year of 2012, while the other years in this pentad were well above average. The index value for 2015 was 80% above the 1901–1960 reference period average and the third highest value in the 120 years of record (after 1998 and 2008).

[INSERT FIGURE 7.4 HERE:]

Figure 7.4: Index of the number of 2-day precipitation events exceeding the station-specific threshold for a 5-year recurrence interval. The annual values are averaged over 5-year periods, with the pentad label indicating the ending year of the period. Annual time series of the number of events are first calculated at individual stations. Next, the grid box time series are calculated as the average of all stations in the grid box. Finally, a national time series is calculated as the average of the grid box time series. Data source: GHCN-Daily. (Figure source: CICS-NC / NOAA NCEI)]

7.1.4 Extratropical Cyclones and Precipitation

A large percentage of the extreme precipitation events in the United States are caused by extratropical cyclones (ETCs) and their associated fronts (Kunkel et al. 2012). In the northern United States, this is the case even in the summer when a sizeable fraction of extreme events occurs. The number of strong ETCs over North America in the summer has decreased since 1979 by more than 35% (Chang et al. 2016), and overall ETC activity has decreased over this same time period. Most climate models simulate little change over this same historical period, but they project a decrease in summer ETC activity during the remainder of the 21st century (Chang et al. 2016). This suggests that in the future there may be fewer opportunities in the summer for extreme precipitation, although increases in water vapor are likely to overcompensate for any decreases in ETCs by increasing the likelihood that an ETC will produce excessive rainfall amounts. An idealized set of climate simulations (Pfahl et al. 2015) suggests that substantial projected warming will lead to a decrease in the number of ETCs but an increase in the intensity of the strongest ETCs. Thus, the most extreme precipitation events associated with ETCs may be even greater in the future.

7.1.5 Detection and Attribution

TRENDS

Detectability of trends (compared to internal variability) for a number of precipitation metrics over the continental United States has been examined, however, trends identified for the United States regions have not been clearly attributed to anthropogenic forcing (Anderson et al. 2015; Easterling et al. 2016). One study concluded that increasing precipitation trends in some north-central U.S. regions and the extreme annual anomalies there in 2013 were at least partly attributable to the combination of anthropogenic and natural forcing (Knutson et al. 2014).

At the global scale there is *medium confidence* that anthropogenic forcing has contributed to global-scale intensification of heavy precipitation over land regions with sufficient data coverage (Bindoff et al. 2013). Global changes in extreme precipitation have been attributed to anthropogenically forced climate change (Min et al. 2011, 2013), including annual maximum 1-day and 5-day accumulated precipitation over northern hemisphere land regions and (relevant to this report) over the North American continent (Zhang et al. 2013). Although the United States was not separately assessed, the parts of North America with sufficient data for their analysis included the continental United States, and parts of southern Canada, Mexico and Central America. Since the covered region was, predominantly over the United States, their detection/attribution findings are applicable to the continental United States.

Analyses of precipitation extreme changes over the U.S. by region (20-year return values of seasonal daily precipitation over 1948–2015, Figure 7.2) show statistically significant increases consistent with theoretical expectations and previous analyses (Westra et al. 2013). Further, a significant increase in the area affected by precipitation extremes over North America has also been detected (Dittus et al. 2015). Extreme rainfall from U.S. landfalling tropical cyclones has been higher in recent years (1994–2008) than the long-term historical average, even accounting for temporal changes in storm frequency (Kunkel et al. 2010).

Based on current evidence it is concluded that detectable but not attributable increases in mean precipitation have occurred over parts of the central United States. Formal detection-attribution studies indicate a human contribution to extreme precipitation increases over the continental United States, but confidence is *low* based on those studies alone due to the short observational period, high natural variability, and model uncertainty.

In summary, based on available studies, it is concluded that for the continental United States there is *high confidence* in the detection of extreme precipitation increases, while there is *low confidence* in attributing the extreme precipitation changes purely to anthropogenic forcing. There is stronger evidence for a human contribution (*medium confidence*) when taking into account process-based understanding (increased water vapor in a warmer atmosphere), evidence from weather and climate models, and trends in other parts of the world.

EVENT ATTRIBUTION

A number of recent heavy precipitation events have been examined to determine the degree to which their occurrence and severity can be attributed to human-induced climate change. Table 7.1 summarizes available attribution statements for recent extreme U.S. precipitation events. Seasonal and annual precipitation extremes occurring in the north-central and eastern U.S. regions in 2013 were examined for evidence of an anthropogenic influence on their occurrence (Knutson et al. 2014). Increasing trends in annual precipitation were detected in the northern tier of states, March–May precipitation in the upper Midwest, and June–August precipitation in the eastern United States since 1900. These trends are attributed to some kind of external forcing (anthropogenic + natural) but could not be directly attributed to anthropogenic forcing alone. However, based on this analysis it is concluded that the probability of these kinds of extremes has been made more likely by anthropogenic forcing.

The human influence on individual storms has been investigated with conflicting results. In particular, Hoerling et al. (2014) find that despite the expected human-induced increase in available moisture, the GEOS-5 model produces fewer extreme storms in Colorado during the fall season and attribute that behavior to changes in the large-scale circulation. However, Pall et al. (2016) find that such coarse models cannot produce the observed magnitude of precipitation due to resolution constraints. Based on a highly conditional set of hindcast simulations imposing the large-scale meteorology and a substantial increase in both the probability and magnitude of the observed precipitation accumulation magnitudes in that particular meteorological situation, their study could not address the question of whether such situations have become more or less probable. Extreme precipitation event attribution is inherently limited by the rarity of the necessary meteorological conditions and the limited number of model simulations that can be performed to examine rare events. This remains an open and active area of research. However, based on these two studies, the anthropogenic contribution to the 2013 Colorado heavy rainfall-flood event is unclear.

[INSERT TABLE 7.1 HERE:]

Table 7.1: A list of U.S. extreme precipitation events for which attribution statements have been made. In the last column, “+” indicates that an attributable human-induced increase in frequency and/or magnitude was found, “-“ indicates that an attributable human-induced decrease in frequency and/or magnitude was found, “0” indicates no attributable human contribution was identified. As in tables 6.1 and 8.2, several of the events were originally examined in the Bulletin of the American Meteorological Society’s (BAMS) State of the Climate Reports and reexamined by Angelil et al. (2016). In these cases, both attribution statements are listed with the original authors first. Source: M. Wehner.]

7.2 Projections

Changes in precipitation in a warmer climate are governed by many factors. Although energy constraints can be used to understand global changes in precipitation, projecting regional changes is much more difficult because of uncertainty in projecting changes in the large-scale circulation that plays important roles in the formation of clouds and precipitation (Shepherd 2014). For the contiguous United States (CONUS), future changes in seasonal average precipitation will include a mix of increases, decreases, or little change, depending on location and season (Figure 7.6). High-latitude regions are generally projected to become wetter while the subtropical zone is projected to become drier. As the CONUS lies between these two regions, there is significant uncertainty about the sign and magnitude of future anthropogenic changes to seasonal precipitation in much of the region, particularly in the middle latitudes of the nation. However, because the physical mechanisms controlling extreme precipitation differ from those controlling seasonal average precipitation (Section 7.1.4), in particular atmospheric water vapor will increase with increasing temperatures, confidence is *high* that projected future precipitation extremes will increase in frequency and intensity throughout the CONUS.

Global climate models used to project precipitation changes exhibit varying degrees of fidelity in capturing the observed climatology and seasonal variations of precipitation across the United States. Global or regional climate models with higher horizontal resolution generally achieve better skill than the CMIP5 models in capturing the spatial patterns and magnitude of winter precipitation in the western and southeastern United States (e.g., Mearns et al. 2012; Wehner 2013; Bacmeister et al. 2014; Wehner et al. 2014), leading to improved simulations of snowpack and runoff (e.g., Rauscher et al. 2008; Rasmussen et al. 2011). Simulation of present and future summer precipitation remains a significant challenge, as current convective parameterizations fail to properly represent the statistics of mesoscale convective systems (Klein et al. 2012). As a result, high-resolution models that still require the parameterization of deep convection exhibit mixed results (Wehner et al. 2014; Sakaguchi et al. 2015). Advances in computing technology are beginning to enable regional climate modeling at the higher resolutions (1–4 km), permitting the direct simulation of convective clouds systems (e.g., Ban et al. 2014) and eliminating the need for this class of parameterization. However, projections from such models are not yet ready for inclusion in this report.

Important progress has been made by the climate modeling community in providing multimodel ensembles such as CMIP5 (Taylor et al. 2012) and NARCCAP (Mearns et al. 2012) to characterize projection uncertainty arising from model differences, and large ensemble simulations such as CESM-LE (Kay et al. 2015) to characterize uncertainty inherent in the climate system due to internal variability.

Projections in this report from the CMIP5 climate model database is based both on model independence and a multivariate measure of skill over North America as described in section 4.4.2. The model skill metrics in simulating seasonal average and extreme precipitation are

shown in figure 7.5. The extreme precipitation index is the seasonal maximum pentad total, defined as *rx5day* in the Expert Team on Climate Change Detection Indices (see climindex.org).

[INSERT FIGURE 7.5 HERE:]

Figure 7.5: Relative performance of the CMIP5 models used in this study in simulating observed North American precipitation indices. Performance in simulating seasonal maxima pentad precipitation is shown in the top four rows. The next four rows show performance in replicating seasonal average precipitation (winter, spring, summer, fall). The bottom row is a combination of all eight precipitation performance metrics. Models are ordered from left (best) to right (worst) as determined by this combined metric. (Figure source: adapted from Sanderson et al., 2016)

7.2.1 Future Changes in U.S. Seasonal Mean Precipitation.

In the United States, projected changes in seasonal mean precipitation span the range from profound decreases to profound increases. And in many regions and seasons, projected changes in precipitation are not large compared to natural variations. The general pattern of change is clear and consistent with theoretical expectations. Figure 7.6 shows the weighted CMIP5 multi-model average seasonal change at the end of the century compared to the present under the RCP8.5 scenario (see Ch. 4: Projections for discussion of RCPs). In this figure, changes projected with high confidence to be larger than natural variations are stippled. Regions where future changes are projected with high confidence to be smaller than natural variations are hashed. In winter and spring, the northern part of the country is projected to become wetter as the global climate warms. In the early to middle parts of this century, this will likely be manifested as increases in snowfall (O’Gorman 2014). Later on, as temperature continues to increase, it will be too warm to snow in many current snow-producing situations, and precipitation will mostly be rainfall. In the southwestern United States, precipitation will decrease in the spring but the changes are only a little larger than natural variations. Many other regions of the country will not experience significant changes in average precipitation. This is also the case over most of the country in the summer and fall.

[INSERT FIGURE 7.6 HERE:]

Figure 7.6: CMIP5 weighted multi-model seasonal average precipitation percent change in the 2070–2100 period relative to the 1976–2005 average under the RCP8.5 pathway. Stippling indicates that changes are assessed to be large compared to natural variations. Hashing indicates that changes are assessed to be small compared to natural variations. Blank regions (if any) are where projections are assessed to be inconclusive. Data source: World Climate Research Program's (WCRP's) Coupled Model Intercomparison Project. (Figure source: NOAA NCEI)].

This pattern of projected precipitation change arises because of changes in locally available water vapor and weather system shifts. In the northern part of the continent, increases in water vapor, together with changes in circulation that are the result of expansion of the Hadley cell,

bring more moisture to these latitudes while maintaining or increasing the frequency of precipitation-producing weather systems. This change in the Hadley circulation also causes the subtropics to be drier in warmer climates as well as moving the mean storm track northward and away from the subtropics, decreasing the frequency of precipitation-producing systems. The combination of these two factors results in precipitation decreases in the southwestern United States, Mexico, and the Caribbean (Collins et al. 2013).

PROJECTED CHANGES IN SNOW

The Third National Climate Assessment (Georgakakos et al. 2014) projected reductions in annual snowpack of up to 40% in the western United States based on the SRES A2 emissions scenario in the CMIP3 suite of climate model projections. Recent research using the CMIP5 suite of climate model projections forced with the RCP8.5 scenario and statistically downscaled for the western United States continues to show the expected declines in various snow metrics, including snow water equivalent, the number of extreme snowfall events, and number of snowfall days (Lute et al. 2015). A northward shift in the rain–snow transition zone in the central and eastern United States was found using statistically downscaled CMIP5 simulations forced with RCP8.5. By the end of the 21st century, large areas that are currently snow-dominated in the cold season are expected to be rainfall dominated (Ning and Bradley 2015).

7.2.2 Extremes

HEAVY PRECIPITATION EVENTS

Studies project that the observed increase in heavy precipitation events will continue in the future (e.g. Janssen et al. 2014, 2016). Similar to observed changes, increases are expected in all regions, even those regions where total precipitation is projected to decline, such as the southwestern United States. Under the RCP8.5 scenario the number of extreme events (exceeding a 5-year return period) increases by 2 to 3 times the historical average in every region (Figure 7.7) by the end of the 21st century, with the largest increases in the Northeast. Under the RCP4.5 scenario, increases are 50%–100%. Research shows that there is strong evidence, both from the observed record and modeling studies, that increased water vapor resulting from higher temperatures is the primary cause of the increases (Kunkel et al. 2013a,b; Wehner 2013). However, additional effects on extreme precipitation due to changes in dynamical processes are poorly understood.

[INSERT FIGURE 7.7 HERE:]

Figure 7.7. Regional extreme precipitation event frequency for RCP4.5 (green) and RCP8.5 (blue) for a 2-day duration and 5-year return. Calculated for 2006–2100 but decadal anomalies begin in 2011. Error bars are ± 1 standard deviation. (Figure source: Janssen et al. 2014)]

Projections of changes in the 20-year return period amount for daily precipitation (Figure 7.8) using LOCA downscaled data also show large percentage increases for both the middle and late

21st century. The lower emissions projections (RCP4.5) show increases of around 10% for mid-century, and up to 14% for the late century projections. The higher emissions projections show even large increases for both mid-century and the late century projections. No region in either emissions scenario shows a decline in heavy precipitation.

[INSERT FIGURE 7.8 HERE:]

Figure 7.8: Projected change in the 20-year return period amount for daily precipitation for mid- and late-21st century for RCP4.5 and RCP8.5 emissions scenarios using LOCA downscaled data.

Figure source: CICS-NC / NOAA NCEI]

HURRICANE PRECIPITATION

For precipitation from hurricanes, several studies have projected increases of precipitation rates over ocean regions (Knutson et al. 2010), including for the Atlantic basin in particular (Knutson et al. 2013). The primary physical mechanism for this increase is the enhanced water vapor content in the warmer atmosphere, which enhances moisture convergence into the storm for a given circulation strength, although a more intense circulation can also contribute (Wang et al. 2015). In a set of idealized forcing experiments, this effect was partly offset by differences in warming rates at the surface and at altitude (Villarini et al. 2014). Regional model projections of precipitation from landfalling tropical cyclones over the United States, based on downscaling of CM3 and CMIP5 model climate changes, suggest that the 21st century CMIP5-based projected occurrence frequency of post-landfall tropical cyclones over the United States showed little change compared to present day, as the reduced frequency of tropical cyclones over the Atlantic domain was mostly offset by a greater landfalling fraction. CM3-based projections showed a reduced occurrence frequency over U.S. land. The average tropical cyclone rainfall rates within 500 km (about 311 miles) of the storm center increased by 8% to 17% in the simulations, which was at least as much as expected from the water vapor content increase factor alone.

TRACEABLE ACCOUNTS

Key Message 1

There are sizeable regional and seasonal differences in precipitation changes since 1901. Annual precipitation has decreased in much of the West, Southwest and Southeast, and increased in most of the Northern and Southern Plains, Midwest and Northeast. A national average increase of 4% in annual precipitation since 1901 is mostly a result of large increases in the fall season. (*Medium confidence*)

Description of evidence base

The key message and supporting text summarizes extensive evidence documented in the climate science peer-reviewed literature. Evidence of long-term changes in precipitation is based on analysis of daily precipitation observations from the U.S. Cooperative Observer Network (<http://www.nws.noaa.gov/om/coop/>) and shown in Figure 7.1. Published work (refs) and Figure 7.1 show important regional and seasonal differences in U.S. precipitation change since 1901.

New Information and remaining uncertainties

The main key issues that relates to uncertainty is the sensitivity of observed precipitation trends to the spatial distribution of observing stations, and to historical changes in station location, rain gauges, and observing practices. These issues are mitigated, somewhat, by new methods to produce spatial grids (Vose et al. 2014) through time.

Assessment of confidence based on evidence

Based on the evidence and understanding of the issues leading to uncertainties, confidence is **high** that average annual precipitation has increased in the U.S. Furthermore, confidence is also **high**, that the important regional and seasonal differences in changes documented in the text and in Figure 7.1 are robust.

Key Message 2

Heavy precipitation events across the United States have increased in both intensity and frequency since 1901. There are important regional differences in trends, with the largest increases occurring in the northeastern United States. (*High confidence*)

Description of evidence base

The key message and supporting text summarizes extensive evidence documented in the climate science peer-reviewed literature. Evidence of long-term changes in precipitation is based on analysis of daily precipitation observations from the U.S. Cooperative Observer Network (<http://www.nws.noaa.gov/om/coop/>) and shown in Figures 7.2, 7.3 and 7.4.

New Information and remaining uncertainties

The main key issues that relates to uncertainty is the sensitivity of observed precipitation trends to the spatial distribution of observing stations, and to historical changes in station location, rain

gauges, and observing practices. These issues are mitigated, somewhat, by methods used to produce spatial grids through gridbox averaging.

Assessment of confidence based on evidence

Based on the evidence and understanding of the issues leading to uncertainties, confidence is **high** that heavy precipitation events have increased in the U.S. Furthermore, confidence is also **high**, that the important regional and seasonal differences in changes documented in the text and in Figures 7.2, 7.3, and 7.4 are robust.

Key Message 3

The frequency and intensity of heavy precipitation events are projected to continue to increase over the 21st century (*high confidence*). However, there are regional and seasonal differences in projected changes in total precipitation with the northern United States, including Alaska getting wetter in the winter and spring, and parts of the southwest United States getting drier in the winter and spring (*medium confidence*).

Description of evidence base

Evidence of future change in precipitation is based on climate model projections and our understanding of the climate system's response to increasing greenhouse gases and on regional mechanisms behind the projected changes.

New information and remaining uncertainties

A key issue is how well climate models simulate precipitation, which is one of the more challenging aspects of weather and climate simulation. In particular, comparisons of model projections for total precipitation (from both CMIP3 and CMIP5, see Sun et al. 2015) by NCA3 region show a spread of responses in some regions (e.g. southwest) such that they are opposite from the ensemble average response. The continental United States is positioned in the transition zone between expected drying in the sub-tropics and wetting in the mid- and higher-latitudes. There are some differences in the location of this transition between CMIP3 and CMIP5 models and thus there remains uncertainty in the exact location of the transition zone.

Assessment of confidence based on evidence

Based on evidence from climate model simulations and our fundamental understanding of the relationship of water vapor to temperature, confidence is **high** that extreme precipitation will increase in all regions of the United States. However, based on the evidence and understanding of the issues leading to uncertainties, confidence is **medium** that that more total precipitation is projected for the northern U.S. and less for the Southwest.

Key Message 4

Northern Hemisphere spring snow cover extent, North America maximum snow depth, and extreme snowfall years in the southern and western United States. have all declined while extreme snowfall years in parts of the northern United States. have increased (*medium confidence*). Projections indicate large declines in snowpack in the western United States and shifts to more precipitation falling as rain than snow in the cold season in many parts of the central and eastern United States (*high confidence*).

Description of evidence base

Evidence of historical changes in snow cover extent and reduction in extreme snowfall years is consistent with our understanding of the climate system's response to increasing greenhouse gases.

Furthermore, climate model continue to consistently show future declines in snowpack in the western United States. Recent model projections for the eastern United States also confirm a future shift from snowfall to rainfall during the cold season in colder portions of the central and eastern United States.

New Information and remaining uncertainties

The main key issues that relates to uncertainty is the sensitivity of observed snow changes to the spatial distribution of observing stations, and to historical changes in station location, rain gauges, and observing practices, particularly for snow. Another key issue is the ability of climate models to simulate precipitation, particularly snow. Future changes in the frequency and intensity of meteorological systems causing heavy snow are less certain than temperature changes.

Assessment of confidence based on evidence

Given the evidence base and uncertainties confidence is **medium**, that snow cover extent has declined in the United States and **medium** that extreme snowfall years have declined in recent years. Confidence is **high** that western United States snowpack will decline in the future, and confidence is **medium** that a shift from snow domination to rain domination will occur in the parts of the central and eastern United States cited in the text.

1 **TABLE**

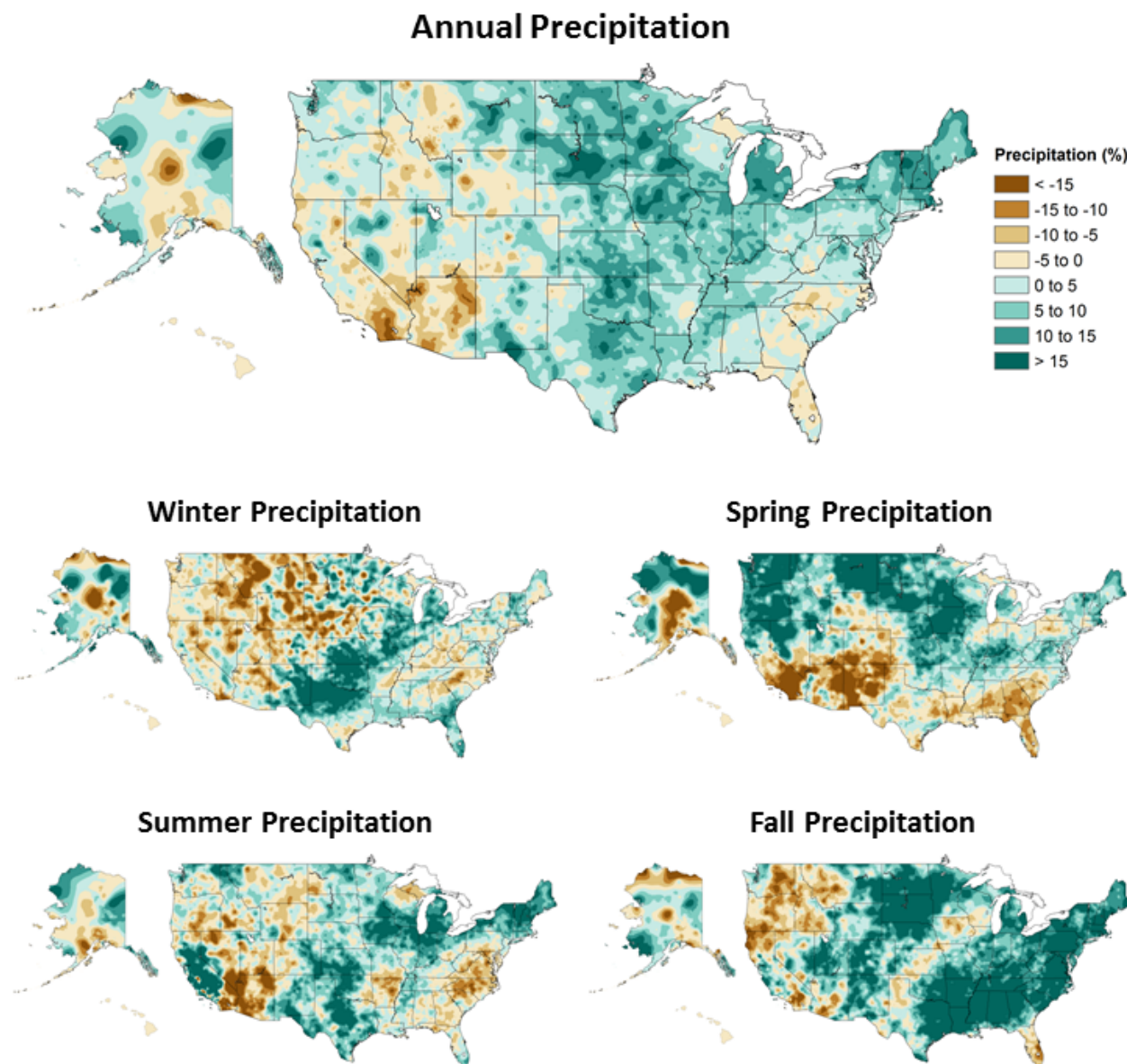
2 **Table 7.1:** A list of U.S. extreme precipitation events for which attribution statements have been
 3 made. In the last column, “+” indicates that an attributable human-induced increase in frequency
 4 and/or magnitude was found, “-“ indicates that an attributable human-induced decrease in
 5 frequency and/or magnitude was found, “0” indicates no attributable human contribution was
 6 identified. As in tables 6.2 and 8.2, several of the events were originally examined in the BAMS
 7 State of the Climate Reports and reexamined by Angelil et al. (2016) In these cases, both
 8 attribution statements are listed with the original authors first. Source: M. Wehner.

Authors	Event year and duration	region	type	Attribution statement
Knutson et al. 2014 / Angelil et al. 2016	ANN 2013	U.S. Northern Tier	Wet	+/0
Knutson et al. 2014 / Angelil et al. 2016	MAM 2013	U.S. Upper Midwest	Wet	+/+
Knutson et al. 2014 / Angelil et al. 2016	JJA 2013	Eastern U.S. Region	Wet	+/-
Edwards et al. 2014	October 4-5, 2013	South Dakota	blizzard	0
Hoerling et al. 2014	September 10-14, 2013	Colorado	Wet	0
Pall et al. 2016	September 10-14, 2013	Colorado	Wet	+

9

10

1 FIGURES



2

3 **Figure 7.1:** Annual and seasonal changes in precipitation over the contiguous United States.
 4 Changes are the average for present-day (1986-2015) minus the average for the first half of the
 5 last century (1901-1960 for the contiguous United States, 1925-1960 for Alaska and Hawaii)
 6 divided by the average for the first half of the century. (Figure source: Panel 1: adapted from
 7 Peterson et al. 2013, © American Meteorological Society. Used with permission; Panels 2-5:
 8 NOAA NCEI, data source: nCLIMDiv)

Observed Change in Daily, 20-year Return Level Precipitation

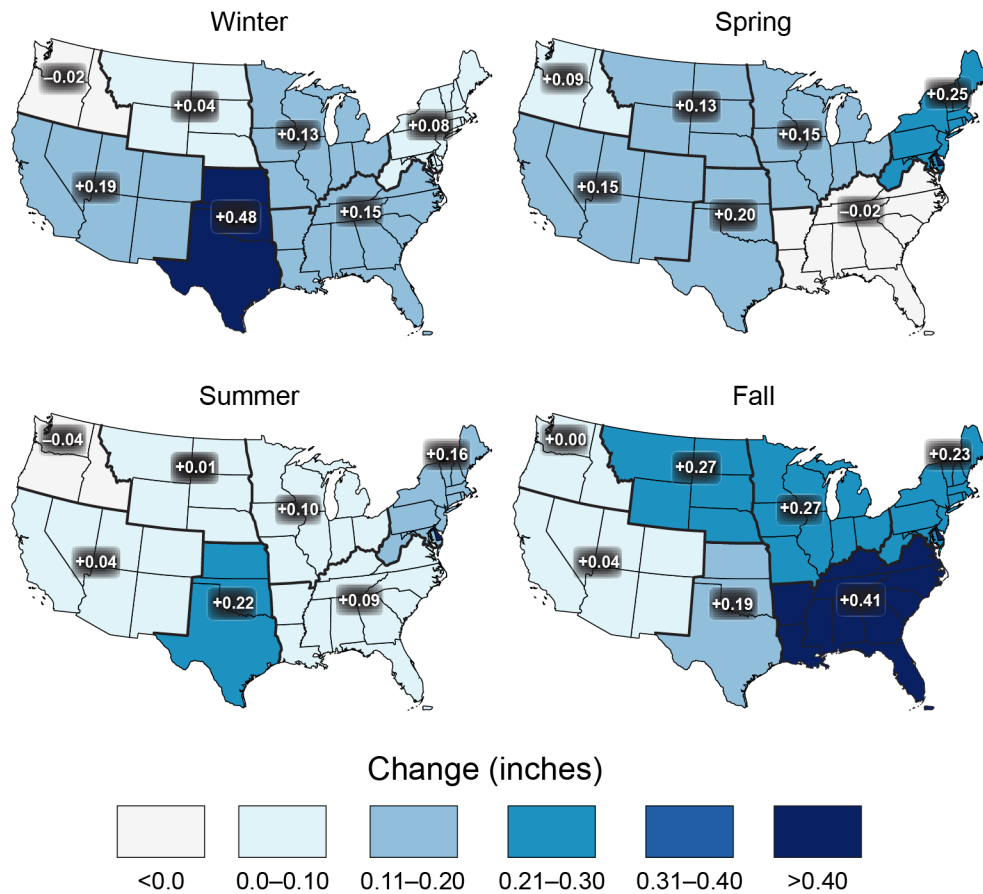


Figure 7.2: Observed changes in the 20-year return value of the seasonal daily precipitation totals over the period 1948 to 2015 using data from the Global Historical Climatology Network (GHCN) dataset. (Figure source: adapted from Kunkel et al. 2013; © American Meteorological Society. Used with permission.)

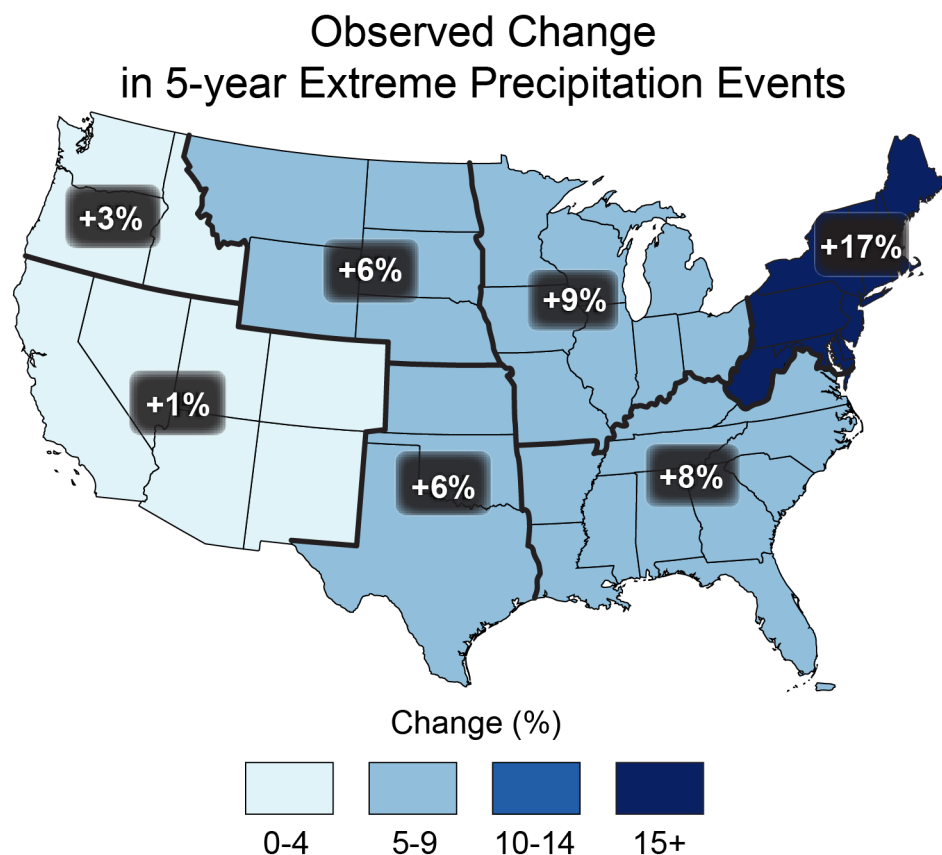


Figure 7.3: Percentage difference between 1901–1960 average and 1981–2015 average of top 20% (events exceeding the threshold for a 5-year return period) of annual maximum daily precipitation values in each period using 930 U.S. stations from the Global Historical Climatology Network (GHCN). The percentages are first calculated for individual stations, then averaged over 2° latitude by 2° longitude grid boxes, and finally averaged over each NCA4 region. (Figure source: CICS-NC / NOAA NCEI)

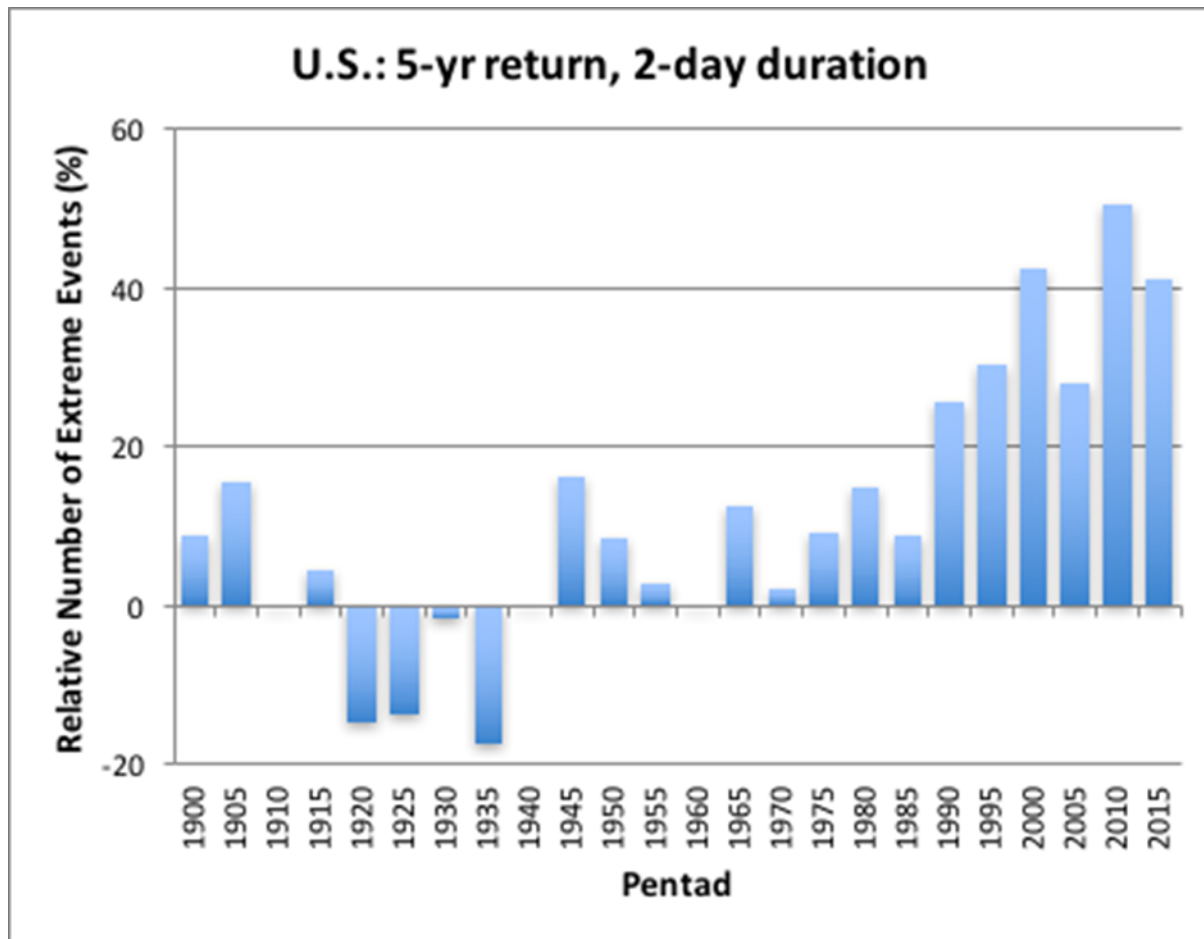


Figure 7.4: Index of the number of 2-day precipitation events exceeding the station-specific threshold for a 5-year recurrence interval. The annual values are averaged over 5-year periods, with the pentad label indicating the ending year of the period. Annual time series of the number of events are first calculated at individual stations. Next, the grid box time series are calculated as the average of all stations in the grid box. Finally, a national time series is calculated as the average of the grid box time series. Data source: GHCN-Daily. (Figure source: CICS-NC / NOAA NCEI)

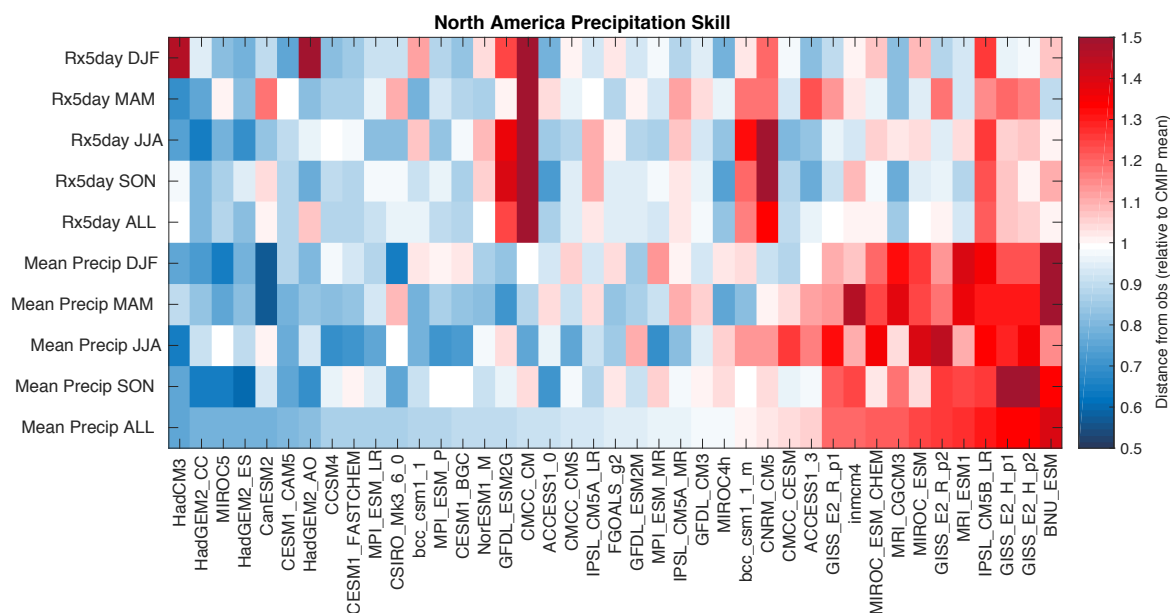


Figure 7.5: Relative performance of the CMIP5 models used in this study in simulating observed North American precipitation indices. Performance in simulating seasonal maxima pentad precipitation is shown in the top four rows. The next four rows show performance in replicating seasonal average precipitation (winter, spring, summer, fall). The bottom row is a combination of all eight precipitation performance metrics. Models are ordered from left (best) to right (worst) as determined by this combined metric. (Figure source: adapted from Sanderson et al., 2016)

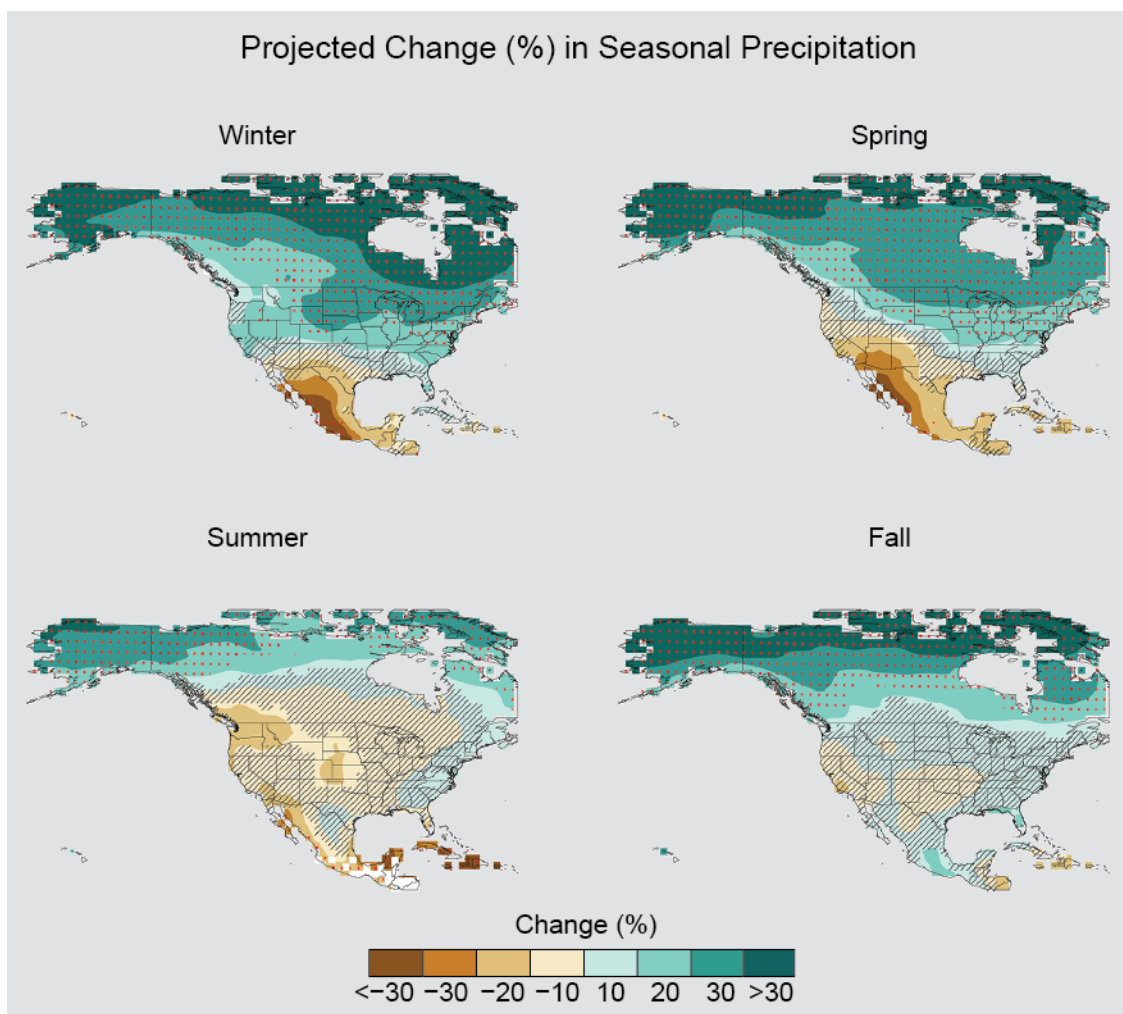


Figure 7.6: CMIP5 weighted multi-model seasonal average precipitation percent change in the 2070–2100 period relative to the 1976–2005 average under the RCP8.5 pathway. Stippling indicates that changes are assessed to be large compared to natural variations. Hashing indicates that changes are assessed to be small compared to natural variations. Blank regions (if any) are where projections are assessed to be inconclusive. Data source: World Climate Research Program's (WCRP's) Coupled Model Intercomparison Project. Figure source: NOAA NCEI.

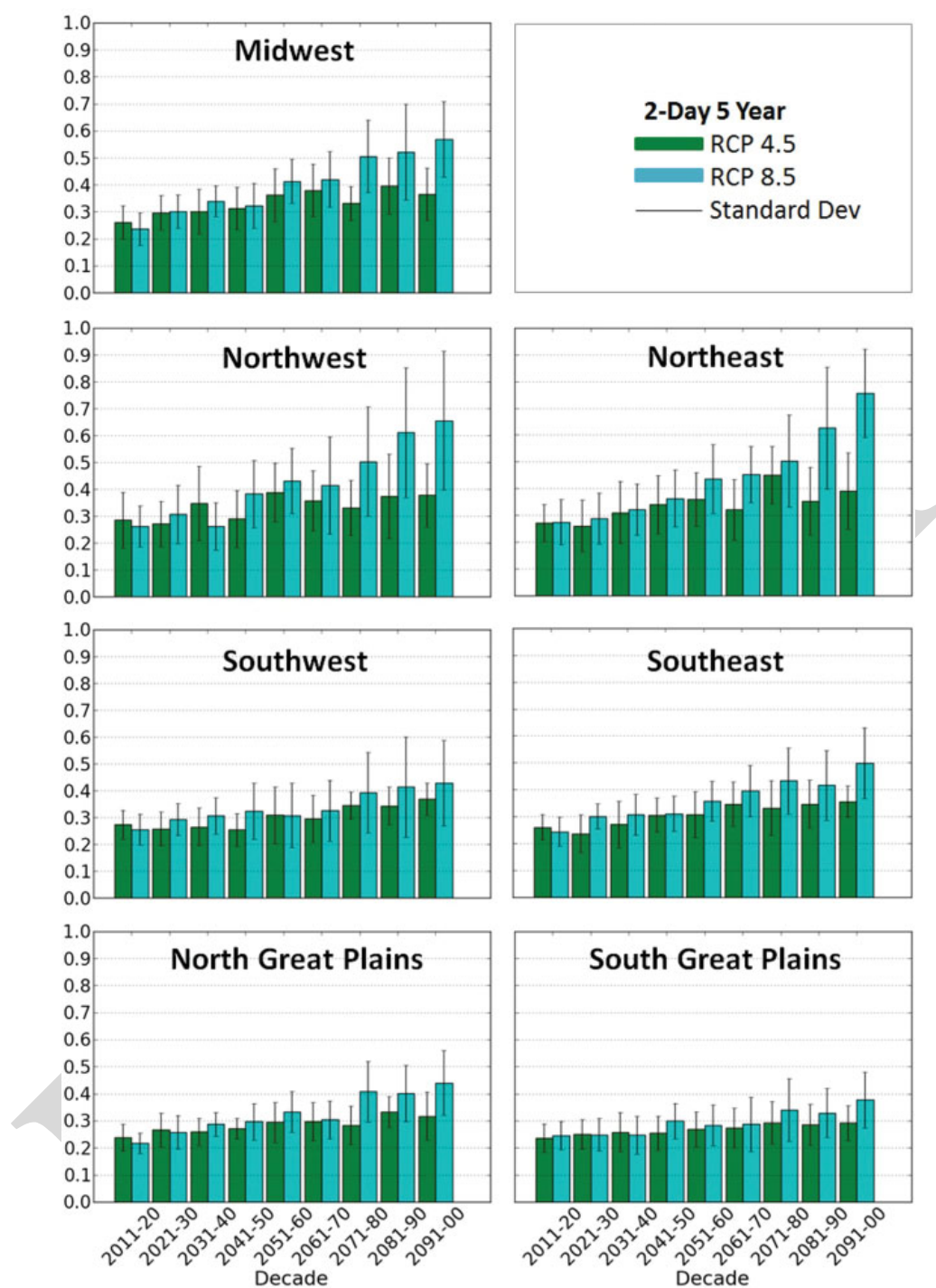
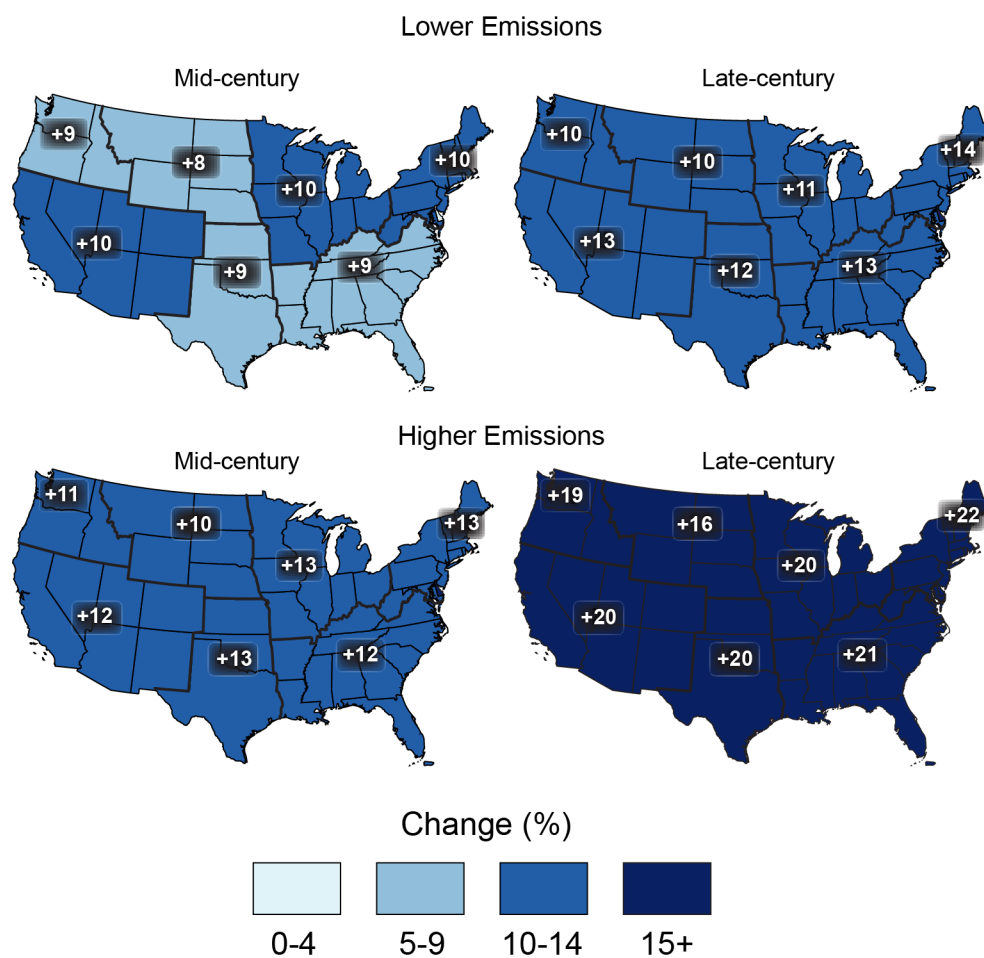


Figure 7.7: Regional extreme precipitation event frequency for RCP4.5 (green) and RCP8.5 (blue) for a 2-day duration and 5-year return. Calculated for 2006–2100 but decadal anomalies begin in 2011. Error bars are ± 1 standard deviation. (Figure source: Janssen et al. 2014)

Projected Change in Daily, 20-year Extreme Precipitation



1

2 **Figure 7.8:** Projected change in the 20-year return period amount for daily precipitation for mid-

3 and late-21st century for RCP4.5 and RCP8.5 emissions scenarios using LOCA downscaled data.

4 Figure source: CICS-NC / NOAA NCEI)

1 REFERENCES

- 2 Anderson, B.T., D.J. Gianotti, and G.D. Salvucci, 2015: Detectability of historical trends in
 3 station-based precipitation characteristics over the continental United States. *Journal of*
 4 *Geophysical Research: Atmospheres*, **120**, 4842-4859.
 5 <http://dx.doi.org/10.1002/2014JD022960>
- 6 Angélil, O., D. Stone, M. Wehner, C.J. Paciorek, H. Krishnan, and W. Collins, 2016: An
 7 independent assessment of anthropogenic attribution statements for recent extreme
 8 temperature and rainfall events. *Journal of Climate*, **in press**, null.
 9 <http://dx.doi.org/10.1175/JCLI-D-16-0077.1>
- 10 Bacmeister, J.T., M.F. Wehner, R.B. Neale, A. Gettelman, C. Hannay, P.H. Lauritzen, J.M.
 11 Caron, and J.E. Truesdale, 2014: Exploratory high-resolution climate simulations using the
 12 Community Atmosphere Model (CAM). *Journal of Climate*, **27**, 3073-3099.
 13 <http://dx.doi.org/10.1175/JCLI-D-13-00387.1>
- 14 Ban, N., J. Schmidli, and C. Schär, 2014: Evaluation of the convection-resolving regional
 15 climate modeling approach in decade-long simulations. *Journal of Geophysical Research:*
 16 *Atmospheres*, **119**, 7889-7907. <http://dx.doi.org/10.1002/2014JD021478>
- 17 Bard, L. and D.A.R. Kristovich, 2012: Trend Reversal in Lake Michigan Contribution to
 18 Snowfall. *Journal of Applied Meteorology and Climatology*, **51**, 2038-2046.
 19 <http://dx.doi.org/10.1175/jamc-d-12-064.1>
 20 <http://journals.ametsoc.org/doi/abs/10.1175/JAMC-D-12-064.1>
- 21 Barnston, A.G. and B. Lyon, 2016: Does the NMME Capture a Recent Decadal Shift toward
 22 Increasing Drought Occurrence in the Southwestern United States? *Journal of Climate*, **29**,
 23 561-581. <http://dx.doi.org/10.1175/JCLI-D-15-0311.1>
- 24 Bindoff, N.L., P.A. Stott, K.M. AchutaRao, M.R. Allen, N. Gillett, D. Gutzler, K. Hansingo, G.
 25 Hegerl, Y. Hu, S. Jain, I.I. Mokhov, J. Overland, J. Perlwitz, R. Sebbari, and X. Zhang, 2013:
 26 Detection and Attribution of Climate Change: from Global to Regional. *Climate Change*
 27 *2013: The Physical Science Basis. Contribution of Working Group I to the Fifth Assessment*
 28 *Report of the Intergovernmental Panel on Climate Change*. Stocker, T.F., D. Qin, G.-K.
 29 Plattner, M. Tignor, S.K. Allen, J. Boschung, A. Nauels, Y. Xia, V. Bex, and P.M. Midgley,
 30 Eds. Cambridge University Press, Cambridge, United Kingdom and New York, NY, USA,
 31 867–952. <http://dx.doi.org/10.1017/CBO9781107415324.022> www.climatechange2013.org
- 32 Chang, E.K.M., C.-G. Ma, C. Zheng, and A.M.W. Yau, 2016: Observed and projected decrease
 33 in Northern Hemisphere extratropical cyclone activity in summer and its impacts on
 34 maximum temperature. *Geophysical Research Letters*, **43**, 2200-2208.
 35 <http://dx.doi.org/10.1002/2016GL068172>

- 1 Collins, M., R. Knutti, J. Arblaster, J.-L. Dufresne, T. Fichefet, P. Friedlingstein, X. Gao, W.J.
2 Gutowski, T. Johns, G. Krinner, M. Shongwe, C. Tebaldi, A.J. Weaver, and M. Wehner,
3 2013: Long-term Climate Change: Projections, Commitments and Irreversibility. *Climate*
4 *Change 2013: The Physical Science Basis. Contribution of Working Group I to the Fifth*
5 *Assessment Report of the Intergovernmental Panel on Climate Change*. Stocker, T.F., D.
6 Qin, G.-K. Plattner, M. Tignor, S.K. Allen, J. Boschung, A. Nauels, Y. Xia, V. Bex, and
7 P.M. Midgley, Eds. Cambridge University Press, Cambridge, United Kingdom and New
8 York, NY, USA, 1029–1136. <http://dx.doi.org/10.1017/CBO9781107415324.024>
9 www.climatechange2013.org
- 10 Dittus, A.J., D.J. Karoly, S.C. Lewis, and L.V. Alexander, 2015: A Multiregion Assessment of
11 Observed Changes in the Areal Extent of Temperature and Precipitation Extremes. *Journal*
12 *of Climate*, **28**, 9206–9220. <http://dx.doi.org/10.1175/JCLI-D-14-00753.1>
- 13 Easterling, D.R., K.E. Kunkel, M.F. Wehner, and L. Sun, 2016: Detection and attribution of
14 climate extremes in the observed record. *Weather and Climate Extremes*, **11**, 17–27.
15 <http://dx.doi.org/10.1016/j.wace.2016.01.001>
- 16 Edwards, L.M., M. Bunkers, J.T. Abatzoglou, D.P. Todey, and L.E. Parker, 2014: October 2013
17 Blizzard in Western South Dakota [in "Explaining Extremes of 2013 from a Climate
18 Perspective"]. *Bulletin of the American Meteorological Society*, **95**, S23–S26.
19 <http://dx.doi.org/10.1175/1520-0477-95.9.S1.1>
- 20 Georgakakos, A., P. Fleming, M. Dettinger, C. Peters-Lidard, T.C. Richmond, K. Reckhow, K.
21 White, and D. Yates, 2014: Ch. 3: Water resources. *Climate Change Impacts in the United*
22 *States: The Third National Climate Assessment*. Melillo, J.M., T.C. Richmond, and G.W.
23 Yohe, Eds. U.S. Global Change Research Program, Washington, D.C., 69–112.
24 <http://dx.doi.org/10.7930/J0G44N6T>
- 25 Hartnett, J.J., J.M. Collins, M.A. Baxter, and D.P. Chambers, 2014: Spatiotemporal Snowfall
26 Trends in Central New York. *Journal of Applied Meteorology and Climatology*, **53**, 2685–
27 2697. <http://dx.doi.org/10.1175/jamc-d-14-0084.1>
28 <http://journals.ametsoc.org/doi/abs/10.1175/JAMC-D-14-0084.1>
- 29 Hoerling, M., K. Wolter, J. Perlwitz, X. Quan, J. Eischeid, H. Want, S. Schubert, H. Diaz, and R.
30 Dole, 2014: Northeast Colorado extreme rains interpreted in a climate change context [in
31 "Explaining Extremes of 2013 from a Climate Perspective"]. *Bulletin of the American*
32 *Meteorological Society*, **95**, S15–S18. <http://dx.doi.org/10.1175/1520-0477-95.9.S1.1>
- 33 Janssen, E., R.L. Sriver, D.J. Wuebbles, and K.E. Kunkel, 2016: Seasonal and regional variations
34 in extreme precipitation event frequency using CMIP5. *Geophysical Research Letters*, **43**,
35 5385–5393. <http://dx.doi.org/10.1002/2016GL069151>

- Janssen, E., D.J. Wuebbles, K.E. Kunkel, S.C. Olsen, and A. Goodman, 2014: Observational- and model-based trends and projections of extreme precipitation over the contiguous United States. *Earth's Future*, **2**, 99-113. <http://dx.doi.org/10.1002/2013EF000185>
- Kay, J.E., C. Deser, A. Phillips, A. Mai, C. Hannay, G. Strand, J.M. Arblaster, S.C. Bates, G. Danabasoglu, J. Edwards, M. Holland, P. Kushner, J.-F. Lamarque, D. Lawrence, K. Lindsay, A. Middleton, E. Munoz, R. Neale, K. Oleson, L. Polvani, and M. Vertenstein, 2015: The Community Earth System Model (CESM) Large Ensemble Project: A Community Resource for Studying Climate Change in the Presence of Internal Climate Variability. *Bulletin of the American Meteorological Society*, **96**, 1333-1349. <http://dx.doi.org/10.1175/BAMS-D-13-00255.1>
- Klein, S.A., X. Jiang, J. Boyle, S. Malyshev, and S. Xie, 2006: Diagnosis of the summertime warm and dry bias over the U.S. Southern Great Plains in the GFDL climate model using a weather forecasting approach. *Geophysical Research Letters*, **33**, n/a-n/a. <http://dx.doi.org/10.1029/2006GL027567>
- Kluver, D. and D. Leathers, 2015: Regionalization of snowfall frequency and trends over the contiguous United States. *International Journal of Climatology*, **35**, 4348-4358. <http://dx.doi.org/10.1002/joc.4292>
- Knutson, T.R., J.L. McBride, J. Chan, K. Emanuel, G. Holland, C. Landsea, I. Held, J.P. Kossin, A.K. Srivastava, and M. Sugi, 2010: Tropical cyclones and climate change. *Nature Geoscience*, **3**, 157-163. <http://dx.doi.org/10.1038/ngeo779>
- Knutson, T.R., J.J. Sirutis, G.A. Vecchi, S. Garner, M. Zhao, H.-S. Kim, M. Bender, R.E. Tuleya, I.M. Held, and G. Villarini, 2013: Dynamical downscaling projections of twenty-first-century Atlantic hurricane activity: CMIP3 and CMIP5 model-based scenarios. *Journal of Climate*, **27**, 6591-6617. <http://dx.doi.org/10.1175/jcli-d-12-00539.1>
- Knutson, T.R., F. Zeng, and A.T. Wittenberg, 2014: Seasonal and annual mean precipitation extremes occurring during 2013: A U.S. focused analysis [in "Explaining Extremes of 2013 from a Climate Perspective"]. *Bulletin of the American Meteorological Society*, **95**, S19-S23. <http://dx.doi.org/10.1175/1520-0477-95.9.S1.1>
- Kunkel, K.E., D.R. Easterling, D.A. Kristovich, B. Gleason, L. Stoecker, and R. Smith, 2012: Meteorological causes of the secular variations in observed extreme precipitation events for the conterminous United States. *Journal of Hydrometeorology*, **13**, 1131-1141. <http://dx.doi.org/10.1175/JHM-D-11-0108.1>
- Kunkel, K.E., D.R. Easterling, D.A.R. Kristovich, B. Gleason, L. Stoecker, and R. Smith, 2010: Recent increases in U.S. heavy precipitation associated with tropical cyclones. *Geophysical Research Letters*, **37**, L24706. <http://dx.doi.org/10.1029/2010GL045164>

- 1 Kunkel, K.E., L. Ensor, M. Palecki, D. Easterling, D. Robinson, K.G. Hubbard, and K.
2 Redmond, 2009: A new look at lake-effect snowfall trends in the Laurentian Great Lakes
3 using a temporally homogeneous data set. *Journal of Great Lakes Research*, **35**, 23-29.
4 <http://dx.doi.org/10.1016/j.jglr.2008.11.003>
5 <http://www.bioone.org/doi/pdf/10.1016/j.jglr.2008.11.003>
- 6 Kunkel, K.E., T.R. Karl, H. Brooks, J. Kossin, J. Lawrimore, D. Arndt, L. Bosart, D. Changnon,
7 S.L. Cutter, N. Doesken, K. Emanuel, P.Y. Groisman, R.W. Katz, T. Knutson, J. O'Brien,
8 C.J. Paciorek, T.C. Peterson, K. Redmond, D. Robinson, J. Trapp, R. Vose, S. Weaver, M.
9 Wehner, K. Wolter, and D. Wuebbles, 2013: Monitoring and understanding trends in extreme
10 storms: State of knowledge. *Bulletin of the American Meteorological Society*, **94**.
11 <http://dx.doi.org/10.1175/BAMS-D-11-00262.1>
- 12 Kunkel, K.E., T.R. Karl, D.R. Easterling, K. Redmond, J. Young, X. Yin, and P. Hennon, 2013:
13 Probable maximum precipitation and climate change. *Geophysical Research Letters*, **40**,
14 1402-1408. <http://dx.doi.org/10.1002/grl.50334>
- 15 Kunkel, K.E., D.A. Robinson, S. Champion, X. Yin, T. Estilow, and R.M. Frankson, 2016:
16 Trends and Extremes in Northern Hemisphere Snow Characteristics. *Current Climate*
17 *Change Reports*, **2**, 65-73. <http://dx.doi.org/10.1007/s40641-016-0036-8>
- 18 Lute, A.C., J.T. Abatzoglou, and K.C. Hegewisch, 2015: Projected changes in snowfall extremes
19 and interannual variability of snowfall in the western United States. *Water Resources*
20 *Research*, **51**, 960-972. <http://dx.doi.org/10.1002/2014WR016267>
- 21 Mearns, L.O., R. Arritt, S. Biner, M.S. Bukovsky, S. Stain, S. Sain, D. Caya, J. J. Correia, D.
22 Flory, W. Gutowski, E.S. Takle, R. Jones, R. Leung, W. Moufouma-Okia, L. McDaniel,
23 A.M.B. Nunes, Y. Qian, J. Roads, L. Sloan, and M. Snyder, 2012: The North American
24 regional climate change assessment program: Overview of phase I results. *Bulletin of the*
25 *American Meteorological Society*, **93**, 1337-1362. [http://dx.doi.org/10.1175/BAMS-D-11-](http://dx.doi.org/10.1175/BAMS-D-11-00223.1)
26 [00223.1](http://dx.doi.org/10.1175/BAMS-D-11-00223.1)
- 27 Min, S.K., X. Zhang, F.W. Zwiers, and G.C. Hegerl, 2011: Human contribution to more-intense
28 precipitation extremes. *Nature*, **470**, 378-381. <http://dx.doi.org/10.1038/nature09763>
- 29 Min, S.-K., X. Zhang, F. Zwiers, H. Shioyama, Y.-S. Tung, and M. Wehner, 2013: Multimodel
30 Detection and Attribution of Extreme Temperature Changes. *Journal of Climate*, **26**, 7430-
31 7451. <http://dx.doi.org/10.1175/JCLI-D-12-00551.1>
- 32 Ning, L. and R.S. Bradley, 2015: Snow occurrence changes over the central and eastern United
33 States under future warming scenarios. *Scientific Reports*, **5**, 17073.
34 <http://dx.doi.org/10.1038/srep17073>

- 1 NOAA, 2016: Climate at a glance. [http://www.ncdc.noaa.gov/cag/time-](http://www.ncdc.noaa.gov/cag/time-series/us/107/0/pdsi/12/12/1895-2016?base_prd=true&firstbaseyear=1901&lastbaseyear=2000)
- 2 [series/us/107/0/pdsi/12/12/1895-](http://www.ncdc.noaa.gov/cag/time-series/us/107/0/pdsi/12/12/1895-2016?base_prd=true&firstbaseyear=1901&lastbaseyear=2000)
- 3 [2016?base_prd=true&firstbaseyear=1901&lastbaseyear=2000](http://www.ncdc.noaa.gov/cag/time-series/us/107/0/pdsi/12/12/1895-2016?base_prd=true&firstbaseyear=1901&lastbaseyear=2000)
- 4 NOAA, 2016: Climate at a glance. [http://www.ncdc.noaa.gov/cag/time-](http://www.ncdc.noaa.gov/cag/time-series/us/4/0/pdsi/12/9/1895-2016?base_prd=true&firstbaseyear=)
- 5 [series/us/4/0/pdsi/12/9/1895-2016?base_prd=true&firstbaseyear=](http://www.ncdc.noaa.gov/cag/time-series/us/4/0/pdsi/12/9/1895-2016?base_prd=true&firstbaseyear=)
- 6 O'Gorman, P.A., 2014: Contrasting responses of mean and extreme snowfall to climate change.
- 7 *Nature*, **512**, 416-418. <http://dx.doi.org/10.1038/nature13625>
- 8 Pall, P.C.M.P., M.F. Wehner, D.A. Stone, C.J. Paciorek, and W.D. Collins, 2016: Diagnosing
- 9 anthropogenic contributions to heavy Colorado rainfall in September 2013. *Weather and*
- 10 *Climate Extremes*, **in review**.
- 11 Peterson, T.C., R.R. Heim, R. Hirsch, D.P. Kaiser, H. Brooks, N.S. Diffenbaugh, R.M. Dole, J.P.
- 12 Giovannetone, K. Guirguis, T.R. Karl, R.W. Katz, K. Kunkel, D. Lettenmaier, G.J. McCabe,
- 13 C.J. Paciorek, K.R. Ryberg, S. Schubert, V.B.S. Silva, B.C. Stewart, A.V. Vecchia, G.
- 14 Villarini, R.S. Vose, J. Walsh, M. Wehner, D. Wolock, K. Wolter, C.A. Woodhouse, and D.
- 15 Wuebbles, 2013: Monitoring and understanding changes in heat waves, cold waves, floods
- 16 and droughts in the United States: State of knowledge. *Bulletin of the American*
- 17 *Meteorological Society*, **94**, 821-834. <http://dx.doi.org/10.1175/BAMS-D-12-00066.1>
- 18 Pfahl, S., P.A. O'Gorman, and M.S. Singh, 2015: Extratropical Cyclones in Idealized
- 19 Simulations of Changed Climates. *Journal of Climate*, **28**, 9373-9392.
- 20 <http://dx.doi.org/10.1175/JCLI-D-14-00816.1>
- 21 Rasmussen, R., C. Liu, K. Ikeda, D. Gochis, D. Yates, F. Chen, M. Tewari, M. Barlage, J.
- 22 Dudhia, W. Yu, K. Miller, K. Arsenault, V. Grubišić, G. Thompson, and E. Gutmann, 2011:
- 23 High-Resolution Coupled Climate Runoff Simulations of Seasonal Snowfall over Colorado:
- 24 A Process Study of Current and Warmer Climate. *Journal of Climate*, **24**, 3015-3048.
- 25 <http://dx.doi.org/10.1175/2010JCLI3985.1>
- 26 Rauscher, S.A., J.S. Pal, N.S. Diffenbaugh, and M.M. Benedetti, 2008: Future changes in
- 27 snowmelt-driven runoff timing over the western US. *Geophysical Research Letters*, **35**,
- 28 L16703. <http://dx.doi.org/10.1029/2008GL034424>
- 29 Sakaguchi, K., L.R. Leung, C. Zhao, Q. Yang, J. Lu, S. Hagos, S.A. Rauscher, L. Dong, T.D.
- 30 Ringler, and P.H. Lauritzen, 2015: Exploring a Multiresolution Approach Using AMIP
- 31 Simulations. *Journal of Climate*, **28**, 5549-5574. [http://dx.doi.org/10.1175/JCLI-D-14-](http://dx.doi.org/10.1175/JCLI-D-14-00729.1)
- 32 [00729.1](http://dx.doi.org/10.1175/JCLI-D-14-00729.1)
- 33 Seager, R., M. Hoerling, S. Schubert, H. Wang, B. Lyon, A. Kumar, J. Nakamura, and N.
- 34 Henderson, 2015: Causes of the 2011–14 California Drought. *Journal of Climate*, **28**, 6997-
- 35 7024. <http://dx.doi.org/10.1175/JCLI-D-14-00860.1>

- 1 Shepherd, T.G., 2014: Atmospheric circulation as a source of uncertainty in climate change
2 projections. *Nature Geoscience*, **7**, 703-708. <http://dx.doi.org/10.1038/ngeo2253>
- 3 Sun, L., K.E. Kunkel, L.E. Stevens, A. Buddenberg, J.G. Dobson, and D.R. Easterling, 2015:
4 Regional Surface Climate Conditions in CMIP3 and CMIP5 for the United States:
5 Differences, Similarities, and Implications for the U.S. National Climate Assessment. NOAA
6 Technical Report NESDIS 144, 111 pp. National Oceanic and Atmospheric Administration,
7 National Environmental Satellite, Data, and Information Service.
8 http://www.nesdis.noaa.gov/technical_reports/NOAA_NESDIS_Technical_Report_144.pdf
- 9 Taylor, K.E., R.J. Stouffer, and G.A. Meehl, 2012: An overview of CMIP5 and the experiment
10 design. *Bulletin of the American Meteorological Society*, **93**, 485-498.
11 <http://dx.doi.org/10.1175/BAMS-D-11-00094.1>
- 12 Villarini, G., D.A. Lavers, E. Scoccimarro, M. Zhao, M.F. Wehner, G.A. Vecchi, T.R. Knutson,
13 and K.A. Reed, 2014: Sensitivity of Tropical Cyclone Rainfall to Idealized Global-Scale
14 Forcings. *Journal of Climate*, **27**, 4622-4641. <http://dx.doi.org/10.1175/JCLI-D-13-00780.1>
- 15 Vose, R.S., S. Applequist, M. Squires, I. Durre, M.J. Menne, C.N.W. Jr., C. Fenimore, K.
16 Gleason, and D. Arndt, 2014: Improved Historical Temperature and Precipitation Time
17 Series for U.S. Climate Divisions. *Journal of Applied Meteorology and Climatology*, **53**,
18 1232-1251. <http://dx.doi.org/10.1175/JAMC-D-13-0248.1>
- 19 Walsh, J., D. Wuebbles, K. Hayhoe, J. Kossin, K. Kunkel, G. Stephens, P. Thorne, R. Vose, M.
20 Wehner, J. Willis, D. Anderson, S. Doney, R. Feely, P. Hennon, V. Kharin, T. Knutson, F.
21 Landerer, T. Lenton, J. Kennedy, and R. Somerville, 2014: Ch. 2: Our changing climate.
22 *Climate Change Impacts in the United States: The Third National Climate Assessment*.
23 Melillo, J.M., T.C. Richmond, and G.W. Yohe, Eds. U.S. Global Change Research Program,
24 Washington, D.C., 19-67. <http://dx.doi.org/10.7930/J0KW5CXT>
- 25 Wang and Kotamarthi, 2014: Missing from list.
- 26 Wang, C.-C., B.-X. Lin, C.-T. Chen, and S.-H. Lo, 2015: Quantifying the Effects of Long-Term
27 Climate Change on Tropical Cyclone Rainfall Using a Cloud-Resolving Model: Examples of
28 Two Landfall Typhoons in Taiwan. *Journal of Climate*, **28**, 66-85.
29 <http://dx.doi.org/10.1175/JCLI-D-14-00044.1>
- 30 Wehner, M.F., 2013: Very extreme seasonal precipitation in the NARCCAP ensemble: Model
31 performance and projections. *Climate Dynamics*, **40**, 59-80.
32 <http://dx.doi.org/10.1007/s00382-012-1393-1>
- 33 Wehner, M.F., K.A. Reed, F. Li, Prabhat, J. Bacmeister, C.-T. Chen, C. Paciorek, P.J. Gleckler,
34 K.R. Sperber, W.D. Collins, A. Gettelman, and C. Jablonowski, 2014: The effect of
35 horizontal resolution on simulation quality in the Community Atmospheric Model, CAM5.1.

- 1 *Journal of Advances in Modeling Earth Systems*, **6**, 980-997.
2 <http://dx.doi.org/10.1002/2013MS000276>
- 3 Westra, S., L.V. Alexander, and F.W. Zwiers, 2013: Global Increasing Trends in Annual
4 Maximum Daily Precipitation. *Journal of Climate*, **26**, 3904-3918.
5 <http://dx.doi.org/10.1175/JCLI-D-12-00502.1>
- 6 Zhang, X., H. Wan, F.W. Zwiers, G.C. Hegerl, and S.-K. Min, 2013: Attributing intensification
7 of precipitation extremes to human influence. *Geophysical Research Letters*, **40**, 5252-5257.
8 <http://dx.doi.org/10.1002/grl.51010>

DRAFT

8. Droughts, Floods, and Hydrology

KEY FINDINGS

1. Recent droughts and associated heat waves have reached record intensity in some regions of the United States, but, by geographical scale and duration, the Dust Bowl era of the 1930s remains the benchmark drought and extreme heat event in the historical record. (*Very high confidence*)
2. The human effect on recent major U.S. droughts is complicated. Little evidence is found for a human influence on observed precipitation deficits but much evidence is found for a human influence on surface soil moisture deficits due to increased evapotranspiration caused by higher temperatures. (*High confidence*)
3. Future decreases in surface soil moisture over most of the United States are *likely* as the climate warms. (*High confidence*)
4. Reductions in western U.S. winter and spring snowpack are projected as the climate warms. Under higher emissions scenarios, and assuming no change to current water-resources management, chronic, long-duration hydrological drought is increasingly possible by the end of this century. (*Very high confidence*)
5. Detectable increases in seasonal flood frequency have occurred in parts of the central United States. This is to be expected in the presence of the increase in extreme downpours known with high confidence to be linked to a warming atmosphere, but formal attribution approaches have not certified the connection of increased flooding to human influences. (*Medium confidence*)

8.1. Drought

The word “drought” brings to mind abnormally dry conditions. However, the meaning of “dry” can be ambiguous and lead to confusion in how drought is actually defined. Three different classes of droughts are defined by NOAA and describe a useful hierarchical set of water deficit characterization, each with different impacts. “Meteorological drought” describes conditions of precipitation deficit. “Agricultural drought” describes conditions of soil moisture deficit. “Hydrological drought” describes conditions of deficit in runoff (NOAA 2008). Clearly these three characterizations of drought are related but are also different descriptions of water scarcity with different target audiences. In particular, agricultural drought is of concern to producers of food while hydrological drought is of concern to water system managers. Soil moisture is a function of both precipitation and evapotranspiration. Because potential evapotranspiration increases with temperature, anthropogenic climate change generally results in drier soils and often less runoff in the long term. In fact, under the RCP8.5 scenario (see Ch. 4 for a description of the RCP scenarios) at the end of the 21st century, no region of the planet is projected to

experience significantly higher levels of annual average surface soil moisture due to the sensitivity of evapotranspiration to temperature, even though much higher precipitation is projected in some regions (Collins et al. 2013). Runoff, on the other hand, is projected to both increase and decrease, depending on location and season under the same conditions, illustrating the complex relationships between the various components of the hydrological system. Hence, it is vital to describe precisely the definition of drought in any public discussion to avoid confusion due to this complexity.

8.1.1. Historical Context

The United States has experienced all three types of droughts in the past, always driven in at least some part by natural variations in seasonal and/or annual precipitation amounts. As the climate changes, we can expect that human activities will alter the effect of these natural variations. The “Dust Bowl” drought of the 1930s is still the most significant meteorological and agricultural drought experienced in the United States in terms of its geographic and temporal extent. However, even though it happened prior to most of the current global warming, human activities exacerbated the dryness of the soil by the farming practices of the time (Bennet et al. 1936). Tree ring archives reveal that such droughts (in the agricultural sense) have occurred periodically over the last 1,000 years (Cook et al. 2004). Long climate model simulations suggest that such droughts lasting several years to decades occur naturally in the southwestern United States (Coats et al. 2015). The IPCC AR5 (Bindoff et al. 2013) concluded “there is low confidence in detection and attribution of changes in (meteorological) drought over global land areas since the mid-20th century, owing to observational uncertainties and difficulties in distinguishing decadal-scale variability in drought from long-term trends.” As they noted, this was a weaker attribution statement than the IPCC AR4, which had concluded “that an increased risk of drought was *more likely than not* due to anthropogenic forcing during the second half of the 20th century.” The weaker statement in AR5 reflected additional studies with conflicting conclusions on global drought trends (e.g., Sheffield et al. 2012; Dai 2013). The western North America region was noted as a region where determining if observed recent droughts were unusual compared to natural variability was particularly difficult, due to evidence from paleoclimate proxies of cases of central U.S. droughts during the past 1,000 years that were longer and more intense than historical U.S. droughts (Masson-Delmotte et al. 2013). Future projections of the anthropogenic contribution to changes in drought risk and severity must be considered in the context of the significant role of natural variability.

8.1.2. Recent Major U.S. Droughts

Meteorological and agricultural drought

The United States has suffered a number of very significant droughts of all types since 2011. Each of these droughts was a result of different persistent, large-scale meteorological patterns of mostly natural origins, with varying degrees of attributable human influence. Table 8.1

summarizes available attribution statements for recent extreme U.S. meteorological and agricultural droughts. Statements about meteorological data are decidedly mixed, revealing the complexities in interpreting the low tail of the distribution of precipitation. Statements about agricultural drought consistently maintain a human influence if only surface soil moisture measures are considered. The single agricultural drought attribution study at root depth comes to the opposite conclusion. In all cases, these attribution statements are made without detection (see Section 3.2). The absence of moisture during the 2011 Texas/Oklahoma drought and heat wave was found to be a naturally occurring event whose likelihood was enhanced by the La Niña state of the ocean, but the human interference in the climate system still doubled the chances of reaching such high temperatures (Hoerling et al. 2013). This study illustrates that the effect of human induced climate change is combined with natural variations and can compound or inhibit the realized severity of any given extreme weather event.

[INSERT TABLE 8.1 HERE:

Table 8.1: A list of U.S. droughts for which attribution statements have been made. In the last column, “+” indicates that an attributable human induced increase in frequency and/or magnitude was found, “– “ indicates that an attributable human induced decrease in frequency and/or magnitude was found, “0” indicates no attributable human contribution was identified. As in tables 6.2 and 7.1, several of the events were originally examined in the Bulletin of the American Meteorological Society’s (BAMS) State of the Climate Reports and reexamined by Angelil et al. (2016). In these cases, both attribution statements are listed with the original authors first.

Source: M. Wehner.]

The Great Plains/Midwest drought of 2012 was the most severe summer meteorological drought in the observational record for that region (Hoerling et al. 2014). An unfortunate string of three different patterns of large-scale meteorology from May through August 2012 precluded the normal frequency of summer thunderstorms but was not predicted by the NOAA seasonal forecasts (Hoerling et al. 2014). Little influence of the global sea surface temperature (SST) pattern on meteorological drought frequency has been found in model simulations (Hoerling et al. 2014). No evidence of a human contribution to the 2012 precipitation deficit in the Great Plains and Midwest is consistently found (Rupp et al. 2013; Hoerling et al. 2014; Angelil et al. 2016). However, again an increase in the chances of the unusually high U.S. 2012 temperatures, partly associated with resultant dry summer soil moisture anomalies, was attributed to the human interference to the climate system (Diffenbaugh and Scherer 2013), indicating the strong feedback between soil moisture and surface air temperature variability from both natural and anthropogenic causes during periods of low precipitation. One study found that most, but not all, of the 2012 surface moisture deficit in the Great Plains was attributable to the precipitation deficit (Livneh and Hoerling 2016). That study also noted that Great Plains deep soil moisture was higher than normal in 2012 despite the surface drying due to wet conditions in prior years, indicating the long timescales relevant below the surface (Livneh and Hoerling 2016).

The current California drought, which began in 2011, is unusual in different respects. In this case, the precipitation deficit from 2011 to 2014 was a result of the “ridiculously resilient ridge” of high pressure. This very stable high-pressure system steered storms towards the north, away from the highly engineered California water resource system (Swain et al. 2014; Seager et al. 2014, 2015). The ridge itself was due to a slow-moving high sea surface temperature (SST) anomaly, referred to as “The Blob”—a result of an anomalous atmospheric circulation pattern (Bond et al. 2015). A principal attribution question regarding the precipitation deficit concerns the causes of this SST anomaly. Observational records are not long enough and the anomaly was unusual enough that similarly long-lived structures have not been often seen before. Hence, attribution statements, such as that about an anthropogenic increase in the frequency of geopotential height anomalies similar to 2012–2014 (e.g., Swain et al. 2014), are without associated detection (Ch. 3: Detection and Attribution). A secondary attribution question concerns the anthropogenic precipitation response in the presence of this SST anomaly. In attribution studies with a prescribed 2013 SST anomaly, a consistent human increase in the chances of very dry California conditions was found (Angelil et al. 2016).

As in 2012, anthropogenic climate change did increase the risk of the high temperatures in California (Seager et al. 2015; Diffenbaugh et al. 2015), further exacerbating the soil moisture deficit and the associated stress on irrigation systems. An anthropogenic contribution to commonly used measures of agricultural drought, including the Palmer Drought Severity Index (PDSI), was found in California (Diffenbaugh et al. 2015; Williams et al. 2015) and is consistent with previous projections of changes in PDSI (Dai et al. 2013; Wehner et al. 2011; Walsh et al. 2014) and with an attribution study (Brown et al. 2008). Due to its simplicity, the PDSI has been criticized as being overly sensitive to higher temperatures and thus may exaggerate the human contribution to soil dryness (Milly and Dunne 2016). In fact, this study also finds that formulations of potential evaporation used in more complicated hydrologic models are similarly biased, undermining confidence in the magnitude but not the sign of projected surface soil moisture changes in a warmer climate. Seager et al. (2013) analyzed climate model output directly finding that precipitation minus evaporation in the southwest United States is projected to experience significant decreases in surface water availability leading to surface runoff decreases in California, Nevada, the Colorado River headwaters and Texas even in the near term. However, the Milly and Dunne criticisms also apply to most of the CMIP5 land surface model evapotranspiration formulations. Analysis of soil moisture at deeper levels reveals less sensitivity to temperature increases than to precipitation variations, which have increased over the 20th century (Cheng et al. 2016). Nonetheless, the warming trend has led to declines in a number of indicators, including Sierra snow water equivalent, that are relevant to hydrological drought (Mao et al. 2015). Attribution of the California drought and heat wave remains an interesting and controversial research topic.

In summary, there has not been a formal identification of a human influence on past changes in United States meteorological drought through the analysis of precipitation trends. Some, but not

all, United States meteorological drought event attribution studies, largely in the “without detection” class, exhibit a human influence. Attribution of a human influence on past changes in U.S. agricultural drought are limited both by availability of soil moisture observations and a lack of sub-surface modeling studies. While a human influence on surface soil moisture trends has been identified with *medium confidence*, its relevance to agriculture may be exaggerated.

Runoff and hydrological drought

Several studies focused on the Colorado River basin in the United States using more sophisticated runoff models driven by the CMIP3 models (Christensen and Lettenmaier 2007; McCabe and Wolock 2007; Barnett and Pierce 2009; Barnett et al. 2008; Hoerling et al. 2009) showed that annual runoff reductions in a warmer climate occur through a combination of evapotranspiration increases and precipitation decreases, with the overall reduction in river flow exacerbated by human water demands on the basin’s supply.

8.1.2. Projections of Future Droughts and Runoff

The future changes in seasonal precipitation shown in Chapter 7: Precipitation Change (Figure 7.6) would indicate that the western United States may experience chronic future precipitation deficits, particularly in the spring. Such deficits are not confidently projected in other portions of the country. However, future higher temperatures will *very likely* lead to greater frequencies and magnitudes of agricultural droughts throughout the continental United States as the resulting increases in evapotranspiration outpace projected precipitation increases (Collins et al. 2013). Figure 8.1 shows the weighted multimodel projection of the percent change in near-surface soil moisture at the end of the 21st century under the RCP8.5 scenario, indicating widespread drying over the entire continental United States. Previous National Climate Assessments (Karl et al. 2009; Walsh et al. 2014) have discussed the implication of these future drier conditions in the context of the Palmer Drought Severity Index (PDSI), finding that the future normal condition would be considered drought at the present time, and that the incidence of “extreme drought” ($PDSI < -4$) would be significantly increased. Confidence that future soils will generally be drier at the surface is *high*, as the mechanisms leading to increased evapotranspiration in a warmer climate are elementary scientific facts. However, the land surface component models in the CMIP5 climate models vary greatly in their sophistication, causing the projected magnitude of both the average soil moisture decrease and the increased risk for agricultural drought to be less certain. The weighted projected seasonal decreases in surface soil moisture are generally towards drier conditions, even in regions and seasons where precipitation is projected to experience large increases (Figure 7.6) due to increases in the evapotranspiration associated with higher temperature. Drying is assessed to be large relative to natural variations in much of the CONUS region in the summer. Significant spring and fall drying is also projected in the mountainous western states, with potential implications for forest and wildfire risk. Also, the combination of significant summer and fall drying in the midwestern states has potential agricultural implications. The largest percent changes are projected in the Southwestern United States and are

1 consistent in magnitude with an earlier study of the Colorado River Basin using more
2 sophisticated macroscale hydrological models (Christensen and Lettenmaier 2007).

3 Despite the important usage of PDSI as an early warning indicator of U.S. drought (e.g., NOAA
4 2016), its suitability as a measure of future agricultural drought in much warmer climates is
5 questionable due to its simplified representation of the water cycle, resulting in overly
6 pessimistic projections (Hoerling et al. 2012). Similarly, a direct CMIP5 multimodel projection
7 of soil moisture such as in Figure 8.1 must be limited to the surface (defined as the top 10 cm of
8 the soil), as the land surface component sub-models vary greatly in their representation of the
9 total depth of the soil. A more relevant projection to agricultural drought would be the soil
10 moisture at the root depth of typical U.S. crops, which is not generally available from the CMIP5
11 models. Few of the CMIP5 land models have detailed ecological representations of
12 evapotranspiration processes, causing the simulation of the soil moisture budget to be less
13 constrained than reality (Williams and Torn 2015). Nonetheless, Figure 8.1 shows a projected
14 drying of surface soil moisture across nearly all of the coterminous United States in all seasons
15 even in regions and seasons where precipitation is projected to increase.

16 Changes in average total seasonal runoff—including surface streamflow and groundwater—
17 differ significantly between the mountainous western United States, Alaska and the rest of the
18 Nation. Figure 8.2 shows the projected end of the 21st century CMIP5 multimodel weighted
19 average percent changes in near-total runoff under the RCP8.5 scenario, revealing increased
20 runoff in Alaska and Northern Canada during winter due to the change from snow to rain in the
21 warmer climate. Projected winter increases are assessed as large (Appendix B) in a small region
22 of the Rockies as well. For the rest of the contiguous United States, the weighted projection for
23 average total runoff is generally to be decreased as a result of increased evapotranspiration.
24 However, these decreases are assessed to be small compared to natural variations in all seasons
25 (Appendix B).

26 Reduced contiguous U.S. snowfall accumulations in much warmer future climates are virtually
27 certain as frozen precipitation is replaced by rain regardless of the projected changes in total
28 precipitation amounts discussed in Chapter 7 (Figure 7.6). Widespread reductions in mean
29 snowfall across North America are projected by the CMIP5 models (O’Gorman 2014). Together
30 with earlier snowmelt at altitudes high enough for snow, disruptions in western U.S. water
31 delivery systems are expected to lead to more frequent hydrological drought conditions (Barnett
32 et al. 2008; Pierce et al. 2008; Barnett and Pierce 2009; Cayan et al. 2010). The elevation of
33 mountains as represented in the CMIP5 models is too low, due to resolution constraints, to
34 adequately represent the effects of future temperature on snowpacks. However, increased model
35 resolution has been demonstrated to have important impacts on future projections of snowpack
36 change in warmer climates and is enabled by recent advances in high performance computing
37 (Kapnick and Delworth 2013). Figure 8.3 and Table 8.2 show a projection of changes in western
38 U.S. mountain winter (December, January, and February) hydrology obtained from a different
39 high-resolution atmospheric model at the middle and end of the 21st century under the RCP8.5

scenario. These projections indicate dramatic reductions in all aspects of snow (Rhoades et al. in review) and are similar to a previous statistically downscaled projections (Cayan et al. 2013; Klos et al. 2014). Given the larger projected increases in temperature at high altitudes compared to adjacent lower altitudes (Pierce and Cayan 2012) and the resulting changes in both snowpack depth and melt timing in very warm future scenarios, and assuming no change to water-resource management, several important western U.S. snowpack reservoirs effectively disappear by 2100 in this dynamical projection, resulting in chronic, long-lasting hydrological drought. This dramatic statement is also supported by a multi-model statistical downscaling of the CMIP5 RCP8.5 ensemble that finds large areal reductions in snow dominated regions of the western United States by mid-century and complete elimination of snow-dominated regions in certain watersheds (Klos et al. 2014).

[INSERT FIGURE 8.1 HERE:

Figure 8.1. Projected end of the 21st century weighted CMIP5 multimodel average percent changes in near surface seasonal soil moisture (mrsos) under the RCP8.5 scenario. Stippling indicates that changes are assessed to be large compared to natural variations. Hashing indicates that changes are assessed to be small compared to natural variations. Blank regions (if any) are where projections are assessed to be inconclusive (Appendix B).]

[INSERT FIGURE 8.2 HERE:

Figure 8.2. Projected end of the 21st century weighted CMIP5 multimodel average percent changes in total seasonal runoff (mrro) under the RCP8.5 emissions scenario. Stippling indicates that changes are assessed to be large compared to natural variations. Hashing indicates that changes are assessed to be small compared to natural variations. Blank regions (if any) are where projections are assessed to be inconclusive (Appendix B).]

[INSERT FIGURE 8.3 HERE:

Figure 8.3. Projected changes in winter (DJF) Snow Water Equivalent at the middle and end of this century under the RCP8.5 scenario from a high-resolution version of the Community Atmospheric Model, CAM5 (Rhoades et al. 2016), Figure source: Lawrence Berkeley National Laboratory.]

8.2. Floods

Flooding damage in the United States can come from flash floods of smaller rivers and creeks, prolonged flooding along major rivers, and coastal flooding from storm surge and the confluence of coastal storms and inland riverine flooding from the same precipitation event (Ch. 12: Sea Level Rise). Flash flooding is associated with extreme precipitation somewhere along the river which may occur upstream of the regions at risk. Flooding of major rivers in the United States usually occurs in the late winter or spring and can result from an unusually heavy seasonal snowfall followed by a “rain on snow” event or from a rapid onset of higher temperatures that leads to rapid snow melting within the river basin. Changes in streamflow rates depend on many

factors, both human and natural, in addition to climate change. Deforestation, urbanization, and changes in agricultural practices can all play a role in past and future changes in flood statistics. Projection of future changes is thus a multivariate problem (Walsh et al. 2014).

Trends in extreme high values of streamflow are mixed across the United States, as reported in the Third National Climate Assessment (Walsh et al. 2014). Recent analysis of annual maximum streamflow shows statistically significant trends only in the upper Mississippi River valley (increasing) and in the Northwest (decreasing) (McCabe and Wolock 2014). This is seemingly in contrast to the much more widespread increasing trends in extreme precipitation over much of the eastern and northern United States. As noted above, floods are poorly explained by precipitation characteristics alone; the relevant mechanisms are more complex, involving processes that are seasonally and geographically variable, including the seasonal cycles of soil moisture content and snowfall/snowmelt (Berghuijs et al. 2016). The northeast United States is an interesting example. Strong increasing trends in extreme precipitation have been observed and appear to be ubiquitous across this region (Walsh et al. 2014; Frei et al. 2015). Trends in maximum streamflow are less dramatic and less spatially coherent (McCabe and Wolock 2014; Frei et al. 2015), although one study found mostly increasing trends (Armstrong et al. 2014) in that region, somewhat at odds with other studies. This apparent disparity is caused by the seasonality of the two phenomena. Extreme precipitation events are larger in the warm season when soil moisture and seasonal streamflow levels are low and less favorable for flooding. By contrast, high streamflow events are larger in the cold season when soil moisture is high and snowmelt and frozen ground can enhance runoff (Frei et al. 2015). A future projection study based on coupling an ensemble of regional climate model output to a hydrology model (Najafi and Moradkhani 2015) finds that the magnitude of very extreme runoff (which can lead to flooding) is decreased in most of the summer months in Washington State, Oregon, Idaho and western Montana but is substantially increased in the other seasons. Projected increases in extreme runoff from the coast to the Cascades are particularly large in the fall and winter.

Thus, apparent disparities between extreme precipitation and flood trends are partially explained by the complex seasonal and geographic processes that affect flooding that go beyond simple precipitation characteristics. This presents a challenge for attribution studies and it has been suggested that additional scientific rigor is needed in flood attribution studies (Merz et al. 2012).

The IPCC WG1 AR5 (Bindoff et al. 2013) did not attribute changes in flooding to anthropogenic influence nor report detectable changes in flooding magnitude or frequency. Analysis of 200 U.S. stream gauges indicates both areas of increasing and decreasing flooding magnitude (Hirsch and Ryberg 2012) but does not provide robust evidence that these trends are detectable or attributable to human influences. Significant increases in flood frequency have been detected in about one-third of stream gauge stations examined for the central United States, with a much stronger signal of change than is found for flood magnitude in these gauges (Mallakpour and Villarini 2015). Although both temperature and precipitation increases were influencing the

1 flooding changes, no attribution of these changes to anthropogenic forcing has been claimed
2 (Mallakpour and Villarini 2015).

3 The nature of the proxy archives complicates the reconstruction of past flood events in a gridded
4 fashion as has been done with droughts. However, reconstructions of past river outflows do exist.
5 For instance, it has been suggested that the mid-20th century river allocations for the Colorado
6 River were made during one of the wettest periods of the past five centuries (Woodhouse et al.
7 2006). For the eastern United States, the Mississippi River has undergone century-scale
8 variability in flood frequency—perhaps linked to the moisture availability in the central United
9 States and the temperature structure of the Atlantic Ocean (Munoz et al. 2015).

10 No studies have clearly attributed long-term changes in observed flooding of major rivers in the
11 United States to anthropogenic forcing. We conclude that there is *medium confidence* that
12 detectable, though not attributable, increases in seasonal flood frequency have occurred in parts
13 of the central United States.

14 Studies of localized extreme flooding events are extremely limited, are confined to changes in
15 the locally responsible precipitation event, and do not include detailed analyses of the events’
16 hydrology. Gochis et al. (2015) describes the massive floods of 2013 along the Colorado front
17 range, estimating that the record rainfall exceeds 1,000-year return values in some regions.
18 Hoerling et al. (2014) analyzed the 2013 northeastern Colorado heavy multiday precipitation
19 event and resulting flood finding little evidence of an anthropogenic influence on its occurrence.
20 However, Pall et al. (2016) challenge their methodology with a more constrained study and find
21 that the thermodynamic response of precipitation in this event due to anthropogenic forcing was
22 substantially increased. The Pall et al. (2016) approach does not rule out that the likelihood of the
23 extremely rare large-scale meteorological pattern responsible for the flood may have changed.

24 8.3 Wildfires

25 Recent decades have seen increased forest fire activity in the western United States and Alaska.
26 For the western United States, one study has estimated that human-caused climate change was
27 responsible for nearly half of the total forest acreage burned by wildfires over 1984 to 2015
28 (Abatzoglou and Williams 2016) while another study found an increased risk of fire in California
29 due to human-caused climate change, based on a model assessment of the 2014 fire season
30 (Yoon et al. 2015). For Alaska, one study found that human caused climate change had increased
31 the risk of severe fire seasons like 2015 by 34%–60% (Partain et al., in review). In Abatzoglou
32 and Williams, modeled increases in temperatures and vapor pressure deficits due to
33 anthropogenic climate change caused increased fire potential by increasing the aridity of forest
34 fuels during the fire season. None of the studies demonstrates that a long term increase in forest
35 fire activity is highly unusual in comparison to natural variability, as they are generally inferring
36 a human-caused climate change contribution to trends or probabilities based on model
37 calculations. The degree of forestry management, which is greater in the western United States

1 than in Alaska, is a confounding factor that complicates attribution of changes to anthropogenic
2 climate change. We conclude that there is *medium confidence* for a human-caused climate
3 change contribution to increased forest fire activity in Alaska in recent decades, but *low*
4 *confidence* for a detectable human climate change contribution in the western United States
5 based on existing studies.

6

DRAFT

TRACEABLE ACCOUNTS

Key Message 1

Recent droughts and associated heat waves have reached record intensity in some regions of the United States, but, by geographical scale and duration, the Dust Bowl era of the 1930s remains the benchmark drought and extreme heat event in the historical record. (*Very high confidence*)

Description of evidence base

Recent droughts are well characterized and described in the literature. The dust bowl is not as well documented, but available observational records support the key finding.

Major uncertainties

Record breaking temperatures are well documented with low uncertainty (Meehl et al 2009). The magnitude of the Dust Bowl relative to present times varies with location. Uncertainty in the key finding is affected by the quality of pre-WW2 observations but is relatively low.

Assessment of confidence based on evidence and agreement

X Very High

☐ High

☐ Medium

☐ Low

Precipitation is well observed in the United States leading to very high confidence.

Summary sentence or paragraph that integrates the above information

The key finding is a statement that recent U.S. droughts, while sometimes long and severe, are not unprecedented in the history of Earth's hydrologic natural variation.

Key Message 2

The human effect on recent major U.S. droughts is complicated. Little evidence is found for a human influence on observed precipitation deficits but much evidence is found for a human influence on surface soil moisture deficits due to increased evapotranspiration caused by higher temperatures. (*High confidence*)

Description of evidence base

Observational records of meteorological drought are not long enough to detect statistically significant trends. Additionally, paleoclimatic evidence suggests that major droughts have occurred throughout the distant past. Surface soil moisture is not well observed throughout the CONUS but numerous event attribution studies attributes enhanced reduction of surface soil moisture during dry periods due to anthropogenic warming and enhanced evapotranspiration.

Major uncertainties

Uncertainties stem from the length of precipitation observations and the lack of surface moisture observations.

Assessment of confidence based on evidence and agreement

☐ Very High

☒ High

☐ Medium

☐ Low

Summary sentence or paragraph that integrates the above information

The precipitation deficit portion of the key finding is a conservative statement reflecting the conflicting and limited event attribution literature on meteorological drought. The soil moisture portion of the key finding is limited to the surface and not the more relevant root depth and is supported by the studies cited in Chapter 8.

Key Message 3

Future decreases in surface soil moisture over most of the United States are *likely* as the climate warms. (*High confidence*)

Description of evidence base

First principles establish that evaporation is at least linearly dependent on temperatures and accounts for much of the surface moisture decrease as temperature increases. Plant transpiration for many non-desert species controls plant temperature and responds to increased temperature by opening stomata to release more water vapor. This water comes from the soil at root depth as the plant exhausts its stored water supply (*very high confidence*).

Major uncertainties

While both evaporation and transpiration changes are of the same sign as temperature increases, the relative importance of each as a function of depth is less well quantified. The amount of transpiration varies considerably among plant species and these are treated with widely varying of sophistication in the land surface components of contemporary climate models. Uncertainty in the sign of the anthropogenic change of root depth soil moisture is low in regions and seasons of projected precipitation decreases (Chapter 7). Uncertainty in the magnitude of the change in soil moisture at all depths and all regions and seasons is not low.

Assessment of confidence based on evidence and agreement

☐ Very High

☒ High

1 ☐ Medium

2 ☐ Low

3 CMIP5 and regional models support the surface soil moisture key finding.

4 **Summary sentence or paragraph that integrates the above information**

5 In the northern United States, surface soil moisture (top 10 cm) is *very likely* to decrease as
6 evaporation outpaces increases in precipitation. In the southwest, the combination of temperature
7 increases and precipitation decreases causes surface soil moisture decreases to be *virtually*
8 *certain*. In this region, decreases in soil moisture at the root depth is *very likely*.

9

10 **Key Message 4**

11 Reductions in western U.S. winter and spring snowpack are projected as the climate warms.
12 Under higher emissions scenarios, and assuming no change to current water-resources
13 management, chronic, long-duration hydrological drought is possible by the end of this century.
14 (*Very high confidence*).

15 **Description of evidence base**

16 First principles tell us that as temperatures rise, minimum snow levels also must rise. Certain
17 changes in western U.S. hydrology have already been reported in the papers following Barnett et
18 al. (2008). The CMIP3/5 models project widespread warming with future increases in
19 atmospheric GHG concentrations, although these are underestimated in the current generation of
20 GCMs at the high altitudes of the western U.S. due to constraints on orographic representation at
21 current GCM spatial resolutions.

22 CMIP5 models were not designed or constructed for direct projection of locally relevant
23 snowpack amounts. However, a high-resolution climate model, selected for its ability to simulate
24 Western U.S. snowpack amounts and extent, projects devastating changes in the hydrology of
25 this region assuming constant water-resource management practices (Rhoades et al 2016). This
26 conclusion is also supported by a statistical downscaling result shown in figure 3.1 of Walsh et
27 al. 2014 and Cayan et al. 2013 and by the more recent statistical downscaling study of Klos et al.
28 2014.

29 **Major uncertainties**

30 The major uncertainty is not so much “if” but rather “when” as changes to precipitation phase
31 (rain or snow) are sensitive to temperature increases that in turn depends on GHG forcing
32 changes. Also, changes to the lower elevation catchments will be realized prior to those at higher
33 elevations that even at 25 km, is not adequately resolved. Uncertainty in the second statement
34 also stems from the usage of one model. However, this simulation is a so-called “prescribed
35 temperature” experiment with the usual uncertainties about climate sensitivity wired in by the

usage of one particular ocean temperature change. Uncertainty in the equator to pole differential ocean warming rate is also a factor.

Assessment of confidence based on evidence and agreement

X Very High

☐ High

☐ Medium

☐ Low

All CMIP5 models project large scale western U.S. warming as GHG forcing increases.

Warming is underestimated in most of the western United States due to elevation deficiencies that are a consequence of coarse model resolution. Snow melts above 32°F.

Summary sentence or paragraph that integrates the above information

Warmer temperatures lead to less snow and more rain if total precipitation remains unchanged. Projected winter/spring precipitation changes are a mix of increases in northern states and decreases in the southwest. In the northern Rockies, snowpack is projected decrease even with a projected precipitation increase due to this phase change effect. This will lead to, at the very least, profound changes to the seasonal and sub-seasonal timing of the western U.S. hydrological cycle even where annual precipitation remains nearly unchanged.

Key Message 5

Detectable increases in seasonal flood frequency have occurred in parts of the central United States. This is to be expected in the presence of the increase in extreme downpours known with high confidence to be linked to a warming atmosphere, but formal attribution approaches have not certified the connection of increased flooding to human influences. (*Medium confidence*).

Description of evidence base

Observed increases are documented by Walsh et al. 2014 and other studies cited in the text. No attribution statements have been made.

Major uncertainties

Floods are highly variable both in space and time. The multi-variate nature of floods complicates detection and attribution.

Assessment of confidence based on evidence and agreement

☐ Very High

☐ High

X Medium

☐ Low

Summary sentence or paragraph that integrates the above information

The key finding is a relatively weak statement reflecting the limited literature on the detection and attribution of anthropogenic changes in US flooding intensity, duration and frequency.

TABLES

Table 8.1: A list of U.S. droughts for which attribution statements have been made. In the last column, “+” indicates that an attributable human induced increase in frequency and/or magnitude was found, “–” indicates that an attributable human induced decrease in frequency and/or magnitude was found, “0” indicates no attributable human contribution was identified. As in tables 6.2 and 7.1, several of the events were originally examined in the Bulletin of the American Meteorological Society’s (BAMS) State of the Climate Reports and reexamined by Angelil et al. (2016). In these cases, both attribution statements are listed with the original authors first. Source: M. Wehner.

Authors	Event Year and Duration	Region or State	Type	Attribution Statement
Rupp and Mote 2012 / Angelil et al. 2016	MAMJJA 2011	Texas	Meteorological	+/+
Hoerling et al. 2013	2012	Texas	Meteorological	+
Rupp et al. 2013 / Angelil et al. 2016	MAMJJA 2012	CO, NE, KS, OK, IA, MO, AR & IL	Meteorological	0/0
Rupp et al. 2013 / Angelil et al. 2016	MAM 2012	CO, NE, KS, OK, IA, MO, AR & IL	Meteorological	0/0
Rupp et al. 2013 / Angelil et al. 2016	JJA 2012	CO, NE, KS, OK, IA, MO, AR & IL	Meteorological	0/+
Hoerling et al. 2014	MJJA 2012	Great Plains/Midwest	Meteorological	0
Swain et al. 2014 / Angelil et al. 2016	ANN 2013	California	Meteorological	+/+
Wang and Schubert 2014 / Angelil et al. 2016	JS 2013	California	Meteorological	0/+
Knutson et al. 2014 / Angelil et al. 2016	ANN 2013	California	Meteorological	+/+
Knutson et al. 2014 / Angelil et al. 2016	MAM 2013	U.S. Southern Plains region	Meteorological	+/+
Diffenbaugh et al. 2014	2012-2014	California	Agricultural	+
Seager et al. 2015	2012-2014	California	Agricultural	+
Cheng et al. 2016	2011-2015	California	Agricultural	-

Table 8.2: Projected changes in western U.S. mountain range winter (DJF) snow-related hydrology variables at the middle and end of this century. Projections are for the RCP8.5 scenario from a high-resolution version of the Community Atmospheric Model, CAM5 (Rhoades et al. 2016).

Mountain Range	Snow Water Equivalent (% Change)		Snow Cover (% Change)		Snowfall (% Change)		Surface Temperature (Change in K)	
	2050	2100	2050	2100	2050	2100	2050	2100
Cascades	-41.5	-89.9	-21.6	-72.9	-10.7	-50.0	0.9	4.1
Klamath	-50.7	-95.8	-38.6	-89.0	-23.1	-78.7	0.8	3.5
Rockies	-17.3	-65.1	-8.2	-43.1	1.7	-8.2	1.4	5.5
Sierra Nevada	-21.8	-89.0	-21.9	-77.7	-4.7	-66.6	1.1	4.5
Wasatch and Uinta	-18.9	-78.7	-14.2	-61.4	4.1	-34.6	1.8	6.1
Western USA	-22.3	-70.1	-12.7	-51.5	-1.6	-21.4	1.3	5.2

FIGURES

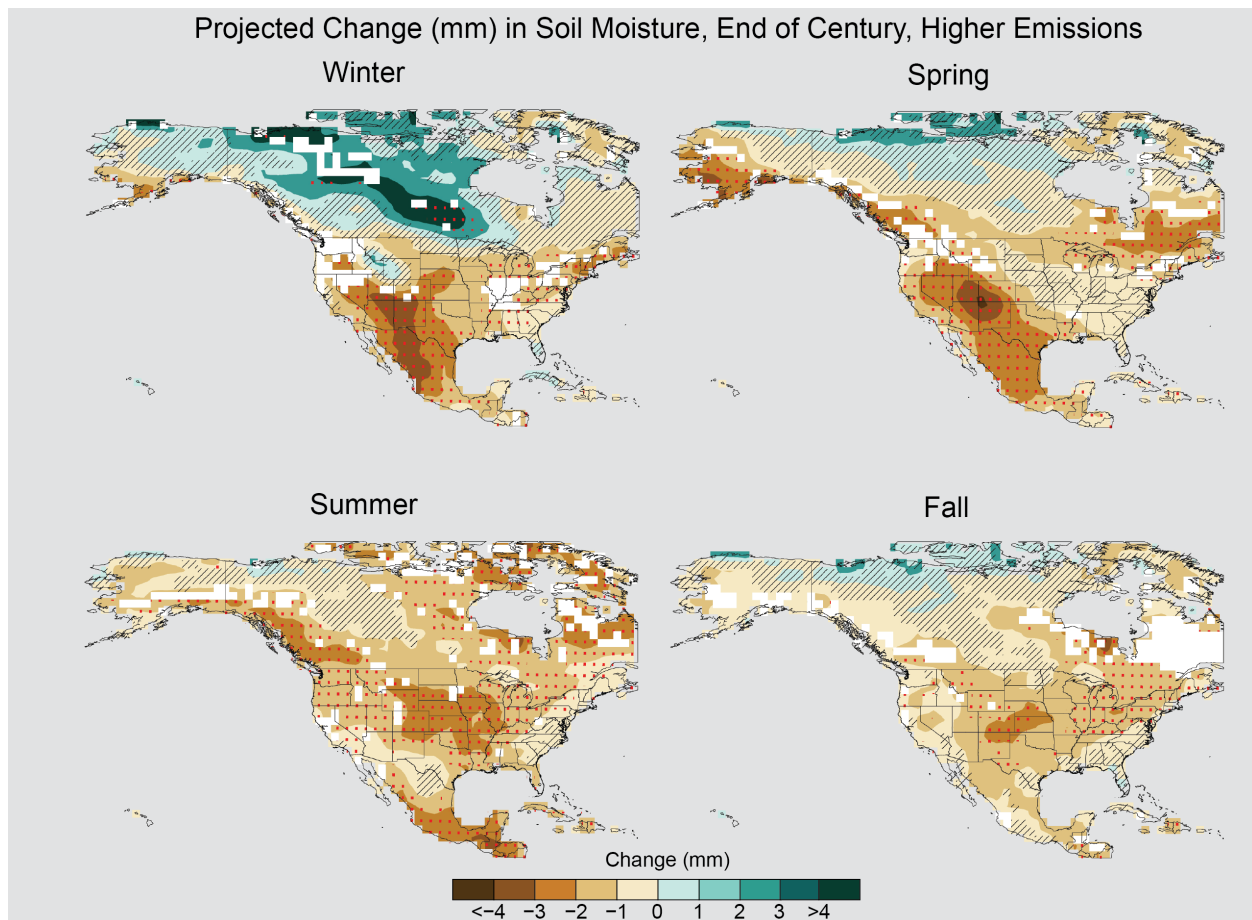


Figure 8.1. Projected end of the 21st century weighted CMIP5 multimodel average percent changes in near surface seasonal soil moisture (mrsos) under the RCP8.5 scenario. Stippling indicates that changes are assessed to be large compared to natural variations. Hashing indicates that changes are assessed to be small compared to natural variations. Blank regions (if any) are where projections are assessed to be inconclusive (Appendix B).

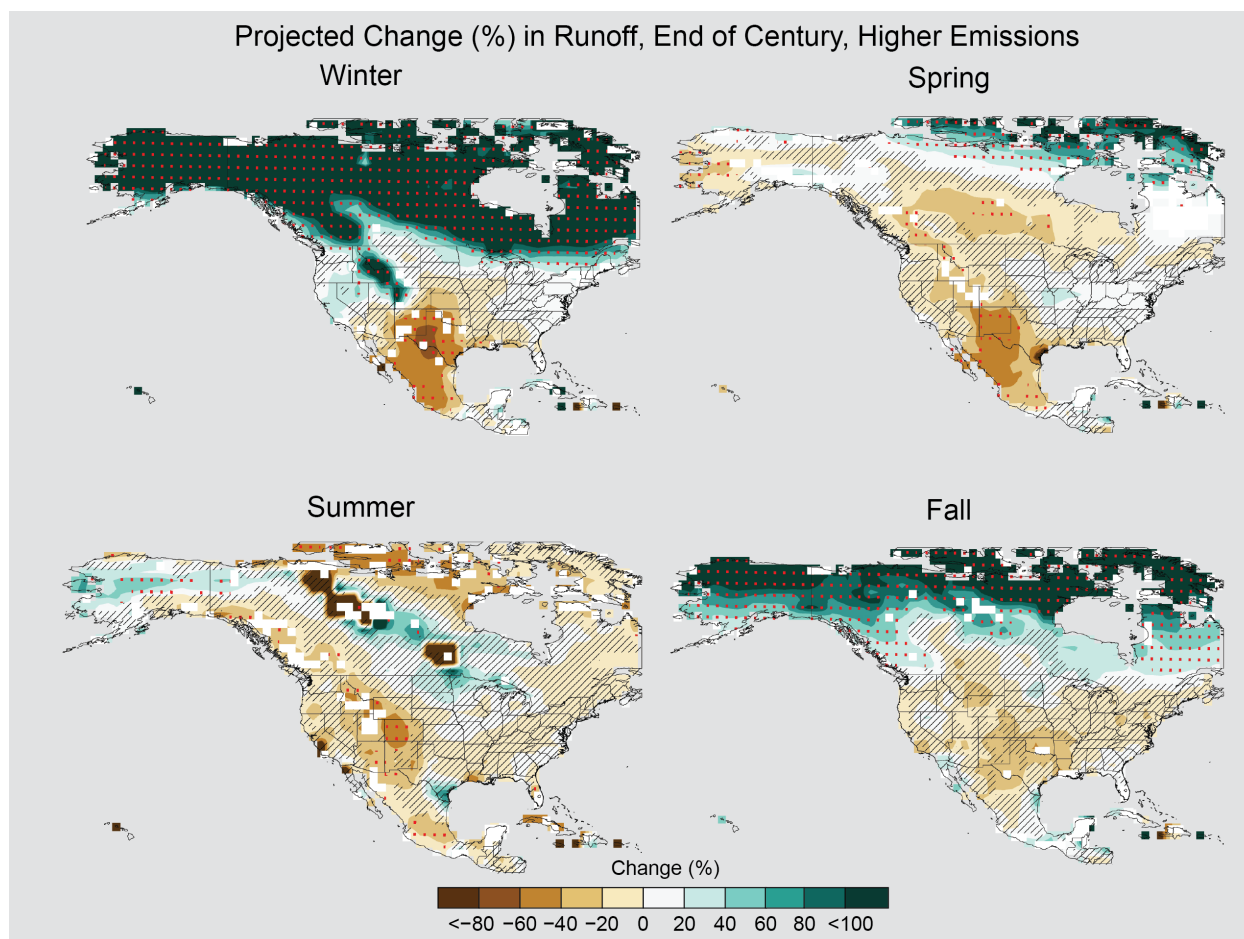


Figure 8.2. Projected end of the 21st century weighted CMIP5 multimodel average percent changes in total seasonal runoff (mmro) under the RCP8.5 scenario. Stippling indicates that changes are assessed to be large compared to natural variations. Hashing indicates that changes are assessed to be small compared to natural variations. Blank regions (if any) are where projections are assessed to be inconclusive (Appendix B).

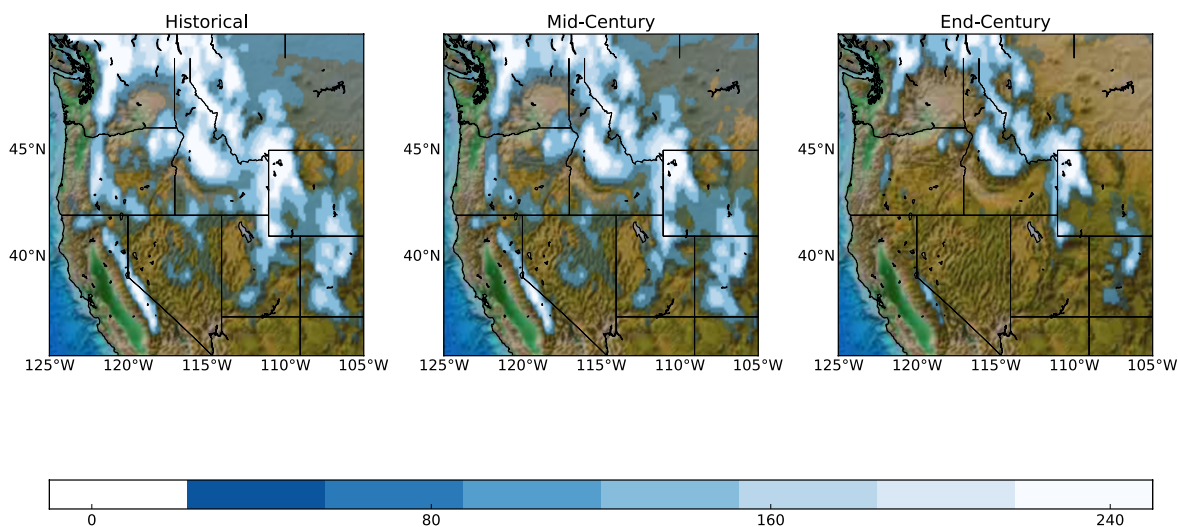


Figure 8.3. Projected changes in winter (DJF) Snow Water Equivalent at the middle and end of this century under the RCP8.5 scenario from a high-resolution version of the Community Atmospheric Model, CAM5 (Rhoades et al. 2016), Figure source: Lawrence Berkeley National Laboratory

1 REFERENCES

- 2 Abatzoglou, J.T. and A.P. Williams, 2016: Impact of anthropogenic climate change on wildfire
3 across western US forests. *Proceedings of the National Academy of Sciences*, **113**, 11770-
4 11775. <http://dx.doi.org/10.1073/pnas.1607171113>
5 <http://www.pnas.org/content/113/42/11770.abstract>
- 6 Angélil, O., D. Stone, M. Wehner, C.J. Paciorek, H. Krishnan, and W. Collins, 2016: An
7 independent assessment of anthropogenic attribution statements for recent extreme
8 temperature and rainfall events. *Journal of Climate*, **in press**, null.
9 <http://dx.doi.org/10.1175/JCLI-D-16-0077.1>
- 10 Armstrong, W.H., M.J. Collins, and N.P. Snyder, 2014: Hydroclimatic flood trends in the
11 northeastern United States and linkages with large-scale atmospheric circulation patterns.
12 *Hydrological Sciences Journal*, **59**, 1636-1655.
13 <http://dx.doi.org/10.1080/02626667.2013.862339>
- 14 Barnett, T.P. and D.W. Pierce, 2009: Sustainable water deliveries from the Colorado River in a
15 changing climate. *Proceedings of the National Academy of Sciences*, **106**, 7334-7338.
16 <http://dx.doi.org/10.1073/pnas.0812762106>
- 17 Barnett, T.P., D.W. Pierce, H.G. Hidalgo, C. Bonfils, B.D. Santer, T. Das, G. Bala, A.W. Wood,
18 T. Nozawa, A.A. Mirin, D.R. Cayan, and M.D. Dettinger, 2008: Human-induced changes in
19 the hydrology of the western United States. *Science*, **319**, 1080-1083.
20 <http://dx.doi.org/10.1126/science.1152538>
- 21 Bennet, H.H., F.H. Fowler, F.C. Harrington, R.C. Moore, J.C. Page, M.L. Cooke, H.A. Wallace,
22 and R.G. Tugwell, 1936: A Report of the Great Plains Area Drought Committee. In: (FERI),
23 N.D.N. (ed.), *Hopkins Papers* Franklin D. Roosevelt Library, Hyde Park, NY.
- 24 Berghuijs, W.R., R.A. Woods, C.J. Hutton, and M. Sivapalan, 2016: Dominant flood generating
25 mechanisms across the United States. *Geophysical Research Letters*, **43**, 4382-4390.
26 <http://dx.doi.org/10.1002/2016GL068070>
- 27 Bindoff, N.L., P.A. Stott, K.M. AchutaRao, M.R. Allen, N. Gillett, D. Gutzler, K. Hansingo, G.
28 Hegerl, Y. Hu, S. Jain, I.I. Mokhov, J. Overland, J. Perlwitz, R. Sebbari, and X. Zhang, 2013:
29 Detection and Attribution of Climate Change: from Global to Regional. *Climate Change*
30 *2013: The Physical Science Basis. Contribution of Working Group I to the Fifth Assessment*
31 *Report of the Intergovernmental Panel on Climate Change*. Stocker, T.F., D. Qin, G.-K.
32 Plattner, M. Tignor, S.K. Allen, J. Boschung, A. Nauels, Y. Xia, V. Bex, and P.M. Midgley,
33 Eds. Cambridge University Press, Cambridge, United Kingdom and New York, NY, USA,
34 867–952. <http://dx.doi.org/10.1017/CBO9781107415324.022> www.climatechange2013.org

- 1 Bond, N.A., M.F. Cronin, H. Freeland, and N. Mantua, 2015: Causes and impacts of the 2014
2 warm anomaly in the NE Pacific. *Geophysical Research Letters*, **42**, 3414-3420.
3 <http://dx.doi.org/10.1002/2015GL063306>
- 4 Brown, P.M., E.K. Heyerdahl, S.G. Kitchen, and M.H. Weber, 2008: Climate effects on
5 historical fires (1630–1900) in Utah. *International Journal of Wildland Fire*, **17**, 28-39.
6 <http://dx.doi.org/10.1071/WF07023>
- 7 Cayan, D., K. Kunkel, C. Castro, A. Gershunov, J. Barsugli, A. Ray, J. Overpeck, M. Anderson,
8 J. Russell, B. Rajagopalan, I. Rangwala, and P. Duffy, 2013: Ch. 6: Future climate: Projected
9 average. *Assessment of Climate Change in the Southwest United States: A Report Prepared*
10 *for the National Climate Assessment*. Garfin, G., A. Jardine, R. Merideth, M. Black, and S.
11 LeRoy, Eds. Island Press, Washington, D.C., 153-196.
12 <http://swccar.org/sites/all/themes/files/SW-NCA-color-FINALweb.pdf>
- 13 Cayan, D.R., T. Das, D.W. Pierce, T.P. Barnett, M. Tyree, and A. Gershunov, 2010: Future
14 dryness in the southwest US and the hydrology of the early 21st century drought.
15 *Proceedings of the National Academy of Sciences*, **107**, 21271-21276.
16 <http://dx.doi.org/10.1073/pnas.0912391107>
- 17 Cheng, L., M. Hoerling, A. AghaKouchak, B. Livneh, X.-W. Quan, and J. Eischeid, 2016: How
18 Has Human-Induced Climate Change Affected California Drought Risk? *Journal of Climate*,
19 **29**, 111-120. <http://dx.doi.org/10.1175/JCLI-D-15-0260.1>
- 20 Christensen, N.S. and D.P. Lettenmaier, 2007: A multimodel ensemble approach to assessment
21 of climate change impacts on the hydrology and water resources of the Colorado River
22 Basin. *Hydrology and Earth System Sciences*, **11**, 1417-1434. [http://dx.doi.org/10.5194/hess-](http://dx.doi.org/10.5194/hess-11-1417-2007)
23 [11-1417-2007](http://dx.doi.org/10.5194/hess-11-1417-2007)
- 24 Coats, S., B.I. Cook, J.E. Smerdon, and R. Seager, 2015: North American pancontinental
25 droughts in model simulations of the last millennium. *Journal of Climate*, **28**, 2025-2043.
26 <http://dx.doi.org/10.1175/JCLI-D-14-00634.1>
- 27 Collins, M., R. Knutti, J. Arblaster, J.-L. Dufresne, T. Fichefet, P. Friedlingstein, X. Gao, W.J.
28 Gutowski, T. Johns, G. Krinner, M. Shongwe, C. Tebaldi, A.J. Weaver, and M. Wehner,
29 2013: Long-term Climate Change: Projections, Commitments and Irreversibility. *Climate*
30 *Change 2013: The Physical Science Basis. Contribution of Working Group I to the Fifth*
31 *Assessment Report of the Intergovernmental Panel on Climate Change*. Stocker, T.F., D.
32 Qin, G.-K. Plattner, M. Tignor, S.K. Allen, J. Boschung, A. Nauels, Y. Xia, V. Bex, and
33 P.M. Midgley, Eds. Cambridge University Press, Cambridge, United Kingdom and New
34 York, NY, USA, 1029–1136. <http://dx.doi.org/10.1017/CBO9781107415324.024>
35 www.climatechange2013.org

- 1 Cook, E.R., C.A. Woodhouse, C.M. Eakin, D.M. Meko, and D.W. Stahle, 2004: Long-Term
2 Aridity Changes in the Western United States. *Science*, **306**, 1015-1018.
3 <http://dx.doi.org/10.1126/science.1102586>
- 4 Dai, A., 2013: Increasing drought under global warming in observations and models. *Nature*
5 *Climate Change*, **3**, 52-58. <http://dx.doi.org/10.1038/nclimate1633>
- 6 Diffenbaugh, N.S. and M. Scherer, 2013: Likelihood of July 2012 U.S. temperatures in pre-
7 industrial and current forcing regimes [in "Explaining Extremes of 2013 from a Climate
8 Perspective"]. *Bulletin of the American Meteorological Society*, **94**, S6-S9.
9 <http://dx.doi.org/10.1175/BAMS-D-13-00085.1>
- 10 Diffenbaugh, N.S., D.L. Swain, and D. Touma, 2015: Anthropogenic warming has increased
11 drought risk in California. *Proceedings of the National Academy of Sciences*, **112**, 3931-
12 3936. <http://dx.doi.org/10.1073/pnas.1422385112>
- 13 Frei, A., K.E. Kunkel, and A. Matonse, 2015: The Seasonal Nature of Extreme Hydrological
14 Events in the Northeastern United States. *Journal of Hydrometeorology*, **16**, 2065-2085.
15 <http://dx.doi.org/10.1175/JHM-D-14-0237.1>
- 16 Gochis, D., R. Schumacher, K. Friedrich, N. Doesken, M. Kelsch, J. Sun, K. Ikeda, D. Lindsey,
17 A. Wood, B. Dolan, S. Matrosov, A. Newman, K. Mahoney, S. Rutledge, R. Johnson, P.
18 Kucera, P. Kennedy, D. Sempere-Torres, M. Steiner, R. Roberts, J. Wilson, W. Yu, V.
19 Chandrasekar, R. Rasmussen, A. Anderson, and B. Brown, 2015: The Great Colorado Flood
20 of September 2013. *Bulletin of the American Meteorological Society*, **96**, 1461-1487.
21 <http://dx.doi.org/10.1175/BAMS-D-13-00241.1>
- 22 Hirsch, R.M. and K.R. Ryberg, 2012: Has the magnitude of floods across the USA changed with
23 global CO₂ levels? *Hydrological Sciences Journal*, **57**, 1-9.
24 <http://dx.doi.org/10.1080/02626667.2011.621895>
- 25 Hoerling, M., J. Eischeid, A. Kumar, R. Leung, A. Mariotti, K. Mo, S. Schubert, and R. Seager,
26 2014: Causes and Predictability of the 2012 Great Plains Drought. *Bulletin of the American*
27 *Meteorological Society*, **95**, 269-282. <http://dx.doi.org/10.1175/BAMS-D-13-00055.1>
- 28 Hoerling, M., D. Lettenmaier, D. Cayan, and B. Udall, 2009: Reconciling future Colorado River
29 flows. *Southwest Hydrology*, **8**.
- 30 Hoerling, M.P., J.K. Eischeid, X.-W. Quan, H.F. Diaz, R.S. Webb, R.M. Dole, and D.R.
31 Easterling, 2012: Is a Transition to Semipermanent Drought Conditions Imminent in the U.S.
32 Great Plains? *Journal of Climate*, **25**, 8380-8386. [http://dx.doi.org/10.1175/JCLI-D-12-](http://dx.doi.org/10.1175/JCLI-D-12-00449.1)
33 [00449.1](http://dx.doi.org/10.1175/JCLI-D-12-00449.1)

- 1 Hoerling, M., M. Chen, R. Dole, J. Eischeid, A. Kumar, J.W. Nielsen-Gammon, P. Pegion, J.
2 Perlwitz, X.-W. Quan, and T. Zhang, 2013: Anatomy of an extreme event. *Journal of*
3 *Climate*, **26**, 2811–2832. <http://dx.doi.org/10.1175/JCLI-D-12-00270.1>
- 4 Kapnick, S.B. and T.L. Delworth, 2013: Controls of Global Snow under a Changed Climate.
5 *Journal of Climate*, **26**, 5537–5562. <http://dx.doi.org/10.1175/JCLI-D-12-00528.1>
- 6 Karl, T.R., J.T. Melillo, and T.C. Peterson, eds. *Global Climate Change Impacts in the United*
7 *States*. ed. Karl, T.R., J.T. Melillo, and T.C. Peterson. 2009, Cambridge University Press:
8 New York, NY. 189. [http://downloads.globalchange.gov/usimpacts/pdfs/climate-impacts-](http://downloads.globalchange.gov/usimpacts/pdfs/climate-impacts-report.pdf)
9 [report.pdf](http://downloads.globalchange.gov/usimpacts/pdfs/climate-impacts-report.pdf)
- 10 Klos, P.Z., T.E. Link, and J.T. Abatzoglou, 2014: Extent of the rain-snow transition zone in the
11 western U.S. under historic and projected climate. *Geophysical Research Letters*, **41**, 4560-
12 4568. <http://dx.doi.org/10.1002/2014GL060500> <http://dx.doi.org/10.1002/2014GL060500>
- 13 Livneh, B. and M.P. Hoerling, 2016: The Physics of Drought in the U.S. Central Great Plains.
14 *Journal of Climate*, **29**, 6783–6804. <http://dx.doi.org/10.1175/JCLI-D-15-0697.1>
- 15 Mallakpour, I. and G. Villarini, 2015: The changing nature of flooding across the central United
16 States. *Nature Climate Change*, **5**, 250–254. <http://dx.doi.org/10.1038/nclimate2516>
- 17 Mao, Y., B. Nijssen, and D.P. Lettenmaier, 2015: Is climate change implicated in the 2013–2014
18 California drought? A hydrologic perspective. *Geophysical Research Letters*, **42**, 2805–2813.
19 <http://dx.doi.org/10.1002/2015GL063456>
- 20 Masson-Delmotte, V., M. Schulz, A. Abe-Ouchi, J. Beer, A. Ganopolski, J.F. González Rouco,
21 E. Jansen, K. Lambeck, J. Luterbacher, T. Naish, T. Osborn, B. Otto-Bliesner, T. Quinn, R.
22 Ramesh, M. Rojas, X. Shao, and A. Timmermann, 2013: Information from Paleoclimate
23 Archives. *Climate Change 2013: The Physical Science Basis. Contribution of Working*
24 *Group I to the Fifth Assessment Report of the Intergovernmental Panel on Climate Change*.
25 Stocker, T.F., D. Qin, G.-K. Plattner, M. Tignor, S.K. Allen, J. Boschung, A. Nauels, Y. Xia,
26 V. Bex, and P.M. Midgley, Eds. Cambridge University Press, Cambridge, United Kingdom
27 and New York, NY, USA, 383–464. <http://dx.doi.org/10.1017/CBO9781107415324.013>
28 www.climatechange2013.org
- 29 McCabe, G.J. and D.M. Wolock, 2014: Spatial and temporal patterns in conterminous United
30 States streamflow characteristics. *Geophysical Research Letters*, **41**, 6889–6897.
31 <http://dx.doi.org/10.1002/2014GL061980>
- 32 Meehl, G.A., C. Tebaldi, G. Walton, D. Easterling, and L. McDaniel, 2009: Relative increase of
33 record high maximum temperatures compared to record low minimum temperatures in the
34 US. *Geophysical Research Letters*, **36**, L23701. <http://dx.doi.org/10.1029/2009GL040736>

- Merz, B., S. Vorogushyn, S. Uhlemann, J. Delgado, and Y. Hundecha, 2012: HESS Opinions "More efforts and scientific rigour are needed to attribute trends in flood time series". *Hydrology and Earth System Sciences*, **16**, 1379-1387. <http://dx.doi.org/10.5194/hess-16-1379-2012>
- Milly, P.C.D. and K.A. Dunne, 2016: Potential evapotranspiration and continental drying. *Nature Climate Change*, **6**, 946-969. <http://dx.doi.org/10.1038/nclimate3046>
- Munoz, S.E., K.E. Gruley, A. Massie, D.A. Fike, S. Schroeder, and J.W. Williams, 2015: Cahokia's emergence and decline coincided with shifts of flood frequency on the Mississippi River. *Proceedings of the National Academy of Sciences*, **112**, 6319-6324. <http://dx.doi.org/10.1073/pnas.1501904112>
- Najafi, M.R. and H. Moradkhani, 2015: Multi-model ensemble analysis of runoff extremes for climate change impact assessments. *Journal of Hydrology*, **525**, 352-361. <http://dx.doi.org/http://dx.doi.org/10.1016/j.jhydrol.2015.03.045> <http://www.sciencedirect.com/science/article/pii/S0022169415002164>
- NOAA, 2008: Drought: Public fact sheet. National Oceanic and Atmospheric Administration, National Weather Service, Washington, D.C. <http://www.nws.noaa.gov/os/brochures/climate/DroughtPublic2.pdf>
- NOAA, 2016: State of the Climate: Drought for June 2016. National Oceanic and Atmospheric Administration, National Centers for Environmental Information, Asheville, NC. <http://www.ncdc.noaa.gov/sotc/drought/201606>
- O'Gorman, P.A., 2014: Contrasting responses of mean and extreme snowfall to climate change. *Nature*, **512**, 416-418. <http://dx.doi.org/10.1038/nature13625>
- Pall, P.C.M.P., M.F. Wehner, D.A. Stone, C.J. Paciorek, and W.D. Collins, 2016: Diagnosing anthropogenic contributions to heavy Colorado rainfall in September 2013. *Weather and Climate Extremes*, **in review**.
- Partain Jr., J.L., S. Alden, U.S. Bhatt, P.A. Bieniek, B.R. Brettschneider, R. Lader, P.Q. Olsson, T.S. Rupp, H. Strader, R.L.T. Jr., J.E. Walsh, A.D. York, and R.H. Zieh, 2016: An assessment of the role of anthropogenic climate change in the Alaska fire season of 2015. *Bulletin of the American Meteorological Society*, **97**, in press. <http://dx.doi.org/10.1175/BAMS-D-16-0149.1>
- Pierce, D.W., T.P. Barnett, H.G. Hidalgo, T. Das, C. Bonfils, B.D. Santer, G. Bala, M.D. Dettinger, D.R. Cayan, A. Mirin, A.W. Wood, and T. Nozawa, 2008: Attribution of declining western US snowpack to human effects. *Journal of Climate*, **21**, 6425-6444. <http://dx.doi.org/10.1175/2008JCLI2405.1>

- 1 Pierce, D.W. and D.R. Cayan, 2013: The Uneven Response of Different Snow Measures to
2 Human-Induced Climate Warming. *Journal of Climate*, **26**, 4148-4167.
3 <http://dx.doi.org/10.1175/jcli-d-12-00534.1>
- 4 Rhoades, C.C., et, and Al., 2016: Projecting 21st Century Snowpack Trends in Western USA
5 Mountains Using Variable-Resolution CESM. *Climate Dynamics*, **In press**.
- 6 Rupp, D.E., P.W. Mote, N. Massey, F.E.L. Otto, and M.R. Allen, 2013: Human influence on the
7 probability of low precipitation in the central United States in 2012 [in "Explaining Extremes
8 of 2013 from a Climate Perspective"]. *Bulletin of the American Meteorological Society*, **94**,
9 S2-S6. <http://dx.doi.org/10.1175/BAMS-D-13-00085.1>
- 10 Seager, R., M. Hoerling, S. Schubert, H. Wang, B. Lyon, A. Kumar, J. Nakamura, and N.
11 Henderson, 2015: Causes of the 2011–14 California Drought. *Journal of Climate*, **28**, 6997-
12 7024. <http://dx.doi.org/10.1175/JCLI-D-14-00860.1>
- 13 Seager, R., M. Hoerling, D.S. Siegfried, h. Wang, B. Lyon, A. Kumar, J. Nakamura, and N.
14 Henderson, 2014: Causes and predictability of the 2011-14 California drought. 40 pp. NOAA
15 Drought Task Force Narrative Team. <http://cpo.noaa.gov/MAPP/californiadroughtreport>
- 16 Sheffield, J., E.F. Wood, and M.L. Roderick, 2012: Little change in global drought over the past
17 60 years. *Nature*, **491**, 435-438. <http://dx.doi.org/10.1038/nature11575>
- 18 Swain, D., M. Tsiang, M. Haughen, D. Singh, A. Charland, B. Rajarthan, and N.S. Diffenbaugh,
19 2014: The extraordinary California drought of 2013/14: Character, context and the role of
20 climate change [in "Explaining Extremes of 2013 from a Climate Perspective"]. *Bulletin of*
21 *the American Meteorological Society*, **95**, S3-S6. [http://dx.doi.org/10.1175/1520-0477-](http://dx.doi.org/10.1175/1520-0477-95.9.S1.1)
22 [95.9.S1.1](http://dx.doi.org/10.1175/1520-0477-95.9.S1.1)
- 23 Walsh, J., D. Wuebbles, K. Hayhoe, J. Kossin, K. Kunkel, G. Stephens, P. Thorne, R. Vose, M.
24 Wehner, J. Willis, D. Anderson, S. Doney, R. Feely, P. Hennon, V. Kharin, T. Knutson, F.
25 Landerer, T. Lenton, J. Kennedy, and R. Somerville, 2014: Ch. 2: Our changing climate.
26 *Climate Change Impacts in the United States: The Third National Climate Assessment*.
27 Melillo, J.M., T.C. Richmond, and G.W. Yohe, Eds. U.S. Global Change Research Program,
28 Washington, D.C., 19-67. <http://dx.doi.org/10.7930/J0KW5CXT>
- 29 Wang, H., S. Schubert, R. Koster, Y.-G. Ham, and M. Suarez, 2014: On the Role of SST Forcing
30 in the 2011 and 2012 Extreme U.S. Heat and Drought: A Study in Contrasts. *Journal of*
31 *Hydrometeorology*, **15**, 1255-1273. <http://dx.doi.org/10.1175/JHM-D-13-069.1>
- 32 Wehner, M., D.R. Easterling, J.H. Lawrimore, R.R. Heim Jr, R.S. Vose, and B.D. Santer, 2011:
33 Projections of future drought in the continental United States and Mexico. *Journal of*
34 *Hydrometeorology*, **12**, 1359-1377. <http://dx.doi.org/10.1175/2011JHM1351.1>

- 1 Williams, A.P., R. Seager, J.T. Abatzoglou, B.I. Cook, J.E. Smerdon, and E.R. Cook, 2015:
2 Contribution of anthropogenic warming to California drought during 2012–2014.
3 *Geophysical Research Letters*, **42**, 6819–6828. <http://dx.doi.org/10.1002/2015GL064924>
- 4 Williams, I.N. and M.S. Torn, 2015: Vegetation controls on surface heat flux partitioning, and
5 land-atmosphere coupling. *Geophysical Research Letters*, **42**, 9416–9424.
6 <http://dx.doi.org/10.1002/2015GL066305>
- 7 Woodhouse, C.A., S.T. Gray, and D.M. Meko, 2006: Updated streamflow reconstructions for the
8 Upper Colorado River Basin. *Water Resources Research*, **42**.
9 <http://dx.doi.org/10.1029/2005WR004455>
- 10 Yoon, J.-H., B. Kravitz, P.J. Rasch, S.-Y.S. Wang, R.R. Gillies, and L. Hipps, 2015: Extreme
11 Fire Season in California: A Glimpse Into the Future? *Bulletin of the American*
12 *Meteorological Society*, **96**, S5–S9. <http://dx.doi.org/10.1175/bams-d-15-00114.1>
13 <http://journals.ametsoc.org/doi/abs/10.1175/BAMS-D-15-00114.1>

9. Extreme Storms

KEY FINDINGS

1. Human activities have contributed substantially to observed ocean-atmosphere variability in the Atlantic Ocean (*medium confidence*), and these changes have contributed to the observed increasing trend in North Atlantic hurricane activity since the 1970s (*medium confidence*).
2. For Atlantic and eastern North Pacific hurricanes and western North Pacific typhoons, increases are projected in precipitation rates (*high confidence*) and intensity (*medium confidence*). The frequency of the most intense of these storms is projected to increase in the Atlantic and western North Pacific (*low confidence*) and in the eastern North Pacific (*medium confidence*).
3. Tornado activity in the United States has become more variable, particularly over the 2000s, with a decrease in the number of days per year experiencing tornadoes, and an increase in the number of tornadoes on these days (*high confidence*). Confidence in past trends for hail and severe thunderstorm winds, however, is *low*. Climate models consistently project environmental changes that would putatively support an increase in the frequency and intensity of severe thunderstorms (a category that combines tornadoes, hail, and winds), especially over regions that are currently prone to these hazards, but confidence in the details of this increase is *low*.
4. There has been a trend toward earlier snowmelt and a decrease in snowstorm frequency on the southern margins of climatologically snowy areas (*medium confidence*). Winter storm tracks have shifted northward since 1950 over the Northern Hemisphere (*medium confidence*). Projections of winter storm frequency and intensity over the United States vary from increasing to decreasing depending on region, but model agreement is poor and confidence is *low*. Potential linkages between the frequency and intensity of severe winter storms in the United States and accelerated warming in the Arctic have been postulated, but they are complex, and, to some extent, controversial, and confidence in the connection is currently *low*.
5. The frequency and severity of landfalling “atmospheric rivers” on the U. S. West Coast (narrow streams of moisture that account for 30%–40% of precipitation and snowpack in the region and are associated with severe flooding events) will increase as a result of increasing evaporation and resulting higher atmospheric water vapor that occurs with increasing temperature. (*Medium confidence*)

9.1 Introduction

Quantifying how broad-scale average climate influences the behavior of extreme storms is particularly challenging, in part because extreme storms are comparatively short-lived events and

1 occur within an environment of largely random variability. Additionally, because the physical
2 mechanisms linking climate change and extreme storms can manifest in a variety of ways, even
3 the sign of the changes in the extreme storms can vary in a warming climate. This makes
4 detection and attribution of trends in extreme storm characteristics more difficult than detection
5 and attribution of trends in the larger environment in which the storms evolve (e.g., Ch. 6:
6 Temperature Change). Despite the challenges, good progress is being made for a variety of storm
7 types, such as tropical cyclones, severe convective storms (thunderstorms), winter storms, and
8 atmospheric river events.

9 **9.2 Tropical Cyclones (Hurricanes, Typhoons)**

10 Detection and attribution (Ch. 3: Detection and Attribution) of past changes in tropical cyclone
11 (TC) behavior remain a challenge due to the nature of the historical data, which are highly
12 heterogeneous in both time and among the various regions that collect and analyze the data
13 (Kossin et al. 2013; Klotzbach and Landsea 2015; Walsh et al. 2016). While there are ongoing
14 efforts to reanalyze and homogenize the data (e.g., Landsea et al. 2015; Kossin et al. 2013), there
15 is still low confidence that any reported long-term (multidecadal to centennial) increases in TC
16 activity are robust, after accounting for past changes in observing capabilities (which is
17 unchanged from the IPCC AR5 assessment statement [Hartmann et al. 2013]). This is not meant
18 to imply that no such increases have occurred, but rather that the data are not of a high enough
19 quality to determine this with much certainty.

20 Both theory and numerical modeling simulations (in general) indicate an increase in TC intensity
21 in a warmer world, and the models generally show an increase in the number of very intense TCs
22 (Bindoff et al. 2013; Christensen et al. 2013; Walsh et al. 2015; Knutson et al. 2015). In some
23 cases, climate models can be used to make attribution statements about TCs without formal
24 detection (see also Ch. 3: Detection and Attribution). For example, there is evidence that, in
25 addition to the effects of El Niño, anthropogenic forcing made the extremely active 2014
26 Hawaiian hurricane season substantially more likely, although no significant rising trend in TC
27 frequency near Hawai‘i was detected (Murakami et al. 2015).

28 Changes in frequency and intensity are not the only measures of TC behavior that may be
29 affected by climate variability and change, and there is evidence that the locations where TCs
30 reach their peak intensity has migrated poleward over the past 30 years in the Northern and
31 Southern Hemispheres, apparently in concert with environmental changes associated with the
32 independently observed expansion of the tropics (Kossin et al. 2014). The poleward migration in
33 the western North Pacific (Kossin et al. 2016), which includes a number of United States
34 Territories, appears particularly robust and remains significant over the past 60–70 years after
35 accounting for the known modes of natural variability in the region (Figure 9.1). The migration,
36 which can substantially change patterns of TC hazard exposure and mortality risk, is also evident
37 in 21st century Coupled Model Intercomparison Project Phase 5 (CMIP5) projections following
38 the RCP8.5 emissions trajectories, suggesting a possible link to human activities. Further

analysis comparing observed past TC behavior with climate model historical forcing runs (and with model control runs simulating multidecadal internal climate variability alone) are needed to better understand this process, but it is expected that this will be an area of heightened future research.

[INSERT FIGURE 9.1 HERE:]

Figure 9.1: Poleward migration, in degrees of latitude, of the location of annual-mean TC peak lifetime intensity in the western N. Pacific ocean, after accounting for the known regional modes of interannual (El Niño–Southern Oscillation; ENSO) and interdecadal (Pacific Decadal Oscillation; PDO) variability. The time series shows residuals of the multivariate regression of annually-averaged latitude of TC peak lifetime intensity onto the mean Niño-3.4 and PDO indices. Data are taken from the Joint Typhoon Warning Center (JTWC). Shading shows 95% confidence bounds for the trend. Annotated values at lower-right show the mean migration rate and its 95% confidence interval in degrees per decade for the period 1945–2013. (Figure source: redrawn from Kossin et al. 2016; © American Meteorological Society. Used with permission.)]

In the Atlantic, observed multidecadal variability of the ocean and atmosphere, which TCs are shown to respond to, has been attributed (Ch. 3: Detection and Attribution) to natural internal variability via meridional overturning ocean circulation changes (Delworth and Mann 2000), natural external variability caused by volcanic eruptions (Thompson and Solomon 2009; Evan 2012) and Saharan dust outbreaks (Evan et al. 2009, 2011), and anthropogenic external forcing via greenhouse gases and sulfate aerosols (Mann and Emanuel 2006; Booth et al. 2012; Dunstone et al. 2013). Determining the relative contributions of each mechanism to the observed multidecadal variability in the Atlantic, and even whether natural or anthropogenic factors have dominated, is presently a very active area of research and debate, and no consensus has yet been reached (Carslaw et al. 2013; Zhang et al. 2013; Tung and Zhao 2013; Mann et al. 2014; Stevens 2015; Sobel et al. 2016). Despite the level of disagreement about the relative magnitude of human influences, there is broad agreement in the literature that human factors have had a measurable impact on the observed oceanic and atmospheric variability in the North Atlantic, and there is *medium confidence* that this has contributed to the observed increase in hurricane activity since the 1970s. This is essentially unchanged from the Intergovernmental Panel on Climate Change Fifth Assessment Report (IPCC AR5) statement (Bindoff et al. 2013), although the post-AR5 literature has only served to further support this statement (Kossin et al. 2015). This is expected to remain an active research topic in the foreseeable future.

The IPCC AR5 consensus TC projections for the late 21st century (IPCC Figure 14.17; Christensen et al. 2013) include an increase in global mean TC intensity, precipitation rate, and frequency of very intense (Saffir-Simpson Category 4–5) TCs, and a decrease, or little change, in global tropical cyclone frequency. Since the IPCC AR5, some studies have provided additional support for this consensus, and some have challenged it. For example, a recent study (Fig. 9.2) projects increased mean TC intensity and occurrence of Saffir-Simpson Category 4–5 storms in the Atlantic Ocean basin and in most, but not all, other TC-supporting basins (Knutson et al.

2015). However, another recent (post-AR5) study proposed that increased thermal stratification of the upper ocean in CMIP5 climate warming scenarios should substantially reduce the warming-induced intensification of TCs estimated in previous studies (Huang et al. 2015). Follow-up studies, however, estimate that the effect of such increased stratification is relatively small, reducing the projected intensification of TCs by only about 10%–15% (Emanuel 2015; Tuleya et al. 2016).

Another recent study challenged the IPCC AR5 consensus projections by simulating increased global TC frequency over the 21st century under the RCP8.5 scenario (Emanuel 2013). However, another modeling study has found that neither direct analysis of CMIP5-class simulations, nor indirect inferences from the simulations (such as those of Emanuel 2013), could reproduce the sign of the change in TC frequency projected in a warmer world by high-resolution TC-permitting climate models (Wehner et al. 2015), which adds uncertainty to the results of Emanuel (2013).

In summary, despite new research that challenges some aspects of the AR5 consensus for late 21st century projected TC activity, it remains *likely* that global mean tropical cyclone maximum wind speeds and precipitation rates will increase; and it is *more likely than not* that the global frequency of occurrence of TCs will either decrease or remain essentially the same. Confidence in projected global increases of intensity and tropical cyclone precipitation rates is *medium* and *high*, respectively, as there is some consistency among studies and at least a fair degree of consensus. Confidence in projected increases in the frequency of very intense TCs is generally lower (*medium* in the eastern North Pacific and *low* in the western North Pacific and Atlantic) due to comparatively fewer studies available and due to the competing influences of projected reductions in overall storm frequency and increased mean intensity on the frequency of the most intense storms. Both the magnitude and sign of projected changes in individual ocean basins appears to depend on the large-scale pattern of changes to atmospheric circulation and ocean surface temperature (e.g., Knutson et al. 2015). Projections of these regional patterns of change — apparently critical for TC projections — are uncertain, leading to uncertainty in regional TC projections.

[INSERT FIGURE 9.2 HERE:]

Figure 9.2: Simulated occurrence of tropical cyclones of at least Category 4 intensity (surface winds of at least 59 m/s [132 mph]) for (a) present-day or (b) late-twenty-first-century (RCP4.5; CMIP5 multimodel ensemble) conditions; unit: storms per decade. Simulated tropical cyclone tracks were obtained using the GFDL hurricane model to resimulate (at higher resolution) the tropical cyclone cases originally obtained from the HiRAM C180 global mode. Occurrence refers to the number of days, over a 20-year period, in which a storm exceeding 59 m/s (132 mph) intensity was centered within the $10^\circ \times 10^\circ$ grid region. (c) Difference in occurrence rate between late twenty-first century and present day [(b) minus (a)]. White regions are regions where no tropical storms occurred in the simulations [in (a) and (b)] or where the difference

between the experiments is zero [in (c)]. (Figure source: redrawn from Knutson et al. 2015; © American Meteorological Society. Used with permission.)]

----- **START BOX 9.1 HERE** -----

Box 9.1: U.S. Landfalling Major Hurricane “Drought”

The last major hurricane (Saffir-Simpson Category 3 or higher) to make landfall in the continental United States was Wilma in 2005. The current 11-year (2006–2016) absence of U.S. major hurricane landfall events (sometimes colloquially referred to as a “hurricane drought”) is unprecedented in the historical records dating back to the mid-19th century, and has occurred in tandem with average to above-average basin-wide major hurricane counts. Is the absence of U.S. landfalling major hurricanes due to random luck, or are there systematic changes in climate driving this?

One recent study indicates that the absence of U.S. landfalling major hurricanes cannot readily be attributed to any sustained changes in the climate patterns that affect hurricanes (Hall and Heried 2015). Based on a statistical analysis of the historical North Atlantic hurricane database, the study found no evidence for memory in major U.S. landfalls from one year to the next and concluded that the 11-year absence of U.S. landfalling major hurricanes is random. Another recent study did identify a systematic pattern of atmosphere/ocean conditions that vary in such a way that conditions conducive to hurricane intensification in the deep tropics occur in concert with conditions conducive to weakening near the U.S. coast (Kossin 2016). This result suggests a possible relationship between climate and hurricanes; increasing basin-wide hurricane counts are associated with decreasing fraction of major hurricanes making U.S. landfall, as major hurricanes approaching the U.S. coast are more likely to weaken during active North Atlantic hurricane periods (such as the present period). It is unclear to what degree this relationship has affected absolute hurricane landfall counts during the recent active hurricane period from the mid-1990s, as the basin-wide number and landfalling fraction are in opposition (that is, there are more major hurricanes but a smaller fraction make landfall as major hurricanes). It is also unclear how this relationship may change as the climate continues to warm.

A third recent study (Hart et al. 2016) shows that the extent of the absence is sensitive to uncertainties in the historical data and even small variations in the definition of a major hurricane, which is somewhat arbitrary. It is also sensitive to the definition of U.S. landfall, which is a geopolitical-border-based constraint and has no physical meaning. In fact, many areas outside of the U.S. border have experienced major hurricane landfalls in the past 11 years. In this sense, the frequency of U.S. landfalling major hurricanes is not a particularly robust metric with which to study questions about hurricane activity and its relationship with climate variability. Furthermore, the 11-year absence of U.S. landfalling major hurricanes is not a particularly relevant metric in terms of coastal hazard exposure and risk. For example, Hurricanes Ike (2008), Irene (2011), and Sandy (2012), and most recently Hurricane Matthew (2016) brought severe

impacts to the U.S. coast despite not making landfall in the United States as major hurricanes. In the case of Hurricane Matthew, the center came within about 40 miles of the Florida coast while Matthew was a major hurricane, which is close enough to significantly impact the coast but not close enough to break the “drought” as it’s defined.

In summary, the 11-year absence of U.S. landfalling major hurricanes is anomalous. There is some evidence that systematic atmosphere/ocean variability has reduced the fraction of hurricanes making U.S. landfall since the mid-1990s, but this is at least partly countered by increased basin-wide numbers, and the net effect on landfall rates is unclear. Moreover, there is a large random element, and the metric itself suffers from lack of physical basis due to the arbitrary intensity threshold and geopolitically based constraints. Additionally, U.S. coastal risk, particularly from storm surge and freshwater flooding, depends strongly on storm size, propagation speed and direction, and rainfall rates. There is some danger, in the form of evoking complacency, in placing too much emphasis on the recent absence of a specific subset of hurricanes.

----- **END BOX 9.1 HERE** -----

9.3 Severe Convective Storms (Thunderstorms)

Tornado and severe thunderstorm events cause significant loss of life and property: more than one-third of the \$1 billion weather disasters in the United States during the past 25 years were due to such events, and relative to other extreme weather, the damages from convective weather hazards have undergone the largest increase (Smith and Katz 2013). A particular challenge in quantifying the existence and intensity of these events arises from the data source: rather than measurements, the occurrence of tornadoes and severe thunderstorms is determined by visual sightings by eyewitnesses (such as “storm spotters” and law enforcement officials). The reporting has been susceptible to changes in population density, modifications to reporting procedures and training, the introduction of video and social media, and so on. These have led to systematic, non-meteorological biases in the long-term data record.

Nonetheless, judicious use of the report database has revealed important information about tornado trends. Since the 1970s, the United States has experienced a decrease in the number of days per year on which tornadoes occur, but an increase in the number of tornadoes that form on such days (Brooks et al. 2014). One important implication is that the frequency of days with large numbers of tornadoes—tornado outbreaks—appears to be increasing (Figure 9.3). The extent of the season over which such tornado activity occurs is increasing as well: although tornadoes in the United States are observed in all months of the year, an earlier calendar-day start to the season of high activity is emerging. In general, there is more interannual variability, or volatility, in tornado occurrence (Tippett 2014; see also Elsner et al. 2015).

[INSERT FIGURE 9.3 HERE:]

Figure 9.3: Annual tornado activity in the United States over the period 1955–2013. The black squares indicate the number of days per year with at least one tornado rated (E)F1 or greater, and the black circles and line show the decadal mean line of such *tornado days*. The red triangles indicate the number of days per year with more than 30 tornadoes rated (E)F1 or greater, and the red circles and line show the decadal mean of these *tornado outbreaks*. (Figure source: redrawn from Brooks et al. 2014)]

Evaluations of hail and (non-tornadic) thunderstorm wind reports have thus far been less revealing. Although there is evidence of an increase in the number of hail days per year, the inherent uncertainty in reported hail size reduces the confidence in such a conclusion (Allen and Tippett 2015). Thunderstorm wind reports have proven to be even less reliable, because, as compared to tornadoes and hail, there is less tangible visual evidence; thus, although the United States has lately experienced several significant thunderstorm wind events (sometimes referred to as “derechos”), the lack of studies that explore long-term trends in wind events and the uncertainties in the historical data preclude any robust assessment.

It is possible to bypass the use of reports by exploiting the fact that the temperature, humidity, and wind in the larger vicinity—or “environment”—of a developing thunderstorm ultimately control the intensity, morphology, and hazardous tendency of the storm. Thus, the premise is that quantifications of the vertical profiles of temperature, humidity, and wind that can be used as a proxy for actual severe thunderstorm occurrence. In particular, a thresholded product of convective available potential energy (CAPE) and vertical wind shear over a surface-to-6 km layer (S06) constitutes one widely used means of representing the frequency of severe thunderstorms (Brooks et al. 2003). This environmental-proxy approach avoids the biases and other issues with eyewitness storm reports and is readily evaluated using the relatively coarse global data sets and global climate models. It has the disadvantage of assuming that a thunderstorm will necessarily form and then realize its environmental potential.

Upon employing Global Climate Models (GCMs) to evaluate CAPE and S06, a consistent finding among a growing number of proxy-based studies is a projected increase in the frequency of severe thunderstorm environments in the United States over the mid- to late 21st century (Van Klooster and Roebber 2009; Diffenbaugh et al. 2013; Gensini et al. 2014; Seely and Romps 2015). The most robust projected increases in frequency are over the central United States, during March-April-May (MAM) (Diffenbaugh et al. 2013). Based on the increased frequency of very high CAPE, increases in storm intensity are also projected over this same period (see also Del Genio et al. 2007).

Key limitations of the environmental proxy approach are being addressed through the applications of high-resolution dynamical downscaling, wherein sufficiently fine model grids are used so that individual thunderstorms are explicitly resolved, rather than implicitly represented (as through environmental proxies). The individually modeled thunderstorms can then be

quantified and assessed in terms of severity (Trapp et al. 2011; Robinson et al. 2013; Gensini and Mote 2014). A comprehensive approach using a dynamically downscaled GCM over 30-year historical and future climate periods showed the following: 1) a relatively large increase in the severe thunderstorm occurrence during the early part of MAM within the southeastern United States; 2) a northward and eastward expansion of the occurrence frequency, especially during MAM; and 3) a significant increase in the frequency in June-July-August (JJA), particularly in the northern Great Plains (Hoogewind et al. 2016).

The computational expense of high-resolution dynamical downscaling makes it difficult to generate model ensembles over long time periods, and thus to assess the uncertainty of the downscaled projections. Because these dynamical downscaling implementations focus on the statistics of storm occurrence rather than on faithful representations of individual events, they have generally been unconcerned with specific extreme convective events in history. So, for example, such downscaling does not address whether the intensity of an event like the Joplin, Missouri, tornado of May 22, 2011, would be amplified under projected future climates. Recently, the “pseudo-global warming” (PGW) methodology (see Schär et al. 1996), which is a variant of dynamical downscaling, has been adapted to address these and related questions. As an example, when the parent “supercell” of select historical tornado events forms under the climate conditions projected during the late 21st century, it becomes a more intense supercell rather than a benign, unorganized thunderstorm (Trapp and Hoogewind 2016). The intensity and, by extension, the severity of these supercells fall short of the expectations based on CAPE. However, the updrafts simulated under PGW are relatively more intense, but not in proportion to the projected higher levels of CAPE.

9.4 Winter Storms

The frequency of large snowfall years has decreased in the southern United States and Pacific Northwest and increased in the northern United States (see Ch. 7: Precipitation Change). The winters of 2013/2014 and 2014/2015 have contributed to this trend. They were characterized by frequent storms and heavier-than-normal snowfalls in the Midwest and Northeast and drought in the western United States. These were related to blocking (a large-scale pressure pattern with little or no movement) of the wintertime circulation in the Pacific sector of the Northern Hemisphere (e.g., Marinaro et al. 2015) that put this part of the United States in the primary winter storm track, while at the same time reducing the number of winter storms in California, causing severe drought conditions (Chang et al. 2015). While some observational studies suggest a linkage between blocking affecting the U.S. climate and enhanced Arctic warming (arctic amplification), specifically for an increase in highly amplified jet stream patterns in winter over the United States (Francis and Skific 2015), other studies show mixed results (Barnes and Polvani 2015; Perlwitz et al. 2015; Screen et al. 2015). Therefore, a definitive understanding of the effects of arctic amplification on midlatitude winter weather remains elusive, and other

explanations have been offered for the weather patterns of recent winters, such as anomalously strong Pacific trade winds (Yang et al. 2015).

Analysis of storm tracks indicates that there has been an increase in winter storm frequency and intensity since 1950, with a slight shift in tracks toward the poles (Wang et al. 2006, 2012; Vose et al. 2014). Current global climate models (CMIP5) do in fact predict an increase in extratropical cyclone (ETC) frequency over the eastern United States, including the most intense ETCs, under the high RCP8.5 emission scenario (Colle et al. 2013). However, there are large model-to-model differences in the realism of ETC simulations and in the projected changes. Moreover, projected ETC changes have large regional variations, including a decreased total frequency in the North Atlantic, further highlighting the complexity of the response to climate change.

9.5 Atmospheric Rivers

The term “atmospheric rivers” (ARs) refers to the relatively narrow streams of moisture transport that often occur within and across midlatitudes (Zhu and Newell 1998) (Figure 9.4), in part because they often transport as much water as in the Amazon River (Newell et al. 1992). While ARs occupy less than 10% of the circumference of the Earth at any given time, they account for 90% of the poleward moisture transport across midlatitudes. In many regions of the world, they account for a substantial fraction of the precipitation (Guan and Waliser 2015), and thus water supply, often delivered in the form of an extreme weather and precipitation event (Figure 9.4). For example, ARs account for 30%–40% of the typical snow pack in the Sierra Nevada mountains and annual precipitation in the U.S. West Coast states (Guan et al. 2010; Dettinger et al. 2011)—an essential summertime source of water for agriculture, consumption, and ecosystem health. However, this vital source of water is also associated with severe flooding, with observational evidence showing a close connection between historically high streamflow events and floods with landfalling AR events, in the west and other sectors of the United States (Ralph et al. 2006; Neiman et al. 2011; Moore et al. 2012). More recently, research has also demonstrated that ARs are often found to be critical in ending droughts in the western United States (Dettinger 2013).

[INSERT FIGURE 9.4 HERE:]

Figure 9.4: (upper left) Atmospheric rivers depicted in Special Sensor Microwave Imager (SSM/I) measurements of total column water vapor leading to extreme precipitation events at landfall locations. (upper right) Annual mean frequency of atmospheric river occurrence (for example, 12% means about 1 every 8 days) and their integrated moisture transport (IVT) (Guan and Waliser 2015). (lower left) ARs are the dominant synoptic storms for the U.S. west coast in terms of extreme precipitation (Ralph and Dettinger 2012) and (lower right) supply a large fraction of the annual precipitation in the U.S. west coast states (Dettinger et al. 2011). [Figure source: (upper left) Ralph et al. 2011, (upper right) Guan and Waliser 2015, (lower left) Ralph

and Dettinger 2012, (lower right), Dettinger et al. 2011; left panels, © American Meteorological Society. Used with permission.]]

Given the important role that ARs play in the water supply of the western United States and their role in weather and water extremes in the west and occasionally other parts of the United States (e.g., Rutz et al. 2014), it is critical to examine how climate change and the expected intensification of the global water cycle and atmospheric transports (e.g., Held and Soden 2006; Lavers et al. 2015) are projected to impact ARs (e.g., Dettinger and Ingram 2013). Under climate change conditions, ARs may be altered in a number of ways, namely their frequency, intensity, duration, and locations. In association with landfalling ARs, any of these would be expected to result in impacts on hazards and water supply given the discussion above. Assessments of ARs in climate change projections for the United States have been undertaken for central California from CMIP3 (Dettinger et al. 2011) and a number of studies for the West Coast of North America (Warner et al. 2015; Payne and Magnusdottir 2015; Gao et al. 2015; Radic et al. 2015; Hagos et al. 2016), and these studies have uniformly shown that ARs are likely to become more frequent and intense in the future. For example, one recent study reveals a large increase of AR days along the West Coast by the end of the 21st century in the RCP8.5 scenario, with fractional increases between 50% and 600%, depending on the seasons and landfall locations (Gao et al. 2015). Results from these studies (and Lavers et al. 2013 for ARs impacting the United Kingdom) show that these AR changes were predominantly driven by increasing atmospheric specific humidity, with little discernible change in the low-level winds. The higher atmospheric water vapor content in a warmer climate is to be expected because of an increase in saturation water vapor pressure with air temperature (Ch. 2: Scientific Basis). While the thermodynamic effect appears to dominate the climate change impact on ARs, leading to projected increases in ARs, there is evidence for a dynamical effect (that is, location change) related to the projected poleward shift of the subtropical jet that diminished the thermodynamic effect in the southern portion of the West Coast of North America (Gao et al. 2015).

The evidence for considerable increases in the number and intensity of ARs depends (as do all climate changes studies based on dynamical models) on the model fidelity in representing ARs and their interactions with the global climate/circulation. Additional confidence comes from studies that show qualitatively similar increases while also providing evidence that the models represent AR frequency, transports, and spatial distributions relatively well compared to observations (Payne and Magnusdottir 2015; Hagos et al. 2016). A caveat associated with drawing conclusions from any given study or differences between two is that they typically use different detection methodologies that are typically tailored to a regional setting (cf. Guan and Waliser 2015). Additional research is warranted to examine these storms from a global perspective, with additional and more in-depth process-oriented diagnostics/metrics. Stepping away from the sensitivities associated with defining atmospheric rivers, one study examined the intensification of the integrated vapor transport (IVT), easily and unambiguously defined (Lavers et al. 2015). That study found that for the RCP8.5 scenario, multimodel mean IVT and the IVT

- 1 associated with extremes above 95% percentile increase by 30%–40% in the North Pacific.
- 2 These results, along with the uniform findings of the studies above examining projected changes
- 3 in ARs for the western North America and the United Kingdom, give *high confidence* that the
- 4 frequency of AR storms will increase in association with rising global temperatures.

5

DRAFT

TRACEABLE ACCOUNTS

Key Finding 1

Human activities have contributed substantially to observed ocean-atmosphere variability in the Atlantic Ocean (*medium confidence*), and these changes have contributed to the observed increasing trend in North Atlantic hurricane activity since the 1970s (*medium confidence*).

Description of evidence base

The Key Finding and supporting text summarizes extensive evidence documented in the climate science literature and are similar to statements made in previous national (NCA3; Melillo et al., 2014) and international (IPCC 2013) assessments. Data limitations are documented in Kossin et al. (2013) and references therein. Contributions of natural and anthropogenic factors in observed multidecadal variability are quantified in Carslaw et al. 2013; Zhang et al. 2013; Tung and Zhao 2013; Mann et al. 2014; Stevens 2015; Sobel et al. 2016; Walsh et al. 2015.

Major uncertainties

Key remaining uncertainties are due to known and substantial heterogeneities in the historical tropical cyclone data and lack of robust consensus in determining the precise relative contributions of natural and anthropogenic factors in past variability of the tropical environment.

Assessment of confidence based on evidence and agreement, including short description of nature of evidence and level of agreement

☐ Very High

☐ High

X Medium

☐ Low

Although the range of estimates of natural versus anthropogenic contributions in the literature is fairly broad, virtually all studies identify a measurable, and generally substantial, anthropogenic influence. This does constitute a consensus for human contribution to the increases in tropical cyclone activity since 1970.

Summary sentence or paragraph that integrates the above information

The key message and supporting text summarizes extensive evidence documented in the climate science peer-reviewed literature. The uncertainties and points of consensus that were described in the NCA3 and IPCC assessments have continued.

Key Finding 2

For Atlantic and eastern North Pacific hurricanes and western North Pacific typhoons, increases are projected in precipitation rates (*high confidence*) and intensity (*medium confidence*). The frequency of the most intense of these storms is projected to increase in the Atlantic and western North Pacific (*low confidence*) and in the eastern North Pacific (*medium confidence*).

Description of evidence base

The Key Finding and supporting text summarizes extensive evidence documented in the climate science literature and are similar to statements made in previous national (NCA3; Melillo et al. 2014) and international (IPCC 2013) assessments. Since these assessments, more recent downscaling studies have further supported these assessments (e.g., Knutson et al. 2015), though pointing out that the changes (future increased intensity and tropical cyclone precipitation rates) may not occur in all basins.

Major uncertainties

A key uncertainty remains the lack of a supporting detectable anthropogenic signal in the historical data to add further confidence to these projections. As such, confidence in the projections is based on agreement among different modeling studies and physical understanding (for example, potential intensity theory for tropical cyclone intensities and the expectation of stronger moisture convergence, and thus higher precipitation rates, in tropical cyclones in a warmer environment containing greater amounts of environmental atmospheric moisture). Additional uncertainty stems from uncertainty in both the projected pattern and magnitude of future sea surface temperatures (Knutson et al. 2015).

Assessment of confidence based on evidence and agreement, including short description of nature of evidence and level of agreement

☐ Very High

☒ High

☒ Medium

☒ Low

Confidence is rated as *high* in tropical cyclone rainfall projections and *medium* in intensity projections since there are a number of publications supporting these overall conclusions, fairly well established theory, generally consistency among different studies, varying methods used in studies, and still a fairly strong consensus among studies. However, a limiting factor for confidence in the results is the lack of a supporting detectable anthropogenic contribution in observed tropical cyclone data.

There is *low to medium confidence* for increased occurrence of the most intense tropical cyclones for most basins, as there are relatively few formal studies that focus on these changes, and the change in occurrence of such storms would be enhanced by increased intensities, but reduced by decreased overall frequency of tropical cyclones.

Summary sentence or paragraph that integrates the above information

Models are generally in agreement that tropical cyclones will be more intense and have higher precipitation rates, at least in most basins. Given the agreement between models and support of theory and mechanistic understanding, there is *medium to high* confidence in the overall projection, although there is some limitation on confidence levels due to the lack of a supporting detectable anthropogenic contribution to tropical cyclone intensities or precipitation rates.

Key Finding 3

Tornado activity in the United States has become more variable, particularly over the 2000s, with a decrease in the number of days per year experiencing tornadoes, and an increase in the number of tornadoes on these days (*high confidence*). Confidence in past trends for hail and severe thunderstorm winds, however, is *low*. Climate models consistently project environmental changes that would putatively support an increase in the frequency and intensity of severe thunderstorms (a category that combines tornadoes, hail, and winds), especially over regions that are currently prone to these hazards, but confidence in the details of this increase is *low*.

Description of evidence base

Evidence for the first and second statement comes from the U.S. database of tornado reports. There are well known biases in this database, but application of an intensity threshold (\geq a rating of 1 on the [Enhanced] Fujita scale) and the quantification of tornado activity in terms of tornado days instead of raw numbers of reports are thought to reduce these biases. It is not known at this time whether the variability and trends are necessarily due to climate change.

The third statement is based on projections from a wide range of climate models, including GCMs and RCMs, run over the past 10 years (e.g., see the review by Brooks 2013). The evidence is derived from an “environmental-proxy” approach, which herein means that severe-thunderstorm occurrence is related to the occurrence of two key environmental parameters, CAPE and vertical wind shear. A limitation of this approach is the assumption that the thunderstorm will necessarily form and then realize its environmental potential. This assumption is indeed violated, albeit at levels that vary by region and season.

Major uncertainties

Regarding the first and second statements, there is still some uncertainty in the database, even when the data are filtered. The major uncertainty in the third statement equates to the aforementioned limitation (that is, the thunderstorm will necessarily form and then realize its environmental potential).

Assessment of confidence based on evidence and agreement, including short description of nature of evidence and level of agreement

High: That the variability in tornado activity has increased.

Medium: That the severe-thunderstorm environmental conditions will change with a changing climate, but

Low: on the precise (geographical and seasonal) realization of the environmental conditions as actual severe thunderstorms.

Summary sentence or paragraph that integrates the above information

Analyses and projections of tornado and severe thunderstorm trends depend on careful treatments of the historical record and on novel approaches on the use of climate model simulations.

Key Finding 4

There has been a trend toward earlier snowmelt and a decrease in snowstorm frequency on the southern margins of climatologically snowy areas (*medium confidence*). Winter storm tracks have shifted northward since 1950 over the Northern Hemisphere (*medium confidence*). Projections of winter storm frequency and intensity over the United States vary from increasing to decreasing depending on region, but model agreement is poor and confidence is *low*. Potential linkages between the frequency and intensity of severe winter storms in the United States and accelerated warming in the Arctic have been postulated, but they are complex, and, to some extent, controversial, and confidence in the connection is currently *low*.

Description of evidence base

The Key Finding and supporting text summarizes evidence documented in the climate science literature.

Evidence for changes in winter storm track changes are documented in a small number of studies (Wang et al. 2006, 2012). Future changes are documented in one study (Colle et al. 2013), but there are large model-to-model differences. The effects of arctic amplification on U.S. winter storms have been studied, but the results are mixed (Francis and Skific 2015; Barnes and Polvani 2015; Perlwitz et al. 2015; Screen et al. 2015), leading to considerable uncertainties.

Major uncertainties

Key remaining uncertainties relate to the sensitivity of observed snow changes to the spatial distribution of observing stations, and to historical changes in station location and observing practices. There is conflicting evidence about the effects of arctic amplification on CONUS winter weather.

Assessment of confidence based on evidence and agreement, including short description of nature of evidence and level of agreement

Very High

☒ High

☒ Medium

☒ Low

There is *high confidence* that warming has resulted in earlier snowmelt and decreased snowfall on the warm margins of areas with consistent snowpack based on a number of observational studies. There is *medium confidence* that Northern Hemisphere storm tracks have shifted north based on a small number of studies. There is *low confidence* in future changes in winter storm frequency and intensity based on conflicting evidence from analysis of climate model simulations.

Summary sentence or paragraph that integrates the above information

Decreases in snowfall on southern and low elevation margins of currently climatologically snowy areas are likely but winter storm frequency and intensity changes are uncertain.

Key Finding 5

The frequency and severity of landfalling “atmospheric rivers” on the U. S. West Coast (narrow streams of moisture that account for 30%–40% of precipitation and snowpack in the region and are associated with severe flooding events) will increase as a result of increasing evaporation and resulting higher atmospheric water vapor that occurs with increasing temperature. (*Medium confidence*)

Description of evidence base

The Key Finding and supporting text summarizes evidence documented in the climate science literature.

Evidence for the expectation of an increase in the frequency and severity of landfalling atmospheric rivers on the US West Coast comes from the CMIP-based climate change projection studies of Dettinger et al. 2011; Warner et al. 2015; Payne and Magnusdottir 2015; Gao et al. 2015; Radic et al. 2015; and Hagos et al. 2016. The close connection between atmospheric rivers and water availability and flooding is based on the present-day observation studies of Guan et al. 2010; Dettinger et al. 2011; Ralph et al. 2006; Neiman et al. 2011; Moore et al. 2012; and Dettinger 2013.

Major uncertainties

A modest uncertainty remains in the lack of a supporting detectable anthropogenic signal in the historical data to add further confidence to these projections. However, the overall increase in atmospheric rivers projected/expected is based to very large degree on the *very high confidence* there is that the atmospheric water vapor will increase. Thus, increasing water vapor coupled with little projected change in wind structure/intensity still indicates increases in the frequency/intensity of atmospheric rivers. A modest uncertainty arises in quantifying the expected change at a regional level (for example, northern Oregon vs southern Oregon) given that there are some changes expected in the position of the jet stream that might influence the degree of increase for different locations along the west coast.

Assessment of confidence based on evidence and agreement, including short description of nature of evidence and level of agreement

☐ Very High

☐ High

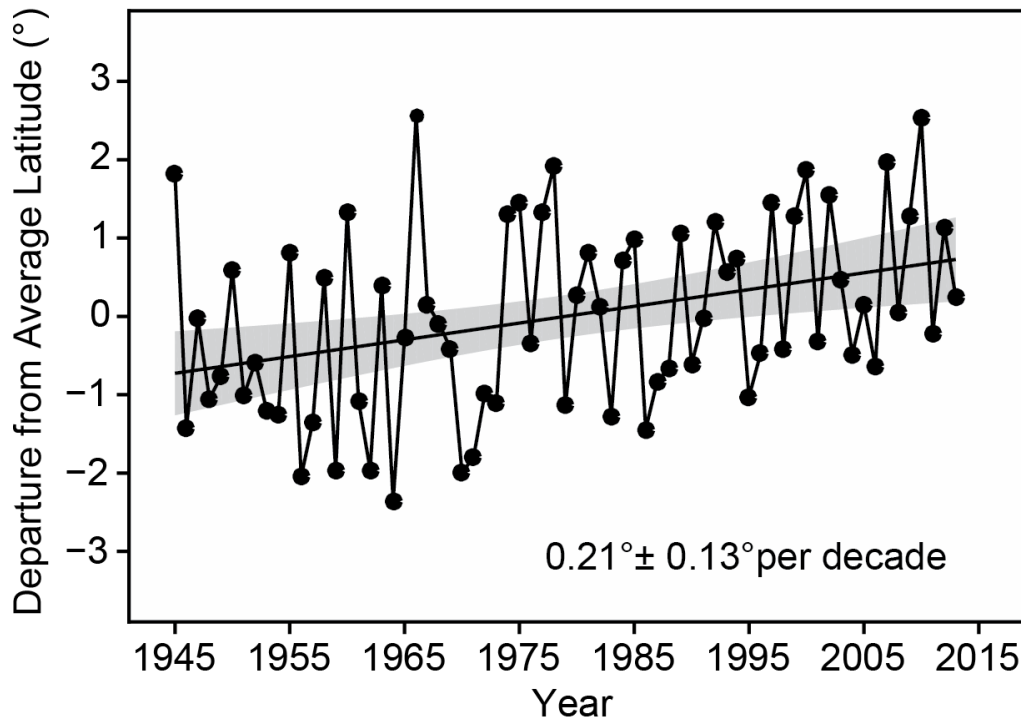
☒ Medium

☐ Low

Summary sentence or paragraph that integrates the above information

Increases in atmospheric river frequency and intensity are expected along the U.S. west coast, leading to the likelihood of more frequent flooding conditions, with uncertainties remaining in the details of the spatial structure of theses along the coast (for example, northern vs southern California)

1 FIGURES



2

3 **Figure 9.1:** Poleward migration, in degrees of latitude, of the location of annual-mean tropical
 4 cyclone (TC) peak lifetime intensity in the western North Pacific Ocean, after accounting for the
 5 known regional modes of interannual (El Niño–Southern Oscillation; ENSO) and interdecadal
 6 (Pacific Decadal Oscillation; PDO) variability. The time series shows residuals of the
 7 multivariate regression of annually-averaged latitude of TC peak lifetime intensity onto the mean
 8 Niño-3.4 and PDO indices. Data are taken from the Joint Typhoon Warning Center (JTWC).
 9 Shading shows 95% confidence bounds for the trend. Annotated values at lower-right show the
 10 mean migration rate and its 95% confidence interval in degrees per decade for the period 1945–
 11 2013. (Figure source: redrawn from Kossin et al. 2016; © American Meteorological Society.
 12 Used with permission.).

Simulated Occurrence of Category 4 and 5 Tropical Cyclones

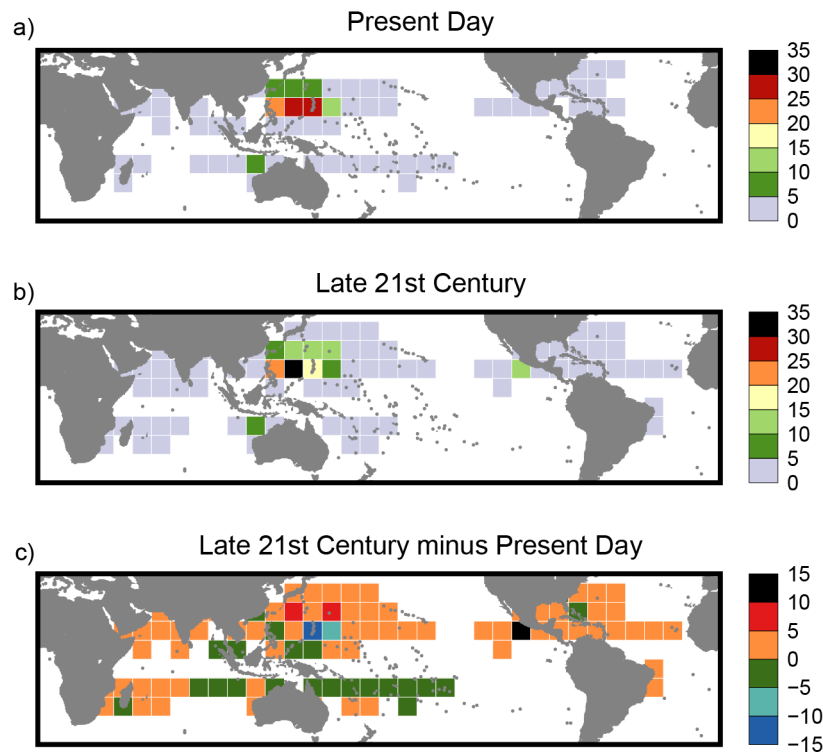


Figure 9.2: Simulated occurrence of tropical cyclones of at least Category 4 intensity (surface winds of at least 59 m/s or 130 mph) for a) present-day or b) late 21st century (RCP4.5; CMIP5 multimodel ensemble) conditions; unit: storms per decade. Simulated tropical cyclone tracks were obtained using the GFDL hurricane model to resimulate (at higher resolution) the tropical cyclone cases originally obtained from the HiRAM C180 global mode. Occurrence refers to the number of days, over a 20-year period, in which a storm exceeding 59 m/s intensity was centered within the $10^\circ \times 10^\circ$ grid region. c) Difference in occurrence rate between late 21st century and present day [(b) minus (a)]. White regions are regions where no tropical storms occurred in the simulations [in (a) and (b)] or where the difference between the experiments is zero [in (c)]. (Figure source: redrawn from Knutson et al. 2015; © American Meteorological Society. Used with permission.).

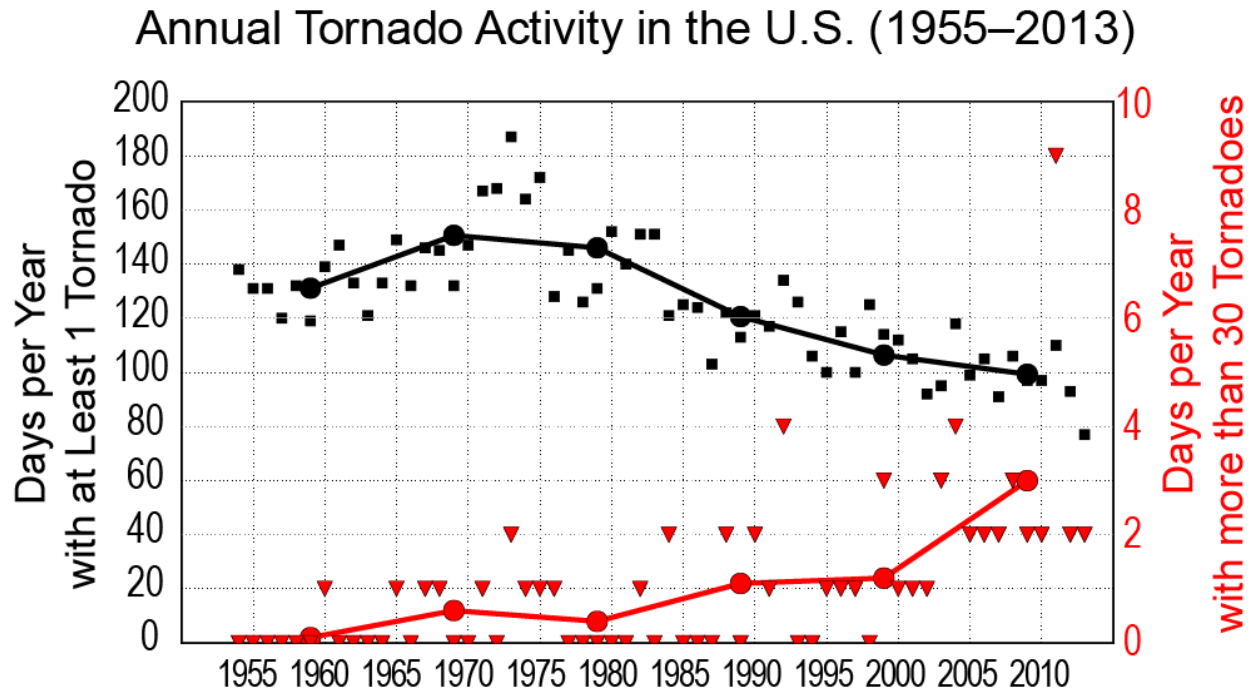


Figure 9.3: Annual tornado activity in the United States over the period 1955–2013. The black squares indicate the number of days per year with at least one tornado rated (E)F1 or greater, and the black circles and line show the decadal mean line of such *tornado days*. The red triangles indicate the number of days per year with more than 30 tornadoes rated (E)F1 or greater, and the red circles and line show the decadal mean of these *tornado outbreaks*. (Figure source: redrawn from Brooks et al. 2014)

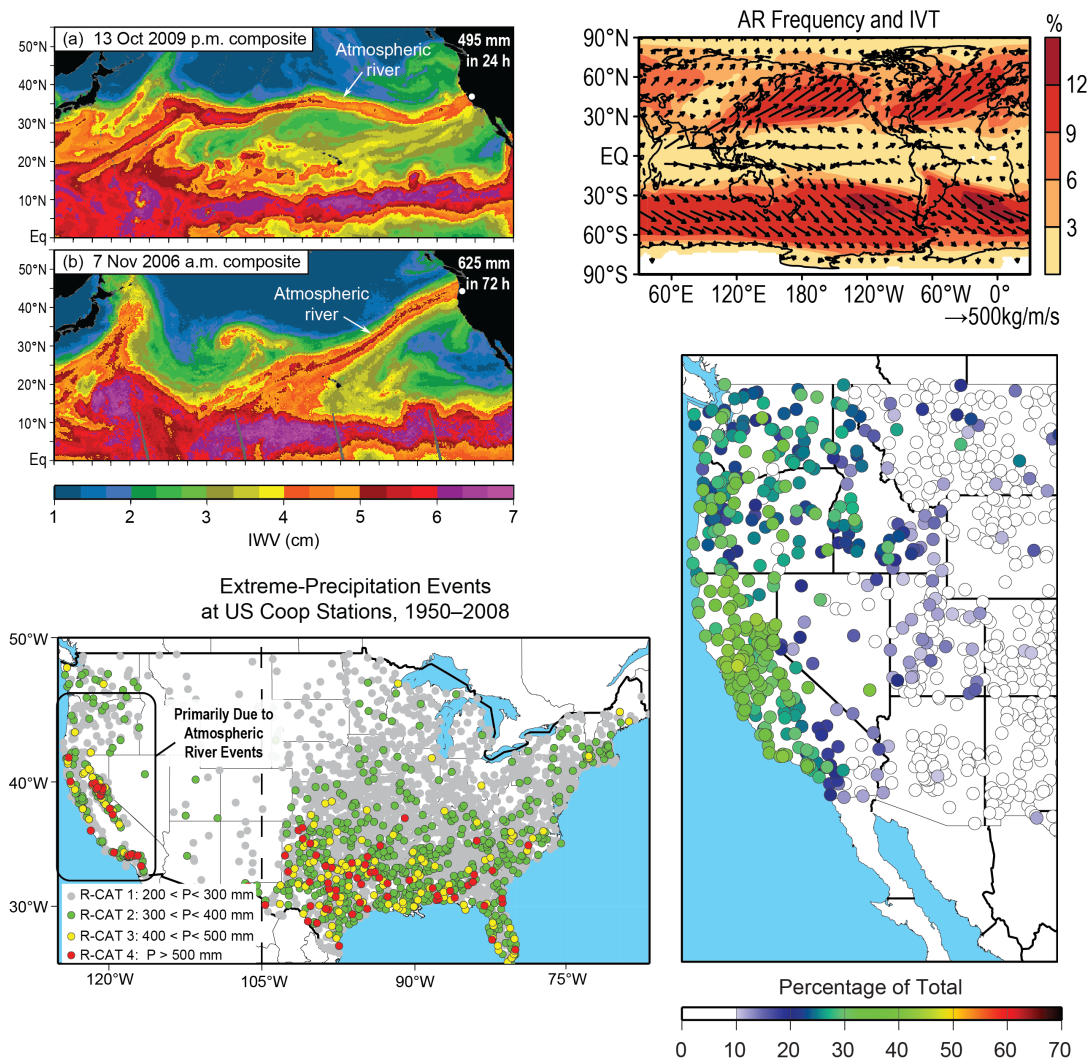


Figure 9.4: (upper left) Atmospheric rivers depicted in Special Sensor Microwave Imager (SSM/I) measurements of SSM/I total column water vapor leading to extreme precipitation events at landfall locations. (upper right) Annual mean frequency of atmospheric river occurrence (for example, 12% means about 1 every 8 days) and their integrated moisture transport (IVT) (Guan and Waliser 2015). (lower left) ARs are the dominant synoptic storms for the U.S. west coast in terms of extreme precipitation (Ralph and Dettinger 2012) and (lower right) supply a large fraction of the annual precipitation in the U.S. west coast states (Dettinger et al. 2011). [Figure source: (upper left) Ralph et al. 2011, (upper right) Guan and Waliser 2015, (lower left) Ralph and Dettinger 2012, (lower right), Dettinger et al. 2011; left panels, © American Meteorological Society. Used with permission.]

1 REFERENCES

- 2 Allen, J.T. and M.K. Tippett, 2015: The Characteristics of United States Hail Reports: 1955-
3 2014. *Electronic Journal of Severe Storms Meteorology*.
- 4 Barnes, E.A. and L.M. Polvani, 2015: CMIP5 Projections of Arctic Amplification, of the North
5 American/North Atlantic Circulation, and of Their Relationship. *Journal of Climate*, 28,
6 5254-5271. <http://dx.doi.org/10.1175/JCLI-D-14-00589.1>
- 7 Bindoff, N.L., P.A. Stott, K.M. AchutaRao, M.R. Allen, N. Gillett, D. Gutzler, K. Hansingo, G.
8 Hegerl, Y. Hu, S. Jain, I.I. Mokhov, J. Overland, J. Perlwitz, R. Sebbari, and X. Zhang, 2013:
9 Detection and Attribution of Climate Change: from Global to Regional. *Climate Change*
10 *2013: The Physical Science Basis. Contribution of Working Group I to the Fifth Assessment*
11 *Report of the Intergovernmental Panel on Climate Change*. Stocker, T.F., D. Qin, G.-K.
12 Plattner, M. Tignor, S.K. Allen, J. Boschung, A. Nauels, Y. Xia, V. Bex, and P.M. Midgley,
13 Eds. Cambridge University Press, Cambridge, United Kingdom and New York, NY, USA,
14 867–952. <http://dx.doi.org/10.1017/CBO9781107415324.022> www.climatechange2013.org
- 15 Booth, B.B.B., N.J. Dunstone, P.R. Halloran, T. Andrews, and N. Bellouin, 2012: Aerosols
16 implicated as a prime driver of twentieth-century North Atlantic climate variability. *Nature*,
17 484, 228-232. <http://dx.doi.org/10.1038/nature10946>
- 18 Brooks, H.E., 2013: Severe thunderstorms and climate change. *Atmospheric Research*, 123, 129-
19 138. <http://dx.doi.org/10.1016/j.atmosres.2012.04.002>
- 20 Brooks, H.E., G.W. Carbin, and P.T. Marsh, 2014: Increased variability of tornado occurrence in
21 the United States. *Science*, 346, 349-352. <http://dx.doi.org/10.1126/science.1257460>
- 22 Brooks, H.E., J.W. Lee, and J.P. Craven, 2003: The spatial distribution of severe thunderstorm
23 and tornado environments from global reanalysis data. *Atmospheric Research*, 67–68, 73-94.
24 [http://dx.doi.org/10.1016/S0169-8095\(03\)00045-0](http://dx.doi.org/10.1016/S0169-8095(03)00045-0)
- 25 Carslaw, K.S., L.A. Lee, C.L. Reddington, K.J. Pringle, A. Rap, P.M. Forster, G.W. Mann, D.V.
26 Spracklen, M.T. Woodhouse, L.A. Regayre, and J.R. Pierce, 2013: Large contribution of
27 natural aerosols to uncertainty in indirect forcing. *Nature*, 503, 67-71.
28 <http://dx.doi.org/10.1038/nature12674>
- 29 Chang, E.K.M., C. Zheng, P. Lanigan, A.M.W. Yau, and J.D. Neelin, 2015: Significant
30 modulation of variability and projected change in California winter precipitation by
31 extratropical cyclone activity. *Geophysical Research Letters*, 42, 5983-5991.
32 <http://dx.doi.org/10.1002/2015GL064424>
- 33 Christensen, J.H., K. Krishna Kumar, E. Aldrian, S.-I. An, I.F.A. Cavalcanti, M. de Castro, W.
34 Dong, P. Goswami, A. Hall, J.K. Kanyanga, A. Kitoh, J. Kossin, N.-C. Lau, J. Renwick, D.B.

- Stephenson, S.-P. Xie, and T. Zhou, 2013: Climate Phenomena and their Relevance for Future Regional Climate Change. *Climate Change 2013: The Physical Science Basis. Contribution of Working Group I to the Fifth Assessment Report of the Intergovernmental Panel on Climate Change*. Stocker, T.F., D. Qin, G.-K. Plattner, M. Tignor, S.K. Allen, J. Boschung, A. Nauels, Y. Xia, V. Bex, and P.M. Midgley, Eds. Cambridge University Press, Cambridge, United Kingdom and New York, NY, USA, 1217–1308.
<http://dx.doi.org/10.1017/CBO9781107415324.028> www.climatechange2013.org
- Colle, B.A., Z. Zhang, K.A. Lombardo, E. Chang, P. Liu, and M. Zhang, 2013: Historical Evaluation and Future Prediction of Eastern North American and Western Atlantic Extratropical Cyclones in the CMIP5 Models during the Cool Season. *Journal of Climate*, 26, 6882–6903. <http://dx.doi.org/10.1175/JCLI-D-12-00498.1>
- Del Genio, A.D., M.S. Yao, and J. Jonas, 2007: Will moist convection be stronger in a warmer climate? *Geophysical Research Letters*, 34, 5. <http://dx.doi.org/10.1029/2007GL030525>
- Delworth, L.T. and E.M. Mann, 2000: Observed and simulated multidecadal variability in the Northern Hemisphere. *Climate Dynamics*, 16, 661–676.
<http://dx.doi.org/10.1007/s003820000075>
- Dettinger, M.D., 2013: Atmospheric Rivers as Drought Busters on the U.S. West Coast. *Journal of Hydrometeorology*, 14, 1721–1732. <http://dx.doi.org/10.1175/JHM-D-13-02.1>
- Dettinger, M.D. and B.L. Ingram, 2013: The Coming Megafloods. *Scientific American*, 308, 64–71. <http://dx.doi.org/10.1038/scientificamerican0113-64>
- Dettinger, M.D., F.M. Ralph, T. Das, P.J. Neiman, and D.R. Cayan, 2011: Atmospheric rivers, floods and the water resources of California. *Water*, 3, 445–478.
<http://dx.doi.org/10.3390/w3020445> <http://www.mdpi.com/2073-4441/3/2/445/pdf>
- Diffenbaugh, N.S., M. Scherer, and R.J. Trapp, 2013: Robust increases in severe thunderstorm environments in response to greenhouse forcing. *Proceedings of the National Academy of Sciences*, 110, 16361–16366. <http://dx.doi.org/10.1073/pnas.1307758110>
- Dunstone, N.J., D.M. Smith, B.B.B. Booth, L. Hermanson, and R. Eade, 2013: Anthropogenic aerosol forcing of Atlantic tropical storms. *Nature Geoscience*, 6, 534–539.
<http://dx.doi.org/10.1038/ngeo1854>
- Elsner, J.B., S.C. Elsner, and T.H. Jagger, 2015: The increasing efficiency of tornado days in the United States. *Climate Dynamics*, 45, 651–659. <http://dx.doi.org/10.1007/s00382-014-2277-3>
- Emanuel, K., 2015: Effect of Upper-Ocean Evolution on Projected Trends in Tropical Cyclone Activity. *Journal of Climate*, 28, 8165–8170. <http://dx.doi.org/10.1175/JCLI-D-15-0401.1>

- 1 Emanuel, K.A., 2013: Downscaling CMIP5 climate models shows increased tropical cyclone
2 activity over the 21st century. *Proceedings of the National Academy of Sciences*, 110, 12219-
3 12224. <http://dx.doi.org/10.1073/pnas.1301293110>
- 4 Evan, A.T., 2012: Atlantic hurricane activity following two major volcanic eruptions. *Journal of*
5 *Geophysical Research*, 117, D06101. <http://dx.doi.org/10.1029/2011JD016716>
- 6 Evan, A.T., G.R. Foltz, D. Zhang, and D.J. Vimont, 2011: Influence of African dust on ocean-
7 atmosphere variability in the tropical Atlantic. *Nature Geoscience*, 4, 762-765.
8 <http://dx.doi.org/10.1038/ngeo1276>
- 9 Evan, A.T., D.J. Vimont, A.K. Heidinger, J.P. Kossin, and R. Bennartz, 2009: The role of
10 aerosols in the evolution of tropical North Atlantic Ocean temperature anomalies. *Science*,
11 324, 778-781. <http://dx.doi.org/10.1126/science.1167404>
- 12 Francis, J. and N. Skific, 2015: Evidence linking rapid Arctic warming to mid-latitude weather
13 patterns. *Philosophical Transactions of the Royal Society A: Mathematical, Physical and*
14 *Engineering Sciences*, 373. <http://dx.doi.org/10.1098/rsta.2014.0170>
- 15 Gao, Y., J. Lu, L.R. Leung, Q. Yang, S. Hagos, and Y. Qian, 2015: Dynamical and
16 thermodynamical modulations on future changes of landfalling atmospheric rivers over
17 western North America. *Geophysical Research Letters*, 42, 7179-7186.
18 <http://dx.doi.org/10.1002/2015GL065435>
- 19 Gensini, V.A. and T.L. Mote, 2014: Estimations of Hazardous Convective Weather in the United
20 States Using Dynamical Downscaling. *Journal of Climate*, 27, 6581-6589.
21 <http://dx.doi.org/10.1175/JCLI-D-13-00777.1>
- 22 Gensini, V.A., C. Ramseyer, and T.L. Mote, 2014: Future convective environments using
23 NARCCAP. *International Journal of Climatology*, 34, 1699-1705.
24 <http://dx.doi.org/10.1002/joc.3769>
- 25 Guan, B., N.P. Molotch, D.E. Waliser, E.J. Fetzer, and P.J. Neiman, 2010: Extreme snowfall
26 events linked to atmospheric rivers and surface air temperature via satellite measurements.
27 *Geophysical Research Letters*, 37, n/a-n/a. <http://dx.doi.org/10.1029/2010GL044696>
- 28 Guan, B. and D.E. Waliser, 2015: Detection of atmospheric rivers: Evaluation and application of
29 an algorithm for global studies. *Journal of Geophysical Research: Atmospheres*, 120, 12514-
30 12535. <http://dx.doi.org/10.1002/2015JD024257>
- 31 Hagos, S.M., L.R. Leung, J.-H. Yoon, J. Lu, and Y. Gao, 2016: A projection of changes in
32 landfalling atmospheric river frequency and extreme precipitation over western North
33 America from the Large Ensemble CESM simulations. *Geophysical Research Letters*, 43,
34 1357-1363. <http://dx.doi.org/10.1002/2015GL067392>

- 1 Hall, T. and K. Hereid, 2015: The frequency and duration of U.S. hurricane droughts.
2 *Geophysical Research Letters*, 42, 3482-3485. <http://dx.doi.org/10.1002/2015GL063652>
- 3 Hart, R.E., D.R. Chavas, and M.P. Guishard, 2016: The Arbitrary Definition of the Current
4 Atlantic Major Hurricane Landfall Drought. *Bulletin of the American Meteorological Society*,
5 97, 713-722. <http://dx.doi.org/10.1175/BAMS-D-15-00185.1>
- 6 Hartmann, D.L., A.M.G. Klein Tank, M. Rusticucci, L.V. Alexander, S. Brönnimann, Y.
7 Charabi, F.J. Dentener, E.J. Dlugokencky, D.R. Easterling, A. Kaplan, B.J. Soden, P.W.
8 Thorne, M. Wild, and P.M. Zhai, 2013: Observations: Atmosphere and Surface. *Climate*
9 *Change 2013: The Physical Science Basis. Contribution of Working Group I to the Fifth*
10 *Assessment Report of the Intergovernmental Panel on Climate Change*. Stocker, T.F., D.
11 Qin, G.-K. Plattner, M. Tignor, S.K. Allen, J. Boschung, A. Nauels, Y. Xia, V. Bex, and
12 P.M. Midgley, Eds. Cambridge University Press, Cambridge, United Kingdom and New
13 York, NY, USA, 159–254. <http://dx.doi.org/10.1017/CBO9781107415324.008>
14 www.climatechange2013.org
- 15 Held, I.M. and B.J. Soden, 2006: Robust responses of the hydrological cycle to global warming.
16 *Journal of Climate*, 19, 5686-5699. <http://dx.doi.org/10.1175/jcli3990.1>
- 17 Hoogewind, K.A., M.E. Baldwin, and R.J. Trapp, 2016: Climate change and hazardous
18 convective weather in the United States: Insights from high-resolution dynamical
19 downscaling. *Journal of Climate*, Submitted.
- 20 Huang, P., I.I. Lin, C. Chou, and R.-H. Huang, 2015: Change in ocean subsurface environment to
21 suppress tropical cyclone intensification under global warming. *Nature Communications*, 6,
22 7188. <http://dx.doi.org/10.1038/ncomms8188> <http://dx.doi.org/10.1038/ncomms8188>
- 23 IPCC, 2013: *Climate Change 2013: The Physical Science Basis. Contribution of Working Group*
24 *I to the Fifth Assessment Report of the Intergovernmental Panel on Climate Change*.
25 Cambridge University Press, Cambridge, UK and New York, NY, 1535 pp.
26 <http://dx.doi.org/10.1017/CBO9781107415324> www.climatechange2013.org
- 27 Klotzbach, P.J. and C.W. Landsea, 2015: Extremely Intense Hurricanes: Revisiting Webster et
28 al. (2005) after 10 Years. *Journal of Climate*, 28, 7621-7629.
29 <http://dx.doi.org/10.1175/JCLI-D-15-0188.1>
- 30 Knutson, T.R., J.J. Sirutis, M. Zhao, R.E. Tuleya, M. Bender, G.A. Vecchi, G. Villarini, and D.
31 Chavas, 2015: Global Projections of Intense Tropical Cyclone Activity for the Late Twenty-
32 First Century from Dynamical Downscaling of CMIP5/RCP4.5 Scenarios. *Journal of*
33 *Climate*, 28, 7203-7224. <http://dx.doi.org/10.1175/JCLI-D-15-0129.1>
- 34 Kossin, J., 2016: Hurricane intensification along U. S. coast suppressed during active hurricane
35 periods. *Nature*, doi:10.1038/nature20783

- 1 Kossin, J.P., K.A. Emanuel, and S.J. Camargo, 2016: Past and Projected Changes in Western
2 North Pacific Tropical Cyclone Exposure. *Journal of Climate*, 29, 5725-5739.
3 <http://dx.doi.org/10.1175/JCLI-D-16-0076.1>
- 4 Kossin, J.P., K.A. Emanuel, and G.A. Vecchi, 2014: The poleward migration of the location of
5 tropical cyclone maximum intensity. *Nature*, 509, 349-352.
6 <http://dx.doi.org/10.1038/nature13278>
- 7 Kossin, J.P., T.R. Karl, T.R. Knutson, K.A. Emanuel, K.E. Kunkel, and J.J. O'Brien, 2015:
8 Reply to "Comments on 'Monitoring and Understanding Trends in Extreme Storms: State of
9 Knowledge'". *Bulletin of the American Meteorological Society*, 96, 1177-1179.
10 <http://dx.doi.org/10.1175/BAMS-D-14-00261.1>
- 11 Kossin, J.P., T.L. Olander, and K.R. Knapp, 2013: Trend analysis with a new global record of
12 tropical cyclone intensity. *Journal of Climate*, 26, 9960-9976.
13 <http://dx.doi.org/10.1175/JCLI-D-13-00262.1>
- 14 Landsea, C., J. Franklin, and J. Beven, 2015: The revised Atlantic hurricane database
15 (HURDAT2) In: (NHC), N.H.C. (ed.). NHC, Miami, FL.
- 16 Lavers, D.A., R.P. Allan, G. Villarini, B. Lloyd-Hughes, D.J. Brayshaw, and A.J. Wade, 2013:
17 Future changes in atmospheric rivers and their implications for winter flooding in Britain.
18 *Environmental Research Letters*, 8, 034010. [http://dx.doi.org/10.1088/1748-](http://dx.doi.org/10.1088/1748-9326/8/3/034010)
19 [9326/8/3/034010](http://dx.doi.org/10.1088/1748-9326/8/3/034010)
- 20 Lavers, D.A., F.M. Ralph, D.E. Waliser, A. Gershunov, and M.D. Dettinger, 2015: Climate
21 change intensification of horizontal water vapor transport in CMIP5. *Geophysical Research*
22 *Letters*, 42, 5617-5625. <http://dx.doi.org/10.1002/2015GL064672>
- 23 Mann, M.E. and K.A. Emanuel, 2006: Atlantic hurricane trends linked to climate change. *Eos*,
24 *Transactions of the American Geophysical Union*, 87, 233-244.
25 <http://dx.doi.org/10.1029/2006EO240001>
- 26 Mann, M.E., B.A. Steinman, and S.K. Miller, 2014: On forced temperature changes, internal
27 variability, and the AMO. *Geophysical Research Letters*, 41, 3211-3219.
28 <http://dx.doi.org/10.1002/2014GL059233>
- 29 Marinaro, A., S. Hilberg, D. Changnon, and J.R. Angel, 2015: The North Pacific–Driven Severe
30 Midwest Winter of 2013/14. *Journal of Applied Meteorology and Climatology*, 54, 2141-
31 2151. <http://dx.doi.org/10.1175/JAMC-D-15-0084.1>
- 32 Melillo, J.M., T.C. Richmond, and G.W. Yohe, eds. *Climate Change Impacts in the United*
33 *States: The Third National Climate Assessment*. 2014, U.S. Global Change Research
34 Program: Washington, D.C. 842. <http://dx.doi.org/10.7930/J0Z31WJ2>.

- 1 Moore, B.J., P.J. Neiman, F.M. Ralph, and F.E. Barthold, 2012: Physical Processes Associated
2 with Heavy Flooding Rainfall in Nashville, Tennessee, and Vicinity during 1–2 May 2010:
3 The Role of an Atmospheric River and Mesoscale Convective Systems. *Monthly Weather*
4 *Review*, 140, 358–378. <http://dx.doi.org/10.1175/MWR-D-11-00126.1>
- 5 Murakami, H., G.A. Vecchi, T.L. Delworth, K. Paffendorf, L. Jia, R. Gudgel, and F. Zeng, 2015:
6 Investigating the Influence of Anthropogenic Forcing and Natural Variability on the 2014
7 Hawaiian Hurricane Season. *Bulletin of the American Meteorological Society*, 96, S115–
8 S119. <http://dx.doi.org/10.1175/BAMS-D-15-00119.1>
- 9 Neiman, P.J., L.J. Schick, F.M. Ralph, M. Hughes, and G.A. Wick, 2011: Flooding in Western
10 Washington: The Connection to Atmospheric Rivers. *Journal of Hydrometeorology*, 12,
11 1337–1358. <http://dx.doi.org/10.1175/2011JHM1358.1>
- 12 Newell, R.E., N.E. Newell, Y. Zhu, and C. Scott, 1992: Tropospheric rivers? – A pilot study.
13 *Geophysical Research Letters*, 19, 2401–2404. <http://dx.doi.org/10.1029/92GL02916>
- 14 Payne, A.E. and G. Magnusdottir, 2015: An evaluation of atmospheric rivers over the North
15 Pacific in CMIP5 and their response to warming under RCP 8.5. *Journal of Geophysical*
16 *Research: Atmospheres*, 120, 11,173–11,190. <http://dx.doi.org/10.1002/2015JD023586>
- 17 Perlwitz, J., M. Hoerling, and R. Dole, 2015: Arctic Tropospheric Warming: Causes and
18 Linkages to Lower Latitudes. *Journal of Climate*, 28, 2154–2167.
19 <http://dx.doi.org/10.1175/JCLI-D-14-00095.1>
- 20 Radić, V., A.J. Cannon, B. Menounos, and N. Gi, 2015: Future changes in autumn atmospheric
21 river events in British Columbia, Canada, as projected by CMIP5 global climate models.
22 *Journal of Geophysical Research: Atmospheres*, 120, 9279–9302.
23 <http://dx.doi.org/10.1002/2015JD023279>
- 24 Ralph, F.M. and M.D. Dettinger, 2012: Historical and National Perspectives on Extreme West
25 Coast Precipitation Associated with Atmospheric Rivers during December 2010. *Bulletin of*
26 *the American Meteorological Society*, 93, 783–790. [http://dx.doi.org/10.1175/BAMS-D-11-](http://dx.doi.org/10.1175/BAMS-D-11-00188.1)
27 [00188.1](http://dx.doi.org/10.1175/BAMS-D-11-00188.1)
- 28 Ralph, F.M., P.J. Neiman, G.A. Wick, S.I. Gutman, M.D. Dettinger, D.R. Cayan, and A.B.
29 White, 2006: Flooding on California's Russian River: Role of atmospheric rivers.
30 *Geophysical Research Letters*, 33, L13801. <http://dx.doi.org/10.1029/2006GL026689>
- 31 Robinson, E.D., R.J. Trapp, and M.E. Baldwin, 2013: The Geospatial and Temporal
32 Distributions of Severe Thunderstorms from High-Resolution Dynamical Downscaling.
33 *Journal of Applied Meteorology and Climatology*, 52, 2147–2161.
34 <http://dx.doi.org/10.1175/JAMC-D-12-0131.1>

- 1 Rutz, J.J., W.J. Steenburgh, and F.M. Ralph, 2014: Climatological Characteristics of
2 Atmospheric Rivers and Their Inland Penetration over the Western United States. *Monthly*
3 *Weather Review*, 142, 905-921. <http://dx.doi.org/10.1175/MWR-D-13-00168.1>
- 4 Schär, C., C. Frei, D. Lüthi, and H.C. Davies, 1996: Surrogate climate-change scenarios for
5 regional climate models. *Geophysical Research Letters*, 23, 669-672.
6 <http://dx.doi.org/10.1029/96GL00265>
- 7 Screen, J.A., C. Deser, and L. Sun, 2015: Projected changes in regional climate extremes arising
8 from Arctic sea ice loss. *Environmental Research Letters*, 10, 084006.
9 <http://dx.doi.org/10.1088/1748-9326/10/8/084006>
- 10 Seeley, J.T. and D.M. Romps, 2015: The Effect of Global Warming on Severe Thunderstorms in
11 the United States. *Journal of Climate*, 28, 2443-2458. <http://dx.doi.org/10.1175/JCLI-D-14->
12 [00382.1](http://dx.doi.org/10.1175/JCLI-D-14-00382.1)
- 13 Smith, A.B. and R.W. Katz, 2013: U.S. billion-dollar weather and climate disasters: Data
14 sources, trends, accuracy and biases. *Natural Hazards*, 67, 387-410.
15 <http://dx.doi.org/10.1007/s11069-013-0566-5>
- 16 Sobel, A.H., S.J. Camargo, T.M. Hall, C.-Y. Lee, M.K. Tippett, and A.A. Wing, 2016: Human
17 influence on tropical cyclone intensity. *Science*, 353, 242-246.
18 <http://dx.doi.org/10.1126/science.aaf6574>
- 19 Stevens, B., 2015: Rethinking the Lower Bound on Aerosol Radiative Forcing. *Journal of*
20 *Climate*, 28, 4794-4819. <http://dx.doi.org/10.1175/JCLI-D-14-00656.1>
- 21 Thompson, D.W.J. and S. Solomon, 2009: Understanding Recent Stratospheric Climate Change.
22 *Journal of Climate*, 22, 1934-1943. <http://dx.doi.org/10.1175/2008JCLI2482.1>
- 23 Tippett, M.K., 2014: Changing volatility of U.S. annual tornado reports. *Geophysical Research*
24 *Letters*, 41, 6956-6961. <http://dx.doi.org/10.1002/2014GL061347>
- 25 Trapp, R.J. and K.A. Hoogewind, 2016: The Realization of Extreme Tornadic Storm Events
26 under Future Anthropogenic Climate Change. *Journal of Climate*, 29, 5251-5265.
27 <http://dx.doi.org/10.1175/JCLI-D-15-0623.1>
- 28 Trapp, R.J., E.D. Robinson, M.E. Baldwin, N.S. Diffenbaugh, and B.R.J. Schwedler, 2011:
29 Regional climate of hazardous convective weather through high-resolution dynamical
30 downscaling. *Climate Dynamics*, 37, 677-688. <http://dx.doi.org/10.1007/s00382-010-0826-y>
- 31 Tuleya, R.E., M. Bender, T.R. Knutson, J.J. Sirutis, B. Thomas, and I. Ginis, 2016: Impact of
32 Upper-Tropospheric Temperature Anomalies and Vertical Wind Shear on Tropical Cyclone

- 1 Evolution Using an Idealized Version of the Operational GFDL Hurricane Model. *Journal of*
2 *the Atmospheric Sciences*, 73, 3803-3820. <http://dx.doi.org/10.1175/JAS-D-16-0045.1>
- 3 Tung, K.-K. and J. Zhou, 2013: Using data to attribute episodes of warming and cooling in
4 instrumental records. *Proceedings of the National Academy of Sciences*.
5 <http://dx.doi.org/10.1073/pnas.1212471110>
- 6 Van Klooster, S.L. and P.J. Roebber, 2009: Surface-Based Convective Potential in the
7 Contiguous United States in a Business-as-Usual Future Climate. *Journal of Climate*, 22,
8 3317-3330. <http://dx.doi.org/10.1175/2009JCLI2697.1>
- 9 Vose, R.S., S. Applequist, M.A. Bourassa, S.C. Pryor, R.J. Barthelmie, B. Blanton, P.D.
10 Bromirski, H.E. Brooks, A.T. DeGaetano, R.M. Dole, D.R. Easterling, R.E. Jensen, T.R.
11 Karl, R.W. Katz, K. Klink, M.C. Kruk, K.E. Kunkel, M.C. MacCracken, T.C. Peterson, K.
12 Shein, B.R. Thomas, J.E. Walsh, X.L. Wang, M.F. Wehner, D.J. Wuebbles, and R.S. Young,
13 2014: Monitoring and understanding changes in extremes: Extratropical storms, winds, and
14 waves. *Bulletin of the American Meteorological Society*, 95, 377-386.
15 <http://dx.doi.org/10.1175/BAMS-D-12-00162.1>
- 16 Walsh, K.J.E., S.J. Camargo, G.A. Vecchi, A.S. Daloz, J. Elsner, K. Emanuel, M. Horn, Y.-K.
17 Lim, M. Roberts, C. Patricola, E. Scoccimarro, A.H. Sobel, S. Strazzo, G. Villarini, M.
18 Wehner, M. Zhao, J.P. Kossin, T. LaRow, K. Oouchi, S. Schubert, H. Wang, J. Bacmeister,
19 P. Chang, F. Chauvin, C. Jablonowski, A. Kumar, H. Murakami, T. Ose, K.A. Reed, R.
20 Saravanan, Y. Yamada, C.M. Zarzycki, P.L. Vidale, J.A. Jonas, and N. Henderson, 2015:
21 Hurricanes and Climate: The U.S. CLIVAR Working Group on Hurricanes. *Bulletin of the*
22 *American Meteorological Society*, 96, 997-1017. [http://dx.doi.org/10.1175/BAMS-D-13-](http://dx.doi.org/10.1175/BAMS-D-13-00242.1)
23 [00242.1](http://dx.doi.org/10.1175/BAMS-D-13-00242.1)
- 24 Walsh, K.J.E., J.L. McBride, P.J. Klotzbach, S. Balachandran, S.J. Camargo, G. Holland, T.R.
25 Knutson, J.P. Kossin, T.-c. Lee, A. Sobel, and M. Sugi, 2016: Tropical cyclones and climate
26 change. *Wiley Interdisciplinary Reviews: Climate Change*, 7, 65-89.
27 <http://dx.doi.org/10.1002/wcc.371>
- 28 Wang, X.L., Y. Feng, G.P. Compo, V.R. Swail, F.W. Zwiers, R.J. Allan, and P.D. Sardeshmukh,
29 2012: Trends and low frequency variability of extra-tropical cyclone activity in the ensemble
30 of twentieth century reanalysis. *Climate Dynamics*, 40, 2775-2800.
31 <http://dx.doi.org/10.1007/s00382-012-1450-9>
- 32 Wang, X.L., V.R. Swail, and F.W. Zwiers, 2006: Climatology and changes of extratropical
33 cyclone activity: Comparison of ERA-40 with NCEP-NCAR reanalysis for 1958-2001.
34 *Journal of Climate*, 19, 3145-3166. <http://dx.doi.org/10.1175/JCLI3781.1>

- 1 Warner, M.D., C.F. Mass, and E.P.S. Jr., 2015: Changes in Winter Atmospheric Rivers along the
2 North American West Coast in CMIP5 Climate Models. *Journal of Hydrometeorology*, 16,
3 118-128. <http://dx.doi.org/10.1175/JHM-D-14-0080.1>
- 4 Wehner, M., Prabhat, K.A. Reed, D. Stone, W.D. Collins, and J. Bacmeister, 2015: Resolution
5 Dependence of Future Tropical Cyclone Projections of CAM5.1 in the U.S. CLIVAR
6 Hurricane Working Group Idealized Configurations. *Journal of Climate*, 28, 3905-3925.
7 <http://dx.doi.org/10.1175/JCLI-D-14-00311.1>
- 8 Yang, X., G.A. Vecchi, T.L. Delworth, K. Paffendorf, L. Jia, R. Gudgel, F. Zeng, and S.D.
9 Underwood, 2015: Extreme North America Winter Storm Season of 2013/14: Roles of
10 Radiative Forcing and the Global Warming Hiatus. *Bulletin of the American Meteorological*
11 *Society*, 96, S25-S28. <http://dx.doi.org/10.1175/BAMS-D-15-00133.1>
- 12 Zhang, R., T.L. Delworth, R. Sutton, D.L.R. Hodson, K.W. Dixon, I.M. Held, Y. Kushnir, J.
13 Marshall, Y. Ming, R. Msadek, J. Robson, A.J. Rosati, M. Ting, and G.A. Vecchi, 2013:
14 Have aerosols caused the observed Atlantic multidecadal variability? *Journal of the*
15 *Atmospheric Sciences*, 70, 1135-1144. <http://dx.doi.org/10.1175/jas-d-12-0331.1>
- 16 Zhu, Y. and R.E. Newell, 1998: A Proposed Algorithm for Moisture Fluxes from Atmospheric
17 Rivers. *Monthly Weather Review*, 126, 725-735. [http://dx.doi.org/10.1175/1520-](http://dx.doi.org/10.1175/1520-0493(1998)126<0725:APAFMF>2.0.CO;2)
18 [0493\(1998\)126<0725:APAFMF>2.0.CO;2](http://dx.doi.org/10.1175/1520-0493(1998)126<0725:APAFMF>2.0.CO;2)

10. Changes in Land Cover and Terrestrial Biogeochemistry

KEY FINDINGS

1. Changes in land use and land cover due to human activities produce changes in surface albedo and in atmospheric aerosol and greenhouse gas concentrations. These combined effects have recently been estimated to account for $40\% \pm 16\%$ of the human-caused global radiative forcing from 1850 to 2010 (*high confidence*). As a whole, the terrestrial biosphere (soil, plants) is a net “sink” for carbon (drawing down carbon from the atmosphere) and this sink has steadily increased since 1980, in part due to CO₂ fertilization (*very high confidence*). The future strength of the land sink is uncertain and dependent on ecosystem feedbacks; the possibility of the land becoming a net carbon source cannot be excluded (*very high confidence*).
2. The increased occurrence and severity of drought has led to large changes in plant community structure with subsequent effects on carbon distribution and cycling within ecosystems (for example, forests, grasslands). Uncertainties about future land use changes (for example, policy or mitigation measures) and about how climate change will affect land cover change make it difficult to project the magnitude and sign of future climate feedbacks from land cover changes. (*High confidence*)
3. Since 1901, the consecutive number of both frost-free days and the length of the corresponding growing season has increased for all regions of the United States. However, there is important variability at smaller scales, with some locations showing decreases of as much as one to two weeks. Plant productivity has not increased linearly with the increased number of frost-free days or with the longer growing season due to temperature thresholds and requirements for growth as well as seasonal limitations in water and nutrient availability (*very high confidence*). Future consequences of changes to the growing season for plant productivity are uncertain.
4. Surface temperatures are often higher in urban areas than in surrounding rural areas, for a number of reasons including the concentrated release of heat from buildings, vehicles, and industry. In the United States, this urban heat island (UHI) effect results in daytime temperatures 0.9°–7.2°F (0.5°–4.0°C) higher and nighttime temperatures 1.8°–4.5°F (1.0°–2.5°C) higher in urban areas, with larger temperature differences in humid regions (primarily the eastern United States) and in cities with larger populations. The UHI effect will strengthen in the future as the spatial extent and population of urban areas grow. (*High confidence*)

10.1 Introduction

Direct changes in land use by humans are contributing to radiative forcing by altering land cover and therefore albedo, contributing to climate change (Chapter 2: Physical Drivers of Climate Change). This forcing is spatially variable in both magnitude and sign; globally averaged it is negative (climate cooling; Figure 2.3). Climate changes, in turn, are altering the biogeochemistry of land ecosystems through extended growing seasons, increased numbers of frost-free days, altered productivity in agricultural and forested systems, longer fire seasons, and urban-induced thunderstorms (Galloway et al. 2014). These changes in land use and land cover interact with local, regional, and global climate processes (Brown et al. 2014). The resulting changes alter Earth's albedo, the carbon cycle, and atmospheric aerosols, constituting a mix of positive and negative feedbacks to climate change (Ward et al. 2014; Figure 10.1 and Chapter 2, Section 2.6.2). Thus, changes to terrestrial ecosystems are a direct driver of climate change and they are altered by climate change in ways that affect both ecosystem productivity and, through feedbacks, the climate itself.

The concept that longer growing seasons are increasing productivity in some agriculture and forested ecosystems was discussed in the Third National Climate Assessment (NCA3; Melillo et al. 2014). However, there are other consequences to a lengthened growing season that can offset these gains in productivity. Here we discuss these emerging complexities (Section 10.3.1) as well as discussing other aspects of how climate change is altering and interacting with terrestrial ecosystems.

[INSERT FIGURE 10.1 HERE:]

Figure 10.1. A graphical representation of climate interactions with land use and land cover. (Figure source: Ward et al. 2014)]

10.2 Terrestrial Ecosystem Interactions with the Climate System

This report discusses changes in temperature (Ch. 6: Temperature Change), precipitation (Ch. 7: Precipitation Change), hydrology (Ch. 8: Droughts, Floods, and Hydrology) and extreme events (Ch. 9: Extreme Storms). The intersections of these topics affect the phenology, or onset of growth through senescence; of land cover and biogeochemistry through biophysical land surface properties such as albedo, energy, and hydrologic processes; and biogeochemical cycles such as carbon, nitrogen, and water (Ward et al. 2014; Figure 10.2). Satellite observations and ecosystem models suggests that biogeochemical interactions of carbon dioxide (CO₂) fertilization and nitrogen (N) deposition and land cover change are responsible for global greening (25%–50%) and 4% of the Earth browning between 1982 and 2009 (Zhu et al. 2016; Mao et al. 2016). A recent analysis shows large-scale greening in the Arctic and boreal regions of North America and browning in the boreal forests of eastern Alaska for the period 1984–2012 (Ju and Masek 2016). While several studies have documented significant green-up periods, the lengthening of the growing season (Chapter 10.3.1) also alters the timing of green-up (onset of growth) and brown-

down (senescence); where ecosystems become depleted of water resources as a result of this, the actual period of productive growth can be truncated (Adams et al. 2015). This section discusses how changes in temperature, the hydrologic cycle, extreme events, and biogeochemistry interact with land cover change.

[INSERT FIGURE 10.2 HERE:]

Figure 10.2. Radiative forcings for land use/land cover change and other anthropogenic impacts estimated for the year 2010 referenced to the year 1850. Total anthropogenic radiative forcings (Myhre et al. 2013) are shown for comparison (yellow). Error lines represent uncertainties in total anthropogenic RF for the IPCC bars and uncertainties in land use/land cover change radiative forcings. The “SUM” bars show the total radiative forcings when all forcing agents are combined. (Figure source: Ward et al. 2014)]

10.2.1 Temperature Change

Interactions between temperature changes, land cover, and biogeochemistry are more complex than commonly assumed. Previous research suggested a fairly direct relationship between increasing temperatures, longer growing seasons (see Section 10.3.1), increasing plant productivity (e.g. Walsh et al. 2014a), and therefore also an increase in CO₂ uptake. Without water or nutrient limitations, increased CO₂ concentrations and warm temperatures have been shown to extend the growing season, which may contribute to longer periods of plant activity and carbon uptake, but do not affect reproduction rates (Reyes-Fox et. al. 2014). However, there are other processes that offset benefits of a longer growing season, such as changes in water availability and demand for water (e.g., Georgakakos et al. 2014; Hibbard et al. 2014). For instance, increased dry conditions can lead to wildfire (e.g., Hatfield et al. 2014; Joyce et al. 2014) and urban temperatures can contribute to urban-induced thunderstorms in the southeastern United States (Ashley et al. 2012). Temperature benefits of early onset of plant development in a longer growing season can be offset by (1) freeze damage caused by late-season frosts; (2) limits to growth because of shortening of the photoperiod later in the season; or (3) by shorter chilling periods required for leaf unfolding by many plants (Fu et al. 2013; Gu et al. 2008). In the case of the 2012 draught, a warm spring reduced the carbon cycle impact of the drought by inducing earlier carbon uptake (Wolf et al. 2016). New evidence points to longer temperature-driven growing seasons for grasslands that may facilitate earlier onset of growth, but also that senescence is typically earlier (Fridley et al. 2016). In addition to changing CO₂ uptake, higher temperatures can also enhance soil decomposition rates, thereby adding more CO₂ to the atmosphere. Similarly temperature, as well as changes in the seasonality and intensity of precipitation, can influence nutrient and water availability (leading to both shortages and excesses) thereby influencing rates and magnitudes of decomposition (Galloway et al. 2014).

10.2.2 Water Cycle Changes

The global hydrological cycle is expected to intensify under climate change as a consequence of increased temperatures in the troposphere. The consequences of the increased water-holding capacity of a warmer atmosphere are longer and more frequent droughts and less frequent but more severe precipitation events and cyclonic activity (see Ch. 9: Extreme Storms for an in-depth discussion of extreme storms). More intense rain events and storms can lead to flooding and ecosystem disturbances, thereby altering ecosystem function and carbon cycle dynamics. For an extensive review of precipitation changes and droughts, floods, and hydrology, see Chapters 7 and 8 in this report.

From the perspective of the land biosphere, drought has strong effects on ecosystem productivity and carbon storage by reducing photosynthesis and increasing the risk of wildfire, pest infestation, and disease susceptibility. Thus, droughts of the future will affect carbon uptake and storage, leading to feedbacks to the climate system (See Chapter 11 for Arctic/climate/wildfire feedbacks; also see Schlesinger et al. 2016). Reduced productivity as a result of extreme drought events can also extend for several years post-drought (i.e., drought legacy effects; Frank et al. 2016; Reichstein et al. 2013; Anderegg et al. 2015). The area of ecosystems under active drought and drought recovery is increasing (Schwalm et al. in review Nature), and recent work suggests that as drought events become more severe and frequent, the period between drought events may become shorter than ecosystem drought recovery time, leading to widespread degradation of land carbon sinks (Schwalm et al. in review Nature). In 2011, the most severe drought on record in Texas led to statewide regional tree mortality of 6.2%, or nearly nine times greater than the average annual mortality in this region (approximately 0.7%) (Moore et al. 2016). The net effect on carbon storage was estimated to be a redistribution of 24–30 Tg C from the live to dead tree carbon pool, which is equal to 6%–7% of pre-drought live tree carbon storage in Texas state forestlands (Moore et al. 2016). Another way to think about this redistribution is that the single Texas drought event equals approximately 36% of annual global carbon losses due to deforestation and land use change (Cias et al. 2013). The projected increases in temperatures and in the magnitude and frequency of heavy precipitation events, changes to snowpack, and changes in the subsequent water availability for agriculture and forestry may lead to similar rates of mortality or changes in land cover. Increasing frequency and intensity of drought across northern ecosystems reduces total observed organic matter export, leads to oxidized wetland soils, and releases stored contaminants into streams after rain events (Szkokan-Emilson et al. 2016). The consequences of drought and changes in the growing season have also increased demand for irrigation water in all major agricultural areas of the United States from 2000 to 2008, resulting in unsustainable use of groundwater resources (Marston et al. 2015).

10.2.3 Biogeochemistry

Terrestrial biogeochemical cycles play a key role in Earth's climate system, including by affecting land–atmosphere fluxes of many aerosol precursors and greenhouse gases, including

1 carbon dioxide (CO₂), methane (CH₄), and nitrous oxide (N₂O). As such, changes in the
2 terrestrial ecosphere can drive climate change. At the same time, biogeochemical cycles are
3 sensitive to changes in climate and atmospheric composition.

4 Historically, increased atmospheric CO₂ concentrations have led to increased plant production
5 (known as CO₂ fertilization) and longer-term storage of carbon in biomass and soils (SOCCR-2
6 Chapter 12). Whether increased atmospheric CO₂ will continue to lead to long-term storage of
7 carbon in terrestrial ecosystems depends on whether CO₂ fertilization simply intensifies the rate
8 of short-term carbon cycling (for example, by stimulating respiration, root exudation, and high
9 turnover root growth) or whether the additional carbon is used by plants to build more wood or
10 tissues that, once senesced, decompose into long-lived soil organic matter (SOCCR-2 Chapter
11 19). Under increased CO₂ concentrations plants have been observed to optimize water use due to
12 reduced stomatal conductance, thereby increasing water use efficiency (Keenan et al. 2013;
13 SOCCR-2 Chapter 17). This change in water use efficiency can affect plants' tolerance to stress
14 and specifically to drought (SOCCR-2 Chapter 17). Due to the complex interactions of the
15 processes that govern terrestrial biogeochemical cycling, terrestrial ecosystem responses to CO₂
16 remains one of the largest uncertainties in predicting future climate change (Chapter 2: Physical
17 Drivers of Climate Change).

18 Nitrogen is a principal nutrient for plant growth and can limit or stimulate plant productivity (and
19 carbon uptake), depending on availability. As a result, increased nitrogen deposition and natural
20 nitrogen-cycle responses to climate change will influence the global carbon cycle. For example,
21 nitrogen limitation can limit the CO₂ fertilization response of plants to elevated atmospheric CO₂
22 (e.g., Norby et al. 2010; Zaehle et al. 2010; SOCCR-2 Chapter 17). Conversely, increased
23 decomposition of soil organic matter in response to climate warming increases nitrogen
24 mineralization. This shift of nitrogen from soil to vegetation can increase ecosystem carbon
25 storage (Melillo et al. 2011; Cias et al. 2013). While the effects of increased nitrogen deposition
26 may counteract some nitrogen limitation on CO₂ fertilization, the importance of nitrogen in
27 future carbon–climate interactions is not clear. Nitrogen dynamics are being integrated into the
28 simulation of land carbon cycle modeling, but only two of the models in CMIP5 included
29 coupled carbon–nitrogen interactions (Knutti and Sedlacek 2013).

30 Many factors, including climate, atmospheric CO₂ concentrations, and nitrogen deposition rates
31 influence the structure of the plant community and therefore the amount and biochemical quality
32 of inputs into soils (Jandl et al. 2007; McLauchlan 2006; Smith et al. 2007; SOCCR-2 Chapter
33 12). For example, though CO₂ losses from soils may decrease with greater nitrogen deposition,
34 increased emissions of other greenhouse gases, such as methane (CH₄) and nitrous oxide (N₂O),
35 can offset the reduction in CO₂ (Liu and Greaver 2009; SOCCR-2 Chapter 12). The dynamics of
36 soil organic carbon under the influences of climate change are poorly understood and therefore
37 not well represented in models. As a result, there is high uncertainty in soil carbon stocks in
38 model simulations (Todd-Brown et al. 2013; Tian et al. 2015; SOCCR-2 Chapter 12).

Future emissions of many aerosol precursors are expected to be affected by a number of climate-related factors, in part because of changes in aerosol and aerosol precursors from the terrestrial biosphere. For example, volatile organic compounds (VOCs) are a significant source of secondary organic aerosols, and biogenic sources of VOCs exceed emissions from the industrial and transportation sectors (Guenther et al. 2006). Isoprene is one of the most important biogenic VOCs, and isoprene emissions are strongly dependent on temperature and light, as well as other factors like plant type and leaf age (Guenther et al. 2006). Higher temperatures are expected to lead to an increase in biogenic VOC emissions. Atmospheric CO₂ concentration can also affect isoprene emissions (e.g., Rosenstiel et al. 2003). Changes in biogenic VOC emissions can impact aerosol formation and feedbacks with climate (Chapter 2: Physical Drivers of Climate Change). Increased biogenic VOC emissions can also impact ozone and the atmospheric oxidizing capacity (Pyle et al. 2007). Conversely, increases in nitrogen oxide (NO_x) pollution produce tropospheric ozone (O₃), which has damaging effects on vegetation. For example, a recent study estimated yield losses for maize and soybean production of up to 5% to 10% due to increases in O₃ (McGrath et al. 2015).

While the climate influences land cover and biogeochemistry, the converse is also true (Kalnay and Cai 2003). Changes in land cover and land use, including deforestation, afforestation, land cultivation, and development together impact surface albedo, CO₂, CH₄, O₃, and aerosols. With all forcing agents considered together, one study estimated that 0.9 W/m², or 40% of the present-day human-caused radiative forcing can be attributed to land use and land cover change (Ward et al. 2014). Continued land-use change is expected to contribute between 0.9 and 1.9 W/m² to direct radiative forcing by 2100 (Ward et al. 2014). The net radiative forcing due specifically to fire, after accounting for short-lived forcing agents O₃ and aerosols, in addition to long-lived greenhouse gases and land albedo change, both now and in the future, is estimated to be near-zero due to regrowth of forests following fires offsetting the release of CO₂ in the fire (Ward and Mahowald 2015).

10.2.4 Extreme Events and Disturbance

This section builds on the physical overview provided in earlier chapters to frame how the intersects of climate, extreme events, and disturbance affect regional land cover and biogeochemistry. In addition to overall trends in temperature (Ch. 7) and precipitation (Ch. 8), changes in modes of variability such as the Pacific Decadal Oscillation (PDO) and the El Niño–Southern Oscillation (ENSO) (Ch. 5: Circulation and Variability) can contribute to drought cycles in the United States, which leads to unanticipated changes in disturbance regimes in the terrestrial biosphere (e.g., Kam et al., 2014). Drought may exacerbate the rate of plant invasions by non-native species in rangelands and grasslands (Moore et al. 2016). Land cover changes such as encroachment and invasion of non-native species can in turn lead to increased frequency of disturbance such as fires. Disturbance events alter soil moisture, which in addition to being affected by evapotranspiration and precipitation (Ch. 8: Droughts, Flood and Hydrology), is controlled by canopy and rooting architecture as well as soil physics. Invasive plants may be

1 directly responsible for changes in fire regimes through increased biomass, changes in the
2 distribution of flammable biomass, increased flammability, and altered timing of fuel drying,
3 while others may be “fire followers” whose abundances increase as a result of shortening the
4 fire return interval (e.g., Lambert et al. 2010). Changes in land cover resulting from fire and
5 alteration of disturbance regimes affects long-term carbon exchange between the atmosphere and
6 biosphere (e.g., Moore et al. 2016). Recent extensive diebacks and changes in plant cover due to
7 drought have interacted with regional carbon cycle dynamics including carbon release from
8 biomass and reductions in carbon uptake from the atmosphere, though plant re-growth may
9 offset emissions (Vose et al. 2016). The current meteorological drought in California (described
10 in Ch. 8: Droughts, Floods and Hydrology), combined with warming, will result in long-term
11 changes in land cover, leading to increased probability of drought and wildfire and in ecosystem
12 shifts (Diffenbaugh et al. 2015). California’s recent drought has also resulted in measureable
13 canopy water losses, posing long-term hazards to forest health and biophysical feedbacks to
14 regional climate (Anderegg et al. 2015; Asner et al. 2016; Mann and Gleick 2015). Multi-year, or
15 severe meteorological and hydrologic (see Ch. 8: Droughts, Floods, and Hydrology for
16 definitions) droughts can also affect stream biogeochemistry and riparian ecosystems by
17 concentrating sediments and nutrients (Vose et al. 2016).

18 Changes in the variability of hurricanes and winter storm events (Ch. 9: Extreme Storms) also
19 affect the terrestrial biosphere, as shown in studies comparing historic and future (projected)
20 extreme events in the western United States and how these translate into changes in the regional
21 water balance, fire, and streamflow. Composited across 10 global climate models (GCMs)
22 summer (June–August) water-balance deficit in the future (2030–2059) increases compared to
23 that under historical (1916–2006) conditions. Portions of the Southwest that have significant
24 monsoon precipitation, and some mountainous areas of the Pacific Northwest are exempt from
25 this deficit (Littell et al. 2016). Projections for 2030–2059 suggest that the Columbia Basin,
26 upper Snake River, southeastern California, and southwestern Oregon may exceed extreme low
27 flows less frequently than they did historically (1916–2006). Given the historical relationships
28 between fire occurrence and drought indicators such as water-balance deficit and streamflow,
29 climate change can be expected to have significant effects on fire occurrence and area burned
30 (Littell et al. 2016, 2011; Elsner et al. 2010).

31 Climate change in the northern high latitudes is directly contributing to increased fire occurrence
32 (Ch. 11: Arctic); in the coterminous United States, climate-induced changes in fires, changes in
33 direct human ignitions, and land management practices all significantly contribute to wildfire
34 trends. Wildfires in the western United States are often ignited by lightning, but management
35 practices such as fire suppression contribute to fuels and amplify the intensity and spread of
36 wildfire. Unintentional ignition by campfires or intentional human ignitions are also
37 compounded by increasingly dry and vulnerable fuels, which build up with fire suppression or
38 human settlements.

10.3 Climate Indicators and Agricultural and Forest Responses

Agricultural production has changed the surface of the Earth and influenced hydrology as well as the flux and distribution of carbon. Recent studies indicate a correlation between the expansion of agriculture and the global amplitude of the CO₂ uptake and emissions (Zeng et al. 2014; Gray et al. 2014). Conversely, agricultural production is increasingly disrupted by climate and extreme weather events, and these impacts are expected to be augmented by mid-century and beyond for most crops (Lobell and Tebaldi 2014; Challinor et al. 2014) and livestock. Precipitation extremes put pressure on agricultural soil and water assets and lead to increased irrigation, shrinking aquifers, and ground subsidence. While human adaptation of crop management has mitigated many near-term consequences, climate change effects on agriculture will have long-term impacts on food security (Brown et al. 2015). Global Climate Models (GCMs) differ with regard to how increasing atmospheric CO₂ concentrations affect plant productivity through CO₂ fertilization or downregulation as well as the strength of carbon cycle feedbacks (Anav et al. 2013; Chapter 2: Physical Drivers of Climate Change). When CO₂ effects on photosynthesis and transpiration are removed from Global Gridded Crop Models, simulated response to climate across the models is comparable, suggesting that model parameterizations representing these process remains uncertain (Rosenzweig et al. 2014).

10.3.1 Changes in the Frost-Free and Growing Seasons

The growing season is the part of the year in which temperatures are favorable to plant growth. A basic metric by which this is measured is the frost-free season. The U. S. Department of Agriculture Natural Resources Conservation Service defines the frost-free period using a range of thresholds. They calculate the average date of the last day with temperature below 24°F, 28°F, and 32°F in the spring and the average date of the first day with temperature below 24°F, 28°F, and 32°F in the fall, at various probabilities. They then define the frost-free season at three index temperatures (32°F, 28°F, and 24°F), also with a range of probabilities. Fixed temperature thresholds (for example, temperature below 32°F) are often used when discussing growing season; however, different plant cover-types (for example, forest, agricultural, shrub, tundra) have different temperature thresholds for growth, and different requirements/thresholds for chilling (Zhang et al. 2011; Hatfield et al. 2014). For the purposes of this report, we use the metric with a 32°F threshold to define the change in the number of “frost-free” days, and a temperature threshold of 41°F as a first-order measure of how the growing season length has changed over the observational record (Zhang et al. 2011).

The NCA3 reported an increase in the growing season by as much as several weeks as a result of higher temperatures occurring earlier and later in the year (e.g., Walsh et al. 2014b; Hatfield et al. 2014; Joyce et al. 2014). NCA3 used a threshold of 32°F—that is to say, the frost-free season—to define the growing season. An update to this finding is presented in Figures 10.3 and 10.4, which show changes in the frost-free and growing season, respectively, as defined above. Overall, the length of the frost-free season has increased in the contiguous United States during

the past century (Figure 10.3). The growing season changes are more variable: Growing season length increased until the late 1930s, declined slightly until the early 1970s, increased again until about 1990, and remained quasi-stable thereafter (Figure 10.4). This contrasts somewhat with changes in the length of the frost-free season presented in NCA3, which showed a continuing increase after 1980. This discrepancy is attributable to the temperature thresholds used in each indicator to define the start and end of a season. Specifically, the growing season length (41°F threshold) is more conservative than the 32°F frost-free threshold because the latter captures more days in winter, which has larger temperature trends.

The lengthening of the growing season has been somewhat greater in the northern and western United States, which had increases of 1–2 weeks in many locations. In contrast, some areas in the Midwest, Southern Great Plains, and the Southeast had decreases of a week or more between the periods 1986–2015 and 1901–1960. These differences reflect the more general pattern of warming and cooling nationwide (Ch. 6: Temperature Changes). Observations and models have verified that the growing season has generally increased plant productivity over most of the United States (Mao et al. 2016).

Consistent with increases in growing season length and the coldest temperature of the year, plant hardiness zones have shifted northward in many areas (Daly et al. 2012). The widespread increase in temperature has also impacted the distribution of other climate zones in parts of the United States. For instance, there have been moderate changes in the range of the temperate and continental climate zones of the eastern United States since 1950 (Chan and Wu 2015) as well as changes in the coverage of some extreme climate zones in the western United States. In particular, the spatial extent of the “alpine tundra” zone has decreased in high-elevation areas (Diaz and Eischeid 2007) while the extent of the “hot arid” zone has increased in the Southwest (Grundstein 2008).

The period over which plants are actually productive, that is, their true growing season, is a function of multiple climate factors including air temperature, number of frost days, and rainfall, as well as biophysical factors including soil physics, daylight hours, and the biogeochemistry of ecosystems (EPA 2016). Further, while growing season length is generally referred to in the context of agricultural productivity, the factors that govern which plant types will grow in a given location are common to all plants whether they are in agricultural, natural, or managed landscapes. Changes in both the length and the seasonality of the growing season, in concert with local environmental conditions, can have multiple effects on agricultural productivity and land cover more generally.

In the context of agriculture, a longer growing season could allow for the diversification of cropping systems or allow multiple harvests within a growing season. For example, shifts in cold-hardy zones across the contiguous United States suggest widespread expansion of thermally suitable areas for the cultivation of cold-intolerant perennial agriculture (Parker and Abatzoglou 2016). However, changes in available water, conversion from dry to irrigated farming, and

changes in sensible and latent heat exchange associated with these shifts need to be considered. Increasingly dry conditions under a longer growing season can alter terrestrial organic matter export and catalyze oxidation of wetland soils, releasing stored contaminants (for example, copper and nickel) into streamflow after rainfall (Szkokan-Emilson et al. 2016). Similarly, a longer growing season, particularly in years where water is limited, is not due to warming alone, but is exacerbated by higher atmospheric CO₂ concentrations that extend the active period of growth by plants (Reyes-Fox et al. 2014). Longer growing seasons can also limit the types of crops that can be grown, encourage invasive species or weed growth, or increase demand for irrigation, possibly beyond the limits of water availability. They could also disrupt the function and structure of a region's ecosystems and could, for example, alter the range and types of animal species in the area.

A longer and seasonally-shifted growing season also affects the role of terrestrial ecosystems in the carbon cycle. Neither seasonality of growing season (spring and summer) nor carbon, water, and energy fluxes should be interpreted separately when analyzing the impacts of climate extremes such as drought (Ch. 8: Droughts, Floods, and Hydrology; Sippel et al. 2016; Wolf et al. 2016). Observations and data-driven model studies suggest that losses in net terrestrial carbon uptake during record warm springs followed by severely hot and dry summers can be largely offset by carbon gains in record-exceeding warmth and early arrival of spring (Wolf et al. 2016). Depending on soil physics and land cover, a cool spring, however, can deplete soil water resources less rapidly, making the subsequent impacts of precipitation deficits less severe (Sippel et al. 2016). Depletion of soil moisture through early plant activity in a warm spring can potentially amplify summer heating, a typical lagged direct effect of an extremely warm spring (Frank et al. 2015). Ecosystem responses to the phenological changes of timing and extent of growing season and subsequent biophysical feedbacks are therefore strongly dependent on the timing of climate extremes (Ch. 8: Droughts, Floods, and Hydrology; Ch. 9: Extreme Storms; Sippel et al. 2016).

The global Coupled Model Intercomparison Project Phase 5 (CMIP5) analyses did not explicitly explore future changes to the growing season. Many projected changes in North American climate are generally consistent across CMIP5 models, but there is substantial inter-model disagreement in projections of some metrics important to biophysical systems' productivity, including the sign of regional precipitation changes and extreme heat events across the northern United States (Maloney et al. 2014).

[INSERT FIGURE 10.3 HERE:]

Figure 10.3. Change in number of days since 1901 between the last spring occurrence of 32°F and first fall occurrence of 32°F for NCA4 regions of the United States. This change is expressed as the difference between the average number of frost-free days in 1986–2015 minus that in 1901–1960. (Figure source: updated from Walsh et al. 2010)]

[INSERT FIGURE 10.4 HERE:]

Figure 10.4. The length of the growing season in the contiguous 48 states compared with a long-term average (1895–2015), where “growing season” is defined by a temperature threshold of 41°F. For each year, the line represents the number of days shorter or longer than average. The line was smoothed using an 11-year moving average. Choosing a different long-term average for comparison would not change the shape of the data over time. (Figure source: Kunkel et al. 2016, EPA 2016)]

10.3.2 Water Availability and Drought

Drought is generally parameterized in most agricultural models as limited water availability, and is an integrated response of both meteorological and agricultural drought, as described in Chapter 8 (Droughts, Floods and Hydrology). However, physiological as well as biophysical processes that influence land cover and biogeochemistry interact with drought through stomatal closure induced by elevated atmospheric CO₂ levels. This has direct impacts on plant transpiration, atmospheric latent heat fluxes, and soil moisture, thereby influencing local and regional climate. Drought is often offset by management through groundwater withdrawals, with increasing pressure on these resources to maintain plant productivity. This results in indirect climate effects by altering land surface exchange of water and energy with the atmosphere (Marston et al. 2015).

10.3.3 Forestry Considerations

Climate change and land cover change in forested areas interact in many ways, such as through changes in mortality rates driven by changes in the frequency and magnitude of fire, insect infestations, and disease. In addition to the direct economic benefits of forestry, unquantified societal benefits include ecosystem services, like protection of watersheds and wildlife habitat, and recreation and human health value. United States forests and related wood products also absorb and store the equivalent of 16% of all CO₂ emitted by fossil fuel burning in the United States each year. Climate change is expected to reduce the carbon sink strength of forests overall.

Effective management of forests offers the opportunity to reduce future climate change (for example, as given in proposals for Reduced Emissions from Deforestation and forest Degradation, or REDD+ (<https://www.forestcarbonpartnership.org/what-redd>), and in the Paris Agreement (see Ch. 14: Mitigation for more on the Paris Agreement) by capturing and storing carbon in forest ecosystems and long-term wood products (Lippke et al. 2011). Afforestation in the United States has the potential to capture and store 225 million tons of additional carbon per year from 2010 to 2110 (EPA 2005; King et al. 2007). However, the projected maturation of United States forests (Wear and Coulston 2015) and land-cover change, in particular the expansion of urban and suburban areas along with projected increased demands for food and bioenergy, threaten the extent of forests and their carbon storage potential (McKinley et al. 2011).

Large-scale die-off and disturbances resulting from climate change have potential effects beyond the biogeochemical and carbon cycle effects. Biogeophysical feedbacks can strengthen or reduce climate forcing. The low albedo of boreal forests provides a positive feedback, but those albedo effects are mitigated in tropical forests through evaporative cooling; for temperate forests, the evaporative effects are less clear (Bonan 2008). Changes in surface albedo, evaporation, and surface roughness can have feedbacks to local temperatures that are larger than the feedback due to the change in carbon sequestration (Jackson et al. 2008). Forest management frameworks (e.g., afforestation, deforestation, avoided deforestation) that account for biophysical (e.g., land surface albedo, surface roughness) properties can be used as climate protection or mitigation strategies (Anderson et al. 2011).

Changes in growing season length, combined with drought and accompanying wildfire are reshaping California's mountain ecosystems. The California drought led to the lowest snowpack in 500 years, the largest wildfires in post-settlement history, greater than 23% stress mortality in Sierra mid-elevation forests, and associated post-fire erosion. It is anticipated that slow recovery, possibly to different ecosystem types, with numerous shifts to species' ranges will result in long-term changes to land surface biophysical as well as ecosystem structure and function in this region (Asner et al. 2016; <http://www.fire.ca.gov/treetaskforce/>).

While changes in forest stocks, composition, and the ultimate use of forest products can influence net emissions and climate, the future net changes in forest stocks continue to be uncertain (US Department of State 2016). This uncertainty is due to a combination of uncertainties in future population size, population distribution and subsequent land-use change, harvest trends, wildfire management practices (for example, large-scale thinning of forests), and the impact of maturing U.S. forests.

10.4 Urban Responses and Feedbacks to Climate Change: Urban Heat Island

The urban heat island (UHI) effect is a well-known phenomenon in which urban environments often retain more heat than nearby rural environments, and it has a profound effect on the quality of life of the world's growing urban population (Shepherd 2013). The UHI is characterized by increased surface and canopy temperatures as a result of heat-retaining asphalt and concrete, a lack of vegetation, and anthropogenic generation of heat and greenhouse gasses (Shepherd 2013). Based on land surface temperature measurements, the UHI effect increases urban temperature by 2.9°C (5.2°F) on average, but it has been measured at 8°C (14.4°F) in cities built in areas dominated by temperate forests (Imhoff et al. 2010). In arid regions, however, urban areas can be greater than 2°C (3.6°F) cooler than surrounding shrublands (Bounoua et al. 2015). Similarly, urban settings lose up to 12% of precipitation through impervious surface runoff, versus just over 3% loss to runoff in vegetated regions. Carbon losses from the biosphere to the atmosphere through urbanization account for almost 2% of the continental total, a significant proportion given that urban areas only account for around 1% of land in the United States (Bounoua et al. 2015).

1 According to the World Bank, over 81% of the United States population currently resides in
2 urban settings (<http://data.worldbank.org/indicator/SP.URB.TOTL.IN.ZS?locations=US>).
3 Mitigation efforts are often stalled by the lack of quantitative data and understanding of the
4 various factors that contribute to UHI. A recent study set out to quantitatively determine
5 contributions to the intensity of UHI across North America (Zhao et al. 2014). The study found
6 that population strongly influenced nighttime UHI, but that daytime UHI varied spatially
7 following precipitation gradients. The model applied in this study indicated that the spatial
8 variation in the UHI signal was controlled most strongly by impacts on the atmospheric
9 convection efficiency. Because of the impracticality of managing convection efficiency, results
10 from Zhao et al. (2014) support albedo management as an efficient strategy to mitigate UHI on a
11 large scale.

12

TRACEABLE ACCOUNTS

Key Finding 1

Changes in land use and land cover due to human activities produce changes in surface albedo and in atmospheric aerosol and greenhouse gas concentrations. These combined effects have recently been estimated to account for $40\% \pm 16\%$ of the human-caused global radiative forcing from 1850 to 2010 (*high confidence*). As a whole, the terrestrial biosphere (soil, plants) is a net “sink” for carbon (drawing down carbon from the atmosphere) and this sink has steadily increased since 1980, in part due to CO₂ fertilization (*very high confidence*). The future strength of the land sink is uncertain and dependent on ecosystem feedbacks; the possibility of the land becoming a net carbon source cannot be excluded (*very high confidence*).

Description of evidence base

Integrative modeling studies that combine climate models with models that simulate changes in land cover and land use have provided updated estimates climate forcing due to feedbacks among climate variables and land. Changes in land cover and land use are estimated to contribute 40% of present climate forcing (0.9 W/m^2), and are estimated to contribute 0.9 to 1.9 W/m^2 in the year 2100 (Ward et al. 2015). This research is grounded in long-term observations that have been documented for over 40 years. For example, studies have documented physical land surface processes such as albedo, surface roughness, sensible and latent heat exchange, and land use and land cover change that interact with regional atmospheric processes (e.g., Marotz et al. 1975; Barnston and Schickendanz 1984; Alpert and Mandel 1986; Pielke and Zeng 1989; Pielke et 2007).

IPCC, 2013: Summary for Policymakers states: “From 1750 to 2011, CO₂ emissions from fossil fuel combustion and cement production have released 375 [345 to 405] Gt C to the atmosphere, while deforestation and other land use change are estimated to have released 180 [100 to 260] GtC. This results in cumulative anthropogenic emissions of 555 [470 to 640] Gt C. {6.3 and WGI, Chapter 14 states for North America: “In summary, it is very likely that by mid-century the anthropogenic warming signal will be large compared to natural variability such as that stemming from the NAO, ENSO, PNA, PDO, and the NAMS in all North America regions throughout the year.”

Major uncertainties

Uncertainty exists in the future land cover and land use change.

Assessment of confidence based on evidence and agreement, including short description of nature of evidence and level of agreement

☐ Certain (100%)

X Very High

☐ High

☐ Medium

☐ Low

The existing impact on climate forcing has *high confidence*. The future forcing has lower confidence because it is difficult to estimate changes in land cover and land use into the future. However, if existing trends in land use and land cover change continue, the contribution of land cover to forcing will increase with high confidence.

If appropriate, estimate likelihood of impact or consequence, including short description of basis of estimate

☐ Greater than 9 in 10 / Very Likely

☐ Greater than 2 in 3 / Likely

☐ About 1 in 2 / As Likely as Not

☐ Less than 1 in 3 / Unlikely

☐ Less than 1 in 10 / Very Unlikely

Summary sentence or paragraph that integrates the above information

The key finding is based on basic physics that has been well established for decades. Specific assessments, however, have not yet been made with regards to land cover and the climate system.

Key Finding 2

The increased occurrence and severity of drought has led to large changes in plant community structure with subsequent effects on carbon distribution and cycling within ecosystems (for example, forests, grasslands). Uncertainties about future land use changes (for example, policy or mitigation measures) and about how climate change will affect land cover change make it difficult to project the magnitude and sign of future climate feedbacks from land cover changes. (*High confidence*)

Description of evidence base

From the perspective of the land biosphere, drought has strong effects on ecosystem productivity and carbon storage by reducing microbial activity and photosynthesis, and increasing the risk of wildfire, pest infestation, and disease susceptibility. Thus, droughts of the future will affect carbon uptake and storage, leading to feedbacks to the climate system (Schlesinger et al. 2016). Reduced productivity as a result of extreme drought events can also extend for several years post-drought (i.e., drought legacy effects; Frank et al. 2016; Reichstein et al. 2013; Anderegg et al. 2015).

The most severe drought on record in Texas led to statewide regional tree mortality of 6.2%, or nearly 9X greater than the average annual mortality in this region of ~0.7% (Moore et al. 2016). The net effect on carbon storage was estimated to be a redistribution of 24–30 Tg C from the live to dead tree carbon pool, which is equal to 6%–7% of pre-drought live tree carbon storage in

Texas state forestlands or (Moore et al. 2016). This redistribution is that one singular event equals ~36% of global carbon losses due to deforestation and land use change (Cias et al. 2013).

Major uncertainties

Major uncertainties include how future land use/land cover changes will occur as a result of policy and/or mitigation strategies in addition to climate change

Assessment of confidence based on evidence and agreement, including short description of nature of evidence and level of agreement

☐ Certain (100%)

☐ Very High

X High

☐ Medium

☐ Low

If appropriate, estimate likelihood of impact or consequence, including short description of basis of estimate

☐ Greater than 9 in 10 / Very Likely

☐ Greater than 2 in 3 / Likely

☐ About 1 in 2 / As Likely as Not

☐ Less than 1 in 3 / Unlikely

☐ Less than 1 in 10 / Very Unlikely

Summary sentence or paragraph that integrates the above information

Future interactions between land cover and the climate system are uncertain and depend on both human decision making and the evolution of the climate system.

Key Finding 3

Since 1901, the consecutive number of both frost-free days and the length of the corresponding growing season has increased for all regions of the United States. However, there is important variability at smaller scales, with some locations showing decreases of as much as one to two weeks. Plant productivity has not increased linearly with the increased number of frost-free days or with the longer growing season due to temperature thresholds and requirements for growth as well as seasonal limitations in water and nutrient availability (*very high confidence*). Future consequences of changes to the growing season for plant productivity are uncertain.

Description of evidence base

Without nutrient limitations, increased CO₂ concentrations and warm temperatures have been shown to extend the growing season, which may contribute to longer periods of plant activity and carbon uptake, but do not affect reproduction rates (Reyes-Fox et. al. 2014). However, other

confounding variables that coincide with climate change (for example, drought, increased ozone, and reduced photosynthesis due to increased or extreme heat) can offset increased growth associated with longer growing seasons (Adams et al. 2015).

Major uncertainties

Uncertainties exist in feedbacks among variables that impact the length of the growing season.

Assessment of confidence based on evidence and agreement, including short description of nature of evidence and level of agreement

☐ Certain (100%)

☒ Very High

☐ High

☐ Medium

☐ Low

If appropriate, estimate likelihood of impact or consequence, including short description of basis of estimate

☐ Greater than 9 in 10 / Very Likely

☐ Greater than 2 in 3 / Likely

☐ About 1 in 2 / As Likely as Not

☐ Less than 1 in 3 / Unlikely

☐ Less than 1 in 10 / Very Unlikely

Summary sentence or paragraph that integrates the above information

Changes in growing season length and interactions with climate, biogeochemistry and land cover were covered in 12 chapters of NCA3, with no real summary statement. This key finding provides a summary of the complex nature of the growing season.

Key Finding 4

Surface temperatures are often higher in urban areas than in surrounding rural areas, for a number of reasons including the concentrated release of heat from buildings, vehicles, and industry. In the United States, this urban heat island (UHI) effect results in daytime temperatures 0.9°–7.2°F (0.5°–4.0°C) higher and nighttime temperatures 1.8°–4.5°F (1.0°–2.5°C) higher in urban areas, with larger temperature differences in humid regions (primarily the eastern United States) and in cities with larger populations. The UHI effect will strengthen in the future as the spatial extent and population of urban areas grow. (*High confidence*)

Description of evidence base

The urban heat island (UHI) effect is correlated with the extent of impervious surfaces, which alter albedo or the saturation of radiation. The urban-rural difference that defines the UHI is

greatest for cities built in temperate forest ecosystems. The average temperature increase is 2.9°C, except for urban areas in biomes with arid and semiarid climates (Imhoff et al. 2010)

Major uncertainties

No major uncertainties.

Assessment of confidence based on evidence and agreement, including short description of nature of evidence and level of agreement

☐ Very High

☒ High

☐ Medium

☐ Low

Land surface temperature estimates are taken from the MODIS-Aqua (MOD11A2) satellite sensor with 99% confidence.

If appropriate, estimate likelihood of impact or consequence, including short description of basis of estimate

☐ Greater than 9 in 10 / Very Likely

☐ Greater than 2 in 3 / Likely

☐ About 1 in 2 / As Likely as Not

☐ Less than 1 in 3 / Unlikely

☐ Less than 1 in 10 / Very Unlikely

Summary sentence or paragraph that integrates the above information

The key finding is based on satellite land surface measurements and analyzed by Imhoff et al. (2010). Bonoua et al. (2015) and Shepherd (2013) provide specific updates with regards to the influence of urban heat islands and their intersects with the climate system.

1 FIGURES

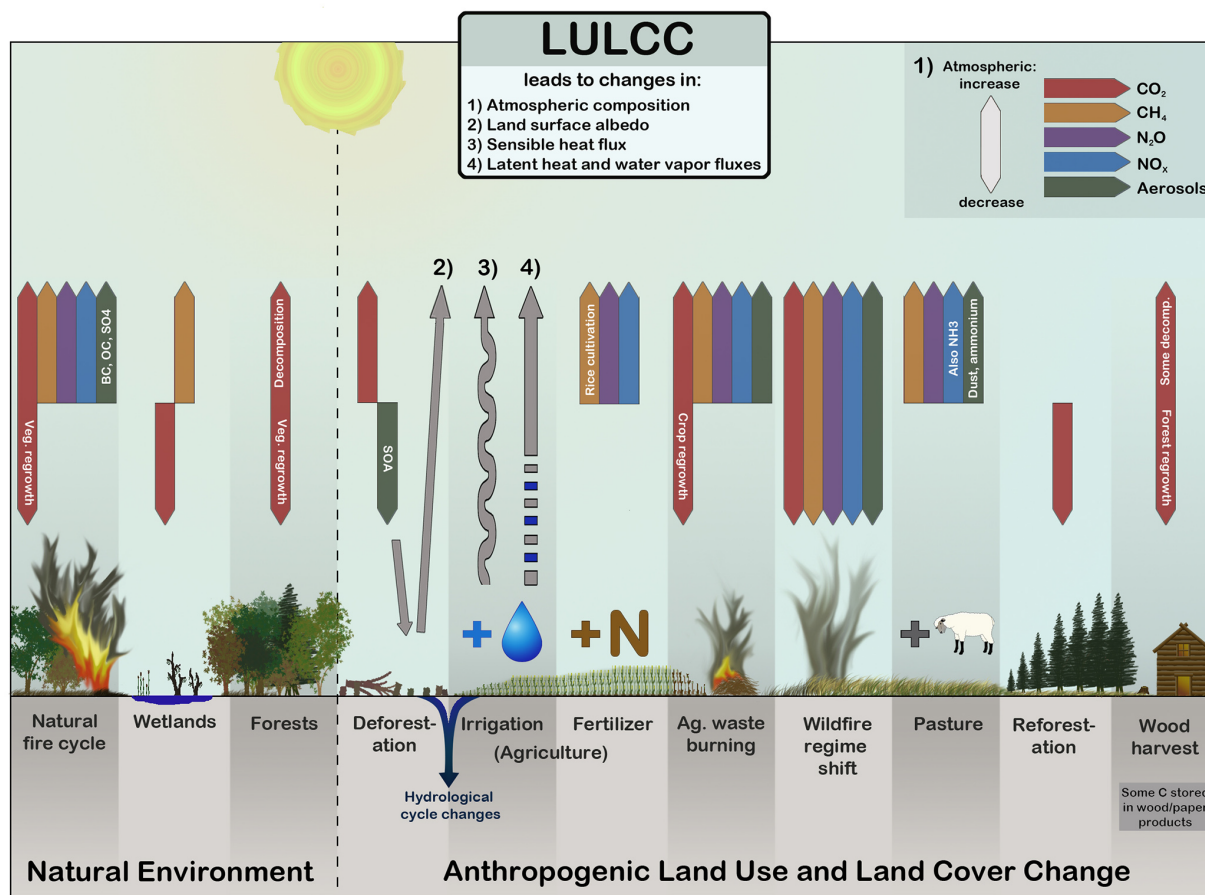


Figure 10.1. A graphical representation of climate interactions with land use and land cover.
(Figure source: Ward et al., 2014)

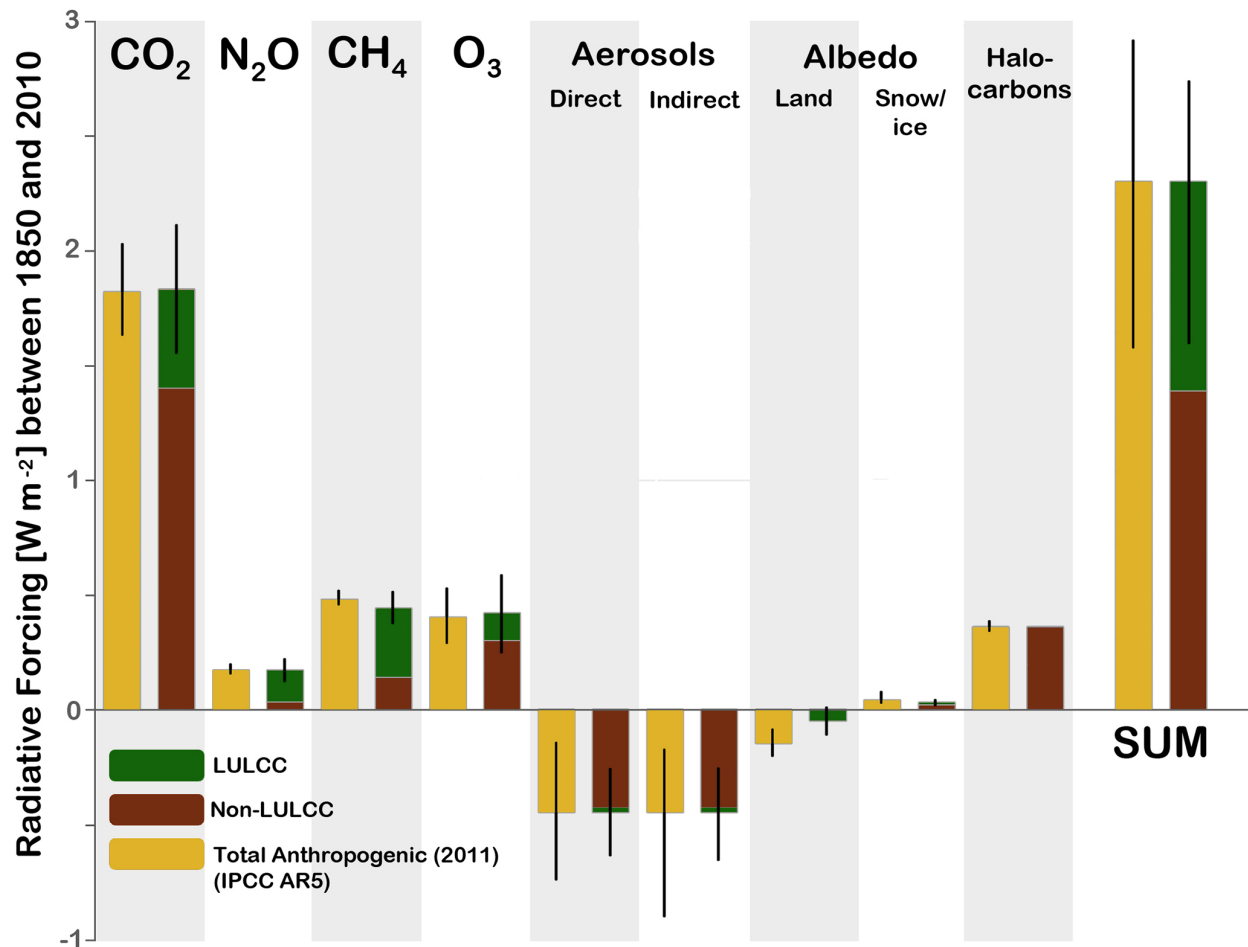


Figure 10.2. Radiative forcings for land use/land cover change and other anthropogenic impacts estimated for the year 2010 referenced to the year 1850 (Ward et al. 2014). Total anthropogenic radiative forcings from (Myhre et al. 2013) are shown for comparison (yellow). Error lines represent uncertainties in total anthropogenic RF for the IPCC bars and uncertainties in land use/land cover change radiative forcings (Ward et al. 2014). The “SUM” bars show the total radiative forcings when all forcing agents are combined. (Figure source: Ward et al. 2014)

Observed Increase in Frost-Free Season Length

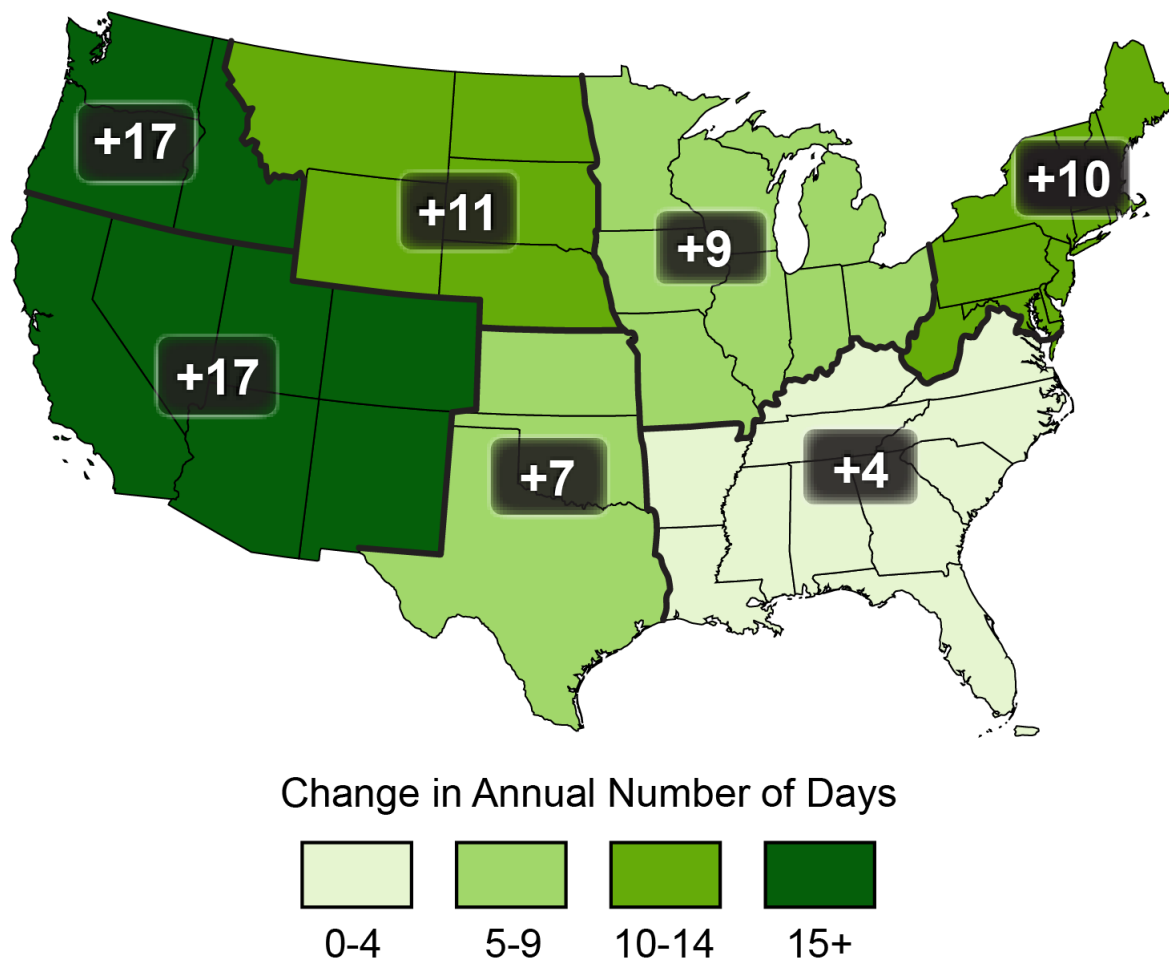


Figure 10.3. Change in number of days since 1901 between the last spring occurrence of 32°F and first fall occurrence of 32°F for NCA4 regions of the United States. This change is expressed as the difference between the average number of frost-free days in 1986-2015 minus that 1901-1960. (Figure source: updated from Walsh et al. 2010).

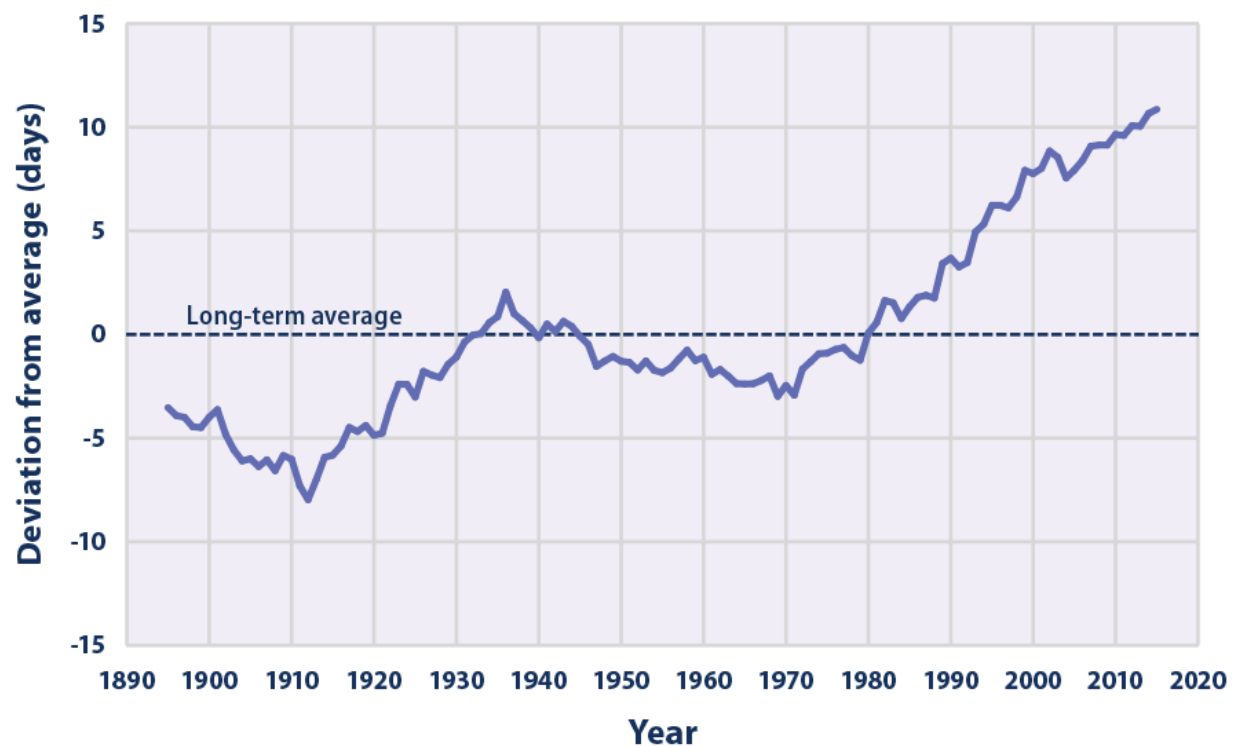


Figure 10.4. The length of the growing season in the contiguous 48 states compared with a long-term average (1895–2015), where “growing season” is defined by a temperature threshold of 41°F. For each year, the line represents the number of days shorter or longer than average. The line was smoothed using an 11-year moving average. Choosing a different long-term average for comparison would not change the shape of the data over time. (Figure source: Kunkel et al. 2016, EPA 2016).

REFERENCES

- Adams, H.D., A.D. Collins, S.P. Briggs, M. Vennetier, L.T. Dickman, S.A. Sevanto, N. Garcia-Forner, H.H. Powers, and N.G. McDowell, 2015: Experimental drought and heat can delay phenological development and reduce foliar and shoot growth in semiarid trees. *Global Change Biology*, **21**, 4210-4220. <http://dx.doi.org/10.1111/gcb.13030>
- Alpert, P. and M. Mandel, 1986: Wind variability — An indicator for a mesoclimatic change in Israel. *Journal of Climate and Applied Meteorology*, **25**, 1568-1576. [http://dx.doi.org/10.1175/1520-0450\(1986\)025<1568:wwifam>2.0.co;2](http://dx.doi.org/10.1175/1520-0450(1986)025<1568:wwifam>2.0.co;2)
- Anav, A., P. Friedlingstein, M. Kidston, L. Bopp, P. Ciais, P. Cox, C. Jones, M. Jung, R. Myneni, and Z. Zhu, 2013: Evaluating the land and ocean components of the global carbon cycle in the CMIP5 earth system models. *Journal of Climate*, **26**, 6801-6843. <http://dx.doi.org/10.1175/jcli-d-12-00417.1>
- Anderegg, W.R.L., C. Schwalm, F. Biondi, J.J. Camarero, G. Koch, M. Litvak, K. Ogle, J.D. Shaw, E. Shevliakova, A.P. Williams, A. Wolf, E. Ziaco, and S. Pacala, 2015: Pervasive drought legacies in forest ecosystems and their implications for carbon cycle models. *Science*, **349**, 528-532. <http://dx.doi.org/10.1126/science.aab1833>
- Anderson, R.G., J.G. Canadell, J.T. Randerson, R.B. Jackson, B.A. Hungate, D.D. Baldocchi, G.A. Ban-Weiss, G.B. Bonan, K. Caldeira, L. Cao, N.S. Diffenbaugh, K.R. Gurney, L.M. Kueppers, B.E. Law, S. Luyssaert, and T.L. O'Halloran, 2011: Biophysical considerations in forestry for climate protection. *Frontiers in Ecology and the Environment*, **9**, 174-182. <http://dx.doi.org/10.1890/090179>
- Ashley, W.S., M.L. Bentley, and J.A. Stallins, 2012: Urban-induced thunderstorm modification in the southeast United States. *Climatic Change*, **113**, 481-498. <http://dx.doi.org/10.1007/s10584-011-0324-1>
- Asner, G.P., P.G. Brodrick, C.B. Anderson, N. Vaughn, D.E. Knapp, and R.E. Martin, 2016: Progressive forest canopy water loss during the 2012–2015 California drought. *Proceedings of the National Academy of Sciences*, **113**, E249-E255. <http://dx.doi.org/10.1073/pnas.1523397113>
- Barnston, A.G. and P.T. Schickedanz, 1984: The effect of irrigation on warm season precipitation in the southern Great Plains. *Journal of Climate and Applied Meteorology*, **23**, 865-888. [http://dx.doi.org/10.1175/1520-0450\(1984\)023<0865:TEOIOW>2.0.CO;2](http://dx.doi.org/10.1175/1520-0450(1984)023<0865:TEOIOW>2.0.CO;2)
- Bonan, G.B., 2008: Forests and climate change: Forcings, feedbacks, and the climate benefits of forests. *Science*, **320**, 1444-1449. <http://dx.doi.org/10.1126/science.1155121>

- Bounoua, L., P. Zhang, G. Mostovoy, K. Thome, J. Masek, M. Imhoff, M. Shepherd, D. Quattrochi, J. Santanello, J. Silva, R. Wolfe, and A.M. Toure, 2015: Impact of urbanization on US surface climate. *Environmental Research Letters*, **10**, 084010. <http://dx.doi.org/10.1088/1748-9326/10/8/084010>
- Brown, D.G., C. Polsky, P. Bolstad, S.D. Brody, D. Hulse, R. Kroh, T.R. Loveland, and A. Thomson, 2014: Ch. 13: Land Use and Land Cover Change. *Climate Change Impacts in the United States: The Third National Climate Assessment*. Melillo, J.M., Terese (T.C.) Richmond, and G.W. Yohe, Eds. U.S. Global Change Research Program, Washington, DC, 318-332. <http://dx.doi.org/10.7930/J05Q4T1Q> <http://nca2014.globalchange.gov/report/sectors/land-use-and-land-cover-change>
- Brown, M.E., J.M. Antle, P. Backlund, E.R. Carr, W.E. Easterling, M.K. Walsh, C. Ammann, W. Attavanich, C.B. Barrett, M.F. Bellemare, V. Dancheck, C. Funk, K. Grace, J.S.I. Ingram, H. Jiang, H. Maletta, T. Mata, A. Murray, M. Ngugi, D. Ojima, B. O'Neill, and C. Tebaldi, 2015: Climate Change, Global Food Security, and the U.S. Food System. 146 pp. U.S. Global Change Research Program. http://www.usda.gov/oce/climate_change/FoodSecurity2015Assessment/FullAssessment.pdf
- Challinor, A.J., J. Watson, D.B. Lobell, S.M. Howden, D.R. Smith, and N. Chhetri, 2014: A meta-analysis of crop yield under climate change and adaptation. *Nature Climate Change*, **4**, 287-291. <http://dx.doi.org/10.1038/nclimate2153>
- Chan, D. and Q. Wu, 2015: Significant anthropogenic-induced changes of climate classes since 1950. *Scientific Reports*, **5**, 13487. <http://dx.doi.org/10.1038/srep13487>
- Ciais, P., C. Sabine, G. Bala, L. Bopp, V. Brovkin, J. Canadell, A. Chhabra, R. DeFries, J. Galloway, M. Heimann, C. Jones, C. Le Quéré, R.B. Myneni, S. Piao, and P. Thornton, 2013: Carbon and Other Biogeochemical Cycles. *Climate Change 2013: The Physical Science Basis. Contribution of Working Group I to the Fifth Assessment Report of the Intergovernmental Panel on Climate Change*. Stocker, T.F., D. Qin, G.-K. Plattner, M. Tignor, S.K. Allen, J. Boschung, A. Nauels, Y. Xia, V. Bex, and P.M. Midgley, Eds. Cambridge University Press, Cambridge, United Kingdom and New York, NY, USA, 465–570. <http://dx.doi.org/10.1017/CBO9781107415324.015> www.climatechange2013.org
- Daly, C., M.P. Widrlechner, M.D. Halbleib, J.I. Smith, and W.P. Gibson, 2012: Development of a new USDA plant hardiness zone map for the United States. *Journal of Applied Meteorology and Climatology*, **51**, 242-264. <http://dx.doi.org/10.1175/2010JAMC2536.1>
- Diaz, H.F. and J.K. Eischeid, 2007: Disappearing “alpine tundra” Köppen climatic type in the western United States. *Geophysical Research Letters*, **34**, n/a-n/a. <http://dx.doi.org/10.1029/2007GL031253>

- 1 Diffenbaugh, N.S., D.L. Swain, and D. Touma, 2015: Anthropogenic warming has increased
2 drought risk in California. *Proceedings of the National Academy of Sciences*, **112**, 3931-3936.
3 <http://dx.doi.org/10.1073/pnas.1422385112>
- 4 Elsner, M.M., L. Cuo, N. Voisin, J.S. Deems, A.F. Hamlet, J.A. Vano, K.E.B. Mickelson, S.Y.
5 Lee, and D.P. Lettenmaier, 2010: Implications of 21st century climate change for the
6 hydrology of Washington State. *Climatic Change*, **102**, 225-260.
7 <http://dx.doi.org/10.1007/s10584-010-9855-0>
- 8 EPA, 2005: Greenhouse Gas Mitigation Potential in U.S. Forestry and Agriculture. EPA 430-R-
9 05-006. U.S. Environmental Protection Agency, Washington, D.C.
- 10 EPA, 2016: Climate Change Indicators in the United States, 2016. 4th edition. EPA 430-R-16-
11 004, 96 pp. U.S. Environmental Protection Agency, Washington, D.C.
12 https://www.epa.gov/sites/production/files/2016-08/documents/climate_indicators_2016.pdf
- 13 Frank, D., M. Reichstein, M. Bahn, K. Thonicke, D. Frank, M.D. Mahecha, P. Smith, M. van der
14 Velde, S. Vicca, F. Babst, C. Beer, N. Buchmann, J.G. Canadell, P. Ciais, W. Cramer, A.
15 Ibrom, F. Miglietta, B. Poulter, A. Rammig, S.I. Seneviratne, A. Walz, M. Wattenbach, M.A.
16 Zavala, and J. Zscheischler, 2015: Effects of climate extremes on the terrestrial carbon cycle:
17 concepts, processes and potential future impacts. *Global Change Biology*, **21**, 2861-2880.
18 <http://dx.doi.org/10.1111/gcb.12916>
- 19 Fridley, J.D., J.S. Lynn, J.P. Grime, and A.P. Askew, 2016: Longer growing seasons shift
20 grassland vegetation towards more-productive species. *Nature Clim. Change*, **6**, 865-868.
21 <http://dx.doi.org/10.1038/nclimate3032>
- 22 Fu, Y.H., H. Zhao, S. Piao, M. Peaucelle, S. Peng, G. Zhou, P. Ciais, M. Huang, A. Menzel, J.
23 Penuelas, Y. Song, Y. Vitasse, Z. Zeng, and I.A. Janssens, 2015: Declining global warming
24 effects on the phenology of spring leaf unfolding. *Nature*, **526**, 104-107.
25 <http://dx.doi.org/10.1038/nature15402>
- 26 Galloway, J.N., W.H. Schlesinger, C.M. Clark, N.B. Grimm, R.B. Jackson, B.E. Law, P.E.
27 Thornton, A.R. Townsend, and R. Martin, 2014: Ch. 15: Biogeochemical Cycles. *Climate*
28 *Change Impacts in the United States: The Third National Climate Assessment*. Melillo, J.M.,
29 Terese (T.C.) Richmond, and G.W. Yohe, Eds. U.S. Global Change Research Program,
30 Washington, DC, 350-368. <http://dx.doi.org/10.7930/J0X63JT0>
31 <http://nca2014.globalchange.gov/report/sectors/biogeochemical-cycles>
- 32 Georgakakos, A., P. Fleming, M. Dettinger, C. Peters-Lidard, T.C. Richmond, K. Reckhow, K.
33 White, and D. Yates, 2014: Ch. 3: Water resources. *Climate Change Impacts in the United*
34 *States: The Third National Climate Assessment*. Melillo, J.M., T.C. Richmond, and G.W.

- Yohe, Eds. U.S. Global Change Research Program, Washington, D.C., 69-112.
<http://dx.doi.org/10.7930/J0G44N6T>
- Gray, J.M., S. Frolking, E.A. Kort, D.K. Ray, C.J. Kucharik, N. Ramankutty, and M.A. Friedl, 2014: Direct human influence on atmospheric CO₂ seasonality from increased cropland productivity. *Nature*, **515**, 398-401. <http://dx.doi.org/10.1038/nature13957>
- Grundstein, A., 2008: Assessing climate change in the contiguous United States using a modified Thornthwaite climate classification scheme. *The Professional Geographer*, **60**, 398-412.
<http://dx.doi.org/10.1080/00330120802046695>
- Gu, L., P.J. Hanson, W. Mac Post, D.P. Kaiser, B. Yang, R. Nemani, S.G. Pallardy, and T. Meyers, 2008: The 2007 eastern US spring freezes: Increased cold damage in a warming world? *BioScience*, **58**, 253-262. <http://dx.doi.org/10.1641/b580311>
- Guenther, A., T. Karl, P. Harley, C. Wiedinmyer, P.I. Palmer, and C. Geron, 2006: Estimates of global terrestrial isoprene emissions using MEGAN (Model of Emissions of Gases and Aerosols from Nature). *Atmospheric Chemistry and Physics*, **6**, 3181-3210.
<http://dx.doi.org/10.5194/acp-6-3181-2006>
- Hatfield, J., G. Takle, R. Grotjahn, P. Holden, R.C. Izaurralde, T. Mader, E. Marshall, and D. Liverman, 2014: Ch. 6: Agriculture. *Climate Change Impacts in the United States: The Third National Climate Assessment*. Melillo, J.M., Terese (T.C.) Richmond, and G.W. Yohe, Eds. U.S. Global Change Research Program, Washington, DC, 150-174.
<http://dx.doi.org/10.7930/J02Z13FR>
<http://nca2014.globalchange.gov/report/sectors/agriculture>
- Hibbard, K., T. Wilson, K. Averyt, R. Harriss, R. Newmark, S. Rose, E. Shevliakova, and V. Tidwell, 2014: Ch. 10: Energy, Water, and Land Use. *Climate Change Impacts in the United States: The Third National Climate Assessment*. Melillo, J.M., Terese (T.C.) Richmond, and G.W. Yohe, Eds. U.S. Global Change Research Program, Washington, DC, 257-281.
<http://dx.doi.org/10.7930/J0JW8BSF> <http://nca2014.globalchange.gov/report/sectors/energy-water-and-land>
- Imhoff, M.L., P. Zhang, R.E. Wolfe, and L. Bounoua, 2010: Remote sensing of the urban heat island effect across biomes in the continental USA. *Remote Sensing of Environment*, **114**, 504-513. <http://dx.doi.org/10.1016/j.rse.2009.10.008>
- IPCC, 2013: Summary for policymakers. *Climate Change 2013: The Physical Science Basis. Contribution of Working Group I to the Fifth Assessment Report of the Intergovernmental Panel on Climate Change*. Stocker, T.F., D. Qin, G.-K. Plattner, M. Tignor, S.K. Allen, J. Boschung, A. Nauels, Y. Xia, V. Bex, and P.M. Midgley, Eds. Cambridge University Press,

- 1 Cambridge, United Kingdom and New York, NY, USA, 1–30.
2 <http://dx.doi.org/10.1017/CBO9781107415324.004>
- 3 Jackson, R.B., J.T. Randerson, J.G. Canadell, R.G. Anderson, R. Avissar, D.D. Baldocchi, G.B.
4 Bonan, K. Caldeira, N.S. Diffenbaugh, C.B. Field, B.A. Hungate, E.G. Jobbágy, L.M.
5 Kueppers, D.N. Marcelo, and D.E. Pataki, 2008: Protecting climate with forests.
6 *Environmental Research Letters*, **3**, 044006. <http://stacks.iop.org/1748-9326/3/i=4/a=044006>
- 7 Jandl, R., M. Lindner, L. Vesterdal, B. Bauwens, R. Baritz, F. Hagedorn, D.W. Johnson, K.
8 Minkinen, and K.A. Byrne, 2007: How strongly can forest management influence soil
9 carbon sequestration? *Geoderma*, **137**, 253–268.
10 <http://dx.doi.org/10.1016/j.geoderma.2006.09.003>
- 11 Joyce, L.A., S.W. Running, D.D. Breshears, V.H. Dale, R.W. Malmshiemer, R.N. Sampson, B.
12 Sohngen, and C.W. Woodall, 2014: Ch. 7: Forests. *Climate Change Impacts in the United*
13 *States: The Third National Climate Assessment*. Melillo, J.M., Terese (T.C.) Richmond, and
14 G.W. Yohe, Eds. U.S. Global Change Research Program, Washington, DC, 175–194.
15 <http://dx.doi.org/10.7930/J0Z60KZC> <http://nca2014.globalchange.gov/report/sectors/forests>
- 16 Ju, J. and J.G. Masek, 2016: The vegetation greenness trend in Canada and US Alaska from
17 1984–2012 Landsat data. *Remote Sensing of Environment*, **176**, 1–16.
18 <http://dx.doi.org/10.1016/j.rse.2016.01.001>
- 19 Kalnay, E. and M. Cai, 2003: Impact of urbanization and land-use change on climate. *Nature*,
20 **423**, 528–531. <http://dx.doi.org/10.1038/nature01675>
- 21 Kam, J., J. Sheffield, and E.F. Wood, 2014: Changes in drought risk over the contiguous United
22 States (1901–2012): The influence of the Pacific and Atlantic Oceans. *Geophysical Research*
23 *Letters*, **41**, 5897–5903. <http://dx.doi.org/10.1002/2014GL060973>
- 24 Keenan, T.F., D.Y. Hollinger, G. Bohrer, D. Dragoni, J.W. Munger, H.P. Schmid, and A.D.
25 Richardson, 2013: Increase in forest water-use efficiency as atmospheric carbon dioxide
26 concentrations rise. *Nature*, **499**, 324–327. <http://dx.doi.org/10.1038/nature12291>
- 27 King, S.L., D.J. Twedt, and R.R. Wilson, 2006: The role of the wetland reserve program in
28 conservation efforts in the Mississippi River alluvial valley. *Wildlife Society Bulletin (1973-*
29 *2006)*, **34**, 914–920. <http://www.jstor.org/stable/4134299>
- 30 Knutti, R. and J. Sedlacek, 2013: Robustness and uncertainties in the new CMIP5 climate model
31 projections. *Nature Climate Change*, **3**, 369–373. <http://dx.doi.org/10.1038/nclimate1716>
- 32 Lambert, A.M., C.M. D'Antonio, and T.L. Dudley, 2010: Invasive species and fire in California
33 ecosystems. *Fremontia*, **38**, 29–36.

- 1 Lippke, B., E. Oneil, R. Harrison, K. Skog, L. Gustavsson, and R. Sathre, 2011: Life cycle
2 impacts of forest management and wood utilization on carbon mitigation : knowns and
3 unknowns. *Carbon management*, **2**, 303-333. <http://dx.doi.org/10.4155/CMT.11.24>
- 4 Littell, J.S., M.M. Elsner, G.S. Mauger, E.R. Lutz, A.F. Hamlet, and E.P. Salathé, 2011:
5 Regional climate and hydrologic change in the northern U.S. Rockies and Pacific Northwest:
6 Internally consistent projections of future climate for resource management. University of
7 Washington, Seattle. [https://cig.uw.edu/publications/regional-climate-and-hydrologic-change-](https://cig.uw.edu/publications/regional-climate-and-hydrologic-change-in-the-northern-u-s-rockies-and-pacific-northwest-internally-consistent-projections-of-future-climate-for-resource-management/)
8 [in-the-northern-u-s-rockies-and-pacific-northwest-internally-consistent-projections-of-future-](https://cig.uw.edu/publications/regional-climate-and-hydrologic-change-in-the-northern-u-s-rockies-and-pacific-northwest-internally-consistent-projections-of-future-climate-for-resource-management/)
9 [climate-for-resource-management/](https://cig.uw.edu/publications/regional-climate-and-hydrologic-change-in-the-northern-u-s-rockies-and-pacific-northwest-internally-consistent-projections-of-future-climate-for-resource-management/)
- 10 Littell, J.S., D.L. Peterson, K.L. Riley, Y.-Q. Liu, and C.H. Luce, 2016: Fire and Drought.
11 *Effects of Drought on Forests and Rangelands in the United States: A comprehensive science*
12 *synthesis*. Vose, J., J.S. Clark, C. Luce, and T. Patel-Weynand, Eds. U.S. Department of
13 Agriculture, Forest Service, Washington Office, Washington, DC, 135-150.
14 <http://www.treesearch.fs.fed.us/pubs/50261>
- 15 Liu, L.L. and T.L. Greaver, 2009: A review of nitrogen enrichment effects on three biogenic
16 GHGs: The CO₂ sink may be largely offset by stimulated N₂O and CH₄ emission. *Ecology*
17 *Letters*, **12**, 1103-1117. <http://dx.doi.org/10.1111/j.1461-0248.2009.01351.x>
- 18 Lobell, D.B. and C. Tebaldi, 2014: Getting caught with our plants down: The risks of a global
19 crop yield slowdown from climate trends in the next two decades. *Environmental Research*
20 *Letters*, **9**, 074003. <http://dx.doi.org/10.1088/1748-9326/9/7/074003>
- 21 Maloney, E.D., S.J. Camargo, E. Chang, B. Colle, R. Fu, K.L. Geil, Q. Hu, X. Jiang, N. Johnson,
22 K.B. Karauskas, J. Kinter, B. Kirtman, S. Kumar, B. Langenbrunner, K. Lombardo, L.N.
23 Long, A. Mariotti, J.E. Meyerson, K.C. Mo, J.D. Neelin, Z. Pan, R. Seager, Y. Serra, A. Seth,
24 J. Sheffield, J. Stroeve, J. Thibeault, S.-P. Xie, C. Wang, B. Wyman, and M. Zhao, 2014:
25 North American climate in CMIP5 experiments: Part III: Assessment of twenty-first-century
26 projections. *Journal of Climate*, **27**, 2230-2270. <http://dx.doi.org/10.1175/JCLI-D-13-00273.1>
- 27 Mann, M.E. and P.H. Gleick, 2015: Climate change and California drought in the 21st century.
28 *Proceedings of the National Academy of Sciences*, **112**, 3858-3859.
29 <http://dx.doi.org/10.1073/pnas.1503667112>
- 30 Mao, J., A. Ribes, B. Yan, X. Shi, P.E. Thornton, R. Seferian, P. Ciais, R.B. Myneni, H.
31 Douville, S. Piao, Z. Zhu, R.E. Dickinson, Y. Dai, D.M. Ricciuto, M. Jin, F.M. Hoffman, B.
32 Wang, M. Huang, and X. Lian, 2016: Human-induced greening of the northern extratropical
33 land surface. *Nature Climate Change*, **6**, 959-963. <http://dx.doi.org/10.1038/nclimate3056>

- 1 Marotz, G.A., J. Clark, J. Henry, and R. Standfast, 1975: Cloud fields over irrigated areas in
2 southwestern Kansas—Data and speculations. *The Professional Geographer*, **27**, 457-461.
3 <http://dx.doi.org/10.1111/j.0033-0124.1975.00457.x>
- 4 Marston, L., M. Konar, X. Cai, and T.J. Troy, 2015: Virtual groundwater transfers from
5 overexploited aquifers in the United States. *Proceedings of the National Academy of Sciences*,
6 **112**, 8561-8566. <http://dx.doi.org/10.1073/pnas.1500457112>
- 7 McGrath, J.M., A.M. Betzelberger, S. Wang, E. Shook, X.-G. Zhu, S.P. Long, and E.A.
8 Ainsworth, 2015: An analysis of ozone damage to historical maize and soybean yields in the
9 United States. *Proceedings of the National Academy of Sciences*, **112**, 14390-14395.
10 <http://dx.doi.org/10.1073/pnas.1509777112>
- 11 McKinley, D.C., M.G. Ryan, R.A. Birdsey, C.P. Giardina, M.E. Harmon, L.S. Heath, R.A.
12 Houghton, R.B. Jackson, J.F. Morrison, B.C. Murray, D.E. Pataki, and K.E. Skog, 2011: A
13 synthesis of current knowledge on forests and carbon storage in the United States. *Ecological*
14 *Applications*, **21**, 1902-1924. <http://dx.doi.org/10.1890/10-0697.1>
15 http://128.104.77.228/documnts/pdf2011/fpl_2011_mckinley001.pdf
- 16 McLauchlan, K., 2006: The nature and longevity of agricultural impacts on soil carbon and
17 nutrients: A review. *Ecosystems*, **9**, 1364-1382. <http://dx.doi.org/10.1007/s10021-005-0135-1>
- 18 Melillo, J.M., S. Butler, J. Johnson, J. Mohan, P. Steudler, H. Lux, E. Burrows, F. Bowles, R.
19 Smith, L. Scott, C. Vario, T. Hill, A. Burton, Y.M. Zhou, and J. Tang, 2011: Soil warming,
20 carbon-nitrogen interactions, and forest carbon budgets. *Proceedings of the National Academy*
21 *of Sciences*, **108**, 9508-9512. <http://dx.doi.org/10.1073/pnas.1018189108>
22 <http://www.pnas.org/content/108/23/9508.full.pdf+html>
- 23 Melillo, J.M., T.C. Richmond, and G.W. Yohe, eds. *Climate Change Impacts in the United*
24 *States: The Third National Climate Assessment*. 2014, U.S. Global Change Research Program:
25 Washington, D.C. 842. <http://dx.doi.org/10.7930/J0Z31WJ2>.
- 26 Moore, G.W., C.B. Edgar, J.G. Vogel, R.A. Washington-Allen, Rosaleen G. March, and R.
27 Zehnder, 2016: Tree mortality from an exceptional drought spanning mesic to semiarid
28 ecoregions. *Ecological Applications*, **26**, 602-611. <http://dx.doi.org/10.1890/15-0330>
- 29 Myhre, G., D. Shindell, F.-M. Bréon, W. Collins, J. Fuglestedt, J. Huang, D. Koch, J.-F.
30 Lamarque, D. Lee, B. Mendoza, T. Nakajima, A. Robock, G. Stephens, T. Takemura, and H.
31 Zhang, 2013: Anthropogenic and Natural Radiative Forcing. *Climate Change 2013: The*
32 *Physical Science Basis. Contribution of Working Group I to the Fifth Assessment Report of*
33 *the Intergovernmental Panel on Climate Change*. Stocker, T.F., D. Qin, G.-K. Plattner, M.
34 Tignor, S.K. Allen, J. Boschung, A. Nauels, Y. Xia, V. Bex, and P.M. Midgley, Eds.

- Cambridge University Press, Cambridge, United Kingdom and New York, NY, USA, 659–740. <http://dx.doi.org/10.1017/CBO9781107415324.018> www.climatechange2013.org
- Norby, R.J., E.H. DeLucia, B. Gielen, C. Calfapietra, C.P. Giardina, J.S. King, J. Ledford, H.R. McCarthy, D.J.P. Moore, R. Ceulemans, P. De Angelis, A.C. Finzi, D.F. Karnosky, M.E. Kubiske, M. Lukac, K.S. Pregitzer, G.E. Scarascia-Mugnozza, W.H. Schlesinger, and R. Oren, 2005: Forest response to elevated CO₂ is conserved across a broad range of productivity. *Proceedings of the National Academy of Sciences of the United States of America*, **102**, 18052-18056. <http://dx.doi.org/10.1073/pnas.0509478102>
- Parker, L.E. and J.T. Abatzoglou, 2016: Projected changes in cold hardiness zones and suitable overwinter ranges of perennial crops over the United States. *Environmental Research Letters*, **11**, 034001. <http://dx.doi.org/10.1088/1748-9326/11/3/034001>
- Pielke, R.A., J. Adegoke, A. Beltrán-Przekurat, C.A. Hiemstra, J. Lin, U.S. Nair, D. Niyogi, and T.E. Nobis, 2007: An overview of regional land-use and land-cover impacts on rainfall. *Tellus B*, **59**, 587-601. <http://dx.doi.org/10.1111/j.1600-0889.2007.00251.x>
- Pielke Sr, R. and X. Zeng, 1989: Influence on severe storm development of irrigated land. *National Weather Digest* **14**, 16-17.
- Pyle, J.A., N. Warwick, X. Yang, P.J. Young, and G. Zeng, 2007: Climate/chemistry feedbacks and biogenic emissions. *Philosophical Transactions of the Royal Society A: Mathematical, Physical and Engineering Sciences*, **365**, 1727-40. <http://dx.doi.org/10.1098/rsta.2007.2041>
- Reichstein, M., M. Bahn, P. Ciais, D. Frank, M.D. Mahecha, S.I. Seneviratne, J. Zscheischler, C. Beer, N. Buchmann, D.C. Frank, D. Papale, A. Rammig, P. Smith, K. Thonicke, M. van der Velde, S. Vicca, A. Walz, and M. Wattenbach, 2013: Climate extremes and the carbon cycle. *Nature*, **500**, 287-295. <http://dx.doi.org/10.1038/nature12350>
- Reyes-Fox, M., H. Steltzer, M.J. Trlica, G.S. McMaster, A.A. Andales, D.R. LeCain, and J.A. Morgan, 2014: Elevated CO₂ further lengthens growing season under warming conditions. *Nature*, **510**, 259-262. <http://dx.doi.org/10.1038/nature13207>
- Rosenstiel, T.N., M.J. Potosnak, K.L. Griffin, R. Fall, and R.K. Monson, 2003: Increased CO₂ uncouples growth from isoprene emission in an agriforest ecosystem. *Nature*, **421**, 256-259. <http://dx.doi.org/10.1038/nature01312>
- Rosenzweig, C., J. Elliott, D. Deryng, A.C. Ruane, C. Müller, A. Arneth, K.J. Boote, C. Folberth, M. Glotter, N. Khabarov, K. Neumann, F. Piontek, T.A.M. Pugh, E. Schmid, E. Stehfest, H. Yang, and J.W. Jones, 2014: Assessing agricultural risks of climate change in the 21st century in a global gridded crop model intercomparison. *Proceedings of the National Academy of Sciences*, **111**, 3268-3273. <http://dx.doi.org/10.1073/pnas.1222463110>

- Schlesinger, W.H., M.C. Dietze, R.B. Jackson, R.P. Phillips, C.C. Rhoads, L.E. Rustad, and J.M. Vose, 2016: Forest biogeochemistry in response to drought. *Effects of Drought on Forests and Rangelands in the United States: A comprehensive science synthesis*. Vose, J., J.S. Clark, C. Luce, and T. Patel-Weynand, Eds. U.S. Department of Agriculture, Forest Service, Washington Office, Washington, DC, 97-106. <http://www.treeseearch.fs.fed.us/pubs/50261>
- Schwalm, C.R., W.R.L. Anderegg, F. Biondi, G. Koch, M. Litvak, K. Ogle, J.D. Shaw, A. Wolf, D.N. Huntzinger, and A.M. Michalak, In review: Global patterns of drought recovery. *Nature*.
- Shepherd, J.M., 2013: Impacts of Urbanization on Precipitation and Storms: Physical Insights and Vulnerabilities *Climate Vulnerability: Understanding and Addressing Threats to Essential Resources*. Academic Press, Oxford, 109-125. <http://dx.doi.org/10.1016/B978-0-12-384703-4.00503-7>
- Sippel, S., J. Zscheischler, and M. Reichstein, 2016: Ecosystem impacts of climate extremes crucially depend on the timing. *Proceedings of the National Academy of Sciences*, **113**, 5768-5770. <http://dx.doi.org/10.1073/pnas.1605667113>
- Smith, P., S.J. Chapman, W.A. Scott, H.I.J. Black, M. Wattenbach, R. Milne, C.D. Campbell, A. Lilly, N. Ostle, P.E. Levy, D.G. Lumsdon, P. Millard, W. Towers, S. Zaehle, and J.U. Smith, 2007: Climate change cannot be entirely responsible for soil carbon loss observed in England and Wales, 1978–2003. *Global Change Biology*, **13**, 2605-2609. <http://dx.doi.org/10.1111/j.1365-2486.2007.01458.x>
- SOCRR-2, To be released in 2017, per website.
- Szokan-Emilson, E.J., B.W. Kielstra, S.E. Arnott, S.A. Watmough, J.M. Gunn, and A.J. Tanentzap, 2016: Dry conditions disrupt terrestrial–aquatic linkages in northern catchments. *Global Change Biology*, **Early view**. <http://dx.doi.org/10.1111/gcb.13361>
- Tian, H., C. Lu, J. Yang, K. Banger, D.N. Huntzinger, C.R. Schwalm, A.M. Michalak, R. Cook, P. Ciais, D. Hayes, M. Huang, A. Ito, A.K. Jain, H. Lei, J. Mao, S. Pan, W.M. Post, S. Peng, B. Poulter, W. Ren, D. Ricciuto, K. Schaefer, X. Shi, B. Tao, W. Wang, Y. Wei, Q. Yang, B. Zhang, and N. Zeng, 2015: Global patterns and controls of soil organic carbon dynamics as simulated by multiple terrestrial biosphere models: Current status and future directions. *Global Biogeochemical Cycles*, **29**, 775-792. <http://dx.doi.org/10.1002/2014GB005021>
- Todd-Brown, K.E.O., J.T. Randerson, W.M. Post, F.M. Hoffman, C. Tarnocai, E.A.G. Schuur, and S.D. Allison, 2013: Causes of variation in soil carbon simulations from CMIP5 Earth system models and comparison with observations. *Biogeosciences*, **10**, 1717-1736. <http://dx.doi.org/10.5194/bg-10-1717-2013>
- U.S. Department of State, 2016: Second Biennial Report of the United States of America. 75 pp., Washington, DC.

http://unfccc.int/files/national_reports/biennial_reports_and_iar/submitted_biennial_reports/application/pdf/2016_second_biennial_report_of_the_united_states.pdf

Vose, J., J.S. Clark, C. Luce, and T. Patel-Weynand, eds. *Effects of Drought on Forests and Rangelands in the United States: A comprehensive science synthesis*. 2016, U.S. Department of Agriculture, Forest Service, Washington Office: Washington, DC. 289.
<http://www.treeseearch.fs.fed.us/pubs/50261>

Walsh, J., D. Wuebbles, K. Hayhoe, J. Kossin, K. Kunkel, G. Stephens, P. Thorne, R. Vose, M. Wehner, J. Willis, D. Anderson, S. Doney, R. Feely, P. Hennon, V. Kharin, T. Knutson, F. Landerer, T. Lenton, J. Kennedy, and R. Somerville, 2014: Ch. 2: Our changing climate. *Climate Change Impacts in the United States: The Third National Climate Assessment*. Melillo, J.M., T.C. Richmond, and G.W. Yohe, Eds. U.S. Global Change Research Program, Washington, D.C., 19-67. <http://dx.doi.org/10.7930/J0KW5CXT>

Walsh, J., D. Wuebbles, K. Hayhoe, J. Kossin, K. Kunkel, G. Stephens, P. Thorne, R. Vose, M. Wehner, J. Willis, D. Anderson, V. Kharin, T. Knutson, F. Landerer, T. Lenton, J. Kennedy, and R. Somerville, 2014: Appendix 4: Frequently Asked Questions. *Climate Change Impacts in the United States: The Third National Climate Assessment*. Melillo, J.M., Terese (T.C.) Richmond, and G.W. Yohe, Eds. U.S. Global Change Research Program, Washington, DC, 790-820. <http://dx.doi.org/10.7930/J0G15XS3>

Ward, D.S. and N.M. Mahowald, 2015: Local sources of global climate forcing from different categories of land use activities. *Earth System Dynamics*, **6**, 175-194.
<http://dx.doi.org/10.5194/esd-6-175-2015>

Ward, D.S., N.M. Mahowald, and S. Kloster, 2014: Potential climate forcing of land use and land cover change. *Atmospheric Chemistry and Physics*, **14**, 12701-12724.
<http://dx.doi.org/10.5194/acp-14-12701-2014>

Wear, D.N. and J.W. Coulston, 2015: From sink to source: Regional variation in U.S. forest carbon futures. *Scientific Reports*, **5**, 16518. <http://dx.doi.org/10.1038/srep16518>

Wolf, S., T.F. Keenan, J.B. Fisher, D.D. Baldocchi, A.R. Desai, A.D. Richardson, R.L. Scott, B.E. Law, M.E. Litvak, N.A. Brunsell, W. Peters, and I.T. van der Laan-Luijkx, 2016: Warm spring reduced carbon cycle impact of the 2012 US summer drought. *Proceedings of the National Academy of Sciences*, **113**, 5880-5885. <http://dx.doi.org/10.1073/pnas.1519620113>

Zaehle, S., P. Friedlingstein, and A.D. Friend, 2010: Terrestrial nitrogen feedbacks may accelerate future climate change. *Geophysical Research Letters*, **37**, L01401.
<http://dx.doi.org/10.1029/2009GL041345>

- 1 Zeng, N., F. Zhao, G.J. Collatz, E. Kalnay, R.J. Salawitch, T.O. West, and L. Guanter, 2014:
2 Agricultural green revolution as a driver of increasing atmospheric CO₂ seasonal amplitude.
3 *Nature*, **515**, 394-397. <http://dx.doi.org/10.1038/nature13893>
- 4 Zhang, X., L. Alexander, G.C. Hegerl, P. Jones, A.K. Tank, T.C. Peterson, B. Trewin, and F.W.
5 Zwiers, 2011: Indices for monitoring changes in extremes based on daily temperature and
6 precipitation data. *Wiley Interdisciplinary Reviews: Climate Change*, **2**, 851-870.
7 <http://dx.doi.org/10.1002/wcc.147>
- 8 Zhao, L., X. Lee, R.B. Smith, and K. Oleson, 2014: Strong contributions of local background
9 climate to urban heat islands. *Nature*, **511**, 216-219. <http://dx.doi.org/10.1038/nature13462>
- 10 Zhu, Z., S. Piao, R.B. Myneni, M. Huang, Z. Zeng, J.G. Canadell, P. Ciais, S. Sitch, P.
11 Friedlingstein, A. Arneeth, C. Cao, L. Cheng, E. Kato, C. Koven, Y. Li, X. Lian, Y. Liu, R.
12 Liu, J. Mao, Y. Pan, S. Peng, J. Penuelas, B. Poulter, T.A.M. Pugh, B.D. Stocker, N. Viovy,
13 X. Wang, Y. Wang, Z. Xiao, H. Yang, S. Zaehle, and N. Zeng, 2016: Greening of the Earth
14 and its drivers. *Nature Climate Change*, **6**, 791-795. <http://dx.doi.org/10.1038/nclimate3004>

11. Arctic Changes and their Effects on Alaska and the Rest of the United States

KEY FINDINGS

1. For both the State of Alaska and for the Arctic as a whole, near-surface air temperature is increasing at a rate more than twice as fast as the global-average temperature. (*Very high confidence*)
2. Rising Alaskan permafrost temperatures are causing permafrost to thaw and become more discontinuous; this releases additional CO₂ and CH₄ resulting in additional warming (*high confidence*). The overall magnitude of the permafrost-carbon feedback is uncertain.
3. Arctic sea ice and Greenland Ice Sheet mass loss are accelerating and Alaskan mountain glaciers continue to melt (*very high confidence*). Alaskan coastal sea ice loss rates exceed the Arctic average (*very high confidence*). Observed sea and land ice loss across the Arctic is occurring faster than climate models predict (*very high confidence*). Melting trends are expected to continue resulting in late summers becoming nearly ice-free for the Arctic ocean by mid-century (*very high confidence*).
4. Human activities have contributed to rising surface temperature, sea ice loss since 1979, and glacier mass loss observed across the Arctic. (*High confidence*)
5. Atmospheric circulation patterns connect the climates of the Arctic and the United States. The mid-latitude circulation influences Arctic climate change (*medium to high confidence*). In turn, current evidence suggests that Arctic warming is influencing mid-latitude circulation over the continental United States and affecting weather patterns, but the mechanisms are not well understood (*low to medium confidence*).

11.1. Introduction

Climate changes in Alaska and across the Arctic continue to outpace changes occurring across the globe. The Arctic is a complex system integral to Earth's climate, influencing global surface energy and moisture budgets, atmospheric and oceanic circulations, and geosphere–biosphere feedbacks. Resulting from its high sensitivity to radiative forcing and its role in amplifying warming, the Arctic cryosphere is a key indicator of the global climate state. Accelerated melting of multiyear sea ice cover, mass loss from the Greenland Ice Sheet (GrIS), reduction of terrestrial snow cover, and permafrost degradation are stark examples of the rapid Arctic system-wide response to global warming. These changes in Arctic sea ice, land ice, surface temperature, and permafrost influence global climate by affecting sea level, the carbon cycle, and potentially atmospheric and oceanic circulation patterns. Arctic climate change has altered the global climate in the past (Knies et al. 2014) and will influence climate in the future. Strongly coupled

to the Arctic, climate change in Alaska is apparent; the connection between climate changes in the Arctic and the continental United States is a topic of current research.

Adaptation, mitigation, and policy decisions depend on projections of future Alaskan and Arctic climate. Aside from uncertainties due to natural variability, scientific uncertainty, and greenhouse gas emissions uncertainty (see Chapter 4), additional unique uncertainties in our understanding of Arctic processes thwart projections, including shortcomings in mixed-phase cloud processes (Wyser et al. 2008); boundary layer processes (Bourassa et al. 2013); sea ice mechanics (Bourassa et al. 2013); and ocean currents, eddies, and tides that affect the advection of heat into and around the Arctic Ocean (Maslowski et al. 2012, 2014). The inaccessibility of the Arctic has made it difficult to sustain the kind of high-quality observations of the atmosphere, ocean, land, and ice required to improve physically based models, stunting scientific progress. Improved data quality and increased observational coverage would help address important Arctic science questions.

Despite these challenges, this chapter documents significant scientific progress and knowledge about how the Alaskan and Arctic climate has changed and will continue to change.

11.2. Arctic Changes

11.2.1. Alaska and Arctic Temperature

Surface temperature—an essential component of the Arctic climate system—both drives and signifies change, fundamentally controlling the melting of sea ice, land ice, and snow. Further, the vertical profile of temperature modulates the exchange of mass, energy, and momentum between the surface and atmosphere, and influences other components such as clouds (Kay and Gettelman 2009; Pavelsky et al. 2011; Taylor et al. 2015). Arctic temperatures exhibit significant spatial and interannual variability resulting from interactions and feedbacks between sea ice, snow cover, atmospheric heat transports, vegetation, clouds, water vapor, and the surface energy budget (Overland et al. 2015b; Johannessen et al. 2016; Overland and Wang 2016).

Satellite observations show that the Arctic has warmed at rates more than twice as fast as the global average—by $+0.60 \pm 0.07^{\circ}\text{C}$ ($1.08^{\circ} \pm 0.13^{\circ}\text{F}$) per decade since 1981—and that North American land regions north of 64°N (including Alaska) have warmed $+0.54 \pm 0.09^{\circ}\text{C}$ ($0.97^{\circ} \pm 0.16^{\circ}\text{F}$) per decade (Hartmann et al. 2013; Overland et al. 2014; Comiso and Hall 2014). Strong surface temperature warming has occurred across Alaska, especially on the North Slope during autumn. For example, Barrow’s warming since 1979 exceeds 3.8°C (7°F) in September, 6.6°C (12°F) in October, and 5.5°C (10°F) in November (Wendler et al. 2014). While Alaska state-wide annual mean temperature changes since 1949 are dominated by decadal variability like the Pacific Decadal Oscillation (Hartmann and Wendler 2005; McAfee 2014; see Ch. 5), records in 2014 and 2015 broke previous marks by more than 0.5°C (1.0°F) (see Ch. 6).

The enhanced warming of Alaska and the Arctic is a robust feature of the climate response to anthropogenic forcing (Collins et al. 2013; Taylor et al. 2013). There is *very likely* an anthropogenic contribution to Alaskan surface temperature warming over the past 50 years (Bindoff et al. 2013; Gillett et al. 2008; Najafi et al. 2015). However, it is *likely* that other anthropogenic forcings (mostly aerosols) have partially offset the greenhouse gas warming since 1913 by up to 60% at high latitudes and that natural forcing has not contributed to the long-term warming in a discernable way (Najafi et al. 2015). According to this study, Arctic warming to date would have been larger without the offsetting aerosols influence. It is *virtually certain* that Arctic surface temperatures continue to increase faster than the global mean through the 21st century (Christensen et al. 2013).

11.2.2. Arctic Sea Ice Change

Arctic sea ice strongly influences Alaskan, Arctic, and global climate by modulating exchanges of mass, energy, and momentum between the ocean and the atmosphere. Variations in Arctic sea ice cover also influence atmospheric temperature and humidity, wind patterns, clouds, ocean temperature, thermal stratification, and ecosystem productivity (Kay and Gettelman 2009; Kay et al. 2010; Pavelsky et al. 2011; Boisvert et al. 2013; Vaughan et al. 2013; Solomon et al. 2014; Taylor et al. 2015; Boisvert et al. 2015a,b; Johannessen et al. 2016). Arctic sea ice exhibits significant interannual, spatial, and seasonal variability driven by atmospheric wind patterns and cyclones, atmospheric temperature and humidity structure, clouds, radiation, sea ice dynamics, and the ocean (Ogi and Wallace 2007; Kwok and Untersteiner 2011; Stroeve et al. 2012a,b; Ogi and Rigor 2013; Carmack et al. 2015). Overwhelming evidence indicates that the character of Arctic sea ice is rapidly changing, marking the beginning of the “New Arctic” era.

Observational evidence indicates Arctic-wide sea ice decline since 1979, accelerating melt since 2000, and the fastest melt along the Alaskan coast (Stroeve et al. 2014a,b; Comiso and Hall 2014; Wendler et al. 2014). Although sea ice loss is found in all months, satellite observations show the fastest loss in late summer and autumn (Stroeve et al. 2014a). Since 1979, the annual average Arctic sea ice extent has decreased at a rate of 3.5%–4.1% per decade, accelerating since 2000 (Vaughan et al. 2013; Stroeve et al. 2014a,b; Comiso and Hall 2014). Regional sea ice melt along the Alaskan coasts exceeds the Arctic average rates with declines in the Beaufort and Chukchi Seas of –4.1% and –4.7% per decade, respectively. The annual minimum and maximum sea ice extent have decreased over the last 35 years by –13.3% and –2.5% per decade, respectively (Perovich et al. 2015). The ten lowest September sea ice extents over the satellite period have all occurred in the last ten years, the lowest in 2012. The 2016 September sea ice minimum tied with 2007 for the second lowest on record, but rapid refreezing resulted in the September monthly average extent being the fifth lowest. Despite the rapid initial refreezing, October and November sea ice extent is again in record low territory due to anomalously warm temperatures in the marginal seas around Alaska.

Other important characteristics of Arctic sea ice have also changed, including thickness, age, and melt season length. Sea ice thickness is monitored using an array of satellite, aircraft, and vessel measurements (Vaughan et al. 2013). The thickness of the Arctic sea ice during winter between 1980 and 2008 has decreased between 1.3 and 2.3 meters (4.3 and 7.5 feet) (Vaughan et al. 2013). The age distribution of sea ice has become younger since 1988 where the extent of first- and multiyear sea ice has decreased in September by $-11.5 \pm 2.1\%$ and $-13.5 \pm 2.5\%$ per decade, respectively (Vaughan et al. 2013; Perovich et al. 2015). Figure 11.1 shows the September sea ice extent and age in 1984 and 2016, illustrating significant reductions in sea ice age (Tschudi et al. 2016). Younger, thinner sea ice is more susceptible to melt, therefore reductions in age and thickness imply a stronger interannual sea ice albedo feedback and larger interannual variability.

[INSERT FIGURE 11.1 HERE:]

Figure 11.1: September sea ice extent (all gray-scale colors) and age shown for (a) 1984 and (b) 2016, illustrating significant reductions in sea ice extent and age (thickness). Bar graph in the lower right of each panel illustrates the sea ice area covered within each age category. (Figure source: NASA Science Visualization Studio (<http://svs.gsfc.nasa.gov/cgi-bin/details.cgi?aid=4489>); data: Tschudi et al. 2016)

Sea ice melt season has lengthened Arctic-wide by at least five days per decade since 1979, with larger regional changes (Stroeve et al. 2014b; Parkinson 2014). Some of the largest observed changes in sea ice melt season (Figure 11.2) are found along Alaska's northern and western coasts, lengthening the melt season by 20–30 days per decade and increasing the annual number of ice-free days by more than 90 (Parkinson 2014). Summer sea ice retreat along coastal Alaska has led to a longer open water seasons making the Alaskan coastline more vulnerable to erosion (Melillo 2014; Gibbs and Richmond 2015).

[INSERT FIGURE 11.2 HERE:]

Figure 11.2: 35-year trends in Arctic sea ice melt season length in days per decade from passive microwave satellite observations, illustrating that the sea ice season has shortened by more than 60 and as much as 90 days in coastal Alaska over the last 30 years. (Figure source: adapted from Parkinson 2014)]

There is *very likely* an anthropogenic contribution to the observed changes in the Alaska and Arctic sea ice since 1979 (Bindoff et al. 2013). Internal climate variability alone could not have caused recently observed record low Arctic sea ice extents (Zhang and Knutson 2013). Additional sea ice loss across the Arctic is *virtually certain* to result in late summers *very likely* becoming nearly ice-free (areal extent less than 10^6 km^2 or approximately $3.9 \times 10^5 \text{ mi}^2$) by mid-century (Collins et al. 2013; Snape and Forster 2014). Natural variability (Wettstein and Deser 2014), future emissions, and model uncertainties (Gagne et al. 2015; Stroeve and Notz, 2015; Swart et al. 2015) all influence sea ice projections. A key message from the Third National Climate Assessment (NCA3; Melillo et al. 2014) was that Arctic sea ice is disappearing. The

fundamental conclusion of this assessment the same, additional research corroborates the NCA3 statement.

11.2.3. Arctic Ocean and Marginal Seas

SEA SURFACE TEMPERATURE

Arctic Ocean sea surface temperatures (SSTs) have increased since 1982. Satellite-observed Arctic Ocean SSTs, poleward of 60°N, exhibit a trend of $+0.09 \pm 0.01^{\circ}\text{C}$ ($+0.16 \pm 0.02^{\circ}\text{F}$) per decade (Comiso and Hall 2014). Arctic Ocean SST is controlled by a combination of factors, including solar radiation and energy transport from ocean currents and atmospheric winds. Summertime Arctic Ocean SST trends and pattern strongly couple with sea ice extent; however, clouds, ocean color, upper-ocean thermal structure, and atmospheric circulation also play a role (Ogi and Rigor 2013; Rhein et al. 2013). Along coastal Alaska, SSTs in the Chukchi Sea exhibit a statistically significant (95% confidence) trend of $0.5 \pm 0.3^{\circ}\text{C}$ ($+0.9 \pm 0.5^{\circ}\text{F}$) per decade (Timmermans and Proshutinsky 2015).

Arctic Ocean temperatures also increased at depth (Polyakov et al. 2012; Rhein et al. 2013). Since 1970, Arctic Ocean Intermediate Atlantic Water (AW)—located between 150 and 900 meters—has warmed by $0.48 \pm 0.05^{\circ}\text{C}$ ($0.86 \pm 0.09^{\circ}\text{F}$) per decade; the most recent decade being the warmest (Polyakov et al. 2012). The observed AW warming is unprecedented in the last 1,150 years (Spielhagen et al. 2011; Jungclaus et al. 2014). The influence of AW warming on future Alaska and Arctic sea ice loss is unclear (Döscher et al. 2014; Carmack et al. 2015).

ALASKAN SEA LEVEL RISE

The Alaskan coastline is vulnerable to sea level rise; however, strong regional variability exists in current trends and future projections. Sea level rise trends from the National Water Level Observation Network around Alaska reveal regional variations in the observed rate of sea level rise, with most stations experiencing slower rises than the global average. Several stations along Alaska's southern coast have observed rises three times slower than the global values due to isostatic rebound and the proximity to Alaskan melting glaciers (Church et al. 2013; Ch. 12: Sea Level Rise). Tide gauge data show sea levels rising faster along the northern coast of Alaska but still slower than the global average. The largest future sea level rise in the Arctic is expected along the North Alaskan coast, exceeding a foot by 2100, but the magnitude depends significantly on the radiative forcing scenario and could reach 0.6 meters (approx. 2 feet) (Church et al. 2013).

SALINITY

Arctic Ocean salinity influences the freezing temperature of sea ice (less salty water freezes more readily) and the density profile representing the integrated effects of freshwater transport, river runoff, evaporation, and sea ice processes. Arctic Ocean salinity exhibits multidecadal variability, hampering the assessment of long-term trends (Rawlins et al. 2010). Emerging

evidence suggests that the Arctic Ocean and marginal sea salinity has decreased in recent years despite short-lived regional salinity increases between 2000 and 2005 (Rhein et al. 2013). Increased river runoff, rapid melting of sea and land ice, and changes in freshwater transport have influenced observed Arctic Ocean salinity (Rhein et al. 2013; Köhl and Serra 2014).

OCEAN ACIDIFICATION

Arctic Ocean acidification is occurring at a faster rate than the rest of the globe (Mathis et al. 2015; Ch. 13: Ocean Acidification). Coastal Alaska and its ecosystems are especially vulnerable to ocean acidification because of the high sensitivity of Arctic Ocean water chemistry to changes in sea ice, respiration of organic matter, upwelling, and increasing river runoff (Mathis et al. 2015). Sea ice loss and a longer melt season contribute to increased vulnerability of the Arctic Ocean to acidification by lowering total alkalinity, permitting greater upwelling, and influencing the primary production characteristics in coastal Alaska (Arrigo et al. 2008; Cai et al. 2010; Hunt et al. 2011; Stabeno et al. 2012; Mathis et al. 2012; Bates et al. 2014). Global-scale modeling studies suggest that the largest and most rapid changes in pH are being observed and will continue to occur along Alaska's coast, indicating that ocean acidification may increase enough by the 2030s to significantly influence coastal ecosystems (Mathis et al. 2015).

11.2.4. Boreal Wildfires

A global phenomenon with natural (lightning) and human-caused ignition sources, wildfire represents a critical ecosystem process that renews terrestrial habitats. Recent decades have seen increased forest fire activity in Alaska. Historically, however, wildfires have been less frequent and smaller in Alaska compared to the rest of the globe (Flannigan et al. 2009; Hu et al. 2015). Shortened land snow cover seasons and higher temperatures make the Arctic more vulnerable to wildfire (Flannigan et al. 2009; Hu et al. 2015; Young et al. 2016). Total area burned and the number of large fires (those with area greater than 1000 km² or 386 mi²) in Alaska exhibits significant interannual and decadal scale variability, from influences of atmospheric circulation patterns and controlled burns, but have *likely* increased since 1959 (Kasischke and Turetsky 2006). The most recent decade has seen an unusually large number of severe wildfire years in Alaska, for which the risk of severe fires has *likely* increased by 33%–50% as a result of anthropogenic climate change (Partain et al. 2016) and is projected to increase by up to a factor of four by the end of the century (Young et al. 2016). Alaska's fire season is also *likely* lengthening—a trend expected to continue (Flannigan et al. 2009; Sanford et al. 2015). Thresholds in temperature and precipitation shape Arctic fire regimes, and projected increases in future lightning activity imply increased vulnerability to future climate change (Flannigan et al. 2009; Young et al. 2016). Alaskan tundra and forest wildfires will *likely* increase under warmer and drier conditions (Sanford et al. 2015; French et al. 2015) and potentially result in a transition into a fire regime unprecedented in the last 10,000 years (Kelly et al. 2013). Total area burned is projected to increase between 25% and 53% by the end of the century (Joly et al. 2012). Existing studies do not demonstrate that the observed increased in forest fire activity over the historical

period has been highly unusual in comparison to natural variability. Rather, these studies have relied on model calculation to infer the human contribution. The degree of forestry management is a confounding factor which complicates attribution of changes to anthropogenic climate change. We conclude that there is *medium confidence* for a human-caused climate change contribution to increased forest fire activity in Alaska in recent decades.

Boreal forests and tundra contain large stores of carbon, approximately 50% of the total global soil carbon (McGuire et al. 2009). Increased fire activity could deplete these stores, releasing them to the atmosphere to serve as an additional source of atmospheric CO₂ and alter the carbon cycle (McGuire et al. 2009; Kelly et al. 2016). Additionally, increased fires in Alaska may also enhance the degradation of Alaska's permafrost, blackening the ground, reducing surface albedo, and removing protective vegetation.

11.2.5. Snow Cover and Permafrost

Snow cover, like sea ice, possesses a high albedo and serves as a climate feedback. Snow cover extent has significantly decreased across the Northern Hemisphere and Alaska over the last decade (Derksen and Brown 2012; see also Ch. 7: Precipitation Change and Ch. 10: Land Cover). Northern Hemisphere June snow cover decreased by more than 50% between 1967 and 2012 (Brown and Robinson 2011; Vaughan et al. 2013), at trend of -19.8% per decade (Derksen et al. 2015). May snow cover has also declined, at -7.3% per decade, due to reduced winter accumulation from warmer temperatures. Regional trends in snow cover duration vary, with some showing earlier onsets while others show later onsets (Derksen et al. 2015). In Alaska, the 2016 May statewide snow coverage 595,000 km² (~372,000 mi²) was the lowest on record dating back to 1967; the snow coverage of 2015 was the second lowest and 2014 was the fourth lowest. Declining snow cover is expected to continue; however, the evolution of Arctic ecosystems, including the observed tundra shrub expansion (Myers-Smith et al. 2011), can alter the snow depth, melt dynamics, and the local surface energy budget influencing melt.

Alaska and Arctic permafrost characteristics have responded to increased temperatures and reduced snow cover in most regions since the 1980s (AMAP 2011; Vaughan et al. 2013). The permafrost warming rate varies regionally; however, colder permafrost is warming faster than warmer permafrost (Vaughan et al. 2013; Romanovsky et al. 2015). This feature is most evident across Alaska, where permafrost on the North Slope is warming more rapidly than in the interior. Permafrost temperatures across the North Slope at various depths ranging from 12 to 20 meters (39 to 65 feet) have warmed between 0.2° and 0.7°C (0.3° and 1.3°F) per decade since 2000 (Figure 11.3; Romanovsky et al. 2016). Trends in the permafrost active layer show strong regional variations (AMAP 2011; Shiklomanov et al. 2012); however, active layer thickness increased across much of the Arctic (Vaughan et al. 2013). Uncertainties in future permafrost warming and active layer deepening in Alaska are due to poorly understood deep soil, ice wedge, and thermokarst processes that may accelerate the thaw (Koven et al. 2015a; Liljedahl et al.

2016). Continued degradation of permafrost and a transition from continuous to discontinuous permafrost is expected over the 21st century (Vaughan et al. 2013).

[INSERT FIGURE 11.3 HERE:]

Figure 11.3: Time series of annual mean permafrost temperatures (units: °F) at various depths from 12 to 20 meters (39 to 65 feet) from 1977 through 2015 at several sites across Alaska, including the North Slope continuous permafrost region, and the discontinuous permafrost in Alaska and northwestern Canada. Solid lines represent the linear trends drawn to highlight that permafrost temperatures are warming faster in the colder, coastal permafrost regions than the warmer interior regions. (Figure Source: adapted from Romanovsky et al. 2016; © American Meteorological Society, used with permission)]

11.2.6. Continental Ice Sheets and Mountain Glaciers

Mass loss from ice sheets and glaciers influences sea level rise (see Ch. 12: Sea Level Rise), the oceanic thermohaline circulation, and the global energy budget. Changes in GrIS can also influence Alaskan climate by altering Arctic-wide and midlatitude circulation patterns (Section 11.3.1). Observational and modeling studies indicate that GrIS and glaciers in Alaska are out of balance with current climate conditions and losing mass (Vaughan et al. 2013; Zemp et al. 2015). In recent years, mass loss has accelerated and is expected to continue (Zemp et al. 2015; Harig and Simons 2016).

Dramatic changes have occurred across GrIS, particularly at its margins. GrIS average annual mass loss from January 2003 to May 2013 was -244 ± 6 Gt per year (Harig and Simons 2016). Increased surface melt, runoff, and increased outlet glacier discharge from warmer surface air temperatures are the primary factors contributing to mass loss (Howat et al. 2008; van den Broeke et al. 2009; Rignot et al. 2010; Straneo et al. 2011; Khan et al. 2014). The effects of warmer air and ocean temperatures on the GrIS mass balance can be amplified by ice dynamical feedbacks, such as faster sliding, greater calving, and increased submarine melting (Joughin et al. 2008; Holland et al. 2008a; Rignot et al. 2010; Bartholomew et al. 2011). Shallow ocean warming and regional changes in the ocean and atmospheric circulation are increasing mass loss (Dupont and Alley 2005; Lim et al. 2016; Tedesco et al. 2016). The underlying mechanisms of the recent speed-up of discharge remain unclear (Straneo et al. 2010; Johannessen et al. 2011); however, warming subsurface ocean temperatures, atmospheric warming (Velicogna 2009; van den Broeke et al. 2009; Andresen et al. 2012), and meltwater penetration to the glacier bed (Johannessen et al. 2011, Mernild et al. 2012) *very likely* contribute.

Annual average ice mass from Arctic-wide glaciers has decreased every year since 1984 (AMAP 2011; Pelto 2015; Zemp et al. 2015), with significant losses in Alaska, especially over the past two decades (Figure 11.4; Vaughan et al. 2013; Sharp et al. 2015; Harig and Simons 2016). Glacial mass loss around the Gulf of Alaska region has declined steadily since 2003 (Harig and Simons 2016). NASA's Gravity Recovery and Climate Experiment (GRACE) indicates mass

loss from the northern and southern parts of the Gulf of Alaska region of -36 ± 4 Gt per year and -4 ± 3 Gt per year, respectively (Harig and Simons 2016). Studies show imbalances in Alaskan glaciers, indicating that melt will continue through the 21st century (Vaughan et al. 2013; Zemp et al. 2015; Mengel et al. 2016). Multiple data sets indicate that it is *extremely likely* that Alaskan glaciers have lost mass over the last 50 years and will continue to do so.

[INSERT FIGURE 11.4 HERE:]

Figure 11.4: Time series of the cumulative climatic mass balance (units: kg/m²) in five Arctic regions and cumulative for the Pan-Arctic from the World Glacier Monitoring Service (WGMS 2016; Wolken et al. 2016; solid lines), and Alaskan glacial mass loss observed from NASA GRACE (Harig and Simons 2016; dashed blue line). (Figure source: Harig and Simons 2016 and Wolken et al. 2016; © American Meteorological Society, used with permission)]

11.3. Arctic Feedbacks on the Lower 48 and Globally

11.3.1. Linkages between Arctic Warming and Lower Latitudes

Midlatitude circulation is an important factor of Arctic climate and climate change (Rigor et al. 2002; Graversen 2006; Perlwitz et al. 2015; Francis et al. 2016; Screen et al. 2012; Park et al. 2015; Lee 2014; Lee et al. 2011; Ding et al. 2014; Screen and Francis 2016; Overland et al. 2016). The extent to which enhanced Arctic surface warming and sea ice loss influence the large-scale atmospheric circulation and midlatitude weather and climate extremes has become an active research area (Francis et al. 2016; Overland et al. 2016). Several pathways have been proposed (see studies referred in Cohen et al. 2014 and Barnes and Screen 2015): reduced meridional temperature gradient, a more sinuous jet-stream, trapped atmospheric waves, modified storm tracks, weakened stratospheric polar vortex. While modeling studies link a reduced meridional temperature gradient to fewer cold temperature extremes in the continental United States (Ayarzagüena and Screen 2016; Sun et al. 2016; Screen et al. 2015a,b), other studies hypothesize that a slower jet stream may amplify Rossby waves and increase the frequency of atmospheric blocking, causing more persistent and extreme weather in midlatitudes (Francis and Vavrus 2012).

Multiple observational studies suggest that the concurrent changes in the Arctic and Northern Hemisphere large-scale circulation since the 1990s did not occur by chance, but were caused by arctic amplification (Cohen et al. 2014; Vihma 2014; Barnes and Screen 2015). Reanalysis data suggest a relationship between arctic amplification and observed changes in persistent circulation phenomena like blocking and planetary wave amplitude (Francis and Skific 2015; Francis and Vavrus 2012; Francis and Vavrus 2015). Robust empirical evidence is lacking because the Arctic sea ice observational record is too short (Overland et al. 2015a) or because the atmospheric response to arctic amplification depends on the prior state of the atmospheric circulation reducing detectability (Overland et al. 2016). Furthermore, it is not possible to draw conclusions regarding the direction of the relationship between Arctic warming and midlatitude circulation

1 based on empirical correlation and covariance analyses alone. Observational analyses have been
2 combined with modeling studies to test causality statements.

3 Studies with simple models and Atmospheric General Circulation Models (AGCMs) provide
4 evidence that Arctic warming can affect midlatitude jet streams and location of storm tracks
5 (Barnes and Screen 2015; Francis et al. 2016; Overland et al. 2016). In addition, analysis of
6 CMIP5 models forced with increasing greenhouse gases suggests that the magnitude of arctic
7 amplification affects the future midlatitude jet position, specifically during boreal winter (Barnes
8 and Polvani 2015). However, the effect of arctic amplification on blocking is not clear (Hoskins
9 and Woollings 2015; Ch. 5: Circulation and Variability).

10 Regarding attribution, AGCM simulations forced with observed changes in Arctic sea ice
11 suggest that the sea ice loss effect on recent circulation changes is small compared to natural
12 variability (Screen et al. 2012; Perlwitz et al. 2015). These simulations do not support the
13 hypothesis that Arctic sea ice loss is the principal factor in the recently emerged “Warm Arctic,
14 Cold Continents” pattern and related enhanced occurrence of cold winters in the continental
15 United States (Sigmond and Fyfe 2016; Sun et al. 2016). While several studies find a significant
16 influence of reduced sea ice in the Barents and Kara Seas (northeast of Scandinavia) on observed
17 cooling over Eurasia (Overland et al. 2016 and references therein), others suggest that the
18 cooling results from an internally generated circulation change (Sun et al. 2016; McCusker et al.
19 2016). Furthermore, models cannot reproduce the observed “Warm Arctic, Cold Continent”
20 trend pattern, nor do they reproduce the linkage between arctic amplification and lower latitude
21 climate due to significant model errors, including incorrect sea ice–atmosphere coupling and
22 poor representation of stratospheric processes (Cohen et al. 2013; Francis et al. 2016). The nature
23 and magnitude of arctic amplification’s influence on U.S. weather over the coming decades
24 remains an open question.

25 **11.3.2. Freshwater Effects on Ocean Circulation**

26 The addition of freshwater to the Arctic Ocean from melting sea ice and land ice can influence
27 ocean salinity, altering ocean circulation, density stratification, and sea ice characteristics. River
28 runoff is increasing into the Arctic Ocean, driven by land ice melt (Nummelin et al. 2016).
29 Changes in the thermohaline circulation that result from freshening the North Atlantic Ocean can
30 be abrupt and occur over just a few decades (see Ch. 15: Potential Surprises).

31 Melting Arctic sea and land ice combined with time-varying atmospheric forcing (Giles et al.
32 2012; Köhl and Serra 2014) control Arctic Ocean freshwater export to the North Atlantic. Large-
33 scale circulation variability in the central Arctic not only controls the redistribution and storage
34 of freshwater in the Arctic (Köhl and Serra 2014) but also the export volume (Morison et al.
35 2012). Increased freshwater fluxes can weaken open ocean convection and deep water formation
36 in the Labrador and Irminger seas, weakening the Atlantic meridional overturning circulation
37 (AMOC; Rahmstorf et al. 2015; Yang et al. 2016). AMOC-associated poleward heat transport

substantially contributes to North American and continental European climate; any AMOC slow-down could have implications for global climate change as well (Smeed et al. 2014).

11.3.3. Thawing permafrost and methane hydrates effects on CO₂ and CH₄ emissions

Permafrost contains large stores of carbon, as do methane hydrates. Though the total contribution of these carbon stores to global methane emission is uncertain, Alaska's permafrost contains some of the richest organic carbon soils in the Arctic (Mishra and Riley 2012; Schuur et al. 2015). Thus, warming Alaska permafrost is not only a concern for the Arctic climate but for the global carbon cycle. Current methane emissions from Alaskan Arctic tundra and boreal forests contribute a small fraction of the global CH₄ budget (Chang et al. 2014). Methane emissions in the cold season (after snowfall) are greater than summer emissions in Alaska, and methane emissions in upland tundra are greater than in wetland tundra (Zona et al. 2016).

The permafrost-carbon feedback represents the additional release of CO₂ and CH₄ from thawing permafrost soils providing additional radiative forcing, a source of a potential surprise (see Ch. 15: Potential Surprises). Thawing permafrost makes previously frozen organic matter available for microbial decomposition, resulting in the release of CO₂ and CH₄. The specific condition under which microbial decomposition occurs, aerobic or anaerobic, determines whether CO₂ or CH₄ is released (Schadel et al. 2016). This distinction has significant implications for future climate change, as CH₄ is more than 20 times stronger a greenhouse gas than CO₂. Combined data and modeling studies suggest a global sensitivity of the permafrost feedback between -14 and -19 GtC per K (approx. 25 to 34 GtC per °F) (Koven et al. 2015a,b) resulting in a 120 ± 85 Gt release of carbon from permafrost and a global temperature increase of $+0.29 \pm 0.21$ °C ($+0.52 \pm 0.38$ °F) by 2100 (Schaefer et al. 2014). In the coming decades, enhanced high-latitude plant growth and its associated CO₂ sink (Friedlingstein et al. 2006) should partially offset the increased emissions from permafrost thaw (Schaefer et al. 2014; Schuur et al. 2015); thereafter, decomposition is expected to dominate uptake. Permafrost thaw is occurring faster than models predict due to poorly understood deep soil, ice wedge, and thermokarst processes (Koven et al. 2015; Liljedahl et al. 2016). There is *high confidence* in the positive sign of the permafrost-carbon feedback, but *low confidence* in the feedback magnitude (Vaughan et al. 2013; Fisher et al. 2014).

Significant stores of CH₄, in the form of methane hydrates (also called clathrates), lie below permafrost and under the global ocean. The estimated total global inventory of methane hydrates ranges from 500 to 3,000 GtC (Archer 2007; Ruppel 2011; Piñero et al. 2013). Methane hydrates are solid compounds formed at high pressures and cold temperatures trapping methane gas within the crystalline structure of water. In the Arctic Ocean and along the shallow coastal Alaskan seas, methane hydrates form on shallow but cold continental shelves and may be vulnerable to small increases in ocean temperature (Bollman et al. 2010; Ruppel 2011).

1 Rising sea levels and warming oceans have a competing influence on methane hydrate stability
2 (Bollman et al. 2010; Hunter et al. 2013). Studies indicate that the temperature effect dominates
3 and that the overall influence is *likely* a destabilizing effect. Projected warming rates for the 21st
4 century Arctic Ocean are not expected to lead to sudden or catastrophic destabilization of sea
5 floor methane hydrates (Kretschmer et al. 2015; AMIP 2015). It is likely that most of the
6 methane hydrate deposits will remain stable for the foreseeable future (the next few thousand
7 years). However, deposits off of coastal Alaska are among the most vulnerable and are expected
8 to begin dissociating and release small amounts of CH₄ during the 21st century (Archer 2007;
9 Ruppel 2011; Hunter et al. 2013; Kretschmer et al. 2015).

10

TRACEABLE ACCOUNTS

Key Finding 1

For both the State of Alaska and for the Arctic as a whole, near-surface air temperature is increasing at a rate more than twice as fast as the global-average temperature. (*Very high confidence*)

Description of evidence base

The Key Finding is supported by observational evidence from ground-based observing stations, satellites, and data-model temperature analyses documented in the climate science literature from multiple sources and analysis techniques (Hartmann et al. 2013; Overland et al. 2014; Comiso and Hall 2014; Wendler et al. 2014). Additionally, climate models have predicted enhanced Arctic warming for more than 40 years, indicating that we have a solid grasp on the underlying physics and positive feedbacks driving the accelerated Arctic warming (Collins et al. 2013; Taylor et al. 2013). These studies are discussed in the chapter text. Lastly, similar statements have been made previously in NCA3 (Melillo et al. 2014), IPCC AR5 (2013), and in other Arctic-specific assessments such as the Arctic Climate Impacts Assessment (ACIA 2005) and Snow, Water, Ice and Permafrost in the Arctic (AMAP 2011).

Major Uncertainties

The lack of high quality and restricted spatial resolution of surface and ground temperature data over many Arctic land regions and essentially no measurements over the Central Arctic Ocean hampers the ability to better refine the rate of Arctic warming and completely restricts our ability to quantify and detect regional trends, especially over the sea ice. Climate models generally produce an Arctic warming between 2 to 3 times the global mean warming. A key uncertainty is our quantitative knowledge of the contributions from individual feedback processes in driving the accelerated Arctic warming. Reducing this uncertainty will help constrain projections of future Arctic warming.

Assessment of confidence based on evidence and agreement, including short description of nature of evidence and level of agreement

x Very High

☐ High

☐ Medium

☐ Low

There is *very high confidence* that the Arctic surface and air temperatures have warmed across Alaska and the Arctic at a much faster rate than the global average. The surface temperature has warmed twice as much as the global average given the combination of observational evidence from multiple sources and the ability of climate models to capture and explain the root causes of the accelerated Arctic warming.

If appropriate, estimate likelihood of impact or consequence, including short description of basis of estimate

☒ Greater than 9 in 10 / Very Likely

☐ Greater than 2 in 3 / Likely

☐ About 1 in 2 / As Likely as Not

☐ Less than 1 in 3 / Unlikely

☐ Less than 1 in 10 / Very Unlikely

It is *very likely* that the accelerated rate of Arctic warming will have a significant consequence for the United States due to accelerated land and sea ice melt driving changes in the ocean including sea level rise threatening our coastal communities and freshening of sea water that is influencing marine ecology and potentially altering the thermohaline circulation.

Summary sentence or paragraph that integrates the above information

It is very likely that surface and air temperatures across Alaska and the Arctic have warmed and will continue to warm faster than the rest of the globe. This Key Finding is supported by a large amount of observational and modeling evidence documented in the climate science peer-reviewed literature. Similar statements have been made previously in international and United States based assessments of Arctic climate change (ACIA 2005; AMAP 2011; IPCC AR5 2013; NCA3). The primary key uncertainty is our inability to provide high quality regional trends of warming in the Arctic due to the lack of high quality surface temperature measurements in isolated land regions and over the Central Arctic Ocean. Accelerated Arctic warming impacts and threatens our coastal community and marine ecosystems.

Key Finding 2

Rising Alaskan permafrost temperatures are causing permafrost to thaw and become more discontinuous; this releases additional CO₂ and CH₄ resulting in additional warming (*high confidence*). The overall magnitude of the permafrost-carbon feedback is uncertain.

Description of evidence base

The Key Finding is supported by observational evidence of warming permafrost temperatures, a deepening active layer, laboratory incubation experiments of CO₂ and CH₄ release, and model studies published in the peer reviewed climate science literature (Vaughan et al. 2013; Fisher et al. 2014; Schuur et al. 2015; Koven et al. 2015a,b; Liljedahl et al. 2016). This evidence is documented in the chapter text.

Major Uncertainties

A major limiting factor is the sparse observations of permafrost in Alaska and remote areas across the Arctic. Major uncertainties are related to deep soil, ice wedging, and thermokarst processes. Uncertainties also exist in relevant soil processes during and after permafrost thaw, especially those that control unfrozen soil carbon storage and plant carbon uptake and net

ecosystem exchange. Many processes with the potential to drive rapid permafrost thaw (such as thermokarst) are not included in current earth system models.

Assessment of confidence based on evidence and agreement, including short description of nature of evidence and level of agreement

☐ Very High

☒ High

☐ Medium

☐ Low

There is *high confidence* that permafrost is thawing, becoming discontinuous, releasing CO₂ and CH₄. Physically based argument indicated that the feedback is positive. This confidence level is justified based on observations of rapidly changing permafrost characteristics.

If appropriate, estimate likelihood of impact or consequence, including short description of basis of estimate

☐ Greater than 9 in 10 / Very Likely

☒ Greater than 2 in 3 / Likely

☐ About 1 in 2 / As Likely as Not

☐ Less than 1 in 3 / Unlikely

☐ Less than 1 in 10 / Very Unlikely

Thawing permafrost has significant impacts to the global carbon cycle and serves as a source of CO₂ and CH₄ emission. Additionally, thawing permafrost will significantly impact Arctic infrastructures as crumbling buildings, roads, and bridges are being observed.

Summary sentence or paragraph that integrates the above information

Permafrost is thawing, becoming more discontinuous, and releasing CO₂ and CH₄. Observational and modeling evidence documented in the peer-reviewed climate literature indicates that the sign of the permafrost feedbacks is (*high confidence*). Although, the magnitude of the permafrost-carbon feedback is uncertain. A number of major uncertainties exist including deep soil and ice wedge processes, plant carbon uptake, and the role of rapid permafrost thaw processes, such as thermokarst. Progress is hindered by the lack of accurate data in remote Arctic regions. Impacts of permafrost thaw are likely significant for both the physical climate system and ecosystem services.

Key Finding 3

Arctic sea ice and Greenland Ice Sheet mass loss are accelerating and Alaskan mountain glaciers continue to melt (*very high confidence*). Alaskan coastal sea ice loss rates exceed the Arctic average (*very high confidence*). Observed sea and land ice loss across the Arctic is occurring faster than climate models predict (*very high confidence*). Melting trends are expected to

continue resulting in late summers becoming nearly ice-free for the Arctic ocean by mid-century (*very high confidence*).

Description of evidence base

The Key Finding is supported by observational evidence from multiple ground-based, satellite observational techniques (passive microwave, laser and radar altimetry, and gravimetry) documented in the climate science literature (Vaughan et al. 2013; Comiso and Hall 2014; Stroeve et al. 2014a; Zemp et al. 2015; Harig and Simons 2016). Multiple sources and independent analysis techniques discussed in the chapter text support the Key Finding. Similar statements have been made previously in NCA3 (Melillo et al. 2014) and IPCC AR5 (Vaughan et al. 2013).

Major uncertainties

Key uncertainties remain in the quantification and modeling of key physical processes that contribute to the acceleration of land and sea ice melting. Climate models are unable to capture the rapid pace of observed sea and land ice melt over the last 15 years; a major factor is our inability to quantify and accurately model the physical processes driving the accelerated melting. The interactions between atmospheric circulation, ice dynamics and thermodynamics, clouds, and specifically the influence on the surface energy budget are key uncertainties. Mechanisms controlling marine-terminating glacier dynamics, specifically the roles of atmospheric warming, seawater intrusions under floating ice shelves, and the penetration of surface meltwater to the glacier bed, are key uncertainties in projecting Greenland Ice Sheet melt.

Assessment of confidence based on evidence and agreement, including short description of nature of evidence and level of agreement

x Very High

☐ High

☐ Medium

☐ Low

There is *very high confidence* that Arctic sea and land ice melt is accelerating given the multiple observational sources and analysis technique documented in the peer reviewed climate science literature.

If appropriate, estimate likelihood of impact or consequence, including short description of basis of estimate

x Greater than 9 in 10 / Very Likely

☐ Greater than 2 in 3 / Likely

☐ About 1 in 2 / As Likely as Not

☐ Less than 1 in 3 / Unlikely

☐ Less than 1 in 10 / Very Unlikely

It is *very likely* that accelerating Arctic land and sea melt impacts the United States. Accelerating Arctic Ocean sea ice melt is affecting coastal erosion in Alaska and important Alaskan fisheries,

by changing Arctic Ocean chemistry and the vulnerability to ocean acidification in the region. Greenland Ice Sheet and Alaska mountain glacier melt drives sea level rise threatening coastal communities in the United State and worldwide, influencing marine ecology, and potentially altering the thermohaline circulation.

Summary sentence or paragraph that integrates the above information

Ice melting across the Arctic continues steadily continues and in some cases is accelerating (*very high confidence*). The Key Finding is supported by observational evidence from multiple data sources and independent analysis techniques documented in the climate science literature. Similar statements have been made previously in international and United States based climate science assessments (Vaughan et al. 2013; Melillo et al. 2014). Key uncertainties remain in the contributions of the sea and land ice melting to individual physical mechanisms and the inability to accurately model the rate of melting. Accelerating Arctic sea and land ice melt impacts our coastal communities and marine ecosystems, especially in Alaska.

Key Finding 4

Human activities have contributed to rising surface temperature, sea ice loss since 1979, and glacier mass loss observed across the Arctic. (*High confidence*).

Description of evidence base

The Key Finding is supported by many attribution studies including a wide array of climate models documented in the climate science literature (Gillett et al. 2008; Bindoff et al. 2013; Christensen et al. 2013; Najafi et al. 2015). Multiple independent analysis techniques and studies discussed in the chapter text support the Key Finding.

Major uncertainties

A major limiting factor in our ability to attribute Arctic sea ice and glacier melt to human activities to the significant natural climate variability in the Arctic. Longer data records and a better understanding of the physical mechanisms that drive natural climate variability in the Arctic are required to reduce this uncertainty. Another major uncertainty is the ability of climate models to capture the relevant physical processes and climate changes at a fine regional scale.

Assessment of confidence based on evidence and agreement, including short description of nature of evidence and level of agreement

x Very High

☐ High

☐ Medium

☐ Low

There is *very high confidence* that human activities have contributed to Arctic sea ice and melting glaciers given the multiple independent studies documented in the peer reviewed climate science literature and discussed in the chapter text.

If appropriate, estimate likelihood of impact or consequence, including short description of basis of estimate

x Greater than 9 in 10 / Very Likely

☐ Greater than 2 in 3 / Likely

☐ About 1 in 2 / As Likely as Not

☐ Less than 1 in 3 / Unlikely

☐ Less than 1 in 10 / Very Unlikely

Arctic sea ice and glacier mass loss impacts the United States by affecting coastal erosion in Alaska and key Alaskan fisheries through an increased vulnerability to ocean acidification. Glacier mass loss is a significant driver of sea level rise threatening coastal communities in the United States and worldwide, influencing marine ecology, and potentially altering the thermohaline circulation.

Summary sentence or paragraph that integrates the above information

It is *very likely* that human activities have contributed to Arctic sea ice and glacier mass loss in recent years. The Key Finding is supported by an array of independent analysis techniques using different climate models documented in the climate science literature. Key uncertainties remain in attribution studies including understanding and characteristics of Arctic climate system natural variability and the modeling of the Arctic climate system. Arctic sea ice and glacier melt influence U.S. coastal communities and marine ecosystems, especially in Alaska.

Key Finding 5

Atmospheric circulation patterns connect the climates of the Arctic and the United States. The mid-latitude circulation influences Arctic climate change (*medium to high confidence*). In turn, current evidence suggests that Arctic warming is influencing mid-latitude circulation over the continental United States and affecting weather patterns, but the mechanisms are not well understood (*low to medium confidence*).

Description of evidence base

The Key Finding addresses recent observations of coherent changes in Arctic climate and midlatitude circulation. While we have a very good understanding of the impact of midlatitude circulation on the Arctic climate (Rigor et al. 2002; Graverson et al. 2006; Screen et al. 2012; Perlwitz et al. 2015), the research on the impact of Arctic climate on midlatitude circulation is rapidly evolving, including observational analysis and modeling studies with several review papers available (Cohen et al. 2014; Barnes and Screen 2015; Vihma 2014). An assessment of current literature is provided in the text.

Major uncertainties

A major limiting factor is our understanding and modeling of natural climate variability in the Arctic. Longer data records and a better understanding of the physical mechanisms that drive

1 natural climate variability in the Arctic are required to reduce this uncertainty. The inability of
2 climate models to accurately capture interactions between sea ice and the atmospheric circulation
3 and polar stratospheric processes limits our current understanding.

4 **Assessment of confidence based on evidence and agreement, including short description of**
5 **nature of evidence and level of agreement**

6 ☐ Very High

7 ☐ High

8 ☐ Medium

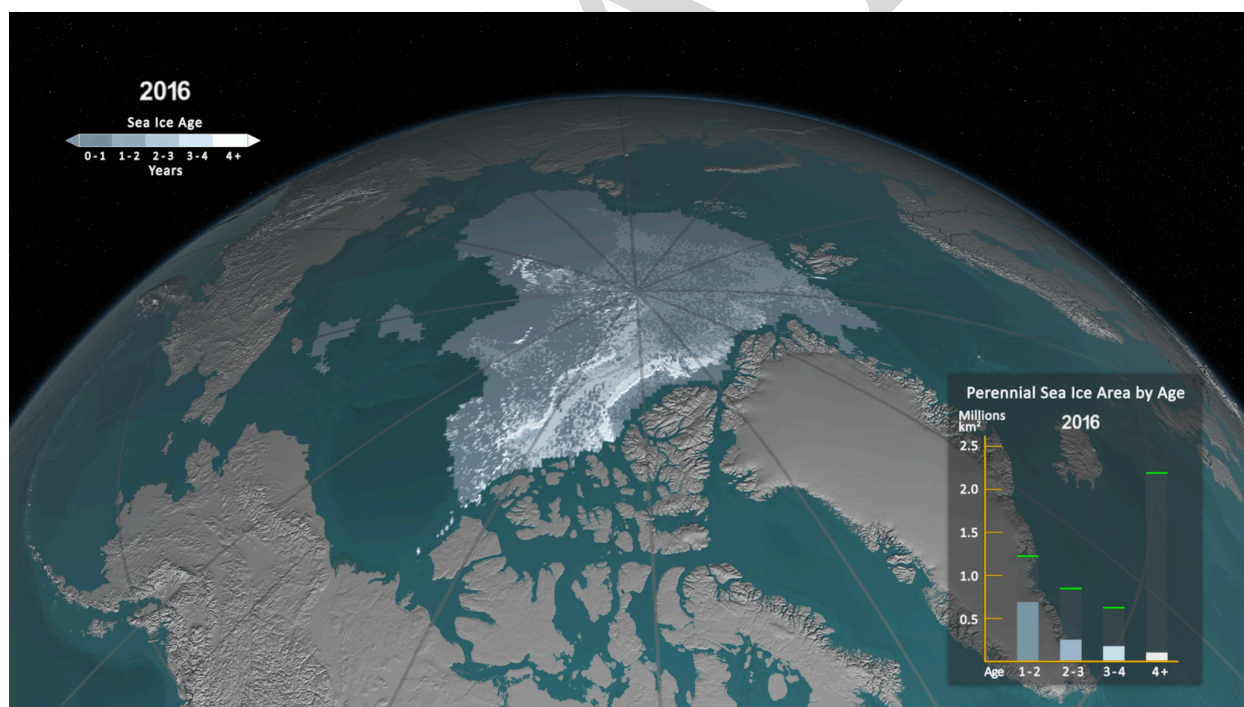
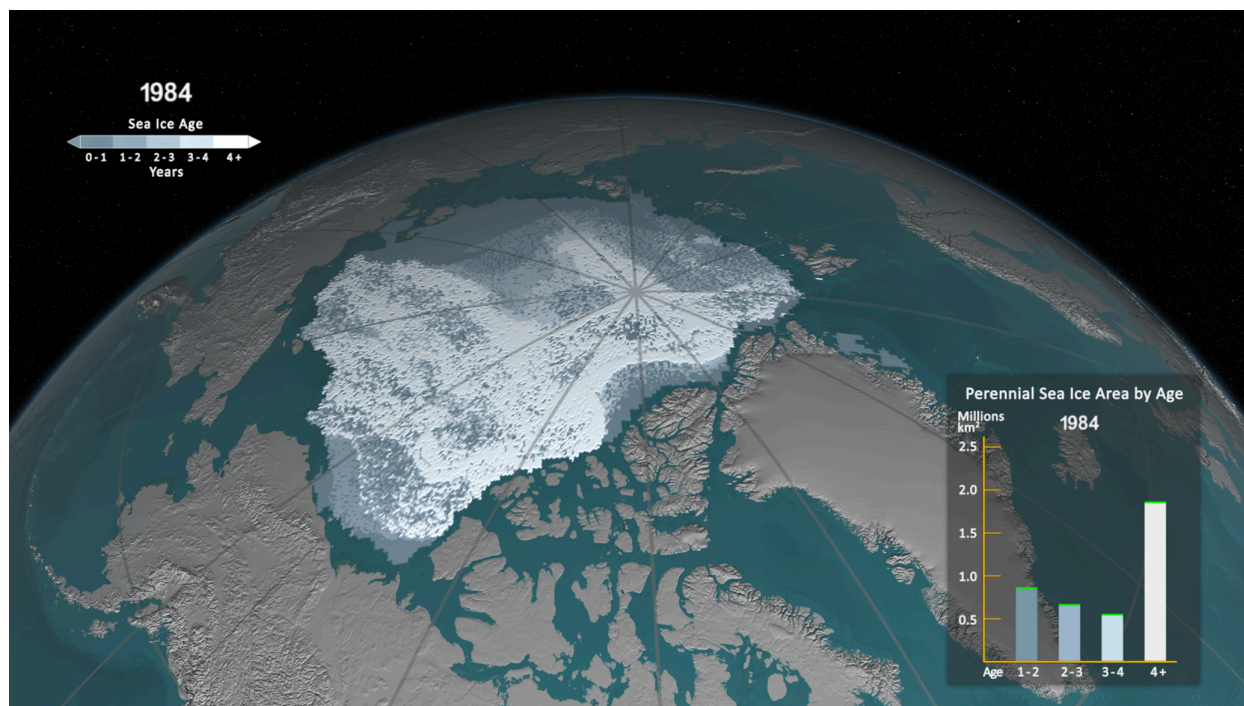
9 ☒ Low

10 *Low confidence* on the detection of an impact of Arctic warming on midlatitude climate is based
11 on short observational data record, model uncertainty, and lack of physical understanding.

12 **Summary sentence or paragraph that integrates the above information**

13 Research on linkages between Arctic and lower latitudes is rapidly evolving with progress
14 limited by short observational data record and model uncertainty.
15

1 FIGURES



4 **Figure 11.1:** September sea ice extent (all gray-scale colors) and age shown for (a) 1984 and (b)
 5 2016, illustrating significant reductions in sea ice extent and age (thickness). Bar graph is the
 6 lower right of each panel illustrates the sea ice area covered within each age category. (Figure
 7 source: NASA Science Visualization Studio ([http://svs.gsfc.nasa.gov/cgi-](http://svs.gsfc.nasa.gov/cgi-bin/details.cgi?aid=4489)
 8 [bin/details.cgi?aid=4489](http://svs.gsfc.nasa.gov/cgi-bin/details.cgi?aid=4489)); data: Tschudi et al. 2016)
 9

Trends in Sea Ice Melt Season

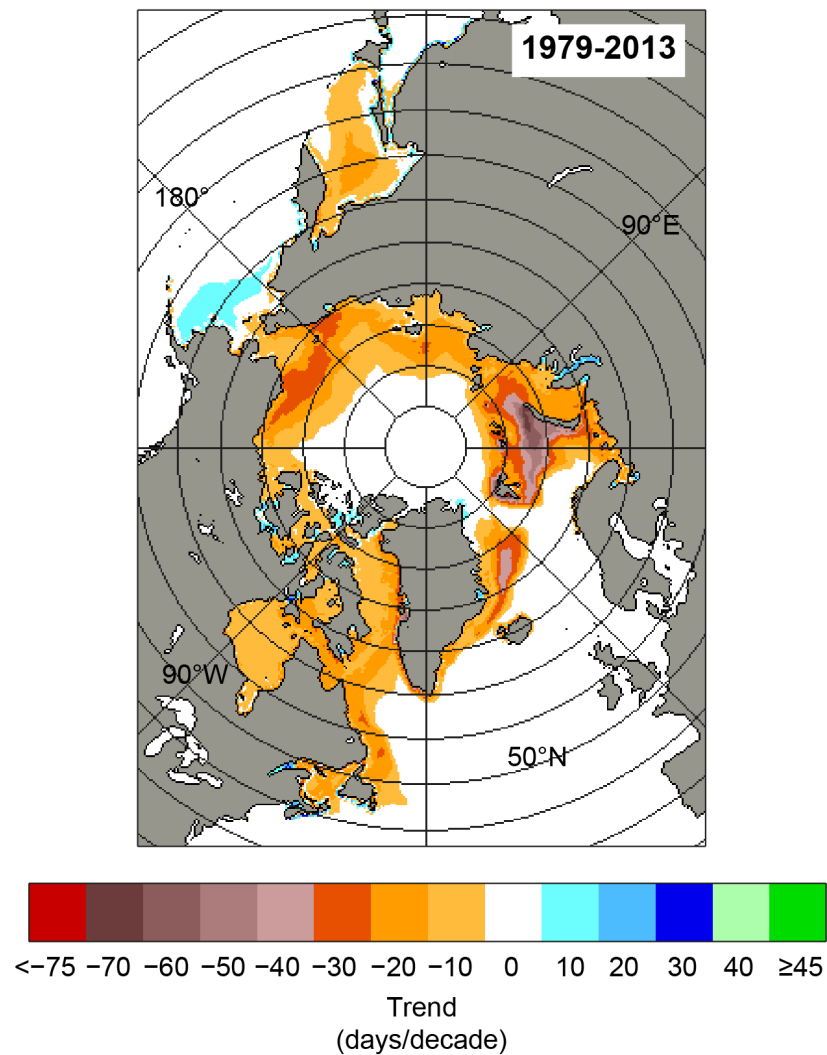


Figure 11.2: 35-year trends in Arctic sea ice melt season length, in days per decade, from passive microwave satellite observations, illustrating that the sea ice season has shortened by more than 60 days in coastal Alaska over the last 30 years. (Figure source: adapted from Parkinson 2014).

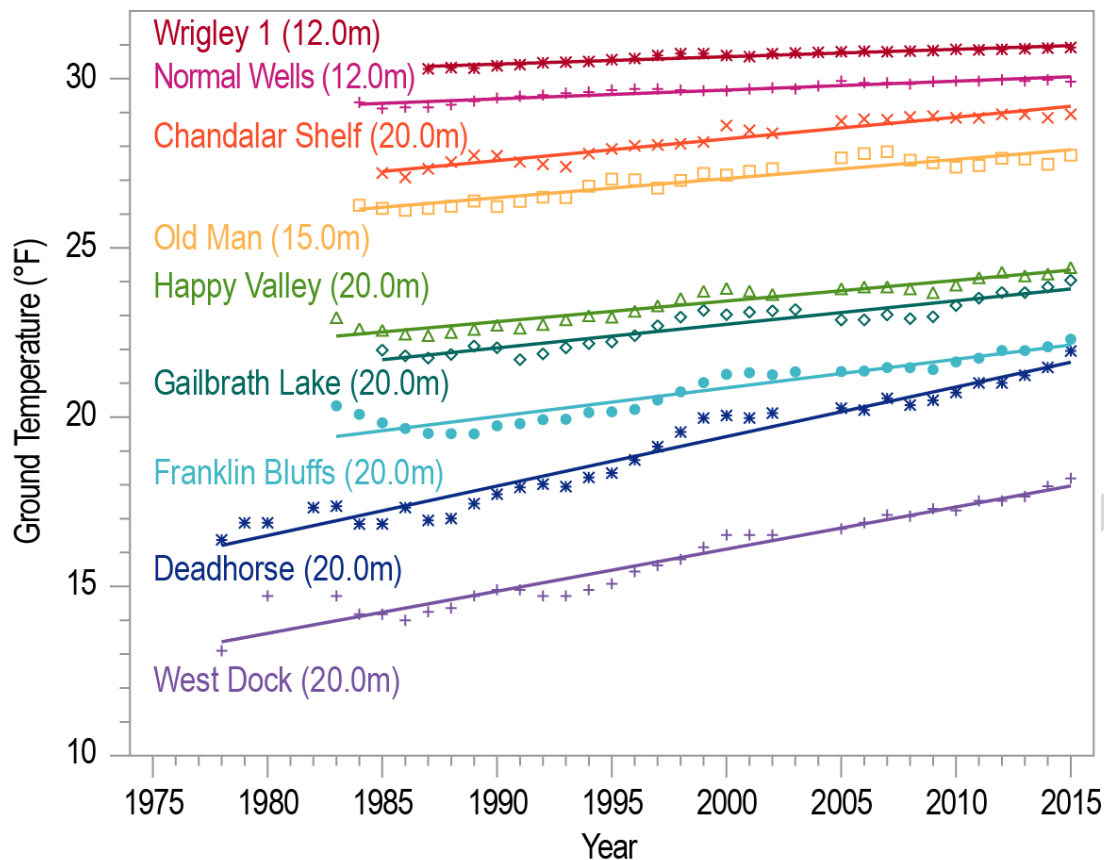


Figure 11.3: Time series of annual mean permafrost temperatures (units: °F) at various depths from 12 to 20 meters (39 to 65 feet) from 1977 through 2015 at several sites across Alaska including the North Slope continuous permafrost region and the discontinuous permafrost in Alaska and northwestern Canada. Solid lines represent the linear trends drawn to highlight that permafrost temperatures are warming faster in the colder, coastal permafrost regions than the warmer interior regions. (Figure Source: adapted from Romanovsky et al. 2016; © American Meteorological Society, used with permission)

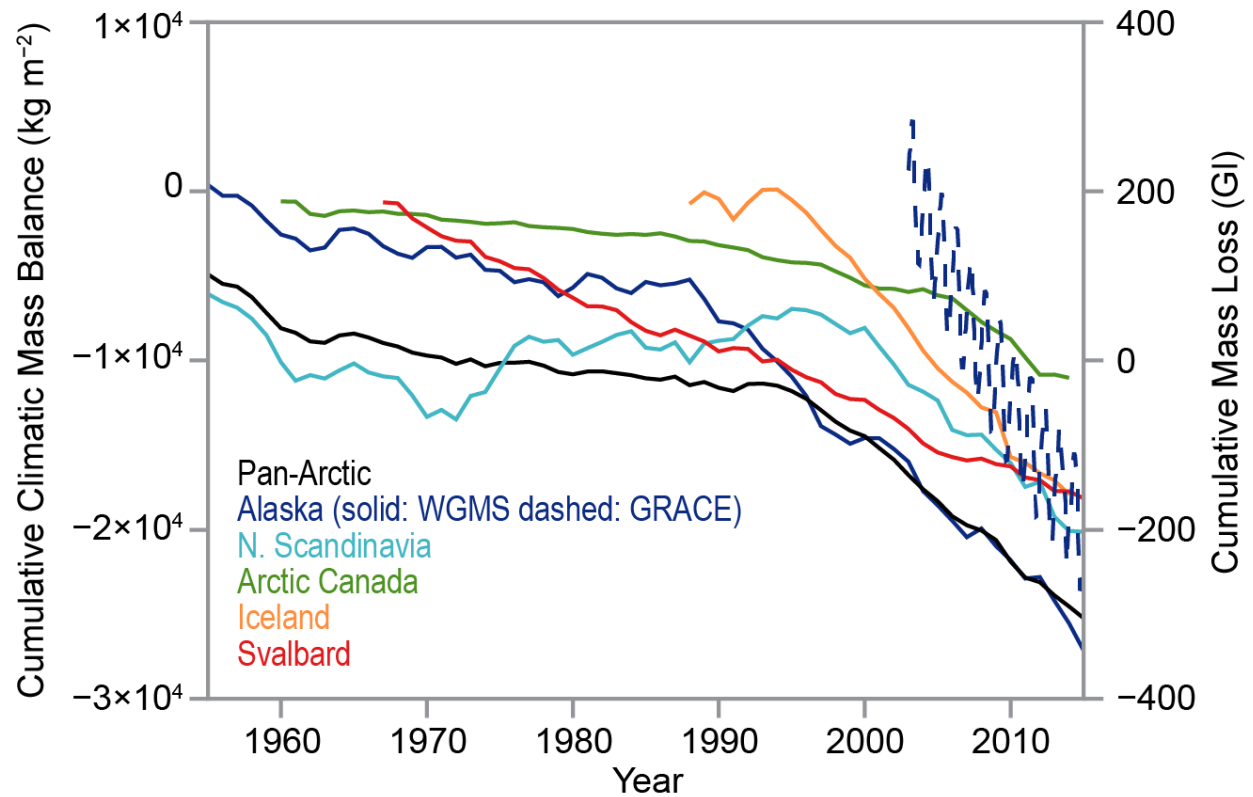


Figure 11.4: Time series of the cumulative climatic mass balance (units: kg/m²) in five Arctic regions and cumulative for the Pan-Arctic from the World Glacier Monitoring Service (WGMS 2016; Wolken et al. 2016; solid lines) and Alaskan glacial mass loss observed from NASA GRACE (Harig and Simons 2016; dashed blue line). (Figure source: Harig and Simons 2016 and Wolken et al. 2016; © American Meteorological Society, used with permission)

1 **REFERENCES**

- 2 ACIA, 2005: Arctic Climate Impact Assessment. 1042 pp. ACIA Secretariat and Cooperative
3 Institute for Arctic Research. <http://www.acia.uaf.edu/pages/scientific.html>
- 4 AMAP, 2011: Snow, Water, Ice and Permafrost in the Arctic (SWIPA): Climate Change and the
5 Cryosphere. 538 pp., Oslo, Norway. <http://www.amap.no/documents/download/1448>
- 6 Andresen, C.S., F. Straneo, M.H. Ribergaard, A.A. Bjork, T.J. Andersen, A. Kuijpers, N.
7 Norgaard-Pedersen, K.H. Kjaer, F. Schjoth, K. Weckstrom, and A.P. Ahlstrom, 2012: Rapid
8 response of Helheim Glacier in Greenland to climate variability over the past century. *Nature*
9 *Geoscience*, **5**, 37-41. <http://dx.doi.org/10.1038/ngeo1349>
- 10 Archer, D., 2007: Methane hydrate stability and anthropogenic climate change. *Biogeosciences*,
11 **4**, 521-544. <http://dx.doi.org/10.5194/bg-4-521-2007>
- 12 Arrigo, K.R., G. van Dijken, and S. Pabi, 2008: Impact of a shrinking Arctic ice cover on marine
13 primary production. *Geophysical Research Letters*, **35**, L19603.
14 <http://dx.doi.org/10.1029/2008GL035028>
- 15 Ayarzagüena, B. and J.A. Screen, 2016: Future Arctic sea ice loss reduces severity of cold air
16 outbreaks in midlatitudes. *Geophysical Research Letters*, **43**, 2801-2809.
17 <http://dx.doi.org/10.1002/2016GL068092>
- 18 Barnes, E.A. and L.M. Polvani, 2015: CMIP5 Projections of Arctic Amplification, of the North
19 American/North Atlantic Circulation, and of Their Relationship. *Journal of Climate*, **28**,
20 5254-5271. <http://dx.doi.org/10.1175/JCLI-D-14-00589.1>
- 21 Barnes, E.A. and J.A. Screen, 2015: The impact of Arctic warming on the midlatitude jet-stream:
22 Can it? Has it? Will it? *Wiley Interdisciplinary Reviews: Climate Change*, **6**, 277-286.
23 <http://dx.doi.org/10.1002/wcc.337>
- 24 Bartholomew, I.D., P. Nienow, A. Sole, D. Mair, T. Cowton, M.A. King, and S. Palmer, 2011:
25 Seasonal variations in Greenland Ice Sheet motion: Inland extent and behaviour at higher
26 elevations. *Earth and Planetary Science Letters*, **307**, 271-278.
27 <http://dx.doi.org/10.1016/j.epsl.2011.04.014>
- 28 Bates, N.R., R. Garley, K.E. Frey, K.L. Shake, and J.T. Mathis, 2014: Sea-ice melt
29 CO₂-carbonate chemistry in the western Arctic Ocean: meltwater contributions
30 to air-sea CO₂ gas exchange, mixed-layer properties and rates of net
31 community production under sea ice. *Biogeosciences*, **11**, 6769-6789.
32 <http://dx.doi.org/10.5194/bg-11-6769-2014>

- 1 Bindoff, N.L., P.A. Stott, K.M. AchutaRao, M.R. Allen, N. Gillett, D. Gutzler, K. Hansingo, G.
 2 Hegerl, Y. Hu, S. Jain, I.I. Mokhov, J. Overland, J. Perlwitz, R. Sebbari, and X. Zhang, 2013:
 3 Detection and Attribution of Climate Change: from Global to Regional. *Climate Change*
 4 *2013: The Physical Science Basis. Contribution of Working Group I to the Fifth Assessment*
 5 *Report of the Intergovernmental Panel on Climate Change*. Stocker, T.F., D. Qin, G.-K.
 6 Plattner, M. Tignor, S.K. Allen, J. Boschung, A. Nauels, Y. Xia, V. Bex, and P.M. Midgley,
 7 Eds. Cambridge University Press, Cambridge, United Kingdom and New York, NY, USA,
 8 867–952. <http://dx.doi.org/10.1017/CBO9781107415324.022> www.climatechange2013.org
- 9 Boisvert, L.N., T. Markus, and T. Vihma, 2013: Moisture flux changes and trends for the entire
 10 Arctic in 2003–2011 derived from EOS Aqua data. *Journal of Geophysical Research:*
 11 *Oceans*, **118**, 5829–5843. <http://dx.doi.org/10.1002/jgrc.20414>
- 12 Boisvert, L.N., D.L. Wu, and C.L. Shie, 2015: Increasing evaporation amounts seen in the Arctic
 13 between 2003 and 2013 from AIRS data. *Journal of Geophysical Research: Atmospheres*,
 14 **120**, 6865–6881. <http://dx.doi.org/10.1002/2015JD023258>
- 15 Boisvert, L.N., D.L. Wu, T. Vihma, and J. Susskind, 2015: Verification of air/surface humidity
 16 differences from AIRS and ERA-Interim in support of turbulent flux estimation in the Arctic.
 17 *Journal of Geophysical Research: Atmospheres*, **120**, 945–963.
 18 <http://dx.doi.org/10.1002/2014JD021666>
- 19 Bollmann, M., T. Bosch, F. Colijn, R. Ebinghaus, R. Froese, K. Güssow, S. Khalilian, S. Krastel,
 20 A. Körtzinger, M. Langenbuch, M. Latif, B. Matthiessen, F. Melzner, A. Oschlies, S.
 21 Petersen, A. Proelß, M. Quaas, J. Reichenbach, T. Requate, T. Reusch, P. Rosenstiel, J.O.
 22 Schmidt, K. Schrottke, H. Sichelschmidt, U. Siebert, R. Soltwedel, U. Sommer, K.
 23 Stattegger, H. Sterr, R. Sturm, T. Treude, A. Vafeidis, C.v. Bernem, J.v. Beusekom, R. Voss,
 24 M. Visbeck, M. Wahl, K. Wallmann, and F. Weinberger, 2010: World ocean review: Living
 25 with the oceans. maribus gGmbH.
- 26 Bourassa, M.A., S.T. Gille, C. Bitz, D. Carlson, I. Cerovecki, C.A. Clayson, M.F. Cronin, W.M.
 27 Drennan, C.W. Fairall, R.N. Hoffman, G. Magnusdottir, R.T. Pinker, I.A. Renfrew, M.
 28 Serreze, K. Speer, L.D. Talley, and G.A. Wick, 2013: High-Latitude Ocean and Sea Ice
 29 Surface Fluxes: Challenges for Climate Research. *Bulletin of the American Meteorological*
 30 *Society*, **94**, 403–423. <http://dx.doi.org/10.1175/BAMS-D-11-00244.1>
- 31 Brown, R.D. and D.A. Robinson, 2011: Northern Hemisphere spring snow cover variability and
 32 change over 1922–2010 including an assessment of uncertainty. *The Cryosphere*, **5**, 219–229.
 33 <http://dx.doi.org/10.5194/tc-5-219-2011>
- 34 Cai, W.-J., L. Chen, B. Chen, Z. Gao, S.H. Lee, J. Chen, D. Pierrot, K. Sullivan, Y. Wang, X.
 35 Hu, W.-J. Huang, Y. Zhang, S. Xu, A. Murata, J.M. Grebmeier, E.P. Jones, and H. Zhang,

- 2010: Decrease in the CO₂ Uptake Capacity in an Ice-Free Arctic Ocean Basin. *Science*, **329**, 556-559. <http://dx.doi.org/10.1126/science.1189338>
- Carmack, E., I. Polyakov, L. Padman, I. Fer, E. Hunke, J. Hutchings, J. Jackson, D. Kelley, R. Kwok, C. Layton, H. Melling, D. Perovich, O. Persson, B. Ruddick, M.-L. Timmermans, J. Toole, T. Ross, S. Vavrus, and P. Winsor, 2015: Toward Quantifying the Increasing Role of Oceanic Heat in Sea Ice Loss in the New Arctic. *Bulletin of the American Meteorological Society*, **96**, 2079-2105. <http://dx.doi.org/10.1175/BAMS-D-13-00177.1>
- Christensen, J.H., K. Krishna Kumar, E. Aldrian, S.-I. An, I.F.A. Cavalcanti, M. de Castro, W. Dong, P. Goswami, A. Hall, J.K. Kanyanga, A. Kitoh, J. Kossin, N.-C. Lau, J. Renwick, D.B. Stephenson, S.-P. Xie, and T. Zhou, 2013: Climate Phenomena and their Relevance for Future Regional Climate Change. *Climate Change 2013: The Physical Science Basis. Contribution of Working Group I to the Fifth Assessment Report of the Intergovernmental Panel on Climate Change*. Stocker, T.F., D. Qin, G.-K. Plattner, M. Tignor, S.K. Allen, J. Boschung, A. Nauels, Y. Xia, V. Bex, and P.M. Midgley, Eds. Cambridge University Press, Cambridge, United Kingdom and New York, NY, USA, 1217–1308. <http://dx.doi.org/10.1017/CBO9781107415324.028> www.climatechange2013.org
- Church, J.A., P.U. Clark, A. Cazenave, J.M. Gregory, S. Jevrejeva, A. Levermann, M.A. Merrifield, G.A. Milne, R.S. Nerem, P.D. Nunn, A.J. Payne, W.T. Pfeffer, D. Stammer, and A.S. Unnikrishnan, 2013: Sea Level Change. *Climate Change 2013: The Physical Science Basis. Contribution of Working Group I to the Fifth Assessment Report of the Intergovernmental Panel on Climate Change*. Stocker, T.F., D. Qin, G.-K. Plattner, M. Tignor, S.K. Allen, J. Boschung, A. Nauels, Y. Xia, V. Bex, and P.M. Midgley, Eds. Cambridge University Press, Cambridge, United Kingdom and New York, NY, USA, 1137–1216. <http://dx.doi.org/10.1017/CBO9781107415324.026> www.climatechange2013.org
- Cohen, J., J. Jones, J.C. Furtado, and E. Tziperman, 2013: Warm Arctic, cold continents: A common pattern related to Arctic sea ice melt, snow advance, and extreme winter weather. *Oceanography*, **26**, 150-160. <http://dx.doi.org/10.5670/oceanog.2013.70> http://tos.org/oceanography/assets/docs/26-4_cohen.pdf
- Cohen, J., J.A. Screen, J.C. Furtado, M. Barlow, D. Whittleston, D. Coumou, J. Francis, K. Dethloff, D. Entekhabi, J. Overland, and J. Jones, 2014: Recent Arctic amplification and extreme mid-latitude weather. *Nature Geoscience*, **7**, 627-637. <http://dx.doi.org/10.1038/ngeo2234>
- Collins, M., R. Knutti, J. Arblaster, J.-L. Dufresne, T. Fichet, P. Friedlingstein, X. Gao, W.J. Gutowski, T. Johns, G. Krinner, M. Shongwe, C. Tebaldi, A.J. Weaver, and M. Wehner, 2013: Long-term Climate Change: Projections, Commitments and Irreversibility. *Climate Change 2013: The Physical Science Basis. Contribution of Working Group I to the Fifth Assessment Report of the Intergovernmental Panel on Climate Change*. Stocker, T.F., D.

- Qin, G.-K. Plattner, M. Tignor, S.K. Allen, J. Boschung, A. Nauels, Y. Xia, V. Bex, and P.M. Midgley, Eds. Cambridge University Press, Cambridge, United Kingdom and New York, NY, USA, 1029–1136. <http://dx.doi.org/10.1017/CBO9781107415324.024>
www.climatechange2013.org
- Comiso, J.C. and D.K. Hall, 2014: Climate trends in the Arctic as observed from space. *Wiley Interdisciplinary Reviews: Climate Change*, **5**, 389-409. <http://dx.doi.org/10.1002/wcc.277>
- Derksen, C. and R. Brown, 2012: Snow [in Arctic Report Card 2012].
<http://www.arctic.noaa.gov/report12/snow.html>
- Derksen, C., R. Brown, L. Mudryk, and K. Luoju, 2015: Terrestrial snow cover [in Arctic Report Card 2015]. http://www.arctic.noaa.gov/reportcard/snow_cover.html
- Ding, Q., J.M. Wallace, D.S. Battisti, E.J. Steig, A.J.E. Gallant, H.-J. Kim, and L. Geng, 2014: Tropical forcing of the recent rapid Arctic warming in northeastern Canada and Greenland. *Nature*, **509**, 209-212. <http://dx.doi.org/10.1038/nature13260>
- Döscher, R., T. Vihma, and E. Maksimovich, 2014: Recent advances in understanding the Arctic climate system state and change from a sea ice perspective: a review. *Atmospheric Chemistry and Physics*, **14**, 13571-13600. <http://dx.doi.org/10.5194/acp-14-13571-2014>
- Dupont, T.K. and R.B. Alley, 2005: Assessment of the importance of ice-shelf buttressing to ice-sheet flow. *Geophysical Research Letters*, **32**, n/a-n/a.
<http://dx.doi.org/10.1029/2004GL020204>
- Fisher, J.B., M. Sikka, W.C. Oechel, D.N. Huntzinger, J.R. Melton, C.D. Koven, A. Ahlström, M.A. Arain, I. Baker, J.M. Chen, P. Ciais, C. Davidson, M. Dietze, B. El-Masri, D. Hayes, C. Huntingford, A.K. Jain, P.E. Levy, M.R. Lomas, B. Poulter, D. Price, A.K. Sahoo, K. Schaefer, H. Tian, E. Tomelleri, H. Verbeeck, N. Viovy, R. Wania, N. Zeng, and C.E. Miller, 2014: Carbon cycle uncertainty in the Alaskan Arctic. *Biogeosciences*, **11**, 4271-4288.
<http://dx.doi.org/10.5194/bg-11-4271-2014> <http://www.biogeosciences.net/11/4271/2014/>
- Flannigan, M., B. Stocks, M. Turetsky, and M. Wotton, 2009: Impacts of climate change on fire activity and fire management in the circumboreal forest. *Global Change Biology*, **15**, 549-560. <http://dx.doi.org/10.1111/j.1365-2486.2008.01660.x>
- Francis, J. and N. Skific, 2015: Evidence linking rapid Arctic warming to mid-latitude weather patterns. *Philosophical Transactions of the Royal Society A: Mathematical, Physical and Engineering Sciences*, **373**. <http://dx.doi.org/10.1098/rsta.2014.0170>
- Francis, J.A. and S.J. Vavrus, 2012: Evidence linking Arctic amplification to extreme weather in mid-latitudes. *Geophysical Research Letters*, **39**, L06801.
<http://dx.doi.org/10.1029/2012GL051000>

- Francis, J.A. and S.J. Vavrus, 2015: Evidence for a wavier jet stream in response to rapid Arctic warming. *Environmental Research Letters*, **10**, 014005. <http://dx.doi.org/10.1088/1748-9326/10/1/014005>
- Francis, J.A., S.J. Vavrus, and J. Cohen, 2016: Amplified Arctic Warming and Mid-Latitude Weather: Emerging ConnectionsWiREs. *WIREs*, **Submitted**.
- French, N.H.F., L.K. Jenkins, T.V. Loboda, M. Flannigan, R. Jandt, L.L. Bourgeau-Chavez, and M. Whitley, 2015: Fire in arctic tundra of Alaska: past fire activity, future fire potential, and significance for land management and ecology. *International Journal of Wildland Fire*, **24**, 1045-1061. <http://dx.doi.org/10.1071/WF14167>
<http://www.publish.csiro.au/paper/WF14167>
- Friedlingstein, P., P. Cox, R. Betts, L. Bopp, W.v. Bloh, V. Brovkin, P. Cadule, S. Doney, M. Eby, I. Fung, G. Bala, J. John, C. Jones, F. Joos, T. Kato, M. Kawamiya, W. Knorr, K. Lindsay, H.D. Matthews, T. Raddatz, P. Rayner, C. Reick, E. Roeckner, K.-G. Schnitzler, R. Schnur, K. Strassmann, A.J. Weaver, C. Yoshikawa, and N. Zeng, 2006: Climate–Carbon Cycle Feedback Analysis: Results from the C4MIP Model Intercomparison. *Journal of Climate*, **19**, 3337-3353. <http://dx.doi.org/10.1175/JCLI3800.1>
- Gagné, M.È., N.P. Gillett, and J.C. Fyfe, 2015: Impact of aerosol emission controls on future Arctic sea ice cover. *Geophysical Research Letters*, **42**, 8481-8488.
<http://dx.doi.org/10.1002/2015GL065504>
- Gibbs, A.E. and B.M. Richmond, 2010: National assessment of shoreline change: Historical shoreline change along the north coast of Alaska, U.S.–Canadian border to Icy Cape. U.S. Geological Survey Open-File Report 2015–1048. 96 pp. U.S. Department of the Interior, U.S. Geological Survey. <http://pubs.usgs.gov/of/2015/1048/pdf/ofr2015-1048.pdf>
- Giles, K.A., S.W. Laxon, A.L. Ridout, D.J. Wingham, and S. Bacon, 2012: Western Arctic Ocean freshwater storage increased by wind-driven spin-up of the Beaufort Gyre. *Nature Geoscience*, **5**, 194-197. <http://dx.doi.org/10.1038/ngeo1379>
- Gillett, N.P., D.A. Stone, P.A. Stott, T. Nozawa, A.Y. Karpechko, G.C. Hegerl, M.F. Wehner, and P.D. Jones, 2008: Attribution of polar warming to human influence. *Nature Geoscience*, **1**, 750-754. <http://dx.doi.org/10.1038/ngeo338>
- Graversen, R.G., 2006: Do Changes in the Midlatitude Circulation Have Any Impact on the Arctic Surface Air Temperature Trend? *Journal of Climate*, **19**, 5422-5438.
<http://dx.doi.org/10.1175/JCLI3906.1>
- Harig, C. and F.J. Simons, 2016: Ice mass loss in Greenland, the Gulf of Alaska, and the Canadian Archipelago: Seasonal cycles and decadal trends. *Geophysical Research Letters*, **43**, 3150-3159. <http://dx.doi.org/10.1002/2016GL067759>

- 1 Hartmann, B. and G. Wendler, 2005: The Significance of the 1976 Pacific Climate Shift in the
2 Climatology of Alaska. *Journal of Climate*, **18**, 4824-4839.
3 <http://dx.doi.org/10.1175/JCLI3532.1>
- 4 Hartmann, D.L., A.M.G. Klein Tank, M. Rusticucci, L.V. Alexander, S. Brönnimann, Y.
5 Charabi, F.J. Dentener, E.J. Dlugokencky, D.R. Easterling, A. Kaplan, B.J. Soden, P.W.
6 Thorne, M. Wild, and P.M. Zhai, 2013: Observations: Atmosphere and Surface. *Climate*
7 *Change 2013: The Physical Science Basis. Contribution of Working Group I to the Fifth*
8 *Assessment Report of the Intergovernmental Panel on Climate Change*. Stocker, T.F., D.
9 Qin, G.-K. Plattner, M. Tignor, S.K. Allen, J. Boschung, A. Nauels, Y. Xia, V. Bex, and
10 P.M. Midgley, Eds. Cambridge University Press, Cambridge, United Kingdom and New
11 York, NY, USA, 159–254. <http://dx.doi.org/10.1017/CBO9781107415324.008>
12 www.climatechange2013.org
- 13 Holland, D.M., R.H. Thomas, B. de Young, M.H. Ribergaard, and B. Lyberth, 2008:
14 Acceleration of Jakobshavn Isbrae triggered by warm subsurface ocean waters. *Nature*
15 *Geoscience*, **1**, 659-664. <http://dx.doi.org/10.1038/ngeo316>
- 16 Hoskins, B. and T. Woollings, 2015: Persistent Extratropical Regimes and Climate Extremes.
17 *Current Climate Change Reports*, **1**, 115-124. <http://dx.doi.org/10.1007/s40641-015-0020-8>
- 18 Howat, I.M., I. Joughin, M. Fahnestock, B.E. Smith, and T.A. Scambos, 2008: Synchronous
19 retreat and acceleration of southeast Greenland outlet glaciers 2000–2011: ice dynamics
20 and coupling to climate. *Journal of Glaciology*, **54**, 646-660.
21 <http://dx.doi.org/10.3189/002214308786570908>
- 22 Hu, F.S., P.E. Higuera, P. Duffy, M.L. Chipman, A.V. Rocha, A.M. Young, R. Kelly, and M.C.
23 Dietze, 2015: Arctic tundra fires: natural variability and responses to climate change.
24 *Frontiers in Ecology and the Environment*, **13**, 369-377. <http://dx.doi.org/10.1890/150063>
- 25 Hunt, G.L., Jr., K.O. Coyle, L.B. Eisner, E.V. Farley, R.A. Heintz, F. Mueter, J.M. Napp, J.E.
26 Overland, P.H. Ressler, S. Salo, and P.J. Stabeno, 2011: Climate impacts on eastern Bering
27 Sea foodwebs: A synthesis of new data and an assessment of the Oscillating Control
28 Hypothesis. *ICES Journal of Marine Science*, **68**, 1230-1243.
29 <http://dx.doi.org/10.1093/icesjms/fsr036>
- 30 Hunter, S.J., D.S. Goldobin, A.M. Haywood, A. Ridgwell, and J.G. Rees, 2013: Sensitivity of
31 the global submarine hydrate inventory to scenarios of future climate change. *Earth and*
32 *Planetary Science Letters*, **367**, 105-115. <http://dx.doi.org/10.1016/j.epsl.2013.02.017>
- 33 IPCC, 2013: *Climate Change 2013: The Physical Science Basis. Contribution of Working Group*
34 *I to the Fifth Assessment Report of the Intergovernmental Panel on Climate Change*.

- Cambridge University Press, Cambridge, UK and New York, NY, 1535 pp.
<http://dx.doi.org/10.1017/CBO9781107415324> www.climatechange2013.org
- Johannessen, O.M., A. Korabely, V. Miles, M.W. Miles, and K.E. Solberg, 2011: Interaction Between the Warm Subsurface Atlantic Water in the Sermilik Fjord and Helheim Glacier in Southeast Greenland. *Surveys in Geophysics*, **32**, 387-396. <http://dx.doi.org/10.1007/s10712-011-9130-6>
- Johannessen, O.M., S.I. Kuzmina, L.P. Bobylev, and M.W. Miles, 2016: Surface air temperature variability and trends in the Arctic: New amplification assessment and regionalisation. *Tellus A*, **68**. <http://dx.doi.org/10.3402/tellusa.v68.28234>
- Joly, K., P.A. Duffy, and T.S. Rupp, 2012: Simulating the effects of climate change on fire regimes in Arctic biomes: implications for caribou and moose habitat. *Ecosphere*, **3**, 1-18. <http://dx.doi.org/10.1890/ES12-00012.1>
- Joughin, I., S.B. Das, M.A. King, B.E. Smith, I.M. Howat, and T. Moon, 2008: Seasonal Speedup Along the Western Flank of the Greenland Ice Sheet. *Science*, **320**, 781-783. <http://dx.doi.org/10.1126/science.1153288>
- Jungclaus, J.H., K. Lohmann, and D. Zanchettin, 2014: Enhanced 20th-century heat transfer to the Arctic simulated in the context of climate variations over the last millennium. *Climate of the Past*, **10**, 2201-2213. <http://dx.doi.org/10.5194/cp-10-2201-2014>
- Kasischke, E.S. and M.R. Turetsky, 2006: Recent changes in the fire regime across the North American boreal region—Spatial and temporal patterns of burning across Canada and Alaska. *Geophysical Research Letters*, **33**, n/a-n/a. <http://dx.doi.org/10.1029/2006GL025677>
- Kay, J.E. and A. Gettelman, 2009: Cloud influence on and response to seasonal Arctic sea ice loss. *Journal of Geophysical Research*, **114**, D18204. <http://dx.doi.org/10.1029/2009JD011773>
- Kay, J.E., K. Raeder, A. Gettelman, and J. Anderson, 2011: The Boundary Layer Response to Recent Arctic Sea Ice Loss and Implications for High-Latitude Climate Feedbacks. *Journal of Climate*, **24**, 428-447. <http://dx.doi.org/10.1175/2010JCLI3651.1>
- Kelly, R., M.L. Chipman, P.E. Higuera, I. Stefanova, L.B. Brubaker, and F.S. Hu, 2013: Recent burning of boreal forests exceeds fire regime limits of the past 10,000 years. *Proceedings of the National Academy of Sciences*, **110**, 13055-13060. <http://dx.doi.org/10.1073/pnas.1305069110>
- Kelly, R., H. Genet, A.D. McGuire, and F.S. Hu, 2016: Palaeodata-informed modelling of large carbon losses from recent burning of boreal forests. *Nature Climate Change*, **6**, 79-82. <http://dx.doi.org/10.1038/nclimate2832>

- 1 Khan, S.A., K.H. Kjaer, M. Bevis, J.L. Bamber, J. Wahr, K.K. Kjeldsen, A.A. Bjork, N.J.
2 Korsgaard, L.A. Stearns, M.R. van den Broeke, L. Liu, N.K. Larsen, and I.S. Muresan, 2014:
3 Sustained mass loss of the northeast Greenland ice sheet triggered by regional warming.
4 *Nature Climate Change*, **4**, 292-299. <http://dx.doi.org/10.1038/nclimate2161>
- 5 Knies, J., P. Cabedo-Sanz, S.T. Belt, S. Baranwal, S. Fietz, and A. Rosell-Melé, 2014: The
6 emergence of modern sea ice cover in the Arctic Ocean. *Nature Communications*, **5**, 5608.
7 <http://dx.doi.org/10.1038/ncomms6608>
- 8 Köhl, A. and N. Serra, 2014: Causes of Decadal Changes of the Freshwater Content in the Arctic
9 Ocean. *Journal of Climate*, **27**, 3461-3475. <http://dx.doi.org/10.1175/JCLI-D-13-00389.1>
- 10 Koven, C.D., D.M. Lawrence, and W.J. Riley, 2015: Permafrost carbon–climate feedback is
11 sensitive to deep soil carbon decomposability but not deep soil nitrogen dynamics.
12 *Proceedings of the National Academy of Sciences*, **112**, 3752-3757.
13 <http://dx.doi.org/10.1073/pnas.1415123112>
- 14 Koven, C.D., E.A.G. Schuur, C. Schädel, T.J. Bohn, E.J. Burke, G. Chen, X. Chen, P. Ciais, G.
15 Grosse, J.W. Harden, D.J. Hayes, G. Hugelius, E.E. Jafarov, G. Krinner, P. Kuhry, D.M.
16 Lawrence, A.H. MacDougall, S.S. Marchenko, A.D. McGuire, S.M. Natali, D.J. Nicolsky, D.
17 Olefeldt, S. Peng, V.E. Romanovsky, K.M. Schaefer, J. Strauss, C.C. Treat, and M. Turetsky,
18 2015: A simplified, data-constrained approach to estimate the permafrost carbon–climate
19 feedback. *Philosophical Transactions of the Royal Society A: Mathematical, Physical and*
20 *Engineering Sciences*, **373**. <http://dx.doi.org/10.1098/rsta.2014.0423>
- 21 Kretschmer, K., A. Biastoch, L. Rüpke, and E. Burwicz, 2015: Modeling the fate of methane
22 hydrates under global warming. *Global Biogeochemical Cycles*, **29**, 610-625.
23 <http://dx.doi.org/10.1002/2014GB005011>
- 24 Kwok, R. and N. Untersteiner, 2011: The thinning of Arctic sea ice. *Physics Today*, **64**, 36-41.
25 <http://dx.doi.org/10.1063/1.3580491>
- 26 Lee, S., 2014: A theory for polar amplification from a general circulation perspective. *Asia-*
27 *Pacific Journal of Atmospheric Sciences*, **50**, 31-43. [http://dx.doi.org/10.1007/s13143-014-](http://dx.doi.org/10.1007/s13143-014-0024-7)
28 [0024-7](http://dx.doi.org/10.1007/s13143-014-0024-7)
- 29 Lee, S., T. Gong, N. Johnson, S.B. Feldstein, and D. Pollard, 2011: On the Possible Link
30 between Tropical Convection and the Northern Hemisphere Arctic Surface Air Temperature
31 Change between 1958 and 2001. *Journal of Climate*, **24**, 4350-4367.
32 <http://dx.doi.org/10.1175/2011JCLI4003.1>
- 33 Liljedahl, A.K., J. Boike, R.P. Daanen, A.N. Fedorov, G.V. Frost, G. Grosse, L.D. Hinzman, Y.
34 Iijma, J.C. Jorgenson, N. Matveyeva, M. Necsoiu, M.K. Reynolds, V.E. Romanovsky, J.
35 Schulla, K.D. Tape, D.A. Walker, C.J. Wilson, H. Yabuki, and D. Zona, 2016: Pan-Arctic

- ice-wedge degradation in warming permafrost and its influence on tundra hydrology. *Nature Geoscience*, **9**, 312-318. <http://dx.doi.org/10.1038/ngeo2674>
- Lim, Y.-K., D.S. Siegfried, M.J.N. Sophie, N.L. Jae, M.M. Andrea, I.C. Richard, Z. Bin, and V. Isabella, 2016: Atmospheric summer teleconnections and Greenland Ice Sheet surface mass variations: insights from MERRA-2. *Environmental Research Letters*, **11**, 024002. <http://dx.doi.org/10.1088/1748-9326/11/2/024002>
- Maslowski, W., J. Clement Kinney, M. Higgins, and A. Roberts, 2012: The future of Arctic sea ice. *Annual Review of Earth and Planetary Sciences*, **40**, 625-654. <http://dx.doi.org/10.1146/annurev-earth-042711-105345>
- Maslowski, W., J. Clement Kinney, S.R. Okkonen, R. Osinski, A.F. Roberts, and W.J. Williams, 2014: The Large Scale Ocean Circulation and Physical Processes Controlling Pacific-Arctic Interactions. *The Pacific Arctic Region: Ecosystem Status and Trends in a Rapidly Changing Environment*. Grebmeier, M.J. and W. Maslowski, Eds. Springer Netherlands, Dordrecht, 101-132. http://dx.doi.org/10.1007/978-94-017-8863-2_5
- Mathis, J.T., J.N. Cross, W. Evans, and S.C. Doney, 2015: Ocean acidification in the surface waters of the Pacific-Arctic boundary regions. *Oceanography*, **28**, 122-135. <http://dx.doi.org/10.5670/oceanog.2015.36> http://tos.org/oceanography/assets/docs/28-2_mathis2.pdf
- Mathis, J.T., R.S. Pickart, R.H. Byrne, C.L. McNeil, G.W.K. Moore, L.W. Juranek, X. Liu, J. Ma, R.A. Easley, M.M. Elliot, J.N. Cross, S.C. Reisdorph, F. Bahr, J. Morison, T. Lichendorf, and R.A. Feely, 2012: Storm-induced upwelling of high pCO₂ waters onto the continental shelf of the western Arctic Ocean and implications for carbonate mineral saturation states. *Geophysical Research Letters*, **39**, L16703. <http://dx.doi.org/10.1029/2012GL051574>
- McAfee, S.A., 2014: Consistency and the Lack Thereof in Pacific Decadal Oscillation Impacts on North American Winter Climate. *Journal of Climate*, **27**, 7410-7431. <http://dx.doi.org/10.1175/JCLI-D-14-00143.1>
- McCusker, K.E., J.C. Fyfe, and M. Sigmond, 2016: Twenty-five winters of unexpected Eurasian cooling unlikely due to Arctic sea-ice loss. *Nature Geosci*, **9**, 838-842. <http://dx.doi.org/10.1038/ngeo2820>
- McGuire, A.D., L.G. Anderson, T.R. Christensen, S. Dallimore, L. Guo, D.J. Hayes, M. Heimann, T.D. Lorenson, R.W. MacDonald, and N. Roulet, 2009: Sensitivity of the carbon cycle in the Arctic to climate change. *Ecological Monographs*, **79**, 523-555. <http://dx.doi.org/10.1890/08-2025.1>

- 1 Melillo, J.M., T.C. Richmond, and G.W. Yohe, eds. *Climate Change Impacts in the United*
2 *States: The Third National Climate Assessment*. 2014, U.S. Global Change Research
3 Program: Washington, D.C. 842. <http://dx.doi.org/10.7930/J0Z31WJ2>.
- 4 Melillo, J.M., T.C. Richmond, and G.W. Yohe, eds. *Highlights of Climate Change Impacts in the*
5 *United States: The Third National Climate Assessment*. 2014, U.S. Global Change Research
6 Program: Washington, DC. 148. <http://dx.doi.org/10.7930/J0H41PB6>.
7 <http://nca2014.globalchange.gov/highlights>
- 8 Mengel, M., A. Levermann, K. Frieler, A. Robinson, B. Marzeion, and R. Winkelmann, 2016:
9 Future sea level rise constrained by observations and long-term commitment. *Proceedings of*
10 *the National Academy of Sciences*, **113**, 2597-2602.
11 <http://dx.doi.org/10.1073/pnas.1500515113>
- 12 Mernild, S.H., J.K. Malmros, J.C. Yde, and N.T. Knudsen, 2012: Multi-decadal marine- and
13 land-terminating glacier recession in the Ammassalik region, southeast Greenland. *The*
14 *Cryosphere*, **6**, 625-639. <http://dx.doi.org/10.5194/tc-6-625-2012>
- 15 Mishra, U. and W.J. Riley, 2012: Alaskan soil carbon stocks: spatial variability and dependence
16 on environmental factors. *Biogeosciences*, **9**, 3637-3645. [http://dx.doi.org/10.5194/bg-9-](http://dx.doi.org/10.5194/bg-9-3637-2012)
17 [3637-2012](http://www.biogeosciences.net/9/3637/2012/) <http://www.biogeosciences.net/9/3637/2012/>
- 18 Morison, J., R. Kwok, C. Peralta-Ferriz, M. Alkire, I. Rigor, R. Andersen, and M. Steele, 2012:
19 Changing Arctic Ocean freshwater pathways. *Nature*, **481**, 66-70.
20 <http://dx.doi.org/10.1038/nature10705>
- 21 Myers-Smith, I.H., B.C. Forbes, M. Wilmking, M. Hallinger, T. Lantz, D. Blok, K.D. Tape, M.
22 Macias-Fauria, U. Sass-Klaassen, E. Lévesque, S. Boudreau, P. Ropars, L. Hermanutz, A.
23 Trant, L.S. Collier, S. Weijers, J. Rozema, S.A. Rayback, N.M. Schmidt, G. Schaepman-
24 Strub, S. Wipf, C. Rixen, C.B. Ménard, S. Venn, S. Goetz, L. Andreu-Hayles, S. Elmendorf,
25 V. Ravolainen, J. Welker, P. Grogan, H.E. Epstein, and D.S. Hik, 2011: Shrub expansion in
26 tundra ecosystems: dynamics, impacts and research priorities. *Environmental Research*
27 *Letters*, **6**, 045509. <http://dx.doi.org/10.1088/1748-9326/6/4/045509>
28 <http://stacks.iop.org/1748-9326/6/i=4/a=045509>
- 29 Najafi, M.R., F.W. Zwiers, and N.P. Gillett, 2015: Attribution of Arctic temperature change to
30 greenhouse-gas and aerosol influences. *Nature Climate Change*, **5**, 246-249.
31 <http://dx.doi.org/10.1038/nclimate2524>
- 32 Nummelin, A., M. Ilicak, C. Li, and L.H. Smedsrud, 2016: Consequences of future increased
33 Arctic runoff on Arctic Ocean stratification, circulation, and sea ice cover. *Journal of*
34 *Geophysical Research: Oceans*, **121**, 617-637. <http://dx.doi.org/10.1002/2015JC011156>

- Ogi, M. and I.G. Rigor, 2013: Trends in Arctic sea ice and the role of atmospheric circulation. *Atmospheric Science Letters*, **14**, 97-101. <http://dx.doi.org/10.1002/asl2.423>
- Ogi, M. and J.M. Wallace, 2007: Summer minimum Arctic sea ice extent and the associated summer atmospheric circulation. *Geophysical Research Letters*, **34**, L12705. <http://dx.doi.org/10.1029/2007GL029897>
- Overland, J., J.A. Francis, R. Hall, E. Hanna, S.-J. Kim, and T. Vihma, 2015: The Melting Arctic and Midlatitude Weather Patterns: Are They Connected? *Journal of Climate*, **28**, 7917-7932. <http://dx.doi.org/10.1175/JCLI-D-14-00822.1>
- Overland, J., E. Hanna, I. Hanssen-Bauer, S.-J. Kim, J. Walsh, M. Wang, and U. Bhatt, 2014: Air temperature [in Arctic Report Card 2014]. http://www.arctic.noaa.gov/report14/air_temperature.html
- Overland, J., E. Hanna, I. Hanssen-Bauer, S.-J. Kim, J. Wlash, M. Wang, and U.S. Bhatt, 2015: [The Arctic] Arctic air temperature [in “State of the Climate in 2014”]. *Bulletin of the American Meteorological Society*, **96**, S128-S129. <http://dx.doi.org/10.1175/2015BAMSStateoftheClimate.1>
- Overland, J.E. and M. Wang, 2016: Recent Extreme Arctic Temperatures are due to a Split Polar Vortex. *Journal of Climate*, **29**, 5609-5616. <http://dx.doi.org/10.1175/JCLI-D-16-0320.1>
- Park, H.-S., S. Lee, S.-W. Son, S.B. Feldstein, and Y. Kosaka, 2015: The Impact of Poleward Moisture and Sensible Heat Flux on Arctic Winter Sea Ice Variability. *Journal of Climate*, **28**, 5030-5040. <http://dx.doi.org/10.1175/JCLI-D-15-0074.1>
- Parkinson, C.L., 2014: Spatially mapped reductions in the length of the Arctic sea ice season. *Geophysical Research Letters*, **41**, 4316-4322. <http://dx.doi.org/10.1002/2014GL060434>
- Partain Jr., J.L., S. Alden, U.S. Bhatt, P.A. Bieniek, B.R. Brettschneider, R. Lader, P.Q. Olsson, T.S. Rupp, H. Strader, R.L.T. Jr., J.E. Walsh, A.D. York, and R.H. Zieh, 2016: An assessment of the role of anthropogenic climate change in the Alaska fire season of 2015. *Bulletin of the American Meteorological Society*, **97**, in press. <http://dx.doi.org/10.1175/BAMS-D-16-0149.1>
- Pavelsky, T.M., J. Boé, A. Hall, and E.J. Fetzer, 2011: Atmospheric inversion strength over polar oceans in winter regulated by sea ice. *Climate Dynamics*, **36**, 945-955. <http://dx.doi.org/10.1007/s00382-010-0756-8>
- Pelto, M.S., 2015: [Global Climate] Alpine glaciers [in “State of the Climate in 2014”]. *Bulletin of the American Meteorological Society*, **96**, S19-S20. <http://dx.doi.org/10.1175/2015BAMSStateoftheClimate.1>

- 1 Perlwitz, J., M. Hoerling, and R. Dole, 2015: Arctic Tropospheric Warming: Causes and
2 Linkages to Lower Latitudes. *Journal of Climate*, **28**, 2154-2167.
3 <http://dx.doi.org/10.1175/JCLI-D-14-00095.1>
- 4 Perovich, D., W. Meier, M. Tschudi, S. Farrell, S. Gerland, and S. Hendricks, 2015: Sea ice [in
5 Arctic Report Card 2015]. http://www.arctic.noaa.gov/reportcard/sea_ice.html
- 6 Piñero, E., M. Marquardt, C. Hensen, M. Haeckel, and K. Wallmann, 2013: Estimation of the
7 global inventory of methane hydrates in marine sediments using transfer functions.
8 *Biogeosciences*, **10**, 959-975. <http://dx.doi.org/10.5194/bg-10-959-2013>
- 9 Polyakov, I.V., A.V. Pnyushkov, and L.A. Timokhov, 2012: Warming of the Intermediate
10 Atlantic Water of the Arctic Ocean in the 2000s. *Journal of Climate*, **25**, 8362-8370.
11 <http://dx.doi.org/10.1175/JCLI-D-12-00266.1>
- 12 Rahmstorf, S., J.E. Box, G. Feulner, M.E. Mann, A. Robinson, S. Rutherford, and E.J.
13 Schaffernicht, 2015: Exceptional twentieth-century slowdown in Atlantic Ocean overturning
14 circulation. *Nature Climate Change*, **5**, 475-480. <http://dx.doi.org/10.1038/nclimate2554>
- 15 Rawlins, M.A., M. Steele, M.M. Holland, J.C. Adam, J.E. Cherry, J.A. Francis, P.Y. Groisman,
16 L.D. Hinzman, T.G. Huntington, D.L. Kane, J.S. Kimball, R. Kwok, R.B. Lammers, C.M.
17 Lee, D.P. Lettenmaier, K.C. McDonald, E. Podest, J.W. Pundsack, B. Rudels, M.C. Serreze,
18 A. Shiklomanov, Ø. Skagseth, T.J. Troy, C.J. Vörösmarty, M. Wensnahan, E.F. Wood, R.
19 Woodgate, D. Yang, K. Zhang, and T. Zhang, 2010: Analysis of the Arctic System for
20 Freshwater Cycle Intensification: Observations and Expectations. *Journal of Climate*, **23**,
21 5715-5737. <http://dx.doi.org/10.1175/2010JCLI3421.1>
- 22 Rhein, M., S.R. Rintoul, S. Aoki, E. Campos, D. Chambers, R.A. Feely, S. Gulev, G.C. Johnson,
23 S.A. Josey, A. Kostianoy, C. Mauritzen, D. Roemmich, L.D. Talley, and F. Wang, 2013:
24 Observations: Ocean. *Climate Change 2013: The Physical Science Basis. Contribution of*
25 *Working Group I to the Fifth Assessment Report of the Intergovernmental Panel on Climate*
26 *Change*. Stocker, T.F., D. Qin, G.-K. Plattner, M. Tignor, S.K. Allen, J. Boschung, A.
27 Nauels, Y. Xia, V. Bex, and P.M. Midgley, Eds. Cambridge University Press, Cambridge,
28 United Kingdom and New York, NY, USA, 255–316.
29 <http://dx.doi.org/10.1017/CBO9781107415324.010> www.climatechange2013.org
- 30 Rignot, E., M. Koppes, and I. Velicogna, 2010: Rapid submarine melting of the calving faces of
31 West Greenland glaciers. *Nature Geoscience*, **3**, 187-191. <http://dx.doi.org/10.1038/ngeo765>
- 32 Rigor, I.G., J.M. Wallace, and R.L. Colony, 2002: Response of Sea Ice to the Arctic Oscillation.
33 *Journal of Climate*, **15**, 2648-2663. [http://dx.doi.org/10.1175/1520-](http://dx.doi.org/10.1175/1520-0442(2002)015<2648:ROSITT>2.0.CO;2)
34 [0442\(2002\)015<2648:ROSITT>2.0.CO;2](http://dx.doi.org/10.1175/1520-0442(2002)015<2648:ROSITT>2.0.CO;2)

- Romanovsky, V.E., S.L. Smith, H.H. Christiansen, N.I. Shiklomanov, D.A. Streletskiy, D.S. Drozdov, G.V. Malkova, N.G. Oberman, A.L. Kholodov, and S.S. Marchenko, 2015: [The Arctic] Terrestrial permafrost [in “State of the Climate in 2014”]. *Bulletin of the American Meteorological Society*, **96**, S139-S141. <http://dx.doi.org/10.1175/2015BAMSStateoftheClimate.1>
- Romanovsky, V.E., S.L. Smith, K. Isaksen, N.I. Shiklomanov, D.A. Streletskiy, A.L. Kholodov, H.H. Christiansen, D.S. Drozdov, G.V. Malkova, and S.S. Marchenko, 2016: [The Arctic] Terrestrial permafrost [in “State of the Climate in 2015”]. *Bulletin of the American Meteorological Society*, **97**, S149-S152. <http://dx.doi.org/10.1175/2016BAMSStateoftheClimate.1>
- Ruppel, C.D., 2011: Methane Hydrates and Contemporary Climate Change. *Nature Education Knowledge*, **3**.
- Sanford, T., R. Wang, and A. Kenwa, 2015: The age of Alaskan wildfires. Climate Central, Princeton, NJ.
- Schadel, C., M.K.F. Bader, E.A.G. Schuur, C. Biasi, R. Bracho, P. Capek, S. De Baets, K. Diakova, J. Ernakovich, C. Estop-Aragones, D.E. Graham, I.P. Hartley, C.M. Iversen, E. Kane, C. Knoblauch, M. Lupascu, P.J. Martikainen, S.M. Natali, R.J. Norby, J.A. O'Donnell, T.R. Chowdhury, H. Santruckova, G. Shaver, V.L. Sloan, C.C. Treat, M.R. Turetsky, M.P. Waldrop, and K.P. Wickland, 2016: Potential carbon emissions dominated by carbon dioxide from thawed permafrost soils. *Nature Climate Change*, **6**, 950-953. <http://dx.doi.org/10.1038/nclimate3054>
- Schaefer, K., H. Lantuit, E.R. Vladimir, E.A.G. Schuur, and R. Witt, 2014: The impact of the permafrost carbon feedback on global climate. *Environmental Research Letters*, **9**, 085003. <http://dx.doi.org/10.1088/1748-9326/9/8/085003>
- Schuur, E.A.G., A.D. McGuire, C. Schadel, G. Grosse, J.W. Harden, D.J. Hayes, G. Hugelius, C.D. Koven, P. Kuhry, D.M. Lawrence, S.M. Natali, D. Olefeldt, V.E. Romanovsky, K. Schaefer, M.R. Turetsky, C.C. Treat, and J.E. Vonk, 2015: Climate change and the permafrost carbon feedback. *Nature*, **520**, 171-179. <http://dx.doi.org/10.1038/nature14338>
- Screen, J.A., C. Deser, and I. Simmonds, 2012: Local and remote controls on observed Arctic warming. *Geophysical Research Letters*, **39**, L10709. <http://dx.doi.org/10.1029/2012GL051598>
- Screen, J.A., C. Deser, and L. Sun, 2015: Reduced Risk of North American Cold Extremes due to Continued Arctic Sea Ice Loss. *Bulletin of the American Meteorological Society*, **96**, 1489-1503. <http://dx.doi.org/10.1175/BAMS-D-14-00185.1>

- 1 Screen, J.A., C. Deser, and L. Sun, 2015: Projected changes in regional climate extremes arising
2 from Arctic sea ice loss. *Environmental Research Letters*, **10**, 084006.
3 <http://dx.doi.org/10.1088/1748-9326/10/8/084006>
- 4 Screen, J.A. and J.A. Francis, 2016: Contribution of sea-ice loss to Arctic amplification is
5 regulated by Pacific Ocean decadal variability. *Nature Climate Change*, **6**, 856-860.
6 <http://dx.doi.org/10.1038/nclimate3011>
- 7 Sharp, M., G. Wolken, D. Burgess, J.G. Cogley, L. Copland, L. Thomson, A. Arendt, B.
8 Wouters, J. Kohler, L.M. Andreassen, S. O'Neel, and M. Pelto, 2015: [Global Climate]
9 Glaciers and ice caps outside Greenland [in "State of the Climate in 2014"]. *Bulletin of the*
10 *American Meteorological Society*, **96**, S135-S137.
11 <http://dx.doi.org/10.1175/2015BAMSStateoftheClimate.1>
- 12 Shiklomanov, N.E., D.A. Streletskiy, and F.E. Nelson. *Northern Hemisphere component of the*
13 *global Circumpolar Active Layer Monitory (CALM) program*. in *Proceedings of the 10th*
14 *International Conference on Permafrost*. 2012. Salekhard, Russia.
- 15 Sigmond, M. and J.C. Fyfe, 2016: Tropical Pacific impacts on cooling North American winters.
16 *Nature Climate Change*, **advance online publication**.
17 <http://dx.doi.org/10.1038/nclimate3069>
- 18 Smeed, D.A., G.D. McCarthy, S.A. Cunningham, E. Frajka-Williams, D. Rayner, W.E. Johns,
19 C.S. Meinen, M.O. Baringer, B.I. Moat, A. Ducheze, and H.L. Bryden, 2014: Observed
20 decline of the Atlantic meridional overturning circulation 2004–2012. *Ocean Science*,
21 **10**, 29-38. <http://dx.doi.org/10.5194/os-10-29-2014>
- 22 Snape, T.J. and P.M. Forster, 2014: Decline of Arctic sea ice: Evaluation and weighting of
23 CMIP5 projections. *Journal of Geophysical Research: Atmospheres*, **119**, 546-554.
24 <http://dx.doi.org/10.1002/2013JD020593>
- 25 Solomon, A., M.D. Shupe, O. Persson, H. Morrison, T. Yamaguchi, P.M. Caldwell, and G.d.
26 Boer, 2014: The Sensitivity of Springtime Arctic Mixed-Phase Stratocumulus Clouds to
27 Surface-Layer and Cloud-Top Inversion-Layer Moisture Sources. *Journal of the Atmospheric*
28 *Sciences*, **71**, 574-595. <http://dx.doi.org/10.1175/JAS-D-13-0179.1>
- 29 Spielhagen, R.F., K. Werner, S.A. Sørensen, K. Zamelczyk, E. Kandiano, G. Budeus, K. Husum,
30 T.M. Marchitto, and M. Hald, 2011: Enhanced Modern Heat Transfer to the Arctic by Warm
31 Atlantic Water. *Science*, **331**, 450-453. <http://dx.doi.org/10.1126/science.1197397>
- 32 Stabeno, P.J., E.V. Farley, Jr., N.B. Kachel, S. Moore, C.W. Mordy, J.M. Napp, J.E. Overland,
33 A.I. Pinchuk, and M.F. Sigler, 2012: A comparison of the physics of the northern and
34 southern shelves of the eastern Bering Sea and some implications for the ecosystem. *Deep*

- 1 *Sea Research Part II: Topical Studies in Oceanography*, **65-70**, 14-30.
2 <http://dx.doi.org/10.1016/j.dsr2.2012.02.019>
- 3 Straneo, F., R.G. Curry, D.A. Sutherland, G.S. Hamilton, C. Cenedese, K. Vage, and L.A.
4 Stearns, 2011: Impact of fjord dynamics and glacial runoff on the circulation near Helheim
5 Glacier. *Nature Geoscience*, **4**, 322-327. <http://dx.doi.org/10.1038/ngeo1109>
- 6 Straneo, F., G.S. Hamilton, D.A. Sutherland, L.A. Stearns, F. Davidson, M.O. Hammill, G.B.
7 Stenson, and A. Rosing-Asvid, 2010: Rapid circulation of warm subtropical waters in a
8 major glacial fjord in East Greenland. *Nature Geoscience*, **3**, 182-186.
9 <http://dx.doi.org/10.1038/ngeo764>
- 10 Stroeve, J., A. Barrett, M. Serreze, and A. Schweiger, 2014: Using records from submarine,
11 aircraft and satellites to evaluate climate model simulations of Arctic sea ice thickness. *The*
12 *Cryosphere*, **8**, 1839-1854. <http://dx.doi.org/10.5194/tc-8-1839-2014>
- 13 Stroeve, J. and D. Notz, 2015: Insights on past and future sea-ice evolution from combining
14 observations and models. *Global and Planetary Change*, **135**, 119-132.
15 <http://dx.doi.org/10.1016/j.gloplacha.2015.10.011>
- 16 Stroeve, J.C., V. Kattsov, A. Barrett, M. Serreze, T. Pavlova, M. Holland, and W.N. Meier,
17 2012: Trends in Arctic sea ice extent from CMIP5, CMIP3 and observations. *Geophysical*
18 *Research Letters*, **39**, L16502. <http://dx.doi.org/10.1029/2012GL052676>
- 19 Stroeve, J.C., T. Markus, L. Boisvert, J. Miller, and A. Barrett, 2014: Changes in Arctic melt
20 season and implications for sea ice loss. *Geophysical Research Letters*, **41**, 1216-1225.
21 <http://dx.doi.org/10.1002/2013GL058951>
- 22 Stroeve, J.C., M.C. Serreze, M.M. Holland, J.E. Kay, J. Malanik, and A.P. Barrett, 2012: The
23 Arctic's rapidly shrinking sea ice cover: A research synthesis. *Climatic Change*, **110**, 1005-
24 1027. <http://dx.doi.org/10.1007/s10584-011-0101-1>
- 25 Sun, L., J. Perlwitz, and M. Hoerling, 2016: What caused the recent "Warm Arctic, Cold
26 Continents" trend pattern in winter temperatures? *Geophysical Research Letters*, **43**, 5345-
27 5352. <http://dx.doi.org/10.1002/2016GL069024>
- 28 Swart, N.C., J.C. Fyfe, E. Hawkins, J.E. Kay, and A. Jahn, 2015: Influence of internal variability
29 on Arctic sea-ice trends. *Nature Climate Change*, **5**, 86-89.
30 <http://dx.doi.org/10.1038/nclimate2483>
- 31 Taylor, P.C., M. Cai, A. Hu, J. Meehl, W. Washington, and G.J. Zhang, 2013: A Decomposition
32 of Feedback Contributions to Polar Warming Amplification. *Journal of Climate*, **26**, 7023-
33 7043. <http://dx.doi.org/10.1175/JCLI-D-12-00696.1>

- 1 Taylor, P.C., S. Kato, K.-M. Xu, and M. Cai, 2015: Covariance between Arctic sea ice and
2 clouds within atmospheric state regimes at the satellite footprint level. *Journal of*
3 *Geophysical Research: Atmospheres*, **120**, 12656-12678.
4 <http://dx.doi.org/10.1002/2015JD023520>
- 5 Tedesco, M., T. Mote, X. Fettweis, E. Hanna, J. Jeyaratnam, J.F. Booth, R. Datta, and K. Briggs,
6 2016: Arctic cut-off high drives the poleward shift of a new Greenland melting record.
7 *Nature Communications*, **7**, 11723. <http://dx.doi.org/10.1038/ncomms11723>
- 8 Timmermans, M.-L. and A. Proshutinsky, 2015: [The Arctic] Sea surface temperature [in “State
9 of the Climate in 2014”]. *Bulletin of the American Meteorological Society*, **96**, S147-S148.
10 <http://dx.doi.org/10.1175/2015BAMSSStateoftheClimate.1>
- 11 Tschudi, M., C. Fowler, J. Maslanik, J.S. Stewart, and W. Meier, 2016: EASE-Grid Sea Ice Age,
12 Version 3. In: NASA (ed.). National Snow and Ice Data Center Distributed Active Archive
13 Center, Boulder, CO.
- 14 van den Broeke, M., J. Bamber, J. Ettema, E. Rignot, E. Schrama, W.J. van de Berg, E. van
15 Meijgaard, I. Velicogna, and B. Wouters, 2009: Partitioning Recent Greenland Mass Loss.
16 *Science*, **326**, 984-986. <http://dx.doi.org/10.1126/science.1178176>
- 17 Vaughan, D.G., J.C. Comiso, I. Allison, J. Carrasco, G. Kaser, R. Kwok, P. Mote, T. Murray, F.
18 Paul, J. Ren, E. Rignot, O. Solomina, K. Steffen, and T. Zhang, 2013: Observations:
19 Cryosphere. *Climate Change 2013: The Physical Science Basis. Contribution of Working*
20 *Group I to the Fifth Assessment Report of the Intergovernmental Panel on Climate Change*.
21 Stocker, T.F., D. Qin, G.-K. Plattner, M. Tignor, S.K. Allen, J. Boschung, A. Nauels, Y. Xia,
22 V. Bex, and P.M. Midgley, Eds. Cambridge University Press, Cambridge, United Kingdom
23 and New York, NY, USA, 317–382. <http://dx.doi.org/10.1017/CBO9781107415324.012>
24 www.climatechange2013.org
- 25 Velicogna, I., 2009: Increasing rates of ice mass loss from the Greenland and Antarctic ice sheets
26 revealed by GRACE. *Geophysical Research Letters*, **36**, L19503.
27 <http://dx.doi.org/10.1029/2009GL040222>
- 28 Vihma, T., 2014: Effects of Arctic Sea Ice Decline on Weather and Climate: A Review. *Surveys*
29 *in Geophysics*, **35**, 1175-1214. <http://dx.doi.org/10.1007/s10712-014-9284-0>
- 30 Wendler, G., B. Moore, and K. Galloway, 2014: Strong Temperature Increase and Shrinking Sea
31 Ice in Arctic Alaska. *The Open Atmospheric Science Journal*, **8**, 7-15.
32 <http://dx.doi.org/10.2174/1874282301408010007>
33 <http://benthamopen.com/contents/pdf/TOASCJ/TOASCJ-8-7.pdf>

- Wettstein, J.J. and C. Deser, 2014: Internal Variability in Projections of Twenty-First-Century Arctic Sea Ice Loss: Role of the Large-Scale Atmospheric Circulation. *Journal of Climate*, **27**, 527-550. <http://dx.doi.org/10.1175/JCLI-D-12-00839.1>
- WGMS, 2016: Fluctuations of Glaciers Database. World Glacier Monitoring Service, Zurich, Switzerland.
- Wolken, G., M. Sharp, L.M. Andreassen, A. Arendt, D. Burgess, J.G. Cogley, L. Copland, J. Kohler, S. O'Neel, M. Pelto, L. Thomson, and B. Wouters, 2016: [The Arctic] Glaciers and ice caps outside Greenland [in "State of the Climate in 2015"]. *Bulletin of the American Meteorological Society*, **97**, S142-S145.
<http://dx.doi.org/10.1175/2016BAMSStateoftheClimate.1>
- Wyser, K., C.G. Jones, P. Du, E. Girard, U. Willén, J. Cassano, J.H. Christensen, J.A. Curry, K. Dethloff, J.-E. Haugen, D. Jacob, M. Køltzow, R. Laprise, A. Lynch, S. Pfeifer, A. Rinke, M. Serreze, M.J. Shaw, M. Tjernström, and M. Zagar, 2008: An evaluation of Arctic cloud and radiation processes during the SHEBA year: simulation results from eight Arctic regional climate models. *Climate Dynamics*, **30**, 203-223. <http://dx.doi.org/10.1007/s00382-007-0286-1>
- Yang, Q., T.H. Dixon, P.G. Myers, J. Bonin, D. Chambers, and M.R. van den Broeke, 2016: Recent increases in Arctic freshwater flux affects Labrador Sea convection and Atlantic overturning circulation. *Nature Communications*, **7**, 10525.
<http://dx.doi.org/10.1038/ncomms10525>
- Young, A.M., P.E. Higuera, P.A. Duffy, and F.S. Hu, 2016: Climatic thresholds shape northern high-latitude fire regimes and imply vulnerability to future climate change. *Ecography*, n/a-n/a. <http://dx.doi.org/10.1111/ecog.02205>
- Zemp, M., H. Frey, I. Gärtner-Roer, S.U. Nussbaumer, M. Hoelzle, F. Paul, W. Haeberli, F. Denzinger, A.P. Ahlstrøm, B. Anderson, S. Bajracharya, C. Baroni, L.N. Braun, B.E. Cáceres, G. Casassa, G. Cobos, L.R. Dávila, H. Delgado Granados, M.N. Demuth, L. Espizua, A. Fischer, K. Fujita, B. Gadek, A. Ghazanfar, J.O. Hagen, P. Holmlund, N. Karimi, Z. Li, M. Pelto, P. Pitte, V.V. Popovnin, C.A. Portocarrero, R. Prinz, C.V. Sangewar, I. Severskiy, O. Sigurðsson, A. Soruco, R. Usabaliev, and C. Vincent, 2015: Historically unprecedented global glacier decline in the early 21st century. *Journal of Glaciology*, **61**, 745-762. <http://dx.doi.org/10.3189/2015JoG15J017>
- Zhang, R. and T.R. Knutson, 2013: The role of global climate change in the extreme low summer Arctic sea ice extent in 2012 [in "Explaining Extremes of 2012 from a Climate Perspective"]. *Bulletin of the American Meteorological Society*, **94**, S23-S26.
<http://dx.doi.org/10.1175/BAMS-D-13-00085.1>

- 1 Zona, D., B. Gioli, R. Commane, J. Lindaas, S.C. Wofsy, C.E. Miller, S.J. Dinardo, S. Dengel,
- 2 C. Sweeney, A. Karion, R.Y.-W. Chang, J.M. Henderson, P.C. Murphy, J.P. Goodrich, V.
- 3 Moreaux, A. Liljedahl, J.D. Watts, J.S. Kimball, D.A. Lipson, and W.C. Oechel, 2016: Cold
- 4 season emissions dominate the Arctic tundra methane budget. *Proceedings of the National*
- 5 *Academy of Sciences*, **113**, 40-45. <http://dx.doi.org/10.1073/pnas.1516017113>

DRAFT

12. Sea Level Rise

KEY FINDINGS

1. Global mean sea level (GMSL) has risen by about 8–9 inches (about 20–23 cm) since 1880, with about 3 of those inches (about 7 cm) occurring since 1990 (*very high confidence*). Human-caused climate change has made a substantial contribution to GMSL rise since 1900 (*high confidence*), contributing to a rate of rise faster than during any comparable period since at least 800 BCE (*medium confidence*).
2. Relative to the year 2000, GMSL is *very likely* to rise by 0.3–0.6 feet (9–18 cm) by 2030, 0.5–1.2 feet (15–38 cm) by 2050, and 1 to 4 feet (30–130 cm) by 2100 (*very high confidence in lower bounds; medium confidence in upper bounds for 2030 and 2050; low confidence in upper bounds for 2100*). Emissions pathways have little effect on projected GMSL rise in the first half of the century, but significantly affect projections for the second half of the century (*high confidence*). Emerging science regarding ice sheet stability suggests that, for high emissions, a GMSL rise exceeding 8 feet (2.4 m) by 2100 cannot be ruled out.
3. Relative sea level (RSL) rise in this century will vary along U.S. coastlines due, in part, to: changes in Earth’s gravitational field and rotation from melting of land ice, changes in ocean circulation, and vertical land motion (*very high confidence*). For almost all future GMSL rise scenarios, RSL rise is *likely* to be greater than the global average in the U.S. Northeast and the western Gulf of Mexico. In intermediate and low GMSL rise scenarios, it is *likely* to be less than the global average in much of the Pacific Northwest and Alaska. For high GMSL rise scenarios, it is *likely* to be higher than the global average along all U.S. coastlines outside Alaska (*high confidence*).
4. The annual occurrences of daily tidal flooding—exceeding local thresholds for minor impacts to infrastructure—have increased 5- to 10-fold since the 1960s in several U.S. coastal cities (*very high confidence*). Rates of increase, which are accelerating in over 25 Atlantic and Gulf Coast cities, are fastest where elevation thresholds are lower, local RSL rise is higher, or extreme variability is less (*very high confidence*). Tidal flooding will continue increasing in depth and frequency in similar manners this century (*very high confidence*).
5. The projected increase in the intensity of hurricanes in the North Atlantic could increase the probability of extreme coastal flooding along the U.S. Atlantic and Gulf Coasts beyond what would be projected based solely on RSL rise. However, there is *low confidence* in the magnitude of the increase in intensity and the associated flood risk amplification, and it could be offset or amplified by other factors, such as changes in hurricane frequency or tracks.

12.1 Introduction

Sea level rise is closely linked to increasing global temperatures. Thus, even as uncertainties remain about just how much sea level may rise this century, it is *virtually certain* that sea level rise this century and beyond will pose a growing challenge to coastal communities, infrastructure, and ecosystems, both through more frequent and extreme coastal flooding and more subtle coastal geomorphological changes associated with increases in mean sea level. Assessment of change requires consideration of physical causes, historical evidence, and projections. Vulnerability and risk-based perspectives point to the need for emphasis on how changing sea levels alter the coastal zone and interact with coastal flood risk at local scales.

12.2 Physical Factors Contributing to Sea Level Rise

Sea level change is driven by a variety of mechanisms operating at different spatial and temporal scales. Global mean sea level (GMSL) rise is primarily driven by two factors: 1) increased volume from thermal expansion of the ocean as it warms, and 2) increased mass from melt additions of ice locked in mountain glaciers and the Antarctic and Greenland ice sheets. Satellite (altimeter and GRACE) and in situ (Argo) measurements show that, since 2005, about one third of GMSL rise has been from steric changes (thermal expansion) and about two-thirds from the addition of mass to the ocean, primarily from melting land-based ice (Llovel et al. 2014; Leuliette 2015; Merrifield et al. 2015; Chambers et al. 2016). The overall amount (mass) of ocean water, and thus sea level, is also affected to a lesser extent by changes in global land water storage associated with dams and reservoirs, groundwater extraction, and global precipitation anomalies (Reager et al. 2016; Rietbroek et al. 2016; Wada et al. 2016), such as associated with the El Niño–Southern Oscillation (ENSO).

Sea level and its changes are not uniform globally, for several reasons. First, atmosphere–ocean dynamics—driven by ocean circulation, winds, and other factors—are associated with differences in the height of the sea surface, as are differences in density arising from the distribution of heat and salinity in the ocean. Changes in any of these factors will affect sea-surface height. For example, a weakening of the Gulf Stream may have contributed to enhanced sea level rise in the ocean environment extending to the northeastern U.S. coast, a trend that many models project will continue into the future (Yin and Goddard 2013).

Second, the location of land ice melting imparts distinct regional “static-equilibrium fingerprints” on sea level, based on gravitational, rotational, and crustal deformation effects (Mitrovica et al. 2011) (Figure 12.1a–d). For example, sea level falls near a melting ice sheet because of the resulting changes in the distribution of mass on the planet and thus in the planet’s gravitational field.

Third, the Earth’s mantle is still moving in response to the loss of the great North American (Laurentide) and European ice sheets of the Last Glacial Maximum; the associated changes in the height of the land, the shape of the ocean basin, and the Earth’s gravitational field give rise to

glacial-isostatic adjustment (Figure 12.1e). For example, underneath the cores of the great ice sheets of the Last Glacial Maximum, such as in Hudson Bay and in Scandinavia, post-glacial rebound of the land is causing relative sea levels (RSL) to fall. Slightly farther away from the cores, such as along most of the east coast of the United States, subsidence of the bulge that flanked the ice sheet is causing RSL to rise. Finally, a variety of other factors can cause local vertical land movement; these include natural sediment compaction, compaction caused by local extraction of groundwater and fossil fuels, and tectonics (Zervas et al. 2013; Kopp et al. 2014, Wöppelmann and Marcos 2016) (Figure 12.1f).

Compared to many climate variables, the trend signal for sea level change tends to be large relative to natural variability. However, at interannual timescales, changes in ocean dynamics, density, and wind can cause substantial sea level variability in some regions. For example, there has been a multidecadal suppression of sea level rise off the Pacific coast (Bromirski et al. 2011) and large year-to-year variations in sea level along the Northeast U.S. coast (Goddard et al. 2015). Local land height changes have also varied dramatically on decadal timescales in some locations, such as along the western Gulf Coast, where rates of subsurface extraction of fossil fuels and groundwater have varied over time (Galloway et al. 1999).

[INSERT FIGURE 12.1 HERE:]

Figure 12.1: (a–d) Static-equilibrium fingerprints of the RSL effect of land ice melt, in units of feet of RSL change per foot of GMSL change, for mass loss from (a) Greenland, (b) West Antarctica, (c) East Antarctica, and (d) the median projected combination of melting glaciers, after Kopp et al. (2014, 2015). (e) Model projections of the rate of RSL rise due to glacial-isostatic adjustment (units of feet.century), after Kopp et al. (2015). (f) Tide gauge-based estimates of the non-climatic, long-term contribution to RSL rise, including the effects of glacial isostatic adjustment, tectonics, and sediment compaction (Kopp et al. 2014) [Figure source: (a)–(d) Kopp et al. (2015), (e) adapted from Kopp et al. (2015); (f) adapted from Sweet et al. (In Review)]

12.3 Paleo Sea Level

Geological records of temperature and sea level indicate that, during past warm periods, GMSL was higher than it is today (Dutton et al. 2015). During the Last Interglacial stage, about 125,000 years ago, global mean temperature was about 1°C (1.8°F) above the preindustrial level (that is, comparable to current temperatures), and polar temperatures were comparable to those projected for 1°C –2°C (1.8°F –3.6°F) of global mean warming above the preindustrial level. At this time, GMSL was about 6–9 meters (about 20–30 feet) higher than today (Dutton and Lambeck 2012; Kopp et al. 2009). This geological benchmark may indicate the probable long-term response of GMSL to the minimum magnitude of temperature change projected for the current century.

Geologists can reconstruct rates of GMSL change over the last few millennia using proxies such as the heights of fossil coral reefs and the different populations of salinity-sensitive microfossils

within salt marsh sediments (Shennan et al. 2015). Since the disappearance of the last remnants of the North American (Laurentide) Ice Sheet about 7,000 years ago (Carlson et al. 2008), GMSL has been relatively stable, with total GMSL rise since 7,000 years ago estimated at about 4 meters (about 13 feet), most of which occurred between 7,000 and 4,000 years ago (Lambeck et al. 2014). The Third National Climate Assessment (NCA3) noted, based on a geological data set from North Carolina (Kemp et al. 2011), that the 20th century GMSL rise was much faster than at any time over the past 2,000 years. Since NCA3, high-resolution sea level reconstructions have been developed for multiple locations, and a new global analysis of such reconstructions strengthens this finding (Kopp et al. 2016). Over the last 2,000 years, prior to the industrial era, GMSL exhibited small fluctuations of about ± 8 cm (3 inches), with a significant decline of about 8 cm (3 inches) between the years 1000 and 1400 CE coinciding with about 0.2°C (0.4°F) of global mean cooling (Kopp et al. 2016). The rate of rise in the last century, about 14 cm/century (5.5 inches/century), was faster than during any century since at least 800 BCE (Kopp et al. 2016; Figure 12.2a).

[INSERT FIGURE 12.2 HERE:]

Figure 12.2: (a) GMSL rise from –500 to 1900 CE, from Kopp et al. (2016)’s geological and tide gauge-based reconstruction [blue], from 1900 to 2010 from Hay et al. (2015)’s tide gauge-based reconstruction [black], and from 1992 to 2015 from the satellite-based reconstruction updated from Nerem et al. (2010) [magenta]; (b) GMSL rise from 1800 to 2100, based on (a) from 1800 to 2015, the six Interagency (Sweet et al., In Review) GMSL scenarios (black, blue, cyan, green, orange and red curves), the *very likely* ranges in 2100 for different RCPs from this chapter (colored boxes), and lines augmenting the *very likely* ranges by the difference between the median Antarctic contribution of Kopp et al. 2014 and the various median Antarctic projections of DeConto and Pollard (2016). (c) Rates of change from 1993 to 2014 in sea surface height from satellite altimetry data; from Kopp et al. (2015) using data updated from Church and White (2011). [Figure source: (a) adapted from Nerem et al. (2010), Kopp et al. (2016) and Hay et al. (2015), (b) adapted from Sweet et al. (In Review), (c) adapted from Kopp et al. (2015)]

12.4 Recent Past Trends (20th and 21st Centuries)

12.4.1 Global Tide Gauge Network and Satellite Observations

A global tide gauge network provides the century-long observations of local RSL, whereas satellite altimetry provides broader coverage of sea surface heights outside the polar regions starting in 1993. GMSL can be estimated through statistical analyses of either data set. GMSL trends over the 1901–1990 period vary slightly (Hay et al. 2015: 1.2 ± 0.2 mm/year [0.5 inches/decade]; Church and White 2011: 1.5 ± 0.2 mm/year [0.6 inches/decade]) with differences amounting to about 1 inch over 90 years. Both data sets indicate similar rates since 1880. Thus, these results indicate about 13–16 cm (5–6 inches) of GMSL rise from 1880 to 1990.

Tide gauge analyses indicate that GMSL rose at a considerably faster rate of about 3 mm/year (1.2 inches/decade) since 1993 (Hay et al. 2015; Church and White 2011), a result supported by satellite data indicating a trend of 3.4 ± 0.4 mm/year (1.3 inches/decade) over 1993–2015 (update to Nerem et al. 2010) (Figure 12.2a). These results indicate an additional GMSL rise of about 7 cm (3 inches) rise since 1990. Thus total GMSL rise since 1880 is about 20–23 cm (8–9 inches).

Comparison of results from a variety of approaches supports the conclusion that a substantial fraction of GMSL rise since 1900 is attributable to human-caused climate change (Kopp et al. 2016; Slangen et al. 2016; Jevrejeva et al. 2009; Dangendorf et al. 2015; Becker et al. 2014; Marcos and Amores, 2014; Slangen et al. 2014; Marzeion et al. 2014; Marcos et al. 2016).

After accounting for background rates inherent in RSL rise rates due to long-term factors like glacial isostatic adjustment, four notable patterns of regional sea surface height variability exist (Figure 12.2c): a slower-than-global increase off of the U.S. Pacific Coast between about 1980 and 2011, with a faster-than-global rise subsequently; a faster-than-global increase in the western tropical Pacific in the 1990s and 2000s, with a slower rise in this decade; a faster-than-global increase in sea level rise in the U.S. Northeast since the 1970s; and a slower-than-global increase in the U.S. Southeast since the 1970s.

The slowdown in sea level rise along the U.S. Pacific Coast and acceleration in the western tropical Pacific was associated with changes in average winds linked to the Pacific Decadal Oscillation (PDO) (Bromirski et al. 2011; Zhang and Church 2012; Merrifield 2011), and appears to have reversed since about 2012 (Hamlington et al. 2016). The acceleration in the U.S. Northeast and slowdown in the U.S. Southeast appear to be tied to changes in the Gulf Stream (Yin and Goddard 2013; Ezer 2013; Kopp 2013; Kopp et al. 2015b), although whether these changes represent natural variability or a long-term trend remains uncertain (Rahmstorf et al. 2015).

12.4.2 Ocean Heat Uptake

About 93% of the global warming due to anthropogenic greenhouse emissions heating since the 1970s has occurred in the ocean (Rhein et al. 2013), leading to temperature increases both at the surface and at depth. This ocean warming acts as a buffer to climate change, slowing down the rate of surface warming (e.g., Nieves et al. 2015), while also leading to ocean thermal expansion and thus contributing to sea level rise.

Between 1970 and 2012, the upper ocean (0–700 meters; 0–2300 feet) warmed by about 0.2°C (0.4°F), corresponding to a heat storage of 0.27 ± 0.04 W/m² (Watts per square meter) (Abraham et al. 2013). For shorter and more recent periods, ocean heat uptake varies: 0.30 ± 0.04 W/m² during 1980–2012 and 0.25 – 0.46 W/m² during 1993–2012. Decadal variability in ocean heat uptake is mostly attributed to volcanic eruptions, which indirectly leads to cooling (for example,

1991 Pinatubo eruption, Fasulo et al. 2016) and to ENSO phases (with El Niños warming and La Niñas cooling) (Abraham et al. 2013).

Previous estimates of the ocean uptake were confined to the upper ocean and had sparse spatial and temporal coverage. Recent studies, based on data from the Argo network of floats that extend to depths of 2000 meters (6600 feet), revise earlier estimates upwards to about 0.4–0.6 W/m² over 2006–2013, with approximately half occurring in the upper 500 m (1600 feet) and half below (Roemmich et al. 2015). This uptake explains about a third of the GMSL rise (Llovel et al. 2014, Leuliette, 2015; Chambers et al. 2016) and corresponds to a steric height increase of about 1.0 ± 0.5 mm/year (0.2 inches/decade) for the period 2005–2013. The role of the deep ocean (below 2,000 meters [3300 feet]) in ocean heat uptake remains uncertain, both in the magnitude but also the sign of the uptake (Purkey and Johnson 2010; Llovel et al. 2014). On interannual scales, ENSO dominates the signal of ocean heat uptake, and the North Atlantic is the most vigorous region for uptake, whereas on decadal timescales the Southern Ocean accounts for about 67%–80% of the uptake (Roemmich et al. 2015; Abraham et al. 2013).

12.4.3 Ice Sheet Gravity and Altimetry and Visual Observations

Since NCA3, Antarctica and Greenland have continued to lose ice mass, with stronger evidence accumulating that mass loss is accelerating.

Studies using repeat gravimetry (GRACE satellites), repeat altimetry, GPS monitoring, and input-output calculations generally agree on accelerating mass loss in Antarctica (Shepherd et al. 2012; Scambos and Shuman 2016; Seo et al. 2015; Martín-Español et al. 2016). Together, these indicate mass loss of roughly 100 Gt/year (gigatonnes/year) over the last decade (a contribution to GMSL of about 0.3 mm/year [0.1 inches/decade]). Positive accumulation-rate anomalies in East Antarctica, especially in Dronning Maud Land, have contributed to the trend of slight growth there (e.g., Seo et al. 2015; Martín-Español et al. 2016), but this is more than offset by mass loss elsewhere, especially in West Antarctica along the coast facing the Amundsen Sea (Sutterley et al. 2014; Mouginot et al. 2014), Totten Glacier in East Antarctica (Khazendar et al. 2013; Li et al. 2015), and along the Antarctic Peninsula (Seo et al. 2015; Martín-Español et al. 2016). Floating ice shelves around Antarctica are losing mass at an accelerating rate (Paolo et al. 2015). Mass loss from floating ice shelves does not directly affect GMSL, but does allow faster flow of ice from the ice sheet into the ocean.

Estimates of mass loss in Greenland based on mass balance from input-output, repeat gravimetry, repeat altimetry, and aerial imagery as discussed in Chapter 11 reveal a recent acceleration (Khan et al. 2014). Mass loss averaged approximately 75 Gt/year (about 0.2 mm/year [0.08 inches/decade] GMSL rise) from 1900 to 1983, continuing at a similar rate of approximately 74 Gt/year through 2003 before accelerating to 186 Gt/year (about 0.5 mm/year [0.2 inches/decade] GMSL rise) from 2003 to 2010 (Kjeldsen et al. 2015). Shorter-term interannual variability exists (see Chapter 11), such as during the exceptional melt year from

April 2012 to April 2013, which produced mass loss of approximately 560 Gt (1.6 mm/year [0.6 inches/decade]) (Tedesco et al. 2013). Accelerating mass loss over the record is clear and has reversed a long-term trend of slow thickening linked to continuing evolution of the ice sheet from the end of the last ice age (MacGregor et al. 2016).

12.5 Projected Sea Level Rise

12.5.1 Scenarios of Global Mean Sea Level Rise

No single physical model is capable of accurately representing all of the major processes contributing to GMSL and regional/local RSL rise. Accordingly, the U.S. Interagency Sea Level Rise Task force (Sweet et al. In Review and henceforth referred to as “Interagency”) has revised the GMSL rise scenarios for the United States, and now provides six scenarios that can be used for assessment and risk-framing purposes (Figure 12.2b; Table 12.1). The low scenario of 30 cm (1 foot) GMSL rise by 2100 is consistent with a continuation of the recent approximately 3 mm/year (1.2 inches/decade) rate of rise through to 2100, while the five other scenarios span a range of GMSL rise between 50 and 250 cm (1.6 and 8.2 feet) in 2100. The highest scenario of 250 cm is consistent with several literature estimates of the maximum physically plausible level of 21st century sea level rise (e.g., Pfeffer et al. 2008; Srivier et al. 2012; Miller et al. 2013; Kopp et al. 2014). The Interagency GMSL scenario interpretations are shown in Table 12.2.

The Interagency scenario approach is similar to local RSL rise scenarios used for all coastal U.S. Department of Defense installations worldwide (Hall et al. 2016). The Interagency approach starts with a probabilistic projection framework to generate time series and regional projections consistent with each GMSL rise scenario for 2100 (Kopp et al. 2014). That framework combines probabilistic estimates of contributions to GMSL and regional RSL rise from ocean processes, cryospheric processes, geological processes, and anthropogenic land-water storage. Pooling the Kopp et al. (2014) projections across RCP2.6, 4.5, and 8.5, the probabilistic projections are filtered to identify pathways consistent with each of these 2100 levels with median (and 17th and 83rd percentiles) picked from each of the filtered subsets.

Table 12.1. The Interagency GMSL rise scenarios, cm (feet) relative to 2000. All values are 19-year averages of GMSL centered at the identified year. To convert from a 1991–2009 tidal datum to the 1983–2001 tidal datum, add 2.4 cm (0.9 inches).

Scenario	2020	2030	2050	2100
Low	6 (0.2)	9 (0.3)	16 (0.5)	30 (1.0)
Intermediate-Low	8 (0.3)	13 (0.4)	24 (0.8)	50 (1.6)

Intermediate	10 (0.3)	16 (0.5)	34 (1.1)	100 (3.3)
Intermediate-High	10 (0.3)	19 (0.6)	44 (1.4)	150 (4.9)
High	11 (0.4)	21 (0.7)	54 (1.8)	200 (6.6)
Extreme	11 (0.4)	24 (0.8)	63 (2.1)	250 (8.2)

1

2 Table 12.2. Interpretations of the Interagency GMSL rise scenarios

Scenario	Interpretation
Low	Continuing current rate of GMSL rise, as calculated since 1993 Low end of <i>very likely</i> range under RCP2.6
Intermediate-Low	Modest increase in rate Middle of <i>likely</i> range under RCP2.6 Low end of <i>likely</i> range under RCP4.5 Low end of <i>very likely</i> range under RCP8.5
Intermediate	High end of <i>very likely</i> range under RCP4.5 High end of <i>likely</i> range under RCP8.5 Middle of <i>likely</i> range under RCP4.5 when accounting for possible ice cliff instabilities
Intermediate-High	Slightly above high end of <i>very likely</i> range under RCP8.5 Middle of <i>likely</i> range under RCP8.5 when accounting for possible ice cliff instabilities
High	High end of <i>very likely</i> range under RCP8.5 when accounting for possible ice cliff instabilities
Extreme	Consistent with estimates of physically possible “worst case”

12.5.2 Probabilities of Different Sea Level Rise Scenarios

Several studies have estimated the probabilities of different amounts of GMSL rise under different emissions pathways (e.g., Church et al. 2013; Kopp et al. 2014; Slangen et al. 2014; Grinsted et al. 2015; Kopp et al. 2016; Mengel et al. 2016) using a variety of methods, including both statistical and physical models. Most of these studies are in general agreement that GMSL rise by 2100 is *very likely* to be between about 25–80 cm (0.8–2.6 feet) under RCP2.6, 35–95 cm (1.1–3.1 feet) under RCP4.5, and 50–130 cm (1.6–4.3 feet) under RCP8.5. The probability of exceeding the amount of GMSL in 2100 under the Interagency scenarios is shown in Table 12.3.

However, emerging science suggests that these projections may understate the probability of faster-than-expected ice sheet melt, particularly for high-end warming scenarios. While these probability estimates are consistent with the assumption that the relationship between global temperature and GMSL in the coming century will be similar to that observed over the last two millennia (Rahmstorf 2007; Kopp et al. 2016), emerging positive feedbacks (self-amplifying cycles) in the Antarctic Ice Sheet especially (Rignot et al. 2014; Joughin et al. 2014) may invalidate that assumption. Physical feedbacks that until recently were not incorporated into ice sheet models (Pollard et al. 2015) could add about 60–110 cm (2.0–3.6 feet) to central estimates of current-century sea level rise under RCP8.5, 20–50 cm (0.7–1.6 feet) to central estimates of sea level rise under RCP4.5, and 0–10 cm (0–0.3 feet) to central estimates of sea level rise under RCP2.6 (DeConto and Pollard 2016). Examples of these interrelated processes include marine ice sheet instability, ice cliff instability, and ice shelf hydrofracturing. Processes underway in Greenland may also be leading to accelerating high-end melt risk. Much of the research has focused on changes in surface albedo driven by the melt-associated unmasking and concentration of impurities in snow and ice (Tedesco et al. 2016). However, ice dynamics at the bottom of the ice sheet may be important as well, through interactions with surface runoff or a warming ocean. As an example of the latter, Jakobshavn Isbræ, Kangerdlugssuaq Glacier, and the Northeast Greenland ice stream may be vulnerable to marine ice sheet instability (Khan et al. 2014).

Table 12.3. Probability of exceeding the Interagency GMSL scenarios in 2100 per Kopp et al. (2014). New evidence regarding the Antarctic ice sheet, if sustained, may significantly increase the probability of the intermediate-high, high and extreme scenarios, particularly for RCP8.5, but these results have not yet been incorporated into a probabilistic analysis.

Scenario	RCP2.6	RCP4.5	RCP8.5
Low	94%	98%	100%
Intermediate-Low	49%	73%	96%

Intermediate	2%	3%	17%
Intermediate-High	0.4%	0.5%	1.3%
High	0.1%	0.1%	0.3%
Extreme	0.05%	0.05%	0.1%

1

2 **12.5.3 Sea Level Rise after 2100**

3 GMSL rise will not stop in 2100, and so it is useful to consider extensions of GMSL rise
4 scenarios beyond this point (e.g., Kopp et al. 2014). By 2200, the 0.3–2.5 meters (1.0–8.2 feet)
5 range spanned by the six Interagency GMSL scenarios increases to 0.3–9.5 meters (1.0–31 feet)
6 as shown in Table 12.4. Excluding the possible effects of still-emerging science regarding ice
7 cliffs and ice shelves, it is very likely that GMSL by 2200 will rise by 1.0–3.7 meters (3.3–12
8 feet) under RCP8.5, 0.4–2.7 meters (1.3–8.9 feet) under RCP4.5, and 0.3–2.4 meters (1.0–7.9
9 feet) under RCP2.6 (Kopp et al. 2014).

10 Under most projections, GMSL rise will also not stop in 2200. The concept of a “sea level rise
11 commitment” refers to the long-term projected sea level rise were the planet’s temperature to be
12 stabilized at a given level. The paleo sea level record suggests that even 2°C (3.6°F) of global
13 average warming above the preindustrial temperature may represent a commitment to several
14 meters of rise, with one modeling study suggesting a 2,000-year commitment of 2.3 m/°C (4.2
15 feet/°F) (Levermann et al. 2013). This relationship suggests that emissions through to 2100
16 would lock in a likely 2,000-year GMSL rise commitment of about 0.7–4.2 meters (2.3–13.8
17 feet) under RCP2.6, about 1.7–5.6 meters (5.6–18.4 feet) under RCP4.5, and about 4.3–9.9
18 meters (14.1–32.5 feet) under RCP8.5 (Strauss et al. 2015). However, as with the 21st century
19 projections, emerging science regarding the sensitivity of the Antarctic Ice Sheet may increase
20 the estimated sea level rise over the next millennium, especially for high-emissions pathways
21 (DeConto and Pollard 2016). Large-scale climate geoengineering might reduce these
22 commitments (Irvine et al. 2009; Applegate and Keller 2015), but may not be able to avoid lock-
23 in of significant change (Lenton 2011; Barrett et al. 2014; Markusson et al. 2014; Sillmann et al.
24 2015).

25

1 **Table 12.4.** Post-2100 extensions of the Interagency GMSL rise scenarios in cm (feet)

Scenario	2100	2120	2150	2200
Low	30 (1.0)	34 (1.1)	37 (1.2)	39 (1.3)
Intermediate-Low	50 (1.6)	60 (2.0)	73 (2.4)	95 (3.1)
Intermediate	100 (3.3)	129 (4.2)	182 (6.0)	283 (9.3)
Intermediate-High	150 (4.9)	203 (6.7)	305 (10.0)	511 (16.8)
High	200 (6.6)	282 (9.3)	434 (14.2)	748 (24.5)
Extreme	250 (8.2)	357 (11.7)	554 (18.2)	972 (31.9)

2

3 **12.5.4 Regional Projections of Sea Level Change**

4 Because the different factors contributing to sea level change give rise to different spatial
 5 patterns, projecting future RSL change at specific locations requires not just an estimate of
 6 GMSL change but estimates of the different processes contributing to GMSL change—each of
 7 which has a different associated spatial pattern—as well as of the processes contributing
 8 exclusively to regional or local change. Based on the process-level projections of the Interagency
 9 scenarios, several key regional patterns are apparent in future U.S. RSL rise as shown for the 1-
 10 meter (3.3 feet) Interagency scenario in 2100 (Figure 12.1 a-f, 12.3a.).

11 (1) RSL rise due to Antarctic Ice Sheet melt is greater than GMSL rise along all U.S.
 12 coastlines due to static-equilibrium effects.

13 (2) RSL rise due to Greenland Ice Sheet melt is less than GMSL rise in the continental U.S.
 14 due to static-equilibrium effects. This effect is especially strong in the Northeast.

15 (3) RSL rise is additionally augmented in the Northeast by the effects of glacial isostatic
 16 adjustment. The Northeast is also exposed to rise due to reductions in the Atlantic
 17 meridional overturning circulation.

18 (4) The western Gulf of Mexico and parts of the U.S. Atlantic Coast south of New York are
 19 currently experiencing significant RSL rise caused by the withdrawal of groundwater

(along the Atlantic Coast) and of both fossil fuels and groundwater (along the Gulf Coast). Continuation of these practices will further amplify RSL rise.

(5) The proximity of the Alaskan glaciers to Alaska and the Pacific Northwest reduces regional RSL rise, due to both the ongoing glacial isostatic adjustment to past glacier shrinkage and to the static-equilibrium effects of projected future losses

(6) Because they are far from all glaciers and ice sheets, RSL rise in Hawai‘i and other Pacific islands due to any source of melting land ice is amplified by the static-equilibrium effects.

[INSERT FIGURE 12.3 HERE:]

Figure 12.3: (a) RSL rise (feet) in 2100 under the median-local Interagency Intermediate (1-meter) Scenario, (b) tidal floods (days per year) exceeding NOAA thresholds for minor impacts at NOAA tide gauges through 2015, from Sweet and Marra (2016), (c) water level heights associated with a local 5-year recurrence probability, after Sweet et al. 2014, and (d) future decade the 5-year becomes a 0.2-year event under the Interagency Intermediate scenario, after Sweet and Park (2014); black dots imply that a 5-year to 0.2-year frequency change does not unfold by 2200 under the Intermediate scenario. [Figure source: (a), (c), and (d) Sweet et al. (In Review), (b) adapted from Sweet and Marra (2016)]

12.6 Extreme Water Levels

12.6.1 Observations

Coastal flooding during extreme high-water events has become deeper due to local RSL rise and more frequent from a fixed-elevation perspective (Menendez and Woodworth 2010; Kemp and Horton 2013; Sweet et al. 2013; Hall et al. 2016). Trends in annual frequencies surpassing local emergency preparedness thresholds for minor tidal flooding (i.e., “nuisance” levels of about 30–60 cm [1–2 feet]) that flood infrastructure and trigger coastal flood “advisories” by NOAA’s National Weather Service (NWS) have increased 5- to 10-fold or more since the 1960s along the U.S. coastline (Sweet et al. 2014), as shown in Figure 12.3b. Locations experiencing such trend changes (based upon fits of flood days per year of Sweet and Park 2014) include Atlantic City and Sandy Hook, NJ; Philadelphia, PA; Baltimore and Annapolis, MD; Norfolk, VA; Wilmington, NC; Charleston, SC; Savannah, GA; Mayport and Key West, FL; Port Isabel, TX, La Jolla, CA and Honolulu, HI. In fact, over the last several decades, minor tidal flood rates have been accelerating within several (> 25) East and Gulf Coast cities with established elevation thresholds for minor (nuisance) flood impacts, fastest where elevation thresholds are lower, local RSL rise is higher, and extreme variability less (Ezer and Atkinson 2014; Sweet et al. 2014; Sweet and Park 2014).

Trends in extreme water levels (for example, monthly maxima) in excess of mean sea levels (for example, monthly means) exist, but are not commonplace (Menendez and Woodworth 2010;

Talke et al. 2014; Wahl and Chambers 2015; Reed et al. 2015; Marcos et al. 2016). More common are regional time dependencies in high-water probabilities, which can co-vary on an interannual basis with climatic and other patterns (Menendez and Woodworth 2010; Grinstead et al. 2013; Marcos et al. 2015; Woodworth and Menendez 2015; Wahl and Chambers 2016; Mawdsley and Haigh 2016; Sweet et al. 2016). These patterns are often associated with anomalous oceanic and atmospheric conditions (Feser et al. 2015; Colle et al. 2015). For instance, the probability of experiencing minor tidal flooding is compounded during El Niño along portions of the West and mid-Atlantic Coasts (Sweet and Park 2014) from a combination of higher sea levels and enhanced synoptic forcing and storm surge frequency (Sweet and Zervas 2011; Thompson et al. 2013; Hamlington et al. 2015; Woodworth and Menendez 2015).

12.6.2 Influence of Projected Sea Level Rise on Coastal Flood Frequencies

The frequency and depth of high-water extreme events experienced locally in the future will continue to increase as local RSL rises (Tebaldi et al. 2012; Kopp et al. 2014; Horton et al. 2011; Woodruff et al. 2013; Buchanan et al. 2016; Hall et al. 2016). Under the probabilistic RSL projections of Kopp et al. 2014, at tide-gauge locations along the contiguous U.S. coastline, a median 8-fold increase (range of 1.1- to 430-fold increase) is expected by 2050 in the annual number of floods exceeding the elevation of the current 100-year flood event (measured with respect to a 1991–2009 baseline sea level) (Buchanan et al. 2016). Under the same forcing, the frequency of minor tidal flooding (with recurrence intervals generally <1 year [Sweet et al. 2014]) will increase even more so in the coming decades (Sweet and Park 2014; Moftakhari et al. 2015). Probabilities of both minor and major high-water events are expected to increase more rapidly at locations with less overall extreme variability and/or greater amounts of local RSL rise (Hunter 2012; Tebaldi et al. 2012; Kopp et al. 2014; Sweet and Park 2014). For example, Figure 12.3d shows the decade in which the frequency of moderate-level flooding—defined as a water level locally with a 5-year recurrence interval (Figure 12.3c) and that typically triggers an issuance of a coastal flood “warning” by NOAA’s NWS (Sweet et al. In Review)—will increase 25-fold in response to local RSL rise associated with the Interagency 1-meter (3.3 feet) scenario for 2100 (Figure 12.3a). Under the 1-meter scenario, many cities along the mid- and Southeast Atlantic, western Gulf, California, and the Island States and Territories may experience a 25-fold increase in moderate flooding over the next three decades.

12.6.3 Waves and Impacts

The combination of a storm surge at high tide with additional dynamical effects from waves (Stockton et al. 2006; Sweet et al. 2015) creates the most damaging coastal hydraulic conditions (Moritz et al. 2015). Simply with higher-than-normal sea levels, wave action increases the likelihood for extensive coastal erosion (Barnard et al. 2011; Theuerkauf et al. 2014; Serafin and Ruggiero 2014) and low-island overwash (Hoeke et al. 2013). Wave runoff is often the largest water level component during extreme events where storm surge is constrained by bathymetry (Tebaldi et al. 2012; Woodruff et al. 2013; Hall et al. 2016), as depicted in Figure 12.3c. On an

interannual basis, wave impacts are correlated across the Pacific Ocean with phases of ENSO (Stopa and Cheung 2014; Barnard et al. 2015). Over the last half century, there has been an increasing trend in wave height and power within the North Pacific Ocean (Bromirski et al. 2013; Erikson et al. 2015) that is modulated by the PDO (Aucan et al. 2012; Bromirski et al. 2013). Resultant increases in wave run-up have been more of a factor than RSL rise in terms of impacts along the U.S. Northwest Pacific Coast over the last several decades (Ruggiero 2013). In the Northwest Atlantic Ocean, no long-term trends in wave power have been observed over the last half century (Bromirski and Cayan 2015), though hurricane activity drives interannual variability (Bromirski and Kossin 2008). In terms of future conditions this century, increases in mean and maximum seasonal wave heights are projected within parts of the northeast Pacific, northwest Atlantic, and Gulf of Mexico (Graham et al. 2013; Wang et al. 2014; Erikson et al. 2015; Shope et al. 2016).

12.6.4 Sea Level Rise, Changing Storm Characteristics, and Their Interdependencies

Future probabilities of extreme coastal floods will depend upon the amount of local RSL rise, changes in coastal storm characteristics, and their interdependencies. For instance, there have been more storms producing concurrent locally extreme storm surge and rainfall (not captured in tide gauge data) along the U.S. East and Gulf Coasts over the last 65 years, with flooding further compounded by local RSL rise (Wahl et al. 2015). Hemispheric-scale extratropical cyclones may experience a northward shift this century, with some studies projecting an overall decrease in storm number (Colle et al. 2015 and references therein). The research is mixed about strong extratropical storms; studies find potential increases in frequency and intensity in some regions, like within the Northeast (Colle et al. 2013), whereas others project decreases in strong extratropical storms in some regions (e.g., Zappa et al. 2013). In terms of tropical cyclones, model projections for the North Atlantic mostly agree that intensities and precipitation rates will increase this century (see Chapter 9), although some model evidence suggests that track changes could dampen the effect in the U.S. Mid-Atlantic and Northeast (Hall and Yonekura 2013). Despite such uncertainties, the combination of sea level rise and tropical cyclone changes is projected to increase extreme coastal flood probabilities along U.S. coastlines (Grinsted et al. 2013; Lin et al. 2012; Little et al. 2015; Knutson et al. 2013, 2015; Lin et al. 2016). In addition, RSL increases are projected to cause a nonlinear increase in storm surge heights in shallow bathymetry environments (Smith et al. 2010; Atkinson et al. 2013; Bilskie et al. 2014; Passeri et al. 2015; Bilskie et al. 2016), and extend wave propagation and impacts landward (Smith et al. 2010; Atkinson et al. 2013).

12.6.5 Interactions between sea level rise and coastal impacts

While outside the scope of this chapter, it is important to note the myriad of other potential impacts associated with RSL rise, wave action, and increases in coastal flooding. These impacts include loss of life, damage to infrastructure and the built environment, salinization of groundwater, mobilization of pollutants, changing sediment budgets, coastal erosion, and

ecosystem changes such as marsh loss and threats to endangered flora and fauna (Wong et al. 2013). While all these impacts are inherently important, some also have the potential to influence local rates of RSL rise and the extent of wave-driven and coastal flooding impacts. For example, there is evidence that wave action and flooding of beaches and marshes can induce changes in coastal geomorphology, such as sediment build up, that may iteratively modify the future flood risk profile of communities and ecosystems (Lentz et al. 2016).

DRAFT

TRACEABLE ACCOUNTS

Key Finding 1

Global mean sea level (GMSL) has risen by about 8–9 inches (about 20–23 cm) since 1880, with about 3 of those inches (about 7 cm) occurring since 1990 (*very high confidence*). Human-caused climate change has made a substantial contribution to GMSL rise since 1900 (*high confidence*), contributing to a rate of rise faster than during any comparable period since at least 800 BCE (*medium confidence*).

Description of evidence base

Multiple researchers, using different statistical approaches, have integrated tide gauge records to estimate GMSL rise since the late nineteenth century (e.g., Church and White 2006, 2011; Hay et al. 2015; Jevrejeva et al. 2009). The most recent published rate estimates are 1.2 ± 0.2 (Hay et al. 2015) or 1.5 ± 0.2 (Church and White 2011) mm/year over 1901–1990. Both data sets indicate similar rates since 1880. Thus, these results indicate about 13–16 cm (5–6 inches) of GMSL rise from 1880 to 1990. Tide gauge analyses indicate that GMSL rose at a considerably faster rate of about 3 mm/year (1.2 inches/decade) since 1993 (Hay et al. 2015; Church and White 2011), a result supported by satellite data indicating a trend of 3.4 ± 0.4 mm/year (1.3 inches/decade) over 1993–2015 (update to Nerem et al. 2010) (Figure 12.2a). These results indicate an additional GMSL rise of about 7 cm (3 inches) rise since 1990. Thus total GMSL rise since 1880 is about 20–23 cm (8–9 inches).

The finding regarding the historical context of the 20th century change is based upon Kopp et al. (2016), who conducted a meta-analysis of geological RSL reconstructions, spanning the last 3000 years, from 24 localities around the world, as well as tide gauge data from 66 sites and the tide gauge based GMSL reconstruction of Hay et al. (2015). By constructing a spatio-temporal statistical model of these data sets, they identified the common global sea level signal over the last three millennia, and its uncertainties. They found a 95% probability that the average rate of GMSL change from 1900–2000 was faster than during any previous century since at least 800 BCE.

The finding regarding the substantial human contribution is based upon several lines of evidence. Kopp et al. (2016), based on the long-term historical relationship between temperature and rate of sea-level change, found that GMSL rise would *extremely likely* have been <59% of observed in the absence of 20th century global warming, and that it is *very likely* that GMSL has been higher since 1960 than it would have been without 20th century global warming. Using a variety of models for individual components, Slangen et al. (2016) found that $69\% \pm 31\%$ out of the $87\% \pm 20\%$ of GMSL rise over 1970–2005 that their models simulated was attributable to anthropogenic forcing, and that $37\% \pm 38\%$ out of $74\% \pm 22\%$ simulated was attributable over 1900–2005. Jevrejeva et al. (2009), using the relationship between forcing and GMSL over 1850 and 2001 and CMIP3 models, found that ~75% of GMSL rise in the 20th century is attributable to anthropogenic forcing. Marcos and Amores (2014), using CMIP5 models, found that ~87% of

ocean heat uptake since 1970 in the top 700 m of the ocean has been due to anthropogenic forcing. Slangen et al. (2014), using CMIP5, found that anthropogenic forcing was required to explain observed thermosteric SLR over 1957–2005. Marzeion et al. (2014) found that $25\% \pm 35\%$ of glacial loss over 1851–2010, and $69\% \pm 24\%$ over 1991–2010, was attributable to anthropogenic forcing. Dangendorf et al (2015), based on time series analysis, found that $>45\%$ of observed GMSL trend since 1900 cannot (with 99% probability) be explained by multi-decadal natural variability. Becker et al. (2014), based on time series analysis, found a 99% probability that at least 1.0 or 1.3 mm/yr of GMSL rise over 1880–2010 is anthropogenic.

Major uncertainties

Uncertainties in reconstructed GMSL change relate to the sparsity of tide gauge records, particularly before the middle of the twentieth century, and to different statistical approaches for estimating GMSL change from these sparse records. Uncertainties in reconstructed GMSL change before the twentieth century also relate to the sparsity of geological proxies for sea level change, the interpretation of these proxies, and the dating of these proxies. Uncertainty in attribution relates to the reconstruction of past changes and the magnitude of unforced variability.

Assessment of confidence based on evidence and agreement, including short description of nature of evidence and level of agreement

x Very High

x High

x Medium

☐ Low

Confidence is *very high* in the rate of GMSL rise since 1900, based on multiple different approaches to estimating GMSL rise from tide gauges and satellite altimetry. It is *high* in the substantial human contribution to GMSL rise since 1900, based on both statistical and physical modeling evidence. It is *medium* that the magnitude of the observed rise since 1900 is unprecedented in the context of the previous 2700 years, based on meta-analysis of geological proxy records.

Summary sentence or paragraph that integrates the above information

This key finding is based upon multiple analyses of tide gauge and satellite altimetry records, on a meta-analysis of multiple geological proxies for pre-instrumental sea level change, and on both statistical and physical analyses of the human contribution to GMSL rise since 1900.

Key Finding 2

Relative to the year 2000, GMSL is *very likely* to rise by 0.3–0.6 feet (9–18 cm) by 2030, 0.5–1.2 feet (15–38 cm) by 2050, and 1 to 4 feet (30–130 cm) by 2100 (*very high confidence in lower bounds; medium confidence in upper bounds for 2030 and 2050; low confidence in upper bounds*).

for 2100). Emissions pathways have little effect on projected GMSL rise in the first half of the century, but significantly affect projections for the second half of the century (*high confidence*). Emerging science regarding ice sheet stability suggests that, for high emissions, a GMSL rise exceeding 8 feet (2.4 m) by 2100 cannot be ruled out.

Description of evidence base

The lower bound of the very likely range is based on a continuation of the observed approximately 3 mm/year rate of GMSL rise. The upper end of the very likely range is based upon estimates for RCP 8.5 from three studies producing fully probabilistic projections across multiple RCPs. Kopp et al. (2014) fused multiple sources of information accounting for the different individual process contributing to GMSL rise. Kopp et al. (2016) constructed a semi-empirical sea level model calibrated to the Common Era sea level reconstruction. Mengel et al. (2016) constructed a set of semi-empirical models of the different contributing processes. All three studies show negligible RCP dependence in the first half of this century, becoming more prominent in the second half of the century.

To estimate the effect of incorporating the DeConto and Pollard (2016) projections of Antarctic ice sheet melt, we note that Kopp et al. (2014)'s median projection of Antarctic melt in 2100 is 4 cm (1.6 inches) (RCP8.5), 5 cm (2 inches) (RCP4.5), or 6 cm (2.4 inches) (RCP2.6). By contrast, DeConto and Pollard (2016)'s ensemble mean projections are (varying the assumptions for the size of Pliocene mass loss and the bias correction in the Amundsen Sea) 64–114 cm (2.1–3.7 feet) for RCP8.5, 26–58 cm (0.9–1.9 feet) for RCP4.5, and 2–14 cm (0.1–0.5 foot) for RCP2.6. Thus we conclude that DeConto and Pollard (2016)'s projection would lead to a 60–110 cm (2.0–3.6 feet) increase in median RCP8.5 projections, a 21–53 cm (0.7–1.7 feet) increase in median RCP4.5 projections, and a –4–10 cm (–0.1–0.3 foot) increase in median RCP2.6 projections.

Very likely ranges, 2030 relative to 2000 in cm (feet)

	Kopp et al. (2014)	Kopp et al. (2016)	Mengel et al. (2016)
RCP8.5	11-18 (0.4-0.6)	8-15 (0.3-0.5)	7-12 (0.2-0.4)
RCP4.5	10-18 (0.3-0.6)	8-15 (0.3-0.5)	7-12 (0.2-0.4)
RCP2.6	10-18 (0.3-0.6)	8-15 (0.3-0.5)	7-12 (0.2-0.4)

1 Very likely ranges, 2050 relative to 2000 in cm (feet)

	Kopp et al. (2014)	Kopp et al. (2016)	Mengel et al. (2016)
RCP8.5	21-38 (0.7-1.2)	16-34 (0.5-1.1)	15-28 (0.5-0.9)
RCP4.5	18-35 (0.6-1.1)	15-31 (0.5-1.0)	14-25 (0.5-0.8)
RCP2.6	18-33 (0.6-1.1)	14-29 (0.5-1.0)	13-23 (0.4-0.8)

2

3 Very likely ranges, 2100 relative to 2000 in cm (feet)

	Kopp et al. (2014)	Kopp et al. (2016)	Mengel et al. (2016)
RCP8.5	55-121 (1.8-4.0)	52-131 (1.7-4.3)	57-131 (1.9-4.3)
RCP4.5	36-93 (1.2-3.1)	33-85 (1.1-2.8)	37-77 (1.2-2.5)
RCP2.6	29-82 (1.0-2.7)	24-61 (0.8-2.0)	28-56 (0.9-1.8)

4

5 **Major uncertainties**

6 Since NCA3, multiple different approaches have been used to generate probabilistic projections
 7 of GMSL rise, conditional upon the RCPs. These approaches are in general agreement. However,
 8 emerging results indicate that marine-based sectors of the Antarctic Ice Sheet are more unstable
 9 than previous modeling indicated. The rate of ice sheet mass changes remains challenging to
 10 project.

11 **Assessment of confidence based on evidence and agreement, including short description of**
 12 **nature of evidence and level of agreement**

- 13 x Very High
 14 x High
 15 x Medium
 16 x Low

There is *very high* confidence that future GMSL rise over the next several decades will be at least as fast as a continuation of the historical trend over the last quarter century would indicate. There is *medium* confidence in the upper end of very likely ranges for 2030 and 2050. Due to possibly large ice sheet contributions, there is *low* confidence in the upper end of very likely ranges for 2100. Based on multiple projection methods, there is *high confidence* that differences between emission scenarios are small before 2050 but significant beyond 2050.

Summary sentence or paragraph that integrates the above information

This key finding is based upon multiple methods for estimating the probability of future sea level change and on new modeling results regarding the stability of the West Antarctic Ice Sheet.

Key Finding 3

Relative sea level (RSL) rise in this century will vary along U.S. coastlines due, in part, to: changes in Earth's gravitational field and rotation from melting of land ice, changes in ocean circulation, and vertical land motion (*very high confidence*). For almost all future GMSL rise scenarios, RSL rise is *likely* to be greater than the global average in the U.S. Northeast and the western Gulf of Mexico. In intermediate and low GMSL rise scenarios, it is *likely* to be less than the global average in much of the Pacific Northwest and Alaska. For high GMSL rise scenarios, it is *likely* to be higher than the global average along all U.S. coastlines outside Alaska (*high confidence*).

Description of evidence base

The processes that cause geographic variability in RSL change are reviewed by Kopp et al. (2015). Long tide gauge data sets show the RSL rise caused by vertical land motion due to glacio-isostatic adjustment and fluid withdrawal along many U.S. coastlines (PSMSL 2016). These observations are corroborated by glacio-isostatic adjustment models, by GPS observations, and by geological data (e.g., Engelhart and Horton 2012). The physics of the gravitational, rotational and flexural "static-equilibrium fingerprint" response of sea level to redistribution of mass from land ice to the oceans is well-established (Farrell and Clark 1976; Mitrovica et al. 2011). GCM studies indicate the potential for a Gulf Stream contribution to sea level rise in the U.S. northeast (Yin et al. 2009; Yin and Goddard 2011). Kopp et al. (2014) and Slangen et al. (2014) accounted for land motion (only glacial isostatic adjustment for Slangen et al.), fingerprint, and ocean dynamic responses. Comparing projections of local RSL change and GMSL change in these studies indicate that local rise is likely to be greater than the global average along the U.S. Atlantic and Gulf coasts and less than the global average in most of the Pacific Northwest.

Sea level rise projections in this report are developed by an Interagency Sea Level Rise Task Force (Sweet et al. In Review)

Major uncertainties

Since NCA3, multiple authors have produced global or regional studies synthesizing the major process that causes global and local sea level change to diverge. The largest sources of uncertainty in the geographic variability of sea-level change are ocean dynamic sea level change and, for those regions where sea level fingerprints for Greenland and Antarctica differ from the global mean in different directions, the relative contributions of these two sources to projected sea level change.

Assessment of confidence based on evidence and agreement, including short description of nature of evidence and level of agreement

x Very High

x High

☐ Medium

☐ Low

Because of the enumerated physical processes, there is *very high* confidence that RSL change will vary across U.S. coastlines. There is *high* confidence in the likely differences of RSL change from GMSL change under different levels of GMSL change, based on projections incorporating the different relevant processes.

Summary sentence or paragraph that integrates the above information

The part of the key finding regarding the existence of geographic variability is based upon a broader observational, modeling, and theoretical literature. The specific differences are based upon the scenarios described by the Interagency Sea Level Rise Task Force (Sweet et al. In Review)

Key Finding 4

The annual occurrences of daily tidal flooding—exceeding local thresholds for minor impacts to infrastructure—have increased 5- to 10-fold since the 1960s in several U.S. coastal cities (*very high confidence*). Rates of increase, which are accelerating in over 25 Atlantic and Gulf Coast cities, are fastest where elevation thresholds are lower, local RSL rise is higher, or extreme variability is less (*very high confidence*). Tidal flooding will continue increasing in depth and frequency in similar manners this century (*very high confidence*).

Description of evidence base

Sweet et al. (2014) examined 45 NOAA tide gauge locations with hourly data since 1980 and Sweet and Park (2014) examined a subset of these (27 locations) with hourly data prior to 1950, all with a National Weather Service elevation threshold established for minor “nuisance” flood impacts. Using linear or quadratic fits of annual number of days exceeding the minor thresholds, Sweet and Park (2014) find differences in trend-derived values since 1960 greater than 10-fold at 8 locations, greater than 5-fold at 6 locations and greater than 3-fold at 7 locations. Sweet et al.

(2014), Sweet and Park (2014), and Ezer and Atkinson (2014) find that annual minor tidal flood frequencies since 1980 are accelerating along locations on the East and Gulf Coasts (> 25 locations, Sweet et al. 2014) due to continued exceedance of a typical high-water distribution above elevation thresholds for minor impacts.

Historical changes over last 60 years in flood probabilities have occurred most rapidly where RSL rates were highest and where tide ranges and extreme variability is less (Sweet and Park 2014). In terms of future rates of changes in extreme event probabilities relative to fixed elevations, Hunter (2012), Tebaldi et al. (2012), Kopp et al. (2014) and Sweet and Park (2014) all find that locations with less extreme variability and higher RSL rise rates are most prone.

Major uncertainties

Minor flooding probabilities has been only assessed where a tide gauge is present with >30 years data and that has a NOAA National Weather Service elevation threshold for impacts established. There are likely many other locations experiencing similar flooding patterns, but an expanded assessment is not possible at this time.

Assessment of confidence based on evidence and agreement, including short description of nature of evidence and level of agreement

☒ Very High

☐ High

☐ Medium

☐ Low

There is *very high* confidence that exceedance probabilities of high-tide flooding at dozens of local-specific elevation thresholds have significantly increased over the last half century, often in an accelerated fashion, and will continue to do this century.

Summary sentence or paragraph that integrates the above information

This key finding is based upon several studies finding historic and projecting future changes in high-water probabilities for local-specific elevation thresholds for flooding.

Key Finding 5

The projected increase in the intensity of hurricanes in the North Atlantic could increase the probability of extreme coastal flooding along the U.S. Atlantic and Gulf Coasts beyond what would be projected based solely on RSL rise. However, there is *low confidence* in the magnitude of the increase in intensity and the associated flood risk amplification, and it could be offset or amplified by other factors, such as changes in hurricane frequency or tracks.

Description of evidence base

Model-based projections of tropical storms and related major storm surges within the North Atlantic mostly agree that intensities and frequencies of the most intense storms will increase this

century (Grinsted et al. 2013; Lin et al. 2012; Little et al. 2015; Knutson et al. 2013; Lin et al. 2016). However, the projection of increased hurricane intensity is more robust across models than the projection of increased frequency of the most intense storms, since a number of models project a decrease in the overall number of tropical storms and hurricanes in the North Atlantic, although high-resolution models generally project increased mean hurricane intensity (e.g., Knutson et al. 2013). In addition, there is model evidence for a change in tropical cyclone tracks in warm years that minimizes the increase in landfalling hurricanes in the U.S. Mid-Atlantic or Northeast (Hall and Yonekura 2013).

Major uncertainties

Uncertainties remain large with respect to the precise change in future risk of a major coastal impact at a specific location from changes in the most intense tropical cyclone characteristics and tracks beyond changes imposed from local sea level rise.

Assessment of confidence based on evidence and agreement, including short description of nature of evidence and level of agreement

☐ Very High

☐ High

☐ Medium

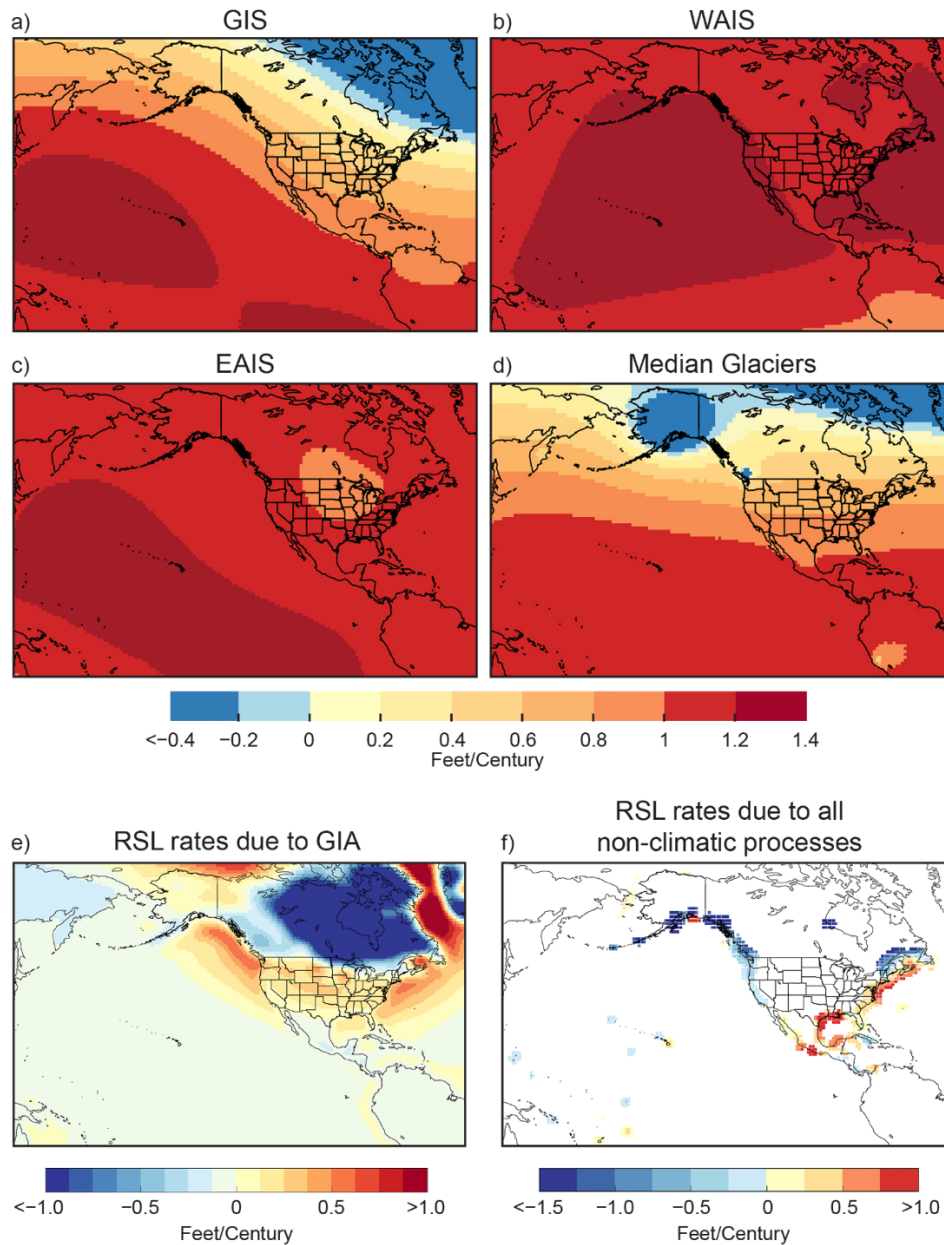
☒ Low

There is *low confidence* that flood risk at specific location will be amplified from a major tropical storm this century.

Summary sentence or paragraph that integrates the above information

This key finding is based upon several modeling studies of future hurricane characteristics and associated increases in major storm surge risk amplification.

1 FIGURES



2

3 **Figure 12.1:** (a–d) Static-equilibrium fingerprints of the RSL effect of land ice melt, in units of
 4 feet of RSL change per foot of GMSL change, for mass loss from (a) Greenland, (b) West
 5 Antarctica, (c) East Antarctica, and (d) the median projected combination of melting glaciers,
 6 after Kopp et al. (2014, 2015). (e) Model projections of the rate of RSL rise due to glacial-
 7 isostatic adjustment (units of feet.century), after Kopp et al. (2015). (f) Tide gauge-based
 8 estimates of the non-climatic, long-term contribution to RSL rise, including the effects of glacial
 9 isostatic adjustment, tectonics, and sediment compaction (Kopp et al. 2014) [Figure source: (a)–
 10 (d) Kopp et al. (2015), (e) adapted from Kopp et al. (2015); (f) adapted from Sweet et al. (In
 11 Review)]

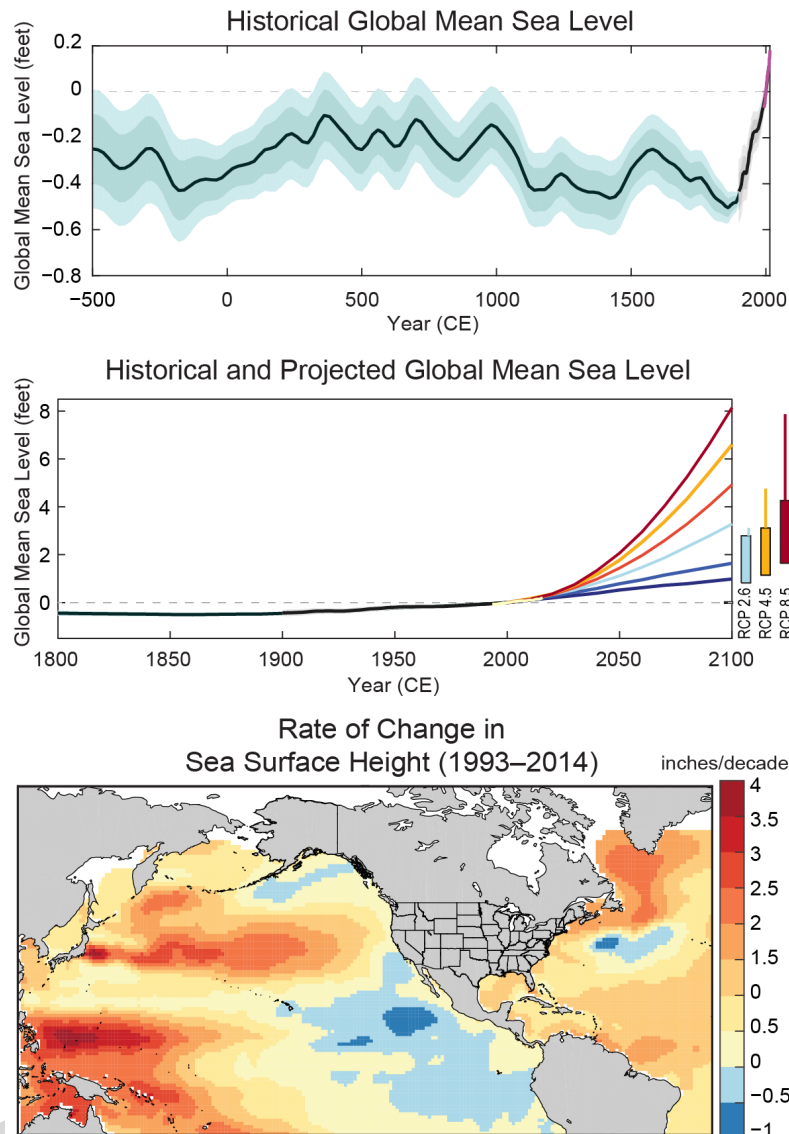


Figure 12.2: (a) GMSL rise from -500 to 1900 CE, from Kopp et al. (2016)'s geological and tide gauge-based reconstruction [blue], from 1900 to 2010 from Hay et al. (2015)'s tide gauge-based reconstruction [black], and from 1992 to 2015 from the satellite-based reconstruction updated from Nerem et al. (2010) [magenta]; (b) GMSL rise from 1800 to 2100, based on (a) from 1800 to 2015, the six Interagency (Sweet et al., In Review) GMSL scenarios (black, blue, cyan, green, orange and red curves), the *very likely* ranges in 2100 for different RCPs from this chapter (colored boxes), and lines augmenting the *very likely* ranges by the difference between the median Antarctic contribution of Kopp et al. 2014 and the various median Antarctic projections of DeConto and Pollard (2016). (c) Rates of change from 1993 to 2014 in sea surface height from satellite altimetry data; from Kopp et al. (2015) using data updated from Church and White (2011). [Figure source: (a) adapted from Nerem et al. (2010), Kopp et al. (2016) and Hay et al. (2015), (b) adapted from Sweet et al. (In Review), (c) adapted from Kopp et al. (2015)]

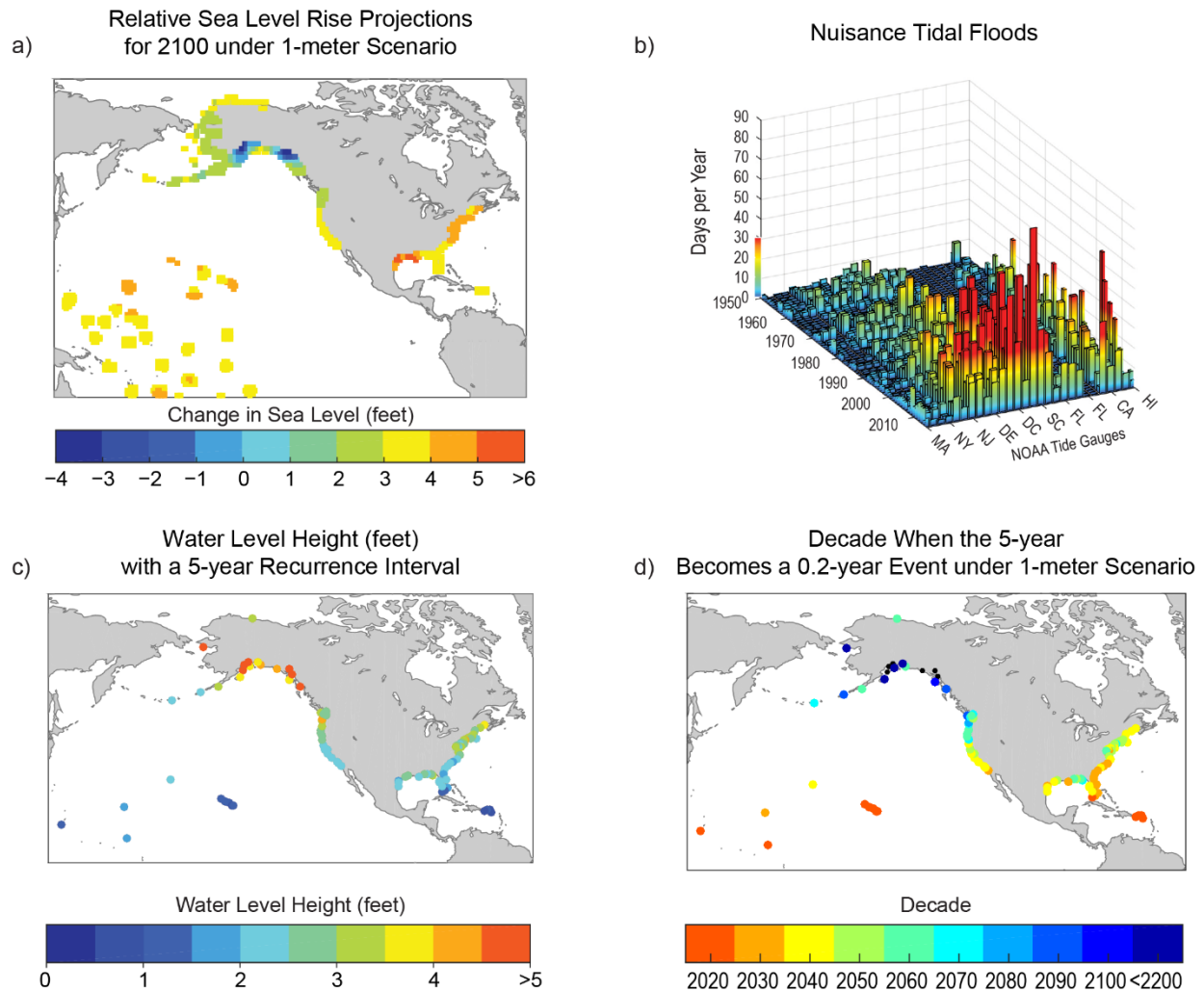


Figure 12.3: (a) RSL rise (feet) in 2100 under the median-local Interagency Intermediate (1-meter) Scenario, (b) tidal floods (days per year) exceeding NOAA thresholds for minor impacts at NOAA tide gauges through 2015, from Sweet and Marra (2016), (c) water level heights associated with a local 5-year recurrence probability, after Sweet et al. 2014, and (d) future decade the 5-year becomes a 0.2-year event under the Interagency Intermediate scenario, after Sweet and Park (2014); black dots imply that a 5-year to 0.2-year frequency change does not unfold by 2200 under the Intermediate scenario. [Figure source: (a), (c), and (d) Sweet et al. (In Review), (b) adapted from Sweet and Marra (2016)]

REFERENCES

- Abraham, J.P., M. Baringer, N.L. Bindoff, T. Boyer, L.J. Cheng, J.A. Church, J.L. Conroy, C.M. Domingues, J.T. Fasullo, J. Gilson, G. Goni, S.A. Good, J.M. Gorman, V. Gouretski, M. Ishii, G.C. Johnson, S. Kizu, J.M. Lyman, A.M. Macdonald, W.J. Minkowycz, S.E. Moffitt, M.D. Palmer, A.R. Piola, F. Reseghetti, K. Schuckmann, K.E. Trenberth, I. Velicogna, and J.K. Willis, 2013: A review of global ocean temperature observations: Implications for ocean heat content estimates and climate change. *Reviews of Geophysics*, **51**, 450-483.
<http://dx.doi.org/10.1002/rog.20022>
- Applegate, P.J. and K. Keller, 2015: How effective is albedo modification (solar radiation management geoengineering) in preventing sea-level rise from the Greenland Ice Sheet? *Environmental Research Letters*, **10**, 084018. <http://dx.doi.org/10.1088/1748-9326/10/8/084018>
- Atkinson, J., J.M. Smith, and C. Bender, 2013: Sea-level rise effects on storm surge and nearshore waves on the Texas coast: Influence of landscape and storm characteristics. *Journal of Waterway, Port, Coastal, and Ocean Engineering*, **139**, 98-117.
[http://dx.doi.org/10.1061/\(ASCE\)WW.1943-5460.0000187](http://dx.doi.org/10.1061/(ASCE)WW.1943-5460.0000187)
- Aucan, J., R. Hoeke, and M.A. Merrifield, 2012: Wave-driven sea level anomalies at the Midway tide gauge as an index of North Pacific storminess over the past 60 years. *Geophysical Research Letters*, **39**, L17603. <http://dx.doi.org/10.1029/2012GL052993>
- Barnard, P.L., J. Allan, J.E. Hansen, G.M. Kaminsky, P. Ruggiero, and A. Doria, 2011: The impact of the 2009–10 El Niño Modoki on U.S. West Coast beaches. *Geophysical Research Letters*, **38**, L13604. <http://dx.doi.org/10.1029/2011GL047707>
- Barnard, P.L., A.D. Short, M.D. Harley, K.D. Splinter, S. Vitousek, I.L. Turner, J. Allan, M. Banno, K.R. Bryan, A. Doria, J.E. Hansen, S. Kato, Y. Kuriyama, E. Randall-Goodwin, P. Ruggiero, I.J. Walker, and D.K. Heathfield, 2015: Coastal vulnerability across the Pacific dominated by /Southern Oscillation. *Nature Geoscience*, **8**, 801-807.
<http://dx.doi.org/10.1038/ngeo2539>
- Barrett, S., T.M. Lenton, A. Millner, A. Tavoni, S. Carpenter, J.M. Anderies, F.S. Chapin Iii, A.-S. Crepin, G. Daily, P. Ehrlich, C. Folke, V. Galaz, T. Hughes, N. Kautsky, E.F. Lambin, R. Naylor, K. Nyborg, S. Polasky, M. Scheffer, J. Wilen, A. Xepapadeas, and A. de Zeeuw, 2014: Climate engineering reconsidered. *Nature Climate Change*, **4**, 527-529.
<http://dx.doi.org/10.1038/nclimate2278>
- Becker, M., M. Karpytchev, and S. Lennartz-Sassinek, 2014: Long-term sea level trends: Natural or anthropogenic? *Geophysical Research Letters*, **41**, 5571-5580.
<http://dx.doi.org/10.1002/2014GL061027>

- 1 Bilskie, M.V., S.C. Hagen, K. Alizad, S.C. Medeiros, D.L. Passeri, H.F. Needham, and A. Cox,
2 2016: Dynamic simulation and numerical analysis of hurricane storm surge under sea level
3 rise with geomorphologic changes along the northern Gulf of Mexico. *Earth's Future*, **4**, 177-
4 193. <http://dx.doi.org/10.1002/2015EF000347>
- 5 Bilskie, M.V., S.C. Hagen, S.C. Medeiros, and D.L. Passeri, 2014: Dynamics of sea level rise
6 and coastal flooding on a changing landscape. *Geophysical Research Letters*, **41**, 927-934.
7 <http://dx.doi.org/10.1002/2013GL058759>
- 8 Bromirski, P.D. and D.R. Cayan, 2015: Wave power variability and trends across the North
9 Atlantic influenced by decadal climate patterns. *Journal of Geophysical Research: Oceans*,
10 **120**, 3419-3443. <http://dx.doi.org/10.1002/2014JC010440>
- 11 Bromirski, P.D., D.R. Cayan, J. Helly, and P. Wittmann, 2013: Wave power variability and
12 trends across the North Pacific. *Journal of Geophysical Research: Oceans*, **118**, 6329-6348.
13 <http://dx.doi.org/10.1002/2013JC009189>
- 14 Bromirski, P.D. and J.P. Kossin, 2008: Increasing hurricane wave power along the U.S. Atlantic
15 and Gulf coasts. *Journal of Geophysical Research*, **113**, C07012.
16 <http://dx.doi.org/10.1029/2007JC004706>
- 17 Bromirski, P.D., A.J. Miller, R.E. Flick, and G. Auad, 2011: Dynamical suppression of sea level
18 rise along the Pacific coast of North America: Indications for imminent acceleration. *Journal*
19 *of Geophysical Research*, **116**, C07005. <http://dx.doi.org/10.1029/2010JC006759>
- 20 Buchanan, M.K., R.E. Kopp, M. Oppenheimer, and C. Tebaldi, 2016: Allowances for evolving
21 coastal flood risk under uncertain local sea-level rise. *Climatic Change*, **137**, 347-362.
22 <http://dx.doi.org/10.1007/s10584-016-1664-7>
- 23 Carlson, A.E., A.N. LeGrande, D.W. Oppo, R.E. Came, G.A. Schmidt, F.S. Anslow, J.M.
24 Licciardi, and E.A. Obbink, 2008: Rapid early Holocene deglaciation of the Laurentide ice
25 sheet. *Nature Geoscience*, **1**, 620-624. <http://dx.doi.org/10.1038/ngeo285>
- 26 Chambers, D.P., A. Cazenave, N. Champollion, H. Dieng, W. Llovel, R. Forsberg, K. von
27 Schuckmann, and Y. Wada, 2016: Evaluation of the Global Mean Sea Level Budget between
28 1993 and 2014. *Surveys in Geophysics*, 1-19. <http://dx.doi.org/10.1007/s10712-016-9381-3>
- 29 Church, J.A., P.U. Clark, A. Cazenave, J.M. Gregory, S. Jevrejeva, A. Levermann, M.A.
30 Merrifield, G.A. Milne, R.S. Nerem, P.D. Nunn, A.J. Payne, W.T. Pfeffer, D. Stammer, and
31 A.S. Unnikrishnan, 2013: Sea Level Change. *Climate Change 2013: The Physical Science*
32 *Basis. Contribution of Working Group I to the Fifth Assessment Report of the*
33 *Intergovernmental Panel on Climate Change*. Stocker, T.F., D. Qin, G.-K. Plattner, M.
34 Tignor, S.K. Allen, J. Boschung, A. Nauels, Y. Xia, V. Bex, and P.M. Midgley, Eds.

- Cambridge University Press, Cambridge, United Kingdom and New York, NY, USA, 1137–1216. <http://dx.doi.org/10.1017/CBO9781107415324.026> www.climatechange2013.org
- Church, J.A. and N.J. White, 2011: Sea-level rise from the late 19th to the early 21st century. *Surveys in Geophysics*, **32**, 585-602. <http://dx.doi.org/10.1007/s10712-011-9119-1>
- Colle, B.A., J.F. Booth, and E.K.M. Chang, 2015: A Review of Historical and Future Changes of Extratropical Cyclones and Associated Impacts Along the US East Coast. *Current Climate Change Reports*, **1**, 125-143. <http://dx.doi.org/10.1007/s40641-015-0013-7>
- Colle, B.A., Z. Zhang, K.A. Lombardo, E. Chang, P. Liu, and M. Zhang, 2013: Historical Evaluation and Future Prediction of Eastern North American and Western Atlantic Extratropical Cyclones in the CMIP5 Models during the Cool Season. *Journal of Climate*, **26**, 6882-6903. <http://dx.doi.org/10.1175/JCLI-D-12-00498.1>
- Dangendorf, S., M. Marcos, A. Müller, E. Zorita, R. Riva, K. Berk, and J. Jensen, 2015: Detecting anthropogenic footprints in sea level rise. *Nature Communications*, **6**, 7849. <http://dx.doi.org/10.1038/ncomms8849>
- DeConto, R.M. and D. Pollard, 2016: Contribution of Antarctica to past and future sea-level rise. *Nature*, **531**, 591-597. <http://dx.doi.org/10.1038/nature17145>
- Dutton, A., A.E. Carlson, A.J. Long, G.A. Milne, P.U. Clark, R. DeConto, B.P. Horton, S. Rahmstorf, and M.E. Raymo, 2015: Sea-level rise due to polar ice-sheet mass loss during past warm periods. *Science*, **349**. <http://dx.doi.org/10.1126/science.aaa4019>
- Dutton, A. and K. Lambeck, 2012: Ice Volume and Sea Level During the Last Interglacial. *Science*, **337**, 216-219. <http://dx.doi.org/10.1126/science.1205749>
- Engelhart, S.E. and Horton, B.P., 2012. Holocene sea level database for the Atlantic coast of the United States. *Quaternary Science Reviews*, **54**, pp.12-25
- Erikson, L.H., C.A. Hegermiller, P.L. Barnard, P. Ruggiero, and M. van Ormondt, 2015: Projected wave conditions in the Eastern North Pacific under the influence of two CMIP5 climate scenarios. *Ocean Modelling*, **96, Part 1**, 171-185. <http://dx.doi.org/10.1016/j.ocemod.2015.07.004>
- Ezer, T., 2013: Sea level rise, spatially uneven and temporally unsteady: Why the U.S. East Coast, the global tide gauge record, and the global altimeter data show different trends. *Geophysical Research Letters*, **40**, 5439-5444. <http://dx.doi.org/10.1002/2013GL057952>
- Ezer, T. and L.P. Atkinson, 2014: Accelerated flooding along the U.S. East Coast: On the impact of sea-level rise, tides, storms, the Gulf Stream, and the North Atlantic Oscillations. *Earth's Future*, **2**, 362-382. <http://dx.doi.org/10.1002/2014EF000252>

- 1 Farrell, W. E., and J. A. Clark, 1976: On postglacial sea level. *Geophys. J. Roy. Astrophys. Soc.*,
2 **46**, 647–667
- 3 Fasullo, J.T., R.S. Nerem, and B. Hamlington, 2016: Is the detection of accelerated sea level rise
4 imminent? *Scientific Reports*, **6**, 31245. <http://dx.doi.org/10.1038/srep31245>
- 5 Feser, F., M. Barcikowska, O. Krueger, F. Schenk, R. Weisse, and L. Xia, 2015: Storminess over
6 the North Atlantic and northwestern Europe—A review. *Quarterly Journal of the Royal
7 Meteorological Society*, **141**, 350–382. <http://dx.doi.org/10.1002/qj.2364>
- 8 Galloway, D., D.R. Jones, and S.E. Ingebritsen, 1999: Land Subsidence in the United States. 6
9 pp. U.S. Geological Survey, Reston, VA.
- 10 Goddard, P.B., J. Yin, S.M. Griffies, and S. Zhang, 2015: An extreme event of sea-level rise
11 along the Northeast coast of North America in 2009–2010. *Nature Communications*, **6**, 6346.
12 <http://dx.doi.org/10.1038/ncomms7346>
- 13 Graham, N.E., D.R. Cayan, P.D. Bromirski, and R.E. Flick, 2013: Multi-model projections of
14 twenty-first century North Pacific winter wave climate under the IPCC A2 scenario. *Climate
15 Dynamics*, **40**, 1335–1360. <http://dx.doi.org/10.1007/s00382-012-1435-8>
- 16 Grinsted, A., S. Jevrejeva, R.E.M. Riva, and D. Dahl-Jensen, 2015: Sea level rise projections for
17 northern Europe under RCP8.5. *Climate Research*, **64**, 15–23.
18 <http://dx.doi.org/10.3354/cr01309>
- 19 Grinsted, A., J.C. Moore, and S. Jevrejeva, 2013: Projected Atlantic hurricane surge threat from
20 rising temperatures. *Proceedings of the National Academy of Sciences*, **110**, 5369–5373.
21 <http://dx.doi.org/10.1073/pnas.1209980110>
- 22 Hall, J.A., S. Gill, J. Obeysekera, W. Sweet, K. Knuuti, and J. Marburger, 2016: Regional Sea
23 Level Scenarios for Coastal Risk Management: Managing the Uncertainty of Future Sea
24 Level Change and Extreme Water Levels for Department of Defense Coastal Sites
25 Worldwide. 224 pp. U.S. Department of Defense, Strategic Environmental Research and
26 Development Program, Alexandria VA.
- 27 Hall, T. and E. Yonekura, 2013: North American Tropical Cyclone Landfall and SST: A
28 Statistical Model Study. *Journal of Climate*, **26**, 8422–8439. <http://dx.doi.org/10.1175/jcli-d-12-00756.1>
- 30 Hamlington, B.D., S.H. Cheon, P.R. Thompson, M.A. Merrifield, R.S. Nerem, R.R. Leben, and
31 K.Y. Kim, 2016: An ongoing shift in Pacific Ocean sea level. *Journal of Geophysical
32 Research: Oceans*, **121**, 5084–5097. <http://dx.doi.org/10.1002/2016JC011815>

- 1 Hamlington, B.D., R.R. Leben, K.Y. Kim, R.S. Nerem, L.P. Atkinson, and P.R. Thompson,
2 2015: The effect of the El Niño-Southern Oscillation on U.S. regional and coastal sea level.
3 *Journal of Geophysical Research: Oceans*, **120**, 3970-3986.
4 <http://dx.doi.org/10.1002/2014JC010602>
- 5 Hay, C.C., E. Morrow, R.E. Kopp, and J.X. Mitrovica, 2015: Probabilistic reanalysis of
6 twentieth-century sea-level rise. *Nature*, **517**, 481-484.
7 <http://dx.doi.org/10.1038/nature14093>
- 8 Hoeke, R.K., K.L. McInnes, J.C. Kruger, R.J. McNaught, J.R. Hunter, and S.G. Smithers, 2013:
9 Widespread inundation of Pacific islands triggered by distant-source wind-waves. *Global*
10 *and Planetary Change*, **108**, 128-138. <http://dx.doi.org/10.1016/j.gloplacha.2013.06.006>
- 11 Horton, R.M., V. Gornitz, D.A. Bader, A.C. Ruane, R. Goldberg, and C. Rosenzweig, 2011:
12 Climate hazard assessment for stakeholder adaptation planning in New York City. *Journal of*
13 *Applied Meteorology and Climatology*, **50**, 2247-2266.
14 <http://dx.doi.org/10.1175/2011JAMC2521.1>
- 15 Hunter, J., 2012: A simple technique for estimating an allowance for uncertain sea-level rise.
16 *Climatic Change*, **113**, 239-252. <http://dx.doi.org/10.1007/s10584-011-0332-1>
- 17 Irvine, P.J., D.J. Lunt, E.J. Stone, and A. Ridgwell, 2009: The fate of the Greenland Ice Sheet in
18 a geoengineered, high CO₂ world. *Environmental Research Letters*, **4**, 045109.
19 <http://dx.doi.org/10.1088/1748-9326/4/4/045109>
- 20 Jevrejeva, S., A. Grinsted, and J.C. Moore, 2009: Anthropogenic forcing dominates sea level rise
21 since 1850. *Geophysical Research Letters*, **36**, n/a-n/a.
22 <http://dx.doi.org/10.1029/2009GL040216>
- 23 Joughin, I., B.E. Smith, and B. Medley, 2014: Marine Ice Sheet Collapse Potentially Under Way
24 for the Thwaites Glacier Basin, West Antarctica. *Science*, **344**, 735-738.
25 <http://dx.doi.org/10.1126/science.1249055>
- 26 Kemp, A.C. and B.P. Horton, 2013: Contribution of relative sea-level rise to historical hurricane
27 flooding in New York City. *Journal of Quaternary Science*, **28**, 537-541.
28 <http://dx.doi.org/10.1002/jqs.2653>
- 29 Kemp, A.C., B.P. Horton, J.P. Donnelly, M.E. Mann, M. Vermeer, and S. Rahmstorf, 2011:
30 Climate related sea-level variations over the past two millennia. *Proceedings of the National*
31 *Academy of Sciences*, **108**, 11017-11022. <http://dx.doi.org/10.1073/pnas.1015619108>
- 32 Khan, S.A., K.H. Kjaer, M. Bevis, J.L. Bamber, J. Wahr, K.K. Kjeldsen, A.A. Bjork, N.J.
33 Korsgaard, L.A. Stearns, M.R. van den Broeke, L. Liu, N.K. Larsen, and I.S. Muresan, 2014:

- 1 Sustained mass loss of the northeast Greenland ice sheet triggered by regional warming.
2 *Nature Climate Change*, **4**, 292-299. <http://dx.doi.org/10.1038/nclimate2161>
- 3 Khazendar, A., M.P. Schodlok, I. Fenty, S.R.M. Ligtenberg, E. Rignot, and M.R. van den
4 Broeke, 2013: Observed thinning of Totten Glacier is linked to coastal polynya variability.
5 *Nature Communications*, **4**, 2857. <http://dx.doi.org/10.1038/ncomms3857>
- 6 Kjeldsen, K.K., N.J. Korsgaard, A.A. Bjørk, S.A. Khan, J.E. Box, S. Funder, N.K. Larsen, J.L.
7 Bamber, W. Colgan, M. van den Broeke, M.-L. Siggaard-Andersen, C. Nuth, A.
8 Schomacker, C.S. Andresen, E. Willerslev, and K.H. Kjær, 2015: Spatial and temporal
9 distribution of mass loss from the Greenland Ice Sheet since AD 1900. *Nature*, **528**, 396-400.
10 <http://dx.doi.org/10.1038/nature16183>
- 11 Knutson, T.R., J.J. Sirutis, G.A. Vecchi, S. Garner, M. Zhao, H.-S. Kim, M. Bender, R.E.
12 Tuleya, I.M. Held, and G. Villarini, 2013: Dynamical downscaling projections of twenty-
13 first-century Atlantic hurricane activity: CMIP3 and CMIP5 model-based scenarios. *Journal*
14 *of Climate*, **27**, 6591-6617. <http://dx.doi.org/10.1175/jcli-d-12-00539.1>
- 15 Knutson, T.R., J.J. Sirutis, M. Zhao, R.E. Tuleya, M. Bender, G.A. Vecchi, G. Villarini, and D.
16 Chavas, 2015: Global Projections of Intense Tropical Cyclone Activity for the Late Twenty-
17 First Century from Dynamical Downscaling of CMIP5/RCP4.5 Scenarios. *Journal of*
18 *Climate*, **28**, 7203-7224. <http://dx.doi.org/10.1175/JCLI-D-15-0129.1>
- 19 Kopp, R.E., 2013: Does the mid-Atlantic United States sea level acceleration hot spot reflect
20 ocean dynamic variability? *Geophysical Research Letters*, **40**, 3981-3985.
21 <http://dx.doi.org/10.1002/grl.50781>
- 22 Kopp, R.E., C.C. Hay, C.M. Little, and J.X. Mitrovica, 2015: Geographic Variability of Sea-
23 Level Change. *Current Climate Change Reports*, **1**, 192-204.
24 <http://dx.doi.org/10.7282/T37W6F4P>
- 25 Kopp, R.E., B.P. Horton, A.C. Kemp, and C. Tebaldi, 2015: Past and future sea-level rise along
26 the coast of North Carolina, USA. *Climatic Change*, **132**, 693-707.
27 <http://dx.doi.org/10.1007/s10584-015-1451-x>
- 28 Kopp, R.E., R.M. Horton, C.M. Little, J.X. Mitrovica, M. Oppenheimer, D.J. Rasmussen, B.H.
29 Strauss, and C. Tebaldi, 2014: Probabilistic 21st and 22nd century sea-level projections at a
30 global network of tide-gauge sites. *Earth's Future*, **2**, 383-406.
31 <http://dx.doi.org/10.1002/2014EF000239>
- 32 Kopp, R.E., A.C. Kemp, K. Bittermann, B.P. Horton, J.P. Donnelly, W.R. Gehrels, C.C. Hay,
33 J.X. Mitrovica, E.D. Morrow, and S. Rahmstorf, 2016: Temperature-driven global sea-level
34 variability in the Common Era. *Proceedings of the National Academy of Sciences*, **113**,
35 E1434-E1441. <http://dx.doi.org/10.1073/pnas.1517056113>

- 1 Kopp, R.E., F.J. Simons, J.X. Mitrovica, A.C. Maloof, and M. Oppenheimer, 2009: Probabilistic
2 assessment of sea level during the last interglacial stage. *Nature*, **462**, 863-867.
3 <http://dx.doi.org/10.1038/nature08686>
- 4 Lambeck, K., H. Rouby, A. Purcell, Y. Sun, and M. Sambridge, 2014: Sea level and global ice
5 volumes from the Last Glacial Maximum to the Holocene. *Proceedings of the National*
6 *Academy of Sciences*, **111**, 15296-15303. <http://dx.doi.org/10.1073/pnas.1411762111>
- 7 Lenton, T.M., 2011: Early warning of climate tipping points. *Nature Climate Change*, **1**, 201-
8 209. <http://dx.doi.org/10.1038/nclimate1143>
- 9 Lentz, E.E., E.R. Thieler, N.G. Plant, S.R. Stippa, R.M. Horton, and D.B. Gesch, 2016:
10 Evaluation of dynamic coastal response to sea-level rise modifies inundation likelihood.
11 *Nature Clim. Change*, **6**, 696-700. <http://dx.doi.org/10.1038/nclimate2957>
- 12 Leuliette, E.W., 2015: The Balancing of the Sea-Level Budget. *Current Climate Change*
13 *Reports*, **1**, 185-191. <http://dx.doi.org/10.1007/s40641-015-0012-8>
- 14 Levermann, A., P.U. Clark, B. Marzeion, G.A. Milne, D. Pollard, V. Radic, and A. Robinson,
15 2013: The multimillennial sea-level commitment of global warming. *Proceedings of the*
16 *National Academy of Sciences*, **110**, 13745-13750.
17 <http://dx.doi.org/10.1073/pnas.1219414110>
- 18 Li, X., E. Rignot, M. Morlighem, J. Mouginot, and B. Scheuchl, 2015: Grounding line retreat of
19 Totten Glacier, East Antarctica, 1996 to 2013. *Geophysical Research Letters*, **42**, 8049-8056.
20 <http://dx.doi.org/10.1002/2015GL065701>
- 21 Lin, N., K. Emanuel, M. Oppenheimer, and E. Vanmarcke, 2012: Physically based assessment of
22 hurricane surge threat under climate change. *Nature Climate Change*, **2**, 462-467.
23 <http://dx.doi.org/10.1038/nclimate1389>
- 24 Lin, N., R.E. Kopp, B.P. Horton, and J.P. Donnelly, 2016: Hurricane Sandy's flood frequency
25 increasing from year 1800 to 2100. *Proceedings of the National Academy of Sciences*, **113**,
26 12071-12075. <http://dx.doi.org/10.1073/pnas.1604386113>
27 <http://www.pnas.org/content/113/43/12071.abstract>
- 28 Little, C.M., R.M. Horton, R.E. Kopp, M. Oppenheimer, and S. Yip, 2015: Uncertainty in
29 Twenty-First-Century CMIP5 Sea Level Projections. *Journal of Climate*, **28**, 838-852.
30 <http://dx.doi.org/10.1175/JCLI-D-14-00453.1>
- 31 Llovel, W., J.K. Willis, F.W. Landerer, and I. Fukumori, 2014: Deep-ocean contribution to sea
32 level and energy budget not detectable over the past decade. *Nature Climate Change*, **4**,
33 1031-1035. <http://dx.doi.org/10.1038/nclimate2387>

- 1 MacGregor, J.A., W.T. Colgan, M.A. Fahnestock, M. Morlighem, G.A. Catania, J.D. Paden, and
2 S.P. Gogineni, 2016: Holocene deceleration of the Greenland Ice Sheet. *Science*, **351**, 590-
3 593. <http://dx.doi.org/10.1126/science.aab1702>
- 4 Marcos, M. and A. Amores, 2014: Quantifying anthropogenic and natural contributions to
5 thermosteric sea level rise. *Geophysical Research Letters*, **41**, 2502-2507.
6 <http://dx.doi.org/10.1002/2014GL059766>
- 7 Marcos, M., F.M. Calafat, Á. Berihuete, and S. Dangendorf, 2015: Long-term variations in
8 global sea level extremes. *Journal of Geophysical Research: Oceans*, **120**, 8115-8134.
9 <http://dx.doi.org/10.1002/2015JC011173>
- 10 Marcos, M., B. Marzeion, S. Dangendorf, A.B.A. Slangen, H. Palanisamy, and L. Fenoglio-
11 Marc, 2016: Internal Variability Versus Anthropogenic Forcing on Sea Level and Its
12 Components. *Surveys in Geophysics*, 1-20. <http://dx.doi.org/10.1007/s10712-016-9373-3>
- 13 Markusson, N., F. Ginn, N. Singh Ghaleigh, and V. Scott, 2014: 'In case of emergency press
14 here': framing geoengineering as a response to dangerous climate change. *Wiley*
15 *Interdisciplinary Reviews: Climate Change*, **5**, 281-290. <http://dx.doi.org/10.1002/wcc.263>
- 16 Martín-Español, A., A. Zammit-Mangion, P.J. Clarke, T. Flament, V. Helm, M.A. King, S.B.
17 Luthcke, E. Petrie, F. Rémy, N. Schön, B. Wouters, and J.L. Bamber, 2016: Spatial and
18 temporal Antarctic Ice Sheet mass trends, glacio-isostatic adjustment, and surface processes
19 from a joint inversion of satellite altimeter, gravity, and GPS data. *Journal of Geophysical*
20 *Research: Earth Surface*, **121**, 182-200. <http://dx.doi.org/10.1002/2015JF003550>
- 21 Marzeion, B., J.G. Cogley, K. Richter, and D. Parkes, 2014: Attribution of global glacier mass
22 loss to anthropogenic and natural causes. *Science*, **345**, 919-921.
23 <http://dx.doi.org/10.1126/science.1254702>
- 24 Mawdsley, R.J. and I.D. Haigh, 2016: Spatial and Temporal Variability and Long-Term Trends
25 in Skew Surges Globally. *Frontiers in Marine Science*, **3**.
26 <http://dx.doi.org/10.3389/fmars.2016.00029>
- 27 Menéndez, M. and P.L. Woodworth, 2010: Changes in extreme high water levels based on a
28 quasi-global tide-gauge data set. *Journal of Geophysical Research*, **115**, C10011.
29 <http://dx.doi.org/10.1029/2009JC005997>
- 30 Mengel, M., A. Levermann, K. Frieler, A. Robinson, B. Marzeion, and R. Winkelmann, 2016:
31 Future sea level rise constrained by observations and long-term commitment. *Proceedings of*
32 *the National Academy of Sciences*, **113**, 2597-2602.
33 <http://dx.doi.org/10.1073/pnas.1500515113>

- 1 Merrifield, M.A., 2011: A shift in western tropical Pacific sea level trends during the 1990s.
2 *Journal of Climate*, **24**, 4126-4138. <http://dx.doi.org/10.1175/2011JCLI3932.1>
- 3 Merrifield, M.A., P. Thompson, E. Leuliette, G.T. Mitchum, D.P. Chambers, S. Jevrejeva, R.S.
4 Nerem, M. Menéndez, W. Sweet, B. Hamlington, and J.J. Marra, 2015: [Global Oceans] Sea
5 level variability and change [in “State of the Climate in 2014”]. *Bulletin of the American*
6 *Meteorological Society*, **96**, S82-S85.
7 <http://dx.doi.org/10.1175/2015BAMSStateoftheClimate.1>
- 8 Miller, K.G., R.E. Kopp, B.P. Horton, J.V. Browning, and A.C. Kemp, 2013: A geological
9 perspective on sea-level rise and its impacts along the U.S. mid-Atlantic coast. *Earth's*
10 *Future*, **1**, 3-18. <http://dx.doi.org/10.1002/2013EF000135>
- 11 Miller, K.G., J.D. Wright, J.V. Browning, A. Kulpecz, M. Kominz, T.R. Naish, B.S. Cramer, Y.
12 Rosenthal, W.R. Peltier, and S. Sosdian, 2012: High tide of the warm Pliocene: Implications
13 of global sea level for Antarctic deglaciation. *Geology*. <http://dx.doi.org/10.1130/g32869.1>
- 14 Mitrovica, J. X., Gomez, N., Morrow, E., Hay, C., Latychev, K., & Tamisiea, M. E. (2011). On
15 the robustness of predictions of sea level fingerprints. *Geophysical Journal International*,
16 **187**(2), 729-742
- 17 Moftakhari, H.R., A. AghaKouchak, B.F. Sanders, D.L. Feldman, W. Sweet, R.A. Matthew, and
18 A. Luke, 2015: Increased nuisance flooding along the coasts of the United States due to sea
19 level rise: Past and future. *Geophysical Research Letters*, **42**, 9846-9852.
20 <http://dx.doi.org/10.1002/2015GL066072>
- 21 Moritz, H., K. White, B. Gouldby, W. Sweet, P. Ruggiero, M. Gravens, P. O'Brien, H. Moritz, T.
22 Wahl, N.C. Nadal-Caraballo, and W. Veatch, 2015: USACE adaptation approach for future
23 coastal climate conditions. *Proceedings of the Institution of Civil Engineers - Maritime*
24 *Engineering*, **168**, 111-117. <http://dx.doi.org/10.1680/jmaen.15.00015>
- 25 Mouginit, J., E. Rignot, and B. Scheuchl, 2014: Sustained increase in ice discharge from the
26 Amundsen Sea Embayment, West Antarctica, from 1973 to 2013. *Geophysical Research*
27 *Letters*, **41**, 1576-1584. <http://dx.doi.org/10.1002/2013GL059069>
- 28 Nerem, R.S., D.P. Chambers, C. Choe, and G.T. Mitchum, 2010: Estimating mean sea level
29 change from the TOPEX and Jason altimeter missions. *Marine Geodesy*, **33**, 435-446.
30 <http://dx.doi.org/10.1080/01490419.2010.491031>
- 31 Nieves, V., J.K. Willis, and W.C. Patzert, 2015: Recent hiatus caused by decadal shift in Indo-
32 Pacific heating. *Science*, **349**, 532-535. <http://dx.doi.org/10.1126/science.aaa4521>
- 33 Paolo, F.S., H.A. Fricker, and L. Padman, 2015: Volume loss from Antarctic ice shelves is
34 accelerating. *Science*, **348**, 327-331. <http://dx.doi.org/10.1126/science.aaa0940>

- 1 Passeri, D.L., S.C. Hagen, S.C. Medeiros, M.V. Bilskie, K. Alizad, and D. Wang, 2015: The
2 dynamic effects of sea level rise on low-gradient coastal landscapes: A review. *Earth's*
3 *Future*, **3**, 159-181. <http://dx.doi.org/10.1002/2015EF000298>
- 4 Pfeffer, W.T., J.T. Harper, and S. O'Neel, 2008: Kinematic constraints on glacier contributions to
5 21st-century sea-level rise. *Science*, **321**, 1340-1343.
6 <http://dx.doi.org/10.1126/science.1159099>
- 7 Pollard, D., R.M. DeConto, and R.B. Alley, 2015: Potential Antarctic Ice Sheet retreat driven by
8 hydrofracturing and ice cliff failure. *Earth and Planetary Science Letters*, **412**, 112-121.
9 <http://dx.doi.org/10.1016/j.epsl.2014.12.035>
- 10 Purkey, S.G. and G.C. Johnson, 2010: Warming of Global Abyssal and Deep Southern Ocean
11 Waters between the 1990s and 2000s: Contributions to Global Heat and Sea Level Rise
12 Budgets. *Journal of Climate*, **23**, 6336-6351. <http://dx.doi.org/10.1175/2010JCLI3682.1>
- 13 Rahmstorf, S., 2007: A Semi-Empirical Approach to Projecting Future Sea-Level Rise. *Science*,
14 **315**, 368-370. <http://dx.doi.org/10.1126/science.1135456>
- 15 Rahmstorf, S., J.E. Box, G. Feulner, M.E. Mann, A. Robinson, S. Rutherford, and E.J.
16 Schaffernicht, 2015: Exceptional twentieth-century slowdown in Atlantic Ocean overturning
17 circulation. *Nature Climate Change*, **5**, 475-480. <http://dx.doi.org/10.1038/nclimate2554>
- 18 Reager, J.T., A.S. Gardner, J.S. Famiglietti, D.N. Wiese, A. Eicker, and M.-H. Lo, 2016: A
19 decade of sea level rise slowed by climate-driven hydrology. *Science*, **351**, 699-703.
20 <http://dx.doi.org/10.1126/science.aad8386>
- 21 Reed, A.J., M.E. Mann, K.A. Emanuel, N. Lin, B.P. Horton, A.C. Kemp, and J.P. Donnelly,
22 2015: Increased threat of tropical cyclones and coastal flooding to New York City during the
23 anthropogenic era. *Proceedings of the National Academy of Sciences*, **112**, 12610-12615.
24 <http://dx.doi.org/10.1073/pnas.1513127112>
- 25 Rhein, M., S.R. Rintoul, S. Aoki, E. Campos, D. Chambers, R.A. Feely, S. Gulev, G.C. Johnson,
26 S.A. Josey, A. Kostianoy, C. Mauritzen, D. Roemmich, L.D. Talley, and F. Wang, 2013:
27 Observations: Ocean. *Climate Change 2013: The Physical Science Basis. Contribution of*
28 *Working Group I to the Fifth Assessment Report of the Intergovernmental Panel on Climate*
29 *Change*. Stocker, T.F., D. Qin, G.-K. Plattner, M. Tignor, S.K. Allen, J. Boschung, A.
30 Nauels, Y. Xia, V. Bex, and P.M. Midgley, Eds. Cambridge University Press, Cambridge,
31 United Kingdom and New York, NY, USA, 255-316.
32 <http://dx.doi.org/10.1017/CBO9781107415324.010> www.climatechange2013.org
- 33 Rietbroek, R., S.-E. Brunnabend, J. Kusche, J. Schröter, and C. Dahle, 2016: Revisiting the
34 contemporary sea-level budget on global and regional scales. *Proceedings of the National*
35 *Academy of Sciences*, **113**, 1504-1509. <http://dx.doi.org/10.1073/pnas.1519132113>

- 1 Rignot, E., J. Mouginot, M. Morlighem, H. Seroussi, and B. Scheuchl, 2014: Widespread, rapid
2 grounding line retreat of Pine Island, Thwaites, Smith, and Kohler glaciers, West Antarctica,
3 from 1992 to 2011. *Geophysical Research Letters*, **41**, 3502-3509.
4 <http://dx.doi.org/10.1002/2014GL060140>
- 5 Roemmich, D., J. Church, J. Gilson, D. Monselesan, P. Sutton, and S. Wijffels, 2015: Unabated
6 planetary warming and its ocean structure since 2006. *Nature Climate Change*, **5**, 240-245.
7 <http://dx.doi.org/10.1038/nclimate2513>
- 8 Ruggiero, P., 2013: Is the Intensifying Wave Climate of the U.S. Pacific Northwest Increasing
9 Flooding and Erosion Risk Faster Than Sea-Level Rise? *Journal of Waterway, Port, Coastal,*
10 *and Ocean Engineering*, **139**, 88-97. [http://dx.doi.org/10.1061/\(ASCE\)WW.1943-](http://dx.doi.org/10.1061/(ASCE)WW.1943-)
11 [5460.0000172](http://dx.doi.org/10.1061/(ASCE)WW.1943-5460.0000172)
- 12 Scambos, T. and C. Shuman, 2016: Comment on ‘Mass gains of the Antarctic ice sheet exceed
13 losses’ by H. J. Zwally and others. *Journal of Glaciology*, **62**, 599-603.
14 <http://dx.doi.org/10.1017/jog.2016.59>
- 15 Seo, K.-W., C.R. Wilson, T. Scambos, B.-M. Kim, D.E. Waliser, B. Tian, B.-H. Kim, and J.
16 Eom, 2015: Surface mass balance contributions to acceleration of Antarctic ice mass loss
17 during 2003–2013. *Journal of Geophysical Research: Solid Earth*, **120**, 3617-3627.
18 <http://dx.doi.org/10.1002/2014JB011755>
- 19 Serafin, K.A. and P. Ruggiero, 2014: Simulating extreme total water levels using a time-
20 dependent, extreme value approach. *Journal of Geophysical Research: Oceans*, **119**, 6305-
21 6329. <http://dx.doi.org/10.1002/2014JC010093>
- 22 Shennan, I., A.J. Long, and B.P. Horton, eds. *Handbook of Sea-Level Research*. 2015, John
23 Wiley & Sons, Ltd. 581. <http://dx.doi.org/10.1002/9781118452547>.
- 24 Shepherd, A., E.R. Ivins, A. Geruo, V.R. Barletta, M.J. Bentley, S. Bettadpur, K.H. Briggs, D.H.
25 Bromwich, R. Forsberg, N. Galin, M. Horwath, S. Jacobs, I. Joughin, M.A. King, J.T.M.
26 Lenaerts, J. Li, S.R.M. Ligtenberg, A. Luckman, S.B. Luthcke, M. McMillan, R. Meister, G.
27 Milne, J. Mouginot, A. Muir, J.P. Nicolas, J. Paden, A.J. Payne, H. Pritchard, E. Rignot, H.
28 Rott, L. Sandberg Sørensen, T.A. Scambos, B. Scheuchl, E.J.O. Schrama, B. Smith, A.V.
29 Sundal, J.H. van Angelen, W.J. van de Berg, M.R. van den Broeke, D.G. Vaughan, I.
30 Velicogna, J. Wahr, P.L. Whitehouse, D.J. Wingham, D. Yi, D. Young, and H.J. Zwally,
31 2012: A reconciled estimate of ice-sheet mass balance. *Science*, **338**, 1183-1189.
32 <http://dx.doi.org/10.1126/science.1228102>
- 33 Shope, J.B., C.D. Storlazzi, L.H. Erikson, and C.A. Hegermiller, 2016: Changes to extreme wave
34 climates of islands within the Western Tropical Pacific throughout the 21st century under

- 1 RCP 4.5 and RCP 8.5, with implications for island vulnerability and sustainability. *Global*
2 *and Planetary Change*, **141**, 25-38. <http://dx.doi.org/10.1016/j.gloplacha.2016.03.009>
- 3 Sillmann, J., T.M. Lenton, A. Levermann, K. Ott, M. Hulme, F. Benduhn, and J.B. Horton, 2015:
4 Climate emergencies do not justify engineering the climate. *Nature Climate Change*, **5**, 290-
5 292. <http://dx.doi.org/10.1038/nclimate2539>
- 6 Slangen, A.B.A., M. Carson, C.A. Katsman, R.S.W. van de Wal, A. Köhl, L.L.A. Vermeersen,
7 and D. Stammer, 2014: Projecting twenty-first century regional sea-level changes. *Climatic*
8 *Change*, **124**, 317-332. <http://dx.doi.org/10.1007/s10584-014-1080-9>
- 9 Slangen, A.B.A., J.A. Church, C. Agosta, X. Fettweis, B. Marzeion, and K. Richter, 2016:
10 Anthropogenic forcing dominates global mean sea-level rise since 1970. *Nature Climate*
11 *Change*, **advance online publication**. <http://dx.doi.org/10.1038/nclimate2991>
- 12 Slangen, A.B.A., J.A. Church, X. Zhang, and D. Monselesan, 2014: Detection and attribution of
13 global mean thermosteric sea level change. *Geophysical Research Letters*, **41**, 5951-5959.
14 <http://dx.doi.org/10.1002/2014GL061356>
- 15 Smith, J.M., M.A. Cialone, T.V. Wamsley, and T.O. McAlpin, 2010: Potential impact of sea
16 level rise on coastal surges in southeast Louisiana. *Ocean Engineering*, **37**, 37-47.
17 <http://dx.doi.org/10.1016/j.oceaneng.2009.07.008>
- 18 Sriver, R. L., N. M. Urban, R. Olson, and K. Keller (2012), Toward a physically plausible upper
19 bound of sea-level rise projections, *Climatic Change*, **115(3-4)**, 893–902,
20 [doi:10.1007/s10584-012-0610-6](https://doi.org/10.1007/s10584-012-0610-6)
- 21 Stockdon, H.F., R.A. Holman, P.A. Howd, and A.H. Sallenger Jr, 2006: Empirical
22 parameterization of setup, swash, and runup. *Coastal Engineering*, **53**, 573-588.
23 <http://dx.doi.org/10.1016/j.coastaleng.2005.12.005>
- 24 Stopa, J.E. and K.F. Cheung, 2014: Periodicity and patterns of ocean wind and wave climate.
25 *Journal of Geophysical Research: Oceans*, **119**, 5563-5584.
26 <http://dx.doi.org/10.1002/2013JC009729>
- 27 Strauss, B.H., S. Kulp, and A. Levermann, 2015: Carbon choices determine US cities committed
28 to futures below sea level. *Proceedings of the National Academy of Sciences*, **112**, 13508-
29 13513. <http://dx.doi.org/10.1073/pnas.1511186112>
- 30 Sutterley, T.C., I. Velicogna, E. Rignot, J. Mouginot, T. Flament, M.R. van den Broeke, J.M.
31 van Wessem, and C.H. Reijmer, 2014: Mass loss of the Amundsen Sea Embayment of West
32 Antarctica from four independent techniques. *Geophysical Research Letters*, **41**, 8421-8428.
33 <http://dx.doi.org/10.1002/2014GL061940>

- 1 Sweet, W., M. Menendez, A. Genz, J. Obeysekera, J. Park, and J. Marra, 2016: In Tide's Way:
2 Southeast Florida's September 2015 Sunny-day Flood [in "Explaining Extremes of 2015
3 from a Climate Perspective"]. *Bulletin of the American Meteorological Society*, **97**, In press.
4 <http://dx.doi.org/10.1175/BAMS-D-16-0117.1>
- 5 Sweet, W., J. Park, J. Marra, C. Zervas, and S. Gill, 2014: Sea Level Rise and Nuisance Flood
6 Frequency Changes around the United States. NOAA Technical Report NOS CO-OPS 073,
7 58 pp. U.S. Department of Commerce, National Oceanic and Atmospheric Administration,
8 National Ocean Service, Silver Spring, MD.
9 [http://tidesandcurrents.noaa.gov/publications/NOAA Technical Report NOS COOPS 073.](http://tidesandcurrents.noaa.gov/publications/NOAA_Technical_Report_NOS_COOPS_073.pdf)
10 [pdf](http://tidesandcurrents.noaa.gov/publications/NOAA_Technical_Report_NOS_COOPS_073.pdf)
- 11 Sweet, W.V., R.E. Kopp, C. Weaver, J. Obeysekera, R. Horton, E.R. Thieler, and C. Zervas, In
12 review: Global and Regional Sea Level Rise Scenarios for the United States. NOAA.
- 13 Sweet, W.V. and J.J. Marra, 2016: State of U.S. Nuisance Tidal Flooding. Supplement to State of
14 the Climate: National Overview for May 2016. 5 pp. NOAA National Centers for
15 Environmental Information. [http://www.ncdc.noaa.gov/monitoring-](http://www.ncdc.noaa.gov/monitoring-content/sotc/national/2016/may/sweet-marra-nuisance-flooding-2015.pdf)
16 [content/sotc/national/2016/may/sweet-marra-nuisance-flooding-2015.pdf](http://www.ncdc.noaa.gov/monitoring-content/sotc/national/2016/may/sweet-marra-nuisance-flooding-2015.pdf)
- 17 Sweet, W.V. and J. Park, 2014: From the extreme to the mean: Acceleration and tipping points
18 of coastal inundation from sea level rise. *Earth's Future*, **2**, 579-600.
19 <http://dx.doi.org/10.1002/2014EF000272>
- 20 Sweet, W.V., J. Park, S. Gill, and J. Marra, 2015: New ways to measure waves and their effects
21 at NOAA tide gauges: A Hawaiian-network perspective. *Geophysical Research Letters*, **42**,
22 9355-9361. <http://dx.doi.org/10.1002/2015GL066030>
- 23 Sweet, W.V. and C. Zervas, 2011: Cool-Season Sea Level Anomalies and Storm Surges along
24 the U.S. East Coast: Climatology and Comparison with the 2009/10 El Niño. *Monthly*
25 *Weather Review*, **139**, 2290-2299. <http://dx.doi.org/10.1175/MWR-D-10-05043.1>
- 26 Sweet, W.V., C. Zervas, S. Gill, and J. Park, 2013: Hurricane Sandy inundation probabilities of
27 today and tomorrow [in "Explaining Extremes of 2012 from a Climate Perspective"]. *Bulletin*
28 *of the American Meteorological Society*, **94**, S17-S20. [http://dx.doi.org/10.1175/BAMS-D-](http://dx.doi.org/10.1175/BAMS-D-13-00085.1)
29 [13-00085.1](http://dx.doi.org/10.1175/BAMS-D-13-00085.1)
- 30 Talke, S.A., P. Orton, and D.A. Jay, 2014: Increasing storm tides in New York Harbor, 1844–
31 2013. *Geophysical Research Letters*, **41**, 3149-3155.
32 <http://dx.doi.org/10.1002/2014GL059574>
- 33 Tebaldi, C., B.H. Strauss, and C.E. Zervas, 2012: Modelling sea level rise impacts on storm
34 surges along US coasts. *Environmental Research Letters*, **7**, 014032.
35 <http://dx.doi.org/10.1088/1748-9326/7/1/014032>

- 1 Tedesco, M., S. Doherty, X. Fettweis, P. Alexander, J. Jeyaratnam, and J. Stroeve, 2016: The
2 darkening of the Greenland ice sheet: trends, drivers, and projections (1981–2100). *The*
3 *Cryosphere*, **10**, 477-496. [http://dx.doi.org/10.5194/tc-](http://dx.doi.org/10.5194/tc-10-477-2016)
4 Tedesco, M., X. Fettweis, T. Mote, J. Wahr, P. Alexander, J.E. Box, and B. Wouters, 2013:
5 Evidence and analysis of 2012 Greenland records from spaceborne observations, a regional
6 climate model and reanalysis data. *The Cryosphere*, **7**, 615-630. [http://dx.doi.org/10.5194/tc-](http://dx.doi.org/10.5194/tc-7-615-2013)
7 7-615-2013
- 8 Theuerkauf, E.J., A.B. Rodriguez, S.R. Fegley, and R.A. Luettich, 2014: Sea level anomalies
9 exacerbate beach erosion. *Geophysical Research Letters*, **41**, 5139-5147.
10 <http://dx.doi.org/10.1002/2014GL060544>
- 11 Thompson, P.R., G.T. Mitchum, C. Vonesh, and J. Li, 2013: Variability of Winter Storminess
12 in the Eastern United States during the Twentieth Century from Tide Gauges. *Journal of*
13 *Climate*, **26**, 9713-9726. <http://dx.doi.org/10.1175/JCLI-D-12-00561.1>
- 14 Wada, Y., M.-H. Lo, P.J.F. Yeh, J.T. Reager, J.S. Famiglietti, R.-J. Wu, and Y.-H. Tseng, 2016:
15 Fate of water pumped from underground and contributions to sea-level rise. *Nature Climate*
16 *Change*, **6**, 777-780. <http://dx.doi.org/10.1038/nclimate3001>
- 17 Wahl, T. and D.P. Chambers, 2015: Evidence for multidecadal variability in US extreme sea
18 level records. *Journal of Geophysical Research: Oceans*, **120**, 1527-1544.
19 <http://dx.doi.org/10.1002/2014JC010443>
- 20 Wahl, T. and D.P. Chambers, 2016: Climate controls multidecadal variability in U. S. extreme
21 sea level records. *Journal of Geophysical Research: Oceans*, **121**, 1274-1290.
22 <http://dx.doi.org/10.1002/2015JC011057>
- 23 Wang, X.L., Y. Feng, and V.R. Swail, 2014: Changes in global ocean wave heights as projected
24 using multimodel CMIP5 simulations. *Geophysical Research Letters*, **41**, 1026-1034.
25 <http://dx.doi.org/10.1002/2013GL058650>
- 26 Wong, P.P. et al. in *Climate Change 2013: The Physical Science Basis*. (eds Stocker, T.F. et al.)
27 361-409 (Cambridge Univ Press, 2014).
- 28 Woodruff, J.D., J.L. Irish, and S.J. Camargo, 2013: Coastal flooding by tropical cyclones and
29 sea-level rise. *Nature*, **504**, 44-52. <http://dx.doi.org/10.1038/nature12855>
- 30 Woodworth, P.L. and M. Menéndez, 2015: Changes in the mesoscale variability and in extreme
31 sea levels over two decades as observed by satellite altimetry. *Journal of Geophysical*
32 *Research: Oceans*, **120**, 64-77. <http://dx.doi.org/10.1002/2014JC010363>

- 1 Wöppelmann, G. and M. Marcos, 2016: Vertical land motion as a key to understanding sea level
2 change and variability. *Reviews of Geophysics*, **54**, 64-92.
3 <http://dx.doi.org/10.1002/2015RG000502>
- 4 Yin, J. and P.B. Goddard, 2013: Oceanic control of sea level rise patterns along the East Coast of
5 the United States. *Geophysical Research Letters*, **40**, 5514-5520.
6 <http://dx.doi.org/10.1002/2013GL057992>
- 7 Yin, J., M.E. Schlesinger, and R.J. Stouffer, 2009: Model projections of rapid sea-level rise on
8 the northeast coast of the United States. *Nature Geoscience*, **2**, 262-266.
9 <http://dx.doi.org/10.1038/ngeo462>
- 10 Zappa, G., L.C. Shaffrey, K.I. Hodges, P.G. Sansom, and D.B. Stephenson, 2013: A Multimodel
11 Assessment of Future Projections of North Atlantic and European Extratropical Cyclones in
12 the CMIP5 Climate Models. *Journal of Climate*, **26**, 5846-5862.
13 <http://dx.doi.org/10.1175/jcli-d-12-00573.1>
- 14 Zervas, C., S. Gill, and W.V. Sweet, 2013: Estimating vertical land motion from long-term tide
15 gauge records. 22 pp. NOAA.
- 16 Zhang, X. and J.A. Church, 2012: Sea level trends, interannual and decadal variability in the
17 Pacific Ocean. *Geophysical Research Letters*, **39**, L21701.
18 <http://dx.doi.org/10.1029/2012GL053240>

13. Ocean Changes: Warming, Stratification, Circulation, Acidification, and Deoxygenation

KEY FINDINGS

1. The world's oceans have absorbed more than 90% of the excess heat caused by greenhouse warming since the mid 20th Century, making them warmer and altering global and regional circulation patterns and climate feedbacks (*very high confidence*). Surface oceans have warmed by about 0.45°F (0.25°C) globally since the 1970s (*very high confidence*). The Atlantic meridional overturning circulation (AMOC) has slowed since preindustrial times (*high confidence*). Regionally, eastern boundary upwelling, such as along the U.S. West Coast, that sustains fisheries and controls local climate has intensified (*high confidence*).
2. The world's oceans are currently absorbing more than a quarter of the carbon dioxide emitted to the atmosphere annually from human activities (*very high confidence*), making them more acidic with potential detrimental impacts to marine ecosystems. The rate of acidification is unparalleled in at least the past 66 million years (*medium confidence*). Acidification is regionally increased along U.S. coastal systems as a result of intensified upwelling (for example, in the Pacific Northwest) (*high confidence*), changes in freshwater inputs (for example, Gulf of Maine) (*medium confidence*), and nutrient input (for example, urbanized estuaries) (*high confidence*).
3. Increasing sea surface temperatures, rising sea levels, and changing patterns of precipitation, winds, nutrients, and ocean circulation are contributing to overall declining oxygen concentrations at intermediate depths in various ocean locations and in many coastal areas. Over the last half century, major oxygen losses have occurred in inland seas, estuaries, and in the coastal and open ocean (*high confidence*).
4. In coastal regions, local biogeochemical processes can result in increased acidification co-occurring with eutrophication and/or where riverine loads include naturally corrosive materials of geological origin. All local areas of deoxygenation also tend to be areas of acidification, due to intensified respiration (*very high confidence*).
5. Under a high future scenario (RCP8.5), the AMOC is projected to decline by 6 Sverdrups ($1 \times 10^6 \text{ m}^3/\text{sec}$), global average ocean acidity is projected to increase by 100% to 150% (*very high confidence*), and ocean oxygen levels are projected to decrease by 4% (*high confidence*) by 2100 relative to preindustrial values. Under a low future scenario (RCP2.6), global average ocean acidity is projected to increase by 35% and oxygen projected to decrease by 2% by 2100. Larger acidity increases and oxygen declines are projected in some regions and in intermediate and mode waters (*medium confidence*).

13.1 Warming, Stratification, and Circulation Changes

13.1.1 General Background

Anthropogenic perturbations to the global earth system have included important changes to the oceans. These changes will be distinguishable from the background natural variability in nearly half of the global open ocean within a decade, with important consequences for marine ecosystems and their services (Gattuso et al. 2015).

As discussed in Chapter 12, between 1971–2010, the upper ocean (0–200 m depth) warmed by about 0.25°C (0.45° F) globally (Rhein et al. 2013). Between 1950 and 2009, the North Atlantic gained heat at the rate of about 0.07°C/decade (Hoegh-Guldberg et al. 2014). Such trends are attributed to the combination of global warming and natural climatic variations, such as the Pacific Decadal Oscillation and the Atlantic Multidecadal Oscillation (Trenberth et al. 2014; Steinman et al. 2015).

The uptake of heat by oceans alleviated some atmospheric warming. However, as the ocean warms, its efficiency in taking up heat and greenhouse gases is decreasing because, among other reasons, the surface ocean has become more stratified. Surface ocean stratification has increased by about 4% during the period 1971 to 2010 (Ciais et al. 2013) due to thermal heating and freshening from increased freshwater inputs (precipitation and evaporation changes, land and sea-ice melting). In addition, changes in stratification are associated with suppression of tropical cyclone intensification (Mei et al. 2015), retreat of the polar ice sheets (Straneo and Heimbach 2013), and reductions of the convective mixing at higher latitudes that ventilates the deep ocean through the Atlantic meridional overturning circulation (AMOC) (Rahmstorf et al. 2015). Ocean heat uptake therefore represents a significant feedback that controls the climate transient response (see Ch. 2) while it is also responsible for one third of the sea level rise (see Ch. 12).

In addition to hydrographic changes, ocean circulation patterns are altered in a warming climate. Through a complex interplay with surface heat fluxes and winds, increased sea surface temperatures (SSTs) have led to intensification and a poleward shift of the western boundary currents in all ocean basins (Yang et al. 2016). The Gulf Stream, in contrast to other western boundary currents, is expected to slow down because of the weakening of the AMOC (Yang et al. 2016). On the other hand, the expected slowdown of the AMOC will be counteracted by the warming of the deep ocean (below 700 m [3000 ft]) which will tend to strengthen the AMOC (Patara and Böning, 2014). Any slowdown of the AMOC will result in less heat and CO₂ absorbed by the ocean from the atmosphere, which is a positive feedback to climate change (see also Ch. 2).

Significant changes to ocean stratification and circulation can also be observed regionally, along the eastern ocean boundaries and the equatorial waveguide. In these areas, wind-driven upwelling brings colder, nutrient- and carbon-rich water to the surface; this upwelled water is more efficient in heat and CO₂ uptake. Some upwelling regions are already experiencing an

intensification and greater number of upwelling events due to climate change (Hoegh-Guldberg et al. 2014), while others, such as the California Current, are experiencing fewer (by about 23%–40%) but stronger upwelling events (Hoegh-Guldberg et al. 2014; Sydeman et al. 2014; Jacox et al. 2014).

The Intergovernmental Panel on Climate Change Fifth Assessment Report (IPCC 2013) concluded that there is low confidence in the current understanding of how eastern upwelling systems will be altered under future climate change because of the obscuring role of multi-decadal climate variability (Ciais et al. 2013). However, subsequent studies showed that by 2100, upwelling is predicted to start earlier, end later, and intensify in three of the four major eastern boundary upwelling systems (not in the California Current; Wang et al. 2015). Southern Ocean upwelling will intensify while the Atlantic equatorial upwelling systems will weaken (Hoegh-Guldberg et al. 2014; Wang et al. 2015). The intensification is attributed to the strengthening of regional coastal winds as observations already show (Sydeman et al. 2014a) and model projections estimate for the 21st Century (Rykaczewski et al. 2015; Wang et al. 2015).

13.1.2 Coastal Changes

Coastal boundary systems have warmed by 0.14°–0.80°C from 1950 to 2009 (Hoegh-Guldberg et al. 2014). This is consistent with changes in adjacent deeper waters. For example, the Gulf of Mexico and Caribbean Sea have warmed by 0.31° and 0.50°C, respectively, from 1982 to 2006 (Chollett et al. 2012; Hoegh-Guldberg et al. 2014; Muller-Karger et al. 2015). Warming in tropical seas is leading to increased rates of stress in biological systems like coral reefs.

Sea level is an important variable that affects coastal ecosystems. Global sea level rose very rapidly at the end of the last glaciation, as glaciers and the polar ice sheets melted at their fringes. On average around the globe, sea level is estimated to have risen at rates exceeding 2.5 mm/year between about 8,000 and 6,000 years before present. These rates steadily decreased to less than 2.0 mm/year through about 4,000 years ago and stabilized at less than 0.4 mm/year through the late 1800s. Global sea level rise has accelerated again within the last 100 years, and now averages about 1 to 2 mm/year (Thompson et al. 2016).

Stronger offshore upwelling combined with cross-shelf advection brings nutrients from the deeper ocean but also increased offshore transport (Bakun et al. 2015). The net nutrient load in the coastal regions is responsible for increased productivity and ecosystem function. There is some evidence that coastal upwelling in mid- to high-latitude eastern boundary regions has increased (Garcia-Reyes et al. 2015), but in more tropical areas of the western Atlantic, such as in the Caribbean Sea, it decreased between 1990 and 2010 (Taylor et al. 2012; Astor et al. 2013). This led to a decrease in primary productivity in the southern Caribbean Sea (Taylor et al. 2012). There is still much uncertainty on the direction in which upwelling systems may go with regards to upwelling strength in different locations. Each coastal upwelling center has unique features and should be evaluated locally in the context of regional changes.

Dust transported from continental desert regions to the marine environment deposits nutrients such as iron, nitrogen and phosphorus, and trace metals that stimulate growth of phytoplankton and increase marine productivity (Jickells and Moore 2015). U.S. continental and coastal regions experience large dust deposition fluxes originating from Sahara on the Eastern boundary and from the Central Asia and China Subcontinent in the Northwest (Chiapello 2014). Greenhouse gas emissions and other anthropogenic interference, such as agricultural activity and land use changes, may play an important role on the variability and strength of these dust sources (e.g., Mulitza et al. 2010).

Additionally, oxidized nitrogen, released during high-temperature combustion over land, and reduced nitrogen, released from intensive agriculture, are emitted in areas of high population in North America and are carried away and deposited through wet or dry deposition over coastal and open ocean ecosystems via the local wind circulation. Wet deposition of pollutants produced in urban areas is known to play an important role in changes of ecosystem structure in coastal and open ocean systems.

13.2 Ocean Acidification

13.2.1 General Background

In addition to causing changes in climate, increasing atmospheric levels of carbon dioxide (CO_2) from the burning of fossil fuels and other human activities (for example, changes in land use and cement production) have a direct effect on the world's oceans' chemistry (Orr et al., 2005; Feely et al. 2009). Chemical changes in seawater as a result of the uptake of CO_2 include increasing concentrations of dissolved inorganic carbon (DIC), the production of carbonic acid (acidification, or lowering of pH), an increase in the partial pressure of CO_2 ($p\text{CO}_{2,\text{sw}}$), and a decrease in the concentration of carbonate ions (Figure 13.1). Ocean surface waters have become 30% more acidic over the last 150 years as they have absorbed large amounts of carbon dioxide from the atmosphere (Feely et al. 2004). Since the preindustrial period, the oceans have absorbed approximately 27% of all carbon dioxide emitted to the atmosphere. The oceans are currently absorbing about a quarter of human-caused carbon dioxide emitted to the atmosphere, leading to ocean acidification and the potential alteration of marine ecosystems (Le Quéré et al. 2015).

[INSERT FIGURE 13.1 HERE:]

Figure 13.1: Trends in surface (< 50 m) ocean carbonate chemistry calculated from observations obtained at the Hawai'i Ocean Time-series (HOT) Program in the North Pacific 1988–2015. Data obtained from the Hawai'i Ocean Time-series Data Organization & Graphical System (HOT-DOGS, <http://hahana.soest.hawaii.edu/hot/hot-dogs/index.html>). Seawater $x\text{CO}_2$ (μatm), pH_{Total} , and carbonate ion concentration ($\mu\text{mol/kg}$) were derived using CO2SYS v2.1 by pairing direct measures of total alkalinity (TA) with dissolved inorganic carbon (DIC) when available ($n = 824$). In cases where this pairing was not possible, then pH and DIC were instead adopted ($n = 16$). As a final option, if neither of those pairings was an option then pH_{Total} and TA were

adopted ($n = 18$). The calculations were performed using K_1 , K_2 from Millero, 2010, the KHSO_4 dissociation constant of Dickon, total scale pH, and Uppstrom, 1974 for $[\text{B}]_{\text{T}}$. Atmospheric mole fraction CO_2 (red) data were obtained from NOAA's Earth System Research Laboratory CarbonTracker (Peters et al. 2007). (Figure source: NOAA)]

13.2.2 Open Ocean Acidification

Open ocean waters experience changes in carbonate chemistry more reflective of large-scale physical oceanic processes, including the global uptake of atmospheric CO_2 and the entrainment of acidified subsurface waters due to vertical mixing and upwelling. The rate of ocean acidification within these waters closely approximates the rate of atmospheric CO_2 increase subsequently modified by multidecadal variability (for example, the Atlantic Multidecadal Oscillation and Pacific Decadal Oscillation) processes thereby exhibiting long-term secular changes in ocean carbonate chemistry, as measured on decadal time-scales (Bates et al. 2014; Gledhill et al. 2015).

13.2.3 Coastal Acidification

In contrast to open ocean waters, coastal shelf and nearshore waters are strongly influenced by a number of additional processes. Along the Pacific Coast, upwelling brings deep waters enriched in CO_2 due to deep water respiration processes, thereby exhibiting much lower pH than that of surface waters (Feely et al. 2009; Harris et al. 2013). Along the East Coast, upwelling is less prominent than along the Pacific Coast but does occur in limited locations. However, the coastal waters of the East Coast and mid-Atlantic are far more influenced by freshwater inputs, which contribute varying amounts of dissolved inorganic carbon (DIC), total alkalinity (TA), dissolved and particulate organic carbon, and nutrients from riverine and estuarine sources, all of which significantly alter the local biogeochemistry of the receiving water mass (Gledhill et al. 2015). Coastal waters can episodically experience riverine plumes that are corrosive to calcium carbonate (Salisbury et al. 2008). While these processes have persisted historically, climate-induced increases in high-intensity precipitation events, particularly in the northeast, can yield larger freshwater plumes extending further from the coast. Nutrient loading promotes organic matter production by autotrophy that can result in intense respiration by heterotrophs and drive up local CO_2 concentrations to a degree dependent upon hydrographic conditions (including stratification and residence time) (Waldbusser & Salisbury 2014). Coastal acidification generally exhibits higher-frequency variability and short-term episodic events relative to open-ocean acidification (Borges & Gypens 2010; Waldbusser & Salisbury 2014; Hendriks et al. 2015). However, long-term changes in nutrient loading and/or precipitation may also impart long-term secular changes in coastal acidification magnitude and occurrence.

13.2.4 Latitudinal Variation

Higher-latitude systems are typically less buffered against pH change and can exhibit low carbonate ion conditions (important in carbonate mineral formation and preservation), in large

part due to their lower temperatures (Gledhill et al. 2015, Bates & Mathis 2009). This means that they will experience seasonally corrosive conditions sooner than low-latitude systems. For example, observations have shown that the northeastern Pacific Ocean, including the Arctic and sub-Arctic seas, is particularly susceptible to ocean acidification because the degree of carbonate mineral supersaturation is reduced due to their lower temperatures (Bates & Mathis 2009). The waters along the northwestern Atlantic, including areas along the Scotian Shelf and Gulf of Maine, are also sensitive to acidification (for example, they exhibit a greater change in pH in response to a given input of CO₂), and have lower buffering capacity due to significant riverine input (Gledhill et al. 2015; Jiang et al. 2010). However, it is important to note that the absolute rate of change in low-latitude systems with respect to carbonate mineral saturation state is considerably faster than that of the higher-latitudes (Friedrich et al. 2012).

13.2.5 Paleo Evidence

Evidence suggests that the current ocean acidification rate is the fastest in the last 66 million years and possibly even the past 300 million years (Honisch et al. 2012; Zeebe et al 2016). There is no known period in the past 66 million years that has shown rates of CO₂ increase similar to those experienced in the late 20th and early 21st centuries. The Paleo-Eocene Thermal Maximum (PETM; around 56 million years ago) is often referenced as the closest analogue to the present CO₂ increase and related change in ocean chemistry. However, at the PETM, only about 2500–4500 PgC of CO₂ were released into the atmosphere over 4000 years. The rate of release was between 0.6 and 1.1 Pg/year (Zeebe et al, 2016) compared to the current 10 Pg/year. Thus, the relatively slower rate of CO₂ increase at the PETM likely led to relatively small change in carbonate ion concentration compared with contemporary acidification, due to the ability of rock weathering to buffer the change (Zeebe et al. 2016). However, others have argued that the PETM may have resulted from an abrupt pulse of CO₂, perhaps even faster than current emission rates, albeit with a lesser total emission volume (Wright and Shaller 2013).

13.2.6 Projected Changes

Projections indicate that in higher emissions pathways, such as SRES A1fi or RCP8.5, pH of the open surface ocean could be reduced from the current, average level of 8.1 to as low as an average of 7.8 by the end of the century (Fig 13.2), and the ocean volume occupied by corrosive waters could expand from 76% in the 1990s to 91% in 2100 (Gattuso et al. 2015). Regional changes in the rate of acidification may vary significantly from the global mean, however, with some regions acidifying faster than others (Turley et al. 2010). Recent observational data from the Arctic Basin show that the Beaufort Sea became undersaturated, for part of the year, with respect to aragonite in 2001, and the other continental shelf seas in the region will all acidify enough to become undersaturated, seasonally, with respect to aragonite by the end of the century (Chukchi Sea in about 2033; Bering Sea in about 2062); this undersaturation will put tremendous pressure on the diverse ecosystems that support some of the largest commercial and subsistence

fisheries in the world (Mathis et al. 2015). The Gulf of Maine will likely experience hypercapnia ($p\text{CO}_2 > 1000 \mu\text{atm}$) throughout much of the fall before 2100 (McNeil & Sasse 2016).

Earth System Models predict that surface waters of the Southern Polar Ocean will be undersaturated with respect to aragonite by 2100 (Caldeira and Wickett 2003; Orr et al. 2005). But, these projections are highly uncertain due to the lack of measurements in the Southern Ocean; more observational data are needed to better constrain the natural variability. Calcium carbonate saturation levels in the Western Antarctic Peninsula and the Arctic Ocean could decrease dramatically if there is increased freshwater from sea ice and glacier melt into the ocean (Chierici and Fransson 2009, Yamamoto-Kawai et al. 2009).

[INSERT FIGURE 13.2 HERE:]

Figure 13.2: Predicted change in pH in 2090–2099 relative to 1990–1999 under RCP8.5, based on the Community Earth System Models–Large Ensemble Experiments CMIP5. (Figure source: adapted from Bopp et al. 2013)]

13.3 Ocean Deoxygenation

13.3.1 General Background

Oxygen is essential to most life in the ocean, governing a host of biogeochemical and biological processes. Oxygen influences metabolic, physiological, reproductive, behavioral, and ecological processes, ultimately shaping the composition, diversity, abundance, and distribution of organisms from microbes to whales. Increasingly, climate-induced oxygen loss (deoxygenation) has become evident locally, regionally, and globally. Deoxygenation can be attributed to anthropogenic nutrient input as well as CO_2 emissions. In addition, acidification (section 13.2) can co-occur with deoxygenation as a result of warming-enhanced biological respiration (Breitburg et al. 2015). As organisms respire, O_2 is consumed and CO_2 is produced. Understanding the combined effect of both low O_2 and low pH on marine ecosystems is an area of active research (Gobler et al. 2014). Warming also raises biological metabolic rates which, in combination with intensified coastal and estuarine stratification, exacerbates eutrophication-induced hypoxia. We now see earlier onset and longer periods of seasonal hypoxia in many eutrophic sites, most of which occur in areas that are also warming (Altieri and Gedan 2015).

13.3.2 Climate Drivers of Ocean Deoxygenation

Global ocean deoxygenation is a direct effect of warming. Ocean warming reduces the solubility of oxygen (that is, warmer water can hold less oxygen). The increased temperature of global oceans accounts for about 15% of current global oxygen loss (Helm et al. 2011), although changes in temperature and oxygen are not uniform throughout the ocean (Roemmich et al. 2015). Warming also exerts direct influence on thermal stratification and enhances salinity stratification through ice melt and climate change-associated precipitation effects. Intensified stratification leads to reduced ventilation (mixing of oxygen into the ocean interior) and accounts

for up to 85% of global ocean oxygen loss (Helm et al. 2011). Effects of ocean temperature change and stratification on oxygen loss are strongest in intermediate or mode waters at bathyal depths (in general, 200–3000 meters), and also nearshore and in the open ocean; these changes are especially evident in tropical and subtropical waters globally, in the Eastern Pacific (Stramma et al. 2010), and in the Southern Ocean (Helm et al. 2011).

There are also other, less direct effects of global temperature increase. Warming on land reduces terrestrial plant water efficiency (through effects on stomata), leading to greater runoff into coastal zones and further enhancing hypoxia potential because greater run off means more nutrient transport (Reay et al. 2008). Warming can induce dissociation of frozen methane in gas hydrates buried on continental margins, leading to further drawdown of oxygen through aerobic methane oxidation in the water column (Boetius and Wenzhöfer 2013). On eastern ocean boundaries, warming enhances the land–sea temperature differential, causing increased upwelling due to higher winds with (a) greater nutrient input leading to production, sinking, decay, and biochemical drawdown of oxygen and (b) upwelling of naturally low-oxygen, high- CO_2 waters onto the upper slope and shelf environments (Sydeman et al. 2014, Feely et al. 2009). Taken together, the effects of warming are manifested as expanding and shoaling oxygen minimum zones (OMZs) in open waters and increased eutrophication-induced hypoxia in coastal areas.

Changes in precipitation, winds, circulation, airborne nutrients, and sea level can also contribute to ocean deoxygenation. Projected increases in precipitation in some regions will intensify stratification, reducing vertical mixing and ventilation, and intensify nutrient input to coastal waters through excess runoff. Coastal wetlands that might remove these nutrients before they reach the ocean may be lost through rising sea level, further exacerbating hypoxia. Some observations of oxygen decline are linked to regional changes in circulation involving low-oxygen water masses. Enhanced fluxes of airborne iron and nitrogen are interacting with natural climate variability and contributing to fertilization, enhanced respiration, and oxygen loss in the tropical Pacific (Ito et al. 2016). In contrast to the many sources of climate-induced oxygen loss, the projected increase in incidence and intensity of cyclones and hurricanes will induce mixing, which can ameliorate hypoxia locally (Rabalais et al. 2009).

13.3.3 Biogeochemical Feedbacks of Deoxygenation to Climate and Elemental Cycles

Climate patterns and ocean circulation have a large effect on global nitrogen and oxygen cycles, which in turn affect phosphorus and trace metal availability and generate feedbacks to the atmosphere and oceanic production. Climate-driven changes in the depth of the tropical and subtropical thermocline control the volume of suboxic waters (< 5 micromolar O_2), which in turn controls loss of fixed nitrogen through denitrification, influencing the supply of nitrite, which limits global ocean productivity (Codispoti et al. 2001; Deutsch et al. 2011). The extent of suboxia also regulates the production of the greenhouse gas nitrous oxide (N_2O); as oxygen declines, greater N_2O production may intensify global warming (Gruber 2008). Production of

hydrogen sulfide (H₂S, which is highly toxic) and intensified phosphorus recycling can occur at low oxygen levels (Wallmann 2003). Other feedbacks may emerge as OMZ shoaling diminishes the depths of diurnal vertical migrations by fish and invertebrates, and as their huge biomass and associated oxygen consumption deplete oxygen (Bianchi et al. 2013).

13.3.4 Past Trends

Over hundreds of millions of years, oxygen has varied dramatically in the atmosphere and ocean, and has been linked to the gain and loss of biodiversity (Knoll and Carroll 1999; McFall-Ngai et al. 2013). Variation in oxygenation in the paleo record is very sensitive to climate—with clear links to temperature and often CO₂ variation (Falkowski et al. 2011). OMZs expand and contract in synchrony with warming and cooling events, respectively (Robinson et al. 2007). Episodic climate events that involve rapid temperature increases over decades, followed by a cool period lasting a few hundred years, lead to major fluctuations in the intensity of Pacific and Indian Ocean oxygen minimum zones. These events are associated with rapid variations in North Atlantic Deep Water formation (Schmittner et al. 2007). Ocean oxygen fluctuates on glacial-interglacial timescales of thousands of years in the Eastern Pacific (Galbraith et al. 2004; Moffitt et al. 2015).

13.3.5 Modern observations (last 50+ years)

Long-term oxygen records made over the last 50 years reflect oxygen declines in inland seas (Justic et al. 1987; Zaitzev 1992; Conley et al. 2011), in estuaries (Brush 2009; Gilbert et al. 2005), and in coastal waters (Rabalais et al. 2007, 2010; Booth et al. 2012; Baden et al. 1990). The number of coastal, eutrophication-induced hypoxic sites in the United States has grown dramatically over the past 40 years (Diaz and Rosenberg 2008, Hypoxia Tracker). Over larger scales, global syntheses show hypoxic waters have expanded by 4.5 million km² at a depth of 200 meters (Stramma et al. 2010), with widespread loss of oxygen in the Southern Ocean (Helm et al. 2011), Western Pacific (Takatani et al. 2012), and North Atlantic (Stendardo and Gruber 2012). Overall oxygen declines have been greater in the coastal ocean than the open ocean (Gilbert et al. 2010) and often greater inshore than offshore (Bograd et al. 2015). The emergence of a deoxygenation signal in regions with naturally high oxygen variability will unfold over longer time periods (20 – 50 years from now) (Long et al. 2016).

13.3.6 Projected changes - Results from ocean models

GLOBAL MODELS

Global models generally agree that ocean deoxygenation is occurring; this finding is also reflected in in situ observations from past 50 years. Compilations of 10 Earth System models predict a global average loss of oxygen of –3.5% (for the RCP8.5 pathway) to –1.8% (RCP2.6) by 2100, but much stronger losses regionally, and in intermediate and mode waters (Bopp et al. 2013) (Figure 13.2). The North Pacific, North Atlantic, Southern Ocean, subtropical South

Pacific, and South Indian Oceans all are expected to experience deoxygenation, with O₂ decreases of as much as 17% in the North Pacific by 2100 for the RCP8.5 pathway. However, the tropical Atlantic and tropical Indian Oceans show increasing O₂ concentrations. In the many areas where oxygen is declining, high natural variability makes it difficult to identify anthropogenically forced trends (Long et al. 2016).

[INSERT FIGURE 13.3 HERE:]

Figure 13.3: Predicted change between the periods 1981–2000 and 2081–2100 in dissolved oxygen, based on the Community Earth System Models – Large Ensemble Experiments. (Figure source: redrawn from Long et al. 2016)]

REGIONAL MODELS

Regional models are critical because many oxygen drivers are local, influenced by bathymetry, winds, circulation, and fresh water and nutrient inputs. Most eastern boundary upwelling areas are predicted to experience intensified upwelling to 2100 (Wang et al. 2015).

Particularly notable for the western United States, variation in trade winds in the eastern Pacific can affect nutrient inputs, leading to centennial periods of oxygen decline or oxygen increase distinct from global oxygen decline (Deutsch et al. 2014). Oxygen dynamics in the Eastern Tropical Pacific are highly sensitive to equatorial circulation changes (Montes et al. 2014).

Regional modeling also shows that year-to-year variability in precipitation in the central United States affects the nitrate–N flux by the Mississippi River and the extent of hypoxia in the Gulf of Mexico (Donner and Scavia 2007). A host of climate influences linked to warming and increased precipitation are predicted to lower dissolved oxygen in Chesapeake Bay (Najjar et al. 2010).

TRACEABLE ACCOUNTS

Key Finding 1

The world's oceans have absorbed more than 90% of the excess heat caused by greenhouse warming since the mid 20th Century, making them warmer and altering global and regional circulation patterns and climate feedbacks (*very high confidence*). Surface oceans have warmed by about 0.45°F (0.25°C) globally since the 1970s (*very high confidence*). The Atlantic meridional overturning circulation (AMOC) has slowed since preindustrial times (*high confidence*). Regionally, eastern boundary upwelling, such as along the U.S. West Coast, that sustains fisheries and controls local climate has intensified (*high confidence*).

Description of evidence base

The Key Finding and supporting text summarizes the evidence documented in climate science literature, including IPCC 2013 and thereafter. The oceanic warming has been documented in a variety of data sources, most notably the WOCE (<http://www.nodc.noaa.gov/woce/wdiu/>) and the ARGO database (<https://www.nodc.noaa.gov/argo/>). The AMOC changes over the 20th Century are inferred from a number of high quality SST observations and a suite of climate models that participated in IPCC 2013 (Rahmstorf et al. 2015). The eastern boundary upwelling trends are based on a number of observational studies which looked at intensification of upwelling favorable winds along the eastern boundaries (Garcia-Reyes et al. 2015, Sydenman et al. 2014a).

Major uncertainties

Uncertainties in the magnitude of ocean warming stem from the disparate measurements over the last century. There is less uncertainty in 0–700 m warming trends, whereas there is only a short record of measurements from 700–2000 m. Data on warming trends in the deep ocean are even more sparse (Roemmich et al. 2015). The estimated change of the strength of the AMOC of about 2 Sv over the 20th Century is made using an inferred method (Rahmstorf et al. 2015) and not direct observations of AMOC. Direct observational records are short (after 2004, RAPID array). There are regional uncertainties in the magnitude of the eastern boundary intensification associated with uncertainties in the measurement of the wind speeds (Sydenman et al. 2014a).

Assessment of confidence based on evidence and agreement, including short description of nature of evidence and level of agreement

x Very High

☐ High

☐ Medium

☐ Low

Confidence on ocean warming is *very high* based on the agreement of different methods. AMOC and eastern boundary upwelling changes are indirectly estimated, but based on high quality measurements, hence the high confidence.

Summary sentence or paragraph that integrates the above information

We have *very high confidence* in measurements that show that the oceans are warming, the overturning circulation is slowing down, and the eastern boundary upwelling is intensified.

Key Finding 2

The world's oceans are currently absorbing more than a quarter of the carbon dioxide emitted to the atmosphere annually from human activities (*very high confidence*), making them more acidic with potential detrimental impacts to marine ecosystems. The rate of acidification is unparalleled in at least the past 66 million years (*medium confidence*). Acidification is regionally increased along U.S. coastal systems as a result of intensified upwelling (for example, in the Pacific Northwest) (*high confidence*), changes in freshwater inputs (for example, Gulf of Maine) (*medium confidence*), and nutrient input (for example, urbanized estuaries) (*high confidence*).

Description of evidence base

The Key Finding and supporting text summarizes the evidence documented in climate science literature, including IPCC 2013 and thereafter. Evidence with regards to the magnitude of the ocean sink is obtained from multiple biogeochemical and transport ocean models, and two observation-based estimates from the 1990s for the uptake of the anthropogenic CO₂. Estimates of the carbonate system (DIC and Alkalinity) were based on multiple survey cruises in the global ocean in the 1990s (WOCE, JGOFS). The data is available from the Carbon Dioxide Information Analysis Center (<http://cdiac.esd.ornl.gov/oceans/>). Rates of change associated with the Palaeocene-Eocene Thermal Maximum (PETM, 56 mya) were derived using stable carbon and oxygen isotope records preserved in the sedimentary record from the New Jersey shelf using time series analysis and carbon cycle–climate modelling. This evidence supports a carbon release during the onset of the PETM over no less than 4,000 years, yielding a maximum sustained carbon release rate of less than 1.1 Pg C yr⁻¹ (Zeebe R. et al. 2016). Evidence for increased upwelling along Pacific Northwest has been documented (Feely et al. 2008; Harris et al. 2013)

Major uncertainties

In 2014 the ocean sink was 2.6 ± 0.5 GtC (10.6 GtCO₂), equivalent to 26% of the total emissions attributed to fossil fuel use and land use changes (Le Quéré et al. 2015). Estimates of PETM ocean acidification event evidenced in the geological record remains a matter of some debate within the community. Evidence for the 1.1 Pg C yr⁻¹ cited by Zeebe et al. (2016), could be biased as a result of brief pulses of carbon input above average rates of emissions where they to transpire on timescales ≤ 40 years.

Assessment of confidence based on evidence and agreement, including short description of nature of evidence and level of agreement

☐ Very High

☒ High

1 ☐ Medium

2 ☐ Low

3 The magnitude of the ocean carbon sink is known at a *high confidence* level because it is
4 estimated using a series of disparate data sources and methods of analysis, while the magnitude
5 of the interannual variability is based only on model studies.

6 **Summary sentence or paragraph that integrates the above information**

7 We have *very high confidence* in evidence that the oceans absorb about a quarter of the carbon
8 dioxide emitted in the atmosphere and hence become more acidic. Current climate acidification
9 is unprecedented in the past 66 million years.

10

11 **Key Finding 3**

12 Increasing sea surface temperatures, rising sea levels, and changing patterns of precipitation,
13 winds, nutrients, and ocean circulation are contributing to overall declining oxygen
14 concentrations at intermediate depths in various ocean locations and in many coastal areas. Over
15 the last half century, major oxygen losses have occurred in inland seas, estuaries, and in the
16 coastal and open ocean (*high confidence*).

17 **Description of evidence base**

18 The Key Finding and supporting text summarizes the evidence documented in climate science
19 literature including IPCC 2013 and thereafter. Evidence arises from extensive global
20 measurements of the World Ocean Circulation Experiment (WOCE) after 1989 and individual
21 profiles before that (Helm et al. 2011). Uncertainties in long-term decreases of the global
22 averaged oxygen concentration amount to 25% in the upper 1000 m for the period 1970–1992
23 and 28% for the period 1993–2003.

24 **Major uncertainties**

25 Remaining uncertainties relate to regional variability driven by mesoscale eddies and intrinsic
26 climate variability such as ENSO.

27 **Assessment of confidence based on evidence and agreement, including short description of
28 nature of evidence and level of agreement**

29 ☐ Very High

30 x High

31 ☐ Medium

32 ☐ Low

33 Confidence levels for the uncertainties quoted above are based on the 90th percentile.

34

Summary sentence or paragraph that integrates the above information

Major ocean deoxygenation is taking place in bodies of water inland, at estuaries, and in the coastal and the open ocean. Regionally, the phenomenon is exacerbated by local changes in weather, ocean circulation and continental inputs to the oceans.

Key Finding 4

In coastal regions, local biogeochemical processes can result in increased acidification co-occurring with eutrophication and/or where riverine loads include naturally corrosive materials of geological origin. All local areas of deoxygenation also tend to be areas of acidification, due to intensified respiration (*very high confidence*).

Description of evidence base

Coastal carbon and acidification surveys have been executed along the U.S. coastal Large Marine Ecosystem since at least 2007, documenting significantly elevated pCO₂ and low pH conditions relative to oceanic waters. Data are archived and available for public access at NOAA NCEI (<http://www.nodc.noaa.gov/oceanacidification/>). Based on these data the relative importance of respiratory DIC has been described within numerous studies including Feely et al. 2008; Hauri et al. 2009 2013; and Gruber et al. 2012.

Major uncertainties

Coastal waters exhibit considerable high frequency variability (both time and space) in carbonate and oxygen dynamics which is poorly constrained by the existing U.S. observing assets, making it difficult to determine the full range of conditions exposed to organisms in these waters. Furthermore, most observing assets provide only surface measures which may underestimate of the corrosive conditions experienced by marine organisms at depth or at the benthos. Quantifying both the magnitudes and trends in nutrient supply to the coast via both terrestrial input and upwelling remains a central challenge to contemporary coastal biogeochemistry and coastal oceanography science.

Assessment of confidence based on evidence and agreement, including short description of nature of evidence and level of agreement

x Very High

☐ High

☐ Medium

☐ Low

The fact that respiratory processes significantly alter the local oxygen and carbonate chemistry conditions has been well established and is documented in the rich history of coastal biogeochemistry literature dating since at least the second half of the twentieth century (Zhang 2014).

Summary sentence or paragraph that integrates the above information

TBD

Key Finding 5

Under a high future scenario (RCP8.5), the AMOC is projected to decline by 6 Sverdrups ($1 \times 10^6 \text{ m}^3/\text{sec}$), global average ocean acidity is projected to increase by 100% to 150%) (*very high confidence*), and ocean oxygen levels are projected to decrease by 4% (*high confidence*) by 2100 relative to preindustrial values. Under a low future scenario (RCP2.6), global average ocean acidity is projected to increase by 35% and oxygen projected to decrease by 2% by 2100. Larger acidity increases and oxygen declines are projected in some regions and in intermediate and mode waters (*medium confidence*).

Description of evidence base

The Key Finding is based on evidence from 10 of the latest generation Earth System Models which include 6 distinct biogeochemical models that were included in the latest IPCC (2014) Assessment Report.

Major uncertainties

Uncertainties (as estimated from the inter-model spread) in the global mean are moderate mainly because when ocean oxygen content exhibits low interannual variability when globally averaged.

Assessment of confidence based on evidence and agreement, including short description of nature of evidence and level of agreement☐ Very High☒ High☐ Medium☐ Low

The confidence level is based on globally integrated O₂ distributions in a variety of ocean models. Although the global mean exhibits low interannual variability, regional contrasts which are large.

Summary sentence or paragraph that integrates the above information

For the 21st Century, ocean overturning circulation is expected to slow down and oceanic pH and oxygen concentrations will continue decrease.

1 FIGURES

Trends in Surface Ocean Carbonate Chemistry

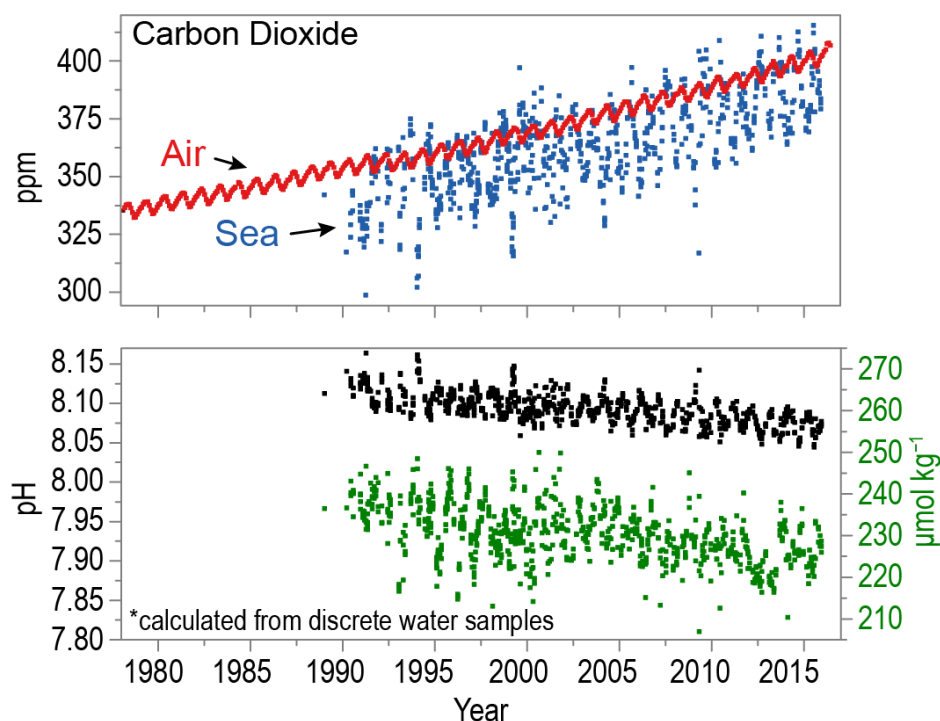


Figure 13.1: Trends in surface (< 50 m) ocean carbonate chemistry calculated from observations obtained at the Hawai‘i Ocean Time-series (HOT) Program in the North Pacific 1988–2015. Data obtained from the Hawai‘i Ocean Time-series Data Organization & Graphical System (HOT-DOGS, <http://hahana.soest.hawaii.edu/hot/hot-dogs/index.html>). Seawater $x\text{CO}_2$ (μatm), pH_{Total} , and carbonate ion concentration ($\mu\text{mol/kg}$) were derived using CO2SYS v2.1 by pairing direct measures of total alkalinity (TA) with dissolved inorganic carbon (DIC) when available ($n = 824$). In cases where this pairing was not possible, then pH and DIC were instead adopted ($n = 16$). As a final option, if neither of those pairings was an option then pH_{Total} and TA were adopted ($n = 18$). The calculations were performed using K_1 , K_2 from Millero, 2010, the KHSO_4 dissociation constant of Dickon, total scale pH, and Uppstrom, 1974 for $[\text{B}]_{\text{T}}$. Atmospheric mole fraction CO_2 (red) were obtained from NOAA’s Earth System Research Laboratory CarbonTracker (Peters et al. 2007). (Figure source: NOAA).

Cites for Figure 13.1:

Peters *et al.*, 2007, "An atmospheric perspective on North American carbon dioxide exchange: CarbonTracker", *PNAS*, November 27, 2007, vol. 104, no. 48, 18925-18930, with updates documented at <http://carbontracker.noaa.gov>.

Dickson, *Journal of Chemical Thermodynamics*, 22:113-127, 1990.

Millero, *Marine and Freshwater Research*, v. 61, p. 139-142, 2010

Dickson, A. G. and Riley, J. P., *Marine Chemistry* 7:89-99, 1979.

Uppstrom, Leif, *Deep-Sea Research* 21:161-162, 1974

b. Surface pH in 2090s (RCP8.5, changes from 1990s)

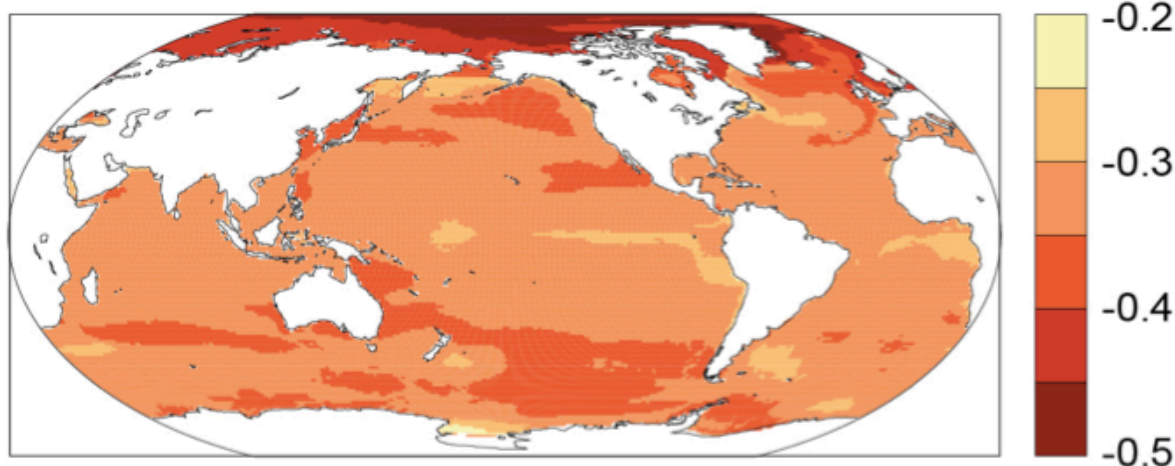


Figure 13.2 Predicted change in pH in 2090–2099 relative to 1990–1999 under RCP8.5, based on the Community Earth System Models – Large Ensemble Experiments CMIP5 (Figure source: adapted from Bopp *et al.* 2013).

Projected Change in Dissolved Oxygen

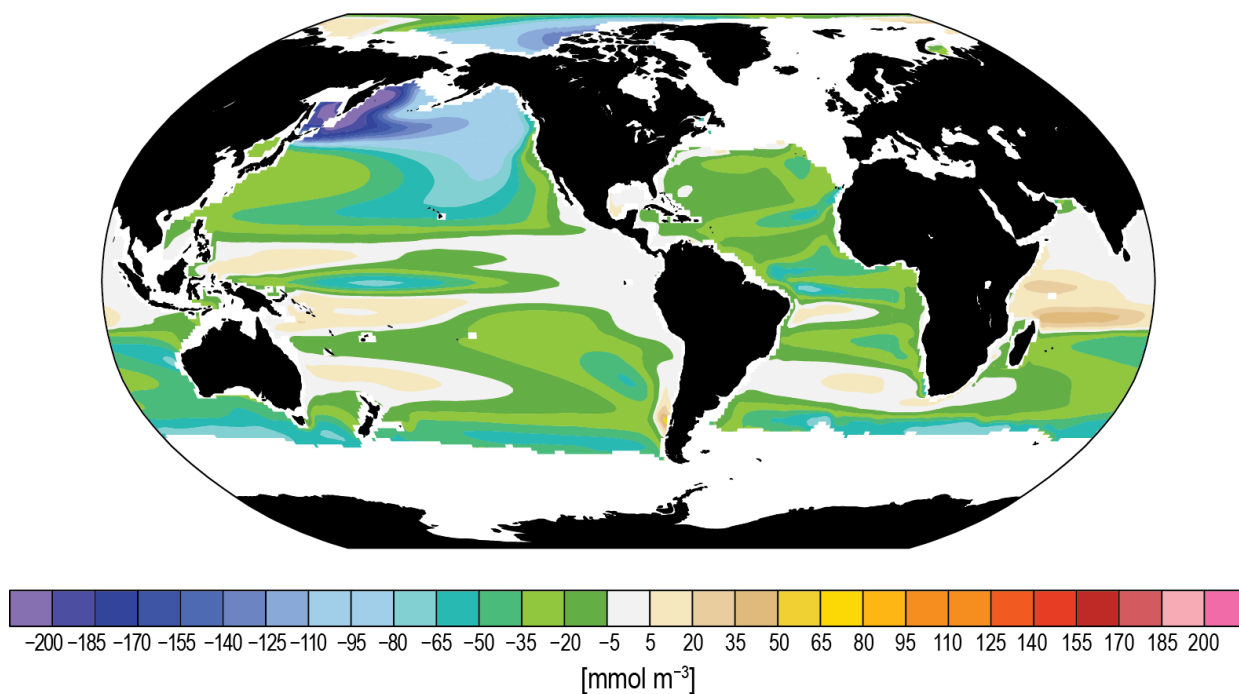


Figure 13.3: Predicted change between the periods 1981–2000 and 2081–2100 in dissolved oxygen, based on the Community Earth System Models – Large Ensemble Experiments (Figure source: redrawn from Long et al. 2016).

1 REFERENCES

- 2 Altieri, A.H. and K.B. Gedan, 2015: Climate change and dead zones. *Global Change Biology*,
 3 **21**, 1395-1406. <http://dx.doi.org/10.1111/gcb.12754>
- 4 Baden, S.P., L.O. Loo, L. Pihl, and R. Rosenberg, 1990: Effects of eutrophication on benthic
 5 communities including fish — Swedish west coast. *Ambio*, **19**, 113-122.
 6 www.jstor.org/stable/4313676
- 7 Bakun, A., B.A. Black, S.J. Bograd, M. García-Reyes, A.J. Miller, R.R. Rykaczewski, and W.J.
 8 Sydeman, 2015: Anticipated Effects of Climate Change on Coastal Upwelling Ecosystems.
 9 *Current Climate Change Reports*, **1**, 85-93. <http://dx.doi.org/10.1007/s40641-015-0008-4>
- 10 Bates, N.R., Y.M. Astor, M.J. Church, K. Currie, J.E. Dore, M. González-Dávila, L. Lorenzoni,
 11 F. Muller-Karger, J. Olafsson, and J.M. Santana-Casiano, 2014: A time-series view of
 12 changing ocean chemistry due to ocean uptake of anthropogenic CO₂ and ocean
 13 acidification. *Oceanography*, **27**, 126–141. <http://dx.doi.org/10.5670/oceanog.2014.16>
- 14 Bates, N.R. and J.T. Mathis, 2009: The Arctic Ocean marine carbon cycle: evaluation of air-sea
 15 CO₂ exchanges, ocean acidification impacts and potential feedbacks.
 16 *Biogeosciences*, **6**, 2433-2459. <http://dx.doi.org/10.5194/bg-6-2433-2009>
- 17 Bianchi, D., E.D. Galbraith, D.A. Carozza, K.A.S. Mislan, and C.A. Stock, 2013: Intensification
 18 of open-ocean oxygen depletion by vertically migrating animals. *Nature Geoscience*, **6**, 545-
 19 548. <http://dx.doi.org/10.1038/ngeo1837>
- 20 Boetius, A. and F. Wenzhofer, 2013: Seafloor oxygen consumption fuelled by methane from
 21 cold seeps. *Nature Geoscience*, **6**, 725-734. <http://dx.doi.org/10.1038/ngeo1926>
- 22 Bograd, S.J., M.P. Buil, E.D. Lorenzo, C.G. Castro, I.D. Schroeder, R. Goericke, C.R. Anderson,
 23 C. Benitez-Nelson, and F.A. Whitney, 2015: Changes in source waters to the Southern
 24 California Bight. *Deep Sea Research Part II: Topical Studies in Oceanography*, **112**, 42-52.
 25 <http://dx.doi.org/10.1016/j.dsr2.2014.04.009>
- 26 Booth, J.A.T., E.E. McPhee-Shaw, P. Chua, E. Kingsley, M. Denny, R. Phillips, S.J. Bograd,
 27 L.D. Zeidberg, and W.F. Gilly, 2012: Natural intrusions of hypoxic, low pH water into
 28 nearshore marine environments on the California coast. *Continental Shelf Research*, **45**, 108-
 29 115. <http://dx.doi.org/10.1016/j.csr.2012.06.009>
 30 www.sciencedirect.com/science/article/pii/S0278434312001653
- 31 Bopp, L., L. Resplandy, J.C. Orr, S.C. Doney, J.P. Dunne, M. Gehlen, P. Halloran, C. Heinze, T.
 32 Ilyina, R. Séférian, J. Tjiputra, and M. Vichi, 2013: Multiple stressors of ocean ecosystems in
 33 the 21st century: projections with CMIP5 models. *Biogeosciences*, **10**, 6225-6245.
 34 <http://dx.doi.org/10.5194/bg-10-6225-2013>

- 1 Borges, A.V. and N. Gypens, 2010: Carbonate chemistry in the coastal zone responds more
2 strongly to eutrophication than ocean acidification. *Limnology and Oceanography*, **55**, 346-
3 353. <http://dx.doi.org/10.4319/lo.2010.55.1.0346>
- 4 Breitburg, D.L., J. Salisbury, J.M. Bernhard, W.-J. Cai, S. Dupont, S.C. Doney, K.J. Kroeker,
5 L.A. Levin, W.C. Long, L.M. Milke, S.H. Miller, B. Phelan, U. Passow, B.A. Seibel, A.E.
6 Todgham, and A.M. Tarrant, 2015: And on Top of All That... Coping with Ocean
7 Acidification in the Midst of Many Stressors. *Oceanography*, **28**, 48-61.
8 <http://dx.doi.org/10.5670/oceanog.2015.31>
- 9 Brush, G.S., 2009: Historical Land Use, Nitrogen, and Coastal Eutrophication: A
10 Paleocological Perspective. *Estuaries and Coasts*, **32**, 18-28.
11 <http://dx.doi.org/10.1007/s12237-008-9106-z>
- 12 Caldeira, K. and M.E. Wickett, 2003: Anthropogenic carbon and ocean pH. *Nature*, **425**, 365.
- 13 Chiapello, I., 2014: Dust Observations and Climatology. *Mineral Dust: A Key Player in the*
14 *Earth System*. Knippertz, P. and J.-B.W. Stuut, Eds. Springer Netherlands, Dordrecht, 149-
15 177. http://dx.doi.org/10.1007/978-94-017-8978-3_7
- 16 Chierici, M. and A. Fransson, 2009: Calcium carbonate saturation in the surface water of the
17 Arctic Ocean: undersaturation in freshwater influenced shelves. *Biogeosciences*, **6**, 2421-
18 2431. <http://dx.doi.org/10.5194/bg-6-2421-2009>
- 19 Chollett, I., F.E. Müller-Karger, S.F. Heron, W. Skirving, and P.J. Mumby, 2012: Seasonal and
20 spatial heterogeneity of recent sea surface temperature trends in the Caribbean Sea and
21 southeast Gulf of Mexico. *Marine Pollution Bulletin*, **64**, 956-965.
22 <http://dx.doi.org/10.1016/j.marpolbul.2012.02.016>
23 www.sciencedirect.com/science/article/pii/S0025326X1200094X
- 24 Ciais, P., C. Sabine, G. Bala, L. Bopp, V. Brovkin, J. Canadell, A. Chhabra, R. DeFries, J.
25 Galloway, M. Heimann, C. Jones, C. Le Quéré, R.B. Myneni, S. Piao, and P. Thornton,
26 2013: Carbon and Other Biogeochemical Cycles. *Climate Change 2013: The Physical*
27 *Science Basis. Contribution of Working Group I to the Fifth Assessment Report of the*
28 *Intergovernmental Panel on Climate Change*. Stocker, T.F., D. Qin, G.-K. Plattner, M.
29 Tignor, S.K. Allen, J. Boschung, A. Nauels, Y. Xia, V. Bex, and P.M. Midgley, Eds.
30 Cambridge University Press, Cambridge, United Kingdom and New York, NY, USA, 465-
31 570. <http://dx.doi.org/10.1017/CBO9781107415324.015> www.climatechange2013.org
- 32 Codispoti, L.A., J.A. Brandes, J.P. Christensen, A.H. Devol, S.W.A. Naqvi, H.W. Paerl, and T.
33 Yoshinari, 2001: The oceanic fixed nitrogen and nitrous oxide budgets: Moving targets as we
34 enter the anthropocene? *Scientia Marina*, **65**, 85-105.

- 1 <http://dx.doi.org/10.3989/scimar.2001.65s285>
2 scientiamarina.revistas.csic.es/index.php/scientiamarina/article/view/684/700
- 3 Conley, D.J., J. Carstensen, J. Aigars, P. Axe, E. Bonsdorff, T. Eremina, B.-M. Haahti, C.
4 Humborg, P. Jonsson, J. Kotta, C. Lännegren, U. Larsson, A. Maximov, M.R. Medina, E.
5 Lysiak-Pastuszek, N. Remeikaitė-Nikienė, J. Walve, S. Wilhelms, and L. Zillén, 2011:
6 Hypoxia Is Increasing in the Coastal Zone of the Baltic Sea. *Environmental Science &*
7 *Technology*, **45**, 6777-6783. <http://dx.doi.org/10.1021/es201212r>
- 8 Deutsch, C., W. Berelson, R. Thunell, T. Weber, C. Tems, J. McManus, J. Crusius, T. Ito, T.
9 Baumgartner, V. Ferreira, J. Mey, and A. van Geen, 2014: Centennial changes in North
10 Pacific anoxia linked to tropical trade winds. *Science*, **345**, 665-668.
11 <http://dx.doi.org/10.1126/science.1252332>
- 12 Deutsch, C., H. Brix, T. Ito, H. Frenzel, and L. Thompson, 2011: Climate-Forced Variability of
13 Ocean Hypoxia. *Science*, **333**, 336-339. <http://dx.doi.org/10.1126/science.1202422>
- 14 Diaz, R.J. and R. Rosenberg, 2008: Spreading dead zones and consequences for marine
15 ecosystems. *Science*, **321**, 926-929. <http://dx.doi.org/10.1126/science.1156401>
- 16 Donner, S.D. and D. Scavia, 2007: How climate controls the flux of nitrogen by the Mississippi
17 River and the development of hypoxia in the Gulf of Mexico. *Limnology and Oceanography*,
18 **52**, 856-861. <http://dx.doi.org/10.4319/lo.2007.52.2.0856>
- 19 Falkowski, P.G., T. Algeo, L. Codispoti, C. Deutsch, S. Emerson, B. Hales, R.B. Huey, W.J.
20 Jenkins, L.R. Kump, L.A. Levin, T.W. Lyons, N.B. Nelson, O.S. Schofield, R. Summons,
21 L.D. Talley, E. Thomas, F. Whitney, and C.B. Pilcher, 2011: Ocean deoxygenation: Past,
22 present, and future. *Eos, Transactions American Geophysical Union*, **92**, 409-410.
23 <http://dx.doi.org/10.1029/2011EO460001>
- 24 Feely, R.A., S.C. Doney, and S.R. Cooley, 2009: Ocean acidification: Present conditions and
25 future changes in a high-CO₂ world. *Oceanography*, **22**, 36-47.
26 <http://dx.doi.org/10.5670/oceanog.2009.95> [www.tos.org/oceanography/archive/22-](http://www.tos.org/oceanography/archive/22-4_feely.pdf)
27 [4_feely.pdf](http://www.tos.org/oceanography/archive/22-4_feely.pdf)
- 28 Feely, R.A., C.L. Sabine, J.M. Hernandez-Ayon, D. Ianson, and B. Hales, 2008: Evidence for
29 Upwelling of Corrosive "Acidified" Water onto the Continental Shelf. *Science*, **320**, 1490-
30 1492. <http://dx.doi.org/10.1126/science.1155676>
- 31 Feely, R.A., C.L. Sabine, K. Lee, W. Berelson, J. Kleypas, V.J. Fabry, and F.J. Millero, 2004:
32 Impact of Anthropogenic CO₂ on the CaCO₃ System in the
33 Oceans. *Science*, **305**, 362-366. <http://dx.doi.org/10.1126/science.1097329>

- 1 Friedrich, T., A. Timmermann, A. Abe-Ouchi, N.R. Bates, M.O. Chikamoto, M.J. Church, J.E.
2 Dore, D.K. Gledhill, M. Gonzalez-Davila, M. Heinemann, T. Ilyina, J.H. Jungclaus, E.
3 McLeod, A. Mouchet, and J.M. Santana-Casiano, 2012: Detecting regional anthropogenic
4 trends in ocean acidification against natural variability. *Nature Climate Change*, **2**, 167-171.
5 <http://dx.doi.org/10.1038/nclimate1372>
- 6 Galbraith, E.D., M. Kienast, T.F. Pedersen, and S.E. Calvert, 2004: Glacial-interglacial
7 modulation of the marine nitrogen cycle by high-latitude O₂ supply to the global
8 thermocline. *Paleoceanography*, **19**, n/a-n/a. <http://dx.doi.org/10.1029/2003PA001000>
- 9 García-Reyes, M., W.J. Sydeman, D.S. Schoeman, R.R. Rykaczewski, B.A. Black, A.J. Smit,
10 and S.J. Bograd, 2015: Under Pressure: Climate Change, Upwelling, and Eastern Boundary
11 Upwelling Ecosystems. *Frontiers in Marine Science*, **2**.
12 <http://dx.doi.org/10.3389/fmars.2015.00109>
- 13 Gattuso, J.-P., A. Magnan, R. Billé, W.W.L. Cheung, E.L. Howes, F. Joos, D. Allemand, L.
14 Bopp, S.R. Cooley, C.M. Eakin, O. Hoegh-Guldberg, R.P. Kelly, H.-O. Pörtner, A.D.
15 Rogers, J.M. Baxter, D. Laffoley, D. Osborn, A. Rankovic, J. Rochette, U.R. Sumaila, S.
16 Treyer, and C. Turley, 2015: Contrasting futures for ocean and society from different
17 anthropogenic CO₂ emissions scenarios. *Science*, **349**.
18 <http://dx.doi.org/10.1126/science.aac4722>
- 19 Gilbert, D., N.N. Rabalais, R.J. Díaz, and J. Zhang, 2010: Evidence for greater oxygen decline
20 rates in the coastal ocean than in the open ocean. *Biogeosciences*, **7**, 2283-2296.
21 <http://dx.doi.org/10.5194/bg-7-2283-2010>
- 22 Gilbert, D., B. Sundby, C. Gobeil, A. Mucci, and G.-H. Tremblay, 2005: A seventy-two-year
23 record of diminishing deep-water oxygen in the St. Lawrence estuary: The northwest Atlantic
24 connection. *Limnology and Oceanography*, **50**, 1654-1666.
25 <http://dx.doi.org/10.4319/lo.2005.50.5.1654>
- 26 Gledhill, D.K., M.M. White, J. Salisbury, H. Thomas, I. Mlsna, M. Liebman, B. Mook, J. Grear,
27 A.C. Candelmo, R.C. Chambers, C.J. Gobler, C.W. Hunt, A.L. King, N.N. Price, S.R.
28 Signorini, E. Stancioff, C. Stymiest, R.A. Wahle, J.D. Waller, N.D. Rebeck, Z.A. Wang, T.L.
29 Capson, J.R. Morrison, S.R. Cooley, and S.C. Doney, 2015: Ocean and coastal acidification
30 off New England and Nova Scotia. *Oceanography*, **28**, 182-197.
31 <http://dx.doi.org/10.5670/oceanog.2015.41> [tos.org/oceanography/assets/docs/28-](http://tos.org/oceanography/assets/docs/28-2_gledhill.pdf)
32 [2_gledhill.pdf](http://tos.org/oceanography/assets/docs/28-2_gledhill.pdf)
- 33 Gobler, C.J., E.L. DePasquale, A.W. Griffith, and H. Baumann, 2014: Hypoxia and Acidification
34 Have Additive and Synergistic Negative Effects on the Growth, Survival, and
35 Metamorphosis of Early Life Stage Bivalves. *PLoS ONE*, **9**, e83648.
36 <http://dx.doi.org/10.1371/journal.pone.0083648>

- 1 Gruber, N., 2008: Chapter 1 - The Marine Nitrogen Cycle: Overview and Challenges. *Nitrogen*
2 *in the Marine Environment (2nd Edition)*. Academic Press, San Diego, 1-50.
3 <http://dx.doi.org/10.1016/B978-0-12-372522-6.00001-3>
- 4 Gruber, N., C. Hauri, Z. Lachkar, D. Loher, T.L. Frölicher, and G.K. Plattner, 2012: Rapid
5 progression of ocean acidification in the California Current System. *Science*, **337**, 220-223.
6 <http://dx.doi.org/10.1126/science.1216773> www.sciencemag.org/content/337/6091/220.short
- 7 Harris, K.E., M.D. DeGrandpre, and B. Hales, 2013: Aragonite saturation state dynamics in a
8 coastal upwelling zone. *Geophysical Research Letters*, **40**, 2720-2725.
9 <http://dx.doi.org/10.1002/grl.50460>
- 10 Hauri, C., N. Gruber, A.M.P. McDonnell, and M. Vogt, 2013: The intensity, duration, and
11 severity of low aragonite saturation state events on the California continental shelf.
12 *Geophysical Research Letters*, **40**, 3424-3428. <http://dx.doi.org/10.1002/grl.50618>
- 13 Hauri, C., N. Gruber, G.-K. Plattner, S. Alin, R.A. Feely, B. Hales, and P.A. Wheeler, 2009:
14 Ocean acidification in the California Current System. *Oceanography*, **22**, 60-71.
15 <http://dx.doi.org/10.5670/oceanog.2009.97>
- 16 Helm, K.P., N.L. Bindoff, and J.A. Church, 2011: Observed decreases in oxygen content of the
17 global ocean. *Geophysical Research Letters*, **38**, n/a-n/a.
18 <http://dx.doi.org/10.1029/2011GL049513>
- 19 Hendriks, I.E., C.M. Duarte, Y.S. Olsen, A. Steckbauer, L. Ramajo, T.S. Moore, J.A. Trotter,
20 and M. McCulloch, 2015: Biological mechanisms supporting adaptation to ocean
21 acidification in coastal ecosystems. *Estuarine, Coastal and Shelf Science*, **152**, A1-A8.
22 <http://dx.doi.org/10.1016/j.ecss.2014.07.019>
- 23 Hoegh-Guldberg, O., R. Cai, E.S. Poloczanska, P.G. Brewer, S. Sundby, K. Hilmi, V.J. Fabry,
24 and S. Jung, 2014: The Ocean--Supplementary material. *Climate Change 2014: Impacts,*
25 *Adaptation, and Vulnerability. Part B: Regional Aspects. Contribution of Working Group II*
26 *to the Fifth Assessment Report of the Intergovernmental Panel of Climate Change*. Barros,
27 V.R., C.B. Field, D.J. Dokken, M.D. Mastrandrea, K.J. Mach, T.E. Bilir, M. Chatterjee, K.L.
28 Ebi, Y.O. Estrada, R.C. Genova, B. Girma, E.S. Kissel, A.N. Levy, S. MacCracken, P.R.
29 Mastrandrea, and L.L. White, Eds. Cambridge University Press, Cambridge, United
30 Kingdom and New York, NY, USA, 1655-1731. [ipcc.ch/pdf/assessment-](http://ipcc.ch/pdf/assessment-report/ar5/wg2/supplementary/WGIIAR5-Chap30_OLSM.pdf)
31 [report/ar5/wg2/supplementary/WGIIAR5-Chap30_OLSM.pdf](http://ipcc.ch/pdf/assessment-report/ar5/wg2/supplementary/WGIIAR5-Chap30_OLSM.pdf)
- 32 Hönisch, B., A. Ridgwell, D.N. Schmidt, E. Thomas, S.J. Gibbs, A. Sluijs, R. Zeebe, L. Kump,
33 R.C. Martindale, S.E. Greene, W. Kiessling, J. Ries, J.C. Zachos, D.L. Royer, S. Barker,
34 T.M.M. Jr., R. Moyer, C. Pelejero, P. Ziveri, G.L. Foster, and B. Williams, 2012: The

- geological record of ocean acidification. *Science*, **335**, 1058-1063.
<http://dx.doi.org/10.1126/science.1208277>
- IPCC, 2014: Climate Change 2013: The Physical Science Basis. Contribution of Working Group I to the Fifth Assessment Report of the Intergovernmental Panel on Climate Change. Stocker, T.F., D. Qin, G.-K. Plattner, M. Tignor, S.K. Allen, J. Boschung, A. Nauels, Y. Xia, V. Bex, and P.M. Midgley (Eds.), 1535 pp. Cambridge University Press, Cambridge, UK and New York, NY. www.climatechange2013.org
- Ito, T., A. Nenes, M.S. Johnson, N. Meskhidze, and C. Deutsch, 2016: Acceleration of oxygen decline in the tropical Pacific over the past decades by aerosol pollutants. *Nature Geosci*, **9**, 443-447. <http://dx.doi.org/10.1038/ngeo2717>
- Jacox, M.G., A.M. Moore, C.A. Edwards, and J. Fiechter, 2014: Spatially resolved upwelling in the California Current System and its connections to climate variability. *Geophysical Research Letters*, **41**, 3189-3196. <http://dx.doi.org/10.1002/2014GL059589>
- Jiang, L.-Q., W.-J. Cai, R.A. Feely, Y. Wang, X. Guo, D.K. Gledhill, X. Hu, F. Arzayus, F. Chen, J. Hartmann, and L. Zhang, 2010: Carbonate mineral saturation states along the U.S. East Coast. *Limnology and Oceanography*, **55**, 2424-2432.
<http://dx.doi.org/10.4319/lo.2010.55.6.2424>
- Jickells, T. and C.M. Moore, 2015: The Importance of Atmospheric Deposition for Ocean Productivity. *Annual Review of Ecology, Evolution, and Systematics*, **46**, 481-501.
<http://dx.doi.org/10.1146/annurev-ecolsys-112414-054118>
- Justić, D., T. Legović, and L. Rottini-Sandrini, 1987: Trends in oxygen content 1911–1984 and occurrence of benthic mortality in the northern Adriatic Sea. *Estuarine, Coastal and Shelf Science*, **25**, 435-445. [http://dx.doi.org/10.1016/0272-7714\(87\)90035-7](http://dx.doi.org/10.1016/0272-7714(87)90035-7)
- Knoll, A.H. and S.B. Carroll, 1999: Early Animal Evolution: Emerging Views from Comparative Biology and Geology. *Science*, **284**, 2129-2137.
<http://dx.doi.org/10.1126/science.284.5423.2129>
- Le Quéré, C., R. Moriarty, R.M. Andrew, J.G. Canadell, S. Sitch, J.I. Korsbakken, P. Friedlingstein, G.P. Peters, R.J. Andres, T.A. Boden, R.A. Houghton, J.I. House, R.F. Keeling, P. Tans, A. Arneeth, D.C.E. Bakker, L. Barbero, L. Bopp, J. Chang, F. Chevallier, L.P. Chini, P. Ciais, M. Fader, R.A. Feely, T. Gkritzalis, I. Harris, J. Hauck, T. Ilyina, A.K. Jain, E. Kato, V. Kitidis, K. Klein Goldewijk, C. Koven, P. Landschützer, S.K. Lauvset, N. Lefèvre, A. Lenton, I.D. Lima, N. Metzl, F. Millero, D.R. Munro, A. Murata, J.E.M.S. Nabel, S. Nakaoka, Y. Nojiri, K. O'Brien, A. Olsen, T. Ono, F.F. Pérez, B. Pfeil, D. Pierrot, B. Poulter, G. Rehder, C. Rödenbeck, S. Saito, U. Schuster, J. Schwinger, R. Séférian, T. Steinhoff, B.D. Stocker, A.J. Sutton, T. Takahashi, B. Tilbrook, I.T. van der Laan-Luijkx,

- 1 G.R. van der Werf, S. van Heuven, D. Vandemark, N. Viovy, A. Wiltshire, S. Zaehle, and N.
2 Zeng, 2015: Global Carbon Budget 2015. *Earth System Science Data*, **7**, 349-396.
3 <http://dx.doi.org/10.5194/essd-7-349-2015>
- 4 Long, M.C., C. Deutsch, and T. Ito, 2016: Finding forced trends in oceanic oxygen. *Global*
5 *Biogeochemical Cycles*, **30**, 381-397. <http://dx.doi.org/10.1002/2015GB005310>
- 6 Mantoura, R.F.C., J.M. Martin, and R. Wollast, eds. *Ocean margin processes in global change*.
7 1991, John Wiley and Sons Ltd. 469.
- 8 Mathis, J.T., S.R. Cooley, N. Lucey, S. Colt, J. Ekstrom, T. Hurst, C. Hauri, W. Evans, J.N.
9 Cross, and R.A. Feely, 2015: Ocean acidification risk assessment for Alaska's fishery sector.
10 *Progress in Oceanography*, **136**, 71-91. <http://dx.doi.org/10.1016/j.pocean.2014.07.001>
11 www.sciencedirect.com/science/article/pii/S0079661114001141
- 12 McFall-Ngai, M., M.G. Hadfield, T.C.G. Bosch, H.V. Carey, T. Domazet-Lošo, A.E. Douglas,
13 N. Dubilier, G. Eberl, T. Fukami, S.F. Gilbert, U. Hentschel, N. King, S. Kjelleberg, A.H.
14 Knoll, N. Kremer, S.K. Mazmanian, J.L. Metcalf, K. Nealson, N.E. Pierce, J.F. Rawls, A.
15 Reid, E.G. Ruby, M. Rumpho, J.G. Sanders, D. Tautz, and J.J. Wernegreen, 2013: Animals
16 in a bacterial world, a new imperative for the life sciences. *Proceedings of the National*
17 *Academy of Sciences*, **110**, 3229-3236. <http://dx.doi.org/10.1073/pnas.1218525110>
- 18 McNeil, B.I. and T.P. Sasse, 2016: Future ocean hypercapnia driven by anthropogenic
19 amplification of the natural CO₂ cycle. *Nature*, **529**, 383-386.
20 <http://dx.doi.org/10.1038/nature16156>
- 21 Mei, W., S.-P. Xie, F. Primeau, J.C. McWilliams, and C. Pasquero, 2015: Northwestern Pacific
22 typhoon intensity controlled by changes in ocean temperatures. *Science Advances*, **1**.
23 <http://dx.doi.org/10.1126/sciadv.1500014>
- 24 Moffitt, S.E., R.A. Moffitt, W. Sauthoff, C.V. Davis, K. Hewett, and T.M. Hill, 2015:
25 Paleooceanographic Insights on Recent Oxygen Minimum Zone Expansion: Lessons for
26 Modern Oceanography. *PLoS ONE*, **10**, e0115246.
27 <http://dx.doi.org/10.1371/journal.pone.0115246>
- 28 Montes, I., B. Dewitte, E. Gutknecht, A. Paulmier, I. Dadou, A. Oschlies, and V. Garçon, 2014:
29 High-resolution modeling of the Eastern Tropical Pacific oxygen minimum zone: Sensitivity
30 to the tropical oceanic circulation. *Journal of Geophysical Research: Oceans*, **119**, 5515-
31 5532. <http://dx.doi.org/10.1002/2014JC009858>
- 32 Mulitza, S., D. Heslop, D. Pittauerova, H.W. Fischer, I. Meyer, J.-B. Stuut, M. Zabel, G.
33 Mollenhauer, J.A. Collins, H. Kuhnert, and M. Schulz, 2010: Increase in African dust flux at
34 the onset of commercial agriculture in the Sahel region. *Nature*, **466**, 226-228.
35 <http://dx.doi.org/10.1038/nature09213>

- Muller-Karger, F.E., J.P. Smith, S. Werner, R. Chen, M. Roffer, Y. Liu, B. Muhling, D. Lindo-Atichati, J. Lamkin, S. Cerdeira-Estrada, and D.B. Enfield, 2015: Natural variability of surface oceanographic conditions in the offshore Gulf of Mexico. *Progress in Oceanography*, **134**, 54-76. <http://dx.doi.org/10.1016/j.pocean.2014.12.007>
www.sciencedirect.com/science/article/pii/S0079661114002171
- Najjar, R.G., C.R. Pyke, M.B. Adams, D. Breitburg, C. Hershner, M. Kemp, R. Howarth, M.R. Mulholland, M. Paolisso, D. Secor, K. Sellner, D. Wardrop, and R. Wood, 2010: Potential climate-change impacts on the Chesapeake Bay. *Estuarine, Coastal and Shelf Science*, **86**, 1-20. <http://dx.doi.org/10.1016/j.ecss.2009.09.026>
- Orr, J.C., V.J. Fabry, O. Aumont, L. Bopp, S.C. Doney, R.A. Feely, A. Gnanadesikan, N. Gruber, A. Ishida, F. Joos, R.M. Key, K. Lindsay, E. Maier-Reimer, R. Matear, P. Monfray, A. Mouchet, R.G. Najjar, G.-K. Plattner, K.B. Rodgers, C.L. Sabine, J.L. Sarmiento, R. Schlitzer, R.D. Slater, I.J. Totterdell, M.-F. Weirig, Y. Yamanaka, and A. Yool, 2005: Anthropogenic ocean acidification over the twenty-first century and its impact on calcifying organisms. *Nature*, **437**, 681-686. <http://dx.doi.org/10.1038/nature04095>
- Patara, L. and C.W. Böning, 2014: Abyssal ocean warming around Antarctica strengthens the Atlantic overturning circulation. *Geophysical Research Letters*, **41**, 3972-3978.
<http://dx.doi.org/10.1002/2014GL059923>
- Peters, W., A.R. Jacobson, C. Sweeney, A.E. Andrews, T.J. Conway, K. Masarie, J.B. Miller, L.M.P. Bruhwiler, G. Pétron, A.I. Hirsch, D.E.J. Worthly, G.R. van der Werf, J.T. Randerson, P.O. Wennberg, M.C. Krol, and P.P. Tans, 2007: An atmospheric perspective on North American carbon dioxide exchange: CarbonTracker. *Proceedings of the National Academy of Sciences*, **104**, 18925-18930. <http://dx.doi.org/10.1073/pnas.0708986104>
- Rabalais, N.N., R.J. Díaz, L.A. Levin, R.E. Turner, D. Gilbert, and J. Zhang, 2010: Dynamics and distribution of natural and human-caused hypoxia. *Biogeosciences*, **7**, 585-619.
<http://dx.doi.org/10.5194/bg-7-585-2010>
- Rabalais, N.N., R.E. Turner, R.J. Díaz, and D. Justić, 2009: Global change and eutrophication of coastal waters. *ICES Journal of Marine Science: Journal du Conseil*, **66**, 1528-1537.
<http://dx.doi.org/10.1093/icesjms/fsp047>
icesjms.oxfordjournals.org/content/66/7/1528.abstract
- Rabalais, N.N., R.E. Turner, B.K. Sen Gupta, D.F. Boesch, P. Chapman, and M.C. Murrell, 2007: Hypoxia in the northern Gulf of Mexico: Does the science support the Plan to Reduce, Mitigate, and Control Hypoxia? *Estuaries and Coasts*, **30**, 753-772.
<http://dx.doi.org/10.1007/bf02841332>

- 1 Reay, D.S., F. Dentener, P. Smith, J. Grace, and R.A. Feely, 2008: Global nitrogen deposition
2 and carbon sinks. *Nature Geoscience*, **1**, 430-437. <http://dx.doi.org/10.1038/ngeo230>
- 3 Rhein, M., S.R. Rintoul, S. Aoki, E. Campos, D. Chambers, R.A. Feely, S. Gulev, G.C. Johnson,
4 S.A. Josey, A. Kostianoy, C. Mauritzen, D. Roemmich, L.D. Talley, and F. Wang, 2013:
5 Observations: Ocean. *Climate Change 2013: The Physical Science Basis. Contribution of*
6 *Working Group I to the Fifth Assessment Report of the Intergovernmental Panel on Climate*
7 *Change*. Stocker, T.F., D. Qin, G.-K. Plattner, M. Tignor, S.K. Allen, J. Boschung, A.
8 Nauels, Y. Xia, V. Bex, and P.M. Midgley, Eds. Cambridge University Press, Cambridge,
9 United Kingdom and New York, NY, USA, 255–316.
10 <http://dx.doi.org/10.1017/CBO9781107415324.010> www.climatechange2013.org
- 11 Robinson, R.S., A. Mix, and P. Martinez, 2007: Southern Ocean control on the extent of
12 denitrification in the southeast Pacific over the last 70 ka. *Quaternary Science Reviews*, **26**,
13 201-212. <http://dx.doi.org/10.1016/j.quascirev.2006.08.005>
14 www.sciencedirect.com/science/article/pii/S0277379106002411
- 15 Roemmich, D., J. Church, J. Gilson, D. Monselesan, P. Sutton, and S. Wijffels, 2015: Unabated
16 planetary warming and its ocean structure since 2006. *Nature Climate Change*, **5**, 240-245.
17 <http://dx.doi.org/10.1038/nclimate2513>
- 18 Salisbury, J., M. Green, C. Hunt, and J. Campbell, 2008: Coastal Acidification by Rivers: A
19 Threat to Shellfish? *Eos, Transactions American Geophysical Union*, **89**, 513-513.
20 <http://dx.doi.org/10.1029/2008EO500001>
- 21 Schmittner, A., E.D. Galbraith, S.W. Hostetler, T.F. Pedersen, and R. Zhang, 2007: Large
22 fluctuations of dissolved oxygen in the Indian and Pacific oceans during Dansgaard-
23 Oeschger oscillations caused by variations of North Atlantic Deep Water subduction.
24 *Paleoceanography*, **22**, n/a-n/a. <http://dx.doi.org/10.1029/2006PA001384>
- 25 Smith, S.V. and J.T. Hollibaugh, 1993: Coastal metabolism and the oceanic organic carbon
26 balance. *Reviews of Geophysics*, **31**, 75-89. <http://dx.doi.org/10.1029/92RG02584>
- 27 Steinman, B.A., M.E. Mann, and S.K. Miller, 2015: Atlantic and Pacific multidecadal
28 oscillations and Northern Hemisphere temperatures. *Science*, **347**, 988-991.
29 <http://dx.doi.org/10.1126/science.1257856>
- 30 Stendardo, I. and N. Gruber, 2012: Oxygen trends over five decades in the North Atlantic.
31 *Journal of Geophysical Research*, **117**, C11004. <http://dx.doi.org/10.1029/2012JC007909>
- 32 Stramma, L., S. Schmidtko, L.A. Levin, and G.C. Johnson, 2010: Ocean oxygen minima
33 expansions and their biological impacts. *Deep Sea Research Part I: Oceanographic Research*
34 *Papers*, **57**, 587-595. <http://dx.doi.org/10.1016/j.dsr.2010.01.005>

- 1 Straneo, F. and P. Heimbach, 2013: North Atlantic warming and the retreat of Greenland's outlet
2 glaciers. *Nature*, **504**, 36-43. <http://dx.doi.org/10.1038/nature12854>
- 3 Sydeman, W.J., M. García-Reyes, D.S. Schoeman, R.R. Rykaczewski, S.A. Thompson, B.A.
4 Black, and S.J. Bograd, 2014: Climate change and wind intensification in coastal upwelling
5 ecosystems. *Science*, **345**, 77-80. <http://dx.doi.org/10.1126/science.1251635>
- 6 Takatani, Y., D. Sasano, T. Nakano, T. Midorikawa, and M. Ishii, 2012: Decrease of dissolved
7 oxygen after the mid-1980s in the western North Pacific subtropical gyre along the 137°E
8 repeat section. *Global Biogeochemical Cycles*, **26**, n/a-n/a.
9 <http://dx.doi.org/10.1029/2011GB004227>
- 10 Taylor, G.T., F.E. Muller-Karger, R.C. Thunell, M.I. Scranton, Y. Astor, R. Varela, L.T.
11 Ghinaglia, L. Lorenzoni, K.A. Fanning, S. Hameed, and O. Doherty, 2012: Ecosystem
12 responses in the southern Caribbean Sea to global climate change. *Proceedings of the*
13 *National Academy of Sciences*, **109**, 19315-19320.
14 <http://dx.doi.org/10.1073/pnas.1207514109> www.pnas.org/content/109/47/19315.abstract
- 15 Thompson, P.R., B.D. Hamlington, F.W. Landerer, and S. Adhikari, 2016: Are long tide gauge
16 records in the wrong place to measure global mean sea level rise? *Geophysical Research*
17 *Letters*, **43**, 10,403-10,411. <http://dx.doi.org/10.1002/2016GL070552>
- 18 Trenberth, K.E., J.T. Fasullo, and M.A. Balmaseda, 2014: Earth's Energy Imbalance. *Journal of*
19 *Climate*, **27**, 3129-3144. <http://dx.doi.org/10.1175/jcli-d-13-00294.1>
- 20 Turley, C., M. Eby, A.J. Ridgwell, D.N. Schmidt, H.S. Findlay, C. Brownlee, U. Riebesell, V.J.
21 Fabry, R.A. Feely, and J.P. Gattuso, 2010: The societal challenge of ocean acidification.
22 *Marine Pollution Bulletin*, **60**, 787-792. <http://dx.doi.org/10.1016/j.marpolbul.2010.05.006>
23 www.sciencedirect.com/science/article/pii/S0025326X1000192X
- 24 Waldbusser, G.G. and J.E. Salisbury, 2014: Ocean Acidification in the Coastal Zone from an
25 Organism's Perspective: Multiple System Parameters, Frequency Domains, and Habitats.
26 *Annual Review of Marine Science*, **6**, 221-247. [http://dx.doi.org/10.1146/annurev-marine-](http://dx.doi.org/10.1146/annurev-marine-121211-172238)
27 [121211-172238](http://dx.doi.org/10.1146/annurev-marine-121211-172238)
- 28 Wallmann, K., 2003: Feedbacks between oceanic redox states and marine productivity: A model
29 perspective focused on benthic phosphorus cycling. *Global Biogeochemical Cycles*, **17**, n/a-
30 n/a. <http://dx.doi.org/10.1029/2002GB001968>
- 31 Walsh, J.J., ed. *On the Nature of Continental Shelves*. 1988, Academic Press. 520.
- 32 Wang, D., T.C. Gouhier, B.A. Menge, and A.R. Ganguly, 2015: Intensification and spatial
33 homogenization of coastal upwelling under climate change. *Nature*, **518**, 390-394.
34 <http://dx.doi.org/10.1038/nature14235>

- 1 Wollast, R., 1998: Evaluation and Comparison of the Global Carbon Cycle in the Coastal Zone
2 and in the Open Ocean. *The Sea: Processes and Methods*. Brink, K.H. and A.R. Robinson,
3 Eds. Harvard University Press, Cambridge, Mass., 213-252.
- 4 Wright, J.D. and M.F. Schaller, 2013: Evidence for a rapid release of carbon at the Paleocene-
5 Eocene thermal maximum. *Proceedings of the National Academy of Sciences*, **110**, 15908-
6 15913. <http://dx.doi.org/10.1073/pnas.1309188110>
7 www.pnas.org/content/110/40/15908.abstract
- 8 Yamamoto-Kawai, M., F.A. McLaughlin, E.C. Carmack, S. Nishino, and K. Shimada, 2009:
9 Aragonite undersaturation in the Arctic ocean: Effects of ocean acidification and sea ice melt.
10 *Science*, **326**, 1098-1100. <http://dx.doi.org/10.1126/science.1174190>
- 11 Yang, H., G. Lohmann, W. Wei, M. Dima, M. Ionita, and J. Liu, 2016: Intensification and
12 poleward shift of subtropical western boundary currents in a warming climate. *Journal of*
13 *Geophysical Research: Oceans*, **121**, 4928-4945. <http://dx.doi.org/10.1002/2015JC011513>
- 14 Zaitsev, Y.P., 1992: Recent changes in the trophic structure of the Black Sea. *Fisheries*
15 *Oceanography*, **1**, 180-189. <http://dx.doi.org/10.1111/j.1365-2419.1992.tb00036.x>
- 16 Zeebe, R.E., A. Ridgwell, and J.C. Zachos, 2016: Anthropogenic carbon release rate
17 unprecedented during the past 66 million years. *Nature Geoscience*, **9**, 325-329.
18 <http://dx.doi.org/10.1038/ngeo2681>
- 19 Zhang, J., 2014: Coastal Biogeochemical Cycles. In: Harff, J., M. Meschede, S. Petersen, and J.
20 Thiede (eds.), *Encyclopedia of Marine Geosciences*. Springer.

14. Perspectives on Climate Change Mitigation

KEY FINDINGS

1. There will be a delay of decades or longer between significant actions that reduce CO₂ emissions and reductions in atmospheric CO₂ concentrations that contribute to surface warming. This delay—the result of the long lifetime of CO₂ in the atmosphere and the time lag in the response of atmospheric CO₂ concentrations following a reduction in emissions—means that near-term changes in climate will be largely determined by past and present greenhouse gas emissions, modified by natural variability. (*Very high confidence*)
2. Limiting the global-mean temperature increase to 3.6°F (2°C) above pre-industrial levels requires significant reductions in global CO₂ emissions relative to present-day emission rates. Given the near-linear relationship between cumulative CO₂ emissions and global temperature response, cumulative emissions would likely have to stay below 1,000 GtC for a 2°C objective, leaving about 400 GtC still to be emitted globally. Assuming future global emissions follow the RCP4.5 scenario, the total, cumulative emissions commensurate with the 2°C objective would likely be reached between 2051 and 2065, while under the RCP8.5 scenario, the timing would likely fall between 2043 and 2050. (*High confidence*)
3. Successful implementation of the first round of National Determined Commitments under the Paris agreement is a large step towards the objective of limiting global warming to 3.6°F (2°C). Even greater greenhouse gas emission reductions are required beyond 2030 in order to increase the likelihood of achieving the 2°C goal; indeed, substantial (although smaller) reductions after 2030 would be required to achieve even the lesser goal of significantly reducing the likelihood of a global mean temperature increase greater than 7.2°F (4°C). (*High confidence*)
4. If projected atmospheric CO₂ concentrations are not sufficiently low to prevent warming of 2°C or more, climate-intervention strategies such as technological CO₂ removal or solar radiation management may gain attention as additional means to limit or reduce temperature increases. Assessing the technical feasibility, costs, risks, co-benefits and governance challenges of these additional measures, which are as-yet unproven at scale, would be of value to decision makers. (*Medium confidence*)

Introduction

This chapter addresses three topics. First, it addresses the science underlying the timing of when and how greenhouse gas (GHG) mitigation activities that occur in the present affect the climate of the future. In other words, when do we see the benefits of a greenhouse gas

emission reduction activity? And how do these benefits manifest themselves? Second, it addresses a number of questions in light of the Paris agreement adopted in December 2015 (UNFCCC 2015) that builds upon the UN Framework Convention on Climate Change (UNFCCC; see Section 14.2): if fully implemented, what is the first round of mitigation commitments under the Paris agreement estimated to achieve in terms of avoiding increases in globally-averaged temperature and associated climate change in the future? And how significant of a role does the Paris agreement play in terms of the oft-cited 2°C (3.6°F) target or even a 1.5°C (2.7°F) target? Third, looking beyond the Paris agreement (which does not set emission reduction targets past the year 2030), what global-scale emissions pathways are estimated to be necessary by mid-century and beyond in order to have a high likelihood of achieving the 2°C or 1.5°C targets? As part of this last question, this chapter briefly addresses the status of climate intervention and geoengineering research and proposals and how these types of mitigation actions could possibly play a role in avoiding future climate change.

14.1 The Timing of Benefits from Mitigation Actions

14.1.1 Inherent Delays in the Climate System

Carbon dioxide (CO₂) concentrations in the atmosphere are directly affected by human activities. The long lifetime of CO₂ in the atmosphere (Joos et al. 2013), coupled with the time lag in the response of the climate system to atmospheric forcing (Tebaldi and Friedlingstein 2013), has timing implications for the benefits of mitigation actions. Benefits of action to improve some environmental issues, such as air or water quality, can be almost immediately detectable and attributable to the specific actions that took place. However, the climate benefits (such as the *avoided* warming) of individual GHG mitigation actions generally will not be discernible in the short term because of an insufficient scale of the mitigation and because changes in climate parameters are generally globally diffuse and occur many decades into the future after the mitigation activity (e.g., Tebaldi and Friedlingstein 2013).

The world is committed to some degree of warming and associated climate change resulting from emissions to date. There is ample literature (Paltsev et al. 2015; IPCC 2013) showing that long-term risks (around and beyond 2050) of climate change can be strongly influenced by the GHG emissions pathways, which includes the emissions path over the near term. In the nearer term, the global climate will not be strongly influenced via changes to the emissions path; natural variability and the earth system response to past and current GHG emissions will be stronger factors. Some studies have nevertheless shown the potential for some near-term benefits. For example, one study found that, even at the regional scale, heat waves would already be significantly more severe by the 2030s in a non-mitigation scenario compared to a moderate mitigation scenario (Tebaldi and Wehner 2016).

The mitigation of short-lived climate pollutants (SLCPs)—such as black carbon, ozone, methane and some hydrofluorocarbons (HFCs)—has been highlighted as a way to achieve more rapid climate benefits (e.g., Zaelke and Borgford-Parnell 2015). SLCPs are substances with an atmospheric lifetime shorter (for example, weeks to a decades) than CO₂. Hence, mitigation of SLCP emissions produce more rapid radiative responses and, in some cases, strong regional (for example, for black carbon) and health co-benefits (for example, for black carbon and methane). Long-term reductions and/or avoidances of methane and HFC emissions could be a significant contribution to staying at or below a 2°C global-mean temperature increase (Hayhoe et al. 1998; Shah 2015). A recent amendment to the Montreal Protocol will regulate global HFC production and consumption in order to avoid substantial CO₂-eq emissions in coming decades. However, given that economic and technological factors tend to couple CO₂ and SLCP emissions, it is thought that significant SLCP emissions reduction would be a co-benefit of CO₂ mitigation, and, conversely, stringent near-term SLCP mitigation could potentially increase allowable CO₂ budgets for avoiding warming beyond 2°C, by up to 25% according to Rogelj et al. (2016).

14.1.2 Stock and Stabilization

Cumulative CO₂ emissions will largely determine long-term global mean temperature change and there is a nearly linear relationship between cumulative CO₂ emissions and global mean temperature increases (IPCC 2013, Figure SPM 10; see Chapter 4.). Thus, for a 2°C (3.6°F) or any desired global mean temperature objective, an estimated range of allowable cumulative CO₂ emissions from the current period onward can be calculated. This issue is illustrated here and discussed in the context of the Paris agreement.

To date, human activities, primarily burning fossil fuels and deforestation, have emitted more than 600 Pg or GtC into the atmosphere since pre-industrial times. To meet the 2°C (3.6°F) objective called for under the Paris Agreement, approximately 400 GtC more CO₂ could be emitted globally. In order to meet the 1.5°C (2.7°F) objective, only about 150 GtC more of CO₂ could be emitted. Assuming a stabilized global emission rate at just under the current value of 10 GtC per year, this would permit around 40 more years of CO₂ emissions for the 2°C objective, and just 15 years for 1.5°C objective. Assuming future global emissions follow the RCP4.5 scenario, the total, cumulative emissions commensurate with the 2°C objective would likely be reached between 2051 and 2065, while under the RCP8.5 scenario, the timing would likely fall between 2043 and 2050. For the 1.5°C objective, the cumulative carbon limit of 750 GtC would likely be reached under RCP4.5 between 2028 and 2041 and under RCP8.5 between 2026 and 2036.

The analysis of remaining CO₂ emissions above is more generally expressed in units of net CO₂-eq emissions, which include a range of climate forcing agents in addition to CO₂ (Chapter 2). Since non-CO₂ forcing agents have projections of net positive forcing, incorporating these agents into the analysis reduces the allowable range of CO₂-only

emissions and increases the uncertainty regarding the amount and timing of net CO₂-eq emissions consistent with achieving specific temperature objectives.

The cumulative carbon emissions estimated to be compatible with a given global temperature objective can be compared to known fossil-fuel reserves, and their associated CO₂ emissions if burnt, to calculate how much of these reserves may be used, in the absence of widespread carbon capture and storage. If the 2°C objective is to be met, no further CO₂ emissions would be allowed for one third of oil reserves, half of gas reserves, and over 80% of coal reserves (McGlade and Ekins 2015).

14.2 Estimated Climate Implications of the Paris Agreement

In December of 2015 in Paris, building upon the UNFCCC, 195 countries adopted the first-ever agreement under which all nations committed to put forward GHG mitigation targets, and to back these targets by domestic measures. Leading up to Paris, nations submitted Intended Nationally Determined Contributions (INDCs), where each country developed its own annual emissions targets, timeframes, and mechanisms that were suited to their own national circumstances. As a country formally joins the Paris agreement, the country's INDC becomes, by default, its first NDC (Nationally Determined Commitment). The first commitments under the Paris agreement extend to 2025 or 2030, and take a wide range of forms. Some, like the U.S. goal of 26% to 28% reductions in annual emissions by 2025 relative to 2005 levels, are absolute emissions reduction goals. Others, like China's goal for its emissions to peak on or before 2030 or India's goal to "to reduce the emissions intensity of its GDP by 33 to 35 percent by 2030 from 2005 level," are relative, not absolute, emissions reduction goals. As a consequence of this country-by-country, bottom-up approach, uncertainty exists as to the net annual emissions reductions implied by this first round of NDCs.

The agreement also contains the objectives of "holding the increase in the global average temperature to well below 2°C above pre-industrial levels and pursuing efforts to limit the temperature increase to 1.5°C above pre-industrial levels." Furthermore, stated goals are to "aim to reach global peaking of greenhouse gas emissions as soon as possible, recognizing that peaking will take longer for developing country Parties, and to undertake rapid reductions thereafter in accordance with best available science, so as to achieve a balance between anthropogenic emissions by sources and removals by sinks of greenhouse gases in the second half of this century." The balance implies net-zero emissions, whereby future CO₂ emissions, for example, would be fully offset through CO₂ removal by terrestrial carbon sinks, other enhanced removal processes, or carbon capture and storage mechanisms.

14.2.1 Temperature Implications from Current Commitments under the Paris Agreement

Analyses have been undertaken to estimate the global emissions and global temperature implications of the successful implementation of the first round of NDCs (Rogelj et al. 2016; Sanderson et al. 2016; Climate Action Tracker 2015; Fawcett et al. 2015; UNFCCC 2015). These estimates generally find that 1) successful implementation of the first round of NDCs would reduce GHG emissions growth by 2030 relative to a situation where these goals did not exist, though global emissions are still not expected to be lower in 2030 than in 2015, and 2) the NDCs are important in order to keep the 2°C objective within reach, but that the NDCs are, by themselves, insufficient to achieve this ambitious objective. According to one study, the NDCs imply a median warming of 2.6°C –3.1°C by 2100, though year 2100 temperature estimates depend on assumed emissions between 2030 and 2100 (Rogelj et al. 2016). For example, Climate Action Tracker, using alternative post-2030 assumptions, put the range at 3.3°C to 3.9°C.

Emissions pathways consistent with the then INDCs were evaluated in the context of likelihood of global mean surface temperature change. It was found that the likelihood of meeting the objective of 2°C or less was enhanced by the INDCs, but depended strongly on subsequent policies and measures. The chief finding was that even without additional emission reductions after 2030, if implemented successfully, the INDCs provided some likelihood (less than 10%) of preventing global mean surface temperature change of 2°C relative to preindustrial levels (that is, an outcome between 1.5°C and 2°C) (by Fawcett et al. 2015). Greater emission reductions beyond 2030 increased the likelihood of achieving the 2°C goal or lower to more than 30%, and significantly reduced the likelihood of a global mean temperature increase greater than 4°C to roughly 1% (Figure 14.1).

[INSERT FIGURE 14.1 HERE:]

Figure 14.1: Global CO₂ emissions and probabilistic temperature outcomes of Paris. (A) Global CO₂ emissions from energy and industry (includes CO₂ emissions from all fossil fuel production and use and industrial processes such as cement manufacture that also produce CO₂ as a byproduct) for emissions scenarios following no policy, current policy, meeting the INDCs with no increased future ambition and meeting the INDCs with continually increasing ambition. (B) Likelihoods of different levels of increase in global mean surface temperature during the 21st century relative to preindustrial levels for the four scenarios. Although (A) shows only CO₂ emissions from energy and industry, temperature outcomes are based on the full suite of GHG, aerosol, and short-lived species emissions across the full set of human activities and physical Earth systems. (Figure source: adapted from Fawcett et al. 2015)]

The way in which near-term goals are achieved also matters to meeting long-term climate goals. Few nations have provided detailed information as to the methods that they will use to accomplish their goals. To the extent that nations have explicitly announced policies that they

1 intend to use to achieve their goals, these policies and measures span a wide range forms,
2 extending from fiscal measures (for example, carbon tax) to regulatory measures (for
3 example, performance standards). This variety in goals and measures raises the prospect of
4 policy interactions that can either enhance others' efforts, (for example, technology
5 development policies), or degrade others' efforts. Also, near-term policies and measures
6 could either help facilitate the deep reductions that need to follow after 2030 to limit global
7 temperature to 2°C or less, or could frustrate that ambition.

8 **14.2.2 Pathways Consistent with Paris Temperature Targets (1.5°C or 2°C)**

9 A robust feature of model climate change simulations, irrespective of the details of the
10 emissions pathway, is the near-linear relationship between cumulative emissions and peak
11 warming in the simulation (see Figure 14.2). To date, humanity has emitted just over 600
12 billion tonnes of carbon, which means that even if emissions were to halt today, temperatures
13 would be expected to stabilize at 1.5°C above the preindustrial average. An exceedance of a
14 trillion tonnes of cumulatively emitted carbon would make it unlikely that temperature
15 increases could remain below 2°C (Allen et al. 2009).

16 **[INSERT FIGURE 14.2 HERE:]**

17 **Figure 14.2: Global mean temperature change for a number of scenarios as a function of**
18 **cumulative CO₂ emissions from preindustrial conditions, with time progressing along each**
19 **individual line for each scenario. (Figure source: IPCC 2013; © IPCC. Used with**
20 **permission.)]**

21 As such, there are only a limited number of pathways which would enable the world to
22 remain below 2°C of warming (see Figure 14.3), and almost all but the most rapid near-term
23 mitigation would be heavily reliant on the implementation of CO₂ removal from the
24 atmosphere later in the century or other climate intervention. If global emissions are in line
25 with the first round of NDCs by 2030, then the world would likely need to reduce effective
26 GHG emissions to zero by 2080, and be significantly net negative by the end of the century
27 (relying on as-yet unproven technologies to remove GHGs from the atmosphere) in order to
28 avoid and not exceed 2°C of warming. Avoiding 1.5°C of warming would require more
29 aggressive action still, with net zero emissions achieved by 2050 and net negative emissions
30 thereafter. In either case, faster near-term action would significantly decrease the
31 requirements for negative emissions in the future.

32 **[INSERT FIGURE 14.3 HERE:]**

33 **Figure 14.3: Global emissions pathways of effective global CO₂ emissions which would be**
34 **consistent with different temperature targets (relative to preindustrial temperatures). (Figure**
35 **source: Sanderson et al. 2016)]**

14.3 The Role of Climate Intervention in Meeting Ambitious Climate Targets

Achieving a 2°C target through emissions reductions or adapting to the impacts of a greater-than-2°C world have been acknowledged as severely challenging tasks by the international science and policy communities. As a consequence, there is increased interest by some scientists and policy makers in exploring measures designed to reduce net radiative forcing through other, as-yet untested actions, which are often referred to as “geoengineering” or “climate intervention” (CI). CI approaches are generally divided into two categories: carbon dioxide (CO₂) removal (CDR) and solar radiation management (SRM). CDR and SRM methods may have future roles in helping meet global temperature targets. Both methods reduce global-average temperature by reducing net global radiative forcing: CDR through reducing atmospheric CO₂ concentrations and SRM through increasing Earth’s albedo. The U.S. National Academy of Sciences completed reports in 2015 examining CDR and SRM (NAS 2015a,b).

By removing CO₂ from the atmosphere, CDR directly addresses the principal cause of climate change. Potential CDR approaches include point-source CO₂ capture, direct air capture, biological methods on land (e.g., afforestation) and in the ocean (e.g., ocean fertilization), and accelerated weathering (e.g., forming calcium carbonate on land or in the oceans). While CDR is technically possible, the primary challenge is achieving the required scale of removal in a cost-effective manner. In principle, at large scale, CDR could reduce CO₂ concentrations (i.e., cause negative emissions). Point-source capture and removal of CO₂ is considered a particularly effective CDR method. The climate value of avoided CO₂ emissions is essentially equivalent to that of the atmospheric removal of the same amount. To realize the climate benefits of CDR, the removal of CO₂ from the atmosphere must be essentially permanent—at least several centuries to millennia. In addition to high costs, CDR has the additional limitation of long implementation times.

By contrast, SRM approaches offer the only CI method of cooling Earth within a few years after inception. An important limitation of SRM is that it would not address damage to ocean ecosystems from increasing ocean acidification due to continued CO₂ uptake. SRM could theoretically have a significant global impact even if implemented by a small number of nations, and by nations who are not also the major emitters of GHGs. Leading SRM concepts would increase Earth’s albedo through injection of sulfur gases or aerosols into the stratosphere (thereby simulating the effects of explosive volcanic eruptions) or marine cloud brightening through aerosol injection near the ocean surface. Injection of solid particles is an alternative to sulfur and yet other SRM methods could be deployed in space. Studies have evaluated the expected effort and effectiveness of various SRM methods have been proposed (NAS 2015b; Keith et al. 2014). For example, model runs

1 were performed in the GeoMIP project using the full CMIP5 model suite to illustrate the
2 effect of reducing top-of-the-atmosphere insolation to offset climate warming from CO₂
3 (Kravitz et al. 2013). The idealized runs, which assumed an abrupt, globally-uniform
4 insolation reduction in a 4×CO₂ atmosphere, show that temperature increases are largely
5 offset, most sea-ice loss is avoided, average precipitation changes are small, and net
6 primary productivity increases. However, important regional changes in climate variables
7 are likely in SRM scenarios as discussed below.

8 As global ambitions increase to avoid or remove CO₂ emissions, probabilities of large
9 increases in global temperatures in 2100 are proportionately reduced (Fawcett et al.
10 2015). Scenarios in which large-scale CDR is used to meet a 2°C limit while allowing
11 business-as-usual consumption of fossil fuels are likely not feasible with present
12 technologies. Model SRM scenarios have been developed that show reductions in
13 radiative forcing up to 1 W/m² with annual stratospheric injections of 1 Mt of sulfur from
14 aircraft or other platforms (Pierce et al. 2010; Tilmes et al. 2016). Preliminary studies
15 suggest that this could be accomplished at a cost as low as a few billion dollars per year
16 using current technology, enabling an individual country or subnational entity to conduct
17 activities having significant global climate impacts.

18 SRM scenarios could be designed to follow a particular radiative forcing trajectory, with
19 adjustments made in response to monitoring of the climate effects (Keith and MacMartin
20 2015). SRM could be used as an interim measure to avoid peaks in global average
21 temperature and other climate parameters. The assumption is often made that SRM
22 measures, once implemented, must continue indefinitely in order to avoid the rapid
23 climate change that would occur if the measures were abruptly stopped. SRM could be
24 used, however, as an interim measure to buy time for the implementation of emissions
25 reductions and/or CDR, and SRM could be phased out as emission reductions and CDR
26 are phased in, to avoid abrupt changes in radiative forcing (Keith and MacMartin 2015).

27 SRM via marine cloud brightening derives from changes in cloud albedo from injection
28 of aerosol into low-level clouds, primarily over the oceans. Clouds with smaller and more
29 numerous droplets reflect more sunlight than clouds with fewer and larger droplets.
30 Current models provide more confidence in the effects of stratospheric injection than in
31 marine cloud brightening (NAS 2015b).

32 Even if the reduction in global-average radiative forcing from SRM was exactly equal to
33 the radiative forcing from greenhouse gases, the regional and temporal patterns of these
34 forcings would vary. Hence, SRM actions are unlikely to fully offset the effects of
35 greenhouse gases, causing potentially important changes in atmospheric circulation and
36 weather patterns. Also, the reduction in sunlight may have effects on agriculture and
37 ecosystems. In general, restoring regional preindustrial temperature and precipitation
38 conditions in response to SRM actions is not expected to be possible based on ensemble

1 modeling studies (Ricke et al. 2010). As a consequence, the optimal climate and
2 geopolitical value of potential SRM actions will likely involve tradeoffs between regional
3 temperature and precipitation changes (MacMartin et al. 2013).

4 CDR and SRM have substantial uncertainties regarding their effectiveness and
5 unintended consequences. CDR on a large scale may disturb natural systems and have
6 important implications for land-use changes. While SRM could rapidly lower global
7 mean temperatures, the effects on precipitation patterns, light availability, crop yields,
8 acid rain, pollution levels, temperature gradients, and atmospheric circulation in response
9 to such actions are less well understood than the effects of GHGs alone. Furthermore, the
10 potential for rapid changes upon initiation (or ceasing) of a CI action would require
11 adaptation on timescales significantly more rapid than what would otherwise be
12 necessary. The NAS (2015a,b) and the Royal Society (Shepherd et al. 2009) recognized
13 that research on the feasibility and consequences of CI actions is incomplete and call for
14 continued research to improve knowledge of the feasibility, risks, and benefits of CI
15 techniques.

16 The evaluation of the suitability and advisability of potential CI actions requires a
17 decision framework that includes important dimensions beyond scientific and technical
18 considerations. Among these dimensions are the development of global and national
19 governance and oversight procedures, geopolitical relations, legality, environmental,
20 economic and societal impacts, ethical considerations, and the relationships to global
21 climate policy and current GHG mitigation and adaptation actions. This report only
22 acknowledges these mostly non-scientific dimensions and must forego a detailed
23 discussion. Furthermore, it is clear that these non-scientific dimensions are likely to be
24 the major part of a decision framework and ultimately control the adoption and
25 effectiveness of CI actions.

26

TRACEABLE ACCOUNTS

Key Finding 1

There will be a delay of decades or longer between significant actions that reduce CO₂ emissions and reductions in atmospheric CO₂ concentrations that contribute to surface warming. This delay—the result of the long lifetime of CO₂ in the atmosphere and the time lag in the response of atmospheric CO₂ concentrations following a reduction in emissions—means that near-term changes in climate will be largely determined by past and present greenhouse gas emissions, modified by natural variability.

Description of evidence base

Joos et al. (2013) describe the climate response of CO₂ pulse emissions. IPCC (2013) stated that the best estimate of the human-induced contribution to observed warming was similar to the observed warming for the period 1951-2010. IPCC (2013) also stated that natural internal variability will continue to be a major influence on climate, particularly in the near term.

Major uncertainties

The Key Finding makes a general statement about the timing of the climate effect following a CO₂ emission reduction activity, without specifying the exact magnitude or timing of the climate effect that could be associated with different timings or levels of CO₂ reductions. Uncertainties affecting the timing of the climate response following a pulse emission (or avoidance of that emission) involve the quantity of emissions, the background concentration of CO₂, and the choice of model.

Assessment of confidence based on evidence and agreement, including short description of nature of evidence and level of agreement

☒ Very High

☐ High

☐ Medium

☐ Low

There is a well-established understanding, based on a robust literature base, of the timing of atmospheric CO₂ concentration effects following an emission of CO₂. There are also well-vetted statements in the scientific literature that the near-term climate can be expected to be most influenced by past and present GHG emissions, and internal natural variability. It follows that the qualitative key finding—that the effects of significant mitigation actions will be delayed—is well supported.

Summary sentence or paragraph that integrates the above information

The qualitative statement that there will be a delay of decades or longer between significant actions that reduce CO₂ emissions and reductions in atmospheric CO₂ concentrations that contribute to surface warming is well supported by the literature.

Key Finding 2

Stabilizing the global-mean temperature increase to 2°C (3.6°F) above pre-industrial levels requires significant reductions in global CO₂ emissions relative to present-day emission rates. Given the near-linear relationship between cumulative CO₂ emissions and global temperature response, cumulative emissions would likely have to stay below 1,000 GtC for a 2°C objective, leaving about 400 GtC to be emitted. Assuming future global emissions follow the RCP4.5 scenario, the total, cumulative emissions commensurate with the 2°C objective would likely be reached between 2051 and 2065, while under the RCP8.5 scenario, the timing would likely fall between 2043 and 2050.

Description of evidence base

The Key Finding is an abbreviated version of the 2°C objective described in section 12.5 of the IPCC WG1 AR5 and section E.8 of its SPM. The 1.5°C objective is a simple linear scaling as described in IPCC WG1 AR5 section 12.5.4.3 on page 1113.

Major uncertainties

The largest uncertainty is the equilibrium response to atmospheric CO₂ increases or “Equilibrium Climate Sensitivity”. Other uncertainties include the ability of the terrestrial and marine biosystems to remove CO₂ from the atmosphere, as well as the effect of reducing the aerosol pollutants associated with the burning of fossil fuels.

Assessment of confidence based on evidence and agreement, including short description of nature of evidence and level of agreement

☐ Very High

X High

☐ Medium

☐ Low

High confidence in the likelihood statement is based on high confidence in the estimate range of the equilibrium climate sensitivity, IPCC WG1 AR5, box 12.2, page 1111.

If appropriate, estimate likelihood of impact or consequence, including short description of basis of estimate

☐ Greater than 9 in 10 / Very Likely

X Greater than 2 in 3 / Likely

☐ About 1 in 2 / As Likely as Not

☐ Less than 1 in 3 / Unlikely

☐ Less than 1 in 10 / Very Unlikely

Likely means that there is a 66% or greater chance that the objective will be met with the stated total cumulative carbon amount (source: IPCC WG1 AR5 SPM section E.8, page 27.)

Summary sentence or paragraph that integrates the above information

The key finding is an abbreviated statement from the IPCC WG1 AR5 that made a thorough assessment of the relevant literature (section 12.5).

Key Finding 3

Successful implementation of the first round of NDCs under the Paris agreement is a large step towards the objective of limiting global warming to 2°C (3.6°F). Even greater GHG emission reductions are required beyond 2030 in order to increase the likelihood of achieving the 2°C goal; indeed, substantial (although smaller) reductions after 2030 would be required to achieve even the lesser goal of significantly reducing the likelihood of a global mean temperature increase greater than 7.2°F (4°C).

Description of evidence base

The primary source supporting this key finding is Fawcett et al. (2015) and is also supported by Rogelj et al. (2016), Sanderson et al. (2016), and Climate Action Tracker. Each of these analyses evaluated the global climate implications of the aggregation of the individual country commitments thus far put forward under the Paris agreement.

Major uncertainties

The largest uncertainty lies in the assumption of “successful implementation” of the first round of NDCs; these are assumed to be fully successful but could either over- or underachieve. This in turn creates uncertainty about the extent of emission reductions that would be needed after the first round of NDCs in order to achieve the 2°C or any other objective. The response of the climate system, the climate sensitivity, is also a source of uncertainty; the Fawcett et al. analysis used the IPCC AR5 range, 1.5 to 4.5°C.

Assessment of confidence based on evidence and agreement, including short description of nature of evidence and level of agreement

☐ Very High

☒ High

☐ Medium

☐ Low

There is high confidence in this key finding because a number of analyses have examined the implications of the first round of national commitments under the Paris agreement and have come to similar conclusions, as captured in this key finding.

Summary sentence or paragraph that integrates the above information

A number of analyses have estimated the implications for global mean temperature of the first round of commitments under the Paris agreement. Assuming successful implementation of this first round of commitments, along with a range of climate sensitivities, these

commitments are a large step towards the objective of limiting global warming to 2°C but greater action will be required.

Key Finding 4

If projected atmospheric CO₂ concentrations are not sufficiently low to prevent warming of 2°C or more, climate-intervention strategies such as technological CO₂ removal or solar radiation management may increasingly gain attention and support as additional means to limit or reduce temperature increases. Assessing the technical feasibility, costs, risks, co-benefits and governance challenges of these additional measures, which are as-yet unproven at scale, would be of value to decision makers.

Description of evidence base

The key finding is a qualitative statement reasonably based on the growing literature addressing this topic.

Major uncertainties

The major uncertainty is how public perception and interest among policymakers in climate intervention may change over time, even independently from the level of progress made towards conventional emission reductions commensurate with the 2°C objective.

Assessment of confidence based on evidence and agreement, including short description of nature of evidence and level of agreement

☐ Very High

☒ High

☐ Medium

☐ Low

There is high confidence that climate intervention strategies may gain attention, especially if efforts to slow the buildup of atmospheric CO₂ are considered inadequate by many in the scientific and policy communities.

Summary sentence or paragraph that integrates the above information

The key finding is a qualitative statement based on the growing literature on this topic. The uncertainty moving forward is the comfort level and desire among numerous stakeholders to research and potentially carry out these climate intervention strategies, particularly in light of progress the global community may make in slowing the atmospheric buildup of CO₂.

1 FIGURES

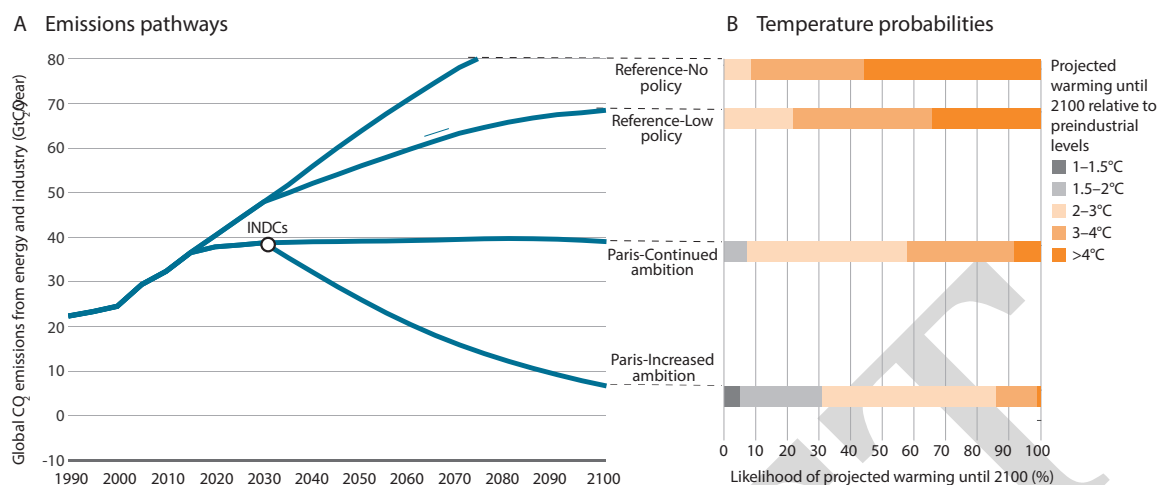
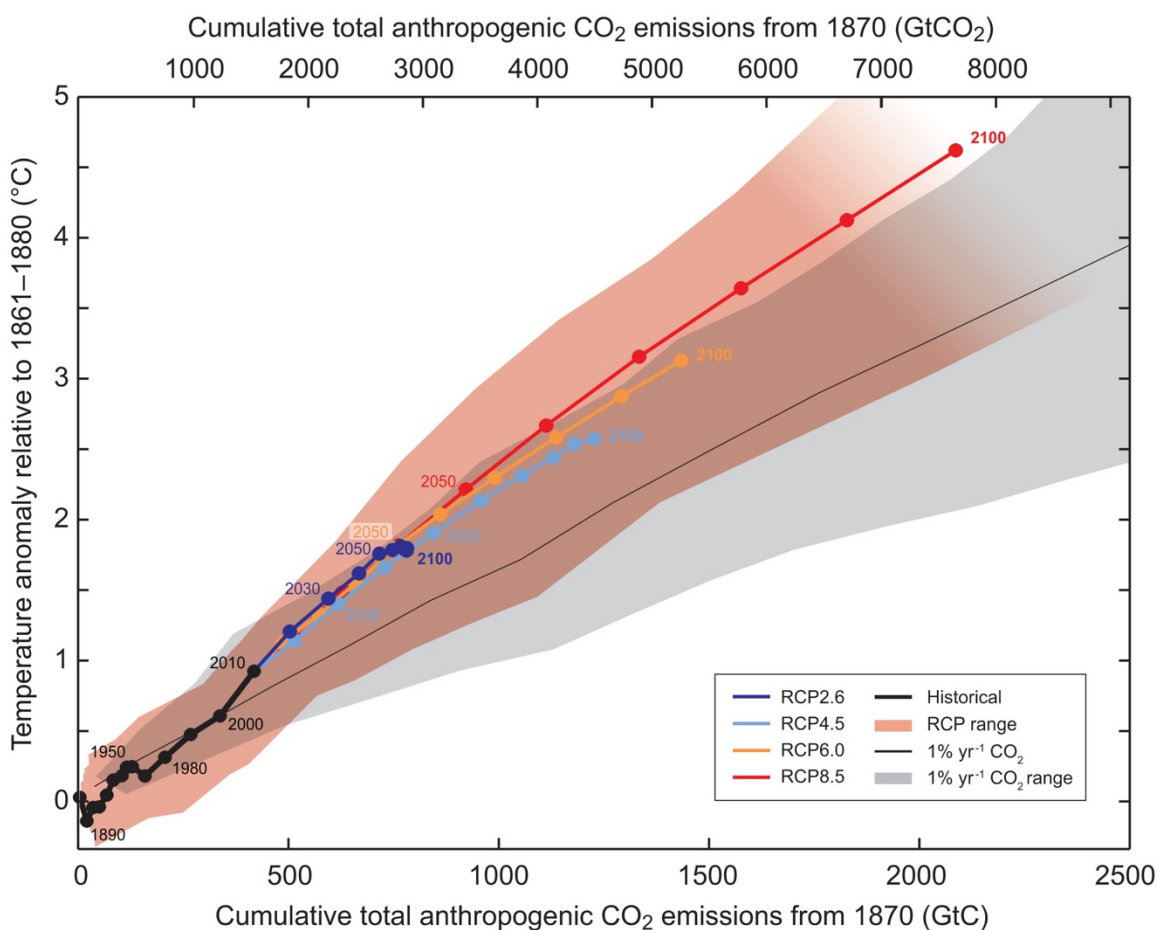


Figure 14.1: Global CO₂ emissions and probabilistic temperature outcomes of Paris. (A) Global CO₂ emissions from energy and industry (includes CO₂ emissions from all fossil fuel production and use and industrial processes such as cement manufacture that also produce CO₂ as a byproduct) for emissions scenarios following no policy, current policy, meeting the INDCs with no increased future ambition and meeting the INDCs with continually increasing ambition. (B) Likelihoods of different levels of increase in global mean surface temperature during the 21st century relative to preindustrial levels for the four scenarios. Although (A) shows only CO₂ emissions from energy and industry, temperature outcomes are based on the full suite of GHG, aerosol, and short-lived species emissions across the full set of human activities and physical Earth systems. (Figure source: Fawcett et al. 2015)



1

2 **Figure 14.2:** Global mean temperature change for a number of scenarios as a function of

3 cumulative CO₂ emissions from preindustrial conditions, with time progressing along each

4 individual line for each scenario. (Figure source: IPCC 2013; © IPCC. Used with

5 permission.)

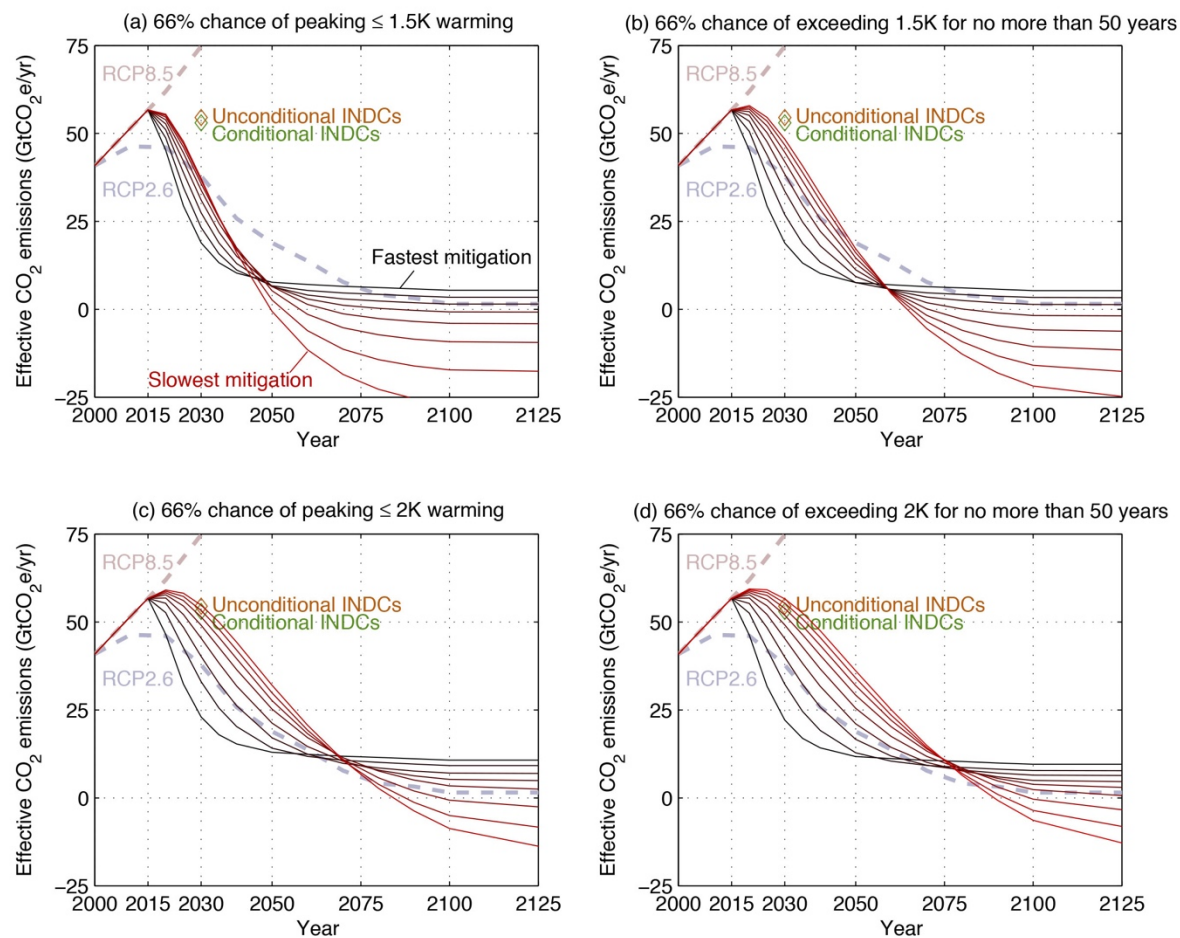


Figure 14.3: Global emissions pathways of effective global CO₂ emissions which would be consistent with different temperature targets (relative to preindustrial temperatures). (Figure source: Sanderson et al. 2016)

REFERENCES

- Allen, M.R., D.J. Frame, C. Huntingford, C.D. Jones, J.A. Lowe, M. Meinshausen, and N. Meinshausen, 2009: Warming caused by cumulative carbon emissions towards the trillionth tonne. *Nature*, **458**, 1163-1166. <http://dx.doi.org/10.1038/nature08019>
- Climate Action Tracker, 2016. <http://climateactiontracker.org/global.html>
- Fawcett, A.A., G.C. Iyer, L.E. Clarke, J.A. Edmonds, N.E. Hultman, H.C. McJeon, J. Rogelj, R. Schuler, J. Alsalam, G.R. Asrar, J. Creason, M. Jeong, J. McFarland, A. Mundra, and W. Shi, 2015: Can Paris pledges avert severe climate change? *Science*, **350**, 1168-1169. <http://dx.doi.org/10.1126/science.aad5761>
- Hayhoe, K.A.S., H.S. Kheshgi, A.K. Jain, and D.J. Wuebbles, 1998: Tradeoffs in fossil fuel use: the effects of CO₂, CH₄, and SO₂ aerosol emissions on climate. *World Resources Review*, **10**.
- IPCC, 2013: *Climate Change 2013: The Physical Science Basis. Contribution of Working Group I to the Fifth Assessment Report of the Intergovernmental Panel on Climate Change*. Cambridge University Press, Cambridge, UK and New York, NY, 1535 pp. <http://dx.doi.org/10.1017/CBO9781107415324> www.climatechange2013.org
- IPCC, 2013: Summary for policymakers. *Climate Change 2013: The Physical Science Basis. Contribution of Working Group I to the Fifth Assessment Report of the Intergovernmental Panel on Climate Change*. Stocker, T.F., D. Qin, G.-K. Plattner, M. Tignor, S.K. Allen, J. Boschung, A. Nauels, Y. Xia, V. Bex, and P.M. Midgley, Eds. Cambridge University Press, Cambridge, United Kingdom and New York, NY, USA, 1–30. <http://dx.doi.org/10.1017/CBO9781107415324.004>
- Joos, F., R. Roth, J.S. Fuglestad, G.P. Peters, I.G. Enting, W. von Bloh, V. Brovkin, E.J. Burke, M. Eby, N.R. Edwards, T. Friedrich, T.L. Frölicher, P.R. Halloran, P.B. Holden, C. Jones, T. Kleinen, F.T. Mackenzie, K. Matsumoto, M. Meinshausen, G.K. Plattner, A. Reisinger, J. Segschneider, G. Shaffer, M. Steinacher, K. Strassmann, K. Tanaka, A. Timmermann, and A.J. Weaver, 2013: Carbon dioxide and climate impulse response functions for the computation of greenhouse gas metrics: a multi-model analysis. *Atmospheric Chemistry and Physics*, **13**, 2793-2825. <http://dx.doi.org/10.5194/acp-13-2793-2013>
- Keith, D.W., R. Duren, and D.G. MacMartin, 2014: Field experiments on solar geoengineering: report of a workshop exploring a representative research portfolio. *Philosophical Transactions of the Royal Society A: Mathematical, Physical and Engineering Sciences*, **372**. <http://dx.doi.org/10.1098/rsta.2014.0175>

- Keith, D.W. and D.G. MacMartin, 2015: A temporary, moderate and responsive scenario for solar geoengineering. *Nature Climate Change*, **5**, 201-206.
<http://dx.doi.org/10.1038/nclimate2493>
- Kravitz, B., K. Caldeira, O. Boucher, A. Robock, P.J. Rasch, K. Alterskjær, D.B. Karam, J.N.S. Cole, C.L. Curry, J.M. Haywood, P.J. Irvine, D. Ji, A. Jones, J.E. Kristjánsson, D.J. Lunt, J.C. Moore, U. Niemeier, H. Schmidt, M. Schulz, B. Singh, S. Tilmes, S. Watanabe, S. Yang, and J.-H. Yoon, 2013: Climate model response from the Geoengineering Model Intercomparison Project (GeoMIP). *Journal of Geophysical Research: Atmospheres*, **118**, 8320-8332. <http://dx.doi.org/10.1002/jgrd.50646>
- MacMartin, D.G., D.W. Keith, B. Kravitz, and K. Caldeira, 2013: Management of trade-offs in geoengineering through optimal choice of non-uniform radiative forcing. *Nature Clim. Change*, **3**, 365-368. <http://dx.doi.org/10.1038/nclimate1722>
- McGlade, C. and P. Ekins, 2015: The geographical distribution of fossil fuels unused when limiting global warming to 2 [deg]C. *Nature*, **517**, 187-190.
<http://dx.doi.org/10.1038/nature14016>
- NAS, 2015: *Climate intervention: Carbon dioxide removal and reliable sequestration*. The National Academies Press, Washington, DC, 154 pp. <http://dx.doi.org/10.17226/18805>
- NAS, 2015: *Climate intervention: Reflecting sunlight to cool earth*. The National Academies Press, Washington, DC, 260 pp. <http://dx.doi.org/10.17226/18988>
- Paltsev, S., E. Monier, J. Scott, A. Sokolov, and J. Reilly, 2015: Integrated economic and climate projections for impact assessment. *Climatic Change*, **131**, 21-33.
<http://dx.doi.org/10.1007/s10584-013-0892-3>
- Pierce, J.R., D.K. Weisenstein, P. Heckendorn, T. Peter, and D.W. Keith, 2010: Efficient formation of stratospheric aerosol for climate engineering by emission of condensable vapor from aircraft. *Geophysical Research Letters*, **37**, L18805.
<http://dx.doi.org/10.1029/2010GL043975>
- Ricke, K.L., M.G. Morgan, and M.R. Allen, 2010: Regional climate response to solar-radiation management. *Nature Geoscience*, **3**, 537-541.
<http://dx.doi.org/10.1038/ngeo915>
- Rogelj, J., M. den Elzen, N. Höhne, T. Fransen, H. Fekete, H. Winkler, R. Schaeffer, F. Sha, K. Riahi, and M. Meinshausen, 2016: Paris Agreement climate proposals need a boost to keep warming well below 2 °C. *Nature*, **534**, 631-639.
<http://dx.doi.org/10.1038/nature18307>

- 1 Sanderson, B.M., B.C. O'Neill, and C. Tebaldi, 2016: What would it take to achieve the Paris
2 temperature targets? *Geophysical Research Letters*, **43**, 7133-7142.
3 <http://dx.doi.org/10.1002/2016GL069563>
- 4 Shah, N., M. Wei, E.L. Virginie, and A.A. Phadke, 2015: Benefits of Leapfrogging to
5 Superefficiency and Low Global Warming Potential Refrigerants in Room Air
6 Conditioning.
- 7 Shepherd, J.G., K. Caldeira, P. Cox, J. Haigh, D. Keith, B. Launder, G. Mace, G.
8 MacKerron, J. Pyle, S. Rayner, C. Redgwell, and A. Watson, 2009: *Geoengineering the*
9 *climate: Science, governance and uncertainty*. Royal Society, 82 pp.
10 http://eprints.soton.ac.uk/156647/1/Geoengineering_the_climate.pdf
- 11 Tebaldi, C. and P. Friedlingstein, 2013: Delayed detection of climate mitigation benefits due
12 to climate inertia and variability. *Proceedings of the National Academy of Sciences*, **110**,
13 17229-17234. <http://dx.doi.org/10.1073/pnas.1300005110>
- 14 Tebaldi, C. and M.F. Wehner, 2016: Benefits of mitigation for future heat extremes under
15 RCP4.5 compared to RCP8.5. *Climatic Change*, 1-13. [http://dx.doi.org/10.1007/s10584-](http://dx.doi.org/10.1007/s10584-016-1605-5)
16 [016-1605-5](http://dx.doi.org/10.1007/s10584-016-1605-5)
- 17 Tilmes, S., B.M. Sanderson, and B.C. O'Neill, 2016: Climate impacts of geoengineering in a
18 delayed mitigation scenario. *Geophysical Research Letters*, **43**, 8222-8229.
19 <http://dx.doi.org/10.1002/2016GL070122>
- 20 UNFCCC, 2015: Paris Agreement. 25 pp. United Nations Framework Convention on Climate
21 Change, [Bonn, Germany].
22 [http://unfccc.int/files/essential_background/convention/application/pdf/english_paris_agr](http://unfccc.int/files/essential_background/convention/application/pdf/english_paris_agreement.pdf)
23 [eement.pdf](http://unfccc.int/files/essential_background/convention/application/pdf/english_paris_agreement.pdf)
- 24 Zaelke, D. and N. Borgford-Parnell, 2015: The importance of phasing down
25 hydrofluorocarbons and other short-lived climate pollutants. *Journal of Environmental*
26 *Studies and Sciences*, **5**, 169-175. <http://dx.doi.org/10.1007/s13412-014-0215-7>

15. Potential Surprises: Compound Extremes and Tipping Elements

KEY FINDINGS

1. Positive feedbacks (self-reinforcing cycles) within the climate system have the potential to accelerate human-induced climate change and even shift the Earth's climate system, in part or in whole, into new states that are very different from those experienced in the recent past (for example, ones with greatly diminished ice sheets or different large-scale patterns of atmosphere or ocean circulation). Some feedbacks and potential state shifts can be modeled and quantified; others can be modeled or identified but not quantified; and some are probably still unknown. (*Very high confidence*)
2. The physical and socioeconomic impacts of compound extreme events (such as simultaneous heat and drought, wildfires associated with hot and dry conditions, or flooding associated with high precipitation on top of snow or waterlogged ground) can be greater than the sum of the parts (*very high confidence*). Few analyses consider the spatial or temporal correlation between extreme events.
3. While climate models incorporate important climate processes that can well quantified, they do not include all of the processes that can contribute to positive feedbacks, correlation of extremes, and abrupt and/or irreversible changes. For this reason, future changes outside the range projected by climate models cannot be ruled out (*very high confidence*), and climate models are more likely to underestimate than to overestimate the amount of future change (*medium confidence*).

15.1 Introduction

Humanity is conducting an unprecedented experiment with the Earth's climate system, through the large-scale combustion of fossil fuels, widespread deforestation, and the resulting release of carbon dioxide (CO₂) into the atmosphere, as well as through emissions of other greenhouse gases and radiatively active substances from human activities (Ch. 2: Scientific Basis). Previous chapters have covered a variety of observed and projected changes in the climate system, including averages and extremes of temperature, precipitation, sea level, and storm events (Chapters 1, 4-13). While the distribution of climate model projections provides insight into the range of possible future change, this range is limited by the fact that models do not include or fully represent some of the known processes and components of the climate system. Therefore, there is a significant potential for our planetary experiment to result in unanticipated surprises, and a broad consensus that the further and the faster the Earth's climate system is pushed towards warming, the greater the risk of such surprises.

The climate system is made up of many subcomponents that interact in complex ways, including some that may be difficult to anticipate. Examples such as Arctic sea ice, Greenland Ice Sheet melt, and Antarctic Ice Sheet instability illustrate how positive feedbacks, or self-reinforcing

cycles, within and between systems have the potential to magnify changes in any given system. Factoring in natural variability and the existence of thresholds beyond which relatively rapid change can occur raises the possibility of a cascading series of impacts throughout the interconnected Earth system and across a broad range of temporal and spatial scales.

This chapter focuses on two potential types of surprises. The first arises from changing correlations in extreme events which, on their own, may not be surprising but which together can increase the likelihood of “perfect storms” of physical and/or socioeconomic impacts. Increasing correlation of extremes, either between types of events (such as paired extremes of droughts and intense rainfall) or over greater spatial or temporal scales (such as a drought occurring in multiple breadbaskets around the world or lasting for multiple decades) are often ignored by analyses that focus solely on one class of extreme. The second type of surprise arises from positive feedbacks in the climate system, which can give rise to “tipping elements” that can exist in multiple, stable but quite different states. Examples of possible tipping elements include modes of atmosphere–ocean circulation like El Niño–Southern Oscillation, ice sheets, and large-scale ecosystems like the Amazon rainforest (Lenton et al. 2008; Kopp et al. 2016).

15.2 Risk Quantification and Its Limits

Quantifying the risk of low-probability, high-impact events, based on models or observations, usually involves examining the tails of a probability distribution function (PDF). Robust detection, attribution, and projection of such events into the future is challenged by multiple factors, including an instrumental record (typically no more than 130 years in length across the United States) that often does not represent the full range of physical possibilities in the climate system, as well as the limitations of the statistical tools, scientific understanding, and models used to describe these processes (Zwiers et al. 2013).

The 2013 Boulder, Colorado, floods and the Dust Bowl of the 1930s in the central United States are two examples of extreme events whose magnitude and/or extent are unprecedented in the observational record. Statistical approaches such as Extreme Value Theory can be used to model and estimate the magnitude of rare events that may not have occurred in the observational record, such as the “1,000-year flood event” (i.e., a flood event with a 0.1% chance of occurrence in any given year) (e.g., Smith 1987). While useful for many applications, these are not physical models: they are statistical models that are typically based on the assumption that observed patterns of natural variability (that is, the sample from which the models derive their statistics) are valid beyond the observational period. Extremely rare events can also be assessed based upon paleoclimate records and physical modeling. In the paleoclimatic record, numerous abrupt changes have occurred since the last deglaciation, many larger than those recorded in the instrumental record. For example, tree ring records of drought in the western United States show abrupt, long-lasting megadroughts that were similar to but more intense and longer-lasting than the 1930s Dust Bowl (Woodhouse and Overpeck 1998).

Since climate models are based on physics rather than observational data, they are not inherently constrained to any given time period or set of physical conditions. They have been used to study the Earth in the distant past, and even the climate of other planets (e.g., Lunt et al. 2012; Navarro et al. 2014). Looking to the future, thousands of years' worth of simulations can be generated and explored to characterize small-probability, high-risk extreme events, as well as correlated extremes (see Section 15.4). However, the likelihood that such model events represent real risks is limited by well-known uncertainties in climate modeling related to parameterizations, model resolution, and limits to scientific understanding (Ch. 4: Projections). For example, conventional convective parameterizations in global climate models systematically underestimate extreme precipitation (Kang et al. 2015). In addition, models often do not accurately capture or even include the processes, such as permafrost feedbacks, by which abrupt, non-reversible change may occur (see Section 15.4). An analysis focusing on physical climate predictions over the last 20 years found a tendency for scientific assessments such as those of the Intergovernmental Panel on Climate Change to under-predict rather than over-predict changes that were subsequently observed (Brysse et al. 2013).

15.3 Compound Extremes

An important aspect of surprise is the potential for compound extreme events. These can be events that occur at the same time, or in sequence (such as consecutive droughts in the same region); and in the same geographic location, or at multiple locations within a given country or around the world (such as the 2009 Australian floods and wildfires). They may consist of multiple extreme events, or of events that by themselves may not be extreme, but together produce a multi-event "occurrence" (such as a heat wave accompanied by drought; Quarantelli 1986). It is possible for the net impact of these events to be less than the sum of the individual events, if their effects cancel each other out. For example, increasing carbon dioxide concentrations and acceleration of the hydrological cycle may mitigate the future impact of extremes in gross primary productivity that currently impact the carbon cycle (Zscheischler et al. 2014). However, our primary concern relates to those whose effects are additive, or even multiplicative, due to compounding influences.

Some areas are susceptible to multiple types of extreme events that can occur simultaneously. For example, some regions are susceptible to both flooding from coastal storms and riverine flooding from snow melt, and a compound event would be the occurrence of both simultaneously. Compound events can also result from shared forcing factors, including natural cycles like El Niño–Southern Oscillation (ENSO); large-scale circulation patterns, such as the ridge observed during the current California Drought (e.g., Swain et al. 2016; see also Ch. 8: Droughts, Floods, and Hydrology); or relatively greater regional sensitivity to global change, as may occur in "hot spots" such as the western United States (Diffenbaugh and Giorgi 2012). Finally, compound events can result from positive feedbacks between individual events leading to mutual reinforcement, such as the relationship between droughts and heat waves in water-limited areas (IPCC 2012). In a changing climate, the probability of compound events can be

1 altered if there is an underlying trend in non-extreme conditions, such as mean temperature,
2 precipitation, or sea level, that alters the baseline conditions or vulnerability of a region. It can
3 also be altered if there is a change in the frequency or intensity of individual extreme events
4 relative to the changing mean (for example, stronger storm surges, more frequent heat waves, or
5 heavier precipitation events).

6 The characterization of compound events in both the historical record and future projections
7 remains challenging and largely incomplete. For example, the relationship between drought and
8 heat, linked through soil moisture and evaporation, is one of the most widespread compound
9 events. Globally, the occurrence of warm/dry and warm/wet conditions has increased since the
10 1950s (Hao et al. 2013). In the future, hot summers will become more frequent, and although it is
11 not always clear for every region whether drought frequency will change, droughts in already dry
12 regions, such as the southwestern United States, are likely to be more intense in a warmer world
13 due to faster evaporation and associated surface drying (Collins et al. 2013; Trenberth et al.
14 2014; Cook et al. 2015). For other regions, however, the picture is not as clear. Recent examples
15 of heat/drought events (in the southern Great Plains in 2011; in California, 2012–2015) have
16 highlighted the inadequacy of traditional univariate risk assessment methods (AghaKouchak et
17 al. 2014); yet an analysis for the contiguous United States of precipitation deficits and positive
18 temperature anomalies in the last 30 years finds no significant trend (Serinaldi 2016).

19 Another compound event frequently discussed in the literature is wildfire driven by the
20 combined effects of high precipitation variability (wet seasons followed by dry), elevated
21 temperature, and low humidity. These factors increase the risk of wildfires, which, if followed by
22 heavy rain, can in turn promote landslides and erosion. They can also radically increase
23 emissions of greenhouse gases, as demonstrated by the amount of carbon dioxide produced by
24 the Fort McMurray fires of May 2016—more than 10% of Canada’s annual emissions (Ch. 11:
25 Arctic Changes).

26 A third compound event involves flooding arising from wet conditions due to precipitation or to
27 snowmelt, which could be exacerbated by warm temperatures. These wet conditions lead to high
28 groundwater levels, saturated soils, and/or elevated river flows, which can increase the risk of
29 flooding associated with a given storm days or even months later (IPCC 2012).

30 Compound events may surprise in two ways. The first is if known types of compound events
31 recur, but are stronger, longer-lasting, and/or more widespread than those experienced in the very
32 limited observational record or projected by model simulations for the future. An example would
33 be simultaneous drought events in different agricultural regions across the country, or even
34 around the world, that challenge the ability of human systems to provide adequate affordable
35 food. The second way in which they could surprise would be the emergence of new types of
36 compound events not observed in the historical record or predicted by model simulations, either
37 due to the limited resolution of models or due to an increase in the frequency of such events as a
38 result of human-induced climate change, or both. An example is Hurricane Sandy, where sea

level rise, anomalously high ocean temperatures, and high tides combined to strengthen both the storm and the magnitude of storm surge associated with it (Reed et al. 2015). At the same time, a blocking ridge over Greenland—a feature whose strength and frequency may be related to both Greenland surface melt and reduced summer sea ice in the Arctic (Liu et al. 2016; see also Ch. 11: Arctic Changes)—redirected the storm inland to what was, coincidentally, an exceptionally high-exposure location.

[INSERT FIGURE 15.1 HERE:]

Figure 15.1: (left) Potential climatic tipping elements affecting the Americas. (right) Wildfire and drought events from the NOAA Billion Dollar Weather Events list (1980–2016), and associated temperature and precipitation anomalies. Dot size scales with the magnitude of impact, as reflected by the cost of the event. These high-impact events occur preferentially under hotter, drier conditions. (Figure source: (left) adapted from Lenton et al. 2008, (right) original analysis.]

15.4 Climatic Tipping Elements

Some potential climatic surprises relate to *critical thresholds*, sometimes called “tipping points”, in different parts of the Earth systems (e.g., Lenton et al. 2008; Collins et al. 2013; NRC 2013; Kopp et al. 2016). These different parts of the Earth system, known as *tipping elements*, have the potential to enter into self-amplifying cycles that commit them to shifting into a new state: for example, from one in which the Arctic Ocean is covered by ice in the summer, to one in which it is ice-free in the summer. In some potential tipping elements, these state shifts occur abruptly; in others, the commitment to a state shift may occur rapidly, but the state shift itself may take decades, centuries, or even millennia to play out. Often, the forcing that commits a tipping element to a shift in state is unknown; sometimes, it is even unclear whether a proposed tipping element actually exhibits tipping behavior. Through a combination of physical modeling, paleoclimate observations, and expert elicitations, scientists have identified possible tipping elements in atmosphere–ocean circulation, the cryosphere, the carbon cycle, and ecosystems (Table 15.1).

[INSERT TABLE 15.1 HERE:]

Table 15.1: Potential tipping elements (adapted from Kopp et al. 2016).]

The Atlantic meridional overturning circulation (AMOC) is a major component of global ocean circulation. Driven by the sinking of cold, dense water in the North Atlantic near Greenland, its strength is projected to decrease with warming due to freshwater input from increased precipitation, glacial melt, and melt of the Greenland Ice Sheet (Rahmstorf et al. 2015; see also discussion in Ch. 11: Arctic Changes). Given sufficient freshwater input, AMOC might collapse entirely, although the large majority of models do not produce an abrupt collapse in the 21st century (NRC 2013). A decrease in AMOC strength is, however, probable and may already be culpable for the “warming hole” observed in the North Atlantic (Rahmstorf et al. 2015), although

1 it is still unclear whether this decrease represents a forced change or internal variability (Cheng
2 et al. 2016).

3 A decrease in the strength of AMOC would accelerate sea level rise off the northeastern United
4 States (Yin and Goddard 2013), while a full collapse could result in as much as approximately
5 0.5 meters (1.6 feet) of regional sea level rise (Gregory and Lowe 2000; Levermann et al. 2005)
6 and a cooling of approximately 0°F–4°F (0°C–2°C) over the United States (Jackson et al. 2015).
7 A slowdown of the AMOC would also lead to a reduction of ocean carbon dioxide uptake, and
8 thus an acceleration of warming (Pérez et al. 2013).

9 The atmospheric–oceanic circulation of the equatorial Pacific drives the state shifts of the El
10 Niño–Southern Oscillation through a set of feedbacks. This is an example of a tipping element
11 that shifts on a sub-decadal, interannual timescale, primarily in response to internal noise.
12 Climate model experiments suggest climate change will reduce the threshold needed to trigger
13 extreme El Niño and extreme La Niña events. As can be seen by examining the impacts of recent
14 El Niño and La Niña events, such a shift would have potential implications for the United States
15 (Cai et al. 2014, 2015; for more on ENSO impacts, see Chapter 5).

16 Arctic sea ice may exhibit abrupt state shifts into summer- and perennially ice-free states.
17 Critical positive feedbacks not captured sufficiently by global climate models could include:
18 greater high-latitude storminess and ocean wave penetration as sea ice declines; more northerly
19 incursions of warm air and water; melting associated with increasing water vapor; loss of
20 multiyear ice; and albedo decreases on the sea ice surface. At the same time, however, the point
21 at which the threshold for an abrupt shift would be crossed also depends on the role of natural
22 variability in a changing system; the relative importance of potential stabilizing negative
23 feedbacks—such as more efficient heat transfer from the ocean to the atmosphere in fall and
24 winter as sea declines; and how sea ice in other seasons, as well as the climate system more
25 generally, will respond once the first “ice free” summer occurs. It is also possible that summer
26 sea ice may not abruptly collapse but instead respond in a manner proportional to increase in
27 temperature (Armour et al. 2011; Ridley et al. 2012; Li et al. 2013; Wagner and Eisenman 2015).
28 Moreover, an abrupt decrease in winter sea ice may result simply from the Arctic Ocean
29 warming above a critical temperature for ice formation, rather than from positive feedbacks
30 (Bathiany et al. 2016).

31 Two possible tipping elements in the carbon cycle also lie in the Arctic. The first is buried in the
32 permafrost, where an estimated 1,300–1,600 Gt C (Schuur et al. 2015) could be released as CO₂
33 or methane as the Arctic warms. The release of permafrost carbon is limited by the freeze–thaw
34 cycle, the rate with which heat diffuses into the permafrost, the potential for organisms to cycle
35 permafrost carbon into new biomass, and limited oxygen availability. Though the release of
36 permafrost carbon would probably not be fast enough to trigger a runaway self-amplifying cycle
37 leading to a permafrost-free Arctic, it still has the potential to significantly amplify both local
38 and global warming, reduce the budget of human-caused CO₂ emissions available to meet global

1 temperature targets such as the Paris Agreement, and drive continued warming even if human
2 emissions stopped altogether (MacDougall et al. 2012, 2015).

3 The second Arctic carbon cycle tipping point is an estimated 1,100 Gt of carbon in methane
4 hydrates (equivalent to about 11,000 Gt C as CO₂ using a 100-year global warming potential)
5 frozen into the sediments of continental shelves of the Arctic Ocean (Kretschmer et al. 2015).
6 While this reservoir has been known and discussed for several decades (e.g., Kvenvolden 1988),
7 only recently has it been hypothesized that warming bottom water temperatures may destabilize
8 the hydrates over timescales shorter than millennia, leading to their release into the water column
9 and eventually the atmosphere (e.g., Archer 2007; Kretschmer et al. 2015). Recent measurements
10 of the release of methane from these sediments in summer find that, while methane is being
11 emitted, these emissions do not appear to reach the ocean surface in sufficient quantity to affect
12 the atmospheric methane budget (Myhre et al. 2016). Future estimates of natural releases to the
13 atmosphere over the next century are only a fraction of present-day anthropogenic methane
14 emissions (Kretschmer et al. 2015; Stranne et al. 2016). These estimates, however, neglect the
15 possibility that humans may insert themselves into the physical feedback systems. With an
16 estimated 53% of global fossil fuel reserves in the Arctic becoming increasingly accessible in a
17 warmer world (Lee and Holder 2001), the risks associated with this carbon being extracted and
18 burned, further exacerbating the influence of humans on global climate, are evident (Jakob and
19 Hilaire 2015; McGlade and Elkins 2015). Of less concern but still relevant, Arctic ocean waters
20 themselves are a source of methane, which could increase as sea ice decreases (Kort et al. 2012).

21 The Antarctic and Greenland Ice Sheets are clear tipping elements, although they respond
22 relatively slowly. The Greenland Ice Sheet exhibits multiple stable states as a result of feedbacks
23 involving the elevation of the ice sheet, atmospheric dynamics, and albedo (Ridley et al. 2010;
24 Robinson et al. 2012; Levermann et al. 2013), with some results suggesting that warming of
25 1.6°C (2.9°F) above a preindustrial baseline could commit Greenland to an 85% reduction in ice
26 volume and a 20 foot (6 meter) contribution to global mean sea level over the course of centuries
27 or millennia (Robinson et al. 2012). In Antarctica, enough ice to raise global mean sea level by
28 23 meters (75.5 feet) sits on bedrock that is below sea level (Fretwell et al. 2013). This ice is
29 vulnerable to collapse due to a variety of feedbacks involving ocean–ice sheet interactions
30 (Schoof 2007; Gomez et al. 2010; Ritz et al. 2015; Mengel and Levermann et al. 2014; Pollard et
31 al. 2015). Observational evidence suggests that ice dynamics already in progress have committed
32 parts of the West Antarctic Ice Sheet to contributing as much as 1.2 meters (3.9 feet) to global
33 mean sea level, probably over the course of many centuries (Joughin et al. 2014; Rignot et al.
34 2014). Plausible physical modeling indicates that, under RCP8.5 (Ch. 4: Projections), Antarctic
35 ice could contribute 1 meter (3.28 feet) or more to global mean sea level over the remainder of
36 this century (DeConto and Pollard 2016), with some authors arguing that rates of change could
37 be even faster (Hansen et al. 2016).

38 Tipping elements also exist in large-scale ecosystems. For example, boreal forests such as those
39 in southern Alaska may expand northward in response to Arctic warming. Because forests are

darker than the tundra they replace, their expansion amplifies regional warming, which in turn accelerates their expansion (Jones et al. 2009). Similarly, coral reef ecosystems, such as those in Florida, are maintained by stabilizing ecological feedbacks among corals, coralline red algae, and grazing fish and invertebrates. However, these stabilizing feedbacks can be undermined by warming, increased risk of bleaching events, spread of disease, and ocean acidification, leading to abrupt reef collapse (Hoegh-Guldberg et al. 2007).

15.5 Paleoclimatic Hints of Additional Potential Surprises

The paleoclimatic record provides evidence for additional state shifts whose driving mechanisms are as yet poorly understood. For example, compared to reconstructions of temperature and CO₂ from the geological record, global climate models have a tendency to underestimate the magnitude of both global mean warming in response to higher CO₂ levels and the amplification of this warming at high latitudes. The late Pliocene (about 3.6–2.6 million years ago), the middle Miocene (about 17–14.5 million years ago), and the early Eocene (about 56–48 million years ago)—all periods well predating the first appearance of *Homo sapiens* around two hundred thousand years ago (Tattersall 2009)—provide three case studies.

Global climate model (GCM) simulations of the late Pliocene systematically underestimate warming north of 30°N (Salzmann et al. 2013). Similarly, GCM simulations of paleoclimate during the middle Miocene (about 17–14.5 million years ago) cannot simultaneously replicate the proxy-estimated global mean temperature (approximately 8°C ± 2°C [14°F ± 4°F] warmer than preindustrial) and the approximately 40% reduction in the pole-to-equator temperature gradient relative to today (Goldner et al. 2014). Although about one-third of the global mean temperature increase can be attributed to changes in geography and vegetation, geological proxies indicate CO₂ concentrations of around 400 ppm (Goldner et al. 2014; Foster et al. 2012), suggesting that as yet unidentified feedbacks must be invoked to explain climate conditions during the middle Miocene.

The early Eocene is characterized by the absence of permanent land ice, CO₂ concentrations peaking around 1400 ± 470 ppm (Anagnostu et al. 2016), and global temperatures about 14°C ± 3°C (25°F ± 5°F) warmer than the preindustrial (Caballero and Huber 2013). Like the late Pliocene and the middle Miocene, it also exhibits about half the meridional temperature gradient of today (Huber and Caballero 2011; Lunt et al. 2012). About one-third of the temperature difference is attributable to changes in geography, vegetation, and ice sheet coverage (Caballero and Huber 2013). To reproduce both the elevated global mean temperature and the reduced pole-to-equator temperature gradient, climate models require CO₂ concentrations approximately 2–5 times that indicated by the proxy record (Lunt et al. 2012).

One possible explanation for this discrepancy is a planetary state shift that, above a particular CO₂ threshold, leads to a significant increase in the sensitivity of the climate to CO₂. One modeling study (Caballero and Huber 2013) suggests that an abrupt change in atmospheric

1 circulation (the onset of equatorial atmospheric superrotation) between 1,120 and 2,240 ppm
2 CO₂ could lead to a reduction in cloudiness and an approximate doubling of climate sensitivity.
3 However, the critical threshold for such a transition is poorly constrained. If it happened at a
4 lower CO₂ level, it might explain the Eocene discrepancy and potentially also the Miocene
5 discrepancy. It could also then pose a threat within the 21st century under the higher RCP8.5
6 emissions pathway (see Ch. 4: Projections for a description of future scenarios). Regardless of
7 the particular mechanism, the systematic paleoclimatic model–data mismatch for past warm
8 climates suggests that GCMs are omitting at least one, and probably more, processes crucial to
9 future warming, especially in polar regions. For this reason, future changes outside the range
10 projected by climate models cannot be ruled out, and climate models are more likely to
11 underestimate than to overestimate the amount of future change (*medium confidence*).
12

TRACEABLE ACCOUNTS

Key Finding 1

Positive feedbacks (self-reinforcing cycles) within the climate system have the potential to accelerate human-induced climate change and even shift the Earth's climate system, in part or in whole, into new states that are very different from those experienced in the recent past. These states might include, for example, ones with greatly diminished ice sheets or different large-scale patterns of atmosphere or ocean circulation. Some feedbacks and potential state shifts can be modeled and quantified; others can be modeled or identified but not quantified; and some are probably still unknown (*very high confidence*).

Description of evidence base

This key finding is based on a large body of scientific literature recently summarized by Lenton et al. (2008), NRC (2013), and Kopp et al. (2016). As NRC (2013, page vii) states, "A study of Earth's climate history suggests the inevitability of 'tipping points'—thresholds beyond which major and rapid changes occur when crossed—that lead to abrupt changes in the climate system" and (page xi), "Can all tipping points be foreseen? Probably not. Some will have no precursors, or may be triggered by naturally occurring variability in the climate system. Some will be difficult to detect, clearly visible only after they have been crossed and an abrupt change becomes inevitable." As IPCC AR5 WG1 Chapter 12, section 12.5.5 (Collins et al. 2013) further states, "A number of components or phenomena within the Earth system have been proposed as potentially possessing critical thresholds (sometimes referred to as tipping points) beyond which abrupt or nonlinear transitions to a different state ensues." Collins et al. (2013) further summarizes critical thresholds that can be modeled and others that can only be identified.

Major uncertainties

The largest uncertainties are: 1) whether proposed tipping elements actually undergo critical transitions, 2) the magnitude and timing of forcing that will be required to initiate critical transitions in tipping elements, 3) the speed of the transition once it has been triggered, 4) the characteristics of the new state that results from such transition, and 5) the potential for new tipping elements to exist that are yet unknown.

Assessment of confidence based on evidence and agreement, including short description of nature of evidence and level of agreement

☒ Very High

☐ High

☐ Medium

☐ Low

Very high confidence in the likelihood of the existence of positive feedbacks and tipping elements statement is based on a large body of literature published over the last 25 years that draws from basic physics, observations, paleoclimate data, and modeling.

Very high confidence that some feedbacks can be quantified, others are known but cannot be quantified, and others may yet exist that are currently unknown.

Summary sentence or paragraph that integrates the above information

The key finding is based on NRC (2013) and IPCC AR4 WG1 Chapter 12 section 12.5.5 (IPCC 2007), which made a thorough assessment of the relevant literature.

Key Finding 2

The physical and socioeconomic impacts of compound extreme events (such as simultaneous heat and drought, wildfires associated with hot and dry conditions, or flooding associated with high precipitation on top of snow or waterlogged ground) can be greater than the sum of the parts (*very high confidence*). Few analyses consider the spatial or temporal correlation between extreme events.

Description of evidence base

This key finding is based on a large body of scientific literature summarized in the 2012 IPCC Special Report on Extremes (IPCC 2012). The report's Summary for Policymakers (page 6) states, "exposure and vulnerability are key determinants of disaster risk and of impacts when risk is realized...extreme impacts on human, ecological, or physical systems can result from individual extreme weather or climate events. Extreme impacts can also result from non-extreme events where exposure and vulnerability are high or from a compounding of events or their impacts. For example, drought, coupled with extreme heat and low humidity, can increase the risk of wildfire."

Major uncertainties

The largest uncertainties are in the temporal congruence of the events and the compounding nature of their impacts.

Assessment of confidence based on evidence and agreement, including short description of nature of evidence and level of agreement

☒ **Very High**

☐ **High**

☐ **Medium**

☐ **Low**

Very high confidence that the impacts of multiple events could exceed the sum of the impacts of events occurring individually.

Summary sentence or paragraph that integrates the above information

The key finding is based on the 2012 IPCC SREX report, particularly section 3.1.3 on compound or multiple events, which presents a thorough assessment of the relevant literature.

Key Finding 3

While climate models incorporate important climate processes that can well quantified, they do not include all of the processes that contribute to positive feedbacks, correlation of extremes, and abrupt and/or irreversible changes. For this reason, future changes outside the range projected by climate models cannot be ruled out (*very high confidence*), and climate models are more likely to underestimate than to overestimate the amount of future change (*medium confidence*).

Description of evidence base

This key finding is based on the conclusions of IPCC AR5 WG1 (IPCC 2013); what is and is not included in the latest generation of CMIP5 models is summarized in Chapter 9 of this report. The second half of this key finding is further supported by the tendency of global climate models to underestimate, relative to geological reconstructions, the magnitude of both global mean warming and the amplification of warming at high latitudes in past warm climates (e.g., Salzmann et al. 2013; Goldner et al. 2014; Caballeo and Huber 2013; Lunt et al. 2012).

Major uncertainties

The largest uncertainties are structural: are the models including all the important components and relationships necessary to model the feedbacks and if so, are these correctly represented in the models?

Assessment of confidence based on evidence and agreement, including short description of nature of evidence and level of agreement

☒ Very High

☐ High

☒ Medium

☐ Low

Very high confidence that the models are incomplete representations of the real world; **medium confidence** that their tendency is to under- rather than over-estimate the amount of future change.

Summary sentence or paragraph that integrates the above information

The key finding is based on the IPCC AR5 WG1 Chapter 9 (IPCC 2013), as well as systematic paleoclimatic model/data comparisons.

1 **TABLE**2 **Table 15.1:** Potential tipping elements (adapted from Kopp et al., 2016).

Candidate Climatic Tipping Element	State Shift	Main impact pathways
<i>Atmosphere–ocean circulation</i>		
Atlantic meridional overturning circulation	Collapse	regional temperature and precipitation; global mean temperature; regional sea level
El Niño–Southern Oscillation	Increase in amplitude	regional temperature and precipitation
Equatorial atmospheric superrotation	Initiation	cloud cover; climate sensitivity
Regional North Atlantic convection	Collapse	regional temperature and precipitation
<i>Cryosphere</i>		
Antarctic Ice Sheet	Collapse in ice volume	sea level; albedo
Arctic sea ice	Collapse in summertime and/or perennial area	regional temperature and precipitation; albedo
Greenland Ice Sheet	Collapse in ice volume	sea level; albedo
<i>Carbon cycle</i>		
Methane hydrates	Massive release	greenhouse gas emissions
Permafrost carbon	Massive release	greenhouse gas emissions
<i>Ecosystem</i>		

Amazon rainforest	Dieback, Transition to grasslands	ecosystem services; greenhouse gas emissions
Boreal forest	Dieback, Transition to grasslands	ecosystem services; greenhouse gas emissions; albedo
Coral reefs	Die-off	ecosystem services

1

DRAFT

FIGURE

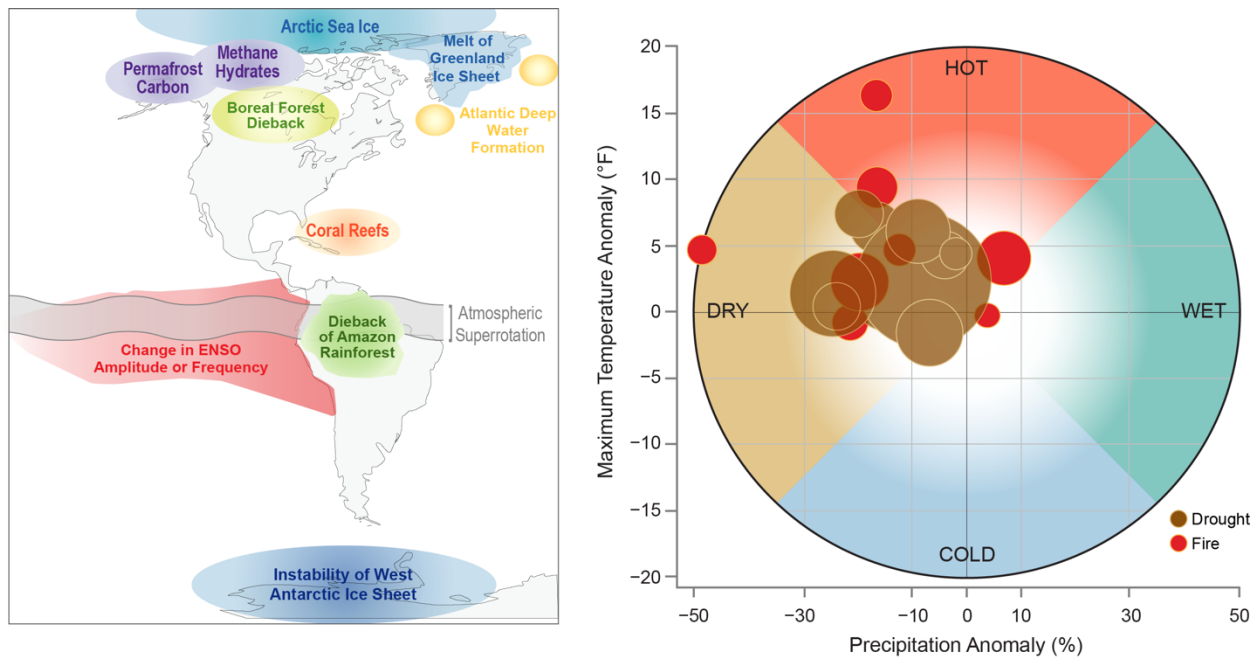


Figure 15.1: (left) Potential climatic tipping elements affecting the Americas (adapted from Lenton et al. 2008). (right) Wildfire and drought events from the NOAA Billion Dollar Weather Events list (1980–2016), and associated temperature and precipitation anomalies. Dot size scales with the magnitude of impact, as reflected by the cost of the event. These high-impact events occur preferentially under hot, dry conditions. (Figure source: adapted from Lenton et al. 2008)

1 REFERENCES

- 2 AghaKouchak, A., L. Cheng, O. Mazdiyasni, and A. Farahmand, 2014: Global warming and
 3 changes in risk of concurrent climate extremes: Insights from the 2014 California drought.
 4 *Geophysical Research Letters*, **41**, 8847-8852. <http://dx.doi.org/10.1002/2014GL062308>
- 5 Anagnostou, E., E.H. John, K.M. Edgar, G.L. Foster, A. Ridgwell, G.N. Inglis, R.D. Pancost,
 6 D.J. Lunt, and P.N. Pearson, 2016: Changing atmospheric CO₂ concentration was the
 7 primary driver of early Cenozoic climate. *Nature*, **533**, 380-384.
 8 <http://dx.doi.org/10.1038/nature17423>
- 9 Archer, D., 2007: Methane hydrate stability and anthropogenic climate change. *Biogeosciences*,
 10 **4**, 521-544. <http://dx.doi.org/10.5194/bg-4-521-2007>
- 11 Armour, K.C., I. Eisenman, E. Blanchard-Wrigglesworth, K.E. McCusker, and C.M. Bitz, 2011:
 12 The reversibility of sea ice loss in a state-of-the-art climate model. *Geophysical Research*
 13 *Letters*, **38**, L16705. <http://dx.doi.org/10.1029/2011GL048739>
- 14 Bathiany, S., D. Notz, T. Mauritsen, G. Raedel, and V. Brovkin, 2016: On the Potential for
 15 Abrupt Arctic Winter Sea Ice Loss. *Journal of Climate*, **29**, 2703-2719.
 16 <http://dx.doi.org/10.1175/JCLI-D-15-0466.1>
- 17 Brysse, K., N. Oreskes, J. O'Reilly, and M. Oppenheimer, 2013: Climate change prediction:
 18 Erring on the side of least drama? *Global Environmental Change*, **23**, 327-337.
 19 <http://dx.doi.org/10.1016/j.gloenvcha.2012.10.008>
- 20 Caballero, R. and M. Huber, 2013: State-dependent climate sensitivity in past warm climates and
 21 its implications for future climate projections. *Proceedings of the National Academy of*
 22 *Sciences*, **110**, 14162-14167. <http://dx.doi.org/10.1073/pnas.1303365110>
- 23 Cai, W., S. Borlace, M. Lengaigne, P. van Rensch, M. Collins, G. Vecchi, A. Timmermann, A.
 24 Santoso, M.J. McPhaden, L. Wu, M.H. England, G. Wang, E. Guilyardi, and F.-F. Jin, 2014:
 25 Increasing frequency of extreme El Nino events due to greenhouse warming. *Nature Climate*
 26 *Change*, **4**, 111-116. <http://dx.doi.org/10.1038/nclimate2100>
- 27 Cai, W., G. Wang, A. Santoso, M.J. McPhaden, L. Wu, F.-F. Jin, A. Timmermann, M. Collins,
 28 G. Vecchi, M. Lengaigne, M.H. England, D. Dommenges, K. Takahashi, and E. Guilyardi,
 29 2015: Increased frequency of extreme La Nina events under greenhouse warming. *Nature*
 30 *Climate Change*, **5**, 132-137. <http://dx.doi.org/10.1038/nclimate2492>
- 31 Cheng, J., Z. Liu, S. Zhang, W. Liu, L. Dong, P. Liu, and H. Li, 2016: Reduced interdecadal
 32 variability of Atlantic Meridional Overturning Circulation under global warming.
 33 *Proceedings of the National Academy of Sciences*, **113**, 3175-3178.
 34 <http://dx.doi.org/10.1073/pnas.1519827113>

- Collins, M., R. Knutti, J. Arblaster, J.-L. Dufresne, T. Fichefet, P. Friedlingstein, X. Gao, W.J. Gutowski, T. Johns, G. Krinner, M. Shongwe, C. Tebaldi, A.J. Weaver, and M. Wehner, 2013: Long-term Climate Change: Projections, Commitments and Irreversibility. *Climate Change 2013: The Physical Science Basis. Contribution of Working Group I to the Fifth Assessment Report of the Intergovernmental Panel on Climate Change*. Stocker, T.F., D. Qin, G.-K. Plattner, M. Tignor, S.K. Allen, J. Boschung, A. Nauels, Y. Xia, V. Bex, and P.M. Midgley, Eds. Cambridge University Press, Cambridge, United Kingdom and New York, NY, USA, 1029–1136. <http://dx.doi.org/10.1017/CBO9781107415324.024>
www.climatechange2013.org
- Cook, B.I., T.R. Ault, and J.E. Smerdon, 2015: Unprecedented 21st century drought risk in the American Southwest and Central Plains. *Science Advances*, **1**.
<http://dx.doi.org/10.1126/sciadv.1400082>
- DeConto, R.M. and D. Pollard, 2016: Contribution of Antarctica to past and future sea-level rise. *Nature*, **531**, 591-597. <http://dx.doi.org/10.1038/nature17145>
- Diffenbaugh, N.S. and F. Giorgi, 2012: Climate change hotspots in the CMIP5 global climate model ensemble. *Climatic Change*, **114**, 813-822. <http://dx.doi.org/10.1007/s10584-012-0570-x>
- Foster, G.L., C.H. Lear, and J.W.B. Rae, 2012: The evolution of pCO₂, ice volume and climate during the middle Miocene. *Earth and Planetary Science Letters*, **341–344**, 243-254.
<http://dx.doi.org/10.1016/j.epsl.2012.06.007>
- Fretwell, P., H.D. Pritchard, D.G. Vaughan, J.L. Bamber, N.E. Barrand, R. Bell, C. Bianchi, R.G. Bingham, D.D. Blankenship, G. Casassa, G. Catania, D. Callens, H. Conway, A.J. Cook, H.F.J. Corr, D. Damaske, V. Damm, F. Ferraccioli, R. Forsberg, S. Fujita, Y. Gim, P. Gogineni, J.A. Griggs, R.C.A. Hindmarsh, P. Holmlund, J.W. Holt, R.W. Jacobel, A. Jenkins, W. Jokat, T. Jordan, E.C. King, J. Kohler, W. Krabill, M. Riger-Kusk, K.A. Langley, G. Leitchenkov, C. Leuschen, B.P. Luyendyk, K. Matsuoka, J. Mouginot, F.O. Nitsche, Y. Nogi, O.A. Nost, S.V. Popov, E. Rignot, D.M. Rippin, A. Rivera, J. Roberts, N. Ross, M.J. Siegert, A.M. Smith, D. Steinhage, M. Studinger, B. Sun, B.K. Tinto, B.C. Welch, D. Wilson, D.A. Young, C. Xiangbin, and A. Zirizzotti, 2013: Bedmap2: improved ice bed, surface and thickness datasets for Antarctica. *The Cryosphere*, **7**, 375-393.
<http://dx.doi.org/10.5194/tc-7-375-2013>
- Goldner, A., N. Herold, and M. Huber, 2014: The challenge of simulating the warmth of the mid-Miocene climatic optimum in CESM1. *Climate of the Past*, **10**, 523-536.
<http://dx.doi.org/10.5194/cp-10-523-2014>

- 1 Gomez, N., J.X. Mitrovica, P. Huybers, and P.U. Clark, 2010: Sea level as a stabilizing factor for
2 marine-ice-sheet grounding lines. *Nature Geoscience*, **3**, 850-853.
3 <http://dx.doi.org/10.1038/ngeo1012>
- 4 Gregory, J.M. and J.A. Lowe, 2000: Predictions of global and regional sea-level rise using
5 AOGCMs with and without flux adjustment. *Geophysical Research Letters*, **27**, 3069-3072.
6 <http://dx.doi.org/10.1029/1999GL011228>
- 7 Hansen, J., M. Sato, P. Hearty, R. Ruedy, M. Kelley, V. Masson-Delmotte, G. Russell, G.
8 Tselioudis, J. Cao, E. Rignot, I. Velicogna, B. Tormey, B. Donovan, E. Kandiano, K.
9 von Schuckmann, P. Kharecha, A.N. Legrande, M. Bauer, and K.W. Lo, 2016: Ice melt, sea
10 level rise and superstorms: evidence from paleoclimate data, climate modeling, and modern
11 observations that 2 °C global warming could be dangerous. *Atmospheric Chemistry and*
12 *Physics*, **16**, 3761-3812. <http://dx.doi.org/10.5194/acp-16-3761-2016>
- 13 Hao, Z., A. AghaKouchak, and T.J. Phillips, 2013: Changes in concurrent monthly precipitation
14 and temperature extremes. *Environmental Research Letters*, **8**, 034014.
15 <http://dx.doi.org/10.1088/1748-9326/8/3/034014>
- 16 Hoegh-Guldberg, O., P.J. Mumby, A.J. Hooten, R.S. Steneck, P. Greenfield, E. Gomez, C.D.
17 Harvell, P.F. Sale, A.J. Edwards, K. Caldeira, N. Knowlton, C.M. Eakin, R. Iglesias-Prieto,
18 N. Muthiga, R.H. Bradbury, A. Dubi, and M.E. Hatziolos, 2007: Coral reefs under rapid
19 climate change and ocean acidification. *Science*, **318**, 1737-1742.
20 <http://dx.doi.org/10.1126/science.1152509>
- 21 Huber, M. and R. Caballero, 2011: The early Eocene equable climate problem revisited. *Climate*
22 *of the Past*, **7**, 603-633. <http://dx.doi.org/10.5194/cp-7-603-2011>
- 23 IPCC, 2007: *Climate Change 2007: The Physical Science Basis. Contribution of Working Group*
24 *I to the Fourth Assessment Report of the Intergovernmental Panel on Climate Change*.
25 Solomon, S., D. Qin, M. Manning, Z. Chen, M. Marquis, K.B. Averyt, M. Tignor, and H.L.
26 Miller, Eds. Cambridge University Press, Cambridge. U.K, New York, NY, USA, 996 pp.
27 [www.ipcc.ch/publications_and_data/publications_ipcc_fourth_assessment_report_wg1_repor](http://www.ipcc.ch/publications_and_data/publications_ipcc_fourth_assessment_report_wg1_report_the_physical_science_basis.htm)
28 [t_the_physical_science_basis.htm](http://www.ipcc.ch/publications_and_data/publications_ipcc_fourth_assessment_report_wg1_report_the_physical_science_basis.htm)
- 29 IPCC, 2012: Managing the Risks of Extreme Events and Disasters to Advance Climate Change
30 Adaptation. A Special Report of Working Groups I and II of the Intergovernmental Panel on
31 Climate Change. Field, C.B., V. Barros, T.F. Stocker, D. Qin, D.J. Dokken, K.L. Ebi, M.D.
32 Mastrandrea, K.J. Mach, G.-K. Plattner, S.K. Allen, M. Tignor, and P.M. Midgley (Eds.),
33 582 pp. Cambridge University Press, Cambridge, UK and New York, NY. [http://ipcc-](http://ipcc-wg2.gov/SREX/images/uploads/SREX-All_FINAL.pdf)
34 [wg2.gov/SREX/images/uploads/SREX-All_FINAL.pdf](http://ipcc-wg2.gov/SREX/images/uploads/SREX-All_FINAL.pdf)

- 1 IPCC, 2013: *Climate Change 2013: The Physical Science Basis. Contribution of Working Group*
2 *I to the Fifth Assessment Report of the Intergovernmental Panel on Climate Change.*
3 Cambridge University Press, Cambridge, UK and New York, NY, 1535 pp.
4 <http://dx.doi.org/10.1017/CBO9781107415324> www.climatechange2013.org
- 5 Jackson, L.C., R. Kahana, T. Graham, M.A. Ringer, T. Woollings, J.V. Mecking, and R.A.
6 Wood, 2015: Global and European climate impacts of a slowdown of the AMOC in a high
7 resolution GCM. *Climate Dynamics*, **45**, 3299-3316. <http://dx.doi.org/10.1007/s00382-015->
8 2540-2
- 9 Jakob, M. and J. Hilaire, 2015: Climate science: Unburnable fossil-fuel reserves. *Nature*, **517**,
10 150-152. <http://dx.doi.org/10.1038/517150a>
- 11 Jones, C., J. Lowe, S. Liddicoat, and R. Betts, 2009: Committed terrestrial ecosystem changes
12 due to climate change. *Nature Geoscience*, **2**, 484-487. <http://dx.doi.org/10.1038/ngeo555>
- 13 Joughin, I., B.E. Smith, and B. Medley, 2014: Marine Ice Sheet Collapse Potentially Under Way
14 for the Thwaites Glacier Basin, West Antarctica. *Science*, **344**, 735-738.
15 <http://dx.doi.org/10.1126/science.1249055>
- 16 Kang, I.-S., Y.-M. Yang, and W.-K. Tao, 2015: GCMs with implicit and explicit representation
17 of cloud microphysics for simulation of extreme precipitation frequency. *Climate Dynamics*,
18 **45**, 325-335. <http://dx.doi.org/10.1007/s00382-014-2376-1>
- 19 Kopp, R.E., R.L. Shwom, G. Wagner, and J. Yuan, 2016: Tipping elements and climate–
20 economic shocks: Pathways toward integrated assessment. *Earth's Future*, **4**, 346-372.
21 <http://dx.doi.org/10.1002/2016EF000362>
- 22 Kort, E.A., S.C. Wofsy, B.C. Daube, M. Diao, J.W. Elkins, R.S. Gao, E.J. Hintsa, D.F. Hurst, R.
23 Jimenez, F.L. Moore, J.R. Spackman, and M.A. Zondlo, 2012: Atmospheric observations of
24 Arctic Ocean methane emissions up to 82[deg] north. *Nature Geoscience*, **5**, 318-321.
25 <http://dx.doi.org/10.1038/ngeo1452>
- 26 Kretschmer, K., A. Biastoch, L. Rüpke, and E. Burwicz, 2015: Modeling the fate of methane
27 hydrates under global warming. *Global Biogeochemical Cycles*, **29**, 610-625.
28 <http://dx.doi.org/10.1002/2014GB005011>
- 29 Kvenvolden, K.A., 1988: Methane hydrate — A major reservoir of carbon in the shallow
30 geosphere? *Chemical Geology*, **71**, 41-51. [http://dx.doi.org/10.1016/0009-2541\(88\)90104-0](http://dx.doi.org/10.1016/0009-2541(88)90104-0)
- 31 Lee, S.-Y. and G.D. Holder, 2001: Methane hydrates potential as a future energy source. *Fuel*
32 *Processing Technology*, **71**, 181-186. [http://dx.doi.org/10.1016/S0378-3820\(01\)00145-X](http://dx.doi.org/10.1016/S0378-3820(01)00145-X)

- 1 Lenton, T.M., H. Held, E. Kriegler, J.W. Hall, W. Lucht, S. Rahmstorf, and H.J. Schellnhuber,
2 2008: Tipping elements in the Earth's climate system. *Proceedings of the National Academy*
3 *of Sciences*, **105**, 1786-1793. <http://dx.doi.org/10.1073/pnas.0705414105>
- 4 Levermann, A., P.U. Clark, B. Marzeion, G.A. Milne, D. Pollard, V. Radic, and A. Robinson,
5 2013: The multimillennial sea-level commitment of global warming. *Proceedings of the*
6 *National Academy of Sciences*, **110**, 13745-13750.
7 <http://dx.doi.org/10.1073/pnas.1219414110>
- 8 Levermann, A., A. Griesel, M. Hofmann, M. Montoya, and S. Rahmstorf, 2005: Dynamic sea
9 level changes following changes in the thermohaline circulation. *Climate Dynamics*, **24**, 347-
10 354. <http://dx.doi.org/10.1007/s00382-004-0505-y>
- 11 Li, C., D. Notz, S. Tietsche, and J. Marotzke, 2013: The Transient versus the Equilibrium
12 Response of Sea Ice to Global Warming. *Journal of Climate*, **26**, 5624-5636.
13 <http://dx.doi.org/10.1175/JCLI-D-12-00492.1>
- 14 Liu, J., Z. Chen, J. Francis, M. Song, T. Mote, and Y. Hu, 2016: Has Arctic Sea Ice Loss
15 Contributed to Increased Surface Melting of the Greenland Ice Sheet? *Journal of Climate*,
16 **29**, 3373-3386. <http://dx.doi.org/10.1175/JCLI-D-15-0391.1>
- 17 Lunt, D.J., T. Dunkley Jones, M. Heinemann, M. Huber, A. LeGrande, A. Winguth, C. Loptson,
18 J. Marotzke, C.D. Roberts, J. Tindall, P. Valdes, and C. Winguth, 2012: A model–data
19 comparison for a multi-model ensemble of early Eocene atmosphere–ocean simulations:
20 EoMIP. *Climate of the Past*, **8**, 1717-1736. <http://dx.doi.org/10.5194/cp-8-1717-2012>
- 21 MacDougall, A.H., C.A. Avis, and A.J. Weaver, 2012: Significant contribution to climate
22 warming from the permafrost carbon feedback. *Nature Geoscience*, **5**, 719-721.
23 <http://dx.doi.org/10.1038/ngeo1573>
- 24 MacDougall, A.H., K. Zickfeld, R. Knutti, and H.D. Matthews, 2015: Sensitivity of carbon
25 budgets to permafrost carbon feedbacks and non-CO₂ forcings. *Environmental Research*
26 *Letters*, **10**, 125003. <http://dx.doi.org/10.1088/1748-9326/10/12/125003>
- 27 McGlade, C. and P. Ekins, 2015: The geographical distribution of fossil fuels unused when
28 limiting global warming to 2 [deg]C. *Nature*, **517**, 187-190.
29 <http://dx.doi.org/10.1038/nature14016>
- 30 Mengel, M. and A. Levermann, 2014: Ice plug prevents irreversible discharge from East
31 Antarctica. *Nature Climate Change*, **4**, 451-455. <http://dx.doi.org/10.1038/nclimate2226>
- 32 Myhre, C.L., B. Ferré, S.M. Platt, A. Silyakova, O. Hermansen, G. Allen, I. Pisso, N.
33 Schmidbauer, A. Stohl, J. Pitt, P. Jansson, J. Greinert, C. Percival, A.M. Fjaeraa, S.J. O'Shea,
34 M. Gallagher, M. Le Breton, K.N. Bower, S.J.B. Bauguitte, S. Dalsøren, S.

- Vadakkepuliyambatta, R.E. Fisher, E.G. Nisbet, D. Lowry, G. Myhre, J.A. Pyle, M. Cain, and J. Mienert, 2016: Extensive release of methane from Arctic seabed west of Svalbard during summer 2014 does not influence the atmosphere. *Geophysical Research Letters*, **43**, 4624-4631. <http://dx.doi.org/10.1002/2016GL068999>
- Navarro, T., J.B. Madeleine, F. Forget, A. Spiga, E. Millour, F. Montmessin, and A. Määttänen, 2014: Global climate modeling of the Martian water cycle with improved microphysics and radiatively active water ice clouds. *Journal of Geophysical Research: Planets*, **119**, 1479-1495. <http://dx.doi.org/10.1002/2013JE004550>
- NRC, 2013: *Abrupt Impacts of Climate Change: Anticipating Surprises*. The National Academies Press, Washington, DC, 222 pp. <http://dx.doi.org/10.17226/18373>
- Pérez, F.F., H. Mercier, M. Vazquez-Rodriguez, P. Lherminier, A. Velo, P.C. Pardo, G. Roson, and A.F. Rios, 2013: Atlantic Ocean CO₂ uptake reduced by weakening of the meridional overturning circulation. *Nature Geoscience*, **6**, 146-152. <http://dx.doi.org/10.1038/ngeo1680>
- Pollard, D., R.M. DeConto, and R.B. Alley, 2015: Potential Antarctic Ice Sheet retreat driven by hydrofracturing and ice cliff failure. *Earth and Planetary Science Letters*, **412**, 112-121. <http://dx.doi.org/10.1016/j.epsl.2014.12.035>
- Quarantelli, E.L., 1986: Disaster Crisis Management. 10 pp. University of Delaware, Newark, DE. <http://udspace.udel.edu/handle/19716/487>
- Rahmstorf, S., J.E. Box, G. Feulner, M.E. Mann, A. Robinson, S. Rutherford, and E.J. Schaffernicht, 2015: Exceptional twentieth-century slowdown in Atlantic Ocean overturning circulation. *Nature Climate Change*, **5**, 475-480. <http://dx.doi.org/10.1038/nclimate2554>
- Reed, A.J., M.E. Mann, K.A. Emanuel, N. Lin, B.P. Horton, A.C. Kemp, and J.P. Donnelly, 2015: Increased threat of tropical cyclones and coastal flooding to New York City during the anthropogenic era. *Proceedings of the National Academy of Sciences*, **112**, 12610-12615. <http://dx.doi.org/10.1073/pnas.1513127112>
- Ridley, J., J.M. Gregory, P. Huybrechts, and J. Lowe, 2010: Thresholds for irreversible decline of the Greenland ice sheet. *Climate Dynamics*, **35**, 1049-1057. <http://dx.doi.org/10.1007/s00382-009-0646-0>
- Ridley, J.K., J.A. Lowe, and H.T. Hewitt, 2012: How reversible is sea ice loss? *The Cryosphere*, **6**, 193-198. <http://dx.doi.org/10.5194/tc-6-193-2012>
- Rignot, E., J. Mouginot, M. Morlighem, H. Seroussi, and B. Scheuchl, 2014: Widespread, rapid grounding line retreat of Pine Island, Thwaites, Smith, and Kohler glaciers, West Antarctica, from 1992 to 2011. *Geophysical Research Letters*, **41**, 3502-3509. <http://dx.doi.org/10.1002/2014GL060140>

- 1 Ritz, C., T.L. Edwards, G. Durand, A.J. Payne, V. Peyaud, and R.C.A. Hindmarsh, 2015:
2 Potential sea-level rise from Antarctic ice-sheet instability constrained by observations.
3 *Nature*, **528**, 115-118. <http://dx.doi.org/10.1038/nature16147>
- 4 Robinson, A., R. Calov, and A. Ganopolski, 2012: Multistability and critical thresholds of the
5 Greenland ice sheet. *Nature Climate Change*, **2**, 429-432.
6 <http://dx.doi.org/10.1038/nclimate1449>
- 7 Salzmann, U., A.M. Dolan, A.M. Haywood, W.-L. Chan, J. Voss, D.J. Hill, A. Abe-Ouchi, B.
8 Otto-Bliesner, F.J. Bragg, M.A. Chandler, C. Contoux, H.J. Dowsett, A. Jost, Y. Kamae, G.
9 Lohmann, D.J. Lunt, S.J. Pickering, M.J. Pound, G. Ramstein, N.A. Rosenbloom, L. Sohl, C.
10 Stepanek, H. Ueda, and Z. Zhang, 2013: Challenges in quantifying Pliocene terrestrial
11 warming revealed by data-model discord. *Nature Climate Change*, **3**, 969-974.
12 <http://dx.doi.org/10.1038/nclimate2008>
- 13 Schoof, C., 2007: Ice sheet grounding line dynamics: Steady states, stability, and hysteresis.
14 *Journal of Geophysical Research*, **112**, F03S28. <http://dx.doi.org/10.1029/2006JF000664>
- 15 Schuur, E.A.G., A.D. McGuire, C. Schadel, G. Grosse, J.W. Harden, D.J. Hayes, G. Hugelius,
16 C.D. Koven, P. Kuhry, D.M. Lawrence, S.M. Natali, D. Olefeldt, V.E. Romanovsky, K.
17 Schaefer, M.R. Turetsky, C.C. Treat, and J.E. Vonk, 2015: Climate change and the
18 permafrost carbon feedback. *Nature*, **520**, 171-179. <http://dx.doi.org/10.1038/nature14338>
- 19 Serinaldi, F., 2016: Can we tell more than we can know? The limits of bivariate drought analyses
20 in the United States. *Stochastic Environmental Research and Risk Assessment*, **30**, 1691-
21 1704. <http://dx.doi.org/10.1007/s00477-015-1124-3>
- 22 Smith, J.A., 1987: Estimating the upper tail of flood frequency distributions. *Water Resources*
23 *Research*, **23**, 1657-1666. <http://dx.doi.org/10.1029/WR023i008p01657>
- 24 Stranne, C., M. O'Regan, G.R. Dickens, P. Crill, C. Miller, P. Preto, and M. Jakobsson, 2016:
25 Dynamic simulations of potential methane release from East Siberian continental slope
26 sediments. *Geochemistry, Geophysics, Geosystems*, **17**, 872-886.
27 <http://dx.doi.org/10.1002/2015GC006119>
- 28 Swain, D.L., D.E. Horton, D. Singh, and N.S. Diffenbaugh, 2016: Trends in atmospheric patterns
29 conducive to seasonal precipitation and temperature extremes in California. *Science*
30 *Advances*, **2**. <http://dx.doi.org/10.1126/sciadv.1501344>
- 31 Tattersall, I., 2009: Human origins: Out of Africa. *Proceedings of the National Academy of*
32 *Sciences*, **106**, 16018-16021. <http://dx.doi.org/10.1073/pnas.0903207106>

- 1 Trenberth, K.E., A. Dai, G. van der Schrier, P.D. Jones, J. Barichivich, K.R. Briffa, and J.
2 Sheffield, 2014: Global warming and changes in drought. *Nature Climate Change*, **4**, 17-22.
3 <http://dx.doi.org/10.1038/nclimate2067>
- 4 Wagner, T.J.W. and I. Eisenman, 2015: How Climate Model Complexity Influences Sea Ice
5 Stability. *Journal of Climate*, **28**, 3998-4014. <http://dx.doi.org/10.1175/JCLI-D-14-00654.1>
- 6 Woodhouse, C.A. and J.T. Overpeck, 1998: 2000 Years of Drought Variability in the Central
7 United States. *Bulletin of the American Meteorological Society*, **79**, 2693-2714.
8 [http://dx.doi.org/10.1175/1520-0477\(1998\)079<2693:YODVIT>2.0.CO;2](http://dx.doi.org/10.1175/1520-0477(1998)079<2693:YODVIT>2.0.CO;2)
- 9 Yin, J. and P.B. Goddard, 2013: Oceanic control of sea level rise patterns along the East Coast of
10 the United States. *Geophysical Research Letters*, **40**, 5514-5520.
11 <http://dx.doi.org/10.1002/2013GL057992>
- 12 Zscheischler, J., M. Reichstein, J. von Buttlar, M. Mu, J.T. Randerson, and M.D. Mahecha, 2014:
13 Carbon cycle extremes during the 21st century in CMIP5 models: Future evolution and
14 attribution to climatic drivers. *Geophysical Research Letters*, **41**, 8853-8861.
15 <http://dx.doi.org/10.1002/2014GL062409>
- 16 Zwiers, F.W., L.V. Alexander, G.C. Hegerl, T.R. Knutson, J.P. Kossin, P. Naveau, N. Nicholls,
17 C. Schär, S.I. Seneviratne, and X. Zhang, 2013: Climate Extremes: Challenges in Estimating
18 and Understanding Recent Changes in the Frequency and Intensity of Extreme Climate and
19 Weather Events. *Climate Science for Serving Society: Research, Modeling and Prediction*
20 *Priorities*. Asrar, G.R. and J.W. Hurrell, Eds. Springer Netherlands, Dordrecht, 339-389.
21 http://dx.doi.org/10.1007/978-94-007-6692-1_13

Appendix A. Observational Datasets Used in Climate Studies

Climate Datasets

Observations, including those from satellites, mobile platforms, field campaigns and ground-based networks, provide the basis of knowledge on many temporal and spatial scales for understanding the changes occurring in the Earth's climate system. These observations also inform the development, calibration, and evaluation of numerical models of the physics, chemistry, and biology being used in analyzing the past changes in climate and for making future projections. As all observational data collected by support from Federal agencies are required to be made available free of charge with machine readable metadata, everyone can access these products for their personal analysis and research, and for informing decisions. Many of these datasets are accessible through web services.

Many long-running observations worldwide have provided us with long-term records necessary for investigating climate change and its impacts. These include many important climate variables such as surface temperature, sea ice extent, sea level rise, and streamflow. Perhaps one of the most iconic climatic datasets, that of atmospheric carbon dioxide measured at Mauna Loa, HI, has been recorded since the 1950s. The U.S. and Global Historical Climatology Networks have been used as authoritative sources of recorded surface temperature increases, with some stations having continuous records going back many decades. Satellite radar altimetry data (for example, NASA's TOPEX/JASON1,2 satellite data) have informed the development of the University of Colorado's authoritative 20+ year record of global sea level changes. In the United States, the USGS (U.S. Geological Survey) National Water Information System contains in some instances decades of daily streamflow records which inform not only climate but land use studies as well. The U.S. Bureau of Reclamation and U.S. Army Corp of Engineers have maintained data about reservoir levels for decades where applicable. Of course, datasets based on shorter-term observations are used in conjunction with longer term records for climate study, and the U.S. programs are aimed at providing continuous data records. Methods have been developed and applied to process these data so as to account for biases, collection method, earth surface geometry, the Urban Heat Island effect, station relocations, and uncertainty (e.g., see Vose et al. 2012; Rennie et al. 2014; Karl et al. 2015).

Even observations not designed for climate have informed climate research. These include ship logs containing descriptions of ice extent, readings of temperature and precipitation provided in newspapers, and harvest records. Today, observations recorded both manually and in automated fashions inform research agendas and are used in climate studies.

The U.S Global Change Research Program (USGCRP) has established the Global Change Information System (GCIS) to better coordinate and integrate the use of federal information products on changes in the global environment and the implications of those changes for society. The GCIS is an open-source, web-based resource for traceable, sound global change data,

information, and products. Designed for use by scientists, decision makers, and the public, the GCIS provides coordinated links to a select group of information products produced, maintained, and disseminated by government agencies and organizations. Currently the GCIS is aimed at the datasets used in Third National Climate Assessment (NCA3) and the USGCRP Climate and Health Assessment. It is to be updated for the datasets used in this report (The Climate Science Special Report, CSSR).

Satellite Temperature Datasets

A special look is given to the satellite temperature datasets because of controversies associated with these datasets. Satellite-borne microwave sounders such as the Microwave Sounding Unit (MSU) and Advanced Microwave Sounding Unit (AMSU) instruments operating on NOAA polar-orbiting platforms make measurements of the temperature of thick layers of the atmosphere with near global coverage. Because the long-term data record requires the piecing together of measurements made by 16 different satellites, accurate instrument intercalibration is of critical importance. Over the mission lifetime of most satellites, the instruments drift in both calibration and local measurement time. Adjustments to counter the effects of these drifts need to be developed and applied before a long-term record can be assembled. For tropospheric measurements, the most challenging of these adjustments is the adjustment for drifting measurement time, which requires knowledge of the diurnal cycle in both atmospheric and surface temperature. Current versions of the sounder-based datasets account for the diurnal cycle by either using diurnal cycles deduced from model output (Mears and Wentz 2009; Zou et al. 2009) or by attempting to derive diurnal cycle from the satellite measurements themselves (an approach plagued by sampling issues and possible calibration drifts) (Christy et al. 2003; Po-Chedley et al. 2015). Recently Mears and Wentz developed a hybrid approach, RSS Version 4.0 (Mears and Wentz 2016), that resulting in an increased warming signal relative to the other approaches, particularly since 2000. Each of these methods has strengths and weaknesses, but neither has sufficient accuracy to construct an unassailable long-term record of atmospheric temperature change. The resulting datasets show a greater spread in decadal-scale trends than do the surface temperature datasets for the same period, suggesting that they may be less reliable. In Figure A.1 shows annual time series for the global mean tropospheric temperature for some recent versions of the satellite datasets. These data have been adjusted to remove the influence of stratospheric cooling (Fu and Johanson 2005). Linear trend values are shown in Table A.1.

[Figure A.1. Annual global (80°S-80°N) mean time series of tropospheric temperature for five recent datasets. Each time series is adjusted so the mean value for the first three years is zero. This accentuates the differences in the long-term changes between the datasets. Figure source: Remote Sensing Systems]

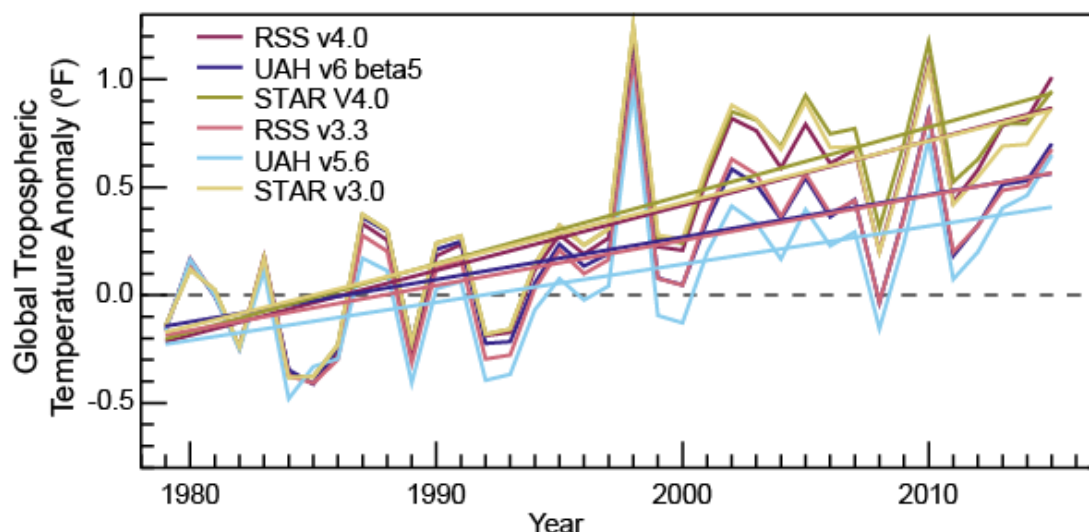
[Table A.1. Global Trends in Temperature Total Troposphere (TTT) since 1979 and 2000. (in degrees F per decade)]

1 **TABLE**

2 **Table A.1.** Global Trends in Temperature Total Troposphere (TTT) since 1979 and 2000 (in
 3 degrees F per decade).

Dataset	Trend (1979–2015) (°F/Decade)	Trend (2000–2015) (°F/Decade)
RSS V4.0	0.301	0.198
UAH V6Beta5	0.196	0.141
STAR V4.0	0.316	0.157
RSS V3.3	0.208	0.105
UAH V5.6	0.176	0.211
STAR V3.0	0.286	0.061

4

1 **FIGURE**

2
3 **Figure A.1.** Annual global (80°S–80°N) mean time series of tropospheric temperature for five
4 recent datasets (see below). Each time series is adjusted so the mean value for the first three
5 years is zero. This accentuates the differences in the long-term changes between the datasets.
6 (Figure source: Remote Sensing Systems)

7 **DATA SOURCES:**

8 All Satellite Data are “Temperature Total Troposphere” time series calculated from TMT and TLS
9 $(1.1 \times \text{TMT}) - (0.1 \times \text{TLS})$. This combination reduces the effect of the lower stratosphere on the tropospheric
10 temperature. (Fu, Qiang et al. "Contribution of stratospheric cooling to satellite-inferred tropospheric
11 temperature trends." *Nature* 429.6987 (2004): 55-58.)

12 UAH. UAH Version 6.0Beta5. Yearly (yyyy) text files of TMT and TLS are available from
13 http://vortex.nsstc.uah.edu/data/msu/v6.0beta/tmt/tmtmonamg.yyyy_6.0beta5
14 http://vortex.nsstc.uah.edu/data/msu/v6.0beta/tls/tlsmonamg.yyyy_6.0beta5
15 Downloaded 5/15/2016.

16 UAH. UAH Version 5.6. Yearly (yyyy) text files of TMT and TLS are available from
17 <http://vortex.nsstc.uah.edu/data/msu/t2/>
18 <http://vortex.nsstc.uah.edu/data/msu/t4/>
19 Downloaded 5/15/2016.

20 RSS. RSS Version 4.0. ftp://ftp.remss.com/msu/data/netcdf/RSS_Tb_Anom_Maps_ch_TTT_V4_0.nc
21 Downloaded 5/15/2016

22 RSS. RSS Version 3.3. ftp://ftp.remss.com/msu/data/netcdf/RSS_Tb_Anom_Maps_ch_TTT_V3.3.nc
23 Downloaded 5/15/2016

24 NOAA STAR. Star Version 3.0.
25 ftp://ftp.star.nesdis.noaa.gov/pub/smcd/emb/mscat/data/MSU_AMSU_v3.0/Monthly_Atmospheric_Layer_Mean_Temperature/Merged_Deep-Layer_Temperature/NESDIS-STAR_TCDR_MSU-AMSUA_V03R00_TMT_S197811_E201604_C20160513.nc
26 ftp://ftp.star.nesdis.noaa.gov/pub/smcd/emb/mscat/data/MSU_AMSU_v3.0/Monthly_Atmospheric_Layer_Mean_Temperature/Merged_Deep-Layer_Temperature/NESDIS-STAR_TCDR_MSU-AMSUA_V03R00_TLS_S197811_E201604_C20160513.nc
27 ftp://ftp.star.nesdis.noaa.gov/pub/smcd/emb/mscat/data/MSU_AMSU_v3.0/Monthly_Atmospheric_Layer_Mean_Temperature/Merged_Deep-Layer_Temperature/NESDIS-STAR_TCDR_MSU-AMSUA_V03R00_TLS_S197811_E201604_C20160513.nc
28 Downloaded 5/18/2016.

REFERENCES

- Christy, J.R., R.W. Spencer, W.B. Norris, W.D. Braswell, and D.E. Parker, 2003: Error estimates of version 5.0 of MSU–AMSU bulk atmospheric temperatures. *Journal of Atmospheric and Oceanic Technology*, **20**, 613-629. [http://dx.doi.org/10.1175/1520-0426\(2003\)20<613:EEOVOM>2.0.CO;2](http://dx.doi.org/10.1175/1520-0426(2003)20<613:EEOVOM>2.0.CO;2)
- Fu, Q. and C.M. Johanson, 2005: Satellite-derived vertical dependence of tropical tropospheric temperature trends. *Geophysical Research Letters*, **32**.
<http://dx.doi.org/10.1029/2004GL022266>
- Karl, T.R., A. Arguez, B. Huang, J.H. Lawrimore, J.R. McMahon, M.J. Menne, T.C. Peterson, R.S. Vose, and H.-M. Zhang, 2015: Possible artifacts of data biases in the recent global surface warming hiatus. *Science*, **348**, 1469-1472. <http://dx.doi.org/10.1126/science.aaa5632>
- Mears, C.A. and F.J. Wentz, 2009: Construction of the Remote Sensing Systems V3.2 atmospheric temperature records from the MSU and AMSU microwave sounders. *Journal of Atmospheric and Oceanic Technology*, **26**, 1040-1056.
<http://dx.doi.org/10.1175/2008JTECHA1176.1>
- Mears, C.A. and F.J. Wentz, 2016: Sensitivity of satellite-derived tropospheric temperature trends to the diurnal cycle adjustment. *Journal of Climate*, **29**, 3629-3646.
<http://dx.doi.org/10.1175/JCLI-D-15-0744.1>
- Po-Chedley, S., T.J. Thorsen, and Q. Fu, 2015: Removing diurnal cycle contamination in satellite-derived tropospheric temperatures: Understanding tropical tropospheric trend discrepancies. *Journal of Climate*, **28**, 2274-2290. <http://dx.doi.org/10.1175/JCLI-D-13-00767.1>
- Rennie, J.J., J.H. Lawrimore, B.E. Gleason, P.W. Thorne, C.P. Morice, M.J. Menne, C.N. Williams, W.G. de Almeida, J.R. Christy, M. Flannery, M. Ishihara, K. Kamiguchi, A.M.G. Klein-Tank, A. Mhanda, D.H. Lister, V. Razuvaev, M. Renom, M. Rusticucci, J. Tandy, S.J. Worley, V. Venema, W. Angel, M. Brunet, B. Dattore, H. Diamond, M.A. Lazzara, F. Le Blancq, J. Luterbacher, H. Mächel, J. Revadekar, R.S. Vose, and X. Yin, 2014: The international surface temperature initiative global land surface databank: monthly temperature data release description and methods. *Geoscience Data Journal*, **1**, 75-102.
<http://dx.doi.org/10.1002/gdj3.8> <http://dx.doi.org/10.1002/gdj3.8>
- Vose, R.S., D. Arndt, V.F. Banzon, D.R. Easterling, B. Gleason, B. Huang, E. Kearns, J.H. Lawrimore, M.J. Menne, T.C. Peterson, R.W. Reynolds, T.M. Smith, C.N. Williams, and D.L. Wuertz, 2012: NOAA's Merged Land-Ocean Surface Temperature Analysis. *Bulletin of the American Meteorological Society*, **93**, 1677-1685. <http://dx.doi.org/10.1175/BAMS-D-11-00241.1>

- 1 Zou, C.-Z., M. Gao, and M.D. Goldberg, 2009: Error structure and atmospheric temperature
- 2 trends in observations from the microwave sounding unit. *Journal of Climate*, **22**, 1661-1681.
- 3 <http://dx.doi.org/10.1175/2008JCLI2233.1>

DRAFT

Appendix B: Weighting Strategy for the Fourth National Climate Assessment

Introduction

This document briefly describes weighting strategy for use with the Climate Model Intercomparison Project, Phase 5 (CMIP5) multimodel archive in the 4th National Climate Assessment which considers both skill in the climatological performance of models over North America as well as the inter-dependency of models arising from common parameterizations or tuning practises. The method exploits information relating to the climatological mean state of a number of projection-relevant variables as well as long-term metrics representing long-term statistics of weather extremes. The weights, once computed, can be used to simply compute weighted mean and significance information from an ensemble containing multiple initial condition members from co-dependent models of varying skill.

Our methodology is based on the concepts outlined in Sanderson et al. (2015), and the specific application to the Fourth National Climate Assessment (NCA4) is also described in that paper. The approach produces a single set of model weights which can be used to combine projections into a weighted mean result, with significance estimates which also treat the weighting appropriately.

The method, ideally, would seek to have two fundamental characteristics:

- If a duplicate of one ensemble member is added to the archive, the resulting mean and significance estimate for future change computed from the ensemble should not change.
- If a demonstrably unphysical model is added to the archive, the resulting mean and significance estimates should also not change.

Method

The analysis requires an assessment of both model skill and an estimate of inter-model relationships – for which inter-model root mean square difference is taken as a proxy. The model and observational data used here is for the contiguous United States (CONUS), and most of Canada, using high resolution data where available. Inter-model distances are computed as simple root mean square differences. Data is derived from a number of mean state fields, and a number of fields, which represent extreme behavior—these are listed in Table B.1. All fields are masked to only include information from CONUS/Canada.

The RMSE between observations and each model can be used to produce an overall ranking for model simulations of the North American climate, Figure B.1 shows how this metric is influenced by different component variables.

[INSERT FIGURE B.1 HERE:]

Figure B.1: A graphical representation of the inter-model distance matrix for CMIP5 and a set of observed values. Each row and column represents a single climate model (or observation). All scores are aggregated over seasons (individual seasons are not shown). Each box represents a pair-wise distance, where warm colors indicate a greater distance. Distances are measured as a fraction of the mean inter-model distance in the CMIP5 ensemble. (Figure source: Sanderson et al. 2016)]

[INSERT FIGURE B.2 HERE:]

Figure B.2: Model skill and independence weights for the CMIP-5 archive evaluated over the North American domain. Contours show the overall weighting, which is the product of the two individual weights. (Figure source: Sanderson et al. 2016)]

Models are downweighted for poor skill if their multivariate combined error is significantly greater than a “skill radius” term, which is a free parameter of the approach, and the calibration of this parameter is determined through a perfect model study (Sanderson et al. 2016). A pairwise distance matrix is computed to assess inter-model RMSE values for each model pair in the archive, and a model is downweighted for dependency if there exists another model with a pairwise distance to the original model significantly smaller than a “similarity radius.” This is the second parameter of the approach, which is calibrated by considering known relationships within the archive. The resulting skill and independence weights are multiplied to give an overall “combined” weight—illustrated in Figure B.2 for the CMIP5 ensemble, and listed in Table B.2.

The weights are used in the Climate Science Special Report (CSSR) to produce weighted mean and significant maps of future change, where the following protocol is used:

Stippling—large changes where the weighted multimodel average change is greater than double the standard deviation of the 20-year mean from control simulations runs and 90% of the weight corresponds to changes of the same sign.

Hatching—No significant change where the weighted multimodel average change is less than the standard deviation of the 20-year means from control simulations runs.

Whited out—Inconclusive where the weighted multimodel average change is greater than double the standard deviation of the 20-year mean from control runs and less than 90% of the weight corresponds to changes of the same sign.

We illustrate the application of this method to future projections of precipitation change under RCP8.5 in Figure B.3. The weights used in the report are chosen to be conservative, minimizing the risk of overconfidence and maximizing out-of-sample predictive skill for future projections. This results (as in Figure B.3) in only modest differences in the weighted and unweighted maps. It is shown in Sanderson et al. (2016) that a more aggressive weighting strategy, or one focused on a particular variable, tends to exhibit a stronger constraint on future change relative to the unweighted case. It is also notable trade-offs exist between skill and replication in the archive (evident in Figure B.2), such that the weighting for both skill and uniqueness has a compensating effect. As such, mean projections using the CMIP5 ensemble are not strongly influenced by the weighting. However, the establishment of the weighting strategy used in the CSSR provides some insurance against a potential case in future assessments where there is a highly replicated, but poorly performing model.

[INSERT FIGURE B.3 HERE:]

Figure B.3: Projections of precipitation change over North America in 2080–2100, relative to 1980–2000 under RCP8.5. (a) shows the simple unweighted CMIP5 multi-model average, using the significance methodology from (IPCC 2013), (b) shows the weighted results as outlined in section 3 for models weighted by uniqueness only, and (c) shows weighted results for models weighted by both uniqueness and skill. (Figure source: Sanderson et al. 2016)]

1 **TABLES**2 **Table B.1:** Observational Datasets used as observations.

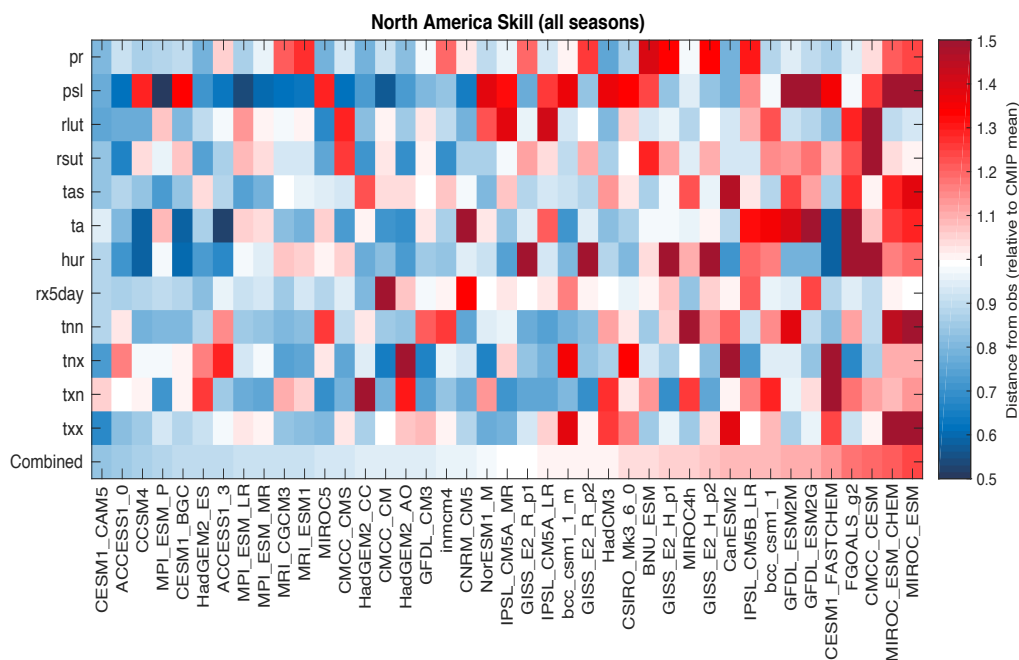
3

Field	Description	Source	Reference	Years
TS	Surface Temperature (seasonal)	Livneh,Hutchinson	(Hopkinson et al. 2012; Hutchinson et al. 2009; Livneh et al. 2013)	1950-2011
PR	Mean Precipitation (seasonal)	Livneh,Hutchinson	(Hopkinson et al. 2012; Hutchinson et al. 2009; Livneh et al. 2013)	1950-2011
RSUT	TOA Shortwave Flux (seasonal)	CERES-EBAF	(NASA 2011)	2000-2005
RLUT	TOA Longwave Flux (seasonal)	CERES-EBAF	(NASA 2011)	2000-2005
T	Vertical Temperature Profile (seasonal)	AIRS*	(Aumann et al. 2003)	2002-2010
RH	Vertical Humidity Profile (seasonal)	AIRS	(Aumann et al. 2003)	2002-2010
PSL	Surface Pressure (seasonal)	ERA-40	(Uppala et al. 2005)	1970-2000
Tnn	Coldest Night	Livneh,Hutchinson	(Hopkinson et al. 2012; Hutchinson et al. 2009; Livneh et al. 2013)	1950-2011
Txn	Coldest Day	Livneh,Hutchinson	(Hopkinson et al. 2012; Hutchinson et al. 2009; Livneh et al. 2013)	1950-2011
Tnx	Warmest Night	Livneh,Hutchinson	(Hopkinson et al. 2012; Hutchinson et al. 2009; Livneh et al. 2013)	1950-2011
Txx	Warmest day	Livneh,Hutchinson	(Hopkinson et al. 2012; Hutchinson et al. 2009; Livneh et al. 2013)	1950-2011
rx5day	seasonal max. 5-day total precip.	Livneh,Hutchinson	(Hopkinson et al. 2012; Hutchinson et al. 2009; Livneh et al. 2013)	1950-2011

4

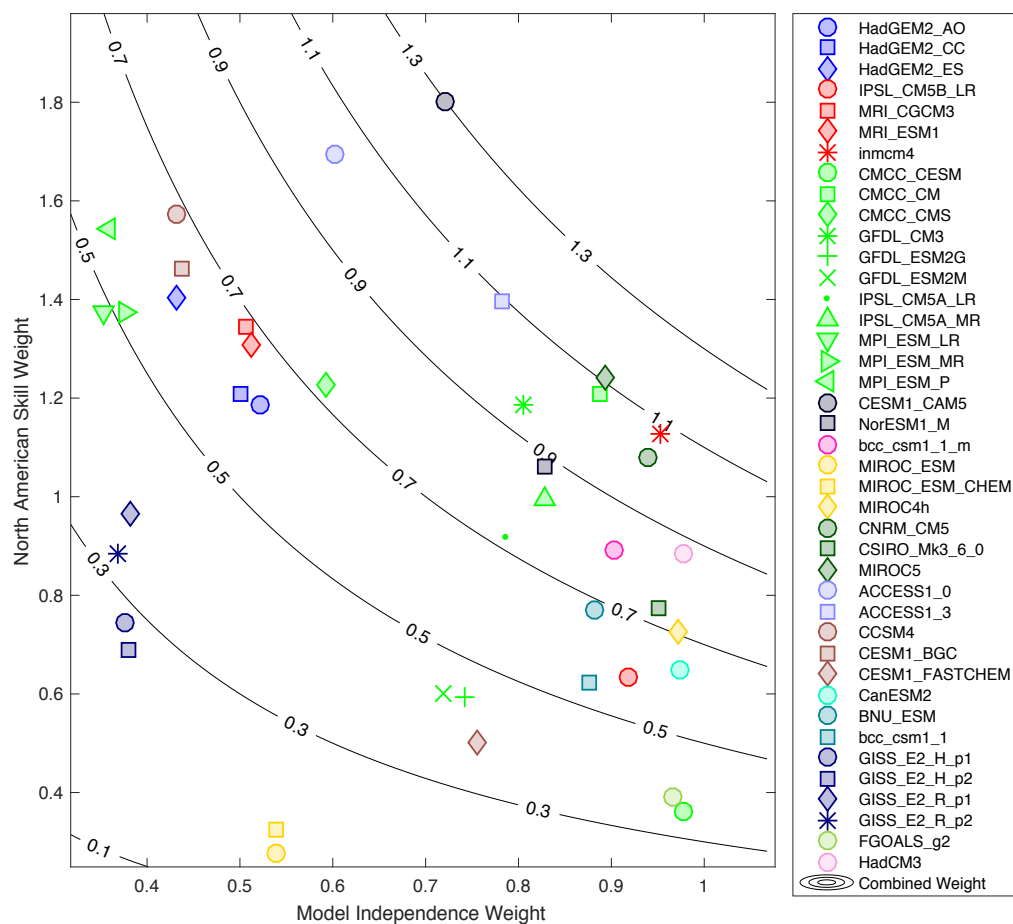
1 **Table B.2:** Uniqueness, Skill and Combined weights for CMIP5

	Uniqueness weight	Skill Weight	Combined
ACCESS1-0	0.60	1.69	1.02
ACCESS1-3	0.78	1.40	1.09
BNU-ESM	0.88	0.77	0.68
CCSM4	0.43	1.57	0.68
CESM1-BGC	0.44	1.46	0.64
CESM1-CAM5	0.72	1.80	1.30
CESM1-FASTCHEM	0.76	0.50	0.38
CMCC-CESM	0.98	0.36	0.35
CMCC-CM	0.89	1.21	1.07
CMCC-CMS	0.59	1.23	0.73
CNRM-CM5	0.94	1.08	1.01
CSIRO-Mk3-6-0	0.95	0.77	0.74
CanESM2	0.97	0.65	0.63
FGOALS-g2	0.97	0.39	0.38
GFDL-CM3	0.81	1.18	0.95
GFDL-ESM2G	0.74	0.59	0.44
GFDL-ESM2M	0.72	0.60	0.43
GISS-E2-H-p1	0.38	0.74	0.28
GISS-E2-H-p2	0.38	0.69	0.26
GISS-E2-R-p1	0.38	0.97	0.37
GISS-E2-R-p2	0.37	0.89	0.33
HadCM3	0.98	0.89	0.87
HadGEM2-AO	0.52	1.19	0.62
HadGEM2-CC	0.50	1.21	0.60
HadGEM2-ES	0.43	1.40	0.61
IPSL-CM5A-LR	0.79	0.92	0.72
IPSL-CM5A-MR	0.83	0.99	0.82
IPSL-CM5B-LR	0.92	0.63	0.58
MIROC-ESM	0.54	0.28	0.15
MIROC-ESM-CHEM	0.54	0.32	0.17
MIROC4h	0.97	0.73	0.71
MIROC5	0.89	1.24	1.11
MPI-ESM-LR	0.35	1.38	0.49
MPI-ESM-MR	0.38	1.37	0.52
MPI-ESM-P	0.36	1.54	0.56
MRI-CGCM3	0.51	1.35	0.68
MRI-ESM1	0.51	1.31	0.67
NorESM1-M	0.83	1.06	0.88
bcc-csm1-1	0.88	0.62	0.55
bcc-csm1-1-m	0.90	0.89	0.80
inmcm4	0.95	1.13	1.08

1 **FIGURES**

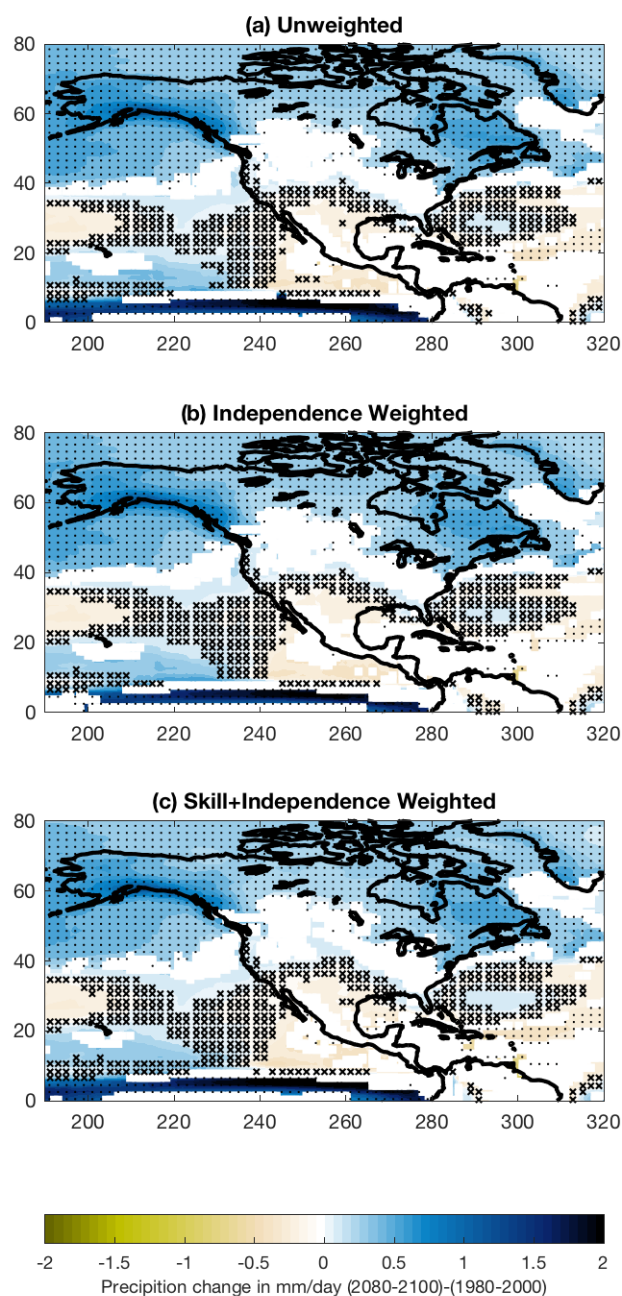
2

3 **Figure B.1:** A graphical representation of the inter-model distance matrix for CMIP5 and
 4 a set of observed values. Each row and column represents a single climate model (or
 5 observation). All scores are aggregated over seasons (individual seasons are not shown).
 6 Each box represents a pair-wise distance, where warm colors indicate a greater distance.
 7 Distances are measured as a fraction of the mean inter-model distance in the CMIP5
 8 ensemble. (Figure source: Sanderson et al. 2016)



1

2 **Figure B.2:** Model skill and independence weights for the CMIP-5 archive evaluated
 3 over the North American domain. Contours show the overall weighting, which is the
 4 product of the two individual weights. (Figure source: Sanderson et al. 2016)



1

2 **Figure B.3:** Projections of precipitation change over North America in 2080–2100,
 3 relative to 1980–2000 under RCP8.5. (a) shows the simple unweighted CMIP5 multi-
 4 model average, using the significance methodology from (IPCC 2013), (b) shows the
 5 weighted results as outlined in section 3 for models weighted by uniqueness only, and (c)
 6 shows weighted results for models weighted by both uniqueness and skill. (Figure source:
 7 Sanderson et al. 2016)

REFERENCES

- Aumann, H.H., M.T. Chahine, C. Gautier, M.D. Goldberg, E. Kalnay, L.M. McMillin, H. Revercomb, P.W. Rosenkranz, W.L. Smith, D.H. Staelin, L.L. Strow, and J. Susskind, 2003: AIRS/AMSU/HSB on the Aqua mission: Design, science objectives, data products, and processing systems. *IEEE Transactions on Geoscience and Remote Sensing*, **41**, 253-264. <http://dx.doi.org/10.1109/TGRS.2002.808356>
- Hopkinson, R.F., M.F. Hutchinson, D.W. McKenney, E.J. Milewska, and P. Papadopol, 2012: Optimizing Input Data for Gridding Climate Normals for Canada. *Journal of Applied Meteorology and Climatology*, **51**, 1508-1518. <http://dx.doi.org/10.1175/JAMC-D-12-018.1>
- Hutchinson, M.F., D.W. McKenney, K. Lawrence, J.H. Pedlar, R.F. Hopkinson, E. Milewska, and P. Papadopol, 2009: Development and Testing of Canada-Wide Interpolated Spatial Models of Daily Minimum–Maximum Temperature and Precipitation for 1961–2003. *Journal of Applied Meteorology and Climatology*, **48**, 725-741. <http://dx.doi.org/10.1175/2008JAMC1979.1>
- IPCC, 2013: *Climate Change 2013: The Physical Science Basis. Contribution of Working Group I to the Fifth Assessment Report of the Intergovernmental Panel on Climate Change*. Cambridge University Press, Cambridge, UK and New York, NY, 1535 pp. <http://dx.doi.org/10.1017/CBO9781107415324> www.climatechange2013.org
- Livneh, B., E.A. Rosenberg, C. Lin, B. Nijssen, V. Mishra, K.M. Andreadis, E.P. Maurer, and D.P. Lettenmaier, 2013: A Long-Term Hydrologically Based Dataset of Land Surface Fluxes and States for the Conterminous United States: Update and Extensions. *Journal of Climate*, **26**, 9384-9392. <http://dx.doi.org/10.1175/JCLI-D-12-00508.1>
- NASA, 2011: CERES EBAF Data Sets. <https://ceres.larc.nasa.gov/products.php?product=EBAF-TOA>
- Sanderson, B.M., R. Knutti, and P. Caldwell, 2015: A Representative Democracy to Reduce Interdependency in a Multimodel Ensemble. *Journal of Climate*, **28**, 5171-5194. <http://dx.doi.org/10.1175/JCLI-D-14-00362.1>
- Sanderson, B.M., M. Wehner, and R. Knutti, 2016: Skill and Independence weighting for multi-model Assessment. *Geoscientific Model Development* **Submitted**.
- Uppala, S.M., P.W. Kållberg, A.J. Simmons, U. Andrae, V.D.C. Bechtold, M. Fiorino, J.K. Gibson, J. Haseler, A. Hernandez, G.A. Kelly, X. Li, K. Onogi, S. Saarinen, N. Sokka, R.P. Allan, E. Andersson, K. Arpe, M.A. Balmaseda, A.C.M. Beljaars, L.V.D. Berg, J. Bidlot, N. Bormann, S. Caires, F. Chevallier, A. Dethof, M. Dragosavac, M.

- 1 Fisher, M. Fuentes, S. Hagemann, E. Hólm, B.J. Hoskins, L. Isaksen, P.A.E.M.
- 2 Janssen, R. Jenne, A.P. McNally, J.F. Mahfouf, J.J. Morcrette, N.A. Rayner, R.W.
- 3 Saunders, P. Simon, A. Sterl, K.E. Trenberth, A. Untch, D. Vasiljevic, P. Viterbo, and
- 4 J. Woollen, 2005: The ERA-40 re-analysis. *Quarterly Journal of the Royal*
- 5 *Meteorological Society*, **131**, 2961-3012. <http://dx.doi.org/10.1256/qj.04.176>

Appendix C. Acronyms and Units

AGCMs	Atmospheric General Circulation Models
AIS	Antarctic Ice Sheet
AMO	Atlantic Multidecadal Oscillation
AMOC	Atlantic meridional overturning circulation
AMSU	Advanced Microwave Sounding Unit
AO	Arctic Oscillation
AOD	aerosol optical depth
ARs	atmospheric rivers
AW	Atlantic Water
BAMS	Bulletin of the American Meteorological Society
BC	black carbon
BCE	Before Common Era
CAM5	Community Atmospheric Model, Version 5
CAPE	convective available potential energy
CCN	cloud condensation nuclei
CCSM3	Community Climate System Model, Version 3 (UCAR)
CDR	carbon dioxide removal
CE	Common Era
CENRS	Committee on Environment, Natural Resources, and Sustainability (National Science and Technology Council, White House)
CESM-LE	Community Earth System Model Large Ensemble Project (UCAR)
CFCs	chlorofluorocarbons
CI	climate intervention
CMIP5	Coupled Model Intercomparison Project, Fifth Phase (also CMIP3 and CMIP6)
CONUS	contiguous United States
CP	Central Pacific
CSSR	Climate Science Special Report
DIC	dissolved inorganic carbon
DJF	December-January-February
DOD SERP	U.S. Department of Defense, Strategic Environmental Research Program
DOE	U.S. Department of Energy
EAIS	East Antarctic Ice Sheet
ECS	equilibrium climate sensitivity
ENSO	El Niño-Southern Oscillation
EOF analysis	empirical orthogonal function analysis
EP	Eastern Pacific

ERF	effective radiative forcing
ESD	empirical statistical downscaling
ESDMs	empirical statistical downscaling models
ESMs	Earth System Models
ESS	Earth system sensitivity
ETC	extra-tropical (or extratropical?) cyclone
ETCCDI	Expert Team on Climate Change Detection Indices
GBI	Greenland Blocking Index
GCIS	Global Change Information System
GCMs	global climate models
GeoMIP	Geoengineering Model Intercomparison Project
GFDL HiRAM	Geophysical Fluid Dynamics Laboratory, global HIgh Resolution Atmospheric Model (NOAA)
GHCN	Global Historical Climatology Network (National Centers for Environmental Information, NOAA)
GHG	greenhouse gas
GMSL	global mean sea level
GMT	global mean temperature
GPS	global positioning system
GRACE	Gravity Recovery and Climate Experiment
GrIS	Greenland Ice Sheet
GWP	global warming potential
HadCM3	Hadley Centre Coupled Model, Version 3
HadCRUT4	Hadley Centre Climatic Research Unit Gridded Surface Temperature Data Set 4
HCFCs	hydrochlorofluorocarbons
HFCs	hydrofluorocarbons
HOT	Hawai'i Ocean Time-series
HOT-DOGS	Hawai'i Ocean Time-series Data Organization & Graphical System
HURDAT2	revised Atlantic Hurricane Database (National Hurricane Center, NOAA)
IAMs	integrated assessment models
IAV	impacts, adaptation, and vulnerability
INDCs	Intended Nationally Determined Contributions
INMCM	Institute for Numerical Mathematics Climate Model
IPCC	Intergovernmental Panel on Climate Change
IPCC AR5	Fifth Assessment Report of the IPCC; also SPM – Summary for Policymakers, and WG1, WG2, WG3 – Working Groups 1-3
IPO	Interdecadal Pacific Oscillation
IQA	Information Quality Act

IVT	integrated vapor transport
JGOFS	U.S. Joint Global Ocean Flux Study
JJA	June-July-August
JTWC	Joint Typhoon Warning Center
LCC	land cover changes
LULCC	land use and land cover change
MAM	March-April-May
MSU	Microwave Sounding Unit
NAM	Northern Annular Mode
NAO	North Atlantic Oscillation
NARCCAP	North American Regional Climate Change Assessment Program (World Meteorological Organization)
NAS	National Academy of Sciences
NASA	National Aeronautics and Space Administration
NCA	National Climate Assessment
NCA3	Third National Climate Assessment
NCA4	Fourth National Climate Assessment
NCEI	National Centers for Environmental Information (NOAA)
NDCs	nationally determined contributions
NOAA	National Oceanic and Atmospheric Administration
NPI	North Pacific Index
NPO	North Pacific oscillation
NPP	net primary production
OMZs	oxygen minimum zones
OSTP	Office of Science and Technology Policy (White House)
PCA	principle component analysis
PDO	Pacific decadal oscillation
PDSI	Palmer Drought Severity Index
PETM	Paleo-Eocene Thermal Maximum
PFCs	perfluorocarbons
PGW	pseudo-global warming
PNA	Pacific North American Pattern
RCMs	regional climate models
RCPs	Representative Concentration Pathways
RF	radiative forcing
RFaci	aerosol-cloud interaction (effect on RF)
RFari	aerosol-radiation interaction (effect on RF)
RMSE	root-mean-square-error
RSL	relative sea level
RSS	remote sensing systems

S06	surface-to-6 km layer
SCE	snow cover extent
SGCR	Subcommittee on Global Change Research (National Science and Technology Council, White House)
SLCFs	short-lived climate forcers
SLCPs	short-lived climate pollutants
SLR	sea level rise
SOC	soil organic carbon
SRES	Special Report on Emissions Scenarios (IPCC, 2000)
SREX	Special Report on Managing the Risks of Extreme Events and Disasters to Advance Climate Change Adaptation (IPCC, 2012)
SRM	solar radiation management
SSC	Science Steering Committee
SSI	solar spectral irradiance
SSPs	Shared Socioeconomic Pathways
SST	sea surface temperature
STAR	Center for Satellite Applications and Research (NOAA)
SWCRE	short-wave cloud radiative effect (on radiative fluxes)
LWCRE	long-wave cloud radiative effect (on radiative fluxes)
TA	total alkalinity
TC	tropical cyclone
TCR	transient climate response
TCRE	transient climate response to cumulative carbon emissions
tOM	total observed organic matter
TOPEX/JASON1,2	Topography Experiment/Joint Altimetry Satellite Oceanography Network satellites (NASA)
TSI	total solar irradiance
TTT	temperature total troposphere
UAH	University of Alabama, Huntsville
UHI	urban heat island (effect)
UNFCCC	United Nations Framework Convention on Climate Change
USGCRP	U.S. Global Change Research Program
USGS	U.S. Geological Survey
UV	ultraviolet
VOCs	volatile organic compounds
WAIS	West Antarctic Ice Sheet
WCRP	World Climate Research Programme
WMGHGs	well-mixed greenhouse gases
WOCE	World Ocean Circulation Experiment (JGOFS)

Abbreviations and Units

C	carbon
CO	carbon monoxide
CH ₄	methane
cm	centimeters
CO ₂	carbon dioxide
°C	degrees celsius
°F	degrees fahrenheit
GtC	gigatonnes of carbon
hPA	hectopascal
H ₂ S	hydrogen sulfide
H ₂ SO ₄	sulfuric acid
km	kilometers
m	meters
mm	millimeters
Mt	megaton
µatm	microatmosphere
N	nitrogen
N ₂ O	nitrous oxide
NO _x	nitrogen oxides
O ₂	molecular oxygen
O ₃	ozone
OH	hydroxyl radical
PgC	petagrams of carbon
ppb	parts per billion
ppm	parts per million
SF ₆	sulfur hexafluoride
SO ₂	sulfur dioxide
TgC	terragrams of carbon (eliminate space in text)
W/m ²	Watts per meters squared